ACTA CHIMICA

ACADEMIAE SCIENTIARUM HUNGARICAE

ADIUVANTIBUS

L. ERDEY, K. POLINSZKY, G. SCHAY

AC

R. BOGNÁR, GY. BRUCKNER, Z. CSŰRÖS, T. ERDEY-GRÚZ, Z. FÖLDI, M. FREUND, Á. GERECS, GY. HARDY, J. HOLLÓ, Á. KISS, M. KORACH, F. MÁRTA, F. NAGY, J. PROSZT, E. PUNGOR, Z. SZABÓ, P. TÉTÉNYI, L. VARGHA, K. VAS

REDIGIT

B. LENGYEL

TOMUS 56 FASCICULUS 1

AKADÉMIAI KIADÓ, BUDAPEST

1968

ACTA CHIM. ACAD. SCI. HUNG.

ACTA CHIMICA

A MAGYAR TUDOMÁNYOS AKADÉMIA KÉMIAI TUDOMÁNYOK OSZTÁLYÁNAK IDEGEN NYELVŰ KÖZLEMÉNYEI

SZERKESZTI

LENGYEL BÉLA

TECHNIKAI SZERKESZTŐK

DEÁK GYULA és TAKÁCS VILMOS

Az Acta Chimica német, angol, francia és orosz nyelven közöl értekezéseket a kémiai tudományok köréből.

Az Acta Chimica változó terjedelmű füzetekben jelenik meg, egy-egy kötet négy füzetből áll. Évente átlag négy kötet jelenik meg.

A közlésre szánt kéziratok a szerkesztőség címére (Budapest 502, postafiók 32) küldendők.

Ugyanerre a címre küldendő minden szerkesztőségi levelezés. A szerkesztőség kéziratokat nem ad vissza.

Az Acta Chimica előfizetési ára kötetenként belföldre 120 Ft, külföldre 165 Ft. Megrendelhető a belföld számára az „Akadémiai Kiadó"-nál (Budapest V., Alkotmány utca 21. Bankszámla 05-915-111-46), a külföld számára pedig a „Kultúra" Könyv- és Hírlap Külkereskedelmi Vállalatnál (Budapest I., Fő utca 32. Bankszámla: 43-790-057-181) vagy annak külföldi képviseleteinél és bizományosainál.

Die Acta Chimica veröffentlichen Abhandlungen aus dem Bereiche der chemischen Wissenschaften in deutscher, englischer, französischer und russischer Sprache.

Die Acta Chimica erscheinen in Heften wechselnden Umfanges. Vier Hefte bilden einen Band. Jährlich erscheinen 4 Bände.

Die zur Veröffentlichung bestimmten Manuskripte sind an folgende Adresse zu senden:

Acta Chimica
Budapest 502, Postafiók 32.

An die gleiche Anschrift ist auch jede für die Redaktion bestimmte Korrespondenz zu richten.

Abonnementspreis pro Band: 165 Forint. Bestellbar bei dem Buch- und Zeitungs-Außenhandels-Unternehmen »*Kultúra*« (Budapest I., Fő utca 32. Bankkonto No. 43-790-057-181) oder bei seinen Auslandsvertretungen und Kommissionären.

ACTA CHIMICA

ACADEMIAE SCIENTIARUM HUNGARICAE

ADIUVANTIBUS

L. ERDEY, K. POLINSZKY, G. SCHAY

AC

R. BOGNÁR, GY. BRUCKNER, Z. CSŰRÖS, T. ERDEY-GRÚZ, Z. FÖLDI, M. FREUND, Á. GERECS, GY. HARDY, J. HOLLÓ, Á. KISS, M. KORACH, F. MÁRTA, F. NAGY, J. PROSZT, E. PUNGOR, Z. SZABÓ, P. TÉTÉNYI, L. VARGHA, K. VAS

REDIGIT

B. LENGYEL

TOMUS 56

AKADÉMIAI KIADÓ, BUDAPEST

1968

ACTA CHIMICA

TOMUS 56

Fasciculus 1: 1968

Fasciculus 2: 1968

Fasciculus 3: 1968

Fasciculus 4: 1968

INDEX

ABOULEZZ, A. F. s. MATKOVICS, B.

AGÓCS, P. s. WEISS, I.

BARTA, M. s. GERECS, A.

BARTÓK, M. and KOVÁCS, K.: Chemical Transformations of Diols and Cyclic Ethers, XXIV. Investigation of the Conversion of 2-monosubstituted Oxetanes in the Presence of Platinum Catalysts by the Microreactor Technique 369

BARTÓK, M. and KOZMA, B.: Chemical Transformations of Diols and Cyclic Ethers, XXV. Investigation of the Conversion of 3,3-dialkyloxetanes in the Presence of Platinum Catalysts by the Microreactor Technique 385

BARTÓK, M., KOVÁCS, K. and SHUIKIN, N. I.: Chemical Transformations of Diols and Cyclic Ethers, XXVI. Investigation of the Conversion of 2,4-Dialkyl-substituted Oxetanes in the Presence of Platinum Catalysts by the Microreactor Technique 395

BÁNSÁGI, T. s. SOLYMOSI, F.

BILLES, F.: The Quadratic Potential Function of the Cyclopentadienyl Anion 131

BILLES, F. s. TÓTH, A.

BITE, P. s. MAGYAR, G.

BOGNÁR, R., SZTARICSKAI, F., SOMOGYI, L., PUSKÁS, M. and MAKLEIT, S.: Investigation of the Hydrolysis Products of Desertomycin 53

Book Reviews 423

BOROS-GYEVI, E. s. TÜDŐS, F.

BORSY, J. s. KIRA, M. A.

BRUCKNER, A. s. KIRA, M. A.

CSÁKVÁRI, B. s. LENGYEL, B.

CSŰRÖS, Z., DEÁK, GY., FENICHEL, L., HOLLY, S. and PÁLINKÁS, J.: Preparation and Investigation of Lewis Acid Complexes, III. The Mechanism of the Preparation of α-Acetochloroglucose from β-Pentaacetylglucose (Preliminary Communication) 325

DEÁK, GY. s. CSŰRÖS, Z.

DUSDORF, W. s. HAHN, G.

ERDEY, L. s. ROKOSZ, A.

ERŐ, J. s. HARDY, GY.

FÁY, L.: On the Extended Damköhler Equation 315

FEHÉR, I. and LŐRINC, M.: Reaction of Xenon Difluoride with Water (Short Communication) 329

FENICHEL, L. s. CSŰRÖS, Z.

FODOR, M. s. POKÓ, Z.

GERECS, Á., BARTA, M., TÓTH, T. und LAY, A.: Indol und Indolderivate III. Die Synthese von 6-RO-Indol- und Indolin-Derivaten 311

HAHN, G. und DUSDORF, W.: Beitrag zur Mangan-(II)-nitrat-Pyrolyse I. Die röntgenographische Zusammensetzung und das Widerstandsverhalten von Pyrolysebraunstein 99

HALMOS, M. s. WEISS, I.

HARDY, GY. and NYITRAI, K.: Polymerisation of Vinylene Carbonate 39

HARDY, GY., NYITRAI, K., NAGY, GY., ERŐ, J. and KISBÉNYI, M.: Investigations in the Field of Radiation-Induced Solid State Polymerisation, XXII. 61

HENNING, O.: Derivatographische Untersuchungen an Aluminathydraten (Kurzmitteilung) 117

HIDEG, K. and HIDEG-HANKOVSZKY, O.: Benzazepines, II. Preparation and Reactions of 2,3-dihydro-6,7-benzo-(1,5)-thiazepines 405

HIDEG-HANKOVSZKY, O. s. HIDEG

HOLLY, S. s. CSŰRÖS, Z.

HŐGYE, I. s. INCZÉDY, J.

ILLY, H. s. KISS, I.

INCZÉDY, J. and PÁSZTLER, É.: The Analytical Use of Ion Exchangers in Organic Solvents, I. Swelling and Salt Splitting in Non-Aqueous Media 9

INCZÉDY, J. and HŐGYE, I.: The Analytical Use of Ion Exchangers in Organic Solvents, II. Swelling and Functioning Properties of Macroporous Ion Exchange Resins.... 109

JANCSÓ, G. s. KISS, I.

JÁKLI, GY. s. KISS, I.

KATONA, F. s. MATKOVICS, B.

KIRA, M. A. and BRUCKNER, A.: Synthesis and Reactions of Heterocyclic Enamines, I. The Vilsmeier Aldehyde Synthesis with 1-Phenyl-3-methyl-5-pyrazolone..... 47

KIRA, M. A., BRUCKNER, A., RUFF, F. and BORSY, J.: Synthesis and Reaction of Enamines, II. Synthesis of Pyrrolenines 189

KISBÉNYI, M. s. HARDY, GY.

KISS, Á.: Theorie der Lichtabsorption der Cyclopentadienyl-Komplexe der Übergangselemente 215

KISS, I., JÁKLI, GY., JANCSÓ, G. and ILLY, H.: Isotopic Effects on Vapour Pressure, III. Deuteration Effect on the Vapour Pressure of Alcohols 271

KOVÁCS, K. s. BARTÓK, M.

KOVÁCS, K. s. WEISS, I.

KOVÁCS, Ö. K. J. s. MATKOVICS, B.

KOZMA, B. s. BARTÓK, M.

LAY, A. s. GERECS, Á.

LENGYEL, B. and CSÁKVÁRI, B.: The Phase Potential between Glass and Liquid Ammonia Solutions of Reduced Vapour Pressure 93

LŐRINC, M. s. FEHÉR, I.

MAGYAR, G. und BITE, P.: Herstellung von 7-Ketosteroidverbindungen..... 303

MAKLEIT, S. s. BOGNÁR, R.

MAROS, L. s. SZAKÁCS-PINTÉR, M.

MATKOVICS, B., ABOULEZZ, A. F., KATONA, F. and KOVÁCS, Ö. K. J.: Steroids, VIII. Syntheses of 2- and 4-CH_2-X Substituted Estrone-3-Alkyl Ethers 361

MEZEI, M. and PULAY, P.: Calculation of Force Constants with the Maximum Overlap Method, I. Tetrahedral Molecules (Short Communication) 67

MEZEI, M. and PULAY, P.: Calculation of Force Constants with the Maximum Overlap Method, II. Molecules with Lone Pair Electrons or Empty Orbitals (Short Communication) 331

NAGY, GY. s. HARDY, GY.

NEMES, A. s. SOHÁR, P.

NEMES, L.: Harmonic Force Field Refinement Calculations for Polyatomic Molecules, II. Force Field Calculations on NO_2F and NO_2Cl Molecules Containing ^{14}N and ^{15}N Isotopes 153

Nyitrai, K. s. Hardy, Gy.

Pálinkás, J. s. Csűrös, Z.

Paulik, F. s. Rokosz, A.

Paulik, J. s. Rokosz, A.

Pásztler, É. s. Inczédy, J.

Pokó, Z., Fodor, M. and Szabó, E.: On Some Properties of Uranium Trioxide Dihydrate (Short Communication) 357

Pulay, P. s. Mezei, M.

Pulay, P. s. Török, F.

Puskás, M. s. Bognár, R.

Rangaswamy, M. and Santappa, M.: Oxidation of Aldehydes by Aqueous Ceric Ions in Perchloric Acid 413

Rokosz, A., Paulik, J., Paulik, F. und Erdey, L.: Beiträge zur quantitativen Differential-Thermoanalyse. Untersuchung des Zusammenhanges zwischen der Spitzenfläche und der Probemenge unter den Versuchsbedingungen der derivatographischen Messung 221

Ruff, F. s. Kira, M. A.

Santappa, M. s. Rangaswamy, M.

Schächter, K. s. Tétényi, P.

Shanmuganathan, Sp. and Sri Rama Rao, D.: Bromine Addition to Some Unsaturated Sulphones 307

Shuikin, N. I. s. Bartók, M.

Sohár, P. and Nemes, A.: NH Stretching Vibration Bands at Wavenumbers Lower than 3000 cm^{-1}, IV. Dimeric Structures, IV. Tautomeric Equilibrium of Isonicotinic Acid Thioamide Derivatives 25

Solymosi, F. and Bánsági, T.: Thermal Stability of Chlorine Oxy-Salts in the Solid State, I. Kinetic Study of the Disproportionation and Explosion of Some Chlorites 251

Solymosi, F. and Bánsági, T.: The Thermal Stability of Chlorine Oxy-Salts in the Solid State, II. Kinetic and Derivatographic Study of the Thermal Decomposition of Some Metal Chlorates 337

Somogyi, L. s. Bognár, R.

Sri Rama Rao, D. s. Shanmuganathan, Sp.

Szabó, E. s. Pokó, Z.

Szakács-Pintér, M. und Maros, L.: Über eine neuere analytische Anwendung der Oxydation von organischen Verbindungen durch Brom, II. Bestimmung des Phenetidins und Phenacetins über das bei der Oxydation mit Brom gebildete Chinon und Ammoniak 1

Szakács-Pintér, M. und Maros, L.: Untersuchung des Mechanismus der zweistufigen Oxydation des Furfurols und Furfurylalkohols mit Brom und Bromchlor in wässriger Lösung 199

Szakács-Pintér, M. und Maros, L.: Über eine neuere analytische Anwendung der Oxydation von organischen Verbindungen durch Brom, III. Bestimmung von Furfurol und Furfurylalkohol 87

Szejtli, J.: Acid-Catalyzed Hydrolysis of Alpha- and Betamethylglucopyranosides 175

Sztaricskai, F. s. Bognár, R.

Tamás, J. and Ujszászy, K.: Mass Spectrum of Tetramethylsilane. Its Decomposition Induced by Electron Bombardement (Preliminary Communication) 125

Tétényi, P. and Schächter, K.: Kinetics of the Catalytic Dehydrogenation of Hydroaromatic Compounds, IX. Catalytic Effect of Various Metals 15

Tétényi, P. and Schächter, K.: Catalytic Degradation of Alcohols on Metals 141

Tóth, A. and Billes, F.: Ultraviolet Spectroscopic Study of the Acid-Base Equilibria of Pyrimidine Derivatives, I. Uracil Derivatives 229

Tóth, T. s. Gerecs, Á.

Török, F. and Pulay, P.: On the Parameter Form of Force Constant Matrix, V. The Maximum and Minimum Values of Force Constants 285

Tüdős, F. and Boros-Gyevi, E.: Kinetics of the Solid State Polymerization of N-Vinylcarbazole 67

Ujszászy, K. s. Tamás, J.

Varsányi, Gy.: Simultaneous Positive and Negative Deviations from the Ideal Behaviour in the System of two Volatile Components (Short Communication) 297

Weiss, I., Agócs, P., Halmos, M. and Kovács, K.: The Effect of the Axial-Substituent on the Quaternisation of Some Cocaine Derivatives (Preliminary Communication) 195

Acta Chimica Academiae Scientiarum Hungaricae Tomus 56 (1), pp. 1—8 (1968)

ÜBER EINE NEUERE ANALYTISCHE ANWENDUNG DER OXYDATION VON ORGANISCHEN VERBINDUNGEN DURCH BROM, II

BESTIMMUNG DES PHENETIDINS UND PHENACETINS ÜBER DAS BEI DER OXYDATION MIT BROM GEBILDETE CHINON UND AMMONIAK

M. SZAKÁCS-PINTÉR und L. MAROS

(Institut für Anorganische und Analytische Chemie der L. Eötvös Universität, Budapest)

Eingegangen am 21. Mai 1967

Die analytische Erfassung der bei der Bromierung entstandenen Reaktionsprodukte ermöglicht die selektive Bestimmung zahlreicher organischer Verbindungen. Das Hydrochinon [1], das *p*-Aminophenol [2], das *p*-Phenylendiamin und die N-alkylierten Derivate des letzteren [3] werden auch mit Brom eindeutig zu Chinon oxydiert und können über dieses bestimmt werden. Vor der jodometrischen Bestimmung des Chinons wird der Bromüberschuß mit Phenol entfernt. Bei der schnellen Zugabe der verhältnismäßig großen Phenolmenge reagiert das Brom unter Bildung des jodometrisch inaktiven Mono- bzw. Dibromphenols, wobei das Chinon unverändert bleibt. Im Falle der *p*-Amino-Derivate bildet sich auch Ammoniak neben dem Chinon, die Messung des Ammoniaks ist zur Bestimmung dieser Verbindungen gleichfalls geeignet.

Im Zusammenhang mit der Oxydation des Anisidins (*p*-Methoxyanilin) mit Brom in wäßriger Lösung stellte WIELAND [4] fest, daß sich gemäß der nachstehenden Gleichung eindeutig Chinon bildet:

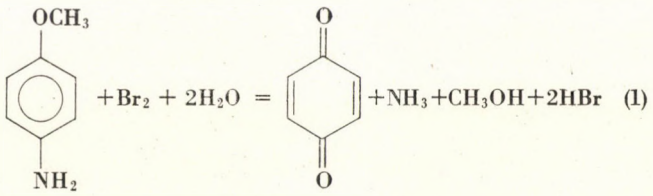

Das bei der Reaktion gebildete Chinon wurde in saurer Lösung mit Zink reduziert, und nach Filtration wurde das Hydrochinon in bicarbonatalkalischer Lösung mit Jodlösung titriert. WIELAND konnte auch das bei der Oxydation entstandene Ammoniak und Methanol nachweisen, zu einer analytischen Verwertung der Reaktion kam es bisher jedoch nicht.

Wir haben die Oxydation des Phenetidins (*p*-Ätoxyanilin) mit Brom eingehend untersucht. Das Acetylderivat dieser Verbindung, das Phenacetin, wird in der Medizin verwendet. Unseren Untersuchungen nach ist die Oxydation des Phenetidins mit Brom in analytisch ausnützbarem Maße eindeutig.

Das bei der Reaktion gebildete Chinon kann, nach Reduktion des Bromüberschusses mit Phenol, auf einfache Weise jodometrisch direkt bestimmt werden. Die genaue Bestimmung der Verbindung ist auch über das bei der Oxydation

Tabelle I

Bestimmung des Phenetidins über das bei der Bromierung gebildete Chinon

Einwaage Phenetidin, g/100 ml	Eingemessene Lösung, ml	Verbr. 0,1 *n* $Na_2S_2O_3$, ml		Gefundenes Phenetidin	
		Einzelwerte	Durchschnitt	mg	%
0,3148	20,07	9,04 9,02 9,01 9,06	9,02	61,87	97,9
	10,04	4,52 4,51 4,52 4,52	4,52	31,00	98,1
	5,02	2,26 2,27 2,26 2,25	2,26	15,51	98,1
		Verbr. 0,01 *n* $Na_2S_2O_3$, ml			
0,06655	10,04	9,57 9,56 9,57	9,57	6,564	98,2
	5,02	4,80 4,81 4,82	4,81	3,299	98,7
	2,01	1,91 1,92 1,91	1,91	1,310	97,9

gebildete Ammoniak möglich. Beide Methoden sind sowohl im 0,1- als auch im 0,01-*n*-Maßstabe zur Bestimmung des Phenetidins geeignet. Reduktionsmittel und andere, Brom verbrauchende organische Stoffe (Olefine, aromatische Amine usw.) stören die Bestimmung nicht.

Die Oxydation ist auch vom Gesichtspunkte der Bildung des Äthanols stöchiometrisch. Das Äthanol kann aber auf einfache Weise analytisch nicht

erfaßt werden, daher ist diese Methode zur quantitativen analytischen Bestimmung nicht zu empfehlen. Bei der Bestimmung des Alkohols reduzierten wir den Bromüberschuß mit Sulfit, danach wurde das Äthanol in 70%ige schwefel-

Tabelle II

Bestimmung des Phenetidins über das bei der Bromierung gebildete Ammoniak

Einwaage Phenetidin, g/100 ml	Eingemessene Lösung, ml	Verbr. 0,1 *n* HCl, ml		Gefundenes Phenetidin	
		Einzelwerte	Durchschnitt	mg	%
		8,65			
	20,00	8,64	8,64	118,5	96,6
		8,63			
		4,36			
0,6135	10,00	4,35	4,35	59,67	97,3
		4,34			
		2,18			
	5,00	2,18	2,18	29,90	97,5
		2,20			
		Verbr. 0,01 *n* HCl, ml			
		9,22			
	9,98	9,24	9,22	12,65	97,5
		9,20			
		4,62			
0,1300	5,02	4,63	4,63	6,35	97,3
		4,65			
		1,82			
	2,00	1,86	1,84	2,52	97,1
		1,84			

saure Chromsäurelösung destilliert. Aus dieser Lösung wird die Essigsäure (nach Verdünnung) mit Wasserdampfdestillation isoliert und nachher titriert.

Die Ergebnisse der Bestimmung des Phenetidins über Chinon und Ammoniak sind in den Tabellen I und II veranschaulicht.

Bei der Bestimmung des Ammoniaks arbeiteten wir nach dem Prinzip der blasenfreien Destillation [5]. Auf solche Weise kann das Ammoniak in Wasser aufgefangen und unmittelbar mit Säurelösung titriert werden. Man kann zur Isolierung des Ammoniaks auch irgendein anderes Destillationsprinzip verwenden.

Das Phenacetin kann mit Brom nicht direkt oxydiert werden, nach saurer Hydrolyse kann man es aber nach dem obigen Prinzip über das aus dem Phenetidin gebildete Chinon bzw. Ammoniak bestimmen.

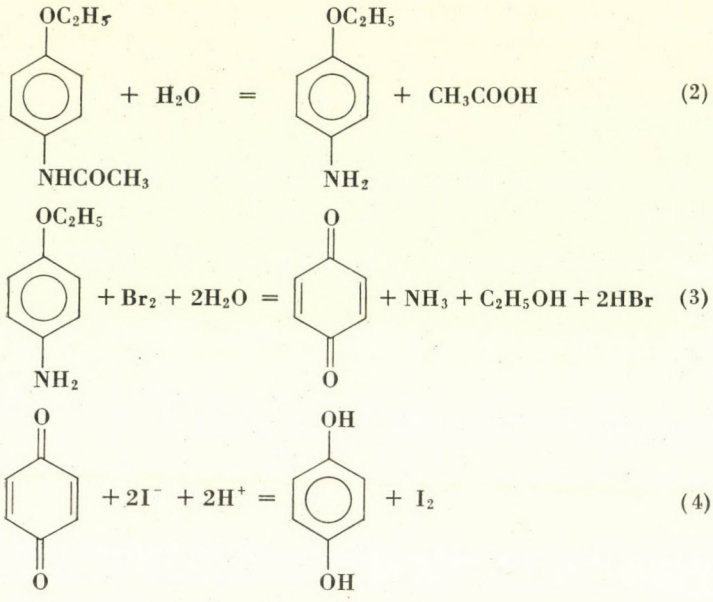

Die Hydrolyse läuft in 20%iger salzsaurer Lösung bei Siedetemperatur binnen 15—20 Minuten vollkommen ab. Die Ergebnisse der Bestimmung des Phenetidins sind in den Tabellen III und IV zusammengestellt.

Die Mehrzahl der zur Bestimmung des Phenacetins empfohlenen Verfahren beruht auf der photometrischen Messung von Azofarbstoffen. Diese Farbreaktionen beruhen auf der Diazotierung und Kupplung des Phenetidins [6, 7, 8]. Auch die photometrische Bestimmung des bei der partiellen Oxydation des Phenetidins entstandenen Farbstoffes wird empfohlen [9]. Zur Bestimmung des Phenetidins bzw. Phenacetins kann weiterhin die Kondensationsreaktion mit 4-Dimethylaminobenzaldehyd benützt werden [10]. Das Verwendungsgebiet dieser Bestimmungen wird aber durch die Gegenwart von verschiedenen organischen Verbindungen begrenzt; in solchen Fällen kann die Bestimmung des Phenacetins erst nach entsprechender Isolierung ausgeführt werden [11].

Um die Selektivität der Chinon-Bestimmung zu beweisen, wurde das Phenacetin auch in Gegenwart der in der medizinischen Praxis mit ihm gemeinsam verwendeten Verbindungen bestimmt. Die Ergebnisse sind in Tabelle V zusammengestellt. Die Gegenwart dieser Verbindungen stört die der Bromierung folgende Bestimmung des Chinons nicht; die Ergebnisse der Messung des

Tabelle III

Bestimmung des Phenacetins nach Hydrolyse über das bei der Bromierung gebildete Chinon

Einwaage Phenacetin, g/100 ml	Eingemessene Lösung, ml	Verbr. 0,1 *n* $Na_2S_2O_3$, ml		Gefundenes Phenacetin	
		Einzelwerte	Durchschnitt	mg	%
		11,45			
	20,00	11,46	11,45	102,6	98,2
		11,44			
		5,73			
	9,98	5,73	5,73	51,35	98,4
		5,73			
0,5227					
		2,87			
	4,99	2,87	2,87	25,72	98,6
		2,86			
		1,15			
	2,00	1,14	1,15	10,31	98,6
		1,16			
		Verbr. 0,01 *n* $Na_2S_2O_3$, ml			
		11,78			
	9,98	11,78	11,78	10,55	98,2
		11,77			
		5,88			
0,1077	4,99	5,87	5,88	5,269	98,0
		5,89			
		2,35			
	2,00	2,36	2,36	2,164	98,2
		2,36			

Ammoniaks werden aber durch die Gegenwart von Coffein und Amidazophen verfälscht.

Erfolgreich kann das Phenacetin über Chinon und Ammoniak in Gegenwart von Acetanilid bestimmt werden. (Durch das bei der Hydrolyse aus dem Acetanilid gebildete Anilin werden die Meßergebnisse der Bestimmung des Chinons und des Ammoniaks nicht beeinflußt.) Die Menge des Acetanilids kann in Gegenwart von Phenacetin nach der Hydrolyse mit der Methode nach KOPPESCHAAR gemessen werden. Die auf Bromierung beruhenden Messungskombinationen sind auch zur Bestimmung dieser Verbindungen nebeneinander geeignet.

Tabelle IV

Bestimmung des Phenacetins nach Hydrolyse über das bei der Bromierung gebildete Ammoniak

Einwaage Phenacetin, g/100 ml	Eingemessene Lösung, ml	Verbr. 0,1 *n* HCl, ml		Gefundenes Phenacetin	
		Einzelwerte	Durchschnitt	mg	%
		3,98			
	9,98	3,97	3,97	71,18	98,2
		3,98			
		1,98			
0,7258	4,99	1,99	1,99	35,67	98,5
		1,99			
		0,80			
	2,00	0,80	0,80	14,34	98,8
		0,78			
		Verbr. 0,01 *n* HCl, ml			
		3,99			
	10,01	4,00	4,00	7,169	98,6
		4,00			
		2,00			
0,0726	5,01	2,02	2,01	3,602	99,1
		2,01			
		0,79			
	2,00	0,80	0,80	1,434	98,8
		0,81			

1. Beschreibung der Verfahren

1. Bestimmung über Chinon

Reagenzien:

0,1 *n* bzw. 0,01 *n* Natriumthiosulfatlösung
20%ige Salzsäure
5%ige Phenollösung
1%ige Stärkelösung als Indikator
Kaliumjodid (fest)

10,00 ml betragende Anteile der 0,05 bzw. 0,005 molaren Lösung des *p*-Phenetidins werden in einen 200 ml fassenden, mit Glasstopfen versehenen Erlenmeyer-Kolben pipettiert. Die Lösung wird mit 3—5 ml Salzsäure angesäuert, dann wird ihr Volumen mit destilliertem Wasser auf 50—60 ml ergänzt. Nun wird Bromwasser tropfenweise so lange zur Lösung gegeben, bis die zuerst vorübergehend auftretende rote Farbe in Gelb übergeht, dann ändert sie sich auf Wirkung von weiterem Brom auf Orangegelb. Nach einer Wartezeit von 10—20 Minuten gießt man 5 ml Phenol schnell in den Kolben, verschließt diesen und schüttelt mehr-

Tabelle V

Bestimmung von Phenacetin neben anderen Verbindungen

Eingewogene Substanz	Bestimmung über das bei der Bromierung gebildete Chinon			Bestimmung über das bei der Bromierung gebildete Ammoniak		
	Eingem. Lösung, ml	Verbr. 0,1 *n* $Na_2S_2O_3$, ml	Gef. Phenacetin, %	Eingem. Lösung, ml	Verbr. 0,1 *n* HCl, ml	Gef. Phenacetin, %
Phenacetin 0,5147 g/100 ml		5,67				
Coffein 0,10 g/100 ml	9,99	5,66	98,7			
Phenacetin 0,4885 g/100 ml		5,40			5,33	
Phenobarb. Na 0,10 g/100 ml	9,99	5,39	99,1	20,0	5,42	98,7
Phenacetin 0,5086 g/100 ml		5,62				
Amidazophen 0,50 g/100 ml	9,99	5,60	98,9			

mals. Der Glasstopfen des Kolbens wird zeitweise gelockert, um auch das am Schliff haftende Brom zu reduzieren. Nach Entfernung des Bromüberschusses wird das Volumen der Lösung mit destilliertem Wasser auf etwa 100 ml ergänzt und 1 g Kaliumjodid eingetragen.

Nach einer Wartezeit von einigen Minuten wird das ausgeschiedene Jod mit 0,1 *n* bzw. 0,01 *n* Natriumthiosulfatlösung — in Gegenwart von Stärkelösung als Indikator — titriert.

Bei der Bestimmung des Phenacetins werden 0,5 g der Probe analytisch genau eingewogen und in einen mit Rückflußkühler versehenen Kolben mit 20 ml 20%iger Salzsäure 20 Minuten gekocht. Nach Abkühlung wird die Lösung in einen 100-ml-Meßkolben gespült und ihr Volumen bis zur Marke ergänzt. In der so vorbereiteten Stammlösung wird das Phenetidin nach Oxydation mit Brom, wie oben beschrieben, bestimmt.

1 ml 0,1 *n* Natriumthiosulfatlösung entspricht 6,859 mg Phenetidin bzw. 8,961 mg Phenacetin.

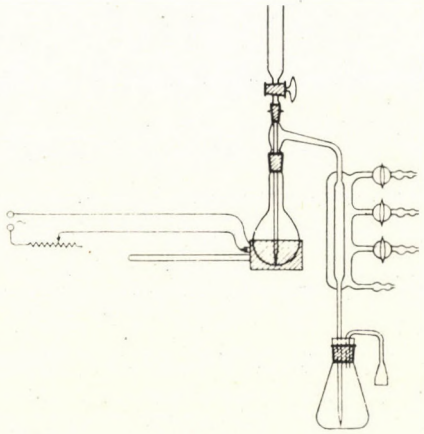

Abb. 1

2. *Bestimmung über Ammoniak*

Reagenzien:

0,1 *n* bzw. 0,01 *n* Salzsäure
20%ige Salzsäure
20%ige Natriumhydroxydlösung
0,1 *n* Natriumhydroxydlösung
gesättigtes Bromwasser
0,2%ige Methylrotlösung als Indikator
Bimsstein

10,00 ml betragende Anteile der zur Chinonbestimmung verwendeten Stammlösung werden in den 150 ml Kolben des Destillierapparats pipettiert (Abb. 1). Die Lösung wird mit 3 ml 20%iger Salzsäure versetzt, dann wird ihr Volumen mit destilliertem Wasser auf 60—70 ml ergänzt. Es wird auf die bei der Bestimmung über Chinon beschriebene Weise mit Bromwasser oxydiert, dann wird die Lösung in Gegenwart einiger Bimssteinkörnchen 10 Minuten gekocht. Nach Abkühlen wird die Lösung in Gegenwart von Methylrot-Indikator mit Natronlauge neutralisiert, dann mit 4—5 Tropfen 20%iger Salzsäure angesäuert.

Nach Zusammenstellung des Destillierapparats wird der Kolben mit einem regulierbaren elektrischen Heizgerät erwärmt. Im Kühler wird das Kühlwasser, bei geschlossenen oberen Hähnen und bei geöffnetem unterem Hahn, nur bis zum unteren Drittel zirkulieren gelassen. Nach einige Minuten dauerndem Kochen wird der Vorlagekolben mittels eines Korkstopfens mit zwei Bohrungen am Kühlerrohr befestigt. Als Vorlagekolben wird ein 100 ml fassender Erlenmeyer-Schliffkolben verwendet, der 20 ml destilliertes Wasser enthält. Das Ende des Kühlerrohres wird vorsichtig an den Boden des Kolbens gedrückt. Zur blasenfreien Destillation wird das Niveau des Kühlwassers durch entsprechendes Einstellen der Hähne erhöht, wobei ein Teil der im Vorlagekolben befindlichen Flüssigkeit in das Innere des Kühlers aufsteigt. Nachher wird die Lösung unter lebhaftem Kochen durch Zugabe von 0,1 *n* NaOH-Lösung, in kleinen Portionen aus einem Hahntrichter, alkalisiert. Nach etwa 20 Minuten dauernder Destillation wird das Niveau des Kühlwassers durch Öffnen des unteren Hahnes gesenkt, dabei fließt die Vorlageflüssigkeit in den Vorlagekolben zurück. Nach Senken des Vorlagekolbens wird die Destillation noch einige Minuten fortgesetzt.

Der Inhalt des Vorlagekolbens wird in Gegenwart von 2 Tropfen Methylrot-Indikator mit 0,1 bzw. 0,01 *n* Salzsäure titriert.

1 ml 0,1 *n* Salzsäure entspricht 13,718 mg Phenetidin bzw. 17,922 mg Phenacetin.

ZUSAMMENFASSUNG

Über das bei seiner Oxydation mit Brom gebildete Chinon und Ammoniak kann das Phenetidin und Phenacetin selektiv bestimmt werden. Das Chinon wird nach der Reduktion des Bromüberschusses mit Phenol jodometrisch, das Ammoniak nach Destillation alkalimetrisch bestimmt. Die Verfahren können sowohl im Makro- als auch im Mikromaßstabe benützt werden.

LITERATUR

1. Schulek, E., Burger, K.: Acta Pharm. Hung. **27,** 5 (1957).
2. Schulek, E., Maros, L., Perl-Molnár, I.: Mikrochim. Acta **1964,** 336.
3. Maros, L., Szakács-Pintér, M.: Acta Chim. Hung. **48,** 161 (1966).
4. Wieland, H.: Ber. **43,** 717 (1910).
5. Maros, L., Schulek, E., Perl-Molnár, I., Szakács-Pintér, M.: Anal. Chim. Acta **25,** 390 (1961).
6. Wirth, C. M. P.: Pharmac. Acta Helv. **35,** 575 (1960).
7. Di Bacco, G.: Bull. chim. farmac. **93,** 366 (1954).
8. Pankratz, R. E., Bandelin, F. J.: J. Am. Pharm. As. **45,** 364 (1956).
9. Affanassjew, B. N.: Aptetschnoe Delo, **2,** 21 (1953).
10. Rózsa, P.: Acta Pharm. Hung. **28,** 1 (1958).
11. Dupcza, K., Kelemen-Küttel, I., Vastagh, G.: Acta Pharm. Hung. **29,** 6 (1959).

Margit Szakács-Pintér
László Maros
} Budapest VIII., Múzeum krt. 4/b.

Acta Chimica Academiae Scientiarum Hungaricae Tomus 56 (1), pp. 9—14 (1968)

THE ANALYTICAL USE OF ION EXCHANGERS IN ORGANIC SOLVENTS, I

SWELLING AND SALT SPLITTING IN NON-AQUEOUS MEDIA

J. INCZÉDY and É. PÁSZTLER

(Institute for General Chemistry, Polytechnical University, Budapest)

Received August 10, 1967

Ion exchange resins, as their name suggests, operate with ions, therefore water proved to be the best solvent in ion exchange processes, considering its high dielectric constant and its polar character. These factors are favourable for electrolytic dissociation.

Many of the organic compounds, however, are not soluble enough in water, and so organic solvents also play an important role in ion exchange processes. Besides their dissolving ability, solvents have to meet two other requirements. The solute should be dissociated, at least to a small extent, and the resin should be swollen slightly in the organic solvent, to make the inner pores and sites for the exchangeable ions accessible. From the kinetic point of view, the low viscosity of the solvent is also an important factor.

The swelling of ion exchange resins is due firstly to the tendency of the fixed ionizable groups to solvation. For the solvation of the active groups more polar solvents are favourable. At the same time, however, the hydrocarbon skeleton of the resin is also able to adsorb molecules. Since the swelling of ion exchangers is due to opposite effects, decided by the dielectric constant, dipole moment, viscosity and other properties of the solvent, one can hardly predict what kind of solvents are the most suitable for certain purposes.

The first thorough investigation into the swelling properties of different resins in different solvents was carried out by BODAMER and KUNIN [1]. They reported the swelling data of several *Amberlite* resins of various forms in many solvents. One can find data about the properties of ion exchange resins in non-aqueous solvents from the literature in connection with new organic analytical procedures. Salt splitting experiments for analytical purposes were carried out in ethanol [2, 3, 4], dimethylformamide [5], pyridine [6], and other solvents. Attempts have been made to use ethanol, isopropanol, dioxan, acetonitrile [7, 8, 9, 10, 11], *etc.* in ion exchange chromatography for the separation of various organic substances. Besides the common microporous resins, the applicability of macroreticular resins was also investigated.

Newly oleophilic ion exchange resins have also been prepared, which have more advantageous properties in non-aqueous media [12, 13, 14].

Some experiments were now carried out to determine the extent of swelling of some conventional polystyrene-divinylbenzene-type strongly acidic and strongly basic ion exchange resins in different solvents. In the selection of the solvents investigated, the following requirements were considered: the solvents should be miscible with water; they should not be of high molar volume; solvents of basic and acidic character should be investigated. To remove water from the organic solvents used in the experiments, a molecular sieve column was used. Besides the swelling experiments, salt splitting experiments were carried out using acetic acid and dimethylformamide as the solvent. The salt splitting methods can be used for the determination of some organic bases and acids in their salts.

Experimental

Ion exchange resins: For the swelling experiments *Dowex 50X8* and *Dowex 50X4* (50—100 mesh) strongly acidic cation exchange resins and *Dowex 1X4* (20—50 mesh) strongly basic anion exchange resins were used. The capacity of the resins was determined by the usual method [15], and found to be as follows: 5.03, 5.02 and 3.53 meq./g, respectively.

The resins were treated in the usual manner with acid and alkali solution before use. Resin samples in the hydrogen and sodium form were prepared from the pretreated and washed cation exchange resins, using 2 *N* hydrochloric acid and 2 *N* sodium chloride solutions, respectively. Hydroxyl-, chloride- and aceta teform resins were prepared from the pretreated and washed anion exchangers using suitable base or salt solutions. The resins were washed out with deionized water, and dried in vacuum. The cation exchange resins and also the chloride form of anion exchange resin samples were dried at 60 °C, while the hydroxyl form of the anion exchanger was dried at room temperature, over phosphorus pentoxide. The water content of the samples was determined by the derivatographic method.

Solvents: The following solvents were used: Deionized water, reagent grade dioxan, methanol, ethanol, dimethylformamide, pyridine, glacial acetic acid, and ethylene glycol.

The dioxan, with the addition of some hydrochloric acid, was boiled for 6 hrs, and potassium hydroxide was added. The next day the liquid was boiled with sodium metal, and finally distilled.

In order to dry the ethanol, dimethylformamide, pyridine and glacial acetic acid, a molecular sieve column (of 70 cm height and 2.4 cm inner diameter) filled with *Zeosorb-4* (*Reanal*, Hungary) was used. The column was provided with an electrical heating jacket and with a central glass tube for a thermocouple. For the regeneration of the molecular sieve bed, the column was kept at 400 °C for 2 hrs under a stream of nitrogen. After the regeneration of the column, the solvent was poured on the cooled column at a rate depending on the water content (0.2 g water/cm^2/hr.). The solvent effluent was collected in a flask equipped with a calcium chloride drying tube [16].

The water content of the organic solvents used in the swelling experiments was determined by the Karl Fischer titration method, and was found to be less than 0.05%, except for ethylene glycol for which it was 1.4%.

Derivatographic measurements: Derivatograph (System *Paulik—Paulik—Erdey; MOM*, Hungary) [17] was used for the determination of the water content of the cation exchange resin samples. 0.5 g of dried resin sample was weighed in the platinum crucible of the apparatus. After inserting the crucible into the oven, the derivatogram was run at a heating rate of 3 °C/min. It was found that the last remainders of water (about 0.6 mole H_2O per g.-eq. resin) could be removed only by a very rigorous drying procedure using phosphorus pentoxide. Unfortunately, the derivatographic method could not be used successfully in the examination of anion exchangers, as the early thermal decomposition of the resin overlaps the water evaporation step on the derivatograms.

Swelling experiments: 0.5—1 g of the resin sample was weighed and placed in a glass vessel with 20 ml of the solvent. This was allowed to stand in the closed vessel for 24 hrs, then it was filtered on a glass filter with suction, and weighed. After weighing it was dried in vacuum, and weighed again. On the basis of the capacity data, the equivalent weights of resins of

different forms were calculated. By using the calculated equivalent weight values and the measured solvent uptake data, the moles of solvent per g-eq. of resin could be calculated. The results of the measurements are summarized in Tables I and II.

Volumetric determination of sodium cholate and sodium cyclamate: An ion exchange resin column was prepared from *Dowex 50X8* (0.6×10 cm) and converted to the H-form using aqueous 2 *N* HCl solution. The column was washed with water, then with 5 ml of a 1 : 1 mixture of water and the solvent, and finally with 25 ml of solvent.

0.1 to 0.2 g of the salt was weighed and dissolved in 20—40 ml of solvent. The solution was poured on the ion exchange column (H-form). After washing the column, the effluent was titrated with 0.1 *M* potassium methoxy standard solution in the presence of Thymol Blue indicator. The results of the determinations are summarized in Table III.

Volumetric determination of salts of organic bases in glacial acetic acid: An ion exchange column (0.6×10 cm) was prepared from *Dowex 1X8* resin, and converted to the OH-form using aqueous 1 *N* NaOH solution. After washing off the excess of the alkali with water, the column was converted to the acetate form using a mixture of water–acetic acid (10 : 1). The water was finally displaced from the column using 50 ml of glacial acetic acid.

50 to 200 mg of the salt sample was weighed and dissolved in 10—25 ml of glacial acetic acid by heating it to 40—60 °C. The resulting clear solution was poured on the ion exchange column in acetate form. After washing the column with about 50 ml of solvent, the collected effluent was titrated with 0.1 *M* perchloric acid in glacial acetic acid standard solution, using Crystal Violet as the indicator. The end-point was also determined by potentiometric measurements using glass and a calomel electrode, which latter contained LiCl in acetic acid.

To compare the results obtained by the ion exchange method, determinations were carried out also by the mercury(II) acetate method [18].

The results of the determinations are shown in Table IV.

Results and discussion

On consideration of the swelling data of the resins investigated (summarized in Table I), one can conclude that water has the best solvent properties. The swelling of the resins is also significant in alcohols (methanol, ethanol, ethylene glycol), but there is a surprisingly great difference between the solvent uptake of the acid form and the salt form cation exchange resins in ethanol.

Table I

The swelling of various forms of the ion exchange resins used in different solvents
(Solvent content of the swollen resin, %)

Solvent	Dowex 50X8		Dowex 50X4		Dowex 1X8	
	(H)	(Na)	(H)	(Na)	(OH)	(Cl)
Water	53.4	58.7	66.8	66.2	49.9	45.1
Ethylene glycol		46.2		61.5	49.1	49.4
Methanol	37.8	24.4	52.2	26.4	38.4	39.0
Ethanol	36.7	6.1	49.2	7.3	31.3	35.4
Dioxan	7.5	6.2	5.8	3.0	9.8	7.8
Dimethylformamide	4.4	4.6	5.6	4.4	5.9	8.2
Pyridine	8.2	8.1	8.3		8.5	7.7
Glacial acetic acid	15.6	13.9	30.3	12.6	49.2*	45.6

* in acetate form

One may assume that the increased ion pair formation of the resin in sodium form is responsible for the very low swelling of the salt form. There is a considerable swelling of the anion exchanger containing quaternary ammonium groups, in glacial acetic acid.

It is interesting to compare the data of Table II, where the adsorbed moles of solvent per g.-eq. of resin (*i.e.* one ionic group) are collected. In the cases

Table II

Solvent uptake of ion exchange resins of different forms
(Mole of solvent per g.-eq. of dry resin)

Solvent				Dowex 50X8		Dowex 50X4		Dowex 1X8	
Name	Molar volume, ml/mole	Dielectr. constant	Dipole moment, 10^{-18} $dyne^{1/2}$ cm^2	(H)	(Na)	(H)	(Na)	(OH)	(Cl)
Water	18	80	1.84	12.6	16.7	22.3	24.1	15.1	12.9
Ethylene glycol	56	41.2	2.28		3.0		5.7	4.1	4.5
Methanol	40	32.4	1.69	3.75	2.2	6.8	2.5	5.1	5.6
Ethanol	58.5	25.8	1.70	2.5	0.3	4.2	0.4	2.6	3.4
Dioxan	86	3	0.4	0.2	0.2	0.1	0.1	0.3	0.3
Dimethylformamide	77.5	26.6		0.1	0.2	0.2	0.2	0.3	0.4
Pyridine	80.5	12.5	2.25	0.2	0.2	0.2		0.3	0.2
Glacial acetic acid	57.2	7	0.83	0.6	0.6	1.4	0.5	5.0*	3.8

* in acetate form

where the data are lower than 0.5, one can hardly call it solvation (dioxan, pyridine, dimethylformamide).

Table III shows that, in spite of the low solvation ability of the cation exchange resins in basic solvents, the splitting of sodium cyclamate can be

Table III

Determination of salts of organic acids

Salt	Solvent used	Weighed, mg	Found, mg	Deviation, %
Sodium salt of cholic acid	ethanol	117.5	117.0	−0.5
		240.8	239.4	−1.4
		99.1	99.0	−0.1
Sodium cyclamate	dimethylformamide	89.7	89.0	−0.7
		104.0	104.5	+0.5
		100.1	100.4	+0.3

carried out successfully in dimethylformamide using an ion exchange column. Since the salt formation of the cation exchange resin is accompanied by remarkable ion association in ethanolic medium, one may say that for salt splitting procedures the use of ethanol is definitely preferable.

For the splitting of salts of organic bases, a strongly basic anion exchange resin column in glacial acetic acid was used. It follows from theoretical considerations that it would be better to use weakly basic anion exchangers in glacial acetic acid, but experiments showed that the latter are not stable in this solvent. The polystyrene–divinylbenzene-type resins containing quaternary ammonium groups are, however, very stable in glacial acetic acid, and they can be used several times without degradation.

The analytical determinations carried out with an ion exchange column in glacial acetic acid medium had satisfactory accuracy. The relative error was not higher than $\pm 1\%$ (see Table IV).

Table IV

Determination of salts of organic bases

Compound	By ion exchange method, %	By mercury(II) acetate method, %
Aniline hydrochloride	70.4	70.2
Betaine hydrochloride	42.8	42.4
Papaverine hydrochloride	90.3	90.4

The authors are indebted to Prof. L. ERDEY, head of the Institute, for his kind support and interest in this work.

SUMMARY

The swelling properties of strongly acidic cation exchange and strongly basic anion exchange resins of different forms have been investigated in water, ethylene glycol, methanol, ethanol, dioxan, dimethylformamide, pyridine and glacial acetic acid.

The splitting and determinations of some salts of organic acids and bases have also been carried out, using ion exchange columns in non-aqueous solvents. The liberated acid or base is titrated in the same media. The error of the determinations was not greater than $\pm$ 1%.

REFERENCES

1. BODAMER, G. W., KUNIN, R.: Ind. Eng. Chem. **45,** 2577 (1953).
2. VÁMOS, E., SIMON, F.: Acta Chim. Acad. Sci. Hung. **27,** 347 (1961).
3. INCZÉDY, J.: Analytische Anwendungen von Ionenaustauschern. Akadémiai Kiadó, Budapest, 1964, p. 237.
4. JINDRA, A., POHORSKY, J.: J. Pharm. Pharmacol. **2,** 361 (1950).
5. VINCENT, M. C., BLAKE, M. I.: J. Am. Pharm. Assoc. Sci. Ed. **48,** 359 (1959).
6. HOWORKA, A. K.: Pharm. Zentralhalle **97,** 521 (1958).
7. PIETRZYK, D. J.: Talanta **13,** 209 (1966).

8. PIETRZYK, D. J.: Talanta **13,** 225 (1966).
9. GORDON, J. E.: J. Phys. Chem. **67,** 19 (1963).
10. GORDON, J. E.: J. Chromatog. **18,** 542 (1965).
11. CASSIDY, J. F., STREULI, C. A.: Anal. Chim. Acta **31,** 86 (1964).
12. GREGOR, H. P., HOESCHELE, G. K., POTENZA, J., TSUK, A. G., FEINLAND, R., SHIDA, M., TEYSSIÉ, PH.: J. Am. Chem. Soc. **87,** 5525 (1965).
13. TSUK, A. G., GREGOR, H. P.: J. Am. Chem. Soc. **87,** 5534 (1965).
14. TSUK, A. G., GREGOR, H. P.: J. Am. Chem. Soc. **87,** 5538 (1965).
15. INCZÉDY, J.: Analytische Anwendungen von Ionenaustauschern. Akadémiai Kiadó, Budapest, 1964, p. 110.
16. KLOPP, G., GÖRÖG, É., SIPOSS, G.: Magy. Kém. Lapja **21,** 607 (1966).
17. PAULIK, F., PAULIK, J., ERDEY, L.: Z. anal. Chem. **160,** 241 (1958).
18. PIFER, CH. W., WOLLISH, E. G.: Anal. Chem. **24,** 300 (1952).

János INCZÉDY
Éva PÁSZTLER
Budapest XI., Gellért tér 4.

Acta Chimica Academiae Scientiarum Hungaricae Tomus 56 (1), pp. 15—23 (1968)

KINETICS OF THE CATALYTIC DEHYDROGENATION OF HYDROAROMATIC COMPOUNDS, IX*

CATALYTIC EFFECT OF VARIOUS METALS

P. TÉTÉNYI and K. SCHÄCHTER

(Institute of Isotopes of the Hungarian Academy of Sciences, Budapest)

Received May 4, 1967

In a former communication [1] we have reported the results of our studies concerning the catalytic activity of eleven metals. It has been found that all the metals studied, *viz.* Fe, Co, Rh, Ni, Pd, Pt, Cu, Ag, Ir, Zn, and W, catalyze the dehydrogenation of six-membered rings. A correlation, similar to that noted by BEECK [2] in connection with the hydrogenation of ethylene, between the lattice constants of the metals and their catalytic activity in the dehydrogenation of cyclohexane has been established.

These results are interesting since catalytic activity in the dehydrogenation of six-membered rings was shown by metals in which dehydrogenation could not proceed according to the sextet mechanism [3, 4]. Thus, a certain measure of activity was found with iron and tungsten, both of body-centered cubic lattice structure, and also with silver, a face-centered structure but having too large atomic diameter (2.8894 Å). For a more thorough elucidation of this phenomenon, we extended our studies to include some further metals, such as vanadium and molybdenum, of body-centered cubic lattice, and also elements with face-centered cubic and hexagonal lattices where the atomic diameters exclude the possibility of dehydrogenation by sextet mechanism, such as gold (2.8841 Å), α-zirconium (3.1790 Å), α-titanium (2.8956 Å), and α-beryllium (2.2260 Å). The catalytic effect of ruthenium was also studied since it was found that metals with a hexagonal lattice show lower catalytic activity in the dehydrogenation of cyclohexane than metals having face-centered cubic structure, even in the case when the atomic diameter would allow dehydrogenation to proceed according to the sextet mechanism.

Thus the catalytic effects of seven further metals not yet studied, or studied but cursorily (ruthenium), were investigated in the dehydrogenation of six-membered rings. This enabled us to experimentally check the relation [1] between the lattice constants and catalytic activity of metals.

* Part VIII, see Acta Chim. Acad. Sci. Hung. **50**, 129 (1966).

Experimental

Reaction rates were measured in a flow reactor described in detail in a former communication [5]. The refractive index of the condensate, formed after conversion and containing benzene and unchanged cyclohexane, served to indicate the quantity of cyclohexane converted per unit time. When the conversion was very low, its extent was established by a chromatogram of the condensate, or, in a few cases, by its ultraviolet spectrum. The degree of conversion of cyclohexene was always determined by chromatography. The chromatograms were obtained on columns 2.7 to 4.4 m long packed with "*Celite 545*" saturated with ethylene glycol, using hydrogen as the carrier gas.

The catalysts studied were the following:

Beryllium. Powder, made by *DEGUSSA*, was prepared for the measurements by heating at 400 °C for 1.5 to 2 hrs in a current of hydrogen. Specific surface area, 0.8 m^2/g.

Gold. From an aqueous solution of $HAuCl_4$ (0.5 g of gold per 1 ml of water) metallic gold was obtained by reduction with formaldehyde, in the presence of potassium hydroxide. The precipitate was washed with distilled water to neutral, then it was dried at 200 to 300 °C in a current of hydrogen. Specific surface area, 0.3 m^2/g.

Molybdenum. Ammonium molybdate was reduced by heating to 1100 to 1200 °C for 1 hr. in a current of hydrogen. Specific surface area, 0.6 m^2/g.

Ruthenium. Ruthenium chloride was reduced to the metal in a current of hydrogen by heating it for 5—10 hrs between 200 and 400 °C so that the temperature was raised by 50 °C steps. Completion of the reduction was checked by allowing the exit gas to bubble through a solution of silver nitrate to indicate the absence of chloride. Specific surface area, 1.6 m^2/g.

Titanium. Commercial titanium sponge was used. Prior to application it was heated at 800 °C for 1 hr. under reduced pressure ($2.5 \cdot 10^{-5}$ torr). Specific surface area, 0.005 m^2/g.

Vanadium. Strips manufactured by Messrs. *Johnson—Matthey* were used. Prior to use these were purified in ether, and heated in a current of hydrogen at 400 °C for 2.5 hrs. Specific surface area, 0.005 m^2/g.

Specific surface area measurements were carried out by adsorption of nitrogen or of krypton gas.*

However, titanium, zirconium, and vanadium had so small specific surface areas that adsorption measurements were not feasible. For these metals the geometric surface was accepted as the actual surface area. The fact that the surface could not be determined by the adsorption of krypton gas, suggests that the specific surface areas of these catalysts were less than $2 \cdot 10^{-2}$ m^2/g, the lowest limit of sensitivity of this method. The figures 3 to $5 \cdot 10^{-3}$ m^2/g for the specific surface areas measured geometrically, compared with the limit value mentioned, indicate that no error exceeding one order of magnitude is committed when the geometrical surface is accepted as the real one for these three metals, and when no account is taken of the surfaces, the real surface area is greater than the value obtained geometrically. The error was diminished by correcting the specific activities found with a roughness factor of 2.5 taken from the literature [6]. This factor has been established by electrochemical and nuclear chemical methods for rolled non-noble metals.

Table I lists data that refer to the purity of the catalysts studied, showing the quantities of trace impurities detected by spectrography.** It can be seen that the catalysts, though some of them were contaminated with a number of various trace impurities, did not contain any element possessing significant catalytic activity in the dehydrogenation of cyclohexane. Thus the possibility that trace impurities should have significantly affected the behaviour of the catalysts as a whole seems to be ruled out.

Distilled cyclohexane and cyclohexene were used in the experiments; the physical constants of these were in good agreement with the data reported in the literature. The purity of the substances was also checked by chromatography.

* The authors are grateful to Dr. L. GUCZI and to Mr. L. ZSINKA for these measurements.

** We are indebted to Mr. B. VORSATZ and Mrs. T. KELEN, of the *Central Physical Research Institute*, for the spectrographic analyses.

Table I

Impurities in the catalysts investigated

Catalyst	Quantity of trace-elements																
	Mg	Al	Si	P	Cr	Mn	Fe	Cu	Zn	Ag	Sn	Sb	Ta	Au	Pb	Bi	Ca
Beryllium	D	—	—	—	—	—	—	A	—	—	—	—	—	—	—	—	C
Gold	A	—	A	—	D	—	C	D	A	A	—	—	—	—	D	—	—
Molybdenum	D	D	C	—	D	D	B	D	—	—	—	—	—	—	—	—	—
Ruthenium	—	—	C	C	—	D	A	A	—	—	D	C	C	—	C	C	—
Titanium	A	—	A	—	—	C	—	C	A	—	—	C	—	B	—	—	—
Vanadium	D	—	A	—	—	—	D	—	—	—	—	—	—	—	—	—	—
Zirconium	—	—	C	—	—	—	—	—	—	—	—	—	—	—	—	—	—

A: 10^{-1}—10^{-2} %
B: 10^{-3}—10^{-4} %
C: 10^{-4}—10^{-5} %
D: 10^{-6} %

Results

The conversion values measured with the different metals studied in the dehydrogenation of cyclohexane and cyclohexene are shown in Tables II and III.

According to the reasons set out in a former communication [1], also in this case the conversion values referred to unit area of the catalytic surface

Table II

Quantity of converted cyclohexane on different catalysts

$$\frac{x}{M} = \frac{\text{NTP ml}}{\text{min g}}; \qquad \frac{x}{s} = \frac{\text{NTP ml}}{\text{min m}^2}$$

Catalyst	t, °C	$\frac{x}{M}$	$\frac{x^*}{s}$
Be	303	$7.5 \cdot 10^{-5}$	$6.0 \cdot 10^{-5}$
Au	303	$4.8 \cdot 10^{-3}$	$1.6 \cdot 10^{-2}$
Mo	303	$2.4 \cdot 10^{-3}$	$4.0 \cdot 10^{-3}$
Ru	303	$9.0 \cdot 10^{-2}$	$5.5 \cdot 10^{-2}$
Ti	377	$9.3 \cdot 10^{-5}$	$7.6 \cdot 10^{-3}$
V	379	$8.2 \cdot 10^{-5}$	$6.0 \cdot 10^{-3}$
Zr	303	$6.6 \cdot 10^{-6}$	$1.5 \cdot 10^{-3}$

* For Ti, V and Zr the $\frac{x}{s}$ values were corrected with the roughness factor.

Table III

Quantity of cyclohexene dehydrogenated on different catalysts

Catalyst	t, °C	$\frac{x}{M}$	$\frac{x}{s}$
Be	400	$2.8 \cdot 10^{-3}$	$3.5 \cdot 10^{-3}$
Au	305	$5.0 \cdot 10^{-3}$	$1.7 \cdot 10^{-2}$
Mo	305	$3.2 \cdot 10^{-2}$	$5.3 \cdot 10^{-2}$
Ru	305	$2.2 \cdot 10^{-1}$	$7.4 \cdot 10^{-2}$
Ti	379	$4.2 \cdot 10^{-1}$	$2.6 \cdot 10^{1}$*
V	412	—	—

* Corrected $\frac{x}{s}$ value

have been used for the characterization of catalytic activity. Since the specific surface area of some of the catalysts was uncertain, in every instance the activity values referred to 1 g of the catalysts are also given.

Table III shows that no benzene was found among the conversion products of cyclohexene in the case of vanadium catalyst, though a slight evolution

Table IV

Kinetic constants of the dehydrogenation of cyclohexane and cyclohexene

Catalyst	Cyclohexane		Cyclohexene	
	E kcal/mole	x_0 ml/m² · min	E kcal/mole	x_0 ml/m² · min
Au	46	$4.22 \cdot 10^{15}$	18	$1.15 \cdot 10^{5}$
Mo	29	$2.40 \cdot 10^{8}$	28	$6.10 \cdot 10^{8}$
Ru	12	$3.20 \cdot 10^{3}$	9	$1.95 \cdot 10^{2}$
Ti	—	—	9	$2.24 \cdot 10^{5}$

of gas could be noted. This fact permits the supposition that benzene that might have formed in the course of the reaction was cracked under the conditions of the process. To elucidate this question, gas chromatographic analyses would have been necessary. However, the minute amounts of gas relative to the volume of the apparatus prevented the detection of the products of cracking.

Whenever strong fluctuation of the activity of the catalyst did not prevent it, the virtual activation energy, E, of the dehydrogenation was determined for all the catalysts studied, together with the values of the pre-exponential factor, x_0, of the ARRHENIUS equation (*cf.* Table IV). The apparent activation energies were calculated from the degree of conversion as a function of tempera-

ture, according to the ARRHENIUS equation. The experimental data satisfied this equation quite well; the logarithms of the conversion values in function of the reciprocals of absolute temperature presented a straight line.

Discussion

From the experimental data listed in Table II it is seen that all the metals studied catalyze the dehydrogenation of cyclohexane, though some have very low activity only. The specific activities of ruthenium and gold are of the same order as that of nickel [1], but they are by several orders of magnitude lower than that of platinum and other highly active metals. In the case of the other metals, beryllium excepted, the reaction rates were by one order of magnitude less than that found for ruthenium and gold, whereas beryllium was found to show very little activity. Perhaps an explanation for this can be found in the fact that the atomic structure of this metal is fundamentally different from that of all the other metals studied. Beryllium belongs into the second period of the periodic table, whereas the other metals studied here are in periods IV—VIII. In any case, it has been found that the dehydrogenation of cyclohexane is catalyzed also by metals, thus there seems to be no justification for the view that this reaction is quite so selective as formerly held [3—7] on the basis of experimental evidence then known.

The extension of studies so as to include a wider domain of metals thus shows that a catalytic effect in the dehydrogenation of cyclohexane is exerted also by metals whose lattice structures differ from the types A1 or A3 (Mo and V, further Fe and W, as reported formerly [1]). Catalytically active are also some metals having the required lattice structure, but possessing atomic diameters outside the range (2.44 to 2.78 Å) postulated as suitable for sextet mechanism (Au, Ti, Zr, Be, and Ag, the latter on grounds of results reported formerly [1]). All this seems to suggest that sextet mechanism is not the only possible pathway for the dehydrogenation of six-membered rings. This conclusion may be arrived at also on the basis of kinetic data [8], and results of isotopic tracer studies [9, 10]. Studies described here and formerly [1], afford direct experimental evidence for the possibility of a stepwise dehydrogenation, as opposed to the exclusive sextet mechanism.

According to the data of Table III, the metals studied — except vanadium — catalyze also the dehydrogenation of cyclohexene. A comparison of Tables II and III shows that the dehydrogenation of cyclohexene proceeds at a much higher rate with some of the catalysts, than does that of cyclohexane. However, with gold and ruthenium, no difference approaching one order of magnitude appears between the rates of dehydrogenation of saturated and unsaturated rings, and this is not so in case of most the metals studied [1]. Then, in the case of vanadium no benzene was found among the conversion

products of cyclohexene; this may be due, as mentioned before, to cracking of the primary reaction products.

It would be premature to look for an explanation of the fact that with ruthenium and gold no significant difference, such as experienced with other metals, was found between the rates of dehydrogenation of cyclohexane and cyclohexene. Perhaps desorption plays a more important part when these two metals are used, and so desorption also becomes a rate determining step, or the rate constants of desorption become commensurable with those of other steps in the process. However, to elucidate this aspect, reaction kinetic studies like those carried out for nickel and for platinum catalysts [5, 11] would be necessary; however, such investigations are not feasible with gold and ruthenium, owing to their low and variable activities.

The values of activation energies listed in Table IV are similar to those found for the other metals reported in a former communication [1]. It should be pointed out that also in the case of gold a rather substantial difference (higher than 25 kcal/mole) is observed between the activation energies of the dehydrogenation reactions of cyclohexane and cyclohexene; a similar difference has been found so far only in the case of copper. However, as it has been seen, this substantial difference is not expressed in the reaction rates. The probable cause of this phenomenon resides in the compensation effect, or in the different degrees of this effect for the dehydrogenation of cyclohexene. The h value characteristic of the degree of the compensation effect is $7.5 \cdot 10^{-4}$ for cyclohexene, as compared with $8.6 \cdot 10^{-4}$ and $11.2 \cdot 10^{-4}$, the values found for cyclohexane. Since the expression

$$x_0 = a\, e^{hE}$$

indicates the connection between the pre-exponential factors, it is understandable that even a small decrease in the h value will cause important changes in x_0, and in the reaction rates. As it was mentioned in our previous communication [1], it was just this important role of the compensation effect that made it expedient to select, instead of the activation energy, the quantity of the substance converted per unit area of the catalyst surface for the characterization of the activity in the dehydrogenation of cyclohexane.

In a discussion of the obtained experimental data the question may be raised which of the properties of the metals studied can be associated with the observed degrees of catalytic activity. The results published in our previous paper [1] suggest that there is a correlation, similar to the one found by BEECK [2], between the lattice constant of the metal and its catalytic activity. Fig. 1 shows that this correlation holds reasonably well also in the case of the metals now included in our study, with the exception of beryllium. Obviously, it must be borne in mind that there have been significant differences in the methods of preparation of the metals, and that with Zn, W, Ti, and V the

degrees of conversion were determined at higher temperatures than in the case of most of the metals.* Due to all this, only a *tendency* characteristic of the correlation between the lattice constant and activity can be suggested. Of course, on the basis of relationships of such character no far-reaching conclusions are justified about the role of a given factor, in this case that of the lattice constant, in catalytic activity. Nothing more is meant, but that in the dehydrogenation of cyclohexane the lattice constant is a characteristic of

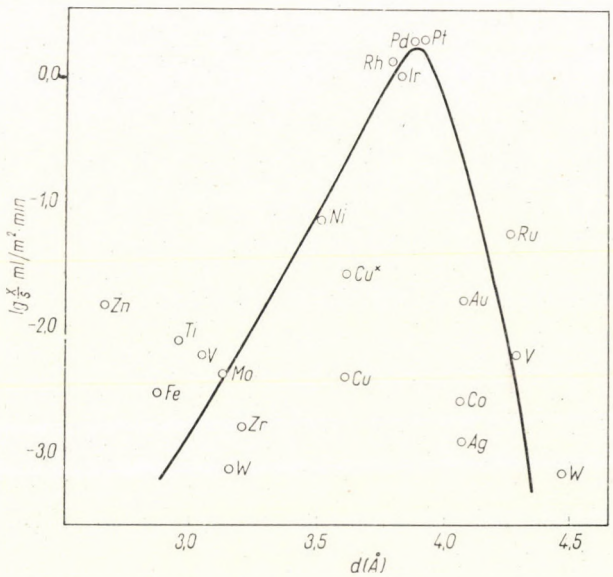

Fig. 1. Rate of the dehydrogenation of cyclohexane as a function of the lattice constants (* Cu, irradiated sample.)

metals nearly enough representative of the properties involved in catalytic activity.

A tendency suggesting a certain relationship between the catalytic activity and some energetical characteristics of metals is also discernible, though there is no immediate parallelism between catalytic activity and the heat of sublimation. Among other things, this is demonstrated by the fact that though Pd and Fe, Pt and V, or Zr, Ru and Mo have very nearly the same heats of sublimation, the dehydrogenation rates of cyclohexane differ with these catalysts by several orders of magnitude.

* In addition to what has been said above, the deviation found in the case of beryllium can also be explained by the fact that the formation of a *d*-bond is impossible with this metal. The absence of unoccupied *d*-sites in copper also significantly reduces activity, producing a deviation from the lattice constant *vs.* activity curve, though in this case a $d \rightarrow s$ electron transfer is feasible requiring relatively small energy. For a more detailed discussion of this point, see our former communication [1]. The values corresponding to the activity of beryllium have been omitted from the Figures for technical reasons.

KEN-ICHI TANAKA, and KENZI TAMARU [12] have found that an unequivocal relation exists between adsorption on metals and their standard enthalpies of oxidation. Later, it has been demonstrated that for several reactions there is a certain connection between the standard enthalpy of oxidation and catalytic activity. Therefore, we have studied the possible existence of a relation between the rate of the dehydrogenation of cyclohexane and the standard enthalpy of oxidation of the metal catalyst (Fig. 2). As it is to be seen, a tendency suggesting a relationship can be found also in this case, though certain deviations, attributable to causes discussed previously, are evident in

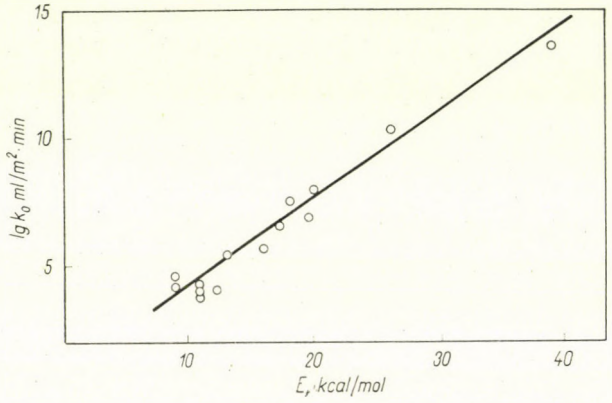

Fig. 2. Rate of the dehydrogenation of cyclohexane *vs.* the standard oxidation enthalpies (ΔH_0) of the metals
(* Cu, irradiated sample.) Temperatures are the same as in Fig. 1

this instance, too. Here again beryllium and copper stand out, in consequence of the causes mentioned above. It should be noted that the curve representing the reaction rate *vs.* the heat of oxidation has a maximum, being similar in character to the curve on which the lattice constant of the metal was shown.

For this reaction no immediate correlation is found between the catalytic activity and electron structure of the metal (cf. [1]). *E.g.*, Fe and Co, further Ni have very different catalytic activities, though the *d*-character of metallic bonding is the same (40%) for all the three metals. Regarding the catalytic activities, there is a difference of about 5 orders of magnitude between Pt and W, though their percentage *d*-character is nearly the same. Conversely, Rh and Pt show nearly identical catalytic activities in spite of the relatively great difference in *d*-character (50% and 44%, respectively). All this proves that for this reaction the relation of lattice constant to catalytic activity cannot be substituted by a correlation between percentage *d*-character of metallic bonding and catalytic activity, as it could be done in the case of the results of BEECK [2] referred to above. However, this is no negation of the role of the electron

structures. The significance of available unoccupied places in the *d*-shell is quite clear from the behaviour of copper, silver, and beryllium, where *d*-bonds are impossible. However, for this reaction the incompleteness of the *d*-shell, or the *d*-character of metallic bonding, does not exert such unequivocal influence on the catalytic activity as in some other reactions, such as the hydrogenation of ethylene, hydrogen-deuterium exchange, etc. [14—16]. In the reaction here studied, rather the lattice constants and oxidation enthalpies might be suggested as the characteristics of the metals which represent features important from the point of view of catalytic activity.

The connection of catalytic activity with the lattice constants and with the oxidation enthalpies of the metals shows that the catalytic properties depend on both geometrical and energetical factors. Further, as it has been pointed out [1], the lattice constant, as a function of the interaction of the metal atoms, represents to a certain extent the energetical, even the electronic properties of the metal. This notion, supported by the correlation shown in Fig. 2, could not have been arrived at without the new data on the catalytic behaviour of the metals investigated in this study.

SUMMARY

The dehydrogenation of cyclohexane in the presence of Be, Au, Mo, Ru, Ti, V, and Zr, and that of cyclohexene in the presence of Be, Au, Mo, Ru, and V have been studied. The kinetic constants characteristic of the reactions with the various catalysts have been determined. All the metals investigated catalyze the dehydrogenation of cyclohexane in spite of the fact that their structures, except for Ru, do not meet the requirements of the sextet mechanism, showing that the dehydrogenation of cyclic hydrocarbons may proceed according to some other mechanism as well.

The catalytic activity of the metals is unequivocally shown to be a function of the lattice constants and of the standard oxidation enthalpies; both functions are represented by maximum curves.

REFERENCES

1. TÉTÉNYI, P., SCHÄCHTER, K.: Acta Chim. Acad. Sci. Hung. **50**, 129 (1966).
2. BEECK, O.: Disc. Far. Soc. **8**, 188 (1950).
3. BALANDIN, A.: Z. phys. Chem. B, **2**, 289 (1929).
4. TRAPNELL, B.: Adv. Catalysis, Vol. 3. New York, 1952. p. 1.
5. TÉTÉNYI, P., BABERNICS, L., PETHŐ, Á.: Acta Chim. Acad. Sci. Hung. **28**, 375 (1961).
6. KING, C. V.: Annals of the New York Academy of Sciences V. **58** Art 6, 910 (1964).
7. BALANDIN, A.: Probl. Kinetiki i Kataliza **10**, 314 (1960).
8. FROST, A., LAPIN, J.: Vestnik MGU 95 (1946).
9. DERBENTSEV, J., BALANDIN, A., ISZAGULJANTS, G.: Kinetika i Kataliz **2**, 741 (1961).
10. TÉTÉNYI, P., BABERNICS, L., THOMSON, S.: Acta Chim. Acad. Sci. Hung. **34**, 335 (1963).
11. TÉTÉNYI, P., BABERNICS, L.: Acta Chim. Acad. Sci. Hung. **35**, 419 (1963).
12. KEN-ICHI TANAKA, KENZI TAMARU: J. Cat. **2**, 366 (1963).
13. KEN-ICHI TANAKA, KENZI TAMARU: Kinetika i Kataliz **7**, 242 (1966).
14. SCHUIT, G.: Disc. Far. Soc. **8**, 118 (1950).
15. AVDEENKO, M., BORESKOV, G., SLINKO, M.: Probl. Kinetiki i Kataliza V, IX, p. 61. Moscow, 1957.
16. KEMBALL, C.: Proc. Roy. Soc. A, 214, 413 (1952).

Pál TÉTÉNYI
Klára SCHÄCHTER
} Budapest XII., Konkoly Thege u.

Acta Chimica Academiae Scientiarum Hungaricae Tomus 56 (1), pp. 25—37 (1968)

NH STRETCHING VIBRATION BANDS AT WAVENUMBERS LOWER THAN 3000 cm^{-1}, IV

DIMERIC STRUCTURES, IV
TAUTOMERIC EQUILIBRIUM OF ISONICOTINIC ACID THIOAMIDE DERIVATIVES

P. SOHÁR and A. NEMES

(Research Institute for Pharmaceutical Chemistry, Budapest)

Received October 16, 1966

Introduction

Our previous investigations have shown that compounds having lactam or analogous structures — corresponding to the general formula **I** — contain in solid state (KBr pellet technique) cyclic dimeric hydrogen bonds, which appear in the spectra as characteristic NH stretching (νNH) bands [1—5] of diffuse form, in the range of unusually small wavenumbers (between 3200 and 2700 cm^{-1}), sometimes including part maxima, too. In primary amides and thioamides this kind of association does not occur, and in accordance with the literature data [6, 7], the band pair of the asymmetric and symmetric stretching vibrations of the NH_2 group ($\nu_{as}NH_2$ and ν_sNH_2) always appears between 3500 and 3050 cm^{-1}, occasionally doubled or sometimes tripled (thus having four or six maxima) because of the simultaneous presence of the monomeric and variously associated molecules [8].

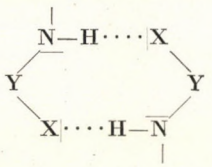

I

In this work the spectra of some isonicotinic acid thioamide derivatives prepared by the authors [9] will be reported. Some of these compounds showed a diffuse νNH band of small wavenumber, characteristic of cyclic dimeric association, although, since the compounds are primary amides, this was not expected.

Thioamide bands

Thioamides and among them isonicotinic acid thioamides have been recently often investigated spectroscopically [10—13]. Assignment of the bands in the spectra is rather difficult, as, on the one hand, not characteristic bond

frequencies but group vibrations* extending to more than one bond are responsible for their appearance, and in consequence, their properties (frequency, intensity, band width, behaviour when altering the physical state of the sample, *etc.*) are very changing and sensitively react also to relatively small changes in the structure of the molecule; on the other hand, the structure of the thioamide group is not unambiguous, as mesomeric (**II** ↔ **III**) and tautomeric (**II** ⇄ **IV**) transformations are both imaginable.

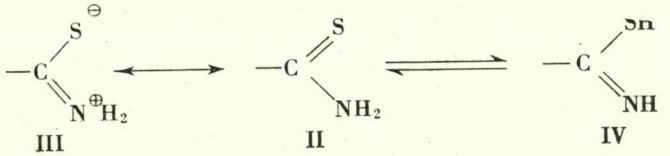

The infrared spectra of about 150 different molecules containing the —N—C=S group were investigated by JENSEN and NIELSEN [10], and seven types of bands (denoted as *A*, *B*, *C*, *etc.*) generally characteristic of thioamides were found:

Band A appears in the 1650—1600 cm^{-1} region and is of analogous origin with the Amide II band, thus it should be assigned as the symmetric in-plane deformation (scissoring) vibration of the NH_2 group ($\beta_s NH_2$ band), which can couple with the νC—N vibration, and then the hybrid band may also appear outside the given frequency range.

The intensive *Band B* is found between 1600 cm^{-1} and 1400 cm^{-1} and is interpreted mainly as νC—N or ν_{as}S=C—N vibration; thus it would be analogous with the Amide I band (when it is regarded as a ν_{as}O=C—N vibration), but while in the latter the νC=O character is predominating, the character of *Band B* is determined by the νC—N, more precisely the $\nu(C{=}N^+ \leftrightarrow C{-}\overline{N})$ vibration mode with increased bond order, according to the mesomeric transformations **II** ↔ **III**. Among the components of this hybrid vibration, some deformation vibration modes (first of all $\beta_s CH_2$, the scissoring vibration type) of the neighbouring aliphatic groups may appear as well.

Band C is generally strong and appears between 1400 and 1200 cm^{-1}. It is assigned as the stretching vibration of the C—C bond connecting the thioamide group to the molecule; however, its coupling with the rocking asymmetric in-plane deformation vibration of the NH_2 group ($\beta_{as} NH_2$) or the νC=S (or νC—S) as well as with some CH deformation vibration modes is also considered possible.

* The group vibrations produced by bonds of different individual frequency values — to distinguish them from the coupled vibrations of bonds with identical frequencies, which are also of the group vibration type — are called hybrid vibrations, and the corresponding bands hybrid bands, pointing to the fact that the properties of the group vibrations reflect the participation of the individual bonds in the group vibration. This nomination should not be confused with that used to denote the vibrational-rotational bands of an asymmetric rotor.

Band D corresponds to the ν_sS=C—N vibration, so it is analogous to the Amide III band. This band of medium intensity appears between 1200 and 1000 cm^{-1}.

Band E, appearing in the range 900—800 cm^{-1} is assigned as $\gamma_s NH_2$ (out-of-plane symmetric NH_2 deformation, wagging) vibration.

Band F, found at about 700 cm^{-1} is supposed to belong to a hybrid vibration resulting from the out-of-plane NH deformation ($\gamma_s NH_2$ or $\gamma_{as} NH_2$: wagging or twisting), νC=S (or νC—S) and νC—N (or νC=N$^+$) vibrations as components.

Finally, *Band G*, as it is the only one of all the bands which shows a significant frequency shift as a result of sulphur-selene exchange in the C=S group, is assigned as a νC=S band. It appears between 800 cm^{-1} and 600 cm^{-1}, and this low frequency value seems to prove the single bond character of the CS bond (thus the increased probability of the mesomeric structure **III**, or the appearance of the thiol tautomeric form **IV**).

Other papers [11, 13, 14, 15] dealing with the thioamide group, with no exception, also regard the characteristic bands of the NCS group as mixed ones. However, concerning the number of bonds participating in the group vibrations and their participation ratios, no uniform opinion has been or could have been developed, since the character of the hybrid bands differs in every group of compounds, even within very small groups containing molecules of closely related structures, owing to the strong inclination of the sulphur and nitrogen atoms for conjugation. So the above-mentioned facts should not be simply generalized, for example, to the isonicotinic acid derivatives, and each band must be investigated to establish if the participating bonds or their participation ratios in the group vibration have remained unchanged or not. The mesomeric equilibrium may also be shifted to different degrees towards one or another limiting structure in different types of molecules, and tautomerism may present another problem. The following investigations aim at clarifying these questions.

Spectrum of ethylisonicotinic acid thioamide

In the spectrum of 2-ethylpyridine-4-thioamide [16] (**V**) (Spectrum 1) a strong, diffuse νNH band of small wavenumbers, indicating cyclic dimeric association, is found in the range from 3100 cm^{-1} to 2400 cm^{-1}, though in primary amides this is not expected. The $\nu_{as} NH_2$ — $\nu_s NH_2$ band pair of primary amides — as mentioned above — should appear between 3500 cm^{-1} and 3050 cm^{-1}, and the distance between the maxima should be 50—200 cm^{-1}. However, in Spectrum 1 between 4000 cm^{-1} and 2000 cm^{-1} there is only one intensive maximum at about 3270 cm^{-1}, in addition to the above-

mentioned diffuse band, but these two bands neither on the basis of the intensity ratio (the diffuse band is at least three or four times more intense than the absorption at 3270 cm^{-1}), nor on the basis of the frequency difference of the maxima (which is about 370 cm^{-1}, taking 2900 cm^{-1} as the centre of

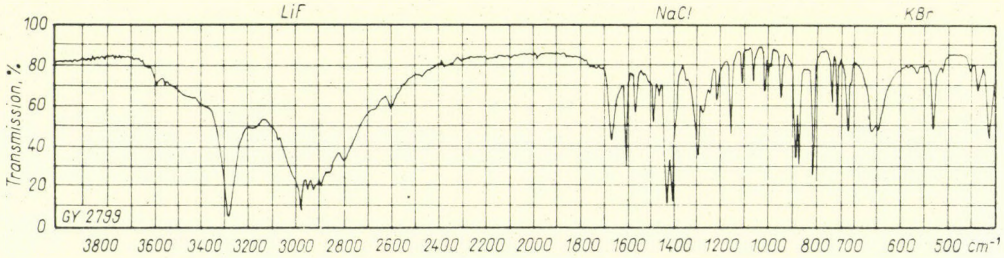

Spectrum 1: 2-Ethylpyridine-4-thioamide

the diffuse band) could be assigned as a $\nu_{as}NH_2$ — ν_sNH_2 band pair. Namely, then the intensities would be of inverse ratio, or two bands of similar intensity would appear in the spectrum. (In general, the $\nu_{as}NH_2$ band at higher wavenumbers is the more intense one; in extreme cases the ν_sNH_2 peak may be so

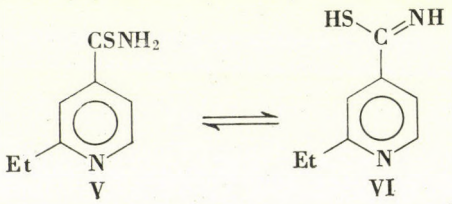

V VI

small that it becomes perfectly covered by the former, or by bands of other OH or NH groups appearing in the same region; on the other hand, intensity ratio displacement in the reversed sense is never so extreme.) The distance between the maxima would also be considerably smaller (see above). In the 4000—2000 cm^{-1} region, in addition to the above-mentioned two strong peaks, there is one maximum at about 3150 cm^{-1} of medium intensity, a weak band at 2595 cm^{-1}, and also bands of stretching vibrations of aliphatic and aromatic CH groups can be found as merged into the diffuse νNH band in the ranges 3100—3000 cm^{-1} and 3000—2800 cm^{-1}.*

These facts are hardly compatible with structure **V** supposing only one NH_2 group, especially when taking into consideration another strong band at 1665 cm^{-1} which would be a *Band A*, according to JENSEN and NIELSEN, when accepting structure **V**. The frequency value of the band is outside the frequency range given for *Band A*. This fact was explained by the above

* At 2800 cm^{-1} there is the first overtone of one of the intensive bands between 1425 and 1405 cm^{-1}, or a combination of them, superimposed on the diffuse band.

authors with the formation of a thiol (**VI**) tautomer, but they maintain to assign it as a $\beta_s NH_2$ band (at least no indication has been given of a different vibration mode). However, this assignment is obviously disputable, because even if limiting structure **III** were predominating, it is not probable that the band of scissoring vibration of the NH_2 group would appear at such a high wavenumber. It is to be noted that in nicotinic acid derivatives even higher frequency values can be observed, *e.g.*, this band of nicotinic acid thioamide [10] appears at 1680 cm^{-1}. (For comparison, two data are given here: the $\beta_s(=NH_2^+)$ band of the $=NH_2^+$ group is found between 1610 and 1570 cm^{-1}, and the $\nu C=N^+$ band between 1690 and 1670 cm^{-1} [17].)

In our opinion a tautomeric equilibrium (**V** $\rightleftharpoons$ **VI**) develops under the circumstances of sample preparation (in KBr pellet); taking this assumption as a starting point, all special features of the spectra can readily be interpreted with the following assignment:

3270 cm^{-1} and 3150 cm^{-1}: the $\nu_{as}NH_2$—$\nu_s NH_2$ band pair of the amide form **V**, with broad contours owing to simple intermolecular association.

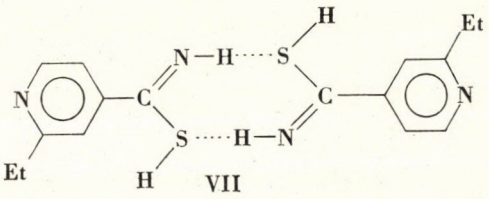

VII

3100—2400 cm^{-1}: νNH band of the thiol tautomeric form **VI**, with a diffuse shape and shifted toward the smaller wavenumber range owing to cyclic dimeric association (**VII**). The formation of hydrogen bonds such as in structure **VII** is quite understandable and expected in the case of structure **VI**, since the latter contains a secondary NH group with a nitrogen atom possessing planar hybrid electron orbitals, furthermore the electron donor character of the sulphur atom is definitely strong; so the formation of a strong hydrogen bond is possible under these circumstances.

3070 cm^{-1}: $\nu(=CH)$ band (of aromatic ring). The assignment holds for both tautomers.

2965, 2940, 2915 and 2880 cm^{-1}: $\nu_{as}CH_3$, $\nu_{as}CH_2$, $\nu_s CH_3$ and $\nu_s CH_2$ bands, resp., for both tautomers.

2595 cm^{-1}: νSH band of "thioimino" hydrin tautomer.

1665 cm^{-1}: this band belongs to the hybrid vibration with $\nu C=N$ character of the thiol tautomer **VI**. The marked asymmetric broadening in the direction of smaller wavenumbers originates from the overlapped *Band A* ($\beta_s NH_2$) of the thioamide tautomer (**V**) with a maximum of far lower intensity at about 1640 cm^{-1}. This clearly shows that the tautomeric equilibrium has been dis-

placed in favour of the thiol form. However, a more accurate determination of the ratio of the quantities of the tautomers is impossible without the knowledge of the spectrum of at least one of the pure tautomers. The intensity ratio of the νNH bands at 3270 cm^{-1} and at about 2900 cm^{-1} also reflects the preponderance of the thiol form. The correct assignment of the band at 1665 cm^{-1} is verified also by the spectrum of the partially deuterated compound (Spectrum 2), in addition to the spectra of other derivatives to be discussed below.

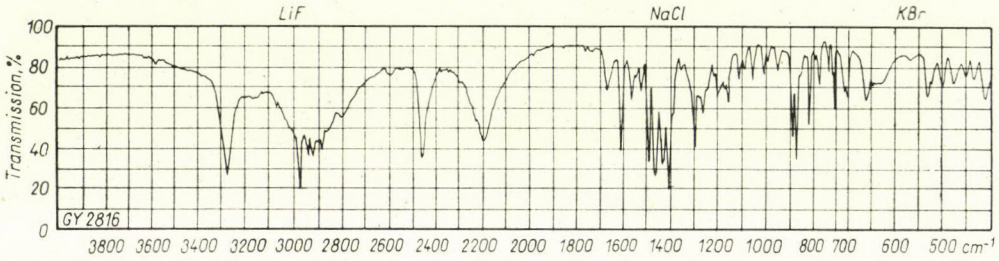

Spectrum 2: Partially deuterated 2-ethylpyridine-4-thioamide

On the basis of the integrated areas under the νNH bands, 40% of the molecules were found to be deuterated.

In the spectrum of the partially deuterated compound the intensity of the 1665 cm^{-1} band — owing to the 40% deuteration — is significantly decreased (almost to the half); the shape of the band, broadening towards the smaller wavenumbers, remains unchanged, indicating the unchanged ratio of tautomers in the deuterated compound. Simultaneously two new bands appear at 1260 cm^{-1} and 1485 cm^{-1}. The first maximum corresponds to the $\beta_s ND_2$ (*A*) band of the thioamide form **V**, and the value of the isotopic shift is almost theoretical (calculated frequency [18]: 1225 cm^{-1}). This shows that the assignment was correct, and *Band A* really belongs to an almost pure $\beta_s NH_2$ vibration.

The maximum at 1485 cm^{-1} belongs to the thiol tautomer (it appears instead of *Band A* of thioamides) and by no means is it possible to assign it to a βND vibration mode. The frequency shift of the isotope is only 180 cm^{-1} (1665—1485) instead of the theoretically expected 440 cm^{-1} (1665—1225). However, the significant isotopic effect shows an assignment as νC=N band also unacceptable. For a pure νC=N bond frequency the theoretical band shift is far smaller:

$$\Delta\nu = \nu C{=}N(H) - \nu C{=}N(D) = 1665\left(1 - \sqrt{\frac{m_{NH}\cdot m_C}{m_{NH}+m_C} \Big/ \frac{m_{ND}\cdot m_C}{m_{ND}+m_C}}\right) =$$

$$= 45 \text{cm}^{-1}$$

It is clear therefore that this is a band of a hybrid vibration involving mainly the C=N and NH bonds, and probably other bonds of the HSC=NH group as well: the hybrid band combines the characteristics of the νC=N and βNH bands. According to our conception [4], it is possible to estimate approximately also the contribution of the βNH vibration, from the theoretically expected (Δ_e) and experimentally observed (Δ_k) band shift values, with the help of the following equation:

$$q = \Delta_k/\Delta_e$$

where Δ_k is the difference of the frequency values determined from the spectra of the light and heavy isotopes, and Δ_e is the difference between the frequency value of the light isotope and its 1.37 part. 100 q gives the percentage contribution of component βNH in the hybrid vibration. In our case it is 40%.

The bands at 1610 and 1480 cm^{-1} belong most probably to the skeletal vibrations of the aromatic ring; the $\beta_s CH_2$ and $\delta_{as} CH_3$ (methyl asymmetric deformational) vibrations absorb overlapped by the latter band and at 1460 cm^{-1}, respectively, corresponding to the two tautomers. These latter two bands overlap each with a band of different origin of the heavy isotope in the spectrum of the partially deuterated derivative; in the case of the maximum at 1480 cm^{-1} the overlapping band is the above-discussed hybrid band belonging to the thiol isomer (corresponding to *Band A* of thioamides).

The maximum at 1560 cm^{-1} holds for *Band B* of the thiol tautomer, and according to this, only a slight isotopic effect is found in the spectrum of the partially deuterated compound (the displaced maximum appears exactly at the theoretically expected wavenumber value, 1516 cm^{-1}, which is by 45 cm^{-1} smaller than the original one).

Between 1450 and 1375 cm^{-1} there is a broad, very intense absorption band having two well separated peaks at 1425 and 1405 cm^{-1}, and a definite shoulder at about 1380 cm^{-1}. This absorption arises at least from four different vibration modes; one of them is the $\delta_s CH_3$ (symmetric methyl deformation) band appearing at the same wavenumber value in both tautomers and giving rise to the shoulder at about 1380 cm^{-1}. The maximum at 1405 cm^{-1} can be assigned to the hybrid vibration of the thiol tautomer which contains also the stretching vibration of the C—C bond connecting the thioiminohydrin group to the ring: the band at 1425 cm^{-1} of similar character is *Band C* of the thioamide group, and under these bands a broad absorption of βNH character appears with no separated maximum because of the broad contour, belonging to the thiol tautomer. These conclusions are confirmed by the spectrum of the partially deuterated compound (Spectrum 2) where the section in question has a radically different structure. The total intensity of the maxima decreases, and at the same time a new broad band appears between 1200 and 1160 cm^{-1} corresponding to a hybrid vibration of βND character. The calcu-

lated frequency is 1050 cm^{-1}. Taking 1420 and 1180 cm^{-1}, resp., as the centres of the bands for the two isotopes, the above facts indicate that component βNH particles in the hybrid vibration in 65%. This is quite evident, as the vibrations of a secondary N—H bond — similarly to amides — are expected to develop a far stronger interaction with the vibrations of the neighbouring bonds than that of a primary NH_2 group, having almost pure bond frequencies, independent from other vibrations. The intensity of the 1425 cm^{-1} band decreases, simultaneously a new maximum appears at 1455 cm^{-1}. This isotopic shift of opposite direction constitutes evidence for a *Band C* character, showing that the main component of the vibration is the stretching vibration of the C—C bond connecting the thioamide group to the ring, which hybridizes with one of the NH deformational vibrations (probably the rocking one) of the light isotope, accompanied by a frequency decrease. In the heavy isotope coupling takes place to a smaller extent because of the smaller wavenumber value of the NH frequencies, or sometimes it is completely missing, owing to the withdrawal of the frequencies of the vibrations which could couple in the light isotope. Thus, the frequency increases: the band is displaced toward higher wavenumbers. The maximum at 1405 cm^{-1} is fundamentally unchanged. It follows that this band of the thiol tautomer is due to an almost pure $\nu C_{aromatic}—C_{thiol}$ vibration. This frequency is unusually high, which may be due to a higher actual C—C bond order. Anyhow, the assignment is uncertain. Naturally, the shoulder at 1380 cm^{-1} remains unchanged.

The assignments of the further bands are much less unambiguous. The absorption bands at about 1300 cm^{-1} probably are $\beta_{as}NH_2$ or *D* bands of the thioamide tautomer, and also a further hybrid band of the thiol group has to appear here.

The peaks at 1150(9a), 1110(13), 1060(18a), 1010(12), 950(ν_{ethyl} C—C), 885(7b), 870(7b), 815(11) and 660(1) cm^{-1}* most probably correspond to the skeletal stretching and deformation, resp. to the out-of-plane CH deformation vibrations of the molecule (first of all of the aromatic ring), the 870, 855 and 815 cm^{-1} bands prove the presence of the 1,2,4-trisubstituted aromatic ring (the 2,4-disubstituted pyridine ring may be regardred as such [19]).

The peak at 645 cm^{-1} (considering the intensities and isotopic shifts) belongs to the γNH (out-of-plane NH deformational) vibration of the thiol tautomer; at 530 and 410 cm^{-1} the $\gamma_s NH_2$ and $\gamma_{as}NH_2$ vibrations of the thioamide molecules absorb.

* In parentheses the probable assignment is given according to WILSON's numbering of the normal vibrations of benzene [20]. Thus the previously mentioned bands at 1610 and 1480 cm^{-1} correspond to the normal vibrations of benzene Nos 8 and 19. The splitting of the 7b vibration is due to the two tautomers.

In addition to the spectrum of the partially deuterated compound, the spectrum in dilute chloroform solution of 2-ethylisonicotinic acid thioamide was also studied (Spectrum 1a). The appearance of the intensive band pair at 3490 and 3375 cm^{-1} and the disappearance of the maxima of 3270, 2900 and about 2595 cm^{-1} prove the perfect displacement of the tautomeric equilibrium in dilute solution favouring the amide form. The doublet at 3490 and 3375 cm^{-1} corresponds to the $\nu_{as}NH_2$ and ν_sNH_2 vibrations of the NH_2 group.

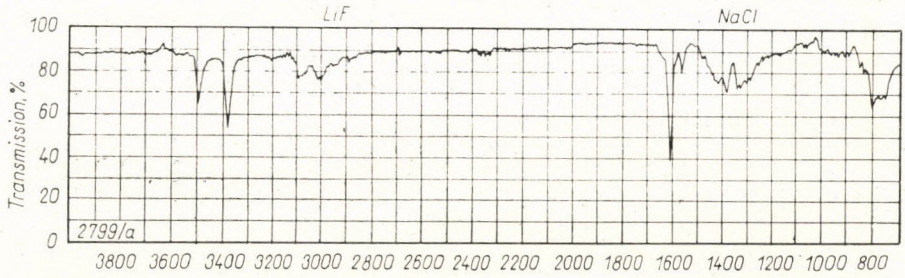

Spectrum 1a: 2-Ethylpyridine-4-thioamide in dilute chloroform solution

The absence of the band at 1665 cm^{-1} in the spectrum of the solution verifies that really the thiol tautomer is responsible for this absorption of the solid sample. The β_sNH_2 band appears — with a lower frequency owing to solvation — at 1610 cm^{-1}, together with the band of aromatic skeletal vibration at 1600 cm^{-1}, as shown by the broadening of the band toward smaller wavenumbers and a considerable increase of the relative intensities (*cf.* Spectrum 1a).

Other isonicotinic acid thioamide derivatives

Starting with the above facts, the effect of different substituents on the tautomeric equilibrium was investigated in some isonicotinic acid thioamide derivatives.

The 2-cyclohexylmethyl (**VIIIa**), 2-benzyl (**VIIIb**) and 2-(*p*-nitrobenzyl) (**VIIIc**) compounds have spectra which are completely analogous to that of the 2-ethyl derivative, indicating the displacement of the tautomeric equilibrium towards the thiol form in these compounds, too. The reversed case is found for the 6-chloro derivatives as in the 2-methyl (**VIIId**), 2-ethyl (**VIIIe**), 2-cyclohexylmethyl (**VIIIf**) and 2-benzyl (**VIIIg**) compounds alike, the amide form is predominating beside an insignificant quantity of the thiol form. The above order shows a displacement of the tautomeric equilibrium in favour of the amide form within narrow limits, however, significant differences occur only between the 6-chloro-substituted and other derivatives.

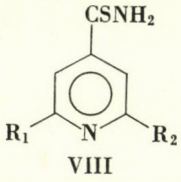

VIII

a: $R_1 = -CH_2-C_6H_5$, $R_2 = H$

b: $R_1 = -CH_2-C_6H_5$, $R_2 = H$

c: $R_1 = -CH_2-C_6H_4-NO_2$, $R_2 = H$

d: $R_1 = -CH_3$, $R_2 = Cl$

e: $R_1 = -CH_2-CH_3$, $R_2 = Cl$

f: $R_1 = -CH_2-C_6H_5$, $R_2 = Cl$

g: $R_1 = -CH_2-C_6H_5$, $R_2 = Cl$

Spectrum of 2-benzyl-6-chloroisonicotinic acid thioamide

The bands of the thioamide tautomer are presented in the spectra of 2-benzyl-6-chloroisonicotinic acid thioamide (Spectrum 3) and its partially deuterated derivative (Spectrum 4), since in the solid state this compound appears as the pure amide tautomer.

The $\nu_{as}NH_2 - \nu_sNH_2$ bands of monomeric or intermolecularly associated primary NH_2 groups appear with both sharp and broader band pairs with maxima at 3380 and 3290 cm^{-1}, further at 3170 and 3080 cm^{-1}, resp. (the associated ν_sNH_2 band is only a shoulder at about 3080 cm^{-1}). At the same time no diffuse band between 3200 and 2700 cm^{-1} due to cyclic dimeric association of the secondary NH groups, neither a νSH band at about 2600 cm^{-1} are found. The band at 1665 cm^{-1}, assigned as a $\nu C{=}N$ band in Spectrum 1 is also missing; on the other hand, there is a considerable intensity increase in the *A* and *B* thioamide bands at 1630 and 1545 cm^{-1}.

Two bands due to aromatic skeletal vibrations appear at 1600, 1500 and 1460 cm^{-1} (in the case of the latter the degenerated vibration pair is split); the β_sCH_2 band occurs at 1440 cm^{-1}.

Band C is found at 1410 cm^{-1}, and *Band D* at 1330 cm^{-1}. The bands at 755 and 695 cm^{-1}, due to out-of-plane CH deformational vibrations, are

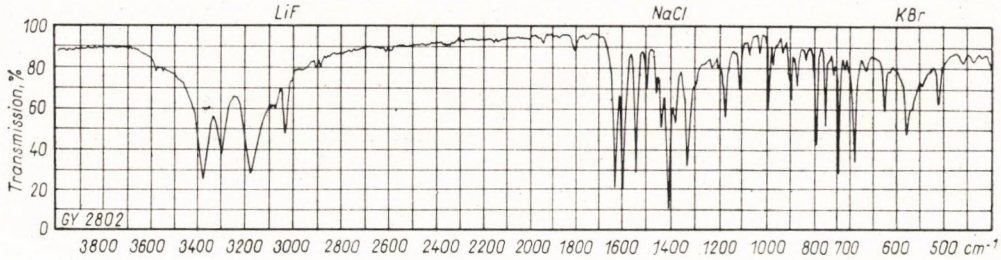

Spectrum 3: 2-Benzyl-6-chloropyridine-4-thioamide

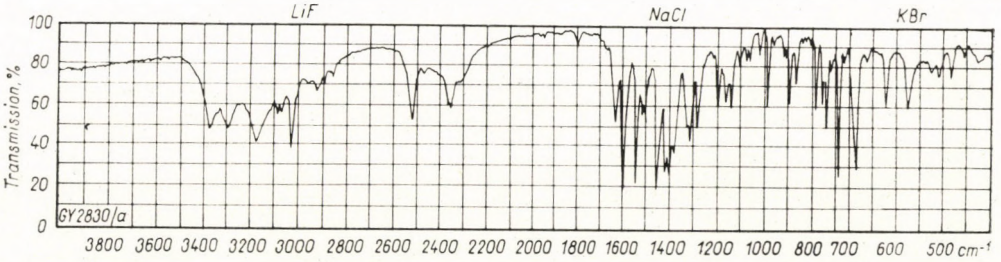

Spectrum 4: Partially deuterated 2-benzyl-6-chloropyridine-4-thioamide

characteristic of monosubstituted aromatic compounds, so the benzyl substituent is responsible for them. The band at 795 cm^{-1} is of similar origin, though this value is slightly outside the usual frequency region [21] of 1,2,3,5-tetrasubstituted derivatives, still this often occurs in aromatic compounds of complicated structures. The out-of-plane deformational vibrations of the NH_2 group give rise to the absorptions at 580 cm^{-1} and 510 cm^{-1}.

In the spectrum of the partially deuterated compound the quartet maxima of stretching vibrations of the monomeric and bonded NH_2 groups appear at about 2525 cm^{-1}, 2470 cm^{-1}, 2370 cm^{-1}, and 2320 cm^{-1}. The degree of deuteration is approximately 42%. The deuterated pair of *Band A* at 1630 cm^{-1} appears at 1290 cm^{-1}, and *Band C*, displaced towards higher wavenumbers, is found at 1460 cm^{-1} in the spectrum of the heavy isotope. The deuterated equivalent of *Band D* appears at 1210 cm^{-1} indicating the contribution of the bonds of the NH_2 group in the corresponding hybrid vibration. An intensity decrease owing to the deuteration was observed in the $\gamma_s NH_2$ and $\gamma_{as} NH_2$ bands at about 580 and 510 cm^{-1}.

Spectrum of N-n-butyl-2-ethylisonicotinic acid thiamide

The spectrum of N-*n*-butyl-2-ethylisonicotinic acid thioamide [22] (Spectrum 5) shows the complete displacement of the tautomeric equilibrium in favour of the amide form. In spite of this fact, cyclic dimeric association rings (**IX**) are formed by the majority of the molecules, so a diffuse νNH band is found at low wavenumbers (between 3100 and 2600 cm^{-1}) in the spectrum,

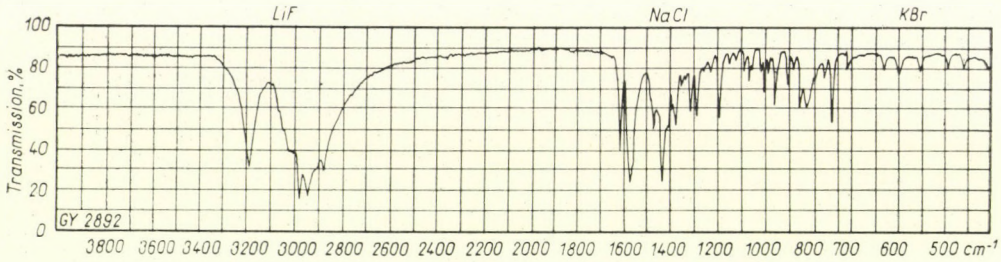

Spectrum 5: N-*n*-butyl-2-ethylisonicotinic acid thioamide

fused with the $\nu_{as}CH_3$, $\nu_{as}CH_2$, ν_sCH_3, and ν_sCH_2 bands of the ethyl and butyl groups (*cf.* the maxima at 2970, 2940 and 2870 cm^{-1}). The maximum at 3170 cm^{-1} belongs to the νNH vibration of the simple intermolecularly associated groups. This result is quite evident, since here a secondary NH group is present instead of a primary NH_2, and the former readily undergoes association to give cyclic dimers.

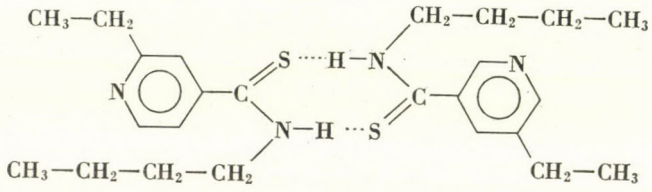

IX

The peaks at about 1550 cm^{-1} and 830 cm^{-1} are βNH and γNH bands; the νC=S band is probably a weak one, so it could not be exactly identified. The spectrum radically differs from that of other compounds containing a thiol or thioamide group, as here the former is missing and the latter contains a secondary NH group instead of the NH_2 group, so the character of the thioamide bands has undergone a complete change.

Experimental

The spectra were recorded on a *Zeiss UR 10* double-beam spectrometer in KBr pellets, and in chloroform solution at about 10^{-1} mole/l concentration in a NaCl cell, of 1 mm thickness.

Partial deuteration was achieved by boiling the compounds in heavy water.

The authors' thanks are due to Prof. Gy. VARSÁNYI (*Polytechnical University*, Budapest) for his valuable advice, and to Miss Zs. LESTYÁNSZKY and Mr. G. TÓTH *(Research Institute for Pharmaceutical Chemistry)* for technical assistance.

SUMMARY

The infrared spectra of some isonicotinic acid thioamide derivatives have been studied. In solid state (in KBr pellets) the thioamide $\rightleftarrows$ thioiminohydrin tautomeric equilibrium was found to change within very wide limits — even to the nearly sole appearance of one or the other tautomer — depending on the other substituents of the pyridine ring. In the 2-alkyl and

2-aralkyl derivatives the thiol form, whereas in the 6-chloro-substituted compounds the amide form is predominating. N-*n*-butyl-2-etyhlisonicotinic acid thioamide is also present as the amide tautomer. The spectra of the latter compound and of the other molecules which are present in thiol form show a diffuse νNH band at low wavenumbers affording evidence for cyclic dimeric association. The molecules appearing in the thiol form in the solid state undergo tautomeric change in dilute chloroform solution to give the amide.

REFERENCES

1. SOHÁR, P.: Acta Chim. Acad. Sci. Hung. **40,** 317 (1964).
2. SOHÁR, P.: Magy. Kém. Foly. **71,** 415 (1965).
3. SOHÁR, P., FARKAS, L.: Acta Chim. Acad. Sci. Hung. **54** 79 (1967).
4. SOHÁR, P.: Infrared Spectroscopic Study of Association Structures. (Post-Doctoral Thesis) Budapest (In Hungarian).
5. SOHÁR, P.: Acta Chim. Acad. Sci. Hung. **54** 91 (1967).
6. JONES, R. N., SÁNDORFY, C.: Infrared and Raman Spectrometry. In WEISSBERGER, A.: Chemical Application of Spectroscopy. Interscience Publ. Inc. New York, 1956, pp. 515—519.
7. CROSS, A. D.: Introduction to Practical Infrared Spectroscopy. Butterworths, London, 1960, pp. 65—67.
8. BELLAY, L. J.: Ultrarot Spektrum und chemische Konstitution. Verlag von dr. Dietrich Steinkopff, Darmstadt, 1955, pp. 162—163.
9. NEMES, A.: Preparation of Sulphur-containing Pyridine Ring Compounds Possessing Pharmaceutical Activity. (Dr. Techn. Thesis) Budapest, 1966 (In Hungarian).
10. JENSEN, K. A., NIELSEN, P. H.: Acta Chem. Scand. **20,** 597 (1966).
11. RAO, C. N. R., VENKATARAGHAVAN, R.: Spectrochim. Acta **18,** 541 (1962).
12. KAKIMOTO, S., SEYDEL, J., WEMPE, E.: Tuberk. Forsch. Borstel, Jahresber. **5,** 233 (1966); C. A. **57,** 15609 (1962).
13. RAO, C. N. R., VENKATARAGHAVAN, R., KASTURI, T. R.: Can. J. Chem. **42,** 36 (1964).
14. SUZUKI, I.: Bull. Chem. Soc. Japan **35,** 1286 (1962).
15. YAMAGOUCHI, A., PENLAND, R. B., MIZUSHIMA, S., LANE, T. J., CURRAN, C., QUAGLIANO, J. V.: J. Am. Chem. Soc. **80,** 527 (1958).
16. LIEBERMANN, B., RIST, N., GRUMBACH, F., CALS, S., MAYEUX, M., ROUAIX, A.: Bull. soc. chim. France **1958,** 687.
17. NAKANISHI, K.: Infrared Absorption Spectroscopy. Holden-Day, San Francisco, 1962, p. 38.
18. NAKANISHI, K.: ibid p. 63.
19. HOLLY, S., SOHÁR, P.: Infrared Spectroscopy. Műszaki Kiadó, Budapest, 1968 (In Hungarian).
20. WILSON, E. B.: Phys. Rev. **45,** 706 (1934).
21. NAKANISHI, K.: Infrared Absorption Spectroscopy. Holden-Day, San Francisco, 1962, p. 27.
22. NEMES, A.: Unpublished results.

Pál SOHÁR
András NEMES
Budapest IV., Szabadságharcosok útja 47—49.



Acta Chimica Academiae Scientiarum Hungaricae Tomus 56 (1), pp. 39—45 (1968)

POLYMERIZATION OF VINYLENE CARBONATE

GY. HARDY and K. NYITRAI

(Research Institute for Plastics, Budapest)

Received March 13, 1967

Vinylene carbonate, as an unsaturated cyclic compound and a 1,2-substituted ethylene derivative, may furnish valuable new theoretical information on the relationship between structure and polymerization ability, and its homopolymers and copolymers may possess special characteristics also from the practical point of view. The laws of polymerization of vinylene carbonate have been investigated so far in solvents only [1, 2]. In addition, the copolymerization reactions of the compound with various monomers have been studied [3—6].

Our present work reports on the laws of the liquid-phase bulk polymerization of vinylene carbonate, initiated by azobisisobutyronitrile (AIBN) and by γ-radiation.

Experimental

The synthesis of vinylene carbonate [7, 8] and the purification of the monomer [9] were carried out as described in literature, with the difference that $LiAlH_4$ was used instead of $NaBH_4$.

Freshly distilled vinylene carbonate used in our experiments had the following physical properties: b.p. 73.5 °C/32 torr; m.p. 22 °C; $n_D^{25} = 1.4190$. Polymerization kinetics were measured by dilatometry; the polymer was precipitated from its solution in acetone by the addition of a 1 : 1 mixture of diethyl ether and petroleum ether, and dried to constant weight in a vacuum oven. The molecular weights of the polymers were determined on the basis of a relationship already reported [1], from the viscosities of the solutions in acetone at 25 °C.

The studies of the polymerization initiated by radiation were made in the same way as it has been described [10], using a ^{60}Co γ-source.

Experimental results and their evaluation

Fig. 1 shows the kinetical curves of the polymerization of vinylene carbonate at various temperatures, and for various AIBN concentrations at 70 °C. The overall activation energy of polymerization, calculated from the tempera-

ture dependence of the polymerization rate, was found to be 22.80 kcal/mole. This is in good agreement with the value of 22.20 kcal/mole, measured in acetone solution [1].

Fig. 2 shows the dependence of the polymerization rate, measured at 70 °C, on the square root of the initiator concentration, which was found to be a linear function. The measured data are listed in Table I. It can be seen that

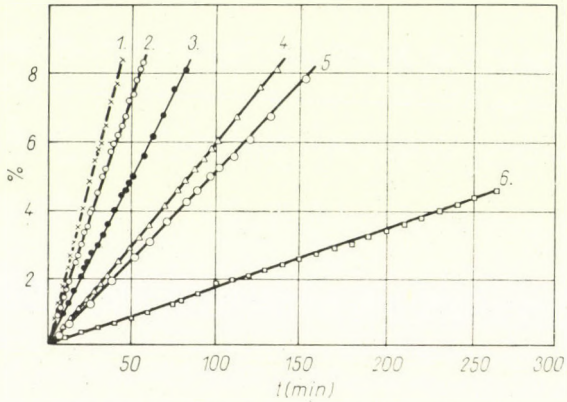

Fig. 1. Kinetical curves of the polymerization of vinylene carbonate at various temperatures and for various initiator concentrations (The numbering of the curves corresponds to the serial numbers in Table I)

Table I

The polymerization of vinylene carbonate initiated by AIBN

No.	Temperature, °C	AIBN concentration, mole/lit.	Monomer concentration, mole/lit.	Polymerization rate, $V \cdot 10^5$ mole/lit. sec.	$\frac{1}{\bar{P}} \cdot 10^3$
1	70	0.149	15.20	42.7	9.47
2	70	0.066	15.20	38.0	9.48
3	70	0.035	15.20	25.3	9.20
4	70	0.016	15.20	15.2	9.48
5	60	0.148	15.35	12.2	7.70
6	50	0.146	15.47	4.5	5.43

the reciprocal of the degree of polymerization of the formed polymers is independent of the initiator concentration, being dependent on the temperature of polymerization only, so that the following relationship [11] is valid:

$$\frac{1}{\bar{P}} = \frac{k_M}{k_p} = C_M$$

where $\bar{P}$ is the average degree of polymerization, k_M and k_p are the reaction rate constants of the chain transfer to the monomer and the chain growth, respectively, and C_M is the so-called constant of chain transfer to the monomer. Therefore, it may be stated that it is the chain transfer process to the monomer molecule which is characteristic of the liquid-phase bulk polymerization of vinylene carbonate. From the temperature dependence of the C_M-values, the

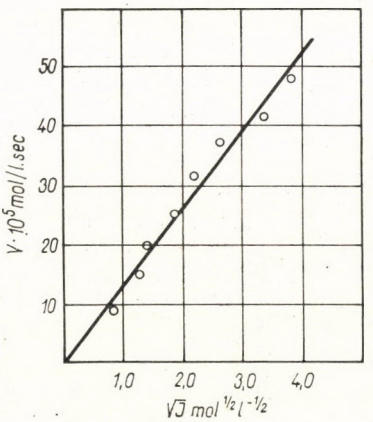

Fig. 2. Dependence of the polymerization rate of vinylene carbonate on the concentration of the initiator at 70 °C

difference in the activation energies of the chain transfer reaction to the monomer and the elementary growth reaction, $E_M - E_p = 5.90$ kcal/mole, can be determined.

Table II

Characteristic data of the polymerization of vinylene carbonate inhibited by Banfield-radicals at 50 °C

No.	AIBN concentration, mole/lit.	Inhibitor concentration, $z_0 \cdot 10^3$, mole/lit.	Inhibition period t_i, sec	Polymerization rate, mole/lit. sec	Rate of initiation, $V_i \cdot 10^7$ mole/lit. sec
7	0.142	0.42	2 880	4.53	1.45
8	0.138	0.82	5 400	4.34	1.51
9	0.140	1.63	10 320	4.66	1.58
10	0.144	2.51	15 300	4.51	1.64
11	0.143	3.40	20 400	4.81	1.66

For a further characterization of the kinetics of polymerization, the rate of initiation was determined with the aid of the so-called BANFIELD radical, which has proved to be helpful for such purposes [10, 12]. Fig. 3 shows the kinetic curves of vinylene carbonate polymerization in the presence of various

concentrations of BANFIELD radicals. In Fig. 4 the magnitude of the inhibition period thus determined is plotted against the concentration of the inhibitor. The data obtained from these measurements are listed in Table II. The average

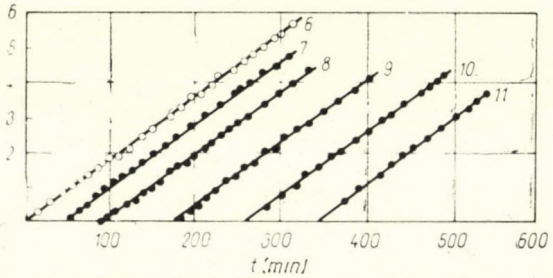

Fig. 3. Effect of the Banfield radical concentration on the polymerization of vinylene carbonate at 50 °C (The numbering of the curves corresponds to the serial numbers in Table II)

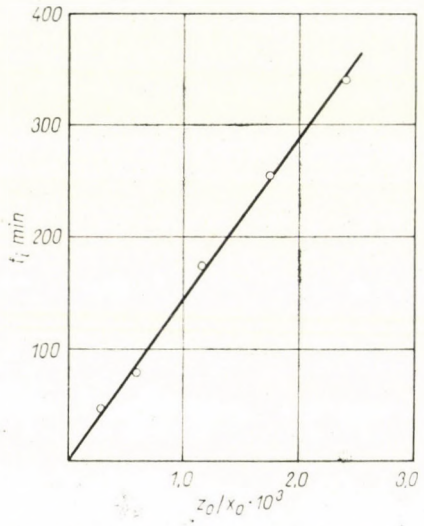

Fig. 4. Dependence of the length of the inhibition period on the concentration of the Banfield radical

value of the rate of the initiation reaction at 50 °C is $1.56 \cdot 10^{-7}$ mole/litre sec. The knowledge of this value permits to determine the value of $\frac{k_p}{k_t^{1/2}}$ at 50 °C, where k_t is the rate constant of the elementary chain termination reaction:

$$\frac{k_p}{k_t^{1/2}} = 0.75 \cdot 10^{-2} \text{ litre}^{1/2} \text{ mole}^{-1/2} \text{ sec}^{-1/2}$$

As it is well known, this value can serve to characterize numerically the activity of the radical formed from the monomer [11]. From this aspect, the above value can be considered very small, being in the same order of magnitude as that for α-methylstyrene [11]. On the other hand, investigations of the copolymerization of vinylene carbonate [3] gave the values $Q = 0.012$ and $e = -0.6$, the order of magnitude of which is similar to the corresponding values of vinyl acetate. The chemical structure of vinylene carbonate and its behaviour in copolymerization substantiate the similarity of this compound

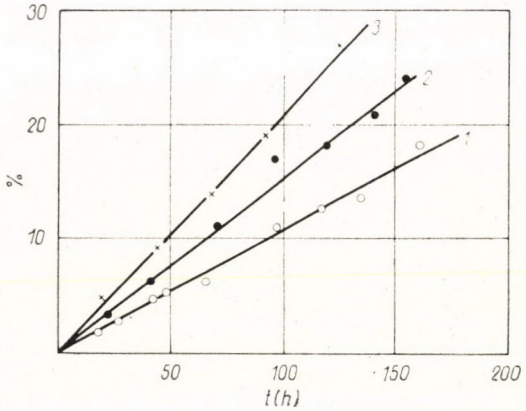

Fig. 5. Kinetic curves of the radiation polymerization of vinylene carbonate at various temperatures (the numbering of the curves corresponds to the serial numbers in Table III)

to vinyl acetate. However, the fact that the value $\frac{k_p}{k_t^{1/2}} = 0.306$, measured for vinyl acetate at 50 °C, is by two orders of magnitude higher [11], seems to be inconsistent with this assumed similarity.

Probably, comparison of vinylene carbonate, a 1,2-substituted ethylene derivative, with vinyl compounds is an unjustified search for analogy, as the value $\frac{k_p}{k_t^{1/2}} = 0.91 \cdot 10^{-2}$, measured at 74.5 °C for the similarly 1,2-substituted maleic anhydride [13], is of the same order of magnitude as that found for vinylene carbonate.

The relatively low reactivity of the monomer molecule is substantiated also by the finding that the radical utilization factor resulting from the above inhibition measurements is $f = 0.29$, *i.e.* a rather low value.

Fig. 5 shows the kinetic curves of the liquid-phase γ-radiation initiated polymerization of vinylene carbonate, irradiated at various temperatures at the same dose rate, and Fig. 6 those obtained at the same temperature, irradiated at various dose rates. In Fig. 7 the rate of radiation polymerization is plotted against the square root of dose rate, giving similarly a linear function.

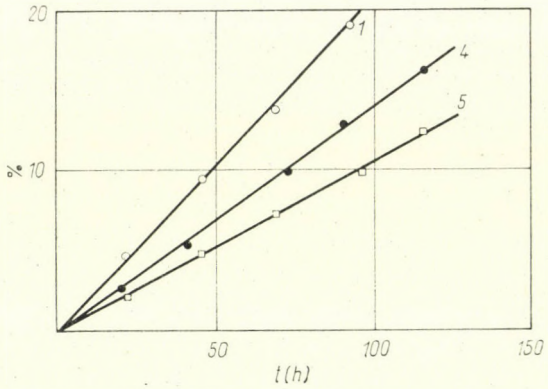

Fig. 6. Kinetic curves of the radiation polymerization of vinylene carbonate at 50 °C at various dose rates (The numbering of the curves corresponds to the serial numbers in Table III)

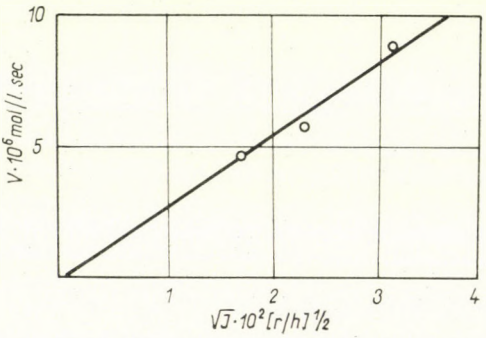

Fig. 7. Dependence of the rate of the radiation polymerization of vinylene carbonate at 50 °C on the dose rate

The conditions of the experiments and characteristic data of the polymers produced are summarized in Table III.

The overall activation energy of the process, calculated from the temperature dependence of the polymerization rate, is $E_p - \frac{1}{2} E_t = 7.40$ kcal/mole. In the knowledge of this value and the data determined earlier, the equation describing the temperature dependence of $\frac{k_p}{k_t^{1/2}}$ can be written as follows:

$$\frac{k_p}{k_t^{1/2}} = 740 \cdot \exp\left(\frac{-7{,}400}{RT}\right)$$

The reciprocal of the degree of polymerization of the formed polymers can be regarded, also in radiation polymerization, as identical with C_M, and a value of $E_M - E_p = 5.10$ kcal/mole is obtained from the temperature dependence. This is in good agreement with the corresponding value given

Table III

Characteristic data of the polymerization of vinylene carbonate initiated by γ-radiation

No.	Temperature, °C	Dose rate, r/h	Monomer concentration, mole/lit.	Polymerization rate, $V \cdot 10^6$ mole/lit. sec	$\frac{1}{\overline{P}} \cdot 10^3$
1	25	93,048	15.94	4.74	5.80
2	35	93,048	15.77	6.56	7.70
3	50	93,048	15.47	11.80	10.70
4	50	52,608	15.47	5.88	10.70
5	50	31,000	15.47	4.42	9.48

earlier, calculated for the process initiated with AIBN. From the data in Table III, the value of G_{init} can be calculated, which is the number of initiating radicals formed by the absorption of an energy of 100 eV. The resulting value, $G_{\text{init}} = 0.16$, is very low, being by an order of magnitude lower than that reported in literature for vinyl acetate [11]. Evidently, this is indicative of the fact that the vinylene carbonate molecule, which contains hydrogen atoms only on the carbon atoms connected by a double bond, is less prone to undergo decomposition by radiolysis.

SUMMARY

The laws of the liquid state polymerization of vinylene carbonate initiated by azobisisobutyronitrile and γ-radiation have been investigated. The chain transfer reaction to the monomer has been found to be characteristic of the process. Values determined by the equation $\frac{k_p}{k^{1/2}} = 740 \cdot \exp\left(\frac{-7{,}400}{RT}\right)$ are different from the corresponding values of vinyl compounds forming reactive radicals, and they are in the same order of magnitude than those of maleic anhydride.

REFERENCES

1. Smets, G., Hayashi, K.: J. Polym. Sci. **29,** 257 (1958).
2. Kazanskaya, V. F., Klimova, O. M.: Zh. Priklad. Khim. **38,** 432 (1965).
3. Hayashi, K., Smets, G.: J. Polym. Sci. **27,** 275 (1958).
4. Judge, J. M., Price, C. C.: J. Polym. Sci. **41,** 435 (1959).
5. Klubikova, L. E., Klimova, O. M., Jarosh, A. V.: Zh. Priklad. Khim. **38,** 1188 (1965).
6. Terteryan, R. A., Zemdin, A. N., Samoilov, S. M., Atakazova, M. H., Monastyrskij, V. N.: Vysokomol. So'ed. **8,** 1721 (1966).
7. Newmann, M. S., Addor, R. W.: J. Am. Chem. Soc. **75,** 1263 (1953).
8. Newmann, M. S., Addor, R. W.: J. Am. Chem. Soc. **77,** 3789 (1955).
9. Field, N. D., Schaefgen, J. R.: J. Polym. Sci. **58,** 533 (1962).
10. Hardy, Gy., Varga, J., Nagy, G., Helcz, A.: Magy. Kém. Foly. **71,** 313 (1965).
11. Bagdasaryan, H. S.: A gyökös polimerizáció elmélete. (The theory of radical polymerization.) (In Hungarian) Akadémiai Kiadó, Budapest 1961.
12. Földes-Berezsnich, T., Tüdős, F.: Magy. Kém. Foly. **70,** 201 (1964).
13. Joshi, R. M.: Makromol. Chem. **53,** 33 (1962).

Gyula Hardy
Károly Nyitrai
Budapest XIV., Hungária krt. 114.

Acta Chimica Academiae Scientiarum Hungaricae Tomus 56 (1), pp. 47—51 (1968)

SYNTHESIS AND REACTIONS OF HETEROCYCLIC ENAMINES, I

THE VILSMEIER ALDEHYDE SYNTHESIS WITH 1-PHENYL-3-METHYL-5-PYRAZOLONE

M. A. KIRA and A. BRUCKNER-WILHELMS

(Department of Organic Chemistry, L. Eötvös University, Budapest)

Received March 18, 1967

Nucleophilic reagents, such as indole [1], pyrrole [2] thiophene [3], *etc.*, are smoothly formylated with phosphorus oxychloride-dimethylformamide (VILSMEIER—HAACK reaction [4]). This method usually gives the respective aldehydes in high yields. SMITH [2] has proposed a mechanism for the formylation of indole in which the eliminated HCl does not take part in the reaction, and has isolated and characterized the intermediate 3-dimethylaminoindolenine. Similar formylations of compounds such as indene, chloro- and bromoacetic acid have been recently described [5].

In accordance with our investigation of reactions of heterocyclic compounds having active methylene groups, we would like to report on the formylation of 1-phenyl-3-methyl-5-pyrazolone (**I**). The latter compound gave with phosphorus oxychloride-dimethylformamide 4-dimethylaminomethylene-1-phenyl-3-methyl-5-pyrazolone (**II**, Scheme A), m.p. 134 °C (perchlorate salt, m.p. 125 °C). The structure assigned to this base is inferred from combustion values, from consideration of its UV and IR absorption spectra, and from its quantitative hydrolysis by boiling aqueous alkali to 4-formyl-1-phenyl-3-methyl-5-pyrazolone (**III**), m.p. 173 °C, a compound which has been previously prepared by an indirect method, namely the alkaline hydrolysis of (1-phenyl-3-methylpyrazole-4-)-(indole-2-)-indigo [6]. The aldehyde **III** showed a broad absorption band in the IR, centered at 2800 cm^{-1}, which indicates its existence in the enolic chelated form.

Acid hydrolysis of the base **II** has now been found to give, in quantitative yield, 4,4'-di-(1-phenyl-3-methyl-5-pyrazolonyl)-methine (**IV**), m.p. 180 °C; found identical with an authentic sample prepared according to the method of KNORR [7].

The mechanism of the formation of **IV** is analogous to that of urorosein hydrochloride [3, 8]. The enamine base **II** is first hydrolyzed to the aldehyde **III**, and the latter condenses with another molecule to give **IV**, according to Scheme B. In accordance with this assumption, the aldehyde **III** has now been found to give compound **IV** on boiling with hydrochlorid acid.

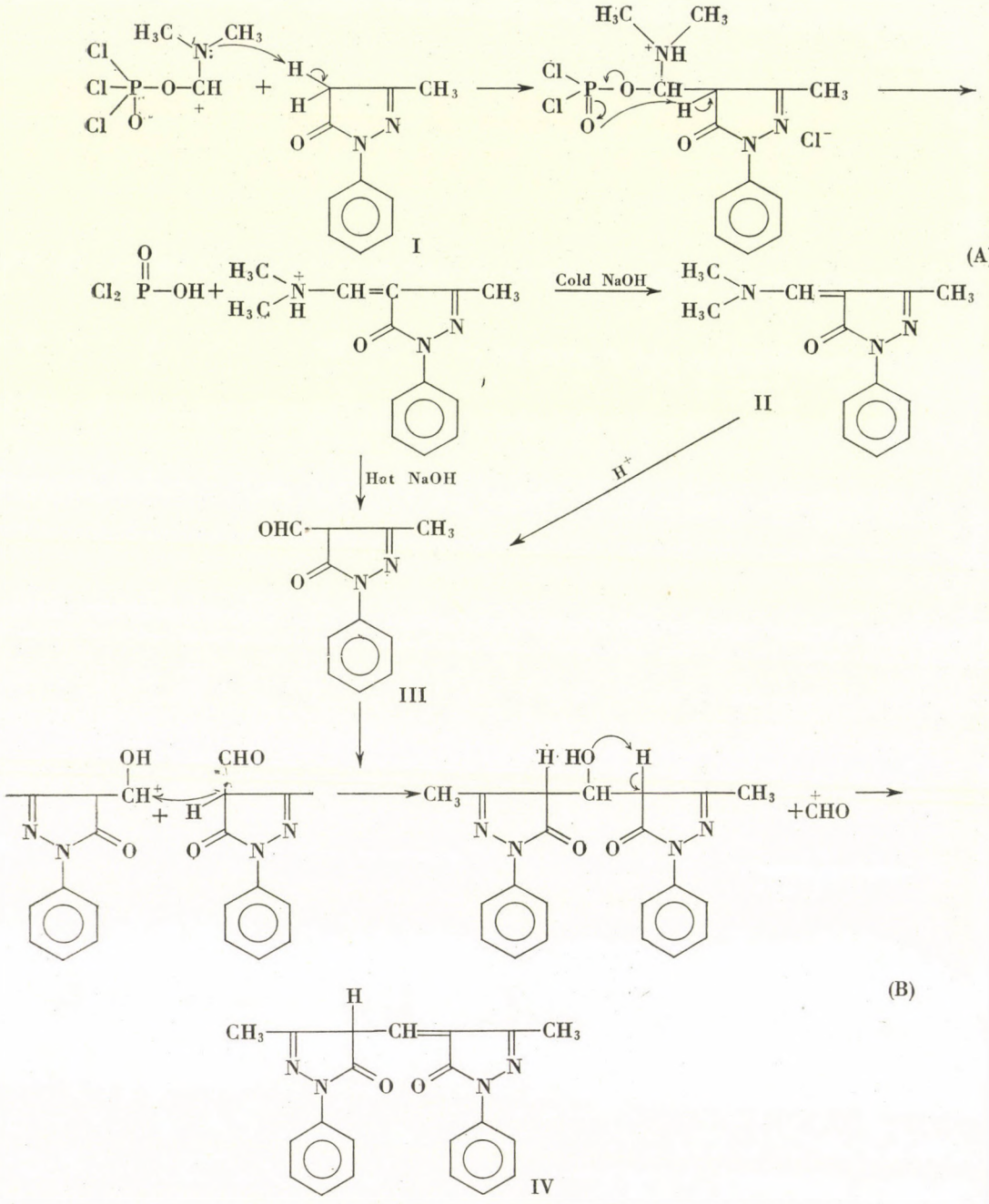
Cold NaOH
Hot NaOH
H+
(A)
(B)
I
II
III
IV

The base **II** is obviously a conjugated enamine. Nucleophilic attack by phenylhydrazine and hydroxylamine hydrochloride in pyridine afforded the phenylhydrazone, m.p. 167 °C [7], and the oxime, m.p. 173 °C, of 4-formyl-1-phenyl-3-methyl-5-pyrazolone, respectively.

The enamine **II** reacted neither with acrylonitrile at 175 °C [9], nor with maleic anhydride at temperatures up to 120 °C; the starting material was recovered in both cases.

The mechanism of the formation of the enamine **II** is apparently similar to the mechanism proposed by SMITH [2] for the formylation of indole (Scheme A); however, since it has now been found that HCl is not evolved in the VILSMEIER aldehyde synthesis either with indole, pyrrole, or with 1-phenyl-3-methyl-5-pyrazolone, it is now obvious that HCl is involved in a salt formation with the amino group (*cf.* Scheme A). In this case the anion PO_2Cl_2 — will then be responsible for the elimination of the second proton, or quaternization of a $N—CH_3$ group, as in the case of the VILSMEIER aldehyde synthesis with N-methylindole [10]. This assumption is favoured by the observation that on the addition of one mole of a strong base, such as triethylamine (in the VILSMEIER aldehyde synthesis with **I**), the enamine **II** was formed under much milder conditions (*cf.* Experimental).

From these considerations, we conclude that in the VILSMEIER aldehyde synthesis with compounds having active methylene groups or with compounds reacting as such, enamines are first formed which are then hydrolyzed to the respective aldehydes [11]. In a similar manner the authors have isolated the respective enamine of pyrrole, namely 2-dimethyl-aminoethylenepyrrolenine* as its perchlorate salt, m.p. 106 °C (λ_{max} 290 mμ), in about 60% yield. Attempted isolation of the free base by careful neutralization of the perchlorate at 0 °C led to the hydrolysis of the enamine with the formation of pyrrole-2-aldehyde in quantitative yield. However, the free base, 2-dimethylaminomethylenepyrrolenine, m.p. 113 °C, λ_{max} 292 mμ, has now been obtained in a yield of 25% by neutralizing an alcoholic solution of the perchlorate salt with triethylamine. The respective picrate salt, m.p. 210 °C, λ_{max} 290 mμ, was directly obtained from the perchlorate salt in about 80% yield.

Experimental**

4-Dimethylaminomethylene-1-phenyl-3-methyl-5-pyrazolone (II)

Phosphorus oxychloride (5.0 ml; 0.055 mole) was added dropwise with stirring to a solution of 8 g (0.11 mole) of dimethylformamide in 30 ml of dry chloroform, the temperature being kept below 10 °C. 1-Phenyl-3-methyl-5-pyrazolone (8.7 g; 0.005 mole) was added slowly

* Dr. G. S. SACH claimed to have isolated from a VILSMEIER aldehyde synthesis with a substituted pyrrole a pyrrolenine which absorbed at 350 mμ both as the free base and its hydrochloride; Tetrahedron 1966, 241, foot-note.

** The reported melting points are uncorrected.

in portions with stirring, the temperature being kept below 20 °C, then heated at 50 °C for 10 min. The yellow reaction solution was cooled in ice and 5g (0.05 mole) of triethylamine was slowly added with stirring. After heating at 45 °C for 2 hrs, the chloroform was evaporated in vacuum, and the viscous oily residue, after cooling, was decomposed with ice (30 g). It was shaken with ether (30 ml) to eliminate traces of chloroform, and the aqueous layer was carefully neutralized with vigorous stirring, by the slow addition of sodium hydroxide (8 g in 80 ml of water), the temperature being kept below —5 °C. The crystalline precipitate was filtered off, washed free from contaminating phosphates with a little cold water, dried in vacuum, and recrystallized from a mixture of methanol–ether (yield 5 g; 45%). It had m. p. 134 °C.

$C_{13}H_{15}N_3O$ (229). Calcd. C 68.11; H 55; N 18.32.
Found C 68.22; H 6.71; N 18.32%.
UV λ_{max} 289 mμ log $\varepsilon = 3.75$ (ethanol).
IR 1670 cm^{-1} (amide-I).

The phenylhydrazone of the aldehyde **III** prepared from the enamine **II** and phenylhydrazine was recrystallized from ethanol, m. p. 167 °C [6].

The oxime of the aldehyde **III** was obtained in almost quantitative yield by heating equimolar amounts of the enamine **II** and hydroxylamine hydrochloride in pyridine for 10 min. on a steam bath. It was recrystallized from methanol, m. p. 173 °C.

$C_{11}H_{11}O_2N_3$ (217). Calcd. N 19.35. Found N 18.89%.

Perchlorate salt of II

The experimental procedure was essentially the same as described above, only dimethylformamide (16 g; 0.22 mole) was substituted for chloroform. After the complete addition of **I**, the reaction solution was heated at 70—80 °C for 4 hrs, cooled and poured onto 30 g of ice. A solution of ice-cold perchloric acid (7.5 ml of 75% $HClO_4$ and 20 ml water) was then added, and the deposited crystalline perchlorate (12 g; 73%) was filtered off, washed with a little cold water, and dried in vacuum. It was recrystallized from methanol to obtain m. p. 125 °C.

$C_{13}H_{16}N_3O_5Cl$ (329.5). Calcd. N 12.76; Cl 10.77.
Found N 12.00; Cl 10.62%.
UV λ_{max} 289 mμ log ε 4.1 (ethanol).

4-Formyl-1-phenyl-3-methyl-5-pyrazolone (III)

(a) One gram of **II** was boiled, with frequent shaking, with 10 ml of 1 *N* NaOH solution until there was no more odour of dimethylamine (about 10 min.). It was neutralized while hot by the addition of 11 ml of HCl, and then cooled in ice. The colourless crystalline precipitate (900 mg; almost quantitative yield) was filtered off, and recrystallized from methanol–water. It shrinked at 158 °C, and melted at 173 °C.*

$C_{11}H_{10}O_2N_2$ (202). Calcd. C 65.33; H 4.96; N 13.87.
Found C 65.64; H 5.12; N 13.73%.

(b) The perchlorate salt of **II** (11 g) was treated as above to give 6.5 g (98%) of 4-formyl-1-phenyl-3-methyl-5-pyrazolone, m. p. 173 °C.

UV λ_{max} 400 mμ, log ε 4.17 (ethanol).
IR broad band centered at 2800 cm^{-1} (chelated OH); 1685 cm^{-1} (amide-I).

4,4′-(1-Phenyl-3-methyl-5-pyrazolonyl)-methine (IV)

A solution of 2.7 g of **II** in 20 ml of 2*N* HCl was heated at steam-bath temperature for 2 hrs. The yellow crystalline precipitate (2.7 g; almost quantitative yield) had m. p. 180 °C, and it gave no depression with a sample prepared according to the method of KNORR [7]. The IR spectra of both samples were found to be identical.

* FRIEDLÄNDER and FELIX reported similar behaviour, *cf.* ref. [6].

2-Dimethylaminomethylenepyrrolenine perchlorate

The experimental procedure was essentially the same as described under the perchlorate salt of **II**. Pyrrole (3.4 g; 0.05 mole) was added dropwise, with stirring; the temperature was kept below 10 °C, then at 35 °C for 1 hr. After cooling, the reaction solution was treated as described under the perchlorate salt of **II**. 2-Dimethylaminomethylenepyrrolenine perchlorate (7 g; 62%), m. p. 106 °C was recrystallized from a mixture of methanol–ether.

$C_7H_{11}N_2O_4Cl$ (222.5). Calcd. N 12.60; Cl 15.97.
Found N 12.0; Cl 15.65%.
UV λ_{max} 290 mμ, log ε 4.2 (ethanol).

2-Dimethylaminoethylenepyrrolenine picrate

To a solution of 2-dimethylaminomethylenepyrrolenine perchlorate (2.2 g; 0.01 mole) in 6 ml of methanol was added a solution of picric acid (2.3 g; 0.01 mole) in 6 ml of the same solvent. The yellow crystalline precipitate (3.5 g; about 80%) was filtered off, and washed with methanol. It was recrystallized from acetone to obtain m. p. 210 °C.

$C_{14}H_{13}N_5O_7$ (363). Calcd. N 19.29. Found N 19.48%.
UV λ_{max} 290 mμ, log ε 4.3 (ethanol).

2-Dimethylaminomethylenepyrrolenine

To a solution of 2-dimethylaminoethylenepyrrolenine perchlorate (2.33 g; 0.01 mole) in 6 ml of abs. methanol was added shaking 1 ml (0.01 mole) of triethylamine, and the solution was kept at room temperature for 15 min. It was triturated with ether (50 ml), and this procedure was repeated several times. Evaporation of the ether in vacuum gave 2-dimethylaminoethylenepyrrolenine (300 mg; 25%). It was recrystallized from benzene, m. p. 113 °C.

$C_7H_{10}N_2$ (122). Calcd. C 68.87; H 8.20; N 22.93.
Found C 69.04; H 8.11; N 22.69%.
UV λ_{max} 292 mμ log ε 4.17 (ethanol).
IR No absorption corresponding to C = N.

SUMMARY

The VILSMEIER aldehyde synthesis with 1-phenyl-3-methyl-5-pyrazolone (**I**) gave 4-dimethylaminomethylene-1-phenyl- 3-methyl-5-pyrazolone (**II**) which was hydrolyzed by aqueous alkali to the 4-formyl derivative **III**. Acid hydrolysis of **II** gave 4,4'-di-(1-phenyl-3--methyl-5-pyrazonyl)-methine.

Similarly, pyrrole gave 2-dimethylaminomethylenepyrrolenine. The mechanism of the VILSMEIER aldehyde synthesis is discussed.

REFERENCES

1. TYSON, F. T., SHAW, J. T.: J. Am. Chem. Soc. **74,** 2273 (1952).
2. SMITH, G. F.: J. Chem. Soc. **1954,** 3842.
3. BUU-HÖI, N. P.: J. Chem. Soc. **1950,** 2130.
4. VILSMEIER, A., HAACK, A.: Chem. Ber. **60,** 119 (1927).
5. ARNOLD, Z.: Collections Czech. Chem. Communs. **30,** 2783 (1965); ibid. **30,** 2125 (1965).
6. FRIEDLÄNDER, P., FELIX, A.: Monatsh. **31,** 72 (1910).
7. KNORR, L.: Ann. **238,** 156 (1887).
8. HARLEY-MASON, J., BU'LOCK, J. D.: Biochem. J. **51,** 430 (1952).
9. STORK, G.: J. Am. Chem. Soc. **78,** 5128 (1956).
10. ANTONY, W. C.: J. Org. Chem. **25,** 2049 (1960).
11. EIDEN, F.: Arch. Pharm. **296,** 104 (1963).

Mohamed A. KIRA
Adrienne BRUCKNER-WILHELMS } Budapest VIII., Múzeum krt. 4/b.

Acta Chimica Academiae Scientiarum Hungaricae Tomus 56 (1), pp. 53—60 (1968)

INVESTIGATION OF THE HYDROLYSIS PRODUCTS OF DESERTOMYCIN

R. Bognár, F. Sztaricskai, L. Somogyi, M. Puskás and S. Makleit

(Research Group for Antibiotics Chemistry, Hungarian Academy of Sciences and Institute for Organic Chemistry, L. Kossuth University, Debrecen)

Received June 15, 1967

It is known from several earlier communications that *Streptomyces flavofungini* [2, 3], a strain of *Streptomyces* isolated by Uri [1] in 1957 from a desert sand originating from the Sahara, produces two antibiotics: flavofungin of antifungal effect [4] and desertomycin, a broad-spectrum antibiotic agent.

In 1958, Uri, Bognár, Békési and Varga [5] described the isolation and the properties of crystalline desertomycin in a preliminary communication. Biological tests showed the *in vitro* antibacterial and antifungal activity of desertomycin, and also revealed a cytostatic activity. It is regrettable that the *in vivo* toxicity of this antibiotic agent proved to be very high. Of later biological investigations [6, 7, 8], the results of Uri and Herpay should be mentioned. These authors have found that desertomycin is a useful tool in differential diagnosis, because it inhibits the multiplication of saprophyte and phytopathogenic fungi at concentrations essentially lower than those which impede the multiplication of fungi infectious to man [8, 9].

Our investigations aimed at elucidating the structure of desertomycin and flavofungin have shown that these two antibiotics produced beside each other, have entirely different chemical structures. Flavofungin which has the lower molecular weight, belongs to the group of polyene polyhydroxy macrolides containing no nitrogen or carbohydrate in its molecule [10, 11]. Desertomycin, in turn, contains both carbohydrate and nitrogen; it has medium molecular weight and amphoteric character, with slightly basic properties.

In 1963, Sztaricskai and Uri [12] reported further work concerning the chemical reactions, hydrolysis, detection and determination of desertomycin.

In the present communication, the results of our recent physical and chemical investigations of desertomycin are reported.

For the purification and recrystallization of desertomycin, *n*-butanol saturated with water and containing 10 to 30% of methanol was found to be the best suitable.

Colour reactions

Desertomycin gives positive EHRLICH, MOLISCH and MALAPRADE tests. A solution in acetone produces with concentrated hydrochloric acid an orange-red colour which, in contrast to erythromycin and carbomycin, cannot be extracted with chloroform.

Vanillin added to a solution of desertomycin in concentrated hydrochloric acid produces a violet colour which becomes dark blue on standing.

In the SAKAGUCHI, PAULY, biuret, MORGAN-ELSON and maltol tests, further in the iron(III) chloride test, desertomycin gives negative reactions.

Hydrolysis of desertomycin

In preliminary tests the acid hydrolysis of desertomycin afforded an amorphous aglycone and a product of the nature of a carbohydrate.

Aglycone

When desertomycin is hydrolyzed with five parts of 1.0 *N* hydrochloric acid at 100 °C for 30—60 minutes, the hydrochloride of "aglycone" separates from the cooled mixture as an amorphous gum. It is, however, dissolved again if some water is added. If the aqueous solution is made slightly alkaline (pH 7.5—8.0), the free aglycone base is precipitated as a light yellow amorphous powder.

No nitrogenous hydrolysis products were detected in the aqueous acid hydrolysate containing the carbohydrate component, whose investigation will be described below. Therefore the nitrogenous structural elements of desertomycin must be contained by the carbohydrate-free "aglycone" of basic character, and desoxyamino sugars cannot be present among the sugar components of desertomycin.

On subjecting the amorphous aglycone to vigorous hydrolysis (6.0 *N* hydrochloric acid, 100 °C, 23 hours), a hydrolysate showing positive ninhydrin reaction is obtained. The gum left behind after the clarification and concentration of the hydrolysate gives a white, crystalline product on treatment with concentrated hydrochloric acid. This, on the evidence of the analytical data, melting point, infrared spectrum and thin-layer chromatogram, has been shown to be identical with the hydrochloride of glutamic acid.

The quantity of glutamic acid in the hydrolysate of desertomycin obtained with 6.0 *N* HCl was determined by quantitative paper chromatography (see Experimental). As a mean value of our measurements, desertomycin contains 3.86% of glutamic acid, corresponding nearly to one molecule of glutamic acid per molecule of the antibiotic. Consequently, the minimum molecular weight of desertomycin should be about 3840.

When a solution of desertomycin in a mixture of water and ethanol (1 : 1) is treated with 2,4-dinitrofluorobenzene in the presence of triethylamine, an amorphous dinitrophenyl derivative is obtained which can be readily purified by recovering recrystallization from its *n*-butanol solution containing 30% of methanol. According to the analytical data, one dinitrophenyl group is linked to the molecule.

Since the hydrolysate of dinitrophenyl-desertomycin obtained with 1.0 *N* hydrochloric acid did not contain any nitrogenous decomposition products and yielded the same results as the original unsubstituted desertomycin, it can be taken for granted that dinitrophenylation had occurred in the aglycone moiety of the desertomycin molecule. This is also confirmed by the experiments in which glutamic acid was found in the hydrolysate obtained by the vigorous hydrolysis of desertomycin that had been deaminated by nitrous acid.

Hydrolysate

The hydrolysate of desertomycin obtained with 1.0 *N* hydrochloric acid (at 100 °C, for 30 minutes, in a sealed ampoule) has been investigated by paper chromatography in several solvent systems under the conditions described in Experimental. The hydrolysate was found to contain only one monosaccharide, an aldohexose. Comparison with a number of known sugars has shown that the sugar component of desertomycin is D-mannose. According to quantitative determinations carried out by spot weight measurements [13] and by extinction measurements after elution of the detected spot [14], about 5.2 to 5.6% of mannose can be split off the molecule of desertomycin by hydrolysis. Accordingly, the calculated minimum molecular weight of desertomycin is about 3200—3500.

The results of the paper chromatographic investigations were unequivocally confirmed also by preparative experiments. The hydrolysate separated from the aglycone was treated in the usual manner with phenylhydrazine to obtain a yellow, crystalline osazone. Elemental analysis, melting point, ultraviolet and infrared spectra showed this compound to be D-glucose phenylosazone which, however, could have formed, besides from D-glucose and D-mannose, also from D-fructose, glucosamine, 2-O-methylglucose or 2-O-methylmannose. The positive rotatory power and negative FOULGER reaction [15] of the hydrolysate exclude the presence of fructose, the negative MORGAN—ELSON reaction that of glucosamine, while the absence of methoxy groups in the original antibiotic excludes the presence of 2-O-methylhexoses. The presence of D-mannose was unequivocally confirmed by treating the hydrolysate at room temperature with phenylhydrazine. The product had the same melting point, elemental analysis, infrared spectrum and other reactions as an authentic sample of crystalline mannose phenylhydrazone.

The presence of mannose has been detected so far only in few antibiotics, and even in those mannose occurred together with other simple sugars. To our knowledge, desertomycin is the first known antibiotic which contains in its molecule D-mannose as the sole carbohydrate component.

Experimental

Recrystallization of desertomycin

16.8 g of crude, amorphous desertomycin of high activity, obtained in a previous isolation from flavofungin-free mycelium, was dissolved in 1700 ml of hot *n*-butanol saturated with water and containing 30% of methanol. A small amount of insoluble material was removed

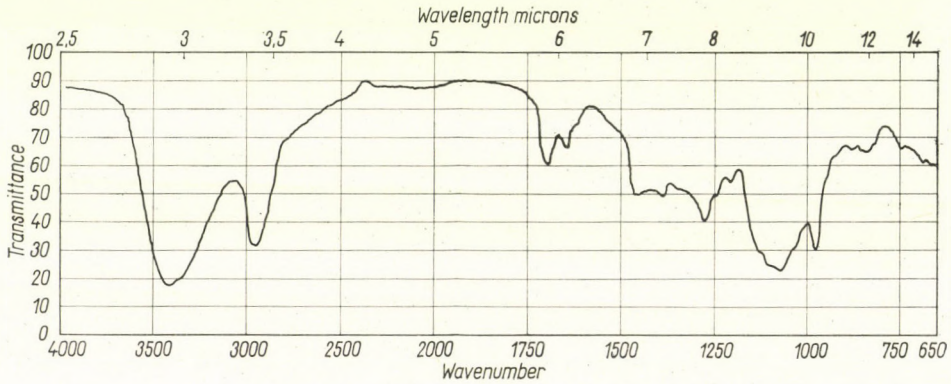

Fig. 1. Infrared spectrum (KBr) of crystalline desertomycin

by filtration, and the filtrate clarified with active carbon. Slow cooling gave 11.80 g of crystalline desertomycin. Products of higher purity may be crystallized from a butanolic solution containing 10% of methanol only.

Pure desertomycin prepared by repeated recrystallizations had m. p. 189—190 °C (d.); $[\alpha]^{20}$ —28.5°(c = 1.0, in pyridine). The infrared spectrum of desertomycin is shown in Fig. 1.

Found: C 56.58; 56.56; H 8.44; 8.45; N 2.40; 2.35%.

Hydrolysis of desertomycin

(a) *Preparation of desertomycin "aglycone"*

1.0 g of crystalline desertomycin (m. p 189—190 °C; d.) was heated with 5.2 mlof 1.0 *N* HCl for 30 min at 100 °C. The aqueous acid phase was separated from the dark greenish-brown amorphous aglycone which was dissolved in water (5.0 ml). The pH of the solution was adjusted with $NaHCO_3$ to 7.5—8.0. A light yellow, amorphous powder precipitated which was dried in a vacuum desiccator (0.53 g). This product was soluble in dilute mineral acids, glacial acetic acid, methanol, pyridine, and in dimethylformamide, being insoluble in acetone, benzene, chloroform and in ethyl acetate.

Found: C 66.40; 66.68; H 9.32; 9.43; N 1.90; 1.85%.

(b) *Isolation of glutamic acid*

300 mg of crystalline desertomycin (m. p. 189—190 °C; d) was heated for 23 hrs in a sealed ampoule with 3.0 ml of 6.0 *N* HCl. The light brown solution was separated from the precipitated dark, amorphous, sticky product, clarified, and evaporated to dryness at room temperature in a vacuum desiccator. Addition of a few drops of conc. HCl to the light yellow gum-like

residue resulted in the separation of white crystals. Recrystallization from 6.0 *N* HCl afforded 3.5 mg of a crystalline substance, m. p. 200 °C (d.) (lit. m. p. of glutamic acid hydrochloride 202—204 °C). The infrared spectrum was identical with that of authentic glutamic acid hydrochloride.

$C_5H_9O_4N \cdot HCl$ (183.60). Calcd. N 7.62. Found N 7.76%.

When the compound obtained as described above was allowed to run on a thin-layer of *Kieselgel G–Cellulose 300 MN* (4 : 10) in a solvent mixture of sec.-butanol–formic acid–water (75 : 13.5 : 11.5), and detected with ninhydrin (10 minutes at 105 °C), an R_f value identical with that of glutamic acid was observed.

(c) *Quantitative determination of glutamic acid by paper chromatography*

0.02—0.03 ml of the hydrolysate of desertomycin obtained as described under (b) was applied on *Schleicher-Schüll 2043 b Mgl* paper, and chromatographed by the descending technique at 20 ± 2 °C, in a solvent mixture of sec.-butanol–formic acid–water (75 : 15 : 10). The developed, dry chromatograms were pulled through a 0.25% acetone solution of ninhydrin, developed for 15 min. at 60 °C, and the colours of the spots were stabilized by treatment with an ethanolic solution of copper(II) nitrate. The individual spots of the chromatograms detected in this way, and blank controls of the corresponding spotless parts were cut out, disintegrated, and extracted for 2 hrs with two consecutive 2-ml portions of 96% ethanol. After rinsing with ethanol, the filtrate was filled up to 5 ml. The extinctions of the solutions were measured at 515 mμ with a *Unicam SP 800* spectrophotometer. The quantity of amino acid in the hydrolysates was then established by means of a calibration curve constructed using pure authentic glutamic acid and proceeding exactly as described above.

A glutamic acid content of 3.86% was found, the error limit of the determination being ±5%.

Deamination and hydrolysis of desertomycin in 6.0 N hydrochloric acid

21.5 mg of desertomycin was dissolved in 1.0 ml of a 1 : 1 mixture of acetic acid and water; 60 mg of sodium nitrite was added in small portions, and the mixture allowed to stand for 24 hrs at room temperature. Excess nitrous acid was decomposed by adding a few crystals of urea, and the solution was evaporated to dryness. The residue was dissolved in 0.5 ml of 6.0 *N* HCl and subjected to hydrolysis in a sealed ampoule for 24 hrs at 105 °C. The hydrolysate was again evaporated to dryness as above, the residue dissolved in water, chromatographed on a thin-layer of *Kieselgel-G* and *Cellulose 300 MN* (4 : 10) in the way described for the isolation of glutamic acid, and glutamic acid was identified in the hydrolysate.

Dinitrophenyl (DNP)-desertomycin

100 mg of desertomycin was dissolved in 4 ml of a 1 : 1 mixture of ethanol and water containing one drop of triethylamine. To this solution 33.9 mg of 2,4-dinitrofluorobenzene in 1 ml of 10% ethanol was added, and the mixture allowed to stand for 1 hr. under cooling in ice. Meanwhile, the pH of the solution was continuously adjusted to 8.0 with triethylamine. The precipitated DNP-desertomycin was filtered off, washed with ice-cool water and with anhydrous ethanol, then dried in a vacuum desiccator at room temperature (91.0 mg). A 50-mg sample was purified by dissolving it in 3 ml of hot *n*-butanol containing 30% of methanol; cooling afforded 25 mg of the product, m. p. 159—160 °C.

Found: C 57.44; 57.49; H 7.93; 7.91; N 3.16; 3.21%.

UV spectrum: λ_{max} 254; 347 mμ (ethanol).

Paper chromatography of the sugar component of desertomycin

In parallel experiments, 10.5, 10.3 10.4 and 9.5 mg samples of crystalline desertomycin (m. p. 189—190 °C; d.) were hydrolyzed with 0.5 ml of 1.0 *N* HCl in a sealed ampoule at 100 °C for periods of 0.5 to 2.0 hrs. In one experiment, after cooling, the ampoule was opened and 0.5 ml of methanol was added to dissolve the precipitated sticky aglycone, too. For the sake of comparison, the hydrolysate was subjected to chromatography in the presence of various simple sugars, employing the descending, once extended technique, on *Schleicher-Schüll 2043 b Mgl* paper, at 21 ±1 °C, in the following solvent mixtures:

I: *n*-butanol–pyridine–water (6 : 4 : 3) [16]
II: *n*-butanol–acetic acid–water (4 : 1 : 5) [17]
III: ethyl acetate–acetic acid–water (44 : 20 : 10) [18]

Detection with aniline hydrogen phthalate (at 105 °C, for 10 minutes) [19] gave a colouring indicating the presence of aldohexoses. In the solvent mixtures I, II and III, the R_M values shown in Table I were obtained.

Table I

R_M values of the sugar component in the hydrolysate of desertomycin and of some simple sugars in different solvent mixtures

Sample	R_M value		
	I	II	III
Hydrolysate of desertomycin	1.00	0.99	1.01
Galactose	0.82	0.80	0.68
Glucose	0.91	0.90	0.82
Mannose	1.00	1.00	1.00
Fructose	1.04	0.95	1.13
Sorbose	0.95	0.97	1.07
Arabinose	1.15	1.03	1.22
Rhamnose	1.81	1.71	1.83
2-O-Methylglucose			1.87

It can be seen that the R_M values of the hydrolysate unequivocally agree with those of mannose.

For the quantitative determination of mannose, aliquots of the hydrolysate were subjected to chromatography in solvent mixture III, in the presence of 5, 10, 15, 20, 25 and 30 μg of mannose. The quantitative determinations were carried out as follows.

(a) *Measuring the weight of spots*

The chromatograms were dried in air and treated with aniline hydrogen phthalate; the spots were marked in ultraviolet light, cut out and weighed. The weights of standard spots were plotted against the logarithms of the known amounts of mannose. With the aid of the calibration curve obtained in this way the mannose content of the hydrolysate could be read from the measured weights of the spots. The following values were found: 6.25 $\pm$0.94; 5.6 $\pm$0.84; 5.2 $\pm$0.78 μg ($\pm$15—20%).

(b) *Elution method*

The chromatogram was dried in air and pulled through aniline hydrogen phthalate reagent; excess reagent was removed by pressing the chromatogram between two sheets of filter paper. Portions of identical areas were cut from the parts containing the spots and of the empty parts of the paper chromatograms. These were cut to small pieces and separately extracted in a closed container by soaking in 4 ml of glacial acetic acid for 18 hrs, filtered, washed with glacial acetic acid and the filtrate diluted to 5 ml. The extinctions of the solutions were measured with a *Beckman DU* spectrophotometer at 380 mμ. A calibration curve was constructed by plotting the extinction values of the eluates from known amounts of mannose against the logarithms of the quantities. The mannose content of the hydrolysate was determined with the aid of this curve, on the basis of the measured extinction values.

In this way a mannose content of 5.42 $\pm$0.27 μg ($\pm$5%) was found.

Precipitation of D-*mannose as phenylosazone*

(a) 1.00 g of crystalline desertomycin (m.p. 189—190 °C; d.) was heated with 5.2 ml of 1.0 *N* HCl for 30 min. on a steam bath. After cooling, the precipitated amorphous aglycone was separated, washed with 1 ml of water, and 0.83 g (6 millimoles) of crystalline sodium acetate was added to the combined aqueous hydrolysate. The cold mixture was clarified, filtered

and diluted with water to 7 ml (in a 10 cm tube, this dilution gave $\alpha = +0.23°$). One ml of phenylhydrazine and 1.0 ml of glacial acetic acid were added, and the mixture was heated for 2 hrs on a water bath. The yellow crystals were filtered off, washed with some ether, then with acetone, and dried in a vacuum desiccator, to obtain 65.0 mg, m. p. 208—209 °C (d.). Recrystallization from 50% ethanol, combined with clarification, did not change the m.p. Lit. m.p. of D-mannose phenylosazone: 209 °C (d.). The ultraviolet spectrum (in anhydrous ethanol) and the infrared spectrum were completely identical with those of authentic D-mannose phenylosazone.

$C_{18}H_{22}N_4O_4$ (358.4). Calcd. C 60.32; H 6.20; N 15.63. Found C 61.56; H 6.05; N 15.68%.

(b) 120 mg of DNP-desertomycin was hydrolyzed with 2.0 ml of 1.0 *N* HCl according to (a). The hydrolysate was separated from the DNP-aglycone, and heated on a water bath for 160 min. with a mixture of 0.408 g of cryst. sodium acetate, 0.10 ml of phenylhydrazine, and 0.10 ml of glacial acetic acid to obtain 5.3 mg of D-mannose phenylosazone, m.p. 211—213 °C (d.).

Isolation of D-*mannose as phenylhydrazone*

To the hydrochloric acid hydrolysate of 0.800 g desertomycin, 0.60 g of cryst. sodium acetate was added, the solution clarified, filtered at room temperature, and treated with 0.20 ml of phenylhydrazine. After about 30 min. crystals began to precipitate from the reaction mixture, which was allowed to stand overnight in a dark place. The crystals were washed with water and with ethyl acetate, and dried in a vacuum desiccator to obtain 80.0 mg (119—128%) of the product, m.p. 186.5 °C. It was treated with decolourizing carbon and recrystallized from 7 ml of hot water containing some isopropanol, to yield 40.0 mg (60 to 64%), m.p. 194—195 °C (lit. m.p. of D-mannosephenylhydrazone: 195—200 °C). The infrared spectrum was identical with that of authentic D-mannosephenylhydrazone.

$C_{12}H_{18}O_5N_2$ (270.28). Calcd. N 10.37. Found N 10.57%.

(Treatment of the mother liquor of the crude mannosephenylhydrazone with 0.8 ml of phenylhydrazine and 0.8 ml of glacial acetic acid on a water bath did not give any osazone, indicating that the precipitation of mannosephenylhydrazone had been practically complete.)

The authors' thanks are expressed to the *Hungarian Academy of Sciences* and to the *Pharmaceutical Works Biogal* for financial support of this work, and to the Analytical Laboratory of the *Institute of Organic Chemistry of the L. Kossuth University*, for the spectral- and microanalyses.

SUMMARY

Desertomycin can be purified by recrystallization from *n*-butanol saturated with water containing 10 to 30% of methanol. Mild acidic hydrolysis of the antibiotic affords an amorphous aglycone of basic character and a carbohydrate component. By means of paper chromatography and preparative methods, this latter was proved to be D-mannose. An amino acid identified as glutamic acid was isolated from the hydrolysate of the aglycone obtained with strong acid. As shown by quantitative paper chromatographic determinations, desertomycin contains 1 mole of D-mannose and 1 mole of glutamic acid. The reaction of desertomycin with 2,4-dinitrofluorobenzene gives DNP-desertomycin.

On the basis of the identified structural components, conclusions have been drawn concerning the size and structure of the desertomycin molecule. Desertomycin is the first known antibiotic which contains D-mannose as the sole carbohydrate component.

REFERENCES

1. URI, J.: Pharmazie **12,** 194 (1957).
2. URI, J., SÁRDY, L., BÉKÉSI, I.: Hung. Pat. 146, 496 (Oct. 3, 1957).
3. SZABÓ, G., PREOBRAZHENSKAYA, T. P.: Antibiotiki **7,** 312 (1962).
4. URI, J., BÉKÉSI, I.: Nature **181,** 908 (1958).
5. URI, J., BOGNÁR, R., BÉKÉSI, I., VARGA, B.: Nature **182,** 401 (1958).
6. URI, J.: Nature **183,** 1188 (1959).
7. VÁLYI-NAGY, T., HERNÁDY, F., SZABÓ, G., JENEY, A.: Antib., Chemo. **11,** 238 (1960).
8. URI, J., HERPAY, ZS.: Nature **191,** 1015 (1961). Mykosan **4,** 128 (1961).
9. FERENCZY, L., ZSOLT, J., URI, J.: Acta Microbiol. Hung. **9,** 183 (1962).

10. BOGNÁR, R.: Chemistry of the flavofungin. Antibiotica congressus cum participatione internationali, 136. (Praha 1964)
11. BOGNÁR, R., FARKAS, I., MAKLEIT, S., RÁKOSI, M., SOLTÉSZ, J., SOMOGYI, L., ZSUPÁN, K.: Antibiotiki **10,** 1059 (1965).
12. SZTARICSKAI, F., URI, J.: Microchimica Acta, Heft 3, 431 (1963); Magy. Kém. Foly. **9,** 484 (1963).
13. BEERSTRECHER, E.: Anal. Chem. **22,** 1200 (1950).
14. BLASS, J., MACHEBOEUF, M., NUNEZ, G.: Bull. Soc. Chim. Biol. **32,** 130 (1950).
15. FOULGER, J. H.: J. Biol. Chem. **99,** 207 (1932); FLARON, W. R., DRUM, J. A.: Analyst. **75,** 56 (1950).
16. LOCK, M. V., ROCHARDS, G. N.: J. Chem. Soc. **1955,** 3024.
17. PATRIDGE, S. M.: Biochemical J. **42,** 238 (1948).
18. PHILIP, J. E., SHENCK, J. R. *et al.*: Antimicrob. Agents. Ann. 10 (1960).
19. PATRIDGE, S. M.: Nature **164,** 443 (1949).

Rezső BOGNÁR
Ferenc SZTARICSKAI
László SOMOGYI
Mária PUSKÁS
Sándor MAKLEIT

Debrecen, 10.

Acta Chimica Academiae Scientiarum Hungaricae Tomus 56 (1), pp. 61—66 (1968)

INVESTIGATIONS IN THE FIELD OF RADIATION-INDUCED SOLID STATE POLYMERIZATION, XXII

POST-POLYMERIZATION OF VINYLENE CARBONATE

GY. HARDY, K. NYITRAI, G. NAGY, (Mrs.) J. ERŐ, and M. KISBÉNYI

(Research Institute for the Plastics, and Department of Plastics and Rubber Technology, Polytechnical University, Budapest)

Received July 3, 1967

It is generally characteristic of the solid state polymerization of saturated cycles that such compounds polymerize within the lattice; the cycles are positioned in the crystal lattice so that when they open up, the contiguous monomer molecules will be linked to each other, without leaving the lattice, to give a polymeric chain. In a former communication [1] we have pointed out that, from the point of view of a study of polymerization processes in the solid state, unsaturated cycles may represent an interesting group of compounds. With unsaturated cyclic compounds there are two possibilities of polymer formation, by the cleavage of the cycles, or by the reactions of the double bonds.

Following our former studies on norbornene derivatives [1, 2], this paper deals with the radiation-induced solid state polymerization of vinylene carbonate. Vinylene carbonate is an unsaturated cyclic compound, a 1,2-disubstituted ethylene derivative.

Experimental

Vinylene carbonate was prepared as described in a former communication [3]; the m.p. of the monomer used was 22 °C. The method of investigation of the polymerization process was the same as discussed previously [4]. After the termination of the post-polymerization, the system was dissolved in acetone that contained 1% benzoquinone. The polymer was precipitated by the addition of a 1 : 1 mixture of diethyl ether and petroleum ether, filtered off, and dried to constant weight under reduced pressure. The molecular weights of the polymers were determined by viscosimetry at 25 °C of their solutions in acetone, and using the equation described earlier [5]. Electron spin resonance studies were carried out with a *J. E. O. L. Spectrometer J. E. S. 3BX*, of the *Central Institute of Physics of the Hungarian Academy of Sciences.*

Results and discussion

First we wanted to study the nature and concentration of the active centres formed in vinylene carbonate under irradiation. Fig. 1 shows the ESR spectrum recorded at —120 °C of a vinylene carbonate sample irradiated at —78 °C with a

total dose of 7.33 Mrad. This spectrum affords little practical information about the primary irradiation products; this may be explained by the diversity of these products and the polycrystalline structure of the irradiated sample. Under the experimental conditions described, the polymerization did not begin yet. However, in a system irradiated as before at −78 °C and then kept at 0 °C for 12 minutes, polymerization did occur. This system was cooled again to −120 °C and the ESR spectrum recorded (Fig. 2). This is an unequivocal triplet

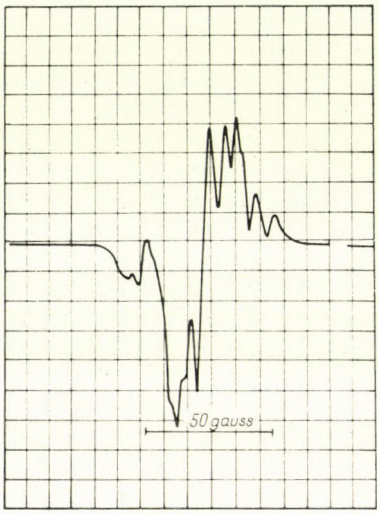

Fig. 1. ESR spectrum, recorded at −120 °C, of vinylene carbonate irradiated with an overall dose of 7.33 Mrad at −78 °C

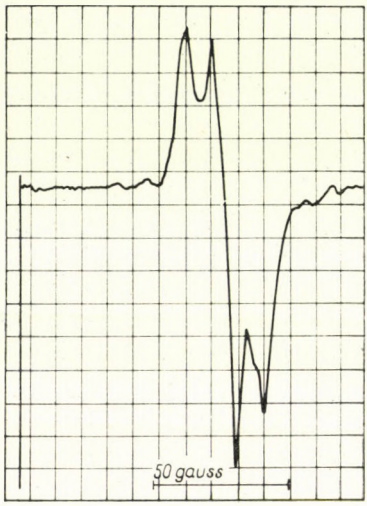

Fig. 2. ESR spectrum of vinylene carbonate irradiated with an overall dose of 7.33 Mrad at −78 °C, then warmed to 0 °C for 12 minutes, and cooled again to −120 °C

spectrum, similar to those observed with other monomers that polymerize according to free radical mechanism in the solid state [6].

Fig. 3 shows the concentration of radicals in vinylene carbonate samples irradiated with the same overall dose, but at different temperatures and various dose rates. Within the interval of the rates studied, the concentration of the radicals formed was independent of the dose rate, and the concentration of radicals was higher at lower temperatures. Fig. 4 represents the change of the concentration of radicals in vinylene carbonate samples irradiated at −78 °C and then warmed to various temperatures. It is to be seen that the limit concentration of radicals decreases steadily with increasing temperatures. Similar findings have been reported for other monomers; obviously the steadily growing mobility due to the higher temperatures, and greater possibilities for the recombination of the frozen radicals in the solid state are responsible for this phenomenon.

Valuable information about the reactions of the primary irradiation products is furnished by an investigation of their further polymerization. Fig. 5 presents kinetic curves of the post-polymerization at 0 °C of vinylene car-

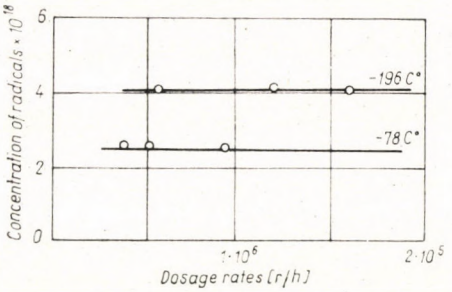

Fig. 3. Concentrations of radicals generated in vinylene carbonate samples irradiated at different dose rates with an overall dose of 5 Mrad, at —78 °C and —196 °C

bonate samples that had been irradiated at —78 °C with different overall doses. It is seen that with increasing overall doses, the velocity and the limit conversion of the post-polymerization grow monotonously, to reach finally a maxi-

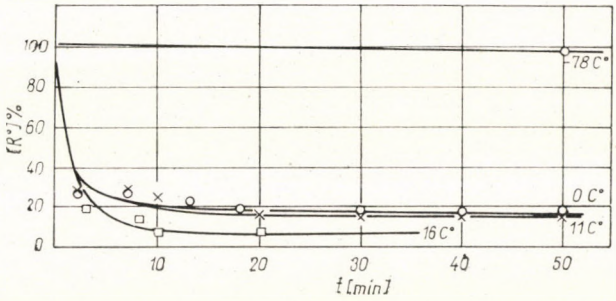

Fig. 4. Concentration of radicals in vinylene carbonate irradiated with an overall dose of 7.9 Mrad at —78 °C, *vs.* time, when heated to different temperatures

mum value somewhat above 5% conversion, under the conditions of our experiments. This shows that with higher overall doses the number of active centres responsible for the initiation of the polymerization is increased, and, in consequence, also the velocity of subsequent polymerization becomes higher. The number of active centres, and mobility restricted by the crystal lattice, allow a conversion only a little higher than 5%. Fig. 6 shows the kinetic curves of the post-polymerization of vinylene carbonate irradiated at —78 °C with an overall dose of 7.9 Mrad, and subsequently warmed to various temperatures. The limit conversion decreases when the temperature of the polymerization is higher. Fig. 7 shows the limit conversion of the post-polymerization as a func-

tion of the temperature: the linear inverse relation is clearly perceivable. This is at variance with the temperature function observed in the cases of monomers polymerized outside a crystal lattice [7], but is in good agreement with the dependence on temperature of the polymerization of trioxane, taking place

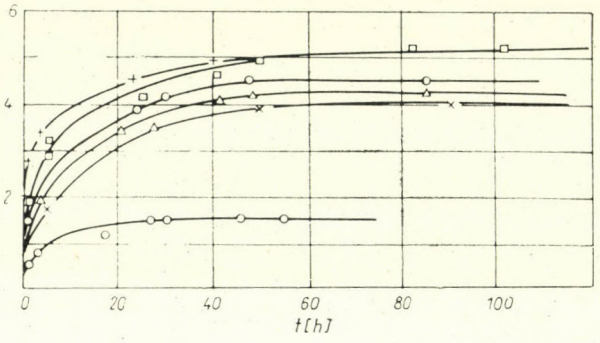

Fig. 5. Kinetic curves of the post-polymerization at 0 °C of vinylene carbonate samples irradiated with various doses at —78 °C. From the bottom upward: 0.9 Mrad; × 3.65 Mrad; △ 4.7 Mrad; ○ 5.22 Mrad; □ 7.9 Mrad; + 11.8 Mrad

within a lattice structure [8], where the limit conversion values of the post-polymerization are rapidly decreasing from a temperature of about 10 °C below the melting point. Thus it may be stated that under the conditions of our experiments vinylene carbonate behaves like monomers that polymerize

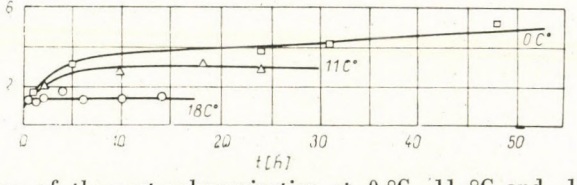

Fig. 6. Kinetic curves of the post-polymerization at 0 °C, 11 °C and 18 °C, of vinylene carbonate irradiated with 7.9 Mrad at —78 °C

within the crystal lattice. A raise of the temperature of the post-polymerization enhances the mobility of the monomer molecules and this affects adversely the rate of this polymerization in the solid state. Another explanation for the lowering of the limit conversion values could be sought in the rapid decrease of the concentration of radicals. However, in a former work [6] we found that in the case of N-vinylsuccinimide the process of heating up from —78 °C to 0 °C resulted in a decrease of the radical concentration to about one fifth of the original value; yet, the limit conversion of the post-polymerization rose with the temperature, since the polymerization of monomers not confined to a lattice structure is enhanced by the increased mobility of the monomer molecules.

Fig. 8 shows, for polymerizations at 0 °C subsequent to irradiation at −78 °C, the concentration of radicals, thel imit conversion values, and the change of the characteristic viscosity of the poly(vinylene carbonate) formed, as functions of the overall dose of irradiation. With increasing overall dose, the concentration of radicals increases, and tends toward a limit value at about 12 Mrad (Curve 3). Curve 1, showing the limit conversion values of the post-polymerization, is of a similar shape, but differs in that, from 8 Mrad on,

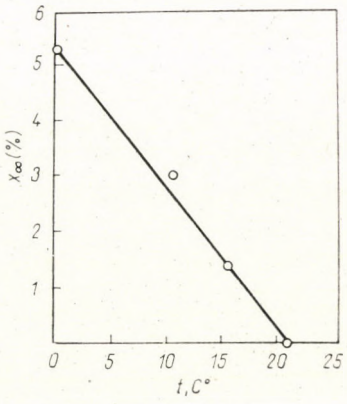

Fig. 7. Dependence of the limit conversions (X_∞) shown in Fig. 6 on the temperature of the post-polymerization

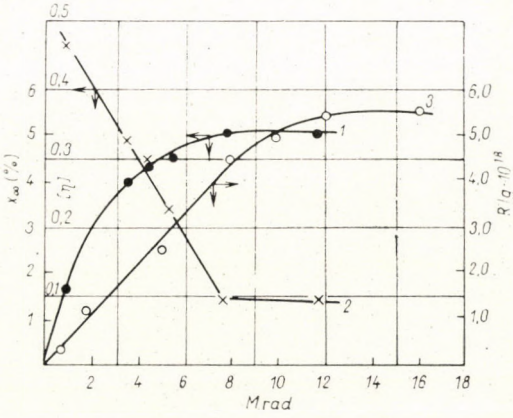

Fig. 8. Concentration of radicals generated by irradiation at −78 °C and determined at 0 °C (Curve 3), the limit conversion of the post-polymerization (Curve 1), and the characteristic viscosity of the polymers formed (Curve 2), as functions of the overall dose of irradiation

the limit value of conversion does not change any more. With increasing radiation doses, the characteristic viscosity of poly(vinylene carbonate) is rapidly reduced to about one fifth of the initial value, and here again a constant limit value is attained at about 8 Mrad, corresponding to the maximum limit conversion (Curve 2). This behaviour unequivocally suggests that the length of the polymer chains is determined, within the limits set by crystal-chemical factors, by the number of active centres produced by the irradiation; these may affect the chain-terminations. This is the cause of the rapid fall of the characteristic viscosity in proportion to the increase of the concentration of radicals.

Curves 1 and 2 reach their respective maxima at an overall dose of 8 Mrad, and Curve 3 at around 12 Mrad. This suggests that irradiation gives rise also to free radicals which have no influence on the polymerization process. This fact further indicates that vinylene carbonate belongs into the group of monomers that polymerize within the lattice, since the active centres formed

at the sites of physical degradation due to higher doses of irradiation affect neither the limit values of post-polymerization, nor the characteristic viscosity of the polymers formed.

SUMMARY

The ESR spectra of the products formed by the irradiation of vinylene carbonate at low temperatures, the change of the concentration of radicals with rising temperature, and the ESR spectrum of the radical detectable in the system undergoing post-polymerization, have been studied. The latter spectrum significantly differs from the spectra of the primary irradiation products. The concentration of radicals, the kinetics of post-polymerization, and the change of the molecular weight of the polymers formed, unequivocally suggest that the post-polymerization of vinylene carbonate in the solid state is a radical process, and that at the conversion values attainable in such polymerization, vinylene carbonate behaves in a manner characteristic of monomers that polymerize within the crystal lattice.

REFERENCES

1. HARDY, GY., NYITRAI, K., SARLÓS, CS.: Magy. Kém. Foly. **72,** 517 (1966).
2. HARDY, GY., NYITRAI, K.: Magy. Kém. Foly. **72,** 522 (1966).
3. HARDY, GY., NYITRAI, K.: Magy. Kém. Foly. **73,** 475 (1967).
4. HARDY, GY., NYITRAI, K., KOVÁCS, G., FEDOROVA, N.: Magy. Kém. Foly. **69,** 437 (1963).
5. SMETS, G., HAYASHI, K.: J. Polymer Sci. **29,** 257 (1958).
6. HARDY, GY., VARGA, J., NAGY, G., CSER, F., (Mrs.) ERŐ, J.: Magy. Kém. Foly. **73,** 55 (1967).
7. HARDY, GY., VARGA, J.: Magy. Kém. Foly. **69,** 441 (1963).
8. HAYASHI, K., OCHI, H., OKAMURA, S.: J. Polymer Sci. **A2,** 2929 (1964).

Gyula HARDY
Károly NYITRAI
Gábor NAGY
Mrs. J. ERŐ
Mária KISBÉNYI

Budapest XIV., Hungária krt. 114.

Acta Chimica Academiae Scientiarum Hungaricae Tomus 56 (1), pp. 67—85 (1968)

KINETICS OF THE SOLID STATE POLYMERIZATION OF N-VINYLCARBAZOLE

F. TÜDŐS and E. BOROS-GYEVI

(Central Research Institute for Chemistry of the Hungarian Academy of Sciences, Budapest)

Received July 18, 1966. Revised manuscript received November 29, 1966

Introduction

In recent years research in the field of solid state polymerization drew attention to the role of several important factors. It turned out that in the determination of chemical reactivity a number of physical features, such as the structure and texture, dimensions and quality of the crystals, the number of defects (dislocations), etc. are just as significant as the common chemical factors (*e.g.* conjugation, steric conditions or polarity). The effect of the physical factors may be just as decisive for the reaction process as chemical effects [1, 2].

In spite of all efforts, several important problems in respect of the kinetics and mechanism of solid state polymerization are still unsolved, and but for some exceptions it is even undecided whether polymerization proceeds by ionic or radical mechanism. This uncertainty is due to the fact that the methods used for the study of liquid phase polymerization (such as dose-rate dependence, inhibitor effect, copolymerization technique, *etc.*), are either inapplicable to solid state reactions, or yield ambiguous results.

Neither are the kinetics of solid state polymerization sufficiently clarified. For the determination of the Arrhenius parameters of these processes the elucidation of the exact relationship between the different elementary processes and the overall reaction rate would be necessary. The solution of this problem, difficult as it is, has to be attempted, because for lack of these relations the dependence of polymerization ability in the solid state on the chemical and physical structure may be interpreted merely qualitatively.

In this respect it seems particularly complicated to elucidate kinetic relations in autocatalytic reactions [3, 4, 5]. The compound of our present investigations, N-vinylcarbazole, also polymerizes according to autocatalytic kinetics. The solid state polymerization of this monomer was first studied in detail by CHAPIRO and HARDY [6].

Experimental

For the experiments a sample of 1—3 g of the monomer was introduced into a glass ampoule. The ampoules were evacuated at 10^{-3} torr, the monomer was rapidly melted on a hot water bath to remove absorbed gases and subsequently frozen in a cold water bath. This

process was repeated three times and the ampoules were then sealed in vacuum. The samples were irradiated at 20 °C by the 500 c Co^{60} source of the Research Institute of Plastics, Budapest. After irradiation, the contents of the ampoules were rapidly dissolved in benzene containing a small quantity of *p*-nitrosodimethylaniline as inhibitor; the polymer was precipitated with excess methanol, filtered off on a *G-3* filter and dried to constant weight.

For chemical initiation azo-bis-obutyronitrile (AIBN) was used. As this system polymerizes rapidly in the melt, the mixture can be melted only once, for some seconds. In every series the quantity of polymer formed during melting was checked by a blind experiment. When working quickly, this quantity did not exceed 0.2 to 0.5%. Polymerization was performed in an ultrathermostat at constant temperature and in practically complete darkness. In other respects the procedure was the same as in the experiments with radiation.

Intrinsic viscosity was determined in 0.4—2 g/100 ml benzene solutions at 25 °C. The degree of polymerization was calculated from UEBERREITER and SPRINGER's equation [7]:

$$\bar{P} = 4.61 \cdot 10^3 [\eta] 1.72$$

where $[\eta]$ is given in 100 ml/g units.

Results

In agreement with previous investigations the conversion–time relation was found to be an S-shaped curve of autocatalytic character (Fig. 1). In spite of slight differences in methodics, our experimental results were in good agree-

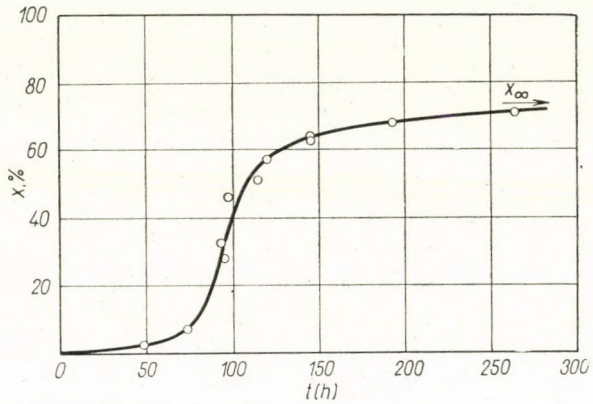

Fig. 1. Conversion–time relation in the γ-radiation induced polymerization of N-vinylcarbazole (I = 250 kr/h, 20 °C)

ment with HARDY's [6] data, so that the latter could be used in the kinetic calculations. Our experimental data are summarized in Tables I to III.

From a comparison of these results with those obtained earlier, one important difference emerges. While in earlier, less detailed examinations the degree of polymerization was found to be constant and independent of time (or of conversion), according to our measurements the polymerization degree increases rapidly at small conversions, and decreases after passing through

a maximum. As the change in polymerization degree is approximately five times higher than the experimental error (10—15%), the observed dependence must certainly be significant (Fig. 2).

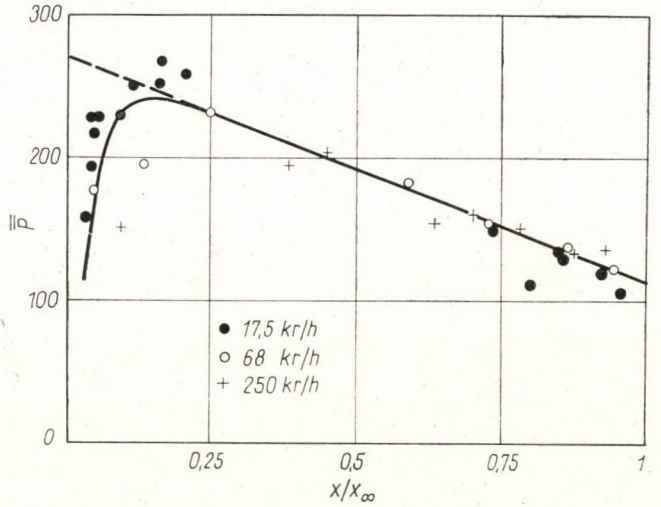

Fig. 2. Polymerization degree *vs.* conversion, at different dose rates

Discussion

(a) *Induction period.* In the conversion–time correlation, two periods of clearly different character can be distinguished. During the initial stage (induction period, t_i) the polymer is formed at a very slow, constant rate

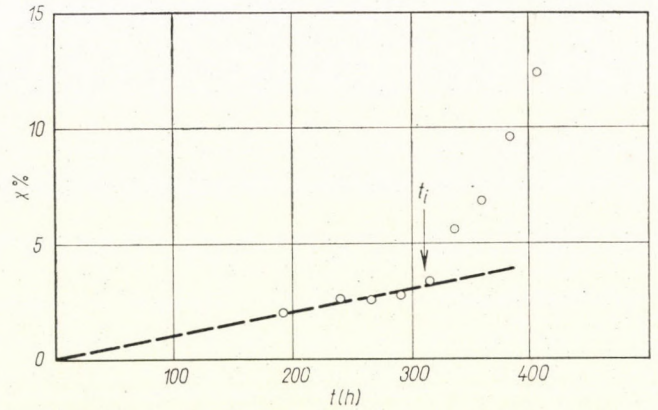

Fig. 3. The first phase of the polymerization (I = 17.5 kr/h, 20 °C)

(Fig. 3). This rate begins to increase when the quantity of the polymer reaches 2.5—3%; after this the increase is very rapid and assumes an exponential character. The induction period is fairly long, *e.g.* at 20 °C it is about 40—60%

of the total reaction time. It should be noted that unlike the second period, the induction period cannot be treated by autocatalytic kinetics.

The length of the induction period (Table IV) depends on the dose rate of radiation in the following manner:

$$t_i = I^{-0.65} \tag{1}$$

The activation energy determined from the temperature dependence is: $E_{t_i} = -12.7$ kcal/mole.

Table I

γ-Radiation induced polymerization of N-vinylcarbazole ($I = 250$ kr/h, 20 °C)
$I = 250$ kr/h

No.	t (h)	$10^2\,\xi$	$\bar{P}$
1	48.8	2.75	—
2	74.5	7.02	151
3	93.3	32.91	204
4	95.9	28.02	195
5	97.8	46.01	155
6	115.4	51.08	160
7	121.1	57.25	151
8	145.2	64.01	134
9	146.2	62.68	—
10	193.3	67.75	137
11	263.4	72.04	299**
—	∞	73*	—

* extrapolated value
** due to cross-linking

From the linear kinetics of the induction period it may be assumed that during this time radiolysis takes place in the organic crystal when the crystal structure is not yet sufficiently disordered for polymerization to occur. Polymerization rate increases only after a sufficient number of crystal defects have developed as a result of the high dose (5—12 Mr) and the short, previously formed polymer chains.

(b) *The rate equation.* For a kinetic treatment of the second period, the rate equation must be known. This may be determined, in principle, in two different ways. If the elementary kinetic steps are known, the rate equation might be derived *theoretically*; otherwise it has to be determined *empirically*.

Table II

γ-Radiation induced polymerization of N-vinylcarbazole (I = 65 kr/h, 20 °C)

$I = 65$ kr/h

No.	t (h)	$10^2\,\xi$	$\bar{P}$
12	70.3	0.99	—
13	110.8	2.10	—
14	119	1.63	—
15	123.8	3.08	176
16	142.2	5.84	—
17	145.8	5.28	—
18	170	8.62	195
19	189.1	28.24	—
20	193.8	16.07	232
21	194.3	33.0	—
22	217.3	38.17	183
23	220.4	47.67	—
24	241.3	47.16	155
25	261.3	52.70	—
26	263	51.80	—
27	284	55.5	—
28	313.7	56.17	138
29	338.2	61.28	122
30	357.6	56.79	—
—	—	65*	—

* extrapolated value

Several researchers have attempted the derivation of the rate equation for solid state polymerization of accelerated character [3, 4, 5] but by the introduction of numerous arbitrary assumptions, such as a stationary process, the kinetic order of the elementary processes, *etc.*, the limit of applicability of these equations is greatly reduced, and the results are not very conclusive. In certain cases no due account was taken of the specific character of the process in the solid matrix. The equation of BAYSAL [3], *e.g.* is nothing else but a relation which may be derived for the initial stage of liquid phase polymerization (where chain termination is yet negligible).

As our knowledge of solid state polymerization is yet very incomplete, it seems more suitable to determine the rate equation empirically. The following procedure was adopted: by the graphical differentiation of the conversion–

Table III

γ-Radiation induced polymerization of N-vinylcarbazole (I = 17.5 kr/h, 20 °C)

$I = 17.5$ kr/h

No.	t (h)	$10^2\,\xi$	$\bar{P}$
31	193.7	2.00	158
32	242	2.62	193
33	266	2.50	229
34	289.5	2.73	216
35	314.5	3.33	228
36	335.9	5.54	229
37	360.5	6.79	250
38	384.5	9.50	252
39	408.1	12.27	258
40	433.4	9.83	267
41	458	44.43	147
42	482	48.11	112
43	505.5	57.39	106
44	530	50.92	134
45	557.9	51.46	130
46	649	55.53	120
—	∞	60*	—

* extrapolated value

Table IV

Induction period in the solid state polymerization of N-vinylcarbazole

T (°C)	I(kr/h)	t_i(h)	$D_i = It_i$ (Mr)
20	250	48	12.0
20	228	47	10.7
20	122	72	8.8
20	65	112	7.6
20	17.5	258	4.5
40	65	26	1.7
60	65	8.7	0.57

time correlations the rates of the process (W_2) were determined from point to point, and the rate–time and rate–conversion curves were analyzed.

Kinetic curves of accelerated character can be described by the general equation* of autocatalysis:

$$W_2 = \frac{dx}{dt} = K' x^m (1 - x)^n \tag{2}$$

where $x = \xi/\xi_\infty$. It should be noted, however, that this equation because of its general character discloses hardly anything about the mechanism of the process; thus it also describes numerous non-autocatalytic branching chain-reactions [8]. Of course, *chemical* autocatalysis is out of question; in the case under investigation it cannot be supposed that the end product, *i.e.* the polymer, exerts by some chemical reaction an accelerating effect. Undoubtedly, we are faced here with *physical* autocatalysis; the polymer formed has a favourable influence on the properties of the solid matrix from the point of view of the reaction. This means at the same time that m and n "reaction orders" cannot be derived from the molecularity of the chemical processes, consequently they are not necessarily whole numbers.

The values of the reaction orders, m and n, were hereupon determined graphically from the relations $\log W_2 - \log x$ (low conversion) and $\log W_2 - \log (1 - x)$ (high conversion). This method yielded as results of three experimental series 1.34; 1.23 and 1.13 for m and 1.86; 1.72 and 1.80 for n.

As a further check on the values of the reaction orders, the functions $W_{calc} = x^m (1 - x)^n$ were calculated, and from these the ratios of W_2/W_{calc} were obtained. According to Equation (2), these ratios have to be independent of the conversion if correct m and n values were used in the calculation. The calculations were carried out for the following pairs of values of $m - n$: 2—2, 3/2—2, 1—2 and for the sake of completeness also for 1—1 (corresponding to the KARGIN—KABANOV equation). As shown in Fig. 4, the best constants are yielded by the combinations 3/2—2 and — except for the very beginning of the reaction — by 1—2. Considerable systematic deviation was found at the beginning of the reaction in the case of the 2—2 combination while 1—1 yielded such deviation at both the beginning and the end. From these considerations the probable values of the reaction orders are $m = 1.2 \pm 0.2$ and $n = 1.9 \pm \pm 0.3$. The reaction orders are independent of the dose rate.

(c) *Polymerization degree.* As it has been mentioned, the degree of polymerization changes according to a maximum type curve. Plotting the experimental data as a function of $x = \xi/\xi_\infty$, within the limits of experimental error,

* Reversible reactions excepted, the equations of reaction kinetics yield always total conversions if $t \to \infty$. If the conversion did not complete up to 100%, account of this must previously be taken in the calculation.

all experimental data fit one curve (Fig. 2). Though the dose rate varied by more than an order of magnitude, polymerization degree and kinetic chain-length were found to be independent of the dose rate. Consequently there is no interaction of the active centres during the process.

From the fact that polymerization degree is a fairly complicated function of time, but a simple and unambiguous function of conversion, it follows that

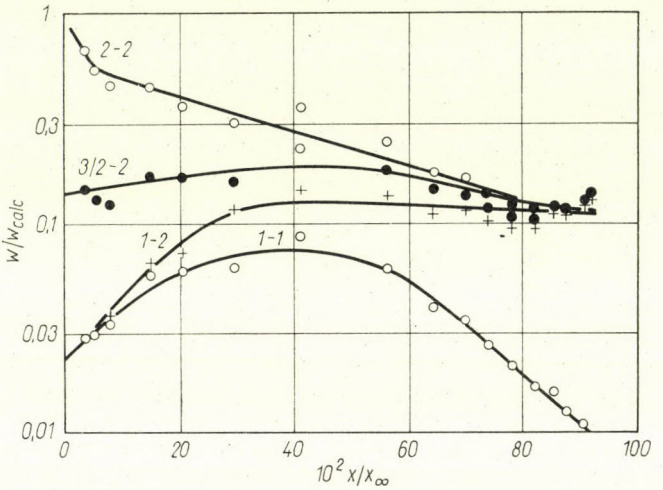

Fig. 4. Determination of the reaction order

at a given temperature the length of the kinetic chain must be determined by the mechanical properties of the matrix. The latter are, however, obviously determined by the composition (monomer/polymer ratio, *i.e.* the conversion).

The experimentally determined polymerization degree is not identical with the actual degree of polymerization, $\overline{P}(x)$, which is an average value already, but rather with its integral mean value, $\overline{\overline{P}}(x)$:

$$\overline{\overline{P}}(x) = \frac{1}{x} \int_0^x \overline{P}(x)\, dx, \tag{3}$$

because the fractions of different degrees of polymerization formed at different conversions are gradually superimposed. However, $\overline{P}(x)$ may also be derived from the experimental data; from Equation (3) we have:

$$\overline{P}(x) = \overline{\overline{P}}(x) + x \frac{d\overline{\overline{P}}}{dx}. \tag{4}$$

It follows from Equation (4) that the value of $\overline{P}(x)$ is zero if $x = 1$. Thus in this system polymerization is stopped before the complete consumption of the monomer, because the kinetic chain length is zero already at $\xi = \xi_\infty$. Probably the residual monomer is dispersed to such an extent in the polymeric mass that owing to hindered mobility the formation of polymer chains is no longer possible. This phenomenon may also be observed in liquid phase polymerization though to a lesser degree, and it is particularly well known in the polymerization of acrylates and methacrylates which give glass-like, extremely hard polymers with 5 to 10% of unchanged monomer at the end of the reaction.

A closer analysis of the experimental data reveals that the following empirical relation gives a good approximation for the polymerization degree:

$$\overline{P}(x) = P_0 x^\beta (1 - x), \tag{5}$$

where P_0 is a constant depending on temperature only. The value of $\beta = 0.2 \pm \pm 0.1$ was found to be the best for the description of the data.

It should be noted, however, that the viscosimetrically determined polymerization degree is surely not equal to the corresponding number-average, as the distribution curve of the polymer formed in the solid state is obviously significantly different from the distribution curves of the samples used for the calibration of the Ueberreiter equation. It may be assumed, however, that the experimental results reflect at least semiquantitatively the trend of the number-average polymerization degree.

From Equation (5) we obtain for $\overline{\overline{P}}(x)$ the following relation:

$$\overline{\overline{P}}(x) = \frac{P_0}{1+\beta} x^\beta \left\{1 - \frac{1+\beta}{2+\beta} x\right\}, \tag{6}$$

which has a maximum at

$$x_{max} = 1 - \frac{1}{(1+\beta)^2}. \tag{7}$$

Earlier less detailed investigations have stated that the polymerization degree in solid state polymerization is constant and independent of the conversion. Actually a similar dependence as shown above is also found in other systems. Thus, according to CHEN, in the solid state polymerization of 2,4-dimethylstyrene the polymerization degree increases with time [9]. In the thoroughly investigated solid state polymerization of acrylamide, the molecular weight changes according to a maximum curve. The data of several authors [3, 10, 11] can be conveniently treated by Equations (5) and (6) where $\beta = 1/2$. An analogous dependence was found by VARGA and HARDY [12, 13] for the poly-

merization of N-vinylsuccinimide ($\beta = 1$). The same holds for the chemically initiated polymerization of N-vinylcarbazole (Fig. 9) but for a slightly higher value of β ($\beta \approx 0.3$).

It seems therefore highly probable that this type of polymerization degree and of kinetic chain length is an important specific feature of autocatalytic polymerization. This type of kinetic chain length formation determines in itself the autocatalytic kinetics of the process.

The rapid increase during the initial period can be interpreted by the increase of the rate, *i.e.* of the rate constant of chain growth. The ordered structure of the initial monomer crystal is unfavourable for such a topoatactic chain growth. During polymerization the disorder of the matrix gradually increases, resulting in an increase of the mobility of the monomer molecules, thus leading to an increased rate of chain growth. In liquid phase polymerization the same phenomenon can be observed, namely that modifications of the physical properties of the matrix cause a change in the rate of the different elementary reactions (gel-effect). The decrease found in the second stage of $\overline{P}(x)$ might probably be interpreted by the decrease of the number of monomer molecules available for polymerization.

(d) *Integration of the rate equations.* The rate Equation (2) can readily be integrated only if m and n are integers or simple fractions. As determinations of the reaction order always contain some errors, such an approximation seems acceptable. By rearranging Equation (2) the following integral may be defined:

$$I_{m,n}(x) = \int \frac{-dx}{x^m(1-x)^n} \tag{8}$$

yielding as the general solution of Equation (2):

$$I_{m,n}(x) = I_{m,n}(x_0) - \int_0^t K' \, dt. \tag{9}$$

If $K' = \text{const.}$, we have

$$\int_0^t K' \, dt = K' t, \tag{10}$$

if, however, $K' = K'' t$, *i.e.* K' is proportional to time, we get

$$\int_0^t K' \, dt = \frac{1}{2} K'' t^2. \tag{11}$$

Any characteristic point of the kinetic curve may be expressed by Equations (9) and (10); *e.g.* the half time, $t_{1/2}$, will be:

$$t_{1/2} = \frac{1}{K'} \{I_{m,n}(x_0) - I_{m,n}(1/2)\}. \tag{12}$$

The integrals according to Equation (8) were calculated for several $m - n$ combinations of practical interest, and are given in the Appendix. By using

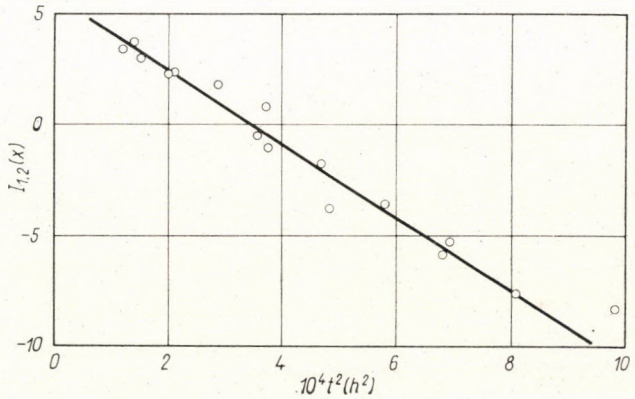

Fig. 5. Linear form of the conversion–time relation (I = 68 kr/h, 20 °C)

the curves of these integrals, a linear conversion–time relation can be easily obtained for the exact determination of the rate constant K'.

Investigations were performed for the combinations 1—2, 3/2—2, and for the sake of comparison, also for 1—1. The correlations were examined as functions of both t and t^2, thus a total of six possibilities were examined. Earlier a further combination, namely 1/2—1—1, was also examined (the third number signifies the exponent of t) but it proved unsuitable, as no linear correlation of the data was obtained with it.

It was established by this method that by the combinations 1—1—1 (KARGIN and KABANOV's equation [5]) or 1—1—2 the S-character of the curves is only partly abolished. Only by the combinations 1—2—1, 3/2—2—1 and 1—2—2 were satisfactorily linear correlations obtained. The combination 3/2—2—2 yielded convex curves, indicating that this combination fails to describe the initial period of the reaction. One of these investigations (combination 1—2—2) is shown in Fig. 5. The values of K' and K'' calculated from the different equations are listed in Table V together with the half-times and the corresponding dose values.

Of the remaining possibilities (firstly of 1—2—1, 3/2—2—1 and 1—2—2), a decision can be reached by the examination of the dose dependence and dose

Table V

Rate constants in the solid state polymerization of N-vinylcarbazole

I(kr/h)	I_{rel}	$t_{1/2}$(h)	$D_{1/2}$ (Mr)	$10^2\ K'(h^{-1})$			$10^4\ K''\ (h^{-2})$	
				1—1—1	1—2—1	3/2—2—1	1—1—2	1—2—2
17.5	1	438	7.66	1.5±0.4	6.8	7.6	0.52	1.10
68	3.89	197	13.4	3.44	7.3	11.4	1.98	3.32
122	6.98	150	18.3	3.80	8.4	14.0	3.55	5.6
228	13.0	103	23.5	5.9	14.9	20.8	8.8	12.6
250	14.3	97	24.2	5.9	14.8	19.8	8.8	12.4

rate dependence of the rate constants. The values of the exponent of the dose rate dependence I^{α} are $\alpha_{1,1,1} = 0.44$, $\alpha_{3/2,2,1} = 0.37$, while the dependence of K_{121} cannot be given in this form (Fig. 6). It would be difficult indeed to attach physical meaning to these dependences.

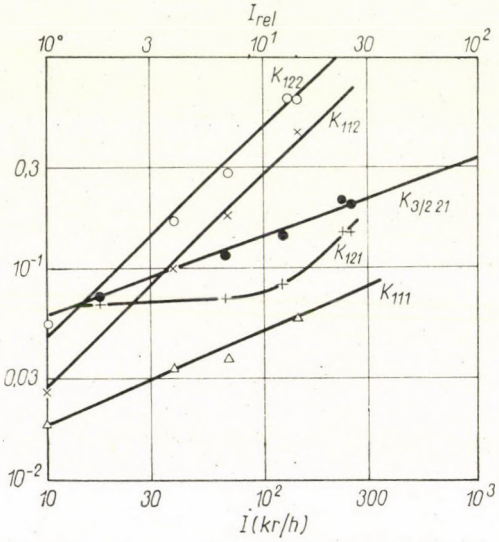

Fig. 6. Dose rate dependence of the overall rate according to different rate equations. (Data are given as the function of I and I_{rel}; to simplify plotting, the values of K_{112} and K_{122} were divided by 2)

More rational dependences are obtained for the constant K'' by means of plotting t^2. The dose rate dependence of both K_{112} and K_{122} may be described with $\alpha = 1$ (Fig. 6).

In agreement with the dose rate independence of the polymerization degree, this is further evidence that the active centres, owing to their reduced mobility in the solid state, cannot interact with one another.

It was to some extent accidental that the data plotted as a function of t showed also a linear correlation. On the other hand, this was a mathematical consequence of the long induction period at the beginning of the reaction ($t = t_i + \Delta t$ and $t^2 = t_i^2 + 2t_i\Delta t + \Delta t^2 \approx t^2{}_i\Delta t$). Constants $K_{m,n,l}$ calculated in this way are proportional to the total dose ($D_{1/2}$) (Table V).

From these considerations and those in section (b), the rate equation of the solid state polymerization of N-vinylcarbazole may be given with great probability as

$$\frac{dx}{dt} = K\,It\,x^{1,2}\,(1 - x)^2, \tag{13}$$

where $K = K''/I$.

(e) *The elementary processes of polymerization.* For all systems (irrespective of their physical state), in which chain growth takes place by individual steps between the active centres and the monomer molecules, the rate of polymerization can be described by the usual equation:

$$W_2 = k_2\,rm, \tag{14}$$

(where k_2 is the rate constant of chain growth, r = concentration of the active centres, and m = concentration of the monomer).* Nevertheless, the expression is hardly applicable here for the time being, as the dependence of k_2, r and m on the conversion is unknown.

Another fundamental relation of the theory of chain reactions [16]

$$W_2 = \nu\,W_1, \tag{15}$$

(where W_1 is the rate of initiation and ν the kinetic chain length) can be used satisfactorily for the analysis of polymerization kinetics.** It can be assumed that ν in this relation is often equal or at least proportional to the polymerization degree. Chain transfer reaction is namely a slow process and according to recent findings [17, 18] cannot take place with aromatic monomers (*e.g.* styrene). Therefore, if we assume that $\nu = \overline{P}(x)$, we have for the rate of initiation:

$$W_1 = W_2/\overline{P}\,(x). \tag{16}$$

* SEMENOV's energy chain [14, 15] is the only exception; however, it is doubtful whether Semenov's energy chain can be considered a chain reaction. According to this mechanism the formation of the polymer chains takes place in one action (and not in individual steps) during 10^{-10} sec. This time interval is equal to the time required for a bimolecular reaction (10^{-10}—10^{-11} sec). Therefore, it seems more correct to regard this mechanism as a polymolecular (or multimolecular) elementary reaction.

** Strictly, this relation is valid only for the quasi-stationary state. In general, the relation $W_2 = \nu W_4$ holds (W_4 being the rate of chain termination). However, if the growing active centres are also regarded as polymer, which is certainly justified experimentally, Equation (15) will hold irrespective whether the process is quasi-stationary or not.

Using Equations (13) and (5) for our system:

$$W_1 = W_1^0 x (1 - x), \tag{17}$$

where

$$W_1^0 = K It/P_0. \tag{18}$$

This relation can be interpreted if we assume that actual initiation (not the formation of primary active centres) takes place at the interface between the polymeric and monomeric phases. The size of this interface will be proportional to the quantities of the polymer already formed and of the monomer not yet used up by the reaction, *i.e.* to $x(1 - x)$. The finding that the rate is proportional to the total dose taken up by the system and not to the dose rate indicates that the primary active centres produced by irradiation are trapped by the lattice and begin to grow only when reached by the polymerization front. Under these conditions the concentration of the primary active centres penetrating into the transitional layer between the monomer and polymer will be proportional to the total dose absorbed by the system during a given time t.

In the given system obviously a termination reaction has also to be taken into account, or else polymerization degree would increase monotonously from the beginning to the end of the reaction, similarly to living polymerization. It has been shown that this is not the case either for N-vinylcarbazole, or for the other monomers examined. Since a bimolecular termination of the active centres is out of question, the most likely interpretation of chain termination is the "burial" mechanism suggested by THOMAS and PELLON [19] for precipitation polymerization, where the active centres become gradually buried by the newly formed polymer, hindering the diffusion of the monomer to the active centre and thus stopping further propagation of the chain. This mechanism indicates a unimolecular termination reaction. The process is not a chemical reaction, but rather a physical process. By reacting with more mobile primary radiolytic reaction products, the buried active centres might perhaps transform into dead molecules, but this does not affect the polymerization. Thus the somewhat curious situation arises that under these conditions a partial quasi-stationary state may occur in spite of the dependence on t^2 and the value of $\alpha = 1$.

As the active centres are buried always under identical conditions at the polymer–monomer interface whose physical properties are unchanged, the rate constant of this process will be independent of the conversion. The rapid increase of the polymerization degree at the beginning of the reaction indicated an increase of the rate constant of chain growth: $k_2 \sim x^{\beta}$.

(f) *The mechanism of polymerization.* The solution of the problem, whether solid state polymerization proceeds by ionic or radical mechanism is extremely difficult. The kinetics of the process, as shown above, cannot be treated without

solving this question. Nevertheless, the clarification of this basic problem is highly interesting.

Our previous investigations [20] indicated that the process has probably radical mechanism. On introducing radical inhibitors, the polymerization rate decreased very markedly in spite of surprisingly low inhibitor concentrations (1—3 mole%).

To settle the question whether N-vinylcarbazole polymerizes in the solid state by radical mechanism, polymerization was studied at 49, 54 and 59 °C in the

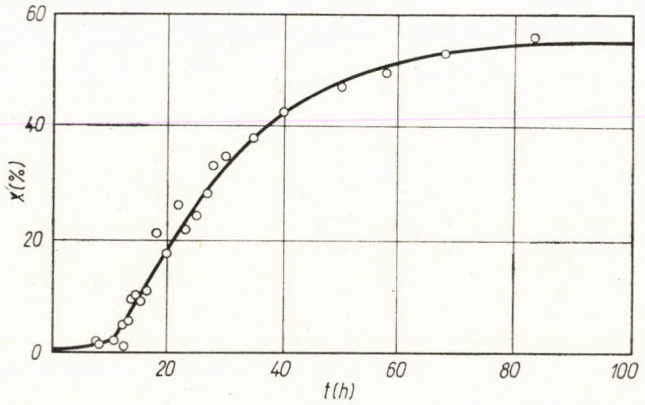

Fig. 7. Conversion–time relation for the AIBN-initiated polymerization of N-vinylcarbazole [1.5% (w/w) AIBN; 54 °C]

presence of AIBN as a radical initiator. Only a short outline of these experiments can be given here. Polymerization is easily initiated by AIBN, though the concentrations used were rather high compared with the concentrations used in liquid phase reactions. As seen in Figs 7, 8 and 9, polymerization kinetics and the polymerization degree essentially agree with the observations made with radiation initiation.

It seems probable that in this case chain growth starts as soon as the primary active centre is formed, and the rate of initiation is

$$W_1 = W_1^0(1 - x).$$

Because of the different temperature the value of β increases, too, and it is 0.3 ± 0.1. The activation energy of the process is extremely high ($\sim$ 40 kcal/mole), caused obviously by the high activation energy of initiation.

In the light of these facts the solid state polymerization of N-vinylcarbazole seems to be a radical process.

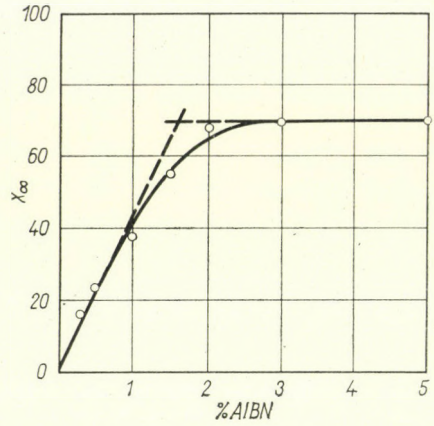

Fig. 8. Limiting conversion *vs.* the concentration of the initiator (54 °C)

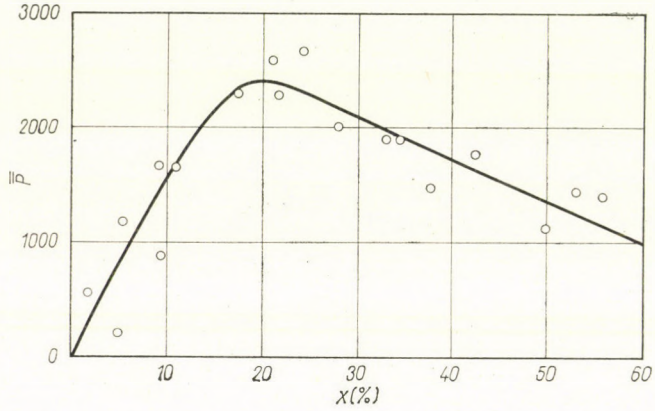

Fig. 9. Polymerization degree *vs.* conversion with chemical initiation [1.5% (w/w) AIBN; 54 °C]

We thank Mrs. B. ZSADON and Miss H. NEUHOLD for their assistance in the experimental work.

Appendix

The $I_{m,n}(x)$ integrals have been determined for the cases: $m = 1$; 3/2 and 2, $n = 1$ and 2. The different integrals are:

1—1 $$I_{1,1}(x) = \log X \qquad (A1)$$

where

3/2—1 $$X = \frac{1}{x} - 1 \qquad (A2)$$

$$2-1 \qquad I_{3/2,1}(x) = 2\left\{\frac{1}{\sqrt{x}} - ArTh\sqrt{x}\right\} \tag{A3}$$

$$1-2 \qquad I_{2,1}(x) = X + \log X \tag{A4}$$

$$3/2-2 \qquad I_{1,2}(x) = \log X - X^{-1} \tag{A5}$$

$$2-2 \qquad I_{3/2,2}(x) = \frac{2}{\sqrt{x}} - \frac{\sqrt{x}}{1-x} - 3\,ArTh\sqrt{x} \tag{A6}$$

$$I_{2,2}(x) = X - X^{-1} + 2\log X \tag{A7}$$

The common feature of all integrals is:

$$\lim_{x\to 0} I_{m,n}(x) = +\infty \tag{A8}$$

and

$$\lim_{x\to 1} I_{m,n}(x) = -\infty \tag{A9}$$

It is to be mentioned that the value $x_0 = 0$ can never exist because in this case the autocatalytic process would not start. At the beginning of the process, x_0 does not denote the amount of polymer, but it means the initial disorder expressed in "polymeric units". Since x_0 is a poorly reproducible quantity, it is barely characteristic for the process or the crystal.

We mention still the following equations:

$$I_{2,2}(x) = I_{1,2}(x) + I_{2,1}(x) \tag{A10}$$

and

$$I_{1,2}(x) = -I_{2,1}(1-x). \tag{A11}$$

SUMMARY

The polymerization of N-vinylcarbazole initiated by γ-radiation and azo-bis-isobutyronitrile, respectively, has been investigated. It has been found that the rate of the process may be described by the following autocatalytic equation:

$$\frac{dx}{dt} = KIt\,x^{1,2}(1-x)^2,$$

where $x = \xi/\xi_\infty$ and ξ denotes the conversion. The polymerization degree changes according to a maximum curve and depends on the conversion in the following manner:

$$\overline{P}(x) = P_0\,x^{\beta}(1-x)$$

where $\beta = 0.2 \pm 0.1$. Thus the rate of initiation can be given as follows:

$$W_1 = \frac{KIt}{P_0}\,x(1-x).$$

The elementary processes of the polymerization are discussed in detail. Initiation and chain growth take place at the interface of the polymeric and monomeric phases, while chain termination most probably occurs by the "burial" mechanism suggested by THOMAS and PELLON.

According to the results obtained with chemical initiation, polymerization kinetics and polymerization degree essentially agree with the observations made with radiation initiation. In the light of these facts the solid state polymerization of N-vinylcarbazole seems to be a adical process.

x	$I_{1,1}(x)$	$I_{3/2,1}(x)$	$I_{2,1}(x)$	$I_{1,2}(x)$	$I_{3/2,2}(x)$	$I_{2,2}(x)$
0	$+\infty$	$+\infty$	$+\infty$	$+\infty$	$+\infty$	$+\infty$
0.01	+4.595	19.80	+103.595	+4.585	19.60	+108.190
0.02	3.833	13.86	52.833	3.813	13.57	56.696
0.03	3.475	11.19	35.475	3.444	10.84	38.919
0.05	2.945	8.50	21.945	2.892	8.04	24.837
0.07	2.589	7.01	15.875	2.514	6.45	18.384
0.1	2.1973	5.67	11.1973	2.0862	4.99	13.2835
0.15	1.7352	4.35	7.4019	1.5590	3.49	8.9609
0.2	1.3863	3.52	5.3863	1.1363	2.48	6.5226
0.25	1.0986	2.90	4.0986	0.7653	1.68	4.8639
0.3	0.8472	2.42	3.1805	0.4186	1.02	3.5991
0.4	0.4055	1.67	1.9055	−0.2612	−0.123	1.6443
0.5	0	1.07	1	−1	−1.23	0
0.6	−0.4055	0.51	0.2612	−1.9055	−2.46	−1.6643
0.7	−0.8472	−0,032	−0.4186	−3.1805	−4.03	−3.5991
0.75	−1.0986	−0.324	−0.7653	−4.0986	−5.11	−4.8639
0.8	−1.3863	−0.643	−1.1363	−5.3863	−6.56	−6.5226
0.85	−1.7352	−1.034	−1.5585	−7.4019	−8.79	−8.9609
0.9	−2.1973	−1.53	−2.0862	−11.1973	−12.84	−13.2835
0.93	−2.589	−1.953	−2.514	−15.875	−17.77	−18.384
0.95	−2.945	−2.317	−2.892	−21.945	−24.02	−24.837
0.97	−3.475	−2.854	−3.444	−35.475	−38.15	−38.919
0.98	−3.833	−3.28	−3.813	−52.833	−55.43	−56.696
0.99	−4.595	−3.99	−4.585	−103.595	−105.99	−108.190
1	$-\infty$	$-\infty$	$-\infty$	$-\infty$	$-\infty$	— —

REFERENCES

1. MAGAT, M.: Polymer. **3,** 449 (1962).
2. CHAPIRO, A.: Effets chimiques et biologiques des radiations, 10 série Masson et Cie, Paris
3. BAYSAL, B., ADLER, G., BALLANTINE, D., COLOMBO, P.: J. Polymer Sci. **44,** 117 (1964).
4. KARGIN, V. A., KABANOV, V. A., PAPISOV, I. M.: J. Polymer Sci. **C4,** 767 (1964).
5. *Каргин, В. А., Кабанов, В. А.:* Журн. Всесоюзн. Хим. Общ. **9,** 602 (1964).
6. CHAPIRO, A., HARDY, GY.: J. Chim. Phys. **59,** 993 (1963).
7. UEBERREITER, K., SPRINGER, J.: Z. phys. Chem. (F/M), **36,** 299 (1963).
8. *Кондратьев, В. Н.:* Кинетика химических газовых реакций. Изд. АН СССР Москва, 1958.
9. HSIA CHEN, C. A.: J. Polymer Sci. **58,** 389 (1962).
10. CHAPIRO, A., ZUMER, M.: J. Chim. Phys. **62,** 947 (1965).
11. TABATA, Y., SUZUKI, T.: Makromol. Chem. **81,** 223 (1965).
12. VARGA, J.: Dissertation, Budapest 1966.
13. HARDY, GY., VARGA, J., CSER, F., DETREKŐY, E.: Eur. Polymer. J. **2,** 41 (1966).
14. *Семёнов, Н Н.:* Химия и Технология Полимеров **4,** 196 (1960).

15. SEMYONOV, N. N.: Paper presented at the XVIIIth Internat. Congress of IUPAC, Montreal. 1961.
16. *Семёнов, Н. Н.:* Цепные реакции (Госхимтехиздат) Ленинград, 1934.
17. TÜDŐS, F.: MTA Kém. Tud. Oszt. Közleményei **21,** 49, 191 (1964); Acta Chim. Acad. Sci. Hung. **43,** 397; **44,** 403 (1965).
18. *Тюдёш, Ф.:* Рассмотрение кинетики радикальной полимеризации на основе гипотезы горячих радикалов (Изд. Мир) Москва, 1966.
19. THOMAS, W. M., PELLON, J. J.: J. Polymer Sci. **13,** 329 (1954).
20. TÜDŐS, F., CHAPIRO, A.: Paper presented at the IUPAC Macromolecular Symposium, Prague, 1965.

Ferenc TÜDŐS
Edit BOROS-GYEVI
Budapest II., Pusztaszeri út 57—69.

INDEX

INORGANIC AND ANALYTICAL CHEMISTRY — ANORGANISCHE UND ANALYTISCHE CHEMIE — НЕОРГАНИЧЕСКАЯ И АНАЛИТИЧЕСКАЯ ХИМИЯ

SZAKÁCS-PINTÉR, M. und MAROS, L.: Über eine neuere analytische Anwendung der Oxydation von organischen Verbindungen durch Brom, II. Bestimmung des Phenetidins und Phenacetins über das bei der Oxydation mit Brom gebildete Chinon und Ammoniak 1

INCZÉDY, J. and PÁSZTLER, É.: The Analytical Use of Ion Exchangers in Organic Solvents, I. Swelling and Salt Splitting in Non-Aqueous Media 9

PHYSICAL CHEMISTRY — PHYSIKALISCHE CHEMIE — ФИЗИЧЕСКАЯ ХИМИЯ

TÉTÉNYI, P. and SCHÄCHTER, K.: Kinetics of the Catalytic Dehydrogenation of Hydroaromatic Compounds, IX. Catalytic Effect of Various Metals 15

SOHÁR, P. and NEMES, A.: NH Stretching Vibration Bands at Wavenumbers Smaller than 3000 cm^{-1}, IV. Dimeric Structures, IV. Tautomeric Equilibrium of Isonicotinic Acid Thioamide Derivatives 25

ORGANIC CHEMISTRY — ORGANISCHE CHEMIE — ОРГАНИЧЕСКАЯ ХИМИЯ

HARDY, GY. and NYITRAI, K.: Polymerization of Vinylene Carbonate 39

KIRA, M. A. and BRUCKNER-WILHELMS, A.: Synthesis and Reactions of Heterocyclic Enamines, I. The Vilsmeier Aldehyde Synthesis with 1-Phenyl-3-methyl-5-pyrazolone 47

BOGNÁR, R., SZTARICSKAI, F., SOMOGYI, L., PUSKÁS, M. and MAKLEIT, S.: Investigation of the Hydrolysis Products of Desertomycin 53

HARDY, GY., NYITRAI, K., NAGY, G., (Mrs.) ERŐ, J. and KISBÉNYI, M.: Investigations in the Field of Radiation-induced Solid State Polymerization, XXII. Post-Polymerization of Vinylene Carbonate 61

TÜDŐS, F. and BOROS-GYEVI, E.: Kinetics of the Solid State Polymerization of N-vinylcarbazole 67

Printed in Hungary

A kiadásért felel az Akadémiai Kiadó igazgatója — Műszaki szerkesztő: Farkas Sándor

A kézirat nyomdába érkezett: 1968. I. 26. — Terjedelem: 7,50 (A/5) ív, 49 ábra

68.65007 Akadémiai Nyomda, Budapest — Felelős vezető: Bernát György

ACTA CHIMICA
ТОМ 56 — ВЫП. 1

РЕЗЮМЕ

Новое аналитическое использование бромистого окисления органических соединений, II

Определение фенетидина и фенацетина через хинон и аммиак, образующиезя при окислении с бромом

М. ПИНТЕР-САКАЧ и Л. МАРОШ

Фенетидин, а также фенацетин селективно определяются с помощью измерения хинона и аммиака, образующихся в ходе их окисления с бромом. После восстановления избытка брома с фенолом хинон измеряется иодометрически, а аммиак после перегонки — алкалиметрически. Методы могут быть использованы как для макро-, так и для микроопределений.

Аналитическое использование ионообменников в органических растворителях, I

Набухание ионообменников и разложение солей ионообменниками в неводных средах

Я. ИНЦЕДИ и Е. ПАСТЛЕР

Исследовалось набухание сильно кислотных катионообменных и сильно основных анионообменных смол в воде, этиленгликоле, метаноле, этаноле, диоксане, диметилформамиде, пиридине и в ледяной уксусной кислоте.

Проводилось также разложение и определение солей некоторых органических кислот и оснований с помощью ионообменной колонки в неводных средах. Выделяющиеся кислоты и основания титровали в неводных средах. Погрешность определения не превышает $\pm 1\%$.

Кинетика каталитического дегидрирования гидроароматических соединений, IX

Каталитическое влияние различных металлов

П. ТЕТЕНИ и К. ШЕХТЕР

Изучалось дегидрирование циклогексана в присутствии Be, Au, Mo, Ru, Ti, V и Zr, а также циклогексена в присутствии Be, Au, Mo, Ru, Ti и V. Были определены кинетические константы, характеризующие реакцию в случае отдельных катализаторов. Установлено, что все исследованные металлы дегидрируют циклогексан, несмотря на то, что их структура— за исключением Ru — не соответствует требованиям секстетного механизма. Это свидетельствует о том, что дегидрирование ароматических углеводородов может протекать и по другому механизму.

Между каталитической активностью металлов и кристаллическим параметром металла-катализатора, а также стандартной энтальпией окисления его, наблюдается однозначная зависимость, описываемая кривой с максимумом.

Полоса валентных колебаний NH в области волновых чисел, меньших 3000 $см^{-1}$, IV. Структуры димера, IV

Таутомерное равновесие для производных тиоамида изоникотиновой кислоты

П. ШОХАР и А. НЕМЕШ

Изучались ик-спектры некоторых тиоамидов изоникотиновой кислоты. Было установлено, что в твердой фазе (снимая спектр в таблетках KBr) таутомерное равновесие тиоамид ⇌ тиоиминогидрин может изменяться в очень широких пределах, вплоть до практически исключительного присутствия одного или другого таутомера, в зависимости от других заместителей пиридинового кольца. Так, в случае 2-алкил- и 2-аралкилпроизводных доминирует тиоловая форма, а в случае соединений, содержащих атом хлора в положении 6 — амидная форма. Амид N-n-бутил-2-этил-изоникотиновой кислоты находится также в форме амидного таутомера. В спектрах последнего соединения и других молекул, находящихся в форме тиола, наблюдается размытая полоса NH с низким волновым числом, что доказывает наличие циклической ассоциации димеров. Молекулы, находящиеся в тиоловой форме в твердой фазе, изомеризуются в амидные таутомеры в разбавленных хлороформных растворах.

Полимеризация винилен-карбоната

ДЬ. ХАРДИ и К. НИТРАИ

Изучались закономерности жидкофазной полимеризации винилен-карбоната, инициированной азо-бис-изобутиронитрилом и гамма-облучением. Было установлено, что процесс характеризуется реакцией переноса цепи на мономер. На основе экспериментальных данных была получена зависимость

$$\frac{k_p}{k^{1/2}} = 740 \cdot \exp\left(\frac{-7{,}400}{RT}\right)$$

величины констант которой отличаются от аналогичных значений, полученных для виниловых соединений, образующих более реакционноспособные радикалы и являются того же порядка, как и в случае ангидрида малеиновой кислоты.

Синтез и реакции энаминов, I

Синтез альдегидов Вилсмэйера с применением 1-феиил-3-метил-5-пиразолона

М. А. КИРА и А. БРУКНЕР (Вилхелмс)

Если в синтезе альдегидов Вилсмэйера применяется 1-фенил-3-метил-5-пиразолон, (I) образуется 4-диметиламинометилен-1-фенил-3-метил-5-пиразолон (II), который при гидролизе с помощью водной щелочи дает 4-формильное производное (III). Кислотный гидролиз II дает 4,4'-ди-(1-фенил-3-метил-5-пиразонил)-метин.

Подобным образом, из пиррола был получен 2-диметиламинометилен-пирроленин. Обсуждается механизм синтеза альдегидов Вилсмэйера.

Изучение продуктов гидролиза дезертомицина

Р. БОГНАР, Ф. СТАРИЧКАИ, Л. ШОМОДИ, М. ПУШКАШ и Ш. МАКЛЕИТ

Дезертомицин может быть очищен перекристаллизацией из *н*-бутанола, содержащего 10—30% метанола. При мягком кислотном гидролизе антибиотика образуются аморфный основной аглюкон и сахароподобный компонент. С помощью бумажной хроматографии и препаративным методом удалось доказать, что последний является D-маннозой. При жестком кислотном гидролизе аглюкона удалось изолировать аминокислоту, которая оказалась глутаминовой кислотой. На основе количественного анализа методом бумажной хроматографии было установлено, что дезертомицин содержит 1 молекулу D-маннозы и 1 молекулу глутаминовой кислоты. С помощью 2,4-динитро-фторбензола может быть приготовлен DNP-дезертомицин.

На основе данных об отдельных составляющих элементах авторами были сделаны заключения о размерах и строении молекулы дезертомицина. Было установлено, что дезертомицин является единственным среди до сих пор известных антибиотиков содержащим в качестве углеводного компонента лишь D-маннозу.

Исследования в области радиационной полимеризации в твердой фазе, XXII

Пост-полимеризация винилен-карбоната

ДЬ. ХАРДИ, К. НИТРАИ, ДЬ. НАДЬ, Й. ЭРЁ и М. КИШБЕНИ

Были изучены спектры ЭПР продуктов, образующихся при низкотемпературном облучении винилен-карбоната, изменение концентрации радикалов в ходе повышения температуры и спектры ЭПР радикалов, образующихся в системе во время пост-полимеризации. Последние спектры значительно отличаются от спектров продуктов, получающихся вначале при облучении. Концентрация радикалов, кинетические закономерности пост-полимеризации и изменения молекулярных весов полученных полимеров указывают на то, что полимеризация винилен-карбоната является радикальным процессом. На основе величин конверсии, достигнутых в течении пост-полимеризации, можно заключить, что поведение винилен-карбоната является подобным поведению мономеров, полимеризующихся в кристаллической решетке.

Кинетика твердофазной полимеризации N-винил-карбазола

Ф. ТЮДЁШ и Э. БОРОШ-ДЬЕВИ

Изучалась инициированная γ-облучением и азо-бис-изобутиронитрилом полимеризация N-винил-карбазола. Было установлено, что скорость процесса описывается следующим автокаталитическим уравнением:

$$\frac{dx}{dt} = K\, It\, x^{1,2}(1-x)^2,$$

где $x = \xi/\xi_\infty$ и ξ — конверсия. Кривая степени полимеризации имеет максимум и зависит от конверсии следующим образом:

$$\overline{P}(x) = P_0\, x^{\beta}\,(1-x).$$

где $\beta = 0{,}2 \pm 0{,}1$. Т. о., скорость инициирования описывается следующим уравнением:

$$W_1 = \frac{K\,It}{P_0}\,x\,(1-x).$$

Подробно обсуждаются элементарные стадии процесса полимеризации. Инициирование и развитие цепи протекают между полимером и мономером в пограничном слое, а процесс обрыва, вероятно, объясняется на основе механизма «погребания», предложенного Томасом и Пеллоном.

На основе исследований с химическим инициированием можно заключить, что кинетика полимеризации и формирование степени полимеризации в основных своих чертах совпадает с наблюдаемым для радиационной полимеризации. Это обстоятельство позволяет заключить, что N-винил-карбазол в твердой фазе полимеризуется по радикальному механизму.

The Acta Chimica publish papers on chemistry in English, German, French and Russian.

The Acta Chimica appear in volumes consisting of four parts of varying size, 4 volumes being published a year.

Manuscripts should be addressed to

Acta Chimica
Budapest 502, Postafiók 32.

Correspondence with the editors should be sent to the same address.

The rate of subscription is 165 forints a volume. Orders may be placed with "*Kultúra*" Foreign Trade Company for Books and Newspapers (Budapest I., Fő utca 32. Account No. 43-790-057-181) or with representatives abroad.

Les Acta Chimica paraissent en français, allemand, anglais et russe et publient des mémoires du domaine des sciences chimiques.

Les Acta Chimica sont publiés sous forme de fascicules. Quatre fascicules seront réunis en un volume (4 volumes par an).

On est prié d'envoyer les manuscrits destinés à la rédaction à l'adresse suivante:

Acta Chimica
Budapest 502, Postafiók 32.

Toute correspondance doit être envoyée à cette même adresse.

Le prix de l'abonnement est de 165 forints par volume.

On peut s'abonner à l'Entreprise pour le Commerce Extérieur de Livres et Journaux «*Kultúra*» (Budapest I., Fő utca 32. Compte-courant No. 43-790-057-181) ou à l'étranger chez tous les représentants ou dépositaires.

«*Acta Chimica*» издают трактаты из области химической науки на русском, французском, английском и немецком языках.

«*Acta Chimica*» выходят отдельными выпусками разного объема. 4 выпуска составляют один том. 4 тома публикуются в год.

Предназначенные для публикации рукописи следует направлять по адресу:

Acta Chimica
Budapest 502, Postafiók 32.

По этому же адресу направлять всякую корреспонденцию для редакции.

Подписная цена «*Acta Chimica*» — 165 форинтов за том. Заказы принимает предприятие по внешней торговле книг и газет «*Kultúra*» (Budapest I., Fő utca 32. Текущий счет № 43-790-057-181) или его заграничные представительства и уполномоченные.

35,— Ft

Reviews of the Hungarian Academy of Sciences are obtainable at the following addresses:

ALBANIA

Ndermarja Shtetnore e Botimeve
Tirana

AUSTRALIA

A. Keesing
Box 4886, GPO
Sydney

AUSTRIA

Globus Buchvertrieb
Salzgries 16
Wien I

BELGIUM

Office International de Librairie
30, Avenue Marnix
Bruxelles 5
Du Monde Entier
5, Place St. Jean
Bruxelles

BULGARIA

Raznoiznos
1, Tzar Assen
Sofia

CANADA

Pannonia Books
2, Spadina Road
Toronto 4, Ont.

CHINA

Waiwen Shudian
Peking
P. O. B. 88

CZECHOSLOVAKIA

Artia
Ve Směčkách 30
Praha 2
Poštovná novinová služba
Dovoz tisku
Vinohradská 46
Praha 2
Mad'arská Kultura
Václavské nám. 2
Praha I
Poštová novinová služba
Dovoz tlače
Leningradská 14
Bratislava

DENMARK

Ejnar Munksgaard
Nörregade 6
Copenhagen

FINLAND

Akateeminen Kirjakauppa
Keskuskatu 2
Helsinki

FRANCE

Office International de Documentation et Librairie
48, rue Gay Lussac
Paris 5

GERMAN DEMOCRATIC REPUBLIC

Deutscher Buch-Export und Import
Leninstraße 16
Leipzig 701
Zeitungsvertriebsamt
Clara Zetkin Straße 62
Berlin N. W.

GERMAN FEDERAL REPUBLIC

Kunst und Wissen
Erich Bieber
Postfach 46
7 Stuttgart S.

GREAT BRITAIN

Collet's Holdings Ltd.
Dennington Estate
London Rd.
Wellingborough. Northants.
Robert Maxwell and Co. Ltd.
Waynflete Bldg. The Plain
Oxford

HOLLAND

Swetz and Zeitlinger
Keizersgracht 471—487
Amsterdam C
Martinus Nijhof
Lange Voorhout 9
The Hague

INDIA

Current Technical Literature
Co. Private Ltd.
India House OPP
GPO Post Box 1374
Bombay I

ITALY

Santo Vanasia
Via M. Macchi 71
Milano
Libreria Commissionaria Sansoni
Via La Marmora 45
Firenze

JAPAN

Nauka Ltd.
92, Ikebukur O-Higashi 1-chome
Toshima-ku
Tokyo
Maruzen and Co. Ltd.
P. O. Box 605
Tokyo-Central
Far Eastern Booksellers
Kanda P. O. Box 72
Tokyo

KOREA

Chulpanmul
Phenjan

NORWAY

Johan Grundt Tanum
Karl Johansgatan 43
Oslo

POLAND

RUCH
ul Wronia 23
Warszawa

ROUMANIA

Cartimex
Str. Aristide Briand 14—18.
București

SOVIET UNION

Mezhdunarodnaya Kniga
Moscow G—200

SWEDEN

Almquist and Wiksell
Gamla Brogatan 26
Stockholm

USA

Stechert Hafner Inc.
31, East 10th Street
New York, N. Y. 10003
Walter J. Johnson
111, Fifth Avenue
New York, N. Y. 10003

VIETNAM

Xunhasaba
19, Tran Quoc Toan
Hanoi

YUGOSLAVIA

Forum
Vojvode Mišića broj 1
Novi Sad
Jugoslovenska Knjiga
Terazije 27
Beograd

29. V. 1968 Index: 26.007

ACTA CHIMICA

ACADEMIAE SCIENTIARUM HUNGARICAE

ADIUVANTIBUS

L. ERDEY, K. POLINSZKY, G. SCHAY

AC

R. BOGNÁR, GY. BRUCKNER, Z. CSŰRÖS, T. ERDEY-GRÚZ, Z. FÖLDI, M. FREUND, Á. GERECS, GY. HARDY, J. HOLLÓ, Á. KISS, M. KORACH, F. MÁRTA, F. NAGY, J. PROSZT, E. PUNGOR, Z. SZABÓ, P. TÉTÉNYI, L. VARGHA, K. VAS

REDIGIT

B. LENGYEL

TOMUS 56 FASCICULUS 2

AKADÉMIAI KIADÓ, BUDAPEST

1968

ACTA CHIM. ACAD. SCI. HUNG.

ACTA CHIMICA

A MAGYAR TUDOMÁNYOS AKADÉMIA KÉMIAI TUDOMÁNYOK OSZTÁLYÁNAK IDEGEN NYELVŰ KÖZLEMÉNYEI

SZERKESZTI

LENGYEL BÉLA

TECHNIKAI SZERKESZTŐK

DEÁK GYULA és TAKÁCS VILMOS

Az Acta Chimica német, angol, francia és orosz nyelven közöl értekezéseket a kémiai tudományok köréből.

Az Acta Chimica változó terjedelmű füzetekben jelenik meg, egy-egy kötet négy füzetből áll. Évente átlag négy kötet jelenik meg.

A közlésre szánt kéziratok a szerkesztőség címére (Budapest 502, postafiók 32) küldendők.

Ugyanerre a címre küldendő minden szerkesztőségi levelezés. A szerkesztőség kéziratokat nem ad vissza.

Az Acta Chimica előfizetési ára kötetenként belföldre 120 Ft, külföldre 165 Ft. Megrendelhető a belföld számára az „Akadémiai Kiadó"-nál (Budapest V., Alkotmány utca 21. Bankszámla 05-915-111-46), a külföld számára pedig a „Kultúra" Könyv- és Hírlap Külkereskedelmi Vállalatnál (Budapest I., Fő utca 32. Bankszámla: 43-790-057-181) vagy annak külföldi képviseleteinél és bizományosainál.

Die Acta Chimica veröffentlichen Abhandlungen aus dem Bereiche der chemischen Wissenschaften in deutscher, englischer, französischer und russischer Sprache.

Die Acta Chimica erscheinen in Heften wechselnden Umfanges. Vier Hefte bilden einen Band. Jährlich erscheinen 4 Bände.

Die zur Veröffentlichung bestimmten Manuskripte sind an folgende Adresse zu senden:

Acta Chimica
Budapest 502, Postafiók 32.

An die gleiche Anschrift ist auch jede für die Redaktion bestimmte Korrespondenz zu richten.

Abonnementspreis pro Band: 165 Forint. Bestellbar bei dem Buch- und Zeitungs-Außenhandels-Unternehmen »*Kultúra*« (Budapest I., Fő utca 32. Bankkonto No. 43-790-057-181) oder bei seinen Auslandsvertretungen und Kommissionären.

Acta Chimica Academiae Scientiarum Hungaricae Tomus 56 (2), pp. 87—91 (1968)

ÜBER EINE NEUERE ANALYTISCHE ANWENDUNG DER OXYDATION VON ORGANISCHEN VERBINDUNGEN DURCH BROM, III

BESTIMMUNG VON FURFUROL UND FURFURYLALKOHOL

M. SZAKÁCS-PINTÉR und L. MAROS

(Institut für Anorganische und Analytische Chemie der L. Eötvös Universität, Budapest)

Eingegangen am 21. Mai 1967

Die zwei ersten Mitteilungen, in denen die auf der Oxydation des Furfurols mit Brom beruhende Bestimmung empfohlen wird, haben abweichende Stöchiometrien. PERVIER und GORTNER [1] titrierten in annähernd 1 *n* salzsaurer bzw. schwefelsaurer Lösung mit Kaliumbromat-Meßlösung unmittelbar und bestimmten das Furfurol nach dem Äquivalentgewicht: Molekulargewicht/2. POWELL und WHITAKKER [2] empfahlen eine in 12%iger salzsaurer Lösung unter Anwendung von Bromat-Bromid-Lösung ausgeführte, auf jodometrischer Titration des Bromüberschusses beruhende Methode. Das Furfurol kann auf diese Weise nach einstündiger Bromierung nach dem Äquivalentgewicht von Molekulargewicht/4 bestimmt werden. Später empfahlen HUGHES und ACREE [3] eine auf der Bestimmung des Bromüberschusses beruhende Methode, bei der das Furfurol mit einem Molekül Brom oxydiert wird. Nach ihren Untersuchungen reagiert das Furfurol bei 0 °C mit einem Molekül Brom rasch, die Reaktion des zweiten Moleküls Brom verläuft auch bei Zimmertemperatur sehr langsam. Die weiteren Mitteilungen über die bromometrische Bestimmung des Furfurols [4, 5, 6, 7, 8] beschäftigen sich im wesentlichen mit der Frage der Anwendbarkeit dieser Verfahren.

Bezüglich der Reaktionsprodukte der Oxydation des Furfurols mit Brom sind in der Fachliteratur wenige Angaben zu finden. HUGHES und ACREE [9] stellten fest, daß bei der Reaktion von einem Molekül Brom 2 Moleküle Bromwasserstoff sowie eine Dioxo-Verbindung entstehen (Bisphenylhydrazon wurde isoliert). Die Reaktion wurde in folgenden Gleichungen beschrieben:

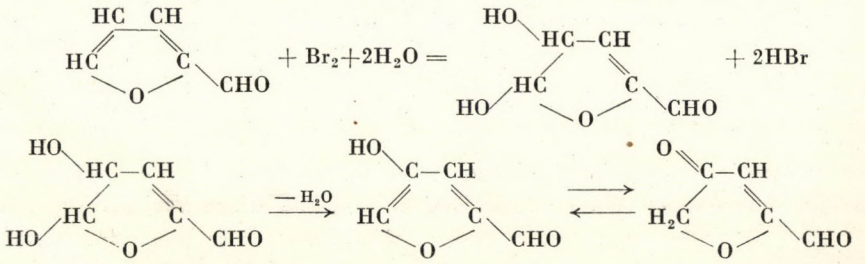

CLAUSON-KAAS und Mitarbeiter [10, 11, 12] haben aus Furanderivativen in alkoholischer und essigsaurer Lösung durch Oxydation mit Brom 2,5-Dialkoxy- bzw. 2,5-Diacetylfuran-Derivate hergestellt. Sie stellten fest, daß bei der Hydrolyse dieser Verbindungen in jedem Fall die 1,4-Dioxo-Verbindung entstand. Z. B.:

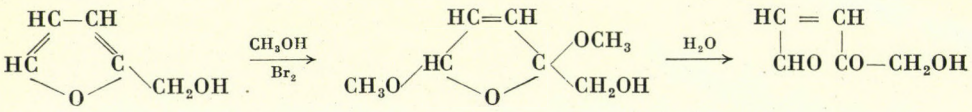

Wir haben den Mechanismus der Oxydation des Furfurols und Furfurylalkohols mit Brom und Bromchlor eingehend untersucht; über die Ergebnisse dieser Arbeit soll in einer späteren Mitteilung berichtet werden. Auf Grund der quantitativen gruppenanalytischen Untersuchungen der Reaktionsprodukte wurde eindeutig bewiesen, daß bei der Oxydation dieser Verbindungen mit 1 Molekül Brom in wäßriger Lösung der Ring sofort gesprengt wird und eine ungesättigte 1,4-Dioxo-Verbindung entsteht. Die Reaktion des zweiten Moleküls Brom bedeutet schon die Oxydation dieser letzteren Verbindung. Die zweistufige Oxydation kann mit folgenden Gleichungen charakterisiert werden:

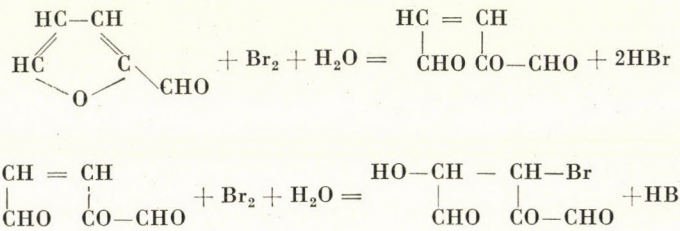

Nach dem gleichen Schema reagiert auch Bromchlor mit Furfurol, und analoge Produkte bilden sich auch bei der Oxydation des Furfurylalkohols mit Brom und Bromchlor. Beide Stufen der Oxydation mit Brom sind säurekatalysierte Vorgänge, ihr Geschwindigkeitsverhältnis ist 1000 : 1. Auch die erste Stufe der Reaktionen mit Bromchlor ist eine säurekatalysierte Reaktion, die zweite Stufe dagegen nicht. In der zweiten Stufe reagiert das Bromchlor mit den ungesättigten Oxoverbindungen um mehrere Größenordnungen schneller als das Brom. Diese Tatsache macht es möglich, Furfurol und Furfurylalkohol auch in mäßig saurer, ja sogar in neutraler Lösung schnell mit Bromchlor zu oxydieren. Unserer Meinung nach ist vom analytischen Gesichtspunkte jene Tatsache von entscheidender Bedeutung, daß diese Verbindungen außer der jodometrischen Messung des Bromchlorüberschusses auch durch die Mes-

sung des bei der Oxydation gebildeten Chlorwasserstoffs bzw. Bromwasserstoffs bestimmt werden können. Im letzteren Fall wird in Gegenwart von Quecksilber-(II)chlorid mit Bromwasser oxydiert, dann titriert man die Säure nach Zugabe

Tabelle I

Jodometrische Bestimmung des Furfurols durch Oxydation mit Bromchlor

Einwaage Furfurol, g/100 ml	Eingemessene Lösung, ml	Verbr. 0.1 *n* BrCl, ml		Gefunden Furfurol	
		Einzelwerte	Durchschnitt	mg	%
		9,64			
	9,99	9,64	9,64	23,16	98,8
		9,65			
		4,80			
0,2347	5,00	4,81	4,81	11,55	98,5
		4,82			
		1,93			
	2,00	1,90	1,93	4,64	98,8
		1,95			

von Kaliumjodid und Natriumthiosulfat. Die Ergebnisse der Bestimmungen von Furfurol und Furfurylalkohol sind in den Tabellen I, II, III und IV zusammengestellt.

Tabelle II

Bestimmung von Furfurol über die bei der Oxydation mit Bromchlor gebildete Säure

Einwaage Furfurol, g/100 ml	Eingemessene Lösung, ml	Verbr. 0.1 *n* NaOH, ml		Gefunden Furfurol	
		Einzelwerte	Durchschnitt	mg	%
		9,98			
	10,00	9,97	9,98	31,96	99,9
		10,00			
		4,98			
0,3199	5,00	5,00	4,98	15,95	99,7
		4,95			
		2,00			
	2,00	2,00	2,00	6,41	100,1
		2,05			

Tabelle III

Jodometrische Bestimmung des Furfurylalkohols durch Oxydation mit Bromchlor

Einwaage Furfuryl-alkohol, g/100 ml	Eingemessene Lösung, ml	Verbr. 0,1 *n* BrCl, ml		Gefunden Furfurylalkohol	
		Einzelwerte	Durchschnitt	mg	%
		10,72			
	10,00	10,71	10,72	26,29	98,7
		10,72			
		5,35			
0,2664	5,00	5,35	5,35	13,12	98,5
		5,34			
		2,17			
	2,00	2,16	2,16	5,30	99,9
		2,16			

Tabelle IV

Bestimmung des Furfurylalkohols über die bei der Oxydation mit Bromchlor gebildete Säure

Einwaage Furfurylalkohol, g/100 ml	Eingemessene Lösung, ml	Verbr. 0,1 *n* NaOH, ml		Gefunden Furfurylalkohol	
		Einzelwerte	Durchschnitt	mg	%
		8,10			
	10,00	8,12	8,12	26,55	99,7
		8,13			
		4,05			
0,2664	5,00	4,05	4,05	13,24	99,4
		4,07			
		1,62			
	2,00	1,60	1,61	5,27	98,8
		1,61			

Beschreibung der Verfahren

1. Jodometrische Bestimmung des Furfurols und des Furfurylalkohols auf Grund der Messung des Bromchlorüberschusses.

Reagenzien:

0,1 *n* Kaliumbromat-Kaliumbromid-Lösung zur Bromchlorierung [13] (2,7835 g Kaliumbromat und 3,9670 g Kaliumbromid in 1000 ml Lösung)

0.1 *n* Natriumthiosulfatlösung

20%ige Salzsäure

Kaliumjodid (fest)
Stärkelösung als Indikator

0,23—0,25 g Furfurol bzw. Furfurylalkohol werden analytisch genau eingewogen und in destilliertem Wasser gelöst. Die Lösung wird in einen 100-ml-Meßkolben gespült und ihr Volumen bis zur Marke ergänzt. Ein 10,00 ml betragender Anteil der Lösung wird in einem 200 ml fassenden, mit Glasstopfen versehenen Erlenmeyerkolben mit 20,00 ml Bromat-Bromid-Lösung versetzt und mit 5 ml Salzsäure angesäuert. Nach einer Wartezeit von 15—20 Minuten werden 0,50 g Kaliumjodid in den Kolben gestreut, und der Kolbeninhalt wird so geschüttelt, daß sich die Flüssigkeit auch am Schliff austauscht. Das Lösungsvolumen wird mit destilliertem Wasser auf etwa 100 ml ergänzt, dann wird das ausgeschiedene Jod mit Natriumthiosulfat-Meßlösung titriert.

1 ml Bromchlor-Lösung entspricht 2,402 mg Furfurol bzw. 2,4525 mg Furfurylalkohol.

2. Bestimmung von Furfurol und Furfurylalkohol über die bei der Oxydation mit Bromchlor gebildete Säure

Reagenzien:

0,1 *n* Natriumhydroxydlösung
gesättigtes Bromwasser
5%ige Quecksilber(II)chloridlösung
0,1 *n* Natriumthiosulfatlösung
0,2%ige alkoholische Methylrotlösung
Kaliumjodid (fest)

10,00 ml betragende Anteile der oben beschriebenen Furfurol- bzw. Furfurylalkohol-Lösung werden in einen 100 ml fassenden, mit Glasstopfen versehenen Erlenmeyerkolben pipettiert. Das Volumen der Lösung wird auf 20—30 ml ergänzt. Nun wird Bromwasser bis zur bleibenden Verfärbung der Lösung in den Kolben getropft, dann werden noch weitere 3—5 ml Bromwasser und 5 ml Quecksilber(II)chloridlösung zugefügt. Nach einer Wartezeit von 20—30 Minuten wird soviel Kaliumjodid in den Kolben gestreut, daß sich das anfangs ausgeschiedene Quecksilber(II)jodid löst. Nach mehrmaligem Schütteln des Kolbeninhaltes gibt man Natriumthiosulfatlösung bis zum Verschwinden der Jodfarbe hinzu, dann titriert man in Gegenwart von Methylrot-Indikator mit Natriumhydroxyd-Meßlösung. (Der eventuelle Säuregehalt der Reagenzien wird mit Blindproben kontrolliert.)

1 ml 0,1 *n* Natriumhydroxydlösung entspricht 3,203 mg Furfurol bzw. 3,270 mg Furfurylalkohol.

ZUSAMMENFASSUNG

Furfurol und Furfurylalkohol reagieren mit Bromchlor in wäßriger Lösung schnell und eindeutig (Äquivalentgewicht = Molekulargewicht/4). Bei der Reaktion bilden sich 3 Äquivalente Säure. Verfasser arbeiteten eine jodometrische und eine auf der Messung der in der Reaktion gebildeten Säure beruhende Methode zur Bestimmung dieser Verbindungen aus. Auch der Mechanismus der Oxydationen mit Brom und Bromchlor wurde untersucht; über diese Untersuchungen wird in einer separaten Mitteilung ausführlich berichtet.

LITERATUR

1. Pervier, N. C., Gortner, R. A.: Ind. Eng. Chem. **15,** 1255 (1923).
2. Powell, W. J., Whitakker, H.: J. Soc. Chem. Ind. **43,** 35T (1924).
3. Hughes, E. E., Acree, S. F.: Ind. Eng. Chem. Anal. Ed. **6,** 123 (1934).
4. Kline, G. M., Acree, S. F.: Bur. Standards J. Research **8,** 25 (1932).
5. Iddles H. A., Robbins, P. J.: Ind. Eng. Chem. Anal. Ed. **5,** 55 (1933).
6. Magisted O. C.: Ind. Eng. Chem. Anal. Ed. **5,** 253 (1933).
7. Hughes, E. E., Acree, S. F.: Ind. Eng. Chem. Anal. Ed. **9,** 318 (1937).
8. Teunissen P. H.: Anal. Chem. **21,** 620 (1949).
9. Hughes, E. E., Acree, S. F.: J. Res. nat. Bur. Standards **24,** 175 (1940); Ch. Z. **1,** 40 (1941).
10. Clauson-Kaas, N., Limborg, F.: Acta Chem. Scand. **1,** 619 (1947).
11. Clauson-Kaas, N.: Acta Chem. Scand. **1,** 379 (1947).
12. Clauson-Kaas, N., Farkstorp, J.: Acta Chem. Scand. **1,** 415 (1947).
13. Schulek, E., Burger, K.: Talanta **1,** 219 (1958); Magy. Tud. Akad. Kém. Tud. Oszt. Közl. **12,** 9 (1959).

Margit Szakács-Pintér
László Maros
} Budapest VIII., Múzeum krt. 4/b.

Acta Chimica Academiae Scientiarum Hungaricae Tomus 56 (2), pp. 93—97 (1968)

THE PHASE POTENTIAL BETWEEN GLASS AND LIQUID AMMONIA SOLUTIONS OF REDUCED VAPOUR PRESSURE

B. LENGYEL and B. CSÁKVÁRI

(Department of General and Inorganic Chemistry, L. Eötvös University and Research Group for Inorganic Chemistry of the Hungarian Academy of Sciences, Budapest)

Received May 17, 1967

The glass electrode is known to be satisfactorily applicable to the measurement of proton or oxonium ion activity as well as to the potentiometric end-point indication of acid-base titrations in anhydrous solvents [1, 2]. After some earlier unsuccessful attempts [3], BAUMANN and SIMON [4] succeeded in applying special, extraordinarily low-resistance glass electrodes (see also LENGYEL and TILL [5]) to the measurement of the activity of the ammonium ion in liquid ammonia, though at −34 °C the resistance of the electrode was still in the order of 10^3 Mohm.

The vapour pressure of liquid ammonia can be considerably reduced by dissolving alkali metal salts in it [6, 7], *e.g.* p_{NH_3} is 430 mm Hg at 20 °C for a solution having the composition of NaI 3,3 NH_3 [8], thus the study of ammoniacal electrolytic cells at normal temperatures is rendered possible. HERLEM [9] studied the behaviour of the hydrogen electrode in liquid ammonia solutions of reduced vapour pressure containing NH_4I. He found that the potential of the hydrogen electrode followed the NERNST equation in the concentration range from $1 \cdot 10^{-1}$ to $1 \cdot 10^{-3}$ mole/l at 20 °C. It was deemed interesting to study the behaviour of the glass electrode in an anhydrous system which contains a relatively high quantity of alkali ions. As the experiment is carried out at normal temperature, there are no particular requirements regarding the glass electrode; therefore, the classical MACINNES—DOLE glass electrode [10] which has been adequately studied in various systems is suitable for the measurements.

The following cell was used for the experiments:

Ag	AgI, $1 \cdot 10^{-2} M$	NH_4I $1 \cdot 10^{-1} M$	glass membrane	NH_4I, c	AgI $1 \cdot 10^{-2} M$	Ag

The "solvent" was NaI 3,3 NH_3, and c was varied between $1 \cdot 10^{-1}$ and $1 \cdot 10^{-3}$ mole/l.

The resistance of the cell was in the order of magnitude of 10 Mohm; the E.M.F. could be measured with good reproducibility. The E.M.F. of the

symmetric cells at $c = 1 \cdot 10^{-1}$ mole/l varied from 1 to 6 mV, indicating that the asymmetry potential of the glass electrode in this system was similar to that encountered in aqueous solutions.

Fig. 1 shows the dependence of the potential of the glass electrode on the ammonium ion concentration (c). It is apparent that a change by one order of magnitude in the ammonium ion concentration causes a change of 58 mV in the potential of the glass electrode, *i.e.* the Nernst correlation is obeyed.

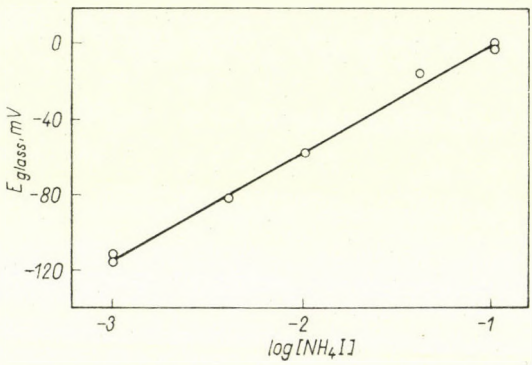

Fig. 1. Potential of the glass electrode *vs.* the ammonium ion concentration

The ammonium ion response of the glass electrode and the hydrogen electrode can be best compared using the following galvanic cell:

$$\mathrm{Ag} \mid \underset{1\cdot10^{-2}M}{\mathrm{AgI}},\ \underset{1\cdot10^{-1}M}{\mathrm{NH_4I}} \mid \underset{\text{membrane}}{\text{glass}} \mid \underset{c}{\mathrm{NH_4I\ or\ NaNH_2}} \mid \underset{p_{H_2}=\text{const.}}{\mathrm{H_2\ (Pt)}}$$

as the E.M.F. of this cell is constant and independent of c when the potential of the glass electrode depends only on the ammonium ion concentration.

Table I

The E.M.F. of the cell containing the glass electrode and the hydrogen electrode

NH_4I c	E. M. F. mV	$NaNH_2$ c	E. M. F. mV
$1 \cdot 10^{-1}$	210	$1 \cdot 10^{-3}$	560
$1 \cdot 10^{-2}$	210	$1 \cdot 10^{-2}$	620
$1 \cdot 10^{-3}$	211	$5 \cdot 10^{-2}$	660

It is apparent from the data in Table I that in acidic media the glass electrode has an ideal ammonium ion response. As the change of the E.M.F. in solutions of basic character corresponds more or less to the ideal potential

change of the hydrogen electrode of the cell, it may be concluded that in these solutions the glass electrode is insensitive to changes in the ammonium ion concentration.

In order to decide whether the presence of other alkali ions had any effect on the potential, the following galvanic cell was studied:

Ag	AgI, $1 \cdot 10^{-2} M$	$NaNH_2$, $5 \cdot 10^{-2} M$	LiBr c	glass membrane	NH_4I, $1 \cdot 10^{-1} M$	AgI $1 \cdot 10^{-2} M$		Ag

In the concentration interval from $c = 0$ to $1 \cdot 10^{-1}$ mole/l the E.M.F. of the cell was constant, indicating that, owing to the high sodium ion concentration, the lithium ions did not influence the electrode potential.

The liquid ammonia solutions of reduced vapour pressure were made by saturating the required quantity of NaI at 0 °C with NH_3 gas, dried over KOH and the solution was dehydrated with Mg_3N_2 according to HERLEM's method [8, 9]. The hydrogen electrode was prepared on the basis of HERLEM's experiments: a Pt electrode coated with platinum in an aqueous solution was used. The sum of the partial vapour pressures of hydrogen and ammonia was one atmosphere. Since the vapour pressure of liquid ammonia solution depends on the salt concentration, the ratio of the partial vapour pressures of H_2 and NH_3 had to be kept constant. This was ensured in the following way: the hydrogen gas prior to be introduced into the measuring cell was bubbled through a washing bottle containing NaI 3,3 NH_3 saturated with $NaNH_2$. The latter ensured the drying of the gas mixture by the reaction:

$$NaNH_2 + H_2O = NaOH + NH_3.$$

The Ag/Ag^+ electrode, used as the reference electrode, was prepared by the method of BADOZ-LAMBLING and HERLEM [11].

The glass electrode was prepared from MACINNES–DOLE glass [10] and soaked in 0.1 N hydrochloric acid as usual. Prior to measurements the air-dried glass electrodes were soaked in NaI 3,3 NH_3 solution for 12 hours.

The E.M.F. was measured with a Radiometer pH-meter 22 type instrument.

The condition of the ammonium ion response of the glass electrode is that a constant proton (ammonium ion) activity be developed in the surface layer of the glass in contact with the liquid ammonia solution. The formation of a considerable amount of Si—OH groups in the silicate glass as a consequence of the action of water during the melting, is a well-known fact [12]. Under the influence of the moisture adsorbed, and during soaking in an aqueous solution the ion exchange $Na^+ \rightleftharpoons H_3O^+$ may occur in the surface layer, which finally results in a given proton activity [13]. If such a glass surface is brought into contact with liquid ammonia, the H_2O molecules can be replaced by NH_3 molecules in the surface layer of the glass, where they may take over the role of the proton acceptor.

It seems theoretically possible that the NH_3 molecules are bound to the silicate skeleton by hydrogen bridges provided steric conditions are favourable. It should be noted that during the interaction of metasilicic acid and liquid ammonia, the bulk of the water content of silicic acid might be replaced by ammonia under formation of an ammoniacate [14].

CHAPMAN and HAIR [15] subjected the surface layer of porous Vycor glass, which had been pretreated with NH_4F, to the action of NH_3 gas and identified the N—H valence vibrations of the NH_4^+ ion in the infrared spectrum of the glass. These authors believe that the ammonium ions are formed on the silanol groups in the surface layer, by the chemosorption of ammonia.

To clarify the role of ammonia, we examined the penetration of ammonia (ammonium ions) in the MACINNES–DOLE electrode glass when it was allowed to stand in liquid ammonia solution.

The quantity of bound nitrogen which had penetrated the surface layer was determined by the following method: rods of a few mm diameter were drawn from the glass; these were subjected to pre-soaking in hydrochloric acid in usual manner, and then dried in air. The rods were placed into the NaI 3,3 NH_3 solution for 12 hours, then immersed in a 1% hydrofluoric acid solution for five seconds and rinsed with distilled water for two seconds. Finally they were etched with 1% hydrofluoric acid solution for 10 minutes. The ammonia content of the etching solution was determined by means of a Parnass—Wagner microdistillation apparatus.

The ammonia content of the rinsing solution was by about half an order of magnitude lower than that of the etching solutions. This excluded the possibility that the ammonia bound on the surface by adsorption had a significant influence on the measured ammonia content of the surface layer. The reproducibility of the results was $\pm 30\%$.

The quantity of the nitrogen expressed as NH_4^+ found in the surface layer of the rods soaked in solutions of $1 \cdot 10^{-2} M$ $NaNH_2$ in NaI 3,3 NH_3, was $2.4 \cdot 10^{-4}$ g NH_4^+ per cm^2 of glass surface; in the case of rods soaked in NH_4NO_3 1,3 NH_3 this value was $2.8 \cdot 10^{-4}$ g NH_4^+ per cm^2.

These data indicate that during soaking in liquid ammonia a considerable quantity of bound nitrogen enters the surface layer. It is noteworthy that the quantity of bound nitrogen in the surface layer is practically independent of the presence of ammonium salts in the solutions used for the soaking. These facts support our theory on the proton acceptor exchange in the surface layer of glass electrodes and its effect on the electrode potential [13].

SUMMARY

The behaviour of the MACINNES–DOLE type glass electrodes has been studied in solutions of liquid ammonia of reduced vapour pressure (NaI 3,3 NH_3). In acid media the potential of the glass electrode depends on the ammonium ion concentration. In basic solutions containing sodium amide, the glass electrode does not exhibit an ammonium ion response.

REFERENCES

1. IZMAILOV, N. A.: Elektrokhimiya Rastvorov. Izd. vtoroye, Izd. Khimiya, Moscow, 1966. p. 498.
2. MATTOCK, G.: pH Measurement and Titration. Heywood Comp. Ltd., London, 1961. p. 336.
3. HEYN, A. H. A., BERGIN, M. J.: J. Am. Chem. Soc. **75,** 5150 (1953).
4. BAUMANN, W. M., SIMON, W.: Z. Anal. Chem. **216,** 273 (1966).
5. LENGYEL, B., TILL, F.: Egypt. J. Chem. **1,** 99 (1958).

6. JANDER, J.: Chemie in nichtwässerigen ionisierenden Lösungsmitteln. Band I, Teilband 1' Anorganische und allgemeine Chemie in flüssigem Ammoniak. Akademie-Verlag' Berlin, 1966. p. 34.
7. SELLERS, D. E., LEONARD, G. W.: Anal. Chem. **34,** 1457 (1962).
8. HERLEM, M.: Réactions acides-bases dans l'ammoniacate d'iodure de sodium et l'ammoniac liquide. Dissertation, Université de Paris, 1966. p. 17.
9. HERLEM, M.: Bull. Soc. Chim. Fr. **1965,** 3329.
10. MACINNES, D. A., DOLE, M.: J. Am. Chem. Soc. **52,** 29 (1930).
11. BADOZ-LAMBLING, J., HERLEM, M.: Bull. Soc. Chim. Fr. **1964,** 90.
12. SCHOLZE, H.: Glastechn. Ber. **32,** 142 (1959).
13. LENGYEL, B., BOKSAY, Z., CSÁKVÁRI, B.: A szilikátüvegek elektromos tulajdonságai. Akadémia Kiadó, Budapest, 1966. p. 137.
14. BILTZ, W., RAHLFS, E.: Z. Anorg. Allg. Chem. **244,** 281 (1940).
15. CHAPMAN, I. D., HAIR, M. L.: Trans. Faraday Soc. **61,** 157 (1965).

Béla LENGYEL
Béla CSÁKVÁRI
} Budapest VIII., Múzeum krt. 6—8.

Acta Chimica Academiae Scientiarum Hungaricae Tomus 56 (2), pp. 99—108 (1968)

BEITRAG ZUR MANGAN-(II)-NITRAT-PYROLYSE, I

DIE RÖNTGENOGRAFISCHE ZUSAMMENSETZUNG UND DAS WIDERSTANDSVERHALTEN VON PYROLYSEBRAUNSTEIN

G. HAHN und W. DUSDORF

(VEB Kondensatorenwerk Freiberg, Abt. Forschung und Entwicklung)

Eingegangen am 7. Juli 1967

1. Einleitung

Das Problem der Herstellung von Braunstein durch thermische Zersetzung von Mangan-(II)-nitrat zeichnet sich in jüngster Zeit durch eine besondere Aktualität seiner Bearbeitung aus. Von grundlegendem Interesse ist hierbei die Reproduzierbarkeit der Herstellung von Mangandioxyd in bezug auf seine chemischen, physikalisch-chemischen und physikalischen Eigenschaften. Neueren Publikationen von HEGEDÜS [1], BRENET [2] sowie GATTOW und GLEMSER [3] ist zu entnehmen, daß bei der Pyrolyse des Mangan-(II)-nitrats Braunsteine unterschiedlicher röntgenografischer Strukturen — wie ε-, η-, β'- und β-MnO_2 — entstehen, die durch wechselnde Intensitätsgänge der einzelnen Röntgenpeaks feststellbar sind (in dieser Arbeit soll die Nomenklatur von GATTOW und GLEMSER [3] zur Anwendung kommen). Aber nicht nur durch Wechsel des Intensitätsgangs entstehen verschiedenartige Röntgendiagramme, sondern auch durch das Auftreten von grundsätzlich anderen Phasen im Pyrolyseprodukt, wie γ-MnOOH und α-Mn_2O_3, erweist sich das ganze Problem der Braunsteinbildung durch Pyrolyse als sehr komplex. So berichtet z. B. BRENET [2], daß bei der thermischen Zersetzung des Mangannitrats bei 150 °C unter Evakuierung der nitrosen Gase β-MnO_2 mit α-Mn_2O_3-Anteilen, bei der Zersetzung in Kontakt mit den nitrosen Gasen der Reaktion hauptsächlich α-Mn_2O_3 neben wenig β-MnO_2 an den oberen Partien des Pyrolysekuchens und bei NO-Atmosphäre während der Zersetzung praktisch nur α-Mn_2O_3 entsteht.

Die Erfahrungen zeigen natürlich, daß sich nicht alle Verhaltensweisen bezüglich der Entstehung von End- und Zwischenprodukten streng wiederholen lassen, und nur die strengste Konstanthaltung aller Versuchsbedingungen (z. B. Temperatur, Gasatmosphäre und -druck) im Hinblick auf röntgenografische Struktur und chemische Zusammensetzung zu weitestgehend ungestörten und reproduzierbar herstellbaren Braunsteinen führen kann, wie den umfangreichen Arbeiten und Überlegungen von HEGEDÜS [1] zu entnehmen ist.

Ziel dieser Bearbeitung war es, den Einfluß der Anwesenheit von niederen Manganoxyden auf das elektrische Leitfähigkeitsverhalten von β-Braunstein-

pulvern festzustellen, wobei zwischen röntgenografischer Zusammensetzung der Proben und chemisch-analytischen Werten eine Relation gefunden werden sollte.

2. Darstellung der Präparate

Bei der thermischen Zersetzung von Mangan-(II)-nitrat bei verschiedenen Temperaturen (180—350 °C) wurde wiederholt die Ausbildung von farblich unterschiedlichen Ringzonen im Pyrolyseprodukt beobachtet, was den Verdacht nahelegte, daß diese Unregelmäßigkeiten von einer differenzierten

Tabelle I

x-Wert der Formel MnO_{1+x} von Pyrolyseproben

Probe Nr.	x-Wert
1	0,674
2	0,839
3	0,853
4	0,877
5	0,882
6	0,958
7	0,973
8	0,985
9	0,990

Zusammensetzung herrühren. Die nähere Auswertung solcher Ringzonen hinsichtlich ihrer chemisch-analytischen Zusammensetzung ergab eine Reproduzierbarkeit dieses Verhaltens insofern, daß stets der mittlere kompakte Teil des Zersetzungsproduktes der Idealzusammensetzung von $MnO_{2,0}$ am nächsten kam, während dünne glasige Stellen an den Rändern des Pyrolyseproduktes immer eine Zusammensetzung in Richtung $MnO_{1,5}$ aufweisen. Ausgehend von diesen Tatsachen erfolgte die Herstellung des Ausgangspräparates für die nachfolgenden Untersuchungen durch Zersetzung von 1 kg $Mn(NO_3)_2 \cdot 6H_2O$ (max. Verunreinigung 0,25%) bei 350 °C über einen Zeitraum von 20 h unter Benutzung einer Porzellanschale in einem Hochtemperaturschrank, aus dem lediglich durch eine angebrachte Öffnung die Zersetzungsgase entweichen konnten, wobei die entstehenden Produkte praktisch immer in Kontakt mit den Zersetzungsgasen standen.

Anschließend wurden an verschiedenen Stellen des Zersetzungsproduktes lokalisierte Proben entnommen und chemisch-analytisch mit Hilfe der KJ Methode der sogenannte »aktive Sauerstoff« bestimmt, dessen Werte in Tabelle

I zusammengestellt sind. Der auf diese Weise ermittelte x-Wert der Formel MnO_{1+x} der Braunsteinproben ist mit einer Genauigkeit von $\pm 0{,}005$ x-Einheiten reproduzierbar.

Die Probe Nr. 1 mit dem x-Wert von 0,674 stammt nicht aus dem gleichen Umsetzungsprodukt, wurde jedoch bei einem anderen Versuch festgestellt und dient an sich im vorliegenden Fall zu einer Komplettierung des angegebenen x-Wertspektrums. Ergänzend wäre noch zu bemerken, daß solche relativ niedrigen x-Werte, die schon fast an die Zusammensetzung des Oxyds Mn_2O_3 mit $x = 0{,}5$ angrenzen, bei Umsetzungen dieser Art selten vorkommen und sich nicht immer isolieren lassen.

3. Röntgenografische Untersuchungen

Das breite x-Wertspektrum warf die Frage nach der röntgenografischen Struktur dieser Braunsteine auf. Die Präparation der Substanzen erfolgte auf durch Deckgläser begrenzte Glasscheiben von jeweils gleicher Fläche (25×15 mm), indem die auf eine Kornfeinheit von < 36 μm abgesiebten Proben auf die mit Vaseline angefettete Glasscheibe schwach angedrückt wurden. Die Feinheit der Proben war besonders wichtig, da die β-MnO_2-Interferenz mit $d = 3{,}11$ sehr texturanfällig ist. Die entsprechenden Röntgenogramme ($Co_{K\alpha}$-Strahlung 30 kV, 16 mA, aufgenommen mit der Iso-Debyeflex I in Verbindung mit dem Berthold-Goniometer) zeigten mit abnehmendem x-Wert eine Steigerung des Gehaltes an α-Mn_2O_3, was an der stärksten Interferenz des α-Mn_2O_3 mit $d = 2{,}70$ erkennbar war. In allen Proben unterhalb $x = 0{,}985$ ließ sich α-Mn_2O_3 einwandfrei nachweisen. MnO und Mn_3O_4 konnten nicht festgestellt werden.

Die kontinuierliche Abhängigkeit des x-Wertes von dem röntgenografisch sichtbaren α-Mn_2O_3-Anteil wurde quantitativ ausgewertet, indem jeweils innerhalb einer Aufnahme die in Millimeter ausgemessene Höhe der Interferenz I_1 des β-MnO_2 ($d = 3{,}11$) ins Verhältnis zur Höhe der Interferenz des α-Mn_2O_3 ($d = 2{,}70$) gesetzt wurde $\left(\frac{I_1}{I_2}\right)$. Die dazu hergestellten Eichproben (Mischung von β-MnO_2 mit $x = 0{,}99$ und α-Mn_2O_3, hergestellt aus β-MnO_2 bei 700 °C) wurden auf diese Weise ausgewertet und in Form einer Eichkurve dargestellt (Abb. 1). Die β-MnO_2-Eichprobe zeigte keine α-Mn_2O_3-Interferenz mit $d = 2{,}70$. Eine genauere quantitative röntgenografische Bestimmung in Form der Methode des inneren Standards bzw. unter Zugrundelegung der Fläche der Peaks war im vorliegenden Falle nicht nötig, wie der weiter unten beschriebene Vergleich zu den chemisch-analytischen Werten zeigen soll.

Mit Hilfe dieser Eichkurve konnten für das x-Wertspektrum folgende α-Mn_2O_3-Anteile ermittelt werden (Tab. II):

Tabelle II

Röntgenografisch ermittelte α-Mn_2O_3-Gehalte der Pyrolyseproben

Probe Nr.	x-Wert	% Mn_2O_3
1	0,674	78
2	0,839	40
3	0,853	44
4	0,877	36
5	0,882	35
6	0,958	13
7	0,973	5
9	0,990	3

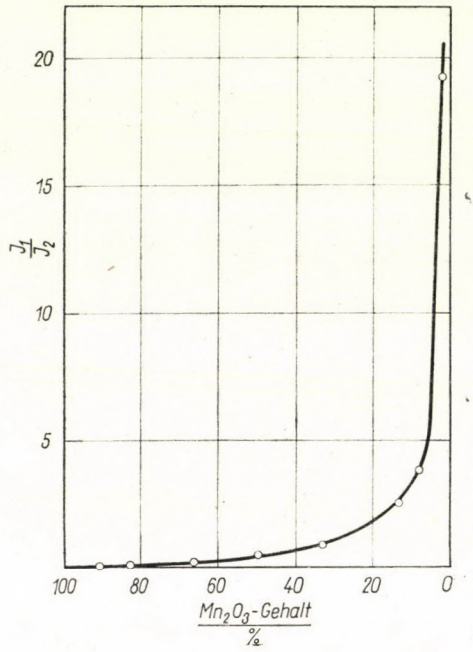

Abb. 1. Eichkurve zur α-Mn_2O_3-Bestimmung in β-Braunsteinproben

Die sehr gute Übereinstimmung der Röntgendiagramme der Eichsubstanzen mit den Untersuchungsproben, die eine prozentual sehr ähnliche Zusammensetzung aufweisen, ist in Abb. 2 zu sehen, wonach bis zu einem Gehalt von 2% α-Mn_2O_3 in den Eichproben dieses noch durch eine Interferenz mit $d = 2{,}70$ wahrzunehmen ist. Hieraus folgt, daß ein Produkt mit reinen β-

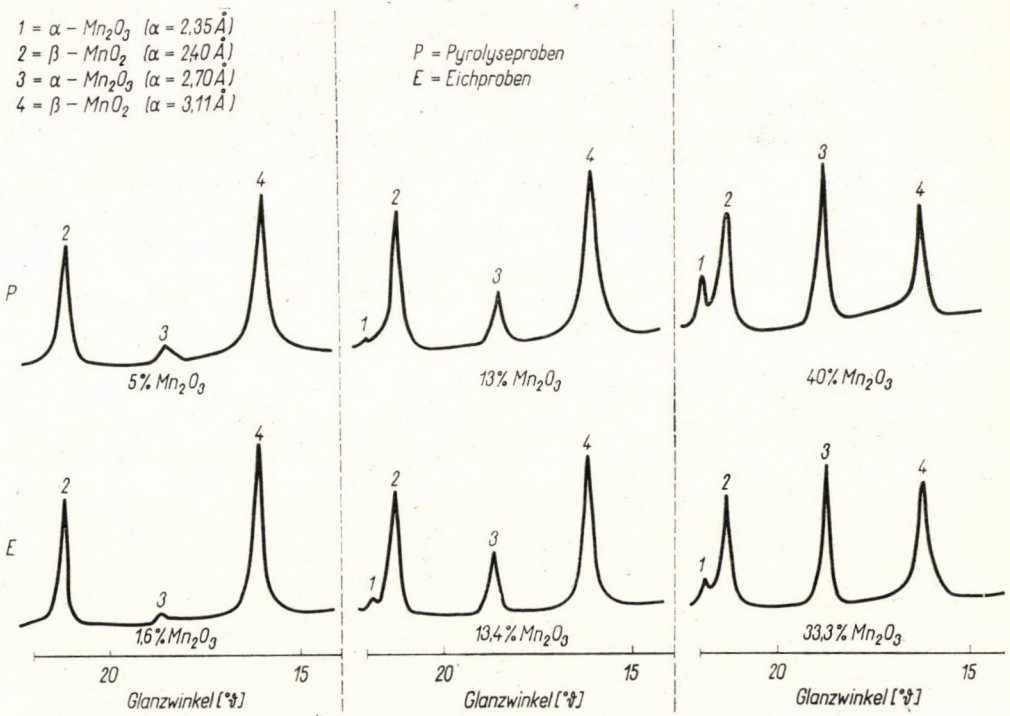

Abb. 2. Röntgenografische Übereinstimmung zwischen Eich- und Untersuchungsproben

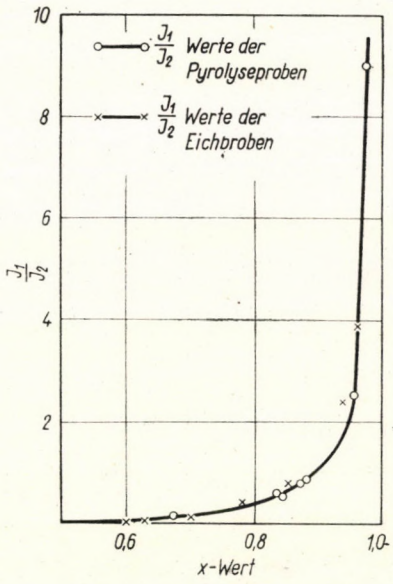

Abb. 3. $\frac{I_1}{I_2}$-Werte der Eich- und Untersuchungsproben in Abhängigkeit von chemisch-analytischer Zusammensetzung

Interferenzen doch noch α-Mn_2O_3 enthalten kann — und damit einen x-Wert $< 2{,}0$ —, welches sich nur der röntgenografischen Nachweisbarkeit entzieht.

Die Versuchsreihe kann ausreichend beweisen, daß die analytisch festgestellte Nichtstöchiometrie auf einen erhöhten bzw. wechselnden α-Mn_2O_3-Gehalt zurückzuführen ist.

Die gute Übereinstimmung im Verhalten zwischen Eich- und Untersuchungsproben ist nochmals aus Abb. 3 ersichtlich, wo die $\frac{I_1}{I_2}$-Verhältnisse der röntgenografischen Messung der Eichproben über ihren theoretisch aus dem Mischungsverhältnis berechneten x-Wert aufgetragen wurden, und zum Vergleich die entsprechende Kurve der Untersuchungsproben beigefügt ist.

Einer Gegenüberstellung der aus den bekannten Mischungsverhältnissen der Eichsubstanzen berechneten x-Werte mit ihren chemisch-analytisch bestimmten x-Werten kann entnommen werden, daß die angewandte KI-Methode eine ausreichende Genauigkeit liefert (Tab. III).

Tabelle III

Vergleich der titrimetrisch ermittelten und theoretisch errechneten x-Werte der Eichproben

x-Wert, theoret.	x-Wert, prakt.
1,000	0,995
0,996	0,981
0,986	0,973
0,964	0,943
0,942	0,933
0,880	0,876
0,855	0,846
0,770	0,771
0,703	0,693
0,588	0,595

Durchgeführte ergänzende Mn-Bestimmungen nach der potentiometrischen Methode zur Ermittlung des O/Mn-Verhältnisses erfüllten bezüglich der Aussagefähigkeit der erhaltenen Werte nicht die in diese Methode gesetzten Erwartungen, so daß der komplexometrischen Methode weiterhin der Vorzug gegeben wurde. Über chemisch-analytische Probleme und derivatografische Untersuchungen zur Ermittlung der Zusammensetzung von β-Braunsteinen soll in einer folgenden Veröffentlichung berichtet werden.

4. Widerstandsmessungen

Die Widerstandsmessungen erfolgten in einer von RACHOW [4] entwikkelten Apparatur und die Auswertung in der von G. KADEN und G. HAHN [5] dargelegten Weise. Die Methode geht davon aus, daß in bestimmten Druck-

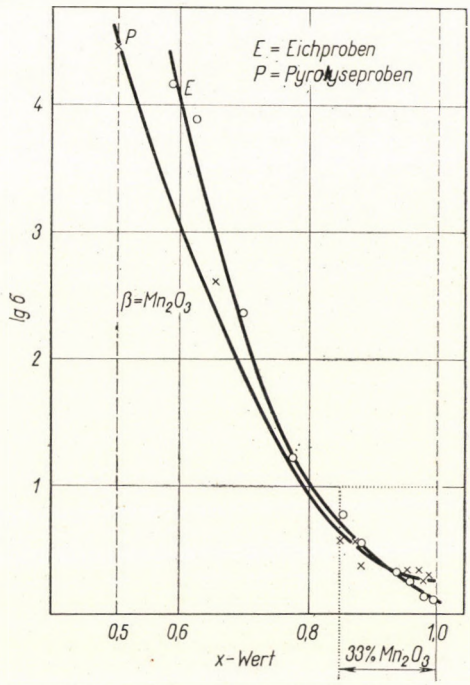

Abb. 4. Spezifischer Widerstand in Abhängigkeit vom x-Wert

bereichen eine lineare Abhängigkeit zwischen dem Logarithmus des spezifischen Widerstandes und dem Logarithmus der Tablettenlänge besteht.

Durch Extrapolation der Widerstandskurve auf einen Wert 1, der sich aus der Dichte des kompakten Körpers berechnen läßt, kann der entsprechende Wert lg σ (σ = spezifischer Widerstand) ermittelt werden. In jedem Fall gelangten Pulver zur Untersuchung, die ein Sieb von < 36 μm Maschenweite passiert hatten. Die Widerstandsmessungen erfolgten mittels einer Kunststoffmatrize von 0,7 cm $\varnothing$ und einer Einsatzmenge von 0,6 g der Untersuchungs- und Eichproben bei 0,6 V durch Strommessung. Aufgrund des identischen Verhaltens der Untersuchungs- und Eichproben in röntgenografischer und chemisch-analytischer Hinsicht war für die Widerstandsmessung ebenfalls eine interessante Abhängigkeit zu erwarten.

In Abb. 4 sind die logarithmischen Werte des spezifischen Widerstandes der Eich- und Untersuchungsproben über dem x-Wert aufgetragen. Danach

weisen die Pyrolyseproben bis zu einem Wert von $x = 0{,}85$ nur geringe Widerstandsänderungen auf ($x = 0{,}99/\sigma = 2{,}0\ \Omega$ cm und $x = 0{,}853/\sigma = 3{,}8\ \Omega$ cm), während nach höheren α-Mn_2O_3-Anteilen hin ($x < 0{,}85$) der spezifische Wider-

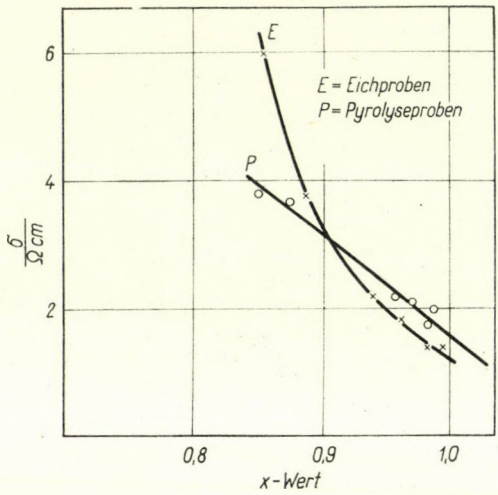

Abb. 5. Vergrößerte Darstellung des spezifischen Widerstandes im Bereich $x = 1{,}00 - 0{,}85$

stand rasch ansteigt, um bei reinem α-Mn_2O_3 schließlich eine um 4 Zehnerpotenzen schlechtere Leitfähigkeit zu erreichen ($\sigma = 30200\ \Omega$ cm).

Die Eichproben bewegen sich in der vergleichbaren Größe der x-Werte auch innerhalb der Größenordnung wie die Pyrolyseproben (reines β-$MnO_2/\sigma =$

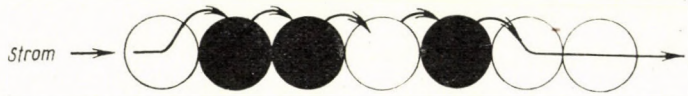

Abb. 6. Schematische Darstellung des Stromflusses in den Eichproben

$= 1{,}3\ \Omega$ cm; $x = 0{,}845/\sigma = 6{,}0\ \Omega$ cm). Unterhalb von $x = 0{,}85$ findet man den gleichen steilen Anstieg des Widerstandes, wie bei den Pyrolyseproben. Die erhaltenen Resultate bestätigen im wesentlichen Beobachtungen von DROTSCHMANN [6], daß der Widerstand von Braunsteinpulvern sich innerhalb weiter Grenzen der chemischen Zusammensetzung (x-Wert) wenig ändert. Die geringfügigen Abweichungen des spezifischen Widerstandes im Gebiet der Zusammensetzung $x = 1{,}00$ bis $x = 0{,}85$ (Abb. 5) zwischen Eich- und Untersuchungsproben können folgendermaßen gedeutet werden: In den Eichproben muß der Strom von Korn zu Korn, also auch über die bedeutend schlechter leitenden Mn_2O_3-Körner, wandern, wobei sich der Widerstand mit zunehmendem Mn_2O_3-Anteil ziemlich stetig vergrößert (vgl. Abb. 4). Den Mechanismus

der Stromleitung könnte man der Abb. 6 entnehmen. Die geringe Abhängigkeit des spezifischen Widerstandes in den Pyrolyseproben bei x-Werten zwischen 0,85 und 1,00 läßt sich aus der Tatsache erklären, daß in diesem Falle sicher nicht nur ein heterogenes, durch Korngrenzen abgeteiltes Gemenge zweier Oxyde vorliegt, sondern vom Prozeß der Pyrolyse her innere oder äußere Schichten oder Bezirke von α-Mn_2O_3 am β-MnO_2-Korn vorliegen. Den Mechanismus der Stromleitung könnte man sich nach Abb. 7 vorstellen:



Abb. 7. Schematische Darstellung des Stromflusses in den Pyrolyseproben

Danach gelingt es, daß der Strom trotz gleicher röntgenografischer Zusammensetzung der Pyrolyse- und Eichproben teilweise Bezirke größeren Widerstandes umgehen kann, so daß als Resultat ein geringerer Faktor des

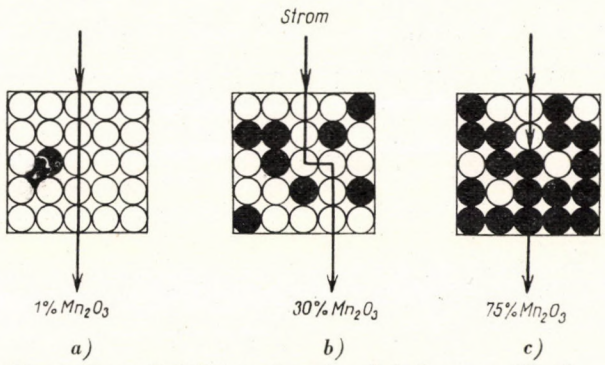

Abb. 8. Stromfluß bei wachsenden Gehalten an α-Mn_2O_3

Anstiegs im x-Bereich 1,00—0,85 beobachtet wird. Bei extrem kleiner Korngröße werden sich beide Modellfälle (Eichproben, Untersuchungsproben) einander nähern, da dann auch im Falle der Untersuchungsproben ein heterogenes Gemenge der beiden Oxyde vorliegt und das Widerstandsverhalten in jedem Fall durch die Übergangswiderstände zwischen den Körnern und der Leitfähigkeit geprägt wird. Beiden Kurven in Abb. 4 gemeinsam ist der steile Anstieg bei x-Werten 0,85 und es ist interessant, daß bei einem Wert von $x = 0{,}85$ bereits 33% des Oxydgemisches als Mn_2O_3 vorliegen. Nach einem in Abb. 8 zweidimensional skizzierten Mechanismus des Stromdurchlaufs ist ersichtlich, daß bei kleinen Prozentgehalten praktisch überhaupt keine Abhängigkeit des Widerstandes auftritt, da der Strom genügend Wege findet, um über sehr gut leitende Körner zu fließen (vgl. Abb. 8a).

Auch bei 30% Mn_2O_3-Gehalt dürften sich immer noch Wege des geringsten Widerstandes finden lassen, obgleich bereits ein geringer Anstieg zu verzeichnen ist (vgl. Abb. 8b). Noch höhere Gehalte (75%) lassen jedoch einen ungehinderten Stromfluß bei homogener Verteilung nicht mehr zu (vgl. Abb. 8c), es kommt zum steilen Anstieg des Widerstandes.

ZUSAMMENFASSUNG

Die Widerstandsmessungen lassen in Verbindung mit den röntgenografischen Phasenbestimmungen einen direkten Zusammenhang erkennen. Im vorliegenden Falle war die in weiten Grenzen schwankende Nichtstöchiometrie röntgenografisch über einen wechselnden Gehalt an α-Mn_2O_3 erklärbar, wobei festgestellt werden konnte, daß Gehalte von 2,0% Mn_2O_3 wahrscheinlich nicht mehr röntgenografisch erfaßbar sind, und somit kleinste Abweichungen von der Stöchiometrie auch auf kleinste Mengen α-Mn_2O_3 zurückgeführt werden können. Diese Resultate ergeben sich eindeutig aus dem Auftreten der für daß β-MnO_2 und α-Mn_2O_3 typischen Röntgen-Interferenzen in allen Proben, und damit hat auch der von der Stöchiometrie abweichende Sauerstoffgehalt seine primäre Ursache in dem beigemengten α-Mn_2O_3. Es liegt somit nahe, daß das Sauerstoffdefizit im Falle der Pyrolyseproben nicht auf Sauerstofffehlstellen — ähnlich des im Rutiltyp kristallisierenden TiO_2 — zurückzuführen ist, d. h. das β-MnO_2-Gitter bei Sauerstoffabgabe in geringsten Mengen zu α-Mn_2O_3 zerfällt. Das Widerstandsverhalten soll in einer weiteren Bearbeitung unter veränderten Parametern (Temperatur, Gasatmosphäre und -druck) verfolgt werden, um weitere Aussagen über den bei der Pyrolyse auftretenden Zersetzungsmechanismus zu erhalten.

LITERATUR

1. Hegedüs, A. J.: Acta chim. Acad. Sci. Hung. **46,** 311—24 (1965).
2. Brenet, J.: C. R. Acad. Sci **259,** 2825—26 (1964).
3. Gattow, G., Glemser, O.: Zeitsch. anorg. allgem. Chem. **309,** 121—50 (1961).
4. Rachow, R.: Diplomarbeit, TH Dresden, 1961.
5. Kaden, G., Hahn, G.: Chem. Techn. **16,** 292—94 (1964).
6. Drotschmann, C.: Batterien **18,** 721—25 (1965).

G. Hahn
W. Dusdorf
92 Freiberg, Silberhofstr. 80. DDR

Acta Chimica Academiae Scientiarum Hungaricae Tomus 56 (2), pp. 109—115 (1968)

THE ANALYTICAL USE OF ION EXCHANGERS IN ORGANIC SOLVENTS, II

SWELLING AND FUNCTIONING PROPERTIES OF MACROPOROUS ION EXCHANGE RESINS

J. INCZÉDY and I. HŐGYE

(Institute of General and Analytical Chemistry, Technical University, Budapest)

Received August 10, 1967

The behaviour of some common ion exchange resins and their analytical use in organic solvents have been reported in an earlier paper [1]. Similar experiments have now been carried out to investigate the swelling and functioning properties of some macroporous ion exchange resins [2, 3] in different organic solvents. On the basis of distribution and kinetic measurements, it has been found that the chromatographic separation of aromatic acids on an ion exchange column is possible using ethanol as the solvent.

Experimental

Ion exchange resins: In the swelling experiments polystyrene-divinylbenzene-type, *Imac C 16 P*, *Imac C 8 P* (*Imacti*, Holland), *Lewatit SP 100* (*Bayer A. G.*, Germany) strongly acid resins, *Lewatit MP 500*, *Lewatit MP 600* strongly basic resins and *Lewatit MP 60*, *Imac A 20 P* weakly basic resins, all of the grain size 20—50 mesh, were used.

The resins were treated in the usual manner with acid and alkali solutions before use. Resin samples in hydrogen- and sodium form were prepared from the pre-treated and washed cation exchangers using 2*N* hydrochloric acid and 2*N* sodium chloride solutions, respectively. Similarly, OH-, Cl- and acetate form resins were prepared from the anion exchange resins using the suitable base or salt solution. The resin samples were washed and dried in vacuum. The capacity of the resins was determined by the usual method [2]. The capacity values found can be seen in Table I. In order to remove interfering soluble impurities from the resin samples used in the distribution and elution experiments, the resins converted to the required form were extracted with ethanol, using a Soxhlet apparatus.

Table I

Capacities of the ion exchange resins used in the experiments

Ion exchange resin	Form	Capacity, meq./g
Imac C 8 P	H	5.03
Imac C 16 P	H	3.57
Lewatit SP 100	H	5.03
Imac A 20 P	Cl	5.23
Lewatit MP 60	Cl	3.26
Lewatit MP 500	Cl	3.84
Lewatit MP 600	Cl	3.44

Solvents: Deionized water and reagent grade ethanol, dimethylformamide, dioxan and glacial acetic acid were used as solvents. The solvents were purified as described before [1].

Derivatographic measurements: To obtain information on the thermal stability of the macroporous resins investigated, derivatographic measurements were carried out with air-dried resin samples. The procedure was similar to that used before [1]. The derivatograms were compared with the derivatograms of conventional ion exchange resins. No significant difference between the thermal properties of the conventional and macroporous resins was found.

Swelling experiments: 0.5—1 g of the formed and dried resin sample was weighed and 20 ml of the solvent added in a glass vessel. The resin with the solvent was allowed to

Table II

Swelling and solvent uptake data of ion exchange resins in water and ethanol

Ion exchange resin (form)	Water		Ethanol	
	%	mole / g. eq.	%	mole / g. eq.
Imac C 8 P (H)	51.4	11.7	37.6	2.6
(Na)	50.4	12.5	3.1	0.2
Imac C 16 P (H)	62.5	26.0	24.3	2.0
(Na)	38.9	10.1	9.9	0.7
Lewatit SP 100 (H)	61.0	17.3	35.2	2.3
(Na)	58.1	17.0	5.9	0.3
Imac A 20 P (OH)	51.6	10.2	69.9	6.3
(Cl)	52.2	11.3	58.3	5.9
Lewatit MP 60 (OH)	52.8	18.0	44.9	5.1
(Cl)	54.9	21.2	41.4	4.8
Lewatit MP 500 (OH)	61.2	21.3	43.7	4.3
(Cl)	58.8	20.6	44.8	4.6
Lewatit MP 600 (OH)	54.7	18.3	35.1	3.2
(Cl)	51.0	16.8	28.2	2.5

Table III

Swelling and solvent uptake data of ion exchangers in dioxan, dimethylformamide and glacial acetic acid

Ion exchange resin (form)	Dioxan		Dimethylformamide		Glacial acetic acid	
	%	mole / g. eq.	%	mole / g. eq.	%	mole / g. eq.
Imac C 16 P (H)	21.3	0.9	19.9	1.0	37.6	2.8
(Na)	10.4	0.4	6,8	0.3	13.1	0.8
Imac A 20 P (OH)	54.4	2.3	55.5	3.0		
(Cl)	35.6	1.2	46.6	2.3	57.1	4.2
Lewatit MP 500 (OH)	27.3	1.1	9.6	0.4	57.6*	6.3*
[Cl]	21.4	0.8	8.4	0.3	41.6	3.1

* acetate form

stand for 24 hrs in the closed vessel, then filtered on a glass filter with short suction, and weighed. After weighing, the resin was dried in vacuum to constant weight, and weighed again. From the data obtained the solvent content of the swollen resin sample could be calculated. On the basis of the capacity values, the equivalent weight of the resins of different forms, and the moles of solvent per g.-eq. of resin were calculated. The results are summarized in Tables II and III.

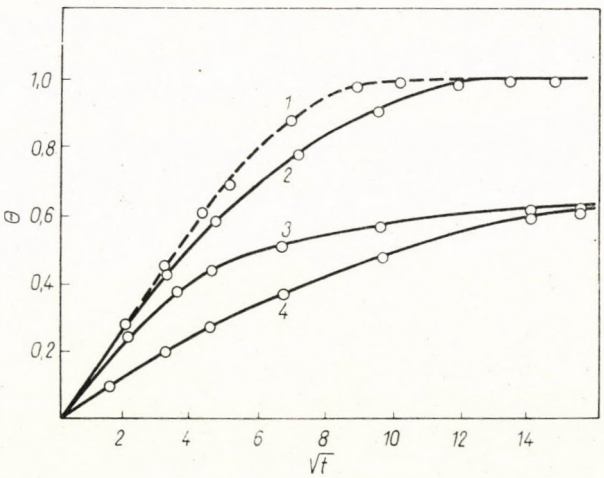

Fig. 1. The absorption of different compounds on ion exchange resins in ethanolic medium. *1* — Pyridine on *Imac C 16* (H) resin, *2* — Hydrochloric acid on *Imac A 20 P* (OH) resin, *3* — Benzoic acid on *Imac A 20 P* (OH) resin, *4* — Salicylic acid on *Imac A 20 P* (OH) resin

Kinetic measurements: Kinetic measurements were carried out with *Imac C 16 P* cation exchange resin (H-form) and *Imac A 20 P* anion exchange resin (OH-form) in ethanolic solution. 0.5 g of the dried resin, moistened with the solvent, was added to a solution (50 ml) containing the compound investigated, and was stirred vigorously with a mechanical stirrer. In each experiment the initial concentration of the solution was the same, always exceeding the total resin capacity. From time to time, a portion of the solution was analyzed by the spectrophotometric method, and on the basis of the data obtained the kinetic curve was constructed (Fig. 1). The calculated exchange ratio values were plotted against the square root of time. From the initial slopes of the curves the diffusion coefficients of the ions were also calculated, using the simplified equation of BOYD, ADAMSON and MEYERS [5], assuming the rate-determining step was the particle diffusion.

$$\Theta = 1.08 \sqrt{\frac{\pi^2 D_r}{r^2}} \sqrt{t},$$

where Θ = exchange ratio (absorbed amount of the ionic compound divided by the total capacity of the resin sample); r = resin particle diameter (cm); t = time (min.); D_r = inner diffusion coefficient.

The calculated diffusion coefficients are summarized in Table IV.

Distribution measurements: In order to determine the distribution ratio of some aromatic acids on the weakly basic *Imac A 20 P* resin in ethanolic solution containing acetic acid of different concentrations, batch experiments were carried out using 0.5 g of resin samples (equilibrated with the acetic acid solution and filtered beforehand) and 50 ml of acetic acid solution containing the aromatic acid. The initial concentration of the aromatic acid was 10^{-3} *M* in each experiment. The solution containing the resin was shaken gently for 24 hrs. After equilibration, the solution was analyzed, and the weight distribution coefficient (D) calculated.

$$D = \frac{\text{species absorbed} \quad \text{meq./g of dry resin}}{\text{species remained} \quad \text{meq./ml of solution}}$$

Table IV

Apparent inner diffusion coefficients of different ions in ethanolic medium, at 22 °C

Ion	Ion exchange resin (form)	D_r, cm²/sec
Chloride	Imac A 20 P (OH)	$8 \cdot 10^{-10}$
Benzoate	Imac A 20 P (OH)	$4 \cdot 10^{-10}$
Salicylate	Imac A 20 P (OH)	$1.1 \cdot 10^{-10}$
Pyridine	Imac C 16 P (H)	$5.7 \cdot 10^{-10}$

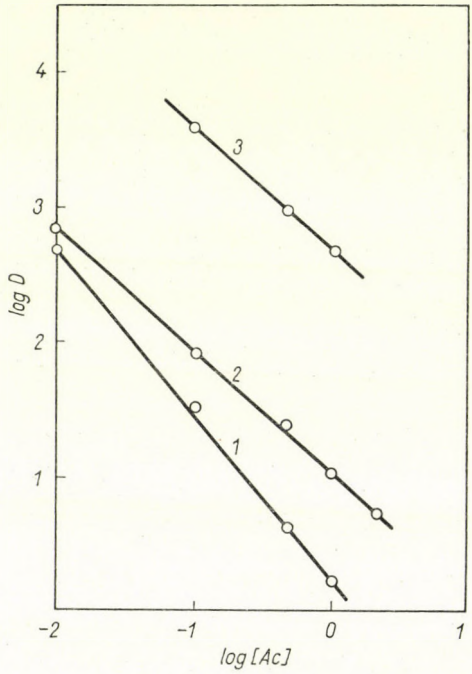

Fig. 2. Change of the distribution coefficients with the eluant concentration in ethanolic medium (*Imac A 20 P* acetate resin). *1* — Benzoic acid, *2*— Anthranilic acid, *3* —Salicylic acid

The distribution coefficients thus obtained were plotted against the concentration of the acetic acid in a logarithmic diagram (Fig. 2).

Elution experiments: For the separation of benzoic acid and anthranilic acid, an ion exchange column (0.6×15.5 cm) was prepared from *Imac A 20 P* resin (acetate-form). The pretreated, extracted resin previously has been ground to a particle size of 0.05—0.1 mm diameter. For each elution experiment 5 μmole acid was dissolved in 0.5 ml of ethanol, and poured on the resin column. The elution of benzoic acid and anthranilic acid was effected with ethanolic acetic acid solutions of 0.5 and of 2 *N* concentration, respectively, at a flow rate of 1 ml/12 min. The effluent was collected in 1-ml portions by means of an automatic fraction collector. Each of the fractions was diluted to 4 ml and analyzed. On the basis of the obtained data, elution diagrams were constructed (Fig. 3).

Determination of aromatic acids and pyridine: The determination of the compounds investigated was carried out by the direct spectrophotometric method. For the determination

of benzoic, anthranilic, salicylic acids and pyridine, the optical density of the ethanolic solutions was measured at 272, 337, 304 and 225 mμ, respectively using the corresponding ethanolic acetic acid solution as a blank. To evaluate quantitatively the optical density data, calibration curves were constructed. A *Spektromom 201 (MOM, Hungary)* instrument was used for the spectrophotometric measurements.

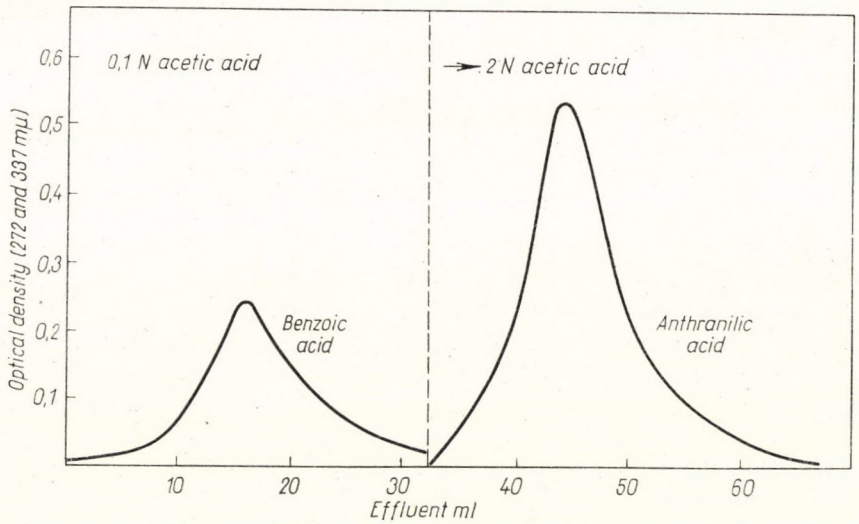

Fig. 3. Chromatographic separation of aromatic acids in ethanolic medium. (Ion exchange column: *Imac A 20 P* acetate; 0.6×15.5 cm)

Results and discussion

The data of the swelling of the macroporous resins investigated show no significant difference from the data of conventional microporous resins. The solvent uptake of the resins is fairly good in ethanol, except in the case of the sodium form of the strongly acid exchangers. In water the strongly acid *Imac C 16 P* in H-form, the strongly basic *Lewatit MP 500* in OH- and Cl-forms, and the weakly basic *Lewatit MP 60* in Cl-form show the highest water uptake values. The resins with lowest values are the weakly basic *Imac A 20 P* in OH-form, and the strongly acid *Imac C 16 P* in Na-form. In ethanol, however, *Imac A 20 P* in OH-form shows the highest solvent uptake, and the strongly acid *Imac C 8 P* and *Lewatit SP 100*, both in Na-form, the lowest. The two latter resins are hardly at all solvated in ethanol.

Comparing the ratio of the water—ethanol uptake values of the resin samples, one finds that the ratio is the smallest in the case of *Imac A 20 P* resin. For the strongly basic resins in both forms, and also for the strongly acid resins in H-form, the ratio is about 4—5. Considering the molar volume ratio of the two solvents (~3.25), one can say that the extent of dissociation of the ionizable group is the most important factor in swelling.

The great difference between the swelling of the sodium form of the cation exchange resins in water and in ethanol shows that the macroporous structure itself is not enough to ensure higher solvent uptake in the resin phase.

In dimethylformamide and dioxan the solvent uptake is significant only in the case of the weakly basic *Imac A 20 P* resin; whereas in glacial acetic acid, as it has been shown before [1], the basic resins have considerable swelling properties.

Kinetic measurements were carried out only with *Imac A 20 P* and *Imac C 16* resins. According to the results, the absorption rate of the aromatic acids does not differ significantly from that of hydrochloric acid on the weakly basic resin. However, the total exchange capacity of the resin cannot be utilized in the case of aromatic acids. For an explanation of this phenomenon one can assume that only a certain fraction of the weakly basic groups is active against the weak acids in the given conditions.

The results of the distribution experiments show that exchange between the aromatic acids and acetate ions takes place according to the exchange mechanism of ions of the same valence. The distribution coefficients found are proportional to the reciprocal value of the eluant concentration.

By choosing the suitable eluant concentration, column size and flow rate, the chromatographic separation of aromatic acids is possible. In the case of separation of benzoic acid and anthranilic acid, the concentration of the eluant was changed from 0.1 to 2 *N*, after the elution of the first acid (Fig. 3). It must be stressed that the volume distribution coefficients, calculated from the peak-eluant volume and resin bed volume data, differ from the volume distribution coefficients calculated from the weight distribution coefficients obtained in static experiments. The difference can be explained by the influence of kinetic factors.

*

The authors express their thanks to the management of *Imacti (Amsterdam, Holland)* and of *Bayer A. G. (Leverkusen, G. F. R.)* for supplying the resin samples used in the experiments. Thanks are expressed also to Prof. L. ERDEY, Head of the Institute, for his advice and attention.

SUMMARY

The swelling properties of some macroporous ion exchange resins in water, ethanol, dimethylformamide, dioxan, and glacial acetic acid were investigated.

On the basis of kinetic and distribution experiments, the chromatographic separation of benzoic and anthranilic acids was achieved on a weakly basic resin column in acetate form, using ethanolic acetic acid solution as the eluant.

REFERENCES

1. INCZÉDY, J., PÁSZTLER, É.: Acta chim. Acad. Sci. Hung. **56,** 115 (1968)
2. KUN, K. A., KUNIN, R.: Polymer Letters **2,** 58 (1964).
3. BARBIER, Y., ROSSET, R.: Bull. Soc. chim. France **1966,** 1388.
4. INCZÉDY, J.: Analytische Anwendungen von Ionenaustauschern, Akadémiai Kiadó, Budapest, 1964. p. 110.
5. BOYD, G. E., ADAMSON, A. W., MYERS, L. S.: J. Am. Chem. Soc. **69,** 2836 (1947).

János INCZÉDY
Irma HŐGYE
Budapest XI., Gellért tér 4.

Acta Chimica Academiae Scientiarum Hungaricae Tomus 56 (2), pp. 117—123 (1968)

DERIVATOGRAPHISCHE UNTERSUCHUNGEN AN ALUMINATHYDRATEN

(KURZMITTEILUNG)

O. HENNING

(Institut für Chemie und Mineralogie der Hochschule für Architektur und Bauwesen, Weimar)

Eingegangen am 17. November 1967

In Zusammenhang mit unseren Untersuchungen über den Hydratationsmechanismus von Erdalkalialuminaten und Tonerdezementen wurde eine Reihe von Aluminathydraten präparativ dargestellt und derivatographisch untersucht. Mit Hilfe der Differential-Thermoanalyse und der Thermogravimetrie sollten als Ergänzung der infrarot-spektroskopischen Ergebnisse [1] folgende Fragen geklärt werden:

— Welche Hydrate treten als Zwischenprodukte bei der Entwässerung anderer, insbesondere höherer Hydrate auf?
— Sind die IR-spektroskopisch ermittelten Bindungsarten des Wassers mit den thermischen Effekten in Zusammenhang zu bringen?

Daß sich die thermische Analyse zur Verfolgung von Hydratationsvorgängen eignet, zeigten TULOWSKAJA und STSCHEGALOWA [2]. Sie stellten zum Beispiel fest, daß bei der Hydratation von C_3A nach anfänglicher Bildung von C_2A- und C_4A-Hydraten diese unter Bildung des stabilen Hexahydrats C_3AH_6 wieder verbraucht werden. In der vorliegenden Arbeit wurden einige Mg-, Ca- und Sr-Aluminathydrate thermoanalytisch untersucht.

Experimentelle Methodik

Die Messungen erfolgten mittels eines Derivatographen *(MOM Budapest)* bei einer Aufheizgeschwindigkeit von 6 °C/min (offene Tiegel). Auf die Wiedergabe der DTG-Kurven wurde in den Abbildungen verzichtet.

Die Darstellung der Aluminathydrate erfolgte nach folgenden Methoden:

M_2AH_6 — 6 g MgO und 4,1 g Al-Pulver werden in 600 ml Wasser 21 Tage am Rückfluß unter CO_2-Ausschluß erhitzt. Das abgesaugte Produkt wird 8 Std. im Vakuum über P_2O_5 bei 140 °C getrocknet.

M_2AH_{12} — 6 g MgO und 4,1 g Al-Pulver werden in 600 ml Wasser 10 Tage bei Zimmertemperatur gerührt, wobei nadelige, doppelbrechende Kristalle entstehen. Das abzentrifugierte feste Reaktionsprodukt wird 2 Tage auf einem Tonteller unter Luftabschluß getrocknet.

$M_3AH_{12,5}$ — 7 g MgO und 3,1 g Al-Pulver werden in 600 ml Wasser 20 Tage am Rückfluß erhitzt.

M_4AH_7 — Dieses Hydrat entsteht bei der Behandlung von M_4AH_{14} 8 Tage über P_2O_5 im Vakuum bei 140 °C.

M_4AH_{14} — 8 g MgO und 2,7 g Al-Pulver werden in 600 ml Wasser 20 Tage am Rückfluß erhitzt. Trocknung wie bei M_2AH_{12}.

M_4AH_{18} — 4 g MgO und 1,35 g Al-Pulver werden in 600 ml Wasser 10 Tage bei Zimmertemperatur gerührt.

$M_7AH_{12,5}$ — Eine dem natürlichen Hydrotalcit in der Zusammensetzung nahe kommende Substanz konnte wie folgt dargestellt werden: Eine Lösung von 25 g NaOH und 5,7 g Al-Späne (Na-Aluminatlösung) wird mit 10,1 g Mg-Pulver 4 Tage am Rückfluß erhitzt.

CAH_6 — 3,5 g Calciumoxyd (aus Calciumhydroxyd p. a. in 6 Std. bei 1000 °C) werden in 1 l frisch destilliertem Wasser von 0 bis 5 °C gelöst bzw. suspendiert. Nach Zugabe von 3 g Al-Pulver *(Riedel de Haën)* wird 72 Std. bei 0 bis 5 °C unter CO_2-Abschluß gerührt, wobei eine weiße kristalline Substanz entsteht. Nach 24 Std. Absetzen, Dekantieren und Absaugen wird die Kristallmasse auf Tontellern getrocknet. Weiterhin wird 3 Wochen über $CuSO_4$ (wasserfrei) und anschließend 140 Std. über $CaCl_2$ getrocknet.

Tabelle I

Chemische Zusammensetzung der untersuchten Aluminathydrate

	MeO	Al_2O_3	H_2O
M_2AH_6	1,90	1,00	6,15
M_2AH_{12}	2,11	1,00	11,76
$M_3AH_{12,5}$	3,06	1,00	12,50
M_4AH_7	3,89	1,00	7,35
M_4AH_{14}	3,89	1,00	14,20
M_4AH_{18}	3,84	1,00	17,79
$M_7AH_{12,5}$	6,84	1,00	12,65
CAH_6	1,13	1,00	6,05
CAH_4	0,91	1,00	4,45
C_2AH_5	1,97	1,00	4,95
C_2AH_9	2,19	1,00	9,20
C_2AH_{13}	1,97	1,00	12,90
C_3AH_6	2,97	1,00	5,96
Sr_3AH_6	3,09	1,00	6,16

CAH_4 — Dieses Hydrat entsteht durch Behandlung der vorstehenden Hexahydrate im Vakuum über P_2O_5 bis zur Gewichtskonstanz (100 Std.).

C_2AH_5 — Das 13-Hydrat wird eine Woche über P_2O_5 im Vakuum getrocknet.

C_2AH_9 — 10 g einer feingemahlenen Schmelze der Zusammensetzung »$C_{9,25}A$« werden in 500 ml Wasser gegeben und 42 Std. bei 0 °C unter CO_2-Abschluß gerührt. Es bilden sich Kristalle, die fest an der Kolbenwandung haften und andere Kristalle, die in der Mutterlauge frei beweglich sind. Letztere werden abgesaugt, je zweimal mit Äthanol und Äther gewaschen und durch mehrmaliges Evakuieren in einem Exsikkator von den Lösungsmittelresten befreit.

C_2AH_{13} — 5,77 g feingepulverte erstarrte Schmelze der Zusammensetzung »C_2A« werden mit 250 ml frisch destilliertem Wasser 50 Std. bei 0 bis 5 °C unter CO_2-Abschluß gerührt. Nach Absaugen und einmaligem kurzem Waschen mit Methanol wird das erhaltene Produkt 40 Std. über $CuSO_4$ (wasserfrei) und 24 Std. über $CaCl_2$ getrocknet.

C_3AH_6 — 2,5 g Al-Pulver werden einer Lösung bzw. Suspension von 7 g CaO in 500 ml Wasser zugegeben. Nach 10 Std. Erhitzen am Rückfluß hat sich das Aluminium vollständig gelöst, wobei ein seidig glänzender Niederschlag entsteht. Dieser wird von der Mutterlauge getrennt, mit Äthanol gewaschen und über KOH getrocknet.

Sr_3AH_6 — Nach Auflösen von 1 g Al-Pulver in einer Lösung von 15,3 g $Sr(OH)_2$ in 1 l Wasser unter Rühren werden 500 ml Wasser abdestilliert. Die dabei an der Kolbenwandung entstehenden würfelförmigen Kristalle werden abgesaugt und mit Äther/Äthanol gewaschen.

In Tabelle I befindet sich eine Zusammenstellung der analytisch gefundenen chemischen Zusammensetzung der präparierten Aluminathydrate.

Ergebnisse

In Bild 1 bis 3 sind die Thermokurven der untersuchten Magnesiumaluminathydrate zusammengestellt. Bei der Entwässerung der Substanz M_2AH_{12} bilden sich Zwischenstufen mit 6, 4,7 und 3 H_2O bei 170—180, 230—240 bzw. 300 °C. Das 4,7- und 3-Hydrat sind auch bei der Entwässerung des M_2AH_6 angedeutet. Der besonders starke Effekt des $M_3AH_{12,5}$ bei 140—150 °C zeigt die Anwesenheit von $Al(OH)_3$ an, das bei 150 °C in Böhmit übergeht. Die DTA-Kurve des M_7AH_{13} zeigt bei 380—390 °C einen starken Effekt, der durch die Zersetzung von $Mg(OH)_2$ verursacht wird. Die festgestellten Hydroxydeffekte sind möglicherweise ein Zeichen dafür, daß in den Strukturen Hydroxydschichten vorliegen.

Die Thermokurven der M_4A-Hydrate zeigen gute Übereinstimmung miteinander. Die beiden im 14- und 18-Hydrat zu erkennenden Effekte bei 110—120 °C und 220—235 °C sind im 7-Hydrat verschwunden. Allen drei Verbindungen ist ein Effekt zwischen 410 und 440 °C gemeinsam. Daraus kann geschlossen werden, daß die ersten 7 H_2O andersartig (fester) gebunden sein müssen als die darüber hinaus vorliegenden Wassermoleküle. Dies stimmt mit der Feststellung überein, daß erst bei mehr als 7 H_2O eine IR-Absorption zwischen 1600 und 1650 cm^{-1} auftritt. Neben dem 11-Hydrat und dem 7-Hydrat erscheinen in den Kurven ein 9- und ein 5-Hydrat, wobei der Bildungstemperaturbereich für das letztere mit 340—360 °C angegeben werden kann.

Die Thermokurven der beiden untersuchten CA-Hydrate stehen ebenfalls mit den Ergebnissen der IR-Untersuchung in Einklang. Während beim 6-Hydrat (Bild 4) noch Effekte bei 130 und 210 °C auftreten, beginnt die Zersetzung des 4-Hydrats erst oberhalb 300 °C. Daß bei der Thermokurve des 6-Hydrats intermediär das 4-Hydrat nicht auftritt, wird darauf zurückgeführt, daß sich der Bindungszustand während der Dehydratation durch Erwärmen ändert (KOHLER [3]) und damit das Entwässerungsverhalten für die folgenden Hydratphasen nicht verbindlich ist.

Ein den CA-Hydraten ähnliches thermisches Verhalten zeigen die C_2A-Hydrate (Bild 5). Auch hier werden die Effekte unter 200 °C mit abnehmendem Wassergehalt kleiner und verschwinden beim 5-Hydrat fast vollständig. Für die bei der thermischen Entwässerung auftretenden Zwischenprodukte gilt das im letzten Abschnitt Gesagte.

Die DTA- und TG-Kurven der Hexahydrate des C_3A und Sr_3A (Bild 6) zeigen große Ähnlichkeit. Beim C_3AH_6 treten Effekte bei 350 °C und 520 °C auf, die KURCZYK [4] bei 330 und 530 °C fand. Sr_3AH_6 weist die analogen Effekte bei 295 und 535 °C auf. Bei den tieferen Temperaturen erfolgt der Übergang zu den entsprechenden Monohydraten. Demgegenüber wurde früher beim C_3A die Bildung eines 1,5-Hydrats (KÖBERICH [5]) und auch eines 2-Hydrats (TRAVERS und ZAHABI [6]) festgestellt. Nach den Ergebnissen der

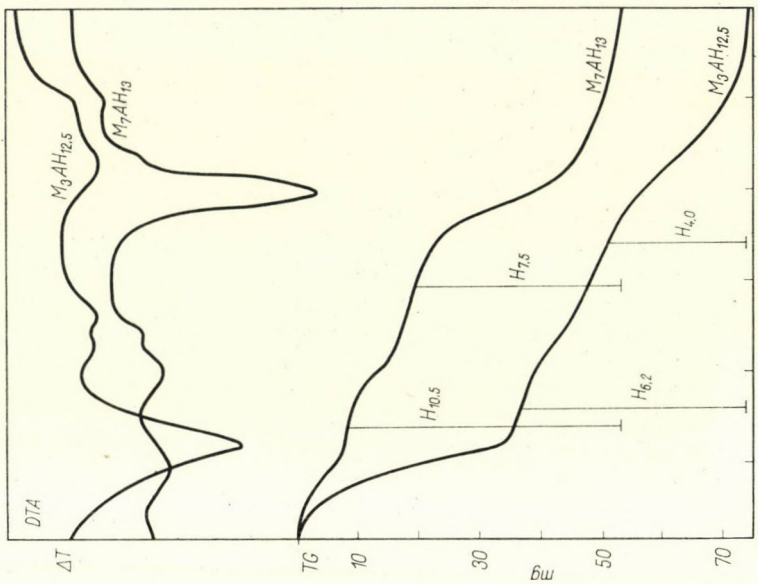

Bild 2. DTA- und TG-Kurven von 3- und 7 MgO · Al_2O_3-Hydraten

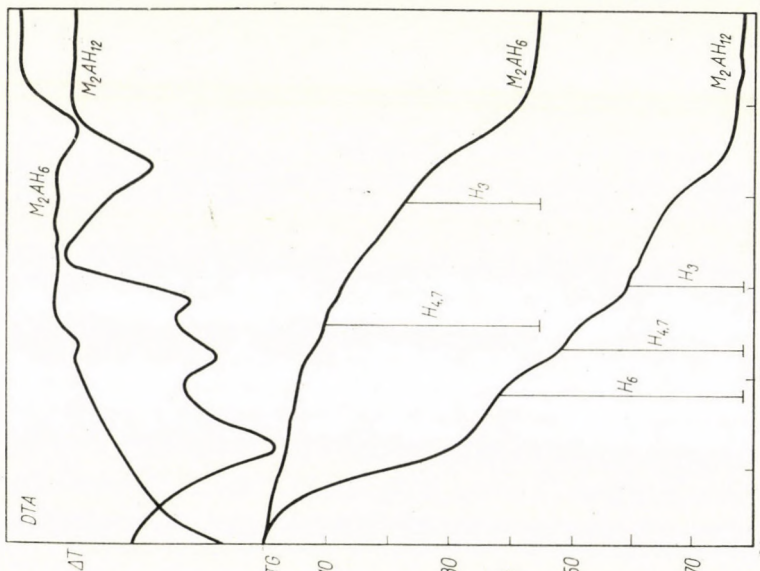

Bild. 1. DTA- und TG-Kurven der 2 MgO · Al_2O_3-Hydrate

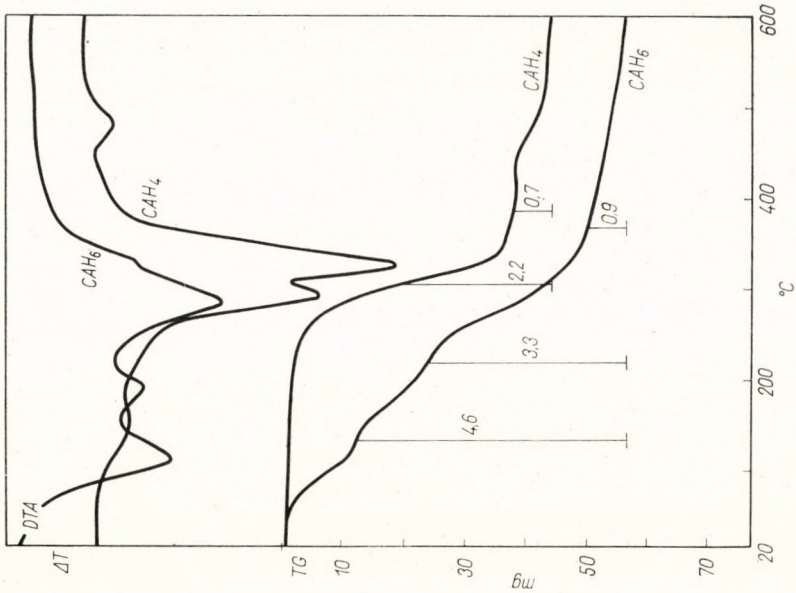

Bild 4. DTA- und TG-Kurven von $CaO \cdot Al_2O_3$-Hydraten

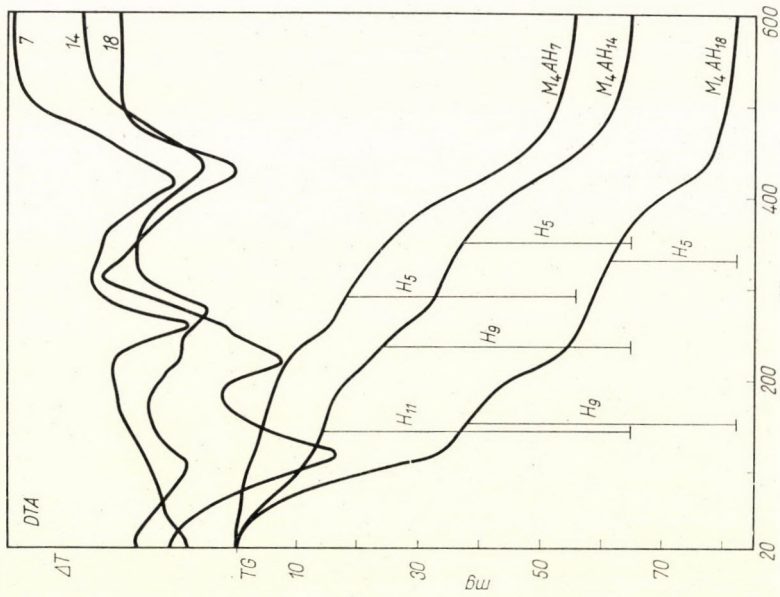

Bild 3. DTA- und TG-Kurven der $4\,MgO \cdot Al_2O_3$-Hydrate

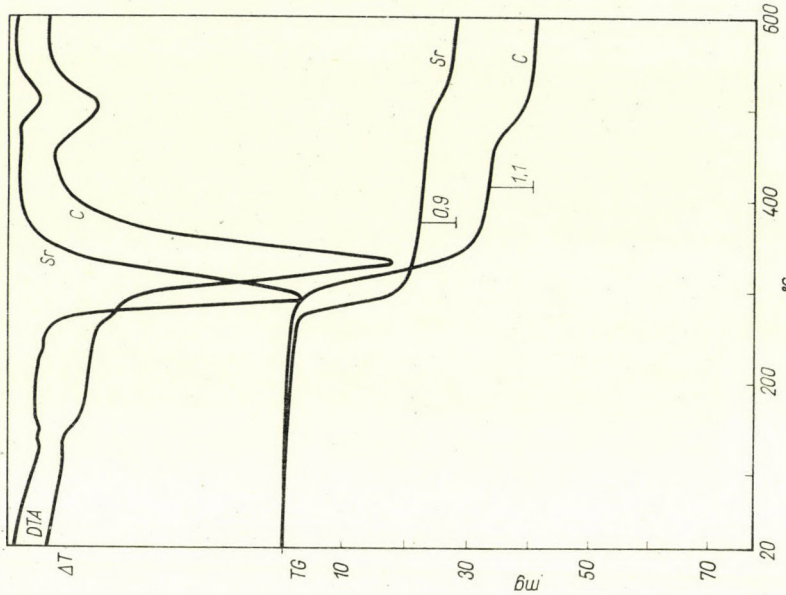

Bild 6. DTA- und TG-Kurven: C_3AH_6, Sr_3AH_6

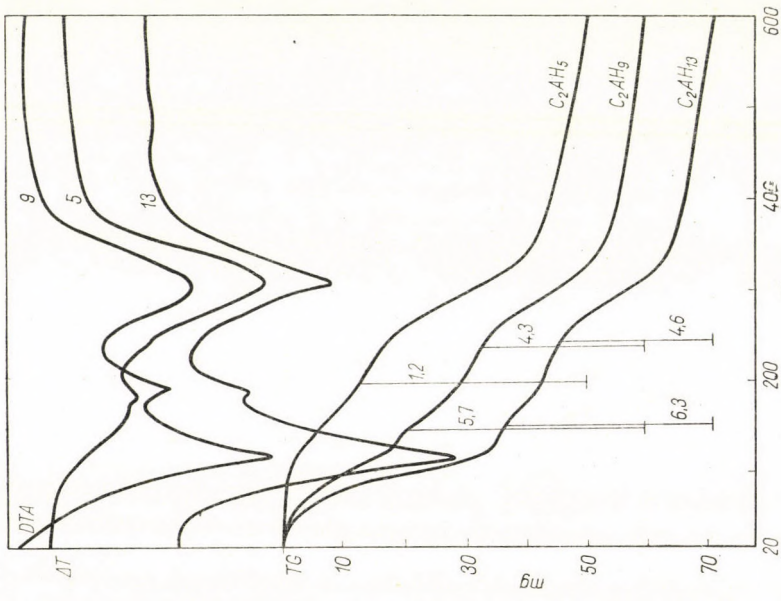

Bild 5. DTA- und TG-Kurven von 2 CaO · Al_2O_3-Hydraten

thermischen Analyse existieren diese beiden Hydrate jedoch nicht. Für die von BARRER und DEMY [7] beschriebene Umwandlung 3 $C_3AH_6 \rightarrow C_4A_3H_3 + + 5\,CH + 10\,H$ bei 200—220 °C ergeben sich im Derivatogramm keine Anhaltspunkte. Als Temperaturbereiche für die Umwandlung in die Monohydrate ergeben sich:

C_3AH_6	300—350 °C
Sr_3AH_6	275—325 °C.

LITERATUR

1. HENNING, O. und VOLKE, K.: Wiss. Z. Hochschule für Architektur u. Bauwesen, Weimar **13,** 557—566 (1966).
2. TULOWSKAJA, S. D. und STSCHEGALOWA, J. J.: J. Angew. Chem. (UdSSR) **37,** 267—275 (1964).
3. KOHLER, K.: Fortschr. Mineralog. **38,** 131 (1960).
4. KURCZYK, H. G.: Dissertation Aachen, 1961.
5. KÖBERICH, F.: Dissertation Berlin, 1934.
6. TRAVERS, A. und ZAHABI, H.: C. R. hebd. Séances Acad. Sci. **206,** 55 (1938).
7. BARRER, R. M. und DEMY, P. J.: J. chem. Soc. (London) 983 **1961.**

Otto HENNING; Institut für Chemie und Mineralogie der Hochschule für Architektur und Bauwesen, Weimar, DDR.

Acta Chimica Academiae Scientiarum Hungaricae Tomus 56 (2), pp. 125—129 (1968)

MASS SPECTRUM OF TETRAMETHYLSILANE. ITS DECOMPOSITION INDUCED BY ELECTRON BOMBARDMENT

(PRELIMINARY COMMUNICATION)

J. TAMÁS and K. ÚJSZÁSZY

(Chemical Structure Research Laboratory of the Hungarian Academy of Sciences, Budapest)

Received October 26, 1966

Papers dealing with the mass spectra of organosilicon compounds are comparatively small in number [1]. Studies in this field have been directed mainly to the investigation of differences between C—C bonds and Si—C bonds, and of atomic groups containing Si attached to a carbon atom [1—9].

The present studies on tetramethylsilane were made as a first step to a mass spectrometric investigation of linear and cyclic methylsiloxanes.

The following papers have been published on the mass spectrum of tetramethylsilane. ASTON *et al.* [10] studied the compound to determine the natural abundances of the isotopes of silicon. This work was followed, eleven years later, by that of DIBELER [3], who published the complete mass spectrum taken at 70 eV energy of bombarding electrons. Further studies, including energetic data and mechanism of formation of some characteristic fragment ions were published by HOBROCK and KISER [5]. In addition to a series of silmethylene compounds, the most intensive peaks of the mass spectrum of tetramethylsilane were investigated by FRITZ *et al.* [6].

The present paper reports the results of our recent studies. Tetramethylsilane of chromatographic purity was made available by the *Inorganic Chemistry Research Group* of the *Hungarian Academy of Sciences*. The mass spectra were taken at 200 °C with an *MH-1303 Type* mass spectrometer of magnetic deflection and scanning, using all-metal inlet system, an accelerating potential of 2 kV and the required filament emission current of 1.50 mA.

The relative intensities of the observed peaks for 30, 50 and 70 eV *nominal* bombarding electron energies, respectively, are given in Table I. To be more exact, the calculated intensities of those peaks are given, which would have been measured if the corresponding fragment ions had contained but one isotope of each element, *i.e.* the isotope of maximum abundance. In other words, the mono-isotope intensities are shown instead of the poly-isotope intensities. For calculating the mono-isotope spectrum, the corresponding data in BEYNON's monograph [11] were used in the case of silicon, and those in the Tables of BEYNON and WILLIAMS [12] in the cases of carbon and hydrogen.

Each silicon-containing ion of an intensity of at least 0.1% relative to

the sum of the intensities of all silicon-containing ions is recorded in Table I. Silicon-free hydrocarbon ions were not taken into account, since — according to studies carried out at a resolving power $(M/\Delta M)_{10\%} = 550$ — their relative amounts remained below 1% in the mass number range 28 to 30.

Table I

m/e	Ion	Relative intensity $(I_i/\sum_{28}^{88} I_i) \cdot 100$		
		30 eV	50 eV	70 eV
28	Si^+	0.73*	1.31*	1.94*
29	SiH^+	0.76	2.66	2.92
30	SiH_2^+	—	0.05	0.09
31	SiH_3^+	1.01	1.85	2.76
41	$SiCH^+$	0.17	0.18	0.31
42	$SiCH_2^+$	0.26	1.15	1.38
43	$SiCH_3^+$	2.19	6.76	6.20
44	$SiCH_3H^+$	1.46	1.93	2.07
45	$SiCH_3H_2^+$	13.3	11.90	12.7
53	$SiCHC^+$	0.12	0.72	1.13
54	$SiCH_2C^+$	0.04	0.19	0.22
55	$SiCH_3C^+$	0.46	1.36	1.29
56	$SiCH_3CH^+$	0.13	0.19	0.17
57	$SiCH_3CH_2^+$	0.72	1.01	0.89
58	$Si(CH_3)_2^+$	0.39	0.73	0.64
59	$Si(CH_3)_2H^+$	1.18	1.28	1.09
70	$Si(CH_3)_2C^+$	0.30	0.26	0.19
71	$Si(CH_3)_2CH^+$	0.28	0.32	0.24
72	$Si(CH_3)_2CH_2^+$	0.74	0.64	0.48
73	$Si(CH_3)_3^+$	74.5	65.0	62.7
88	$Si(CH_3)_4^+$	0.58	0.48	0.46

* Owing to background intensity, the accuracy is 2—5%.

The measured intensity ratios were found to be independent within ±2% of the sample pressure in the ion source. At the only value of 70 eV ionization electron energy where comparison was possible, deviations were found in the intensity ratios as compared to data in the literature [3], particularly in the cases of more intensive peaks.

The most striking difference occurred in the ratio of the peaks 43/45, where we obtained a value of 1/2 as against 4/3 (DIBELER's value [3]). FRITZ *et al.* [6] observed a difference in the same direction.

As it is seen from Table I, the two peaks of maximum intensity correspond to fragment ions containing most probably triply bonded silicon, and those ions with tervalent silicon carry 80 to 90% of the ion current, depending on the bombarding electron energy. Finally, the ions containing even number of electrons yield over 90% of the total intensity.

Ions formed by rearrangement involving one, two or three hydrogen atoms have also been detected in the spectrum. On the other hand, no such quadruply bonded silicon-containing ions were found whose formation involved hydrogen atom rearrangements.

A further characteristic of the mass spectrum of tetramethylsilane, which has not been reported in the literature, is its richness in metastable peaks due to ions partly decomposing during their passage towards the collector. Such ions may be used in studies of decompositions induced by electron bombardment [11, 13, 14]. Thus, for example, the chemical way of formation and decomposition of certain ions and the composition of the neutral products of these reactions can be determined. In such studies the relation

$$m^* = \frac{m_2^2}{m_1} \tag{1}$$

between the mass number of the metastable peak (m^*) and the decomposing and the formed ion (m_1 and m_2, respectively) can be very useful.

Table II

Metastable peaks (m^+)	Decomposition reactions		
60.6	$Si(CH_3)_4^+$	$\rightarrow Si(CH_3)_3^+$	$+ CH_3$
58.9		$\rightarrow Si(CH_3)_2\,CH_2^+$	$+ CH_4$
27.7	$Si(CH_3)_3^+$	$\rightarrow SiCH_3\,H_2^+$	$+ C_2H_4$
46.1		$\rightarrow Si(CH_3)_2^+$	$+ CH_3$
44.5		$\rightarrow SiCH_3\,CH_2^+$	$+ CH_4$
25.3		$\rightarrow SiCH_3^+$	$+ C_2H_6$
68.1	$Si(CH_3)_2\,CH_2^+$	$\rightarrow Si(CH_3)_2\,C^+$	$+ H_2$
26.9		$\rightarrow SiCH_3\,H^+$	$+ C_2H_4$
53.1	$SiCH_3\,CH_2^+$	$\rightarrow SiCH_3\,C^+$	$+ H_2$
30.9		$\rightarrow SiCH_2^+$	$+ CH_3$
14.7		$\rightarrow SiH^+$	$+ C_2H_4$
51.1	$SiCH_3\,C^+$	$\rightarrow Si\,CH\,C^+$	$+ H_2$
16.3	$Si(CH_3)_2\,H^+$	$\rightarrow SiH_3^+$	$+ C_2H_4$
31.9	$Si(CH_3)_2^+$	$\rightarrow Si\,CH_3^+$	$+ CH_3$
17.8	$SiCH_3H^+$	$\rightarrow Si^+$	$+ CH_4$
18.2	$SiCH_3^+$	$\rightarrow Si^+$	$+ CH_3$

Table II shows the mass numbers of the observed metastable peaks of tetramethylsilane. The reaction equations derived from these by the use of Eq. (1) are given in column 2. For all peaks exceeding 1% of the total intensity, formation reaction could be determined by this method, with the exception of $Si(CH_3)_2H^+$ (mass number 59), for no metastable peak could be found cor-

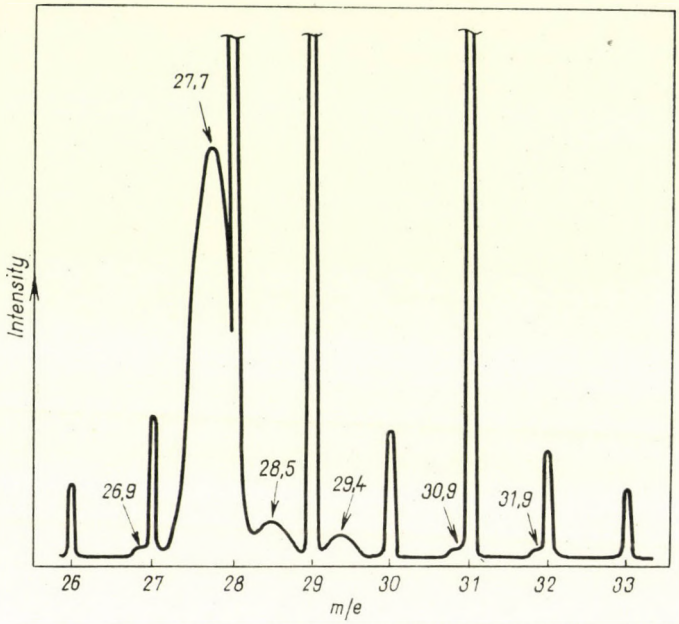

Fig.1. A scan of masses 26 to 33 from the spectrum of tetramethylsilane showing the appearance of metastable peaks in this mass range at 30 eV. The ionic repeller potential was adjusted previously to the intensity maximum of the metastable peak at mass number 27.7, which is due to the transition $Si(CH_3)_3^+ \rightarrow SiC_2H_5^+ + C_2H_4$. The metastable peaks at 28.5 and 29.4 correspond to the heavier isotope ions of the same transition

responding to any of the possible formation reactions in the latter case. Similarly, no metastable peaks corresponding to the splitting-off of a hydrogen atom were found in the spectra.

It is particularly remarkable that the hydrogen rearrangement reactions found always involve the splitting-off of C_2H_4 groups, *i.e.* the simultaneous splitting of two carbon-silicon bonds (corresponding to the metastable peaks 27.7; 26.9; 16.3; and 14.7). A second remarkable feature to be mentioned is that many of the neutral products (such as H_2, CH_4, C_2H_4 and C_2H_6) are identical both in decomposition by electron bombardment and thermal decomposition [15].

The decomposition mechanisms shown in Table II prove HOBROCK's and KISER's theory [5] concerning the formation of the ions $Si(CH_3)_3^+$, $Si(CH_3)_2^+$, $SiCH_3^+$ and Si^+ based on energetical measurements. According to

this theory, the formation of these ions is the result of the splitting-off of methyl radicals. Table II shows furthermore that there are also other ways which may lead to these ions.

The intensity data of Table I also support the decomposition schemes shown in Table II. It should be finally mentioned that there are breaks on the ion-current *versus* ionizing electron energy curves (not published here) which correspond to the decomposition processes given in Table II. These breaks, on the other hand, increase the difficulties in the determination of the appearance potentials.

REFERENCES

1. Bazant, V., Chvalovsky, V., Rathousky, J.: Organosilicon Compounds. Vol. 1, Publ. House Czechosl. Acad. Sci., Prague. 1965.
2. Sommer, L. H.: Stereochemistry, Mechanism and Silicon. McGraw-Hill Book Co., New York, 1965.
3. Dibeler, V. H.: J. Research Natl. Bur. Stands. **49,** 235 (1952).
4. Polyakova, A. A., Zimina, K. I., Petrov, A. A., Khmelnitskii, R. A.: D. A. N. USSR, **134,** 833 (1960).
5. Hobrock, B. G., Kiser, R. W.: J. Phys. Chem. **65,** 2186 (1961).
6. Fritz, G., Buhl, H., Grobe, J., Aulinger, F., Reering, W.: Z. anorg. allg. Chem. **312,** 202 (1961).
7. Steele, W. C., Nichols, L. D., Stone, F. G. A.: J. Am. Chem. Soc. **84,** 4441 (1962).
8. Hobrock, B. G., Kiser, R. W.: J. Phys. Chem. **66,** 155 (1962).
9. Aulinger, F., Reering, W.: Z. anal. Chem. **197,** 24 (1963).
10. Aston, J. G., Kennedy, R. M., Messerly, G. H.: J. Am. Chem. Soc. **63,** 2343 (1941).
11. Beynon, J. H.: Mass Spectrometry and its Application to Organic Chemistry. Elsevier Publ. Co., Amsterdam, 1960.
12. Beynon, J. H., Williams, A. E.: Mass and Abundance Tables for Use in Mass Spectrometry. Elsevier Publ. Co., Amsterdam, 1963.
13. Field, F. H., Franklin, J. L.: Electron Impact Phenomena. Academic Press Inc., New York, 1957.
14. Reed, R. I.: Ion Production by Electron Impact. Academic Press, London, 1962.
15. Fritz, G., Raabe, B.: Z. anorg. allg. Chem. **286,** 149 (1956); **299,** 232 (1959).

József Tamás
Kálmán Újszászy } Budapest VIII., Puskin u. 11—13.

Acta Chimica Academiae Scientiarum Hungaricae Tomus 56 (2), pp. 131—139 (1968)

THE QUADRATIC POTENTIAL FUNCTION OF THE CYCLOPENTADIENYL ANION

F. BILLES

(Department of Physical Chemistry, Technical University, Budapest)

Received April 15, 1967

Introduction

Two studies have been published so far on the normal coordinate analysis of the cyclopentadienyl anion [1, 2]. NELSON, FATELEY and LIPPINCOTT [1] used the frequencies of ferrocene and deuterized ferrocene in their calculations, while SADÔ, WEST, FRITZ and SCHÄFER [2] employed potassium cyclopentadienylide and its perdeuterated derivative. Neither of the studies includes the complete matrix **F**, only its diagonal elements in symmetry coordinate representation and a single interaction force constant in the same representation are given (Table IV).

SADÔ *et al.* have calculated the C—H and C—C force constants in internal coordinate representation. For the C—C force constant they obtained 5.565 mdyn/A; calculated from the data of NELSON *et al.*, 5.79 mdyn/A is obtained for the same constant. In the light of the following arguments, both values seem, to say the least, dubious. If in the cyclopentadienyl anion, similarly to benzene, a complete delocalization of the π-electrons is assumed, the π-electron density for one bond C—C is 1.2, while in benzene it is 1. Taking into account that the C—C valence force constant increases monotonously with increasing π-electron density [3] it can hardly be supposed that the C—C valence force constant in the cyclopentadienyl anion is smaller than in benzene (6.842 mdyn/A [4] or 6.635 mdyn/A [5]). It seems probable that in the two papers mentioned [1, 2] the authors used incorrect sets of force constants in their calculations leading to an incorrect value of the C—C force constant. In the following, we shall examine various sets for the force constants of the cyclopentadienyl anion to select the physically most probable one.

Fundamental frequencies

The fundamental frequencies of the cyclopentadienyl anion were determined on basis of the investigations of FRITZ and SCHÄFER [9] who determined the infrared spectra of various alkali cyclopentadienylides and their deuterated derivatives in Nujol suspension, as well as the infrared and Raman spectra of potassium cyclopentadienylide in ether solution. In the case of the cyclopentadienyl anion, the bands were assigned only on the basis of the spectrum

of the solution in ether, while assignments for the perdeuterated derivative were based on the infrared spectra of the suspension in Nujol.

In potassium cyclopentadienylide the bond K—C cannot be considered completely ionic. If the frequencies of vibrations ν(C—C) of the lithium, potassium and caesium salts of cyclopentadien are compared [9], then, *e.g.*, for the asymmetric valence vibrations the following series is obtained: 1426 cm^{-1}, 1455 cm^{-1}, 1494 cm^{-1}, indicating that the value of the vibration frequency depends on the nature of the alkali metal. This, however, is only possible if the metal-carbon bonds are partially covalent.

As a consequence of the not completely ionic character of the bond K—C, the spectrum in Nujol suspension also shows the bands belonging to the species A_1', A_2', E_2', E_1'' and E_2'', which are forbidden by symmetry D_{5h}, since the symmetry is reduced to C_{2v}. It was, however, impossible to assign all bands pertaining to species E_2''.

Assignments have been made in this work on the basis of the infrared spectrum of potassium cyclopentadienylide in Nujol suspension, and in some cases from the Raman spectrum of the ether solution. The results are shown in Table I. The same Table contains the measured and calculated frequency product ratios.

Table I

Vibrational frequencies of the cyclopentadienyl anion and of the perdeuterated cyclopentadienyl anion

Species	$\frac{\pi(\nu_D)}{\pi(\nu_H)}$		Fundamental vibrations (cm^{-1}) measured	
	Calculated	Measured	$C_5H_5^-$	$C_5D_5^-$
A_1'	0.7073	0.7126	3048	2309
			977	919
A_2'	0.7860	0.8016	1381	1107
E_1'	0.5193	0.5189	3039	2267
			1455	1321
			1009	773
E_2'	0.5003	0.5014	3096	2309
			1455	1393
			1050	798
			565	522
A_1''	—	—	—	—
A_2''	0.7342	0.7436	702	522 (?)
E_1''	0.7858	0.7873	663	522 (?)
E_2''	0.7073	—	913	840 (?)
			—	395 (?)

Calculation of the force constants

As the geometrical parameters of the molecule are unknown, it has been assumed that the lengths of the bonds C—H and C—C are the same as in benzene (1.08 and 1.39 A, respectively), and that the shape of the molecule is a regular pentagon with internal angles of 108°, where the valence lines C—H halve the angles (*i.e.*, the valence angles H—C—C are 126°).

The symbols used to denote the geometrical elements of the molecule are shown in Fig. 1.

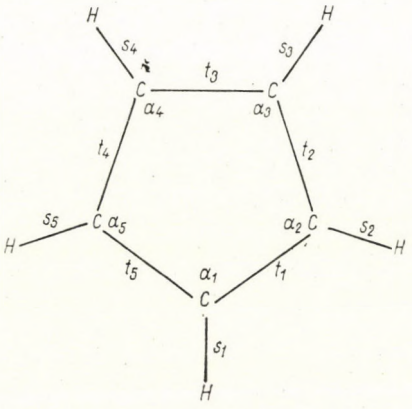

Fig. 1

The following geometrical elements of the molecule are not shown in Fig. 1: the torsional angle of the valence line t_i, δ_i, (the same direction was regarded as positive for the torsion of all valence lines); the directional *(azimuthal)* angles γ_j, pertaining to the valence lines s_j (where the direction of the increase of the angles was chosen to be always identical).

Table II gives the symmetry coordinates (symmetry D_{5h}) of cyclopentadienyl.

The Table includes the redundance coordinates, too. Redundance conditions were determined according to [6]. In the knowledge of the symmetry coordinates, the force constants could be produced in symmetry coordinate representation (Table III).

Using the matrix **G** and the fundamental frequencies (Tables IV and I), the elements of the matrix **F** were produced in symmetry coordinate representation. The calculations were based on the correlation:

$$| \mathbf{F} - \lambda \mathbf{G}^{-1} | = 0 .$$

For the determination of all independent force constants of species E_1', there were five data only instead of the necessary six. It was therefore supposed that $\mathbf{F}_{s\beta}^{E_1'} = 0$. For the determination of the ten independent force constants

Table II

Symmetry coordinates

Species	Symmetry coordinate
A_1'	$\frac{1}{\sqrt{5}}(s_1 + s_2 + s_3 + s_4 + s_5)$
	$\frac{1}{\sqrt{5}}(t_1 + t_2 + t_3 + t_4 + t_5)$
	$\frac{1}{\sqrt{5}}(\alpha_1 + \alpha_2 + \alpha_3 + \alpha_4 + \alpha_5)$
A_2'	$\frac{1}{\sqrt{5}}(\beta_1 + \beta_2 + \beta_3 + \beta_4 + \beta_5)$
E_1'	$\frac{1}{\sqrt{2.5}}(s_1 + 0.3090\, s_2 - 0.8090\, s_3 - 0.8090\, s_4 + 0.3090\, s_5)$
	$\frac{1}{\sqrt{6.5451}}(1.3090\, t_1 - 0.5\, t_2 - 1.6080 t_3 - 0.5\, t_4 + 1.3090\, t_5)$
	$\frac{1}{\sqrt{2.5}}(\alpha_1 + 0.3090\, \alpha_2 - 0.8090\, \alpha_3 - 0.8090\, \alpha_4 + 0.3090\, \alpha_5)$*
	$\frac{1}{\sqrt{9.0451}}(1.8090\, \beta_2 + 1.1180\, \beta_3 - 1.1180\, \beta_4 - 1.8090\, \beta_5)$
E_2'	$\frac{1}{\sqrt{2.5}}(s_1 - 0.8090\, s_2 + 0.3090\, s_3 + 0.3090\, s_4 - 0.8090\, s_5)$
	$\frac{1}{\sqrt{0.9549}}(0.1910\, t_1 - 0.5\, t_2 + 0.6180\, t_3 - 0.5\, t_4 + 0.1910\, t_5)$
	$\frac{1}{\sqrt{2.5}}(\alpha_1 - 0.8090\, \alpha_2 + 0.3090\, \alpha_3 + 0.3090\, \alpha_4 - 0.8090\, \alpha_5)$
	$\frac{1}{\sqrt{3.4550}}(0.6910\, \beta_2 - 1.1180\, \beta_3 + 1.1180\, \beta_4 - 0.6910\, \beta_5)$
A_1''	$\frac{1}{\sqrt{5}}(\delta_1 + \delta_2 + \delta_3 + \delta_4 + \delta_5)$*
A_2''	$\frac{1}{\sqrt{5}}(\gamma_1 + \gamma_2 + \gamma_3 + \gamma_4 + \gamma_5)$
E_1''	$\frac{1}{\sqrt{2.5}}(\gamma_1 + 0.3090\, \gamma_2 - 0.8090\, \gamma_3 - 0.8090\, \gamma_4 - 0.3090\, \gamma_5)$
	$\frac{1}{\sqrt{3.4550}}(0.6910\, \delta_1 + 1.1180\, \delta_2 - 1.1180\, \delta_4 - 0.6910\, \delta_5)$*
E_2''	$\frac{1}{\sqrt{2.5}}(\gamma_1 - 0.8090\, \gamma_2 + 0.3090\, \gamma_3 + 0.3090\, \gamma_4 - 0.8090\, \gamma_5)$
	$\frac{1}{\sqrt{9.0451}}(1.8090\, \delta_1 - 1.1180\, \delta_2 + 1.1180\, \delta_4 - 1.8090\, \delta_5)$

*Redundancy coordinates

of species E_2', only seven data were available. The following assumptions were therefore used: $F_s^{E_2'} = 0$, while the values of $\mathbf{F}_{st}^{E_2'}$ and $\mathbf{F}_{t\beta}^{E_2'}$ were calculated from the force constants of benzene [4], and these were not changed during the calculation.

Table III

Force constants pertaining to the various species in symmetry coordinate representation as the linear combinations of the constants expressed in internal coordinate representation (using Wilson's [5] symbols)

A_1'	$F_{ss} = F_s^1 + 2F_s^2 + 2F_s^3$	A_1'' $F_{\delta\delta} = F_\delta^1 + 2F_\delta^2 + 2F_\delta^3$*
	$F_{tt} = F_t^1 + 2F_t^2 + 2F_t^3$	
	$F_{\alpha\alpha} = F_\alpha^1 + 2F_\alpha^2 + 2F_\alpha^3$*	
	$F_{st} = 2F_{st}^1 + 2F_{st}^2 + F_{st}^3$	
	$F_{s\alpha} = F_{s\alpha}^1 + 2F_{s\alpha}^2 + 2F_{s\alpha}^3$*	
	$F_{t\alpha} = 2F_{t\alpha}^1 + 2F_{t\alpha}^2 + F_{t\alpha}^3$*	
A_2'	$F_{\beta\beta} = F_\beta^1 + 2F_\beta^2 + 2F_\beta^3$	A_2'' $F_{\gamma\gamma} = F_\gamma^1 + 2F_\gamma^2 + 2F_\gamma^3$
E_1'	$F_{ss} = F_s^1 + 0.6180F_s^2 - 1.6180F_s^3$	E_2' $F_{ss} = F_s^1 - 1.6180F_s^2 + 0.6180F_s^3$
	$F_{tt} = F_t^1 + 0.6180F_t^2 - 1.6180F_t^3$	$F_{tt} = F_t^1 - 1.6180F_t^2 + 0.6180F_t^3$
	$F_{\alpha\alpha} = F_\alpha^1 + 0.6180F_\alpha^2 - 1.6180F_\alpha^3$*	$F_{\alpha\alpha} = F_\alpha^1 - 1.6180F_\alpha^2 + 0.6180F_\alpha^3$
	$F_{\beta\beta} = F_\beta^1 + 0.6180F_\beta^2 - 1.6180F_\beta^3$	$F_{\beta\beta} = F_\beta^1 - 1.6180F_\beta^2 + 0.6180F_\beta^3$
	$F_{st} = 1.6180F_{st}^1 - 0.6180F_{st}^2 - F_{st}^3$	$F_{st} = 0.6180F_{st}^1 - 1.6180F_{st}^2 + F_{st}^3$
	$F_{s\alpha} = F_{s\alpha}^1 + 0.6180F_{s\alpha}^2 - 1.6180F_{s\alpha}^3$*	$F_{s\alpha} = F_{s\alpha}^1 - 1.6180F_{s\alpha}^2 + 0.6180F_{s\alpha}^3$
	$F_{s\beta} = 1.9021F_{s\beta}^1 + 1.1756F_{s\beta}^2$	$F_{s\beta} = 1.1756F_{s\beta}^1 - 1.9021F_{s\beta}^2$
	$F_{t\alpha} = 1.6180F_{t\alpha}^1 - 0.6180F_{t\alpha}^2 - F_{t\alpha}^3$*	$F_{t\alpha} = 0.6180F_{t\alpha}^1 - 1.6180F_{t\alpha}^2 + F_{t\alpha}^3$
	$F_{t\beta} = -1.1756F_{t\beta}^1 + 1.9021F_{t\beta}^2$	$F_{t\beta} = -1.9021F_{t\beta}^1 - 1.1756F_{t\beta}^2$
	$F_{\alpha\beta} = 1.9021F_{\alpha\beta}^1 + 1.1756F_{\alpha\beta}^2$*	$F_{\alpha\beta} = 1.1756F_{\alpha\beta}^1 - 1.9021F_{\alpha\beta}^2$
E_1''	$F_{\gamma\gamma} = F_\gamma^1 + 0.6180F_\gamma^2 - 1.6180F_\gamma^3$	E_2'' $F_{\gamma\gamma} = F_\gamma^1 - 1.6180F_\gamma^2 + 0.6180F_\gamma^3$
	$F_{\delta\delta} = F_\delta^1 + 0.6180F_\delta^2 - 1.6180F_\delta^3$*	$F_{\delta\delta} = F_\delta^1 - 1.6180F_\delta^2 + 0.6180F_\delta^3$
	$F_{\gamma\delta} = 1.1756F_{\gamma\delta}^1 + 1.9021F_{\gamma\delta}^2$*	$F_{\gamma\delta} = 1.9021F_{\gamma\delta}^1 - 1.1756F_{\gamma\delta}^2$

* Redundancy correlations

Table IV shows the sets of force constants with a possible physical meaning. Two such sets were obtained for each of the species E_1' and E_2'', while in all other species only one force constant with physical meaning was found.

The correlations of Table III and the force constant values in internal coordinate representation, calculated from the data of Table IV, are given in Table V.

The calculated frequencies are shown in Table VI.

For the calculations a *NE* 803*B* electronic computer was used.

Table IV

Matrices **G** *and* **F** *of the cyclopentadienyl anion in symmetry coordinate representation*

Species	Symmetry coordinate pair	G_{ij} (mole^{-1})	F_{ij} (mdyn/A)			
			Calculated		Sadó *et al.* [2]	Nelson *et al.* [1]
A_1'	ss	1.0754	4.9273		5.030	4.99
	st	—0.0979	—0.5126			
	tt	0.1150	5.5241		5.419	6.97
A_2'	$\beta\beta$	1.1101	0.9360			
			set A	set B		
E_1'	ss	1.0754	5.0083	4.9850	5.012	5.18
	st	—0.0792	0.0415	—0.1659	0.079	
	sβ	0.0461	0	0		
	tt	0.1506	10.1805	6.2736	6.337	5.50
	tβ	—0.1610	1.8675	0.1537		1.52
	$\beta\beta$	1.0583	0.9219	0.9490	0.779	0.639
E_2'	ss	1.0754	5.2727	5.1013	5.228	5.218
	st	—0.0303	—0.1892	0		
	sα	0.1753	—0.3502	0.3545		
	sβ	0.0285	0	0		
	tt	0.2081	1.9895	5.8285	4.866	5.50
	tα	—0.1274	—0.7401	1.2019		
	tβ	—0.1393	0.1066	0		
	$\alpha\alpha$	0.3897	2.5408	0.8694	0.358	0.935
	$\alpha\beta$	0.1016	—0.2790	0.1051		
	$\beta\beta$	0.9447	0.7043	0.9042	0.705	0.633
A_2''	$\gamma\gamma$	0.9219	0.3149		0.2762	0.279
E_1''	$\gamma\gamma$	1.1118	0.2070		0.1774	
E_2''	$\gamma\gamma$	1.6714	0.3508			
	$\gamma\delta$	—0.8411	0.6441			
	$\delta\delta$	0.8618	1.3390			

Discussion

In Table V four calculated sets of force constants of the cyclopentadienyl anion are shown for in-plane vibrations, together with the corresponding force constants of benzene [4, 5, 7, 8]. Only a single set — the one denoted by AB — satisfies the requirements given in the Introduction. This was calculated from set A of species E_1', and set B of species E_2'. Here the value of the force constant of the bond C—C is $\mathbf{F}_t^1 = 7.508$ mdyn/A, which is in satisfactory agreement with the corresponding force constants of benzene.

Table V

Force constants of cyclopentadyenyl anion and benzene in internal coordinate represantation (mdyn/A)

Force constant	Cyclopentadienyl anion				Benzene	
	AA	*AB*	*BA*	*BB*	KOVNER [4, 7]	CRAWFORD *and* MILLER [5, 8]
F_s^1	5.0979	5.0293	5.0885	5.0200	5.185	5.048
F_s^2	—0.1018	—0.0463	—0.1046	—0.0492	0	0.017
F_s^3	0.0165	—0.0047	0.0240	0.0030	0	—0.031
F_s^4	—	—	—	—	0	—0.018
F_{st}^1	—0.1125	—0.1796	—0.0891	—0.1562	0.0733	—0.700
F_{st}^2	—0.0464	—0.0208	—0.1077	—0.0820	0.1453	—0.700
F_{st}^3	—0.1948	—0.1118	—0.1191	—0.0362	0.0006	—0.700
$F_{s\alpha}^1$	—0.1541	0.1258	—0,0840	0.1979	—0.0963	0.216
$F_{s\alpha}^2$	0.1090	—0.1185	0.1307	—0.0974	0.0962	—0.216
$F_{s\alpha}^3$	—0.0320	0.0557	—0.0887	—0.0016	—0.0038	0.216
$F_{s\alpha}^4$	—	—	—	—	—0.0867	—0.216
$F_{s\beta}^1$	0	0	0	0	0	0
$F_{s\beta}^2$	0	0	0	0	0	0
F_t^1	5.9728	7.5084	4.4101	5.9459	6.842	6.635
F_t^2	1.7194	0.4771	1.2365	—0.0059	0.442	0.834
F_t^3	—1.9437	—1.4692	—0.6794	—0.2049	—0.336	—0.112
F_t^4	—	—	—	—	0.446	—0.251
$F_{t\alpha}^1$	—2.6646	—2.6376	—1.8184	—1.5684	—2.674	—2.860
$F_{t\alpha}^2$	1.0907	0.6753	0.8953	0.2669	0.1847	0.0839
$F_{t\alpha}^3$	3.1478	3.9246	1.8262	2.6030	2.480	2.776
$F_{t\beta}^1$	—0.4796	—0.4391	—0.0767	—0.0361	—0.1477	0.0011
$F_{t\beta}^2$	0.6854	0.7104	0.0334	0.0585	0.1483	0.170
$F_{t\beta}^3$	—	—	—	—	—0.0997	—0.0011
F_α^1	3.9288	3.2602	2.8111	2.1425	1.818	2.091
F_α^2	0.0788	0.6187	—0.2677	0.2733	0.227	0.198
F_α^3	—2.0332	—2.2488	—1.1380	—1.3445	—0.619	—0.719
F_α^4	—	—	—	—	—1.070	—1.048
$F_{\alpha\beta}^1$	—0.6736	—0.5833	—0.1151	—0.0247	—0.0887	—0.181
$F_{\alpha\beta}^2$	—0.2652	—0.4113	0.0756	—0.0705	—0.1505	0.0281
F_β^1	0.8377	0.9176	0.8485	0.9285	1.057	1.017
F_β^2	0.0732	0.0086	0.0766	0.0121	—0.0228	0.0243
F_β^3	—0.0241	0.0006	—0.0329	—0.0084	—0.0025	0.0147
F_β^4	—	—	—	—	—0.0567	—0.0284
F_γ^1		0.2861			0.451	0.441
F_γ^2		—0.0250			—0.0733	—0.0665

Table V continued

Force constant	Cyclopentadienyl anion				Benzene	
	AA	*AB*	*BA*	*BB*	KOVNER [4, 7]	CRAWFORD *and* MILLER [5, 8]
F_{γ}^{3}		0.0394			—0.0057	0.0082
F_{γ}^{4}		—			—0.0136	—0.0296
$F_{\gamma\delta}^{1}$		0.2450			—0.1483	—0.0939
$F_{\gamma\delta}^{2}$		—0.1514			—0.0952	—0.1307
$F_{\gamma\delta}^{3}$		—			0.3386	0.3185
F_{δ}^{1}		0.5356			0.6194	0.5967
F_{δ}^{2}		—0.4333			—0.3659	0.3529
F_{δ}^{3}		0.1655			—0.1413	—0.1346
F_{δ}^{4}		—			0.3948	0.3784

Table VI

Measured and calculated fundamental frequencies of C_5H_5 (cm^{-1})

Species	Vibration	Measured	Calculated	
			A	*B*
A_1'	ν CH	3048	3048.0	
	ν CC	977	976.9	
A_2'	δ CH	1381	1381.0	
E_1'	ν CH	3039	3039.0	3039.0
	ν CC	1455	1455.0	3039.0
	δ CH	1009	1009.0	1009.0
E_2'	ν CH	3096	3096.0	3096.0
	ν CC	1455	1455.1	1455.0
	δ CH	1050	1049.9	1050.0
	δ CC	565	565.0	565.0
A_2''	γ CH	702	702.0	
E_1''	γ CH	663	663.0	
E_2''	γ CH	913	913.0	
	γ CC	—	514.0	

According to expectation, the force constants pertaining to in-plane vibrations which do not belong to the geometrical elements of the ring (which pertain to coordinates of types s and β only) change but slightly, as for these the strain of the ring is manifest only slightly or not at all. The strain is due to the hybridization sp^2 of the carbon atoms corresponding, instead of the 108° valence angle C—C—C of the ring, to a valence angle of 120°. Owing to the strain the deformation of the ring is more hindered than in benzene.

Thus all force constants belonging to coordinates of type α (firstly), of course F_{α}^{1} have higher absolute values than the force constants of benzene.

In general, the values of the force constants pertaining to out-of-plane vibrations are lower for cyclopentadienyl anion than for benzene, indicating that despite the strain in the ring, out-of-plane deformation is carried out easier.

Of all five-membered aromatic rings, cyclopentadienyl anion has the highest symmetry, so that its force constants expressed in internal coordinate representation afford a useful basis for the calculation of vibrational force constants of five-membered heteroatomic rings.

SUMMARY

The matrix **F** set of the cyclopentadienyl anion has been determined, and the matrix has been selected in which the force constant of the bond C—C corresponds to a higher π-electron density than that found in benzene. An analysis of the force constants obtained is given.

REFERENCES

1. NELSON, R. D., FATELEY, W. G., LIPPINCOTT, E. R.: J. Am. Chem. Soc. **78,** 4870 (1956).
2. SADÔ, A., WEST, R., FRITZ, H. P., SCHÄFER, L.: Spectrochim. Acta **22,** 509 (1966).
3. WILSON, E. B., DECIUS, J. C., CROSS, P. C.: Molecular Vibrations. McGraw-Hill, London, 1955.
4. KOVNER, M. A.: Doklady A. N. SSSR **91,** 499 (1953).
5. CRAWFORD, B. A., MILLER, F. A.: J. Chem. Phys. **17,** 249 (1949).
6. BILLES, F.: Acta chim. Acad. Sci. Hung. **49,** 97 (1966).
7. KOVNER, M. A.: Doklady A. N. SSSR **97,** 65 (1954).
8. MILLER, F. A., CRAWFORD, B. L.: J. Chem. Phys. **14,** 282 (1946).
9. FRITZ, H. P., SCHÄFER, L.: Chem. Ber. **97,** 1829 (1964).

Ferenc BILLES: Budapest XI., Budafoki-út 8.

Acta Chimica Academiae Scientiarum Hungaricae Tomus 56 (2), pp. 141—152 (1968)

CATALYTIC DEGRADATION OF ALCOHOLS ON METALS

P. TÉTÉNYI and K. SCHÄCHTER

(Institute of Isotopes of the Hungarian Academy of Sciences, Budapest)

Received May 29, 1967

Dehydrogenation has been up to now the most extensively studied decomposition reaction of alcohols on metals [1—4]. Except for a relatively detailed comparative investigation by BALANDIN and one of the present authors [5] dealing with seven metals, most of the researches in this field have been confined to one or another metal catalyst.

In earlier communications we have pointed out the possibility of applying various metals as dehydration of *t*-butyl alcohol on platinum and on nickel catalysts prepared in various ways [9], as well as in the presence of Fe, Co, Ni, Cu, Rh, Ag, Pd and Pt catalysts. It has been found that all these metals catalyze the dehydration of *t*-butyl alcohol to a lesser or greater degree.

In the present paper we wish to report on a more extensive study of the catalytic degradation of alcohols on metals. In these investigations we have set ourselves the following aims:

(1) Study of the parallel dehydrogenation and dehydration of isopropyl alcohol in the presence of Be, Ti, V, Fe, Co, Ni, Cu, Zn, Zr, Mo, Ru, Rh, Pd, Ag, W, Ir, Pt and Au. To the best of our knowledge no research has been done so far on the dehydration of secondary or primary alcohols, which are capable of dehydrogenation, in the presence of metal catalysts. In accordance with the findings of other authors [1—4], we have observed earlier [5], by the analysis of the evolved gas, a selective dehydrogenation of isopropyl alcohol on metal catalysts. The fact that both water and alcohol may absorb fairly significant quantities of unsaturated hydrocarbons [10] necessitated a revision of these results by way of the chromatographic analysis of the liquid product. Data on the parallel dehydrogenation and dehydration of isopropyl alcohol made possible a direct comparison of the dehydrogenating and dehydrating activities of the metals under investigation.

(2) Extension of the scope of the metal catalysts. With this aim in mind the dehydration of *t*-butyl alcohol was studied in the presence of all the above-mentioned metals on which data have not been reported in our earlier communication [9].

(3) From the data in this paper and in our earlier communication [9], a comparison can be made of the catalytic activity and the bulk properties of these metals.

Experimental

The method of preparation of the catalysts used in the experiments has been described elsewhere [11, 12]. The values of the specific surfaces are listed again in this paper, as in some cases, there are discrepancies between

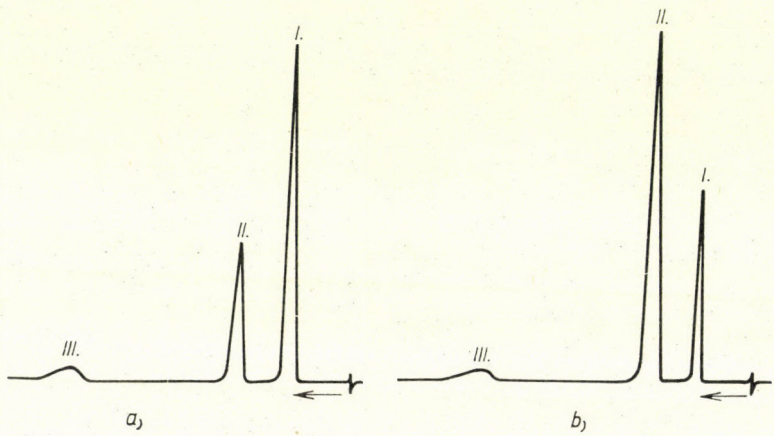

Fig. 1. Chromatogram of products obtained in the conversion of isopropyl alcoho lin the pres ence of (a) nickel and (b) ruthenium catalysts. I: acetone; II: isopropyl alcohol; III: water

the recently obtained values and those found earlier. Data on trace impurities in the catalysts have also been reported [11, 12].

The materials used for the measurements were "*spectroscopic grade*" *(Merck)* isopropyl alcohol and *analytic grade* *t*-butyl alcohol *(Reanal)* whose purity was checked by chromatography. Water was removed from the butyl alcohol by refluxing on calcium oxide, followed by distillation. Good agreement of the physical constants with the literature data and the chromatographic tests proved the satisfactory purity of the reagents.

The measurements were carried out in a flow system reactor which has been described in detail previously [13]. Constancy of the reaction rate (attaining of the stationary state) was checked by measuring the evolution of the gas. In the case of isopropyl alcohol, the quantities of the products formed during the reaction were calculated from the chromatographically determined percentage composition of the condensate and the flow rate of the alcohol. The chromatograms were obtained with a *Griffin B* apparatus using a 2.7 m long *Celite 545* column containing polyethyleneglycol. Fig. 1 shows a few

examples of the chromatograms of the products obtained in the conversion of isopropyl alcohol.

The degree of dehydration of *t*-butyl alcohol was determined from the refractive index of the product by using the calibration curve described earlier [7]. The refractive index was measured with a *Zeiss* immersion refractometer (accuracy $\pm$ 0.00002). The composition of the product was also checked by chromatography, on a column similar to that used for the products of isopropyl alcohol.

The apparent rate constants of dehydrogenation and dehydration were calculated from the conversion (x) and the corresponding value of the flow rate (v_1), according to the equation:

$$k = v_1 \ln \frac{v_1}{v_1 - x}. \tag{1}$$

This expression has been used by several authors in studying the dehydrogenation and dehydration of alcohols [14—16], and its applicability was verified in the dehydrogenation of alcohol on copper and in the dehydration of the same on aluminium oxide. Eq. (1) is obtained from the expression

$$k = \left(\frac{b_2}{b_1} + \frac{b_3}{b_1}\right) v_1 \ln \frac{v_1}{v_1 - x} - \left(\frac{b_2}{b_1} + \frac{b_3}{b_1} - 1\right) x \tag{2}$$

for

$$b_2 + b_3 = b_1 \tag{3}$$

where b_1 is the adsorption equilibrium constant of the alcohol, and b_2 and b_3 are those of the products. Though it has been shown repeatedly [18] that condition (3) is not strictly valid, the discrepancies are generally not too significant, and the sum $\frac{b_2}{b_1} + \frac{b_3}{b_1}$ is only slightly dependent on temperature. Therefore, the differences found between the activation energies calculated from the temperature dependence of the rate constants by means of Eq. (2) and Eq. (3), are quite insignificant [5]. It seemed therefore permissible to calculate the apparent rate constants from Eq. (1), especially since a detailed study beyond the determination of the conversion values was impossible for the majority of the metals investigated, owing to the great fluctuations in catalytic activity.

Results

First the decomposition of isopropyl alcohol on the mentioned 18 metal catalysts was investigated. The rate of the decomposition reaction was measured always on fresh samples, usually at 235 °C. However, owing to the

low reaction rate, no reproducible results were obtained at 235 °C with some of the metals. In these cases, the catalytic activity had to be measured at higher temperatures, which, however, did not exceed 300 °C.

Table I shows the rates of decomposition of isopropyl alcohol on different metals. It may be seen that the decomposition (dehydrogenation or dehydration) of the alcohol is catalyzed by all the metals examined. At the given temperature all metals — with the exception of iron — bring about a more or less extensive dehydration of isopropyl alcohol. Titanium, zirconium, tungsten and vanadium only dehydrate the alcohol; also molybdenum and beryllium are potent dehydrating catalysts. (In expressing the conversion values per one square metre, the geometrically measured surfaces of Ti, Zr and V have been corrected by a roughness factor, similarly to the method described in [12].)

Table I

*Conversion of isopropyl alcohol on metals**

(Flow rate of the alcohol: $v_l = 45$ NTP/ml/min.)

Catalyst	Specific surface, m^2/g	Temp., °C	x_{ac}	x_{H_2O}	k_H	k_{H_2O}	M_H	M_{H_2O}
Be	0.8	296	$9.6 \cdot 10^{-4}$	$6 \cdot 10^{-2}$	$9.7 \cdot 10^{-4}$	0.06	1.7	98.3
Ti	$3 \cdot 10^{-3}$	235	—	23.5	—	33.2	—	100
V	$5 \cdot 10^{-3}$	235	—	1.55	—	1.56	—	100
Fe	21.3	235	$6.51 \cdot 10^{-2}$	—	$6.53 \cdot 10^{-2}$	—	100	—
Co	28.2	235	0.32	0.08	0.40	0.08	80	20
Ni	18.6	235	6.65	0.72	10.50	0.73	90.3	9.7
Cu	2.9	235	3.17	0.48	3.99	0.49	86.8	13.2
Zn	0.2	235	0.32	0.42	0.36	0.43	43.5	56.5
Zr	$3 \cdot 10^{-3}$	260	—	1.13	—	1.14	—	100
Mo	0.6	235	$9.5 \cdot 10^{-2}$	1.99	0.10	2.08	0.8	99.2
Ru	1.6	235	1.50	0.34	1.69	0.35	81.6	18.4
Rh	5.7	235	0.63	0.16	0.67	0.16	81.6	18.4
Pd	0.8	232	7.92	0.39	9.40	0.40	95 4	4.6
Ag	2.5	235	0.57	0.14	0.60	0.14	79.7	20.3
W	0.6	241	—	2.18	—	2.28	—	100
Ir	1.0	235	1.87	0.67	1.96	0.69	73.6	26.4
Pt	12.6	235	1.52	0.19	1.68	0.20	88.9	11.1
Au	0.3	235	$6.9 \cdot 10^{-2}$	0.27	$7.1 \cdot 10^{-2}$	0.28	20.4	79.6

* x_{ac} and x_{H_2O}: quantity of acetone and water, respectively, formed in unit time (NTP ml/m^2/min.)
k_H and k_{H_2O}: dehydrogenation and dehydration rate constants of the alcohol (NTP ml/m^2/min.)
M_H and M_{H_2O}: mole-% of dehydrogenation and dehydration

From the conversion values of the dehydrogenation of isopropyl alcohol at different temperatures, we calculated the k values according to Eq. (1). From these, with the help of the ARRHENIUS equation, the values of the activation energy of dehydrogenation (ε_H) and the pre-exponential factor (k_0) were

Table II

Arrhenius constants of the dehydrogenation of isopropyl alcohol on various metal catalysts

Catalyst	ε_{H_2O} kcal/mole	k_0 ml/sp. m. min.
Be	39	$7.2 \cdot 10^{13}$
V	26	$1.1 \cdot 10^{10}$
Mo	11	$5.7 \cdot 10^{3}$
Ru	9	$1.3 \cdot 10^{4}$
Rh	13	$3.0 \cdot 10^{5}$
Ir	11	$1.1 \cdot 10^{5}$
Au	16	$5.6 \cdot 10^{5}$

obtained. These data are given in Table II. Because of the fluctuating activity, the activation energy on Zn could not be determined. Of the metals shown in Table I, Ti, Zr and W failed to catalyze the dehydrogenation of isopropyl

Table III

Arrhenius constants of the dehydration of isopropyl alcohol on various metal catalysts

Catalyst	ε_{H_2O} kcal/mole	k_0 ml/m²/min.
Be	18	$5.4 \cdot 10^{5}$
Ti	22	$1.4 \cdot 10^{11}$
Zr	13	$2.6 \cdot 10^{5}$
Mo	25	$1.4 \cdot 10^{11}$
Ru	11	$2.0 \cdot 10^{4}$
W	11	$1.2 \cdot 10^{5}$

alcohol, thus the activation energy for these metals could not be determined. From the series of experiments published in [5] and [18], the ε_H and k_0 values of Fe, Co, Ni, Cu, Pd, Ag and Pt were already known, thus their determination was unnecessary.

The ARRHENIUS constants characteristic of the dehydration of isopropyl alcohol were determined in a similar way for some of the metals. The results are contained in Table III.

An attempt was made to determine the kinetic constants of the dehydration reaction of *t*-butyl alcohol in the presence of all the metals listed in Table I for which this had not been done earlier [9]. The data are shown in Table IV. This determination was not possible for Mo and W, as these two metals catalyze the dehydration to such a great extent, that the conversion could not be calculated by the usual procedure from the refractive index of the mixture, obtained by condensation.

Table IV

Kinetic constants of the dehydration of tertiary butyl alcohol on various metal catalysts

Catalyst	k'_{H_2O} ml/m²/min.	k_0 ml/m²/min.	ε_{H_2O} kcal/mole
Be	0.152	$2.4 \cdot 10^{10}$	26
Ti	5.02	$5.6 \cdot 10^{9}$	21
V	1.70	$1.1 \cdot 10^{8}$	19
Zn	0.453	$1.3 \cdot 10^{9}$	22
Zr	1.580	$2.0 \cdot 10^{9}$	23
Ru	0.457	$7.2 \cdot 10^{7}$	19
Mo	1.746	—	—
Ir	0.972	$2.6 \cdot 10^{9}$	22
Au	0.063	$1.9 \cdot 10^{8}$	22

For a numerical determination of the degree of compensation between the ARRHENIUS constants, the $\lg k_0$ values were plotted as a function of the activation energy. The linear correlation expected from the formula

$$k_0 = ae^{h\varepsilon} \tag{4}$$

holds good for all the three above-discussed reactions on the metal catalysts under investigation, as it is illustrated in Fig. 2, by way of example, for the dehydrogenation reaction of isopropanol. The values of the constants in Eq. (4) are:

	a	h
for the dehydrogenation of i-C_3H_7OH	0.9	$8.1 \cdot 10^{-4}$
for the dehydration of i-C_3H_7OH	0.2	$12.0 \cdot 10^{-4}$
for the dehydration of t-C_4H_9OH	4.9	$8.4 \cdot 10^{-4}$

The h values for the dehydrogenation of i-C_3H_7OH and for the dehydration of t-C_4H_9OH are practically identical with those obtained from the kinetic constants for the other metals [9], but there is a significant difference between the a and h values characterizing the dehydration of the two alcohols.

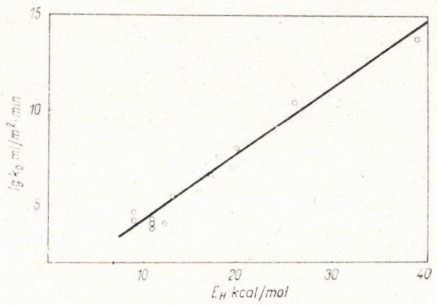

Fig. 2. Compensation effect between the constants of the ARRHENIUS equation in the case of the dehydrogenation of isopropyl alcohol

Discussion

It may be unequivocally established from the results of these experiments that in the presence of metals alcohols undergo both dehydrogenation and dehydration. Dehydration occurs not only in the case of tertiary butyl alcohol which is incapable of dehydrogenation, but takes place parallel to dehydrogenation, as shown on the example of isopropyl alcohol. In the presence of certain metals, isopropyl alcohol suffers selective dehydration.

The fact that alcohols may undergo dehydration is further experimental evidence in support of the possible stepwise dehydrogenation of hydrocarbons as envisaged by us earlier [11, 12, 20]. The surface complexes formed during the stepwise dehydrogenation of hydrocarbons and the dehydration of alcohols are the following:

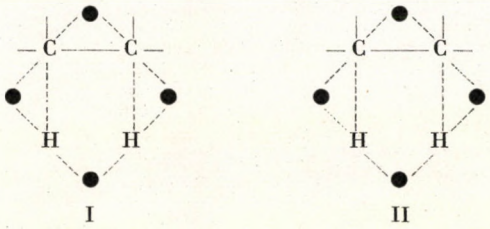

(where ● stands for the atoms of the catalyst surface).

In the case of both structures I and II the vertical bonds open during the reaction, and two horizontal bonds are formed. No significant difference between the two structures is expected from the point of view of hydrogen and water elimination. The energy required for the cleavage of the C—O bond is by about 5 kcal lower than the energy of the C—H bond in cyclohexane [21]. On the other hand, according to calculations [22], there is no significant difference (maximum $\pm$ 5 kcal) between the energies of the Me—O and He—H bonds. Thus the difference to be expected between the energies required for

the rupture of the C—H and C—O bonds is not sufficiently great to justify the preference of either of the two reactions by metal catalysts. Such a case could be explained only by a special mechanism — for instance sextet mechanism — of dehydrogenation, which is impossible for the dehydration of the alcohol. According to the mechanism of a stepwise removal of hydrogen it follows that there is no obstacle to the dehydration of alcohols, either. This conclusion has been confirmed by the experiments described here.

It may be expedient to examine more closely the correlation between the dehydrogenating and dehydrating properties of the various catalysts. It is

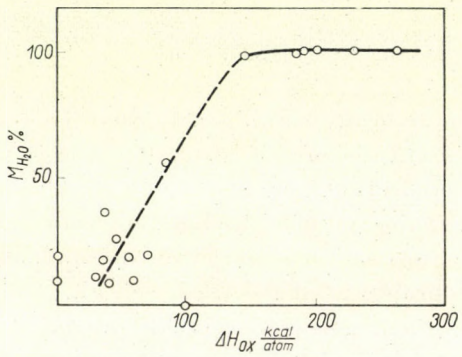

Fig. 3. Correlation between the dehydration ratio of the alcohol and the oxidation enthalpy of the metal

seen from the data in Table I that the catalysts under investigation can be classified into two distinctly different groups: at the temperature chosen for comparison, the catalysts in the one group promote mainly dehydration, while the members of the other group further mainly dehydrogenation. There is but one metal (Zn) which catalyzes both processes to about the same degree. One third of the metals under investigation may be regarded as practically exclusively dehydrating catalysts. It is noteworthy that Be, Ti, V, Zr, Mo and W which can be considered selective dehydrating catalysts, are highly liable to oxidation and their oxides are difficult to reduce. This is clearly visible from Fig. 3 which shows the percentage dehydration *vs.* the oxidation enthalpy of the various metals. There are a few cases only which deviate from the general slope of the curve. The oxidation enthalpy of the selectively dehydrating metals is in each case higher than 140 kcal/g-atom. It seems possible that the correlation observed by Japanese authors [23—25] between catalytic activity and the standard oxidation enthalpy of metals is also valid for the dehydration of alcohols. Fig. 4 supports the existence of some similar correlation; further evidence is given by the fact that in the case of higher ΔH_{ox} values the oxide layer formed on the surface is more stable, and the oxide is more

favourable from the point of view of dehydration than the metal. It is probable that the presence of the oxide layer has a stabilizing effect on catalytic activity, but this alone is not sufficient to explain the dehydrating action of the metals. This explanation would namely exclude a dehydrating action of metals resistant to oxidation, whose oxides are readily reduced in the presence of hydrogen, such as silver, gold, platinum or palladium.

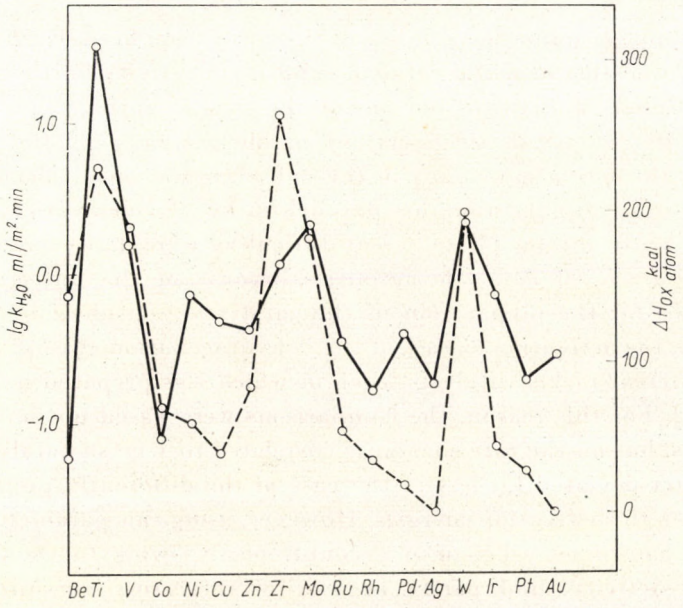

Fig. 4. The rate constant of dehydration of isopropyl alcohol *vs.* the oxidation enthalpy of the metal catalyst

The selective dehydrating effect of Ti, V, Zr, Mo and W may also be explained by the very great atomic distances in the lattices of these metals. RUBINSTEIN and PRIBITKOVA [26] have reported relatively increased dehydration with increasing crystal lattice parameter. This fact is in agreement with the conception that the dehydrogenation of an alcohol takes place through the formation of the following surface complex [27]:

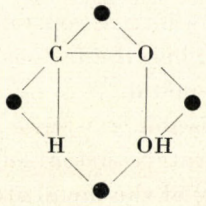

III

The O—H bond is namely much shorter than the C—O bond which has to open during dehydration (Structure II).

It is reasonable that both the oxidation enthalpy and the lattice constants play a part in the explanation of the dehydrating activity. The situation is the same as in the dehydrogenation of cyclohexane: the catalytic activity could be explained both in terms of structure and crystal lattice, since the energetic, structural and electron distribution parameters are correlated with one another.

Let us now examine the validity of the correlation between the characteristic bulk parameters of metal catalysts and their activity in the dehydrogenation of alcohols. BALANDIN and one of the present authors have shown [5] for seven different metals the apparent parallelism between the atomic diameter and the activation energy in the dehydrogenation of alcohols. It was interesting to investigate now this parallelism for a wider variety of metals using the recently obtained data. Great difficulties were, however, encountered in the comparison of catalytic activities because of the differences in the methods used for the preparation of the catalysts. Considerable discrepancy was found in the activation energy of the dehydrogenation of isopropyl alcohol with ten different nickel catalysts, each of which was prepared by a different method [28]. For this reason, the comparisons were based not on the activation energies, but on the rate constants correlated to 1 m^2 of catalytic surface, as these latter deviated far less in the case of the differently prepared nickel catalysts than the activation energies. However, using this parameter, a greater uncertainty has to be taken into account, partly owing to the fluctuations of catalytic activity, and partly because of the errors committed in measuring the surface area, as compared with the case when the activation energies are determined from data pertaining to several different temperatures.

Fig. 5 shows the rate constants of the dehydrogenation of isopropyl alcohol *vs.* the lattice constants of the different metals. It can be seen that similarly to the case of cyclohexane, here again a correlation characterized by a maximum curve is found, though for some metals — probably for reasons discussed above — the deviation from the general shape of the curve is quite considerable. In this respect the case of beryllium should be mentioned whose activity — just as for cyclohexane dehydrogenation — is considerably lower than might be expected from its lattice constant. This is probably due to the fact that the atomic structure of beryllium — as it has been pointed out [12] — differs from that of any other metal.

We also examined the possible existence of a correlation and its extent between the dehydrogenation rate constant of the alcohol and the value of the standard oxidation enthalpy of the metal atom (Fig. 6). A tendency indicative of such a correlation has been found. The curve which represents this,

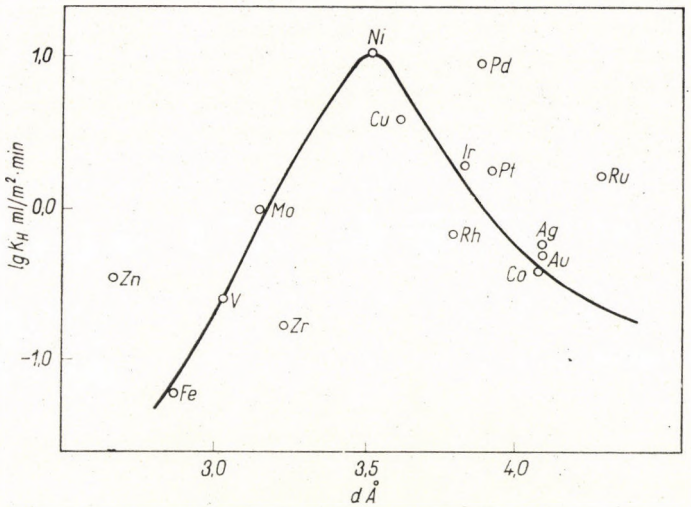

Fig. 5. Correlation between the lattice constant of the catalyst and the rate constant of dehydrogenation of isopropyl alcohol

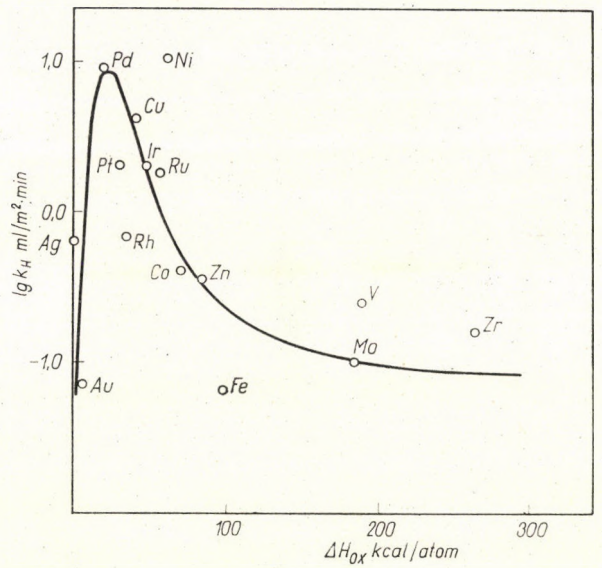

Fig. 6. Correlation between the rate constant of dehydrogenation of isopropyl alcohol and the oxidation enthalpy of the metal catalyst

has a shape very similar to that of the curve obtained for cyclohexane [12]. This curve, like the one shown in Fig. 5, has a definite maximum.

The observed connection of catalytic activity with both the lattice constants and oxidation enthalpies of the metals and the similar character

of the correlations prove again the joint action of energetic and structural factors in catalytic activity, as it has been pointed out in the discussion of the dehydrogenation of cyclohexane.

SUMMARY

The possibility of the parallel dehydrogenation and dehydration of isopropyl alcohol in the presence of Be, Ti, V, Fe, Co, Ni, Cu, Zn, Zr, Mo, Ru, Rh, Pd, Ag, W, Ir, Pt and Au has been investigated. The majority of these metals catalyze both reactions in the temperature range between 230° and 300 °C. Iron is a selective dehydrogenation catalyst, whereas Be, Ti, V, Zr and W are selective dehydrating catalysts. The kinetic constants of the dehydration of tertiary butyl alcohol in the presence of Be, Ti, V., Zn, Zr, Ru, Ir and Au have also been determined.

A correlation has been found between the catalytic activity and the standard oxidation enthalpy of the metals in the case of both reactions. A similar correlation exists in the dehydrogenation of isopropyl alcohol between catalytic activity and the lattice constant of the metal catalyst.

REFERENCES

1. SABATIER, P., SENDERENS, J.: Compt. rend. **136,** 738, 983 (1903).
2. SABATIER, P., SENDERENS, J.: Compt. rend. **137,** 16 (1903).
3. PALMER, W., CONSTABLE, F.: Proc. Roy. Soc. (A) **107,** 255 (1925).
4. THONON, Cl., JUNGERS, J.: Bull. Soc. chim. Belg. **58,** 331 (1949).
5. BALANDIN, A., TÉTÉNYI, P.: Probl. Kinetiki i Kataliza **10,** 339 (1960).
6. TÉTÉNYI, P., SCHÄCHTER, K.: Dokl. Akad. Nauk. USSR **146,** 621 (1962).
7. TÉTÉNYI, P., SCHÄCHTER, K., BABERNICS, L.: Magyar Kém. Foly. **69,** 181 (1963).
8. TÉTÉNYI, P., SCHÄCHTER, K., BABERNICS, L.: Acta chim. Acad. Sci. Hung. **43,** 387 (1965).
9. SCHÄCHTER, K., TÉTÉNYI, P.: Acta chim. Acad. Sci. Hung. **46,** 229 (1965).
10. HODGMAN, C.: Handbook of Chemistry and Physics. Chem. Rubber Publ. Co., Cleveland, 1964.
11. TÉTÉNYI, P., SCHÄCHTER, K.: Acta chim. Acad. Sci. Hung. **50,** 129 (1966).
12. TÉTÉNYI, P., SCHÄCHTER, K.: Acta chim. Acad. Sci. Hung. (In the press.)
13. TÉTÉNYI, P., BABERNICS, L., PETHŐ, Á.: Acta chim. Acad. Sci. Hung. **28,** 375 (1961).
14. BORK, A.: Thesis for D. Sc. Moscow, 1936.
15. BORK, A., TOLSTOPYATOVA, A.: Zh. Fiz. Khim. **12,** 227 (1938).
16. BORK, A., BALANDIN, A.: Z. phys. Chem. **B, 33,** 54, 73, 435 (1936).
17. BALANDIN, A.: Zh. Obshchei Khim. **12,** 153 (1942).
18. BALANDIN, A., TÉTÉNYI, P.: MTA Kém. Tud. Oszt. Közl. **11,** 299 (1959).
19. CREMER, E.: Adv. Catalysis **7,** 75 (1955).
20. TÉTÉNYI, P.: Acta chim. Acad. Sci. Hung. **40,** 157 (1964).
21. SZWARCZ, M.: Chem. Rev. **47,** 75 (1951).
22. MATJUSENKO, V.: Dokl. Akad. Nauk. USSR **128,** 99 (1959).
23. KEN-ICHI TANAKA, KENZI TAMARU: J. Catalysis **2,** 366 (1963).
24. KEN-ICHI TANAKA, KENZI TAMARU: Kinetika i Kataliz **7,** 242 (1966).
25. YOSHIHIKO MORO-OKA, YUTAKA MORIKAWA, ATSUMU OZAKI: J. Catalysis **7,** 23 (1967).
26. RUBINSTEIN, A., PRIBITKOVA, N.: Izvest. Akad. Nauk SSSR. Otdel Khim. Nauk. 509 (1945).
27. BALANDIN, A.: Dokl. Akad. Nauk USSR **97,** 449 (1954).
28. TÉTÉNYI, P., SCHÄCHTER, K., BABERNICS, L.: Acta chim. Acad. Sci. Hung. **42,** 325 (1964).

Pál TÉTÉNYI
Klára SCHÄCHTER
Budapest XII., Konkoly-Thege u.

Acta Chimica Academiae Scientiarum Hungaricae Tomus 56 (2), pp. 153—165 (1968)

HARMONIC FORCE FIELD REFINEMENT CALCULATIONS FOR POLYATOMIC MOLECULES, II

FORCE FIELD CALCULATIONS ON NO_2F AND NO_2Cl MOLECULES CONTAINING ^{14}N AND ^{15}N ISOTOPES

L. NEMES

(Central Research Institute for Chemistry, Hungarian Academy of Sciences, Budapest)

Received July 3, 1967

1. Introduction

In previous papers [1, 2, 3] a method was described for establishing symmetry force constant ranges for nitric acid and its halides, and the application of the hybrid orbital force field model proposed by MILLS [4] for the above molecules was reported. The normal frequency assignment used in our former calculations has been revised by BERNITT, MILLER and HISATSUNE [5] on the ground of the vibrational analysis of NO_2F and NO_2Cl molecules substituted by ^{14}N and ^{15}N isotopes. These authors also gave results for valence force field and UREY-BRADLEY field calculations. The present work reports force field calculations with the help of a least-squares refinement program [6], utilizing isotopic frequency data and the modified vibrational assignment. In the previous calculations [1, 2, 3] such symmetry coordinates were used whose application caused redundancy problems; in the present paper calculations in a more simple coordinate system are also reported, and a comparison of the results obtained in the two types of coordinate systems is given.

2. Comparison of the symmetry coordinate systems

In the following, the two types of symmetry coordinates are shown for planar XZY_2 molecules (Set I and Set II):

Set I

Species A_1:

$$S_1 = \frac{1}{\sqrt{3}}(D + d_1 + d_2)$$

$$S_2 = \frac{1}{\sqrt{6}}(2D - d_1 - d_2)$$

$$S_3 = \frac{d_0}{\sqrt{6}}\left[2d_0 A - \sqrt{d_0 D_0}\,(a_1 + a_2)\right].$$

Set II

Species A_1:

$$S_1 = \frac{1}{\sqrt{2}}(d_1 + d_2)$$

$$S_2 = D$$

$$S_3 = d_0 A.$$

In species B_1 there is only one set of coordinates:

$$S_4 = \frac{1}{\sqrt{2}}(d_1 - d_2)$$

$$S_5 = \frac{\sqrt{d_0 D_0}}{\sqrt{2}}(a_1 - a_2),$$

where D and d denote the N—X and N—O bonds, and A and a are the ONO and XNO angles, respectively (see [1]).

While Set I contains a redundant coordinate (not given here, but denoted as S_4 in [1]), Set II does not, as it is not necessary for symmetry C_{2v} [8]. The particular scaling of the symmetry coordinates, used in order to give a uniform dimension for all force field elements, arises from the conventions of the G-matrix computing program elaborated by S. J. CYVIN* and co-workers [14].

3. Isotopic frequency data and molecular geometry

The following table shows the assignments given by BERNITT, MILLER and HISATSUNE [5] for the molecules treated here.

Table I

Frequency assignments for nitryl halides

Molecule / Normal mode	$^{14}NO_2F$	$^{15}NO_2F$	$^{14}NO_2Cl$	$^{15}NO_2Cl$
ν_1	1309.6(13)	1298.0(13)	1286.0*(13)	1275.8*(13)
ν_2	822.4(6)	808.5(8)	792.6(8)	782.0(8)
ν_3	567.8(6)	567.1(6)	369.6(4)	367.4(4)
ν_4	1791.5(18)	1750.5(18)	1684.6(17)	1646.8(17)
ν_5	559.6(6)	558.9(6)	408.1(4)	(408) (10)

* The author would like to express his thanks to Professor S. J. CYVIN, *Department of Theoretical Chemistry, Technical University of Norway, Trondheim*, for the copies of programs.

The numbers in brackets following the frequencies are the estimated (systematic) uncertainties in the refinement calculations. The ν_1 fundamental frequencies of the NO_2Cl isotopic species (denoted by asterisks in Table I) are values corrected for Fermi resonance (see [5] and [7]). In the case of $^{15}NO_2Cl$ the ν_5 fundamental frequency was estimated from the overtone.

The molecular geometry data used here are the same as in [2].

4. Hybrid orbital force field results in species A_1

In species A_1 the H.O.F.F. model fixes two off-diagonal force field elements (see [2]). These relations are summarized below for Set I and Set II coordinates:

Set I

$$F_{13} = \frac{2}{d_0\sqrt{3}}\left[\left(\frac{\partial d}{\partial \lambda}\right) - \left(\frac{\partial D}{\partial \lambda_x}\right)\right] F_{11}$$
$$F_{23} = -\frac{\sqrt{2}}{d_0\sqrt{3}}\left[\left(\frac{\partial d}{\partial \lambda}\right) + \left(\frac{\partial D}{\partial \lambda_x}\right)\right] F_{22} \qquad (1)$$

Set II

$$F_{13} = \frac{\sqrt{3}}{d_0}\left(\frac{\partial d}{\partial \lambda}\right) F_{11}$$
$$F_{23} = -\frac{\sqrt{6}}{d_0}\left(\frac{\partial D}{\partial \lambda_x}\right) F_{22} \qquad (2)$$

If it is assumed that $(\partial d/\partial\lambda)$ and $(\partial D/\partial\lambda_x)$ are positive quantities, and of similar magnitude, it can be seen that the value of F_{13} obtained in Set I is very small Since this constant describes the interaction of the NO_2 symmetric stretching and the NO_2 scissoring coordinates, it is probable, even apart from H.O.F.F. considerations, that F_{13} has a small value. Accordingly, in all subsequent calculations the constraint $F_{13} = 0$ was used, even for Set II coordinates. Several values were tried for the proportionality constant k in the relation

$$F_{23} = -kF_{22}$$

based on H.O.F.F. considerations. For Set II coordinates the values taken for k were 0.07, 0.10 and 0.13, while for Set I coordinates (given here only for the sake of comparison) the value used was $k = 0.10$. As it will be seen,

the weighted sum of error squares is quite a sensitive function of k. Different values for k mean, of course, different values of the $(\partial k/\partial\lambda)$ type parameters, but this is not inconsistent with the basic assumptions of the H.O.F.F. model [4].

The converged force field data obtained using Set II coordinates are summarized below for different k values. In these calculations the convergence damping possibilities of the program described in [6] have been utilized, and the value of the damping parameter used throughout is 800. For this reason the statistical dispersion values for the force constants obtained are too low, so they have but relative significance.

Table II

NO_2F force constants (Set II), mdyn/A

		$k = 0.07$	$k = 0.10$	$k = 0.13$
F_{11}		10.567±0.090	10.831±0.039	11.033±0.012
F_{12}		0.786±0.085	0.973±0.037	1.088±0.011
F_{13}	(constrained)	0 ± 0	0 ± 0	0 ± 0
F_{22}		3.547±0.088	3.724±0.038	4.066±0.011
F_{23}		−0.248±0.006	−0.373±0.004	−0.529±0.001
F_{33}		1.134±0.057	1.072±0.023	0.989±0.006
$\sum_i \varepsilon_i^2 W_i$		27.045	5.039	0.461
Det(Z'J'WJZ)		$1.494 \cdot 10^{12}$	$1.715 \cdot 10^{12}$	$2.350 \cdot 10^{12}$
$\prod_i (Z'J'WJZ)_{ii}$		$1.674 \cdot 10^{12}$	$1.904 \cdot 10^{12}$	$2.500 \cdot 10^{12}$

The errors of the calculated frequencies obtained by using the above-described force field leading to the smallest errors, and the errors of the calculated nitrogen isotopic shifts are tabulated below.

Frequency errors (exp.—calcd.), cm^{-1}

$$^{14}N: \Delta\nu_1 = -5.97 \quad \Delta\nu_2 = 2.89 \quad \Delta\nu_3 = 0.04$$

$$^{15}N: \Delta\nu_1 = 1.61 \quad \Delta\nu_2 = -2.55 \quad \Delta\nu_3 = 0.25$$

Isotopic frequency shift reproduction, cm^{-1}

$k = 0.13$

Experimental: $\nu_1^{14}-\nu_1^{15}$: 11.6 $\quad \nu_2^{14}-\nu_2^{15}$: 13.9 $\quad \nu_3^{14}-\nu_3^{15}$: 0.7

Calculated: $\nu_1^{14}-\nu_1^{15}$: 19.2 $\quad \nu_2^{14}-\nu_2^{15}$: 8.5 $\quad \nu_3^{14}-\nu_3^{15}$: 0.9

Table III

NO_2Cl force constants (Set II), mdyn/Å

		$k = 0.07$	$k = 0.10$	$k = 0.13$
F_{11}		9.210±0.018	9.409±0.015	9.581±0.018
F_{12}		0.332±0.017	0.353±0.014	0.365±0.017
F_{13}	(constrained)	0 ± 0	0 ± 0	0 ± 0
F_{22}		6.088±0.018	6.377±0.014	6.648±0.017
F_{23}		−0.426±0.001	−0.638±0.001	−0.864±0.002
F_{33}		0.439±0.004	0.442±0.003	0.464±0.003
$\sum_i \varepsilon_i^2 w_i$		1.161	0.725	1.095
Det(Z'J'WJZ)		$1.458 \cdot 10^{13}$	$1.759 \cdot 10^{13}$	$2.086 \cdot 10^{13}$
$\prod_i^i (Z'J'WJZ)_i^i$		$1.467 \cdot 10^{13}$	$1.768 \cdot 10^{13}$	$2.105 \cdot 10^{13}$

The frequency errors obtained by using the above-described force field leading to minimal errors, and the errors of the calculated N isotopic shifts are compiled below.

Frequency errors (exp.—calcd.), cm^{-1}

$k = 0.10$

^{14}N : $\Delta\nu_1 = -5.95$ $\Delta\nu_2 = 2.80$ $\Delta\nu_3 = 0.47$

^{15}N : $\Delta\nu_1 = 6.84$ $\Delta\nu_2 = -2.38$ $\Delta\nu^3 = -0.48$

Isotopic frequency shift reproduction, cm^{-1}

$k = 0.10$

Experimental: $\nu_1^{14}-\nu_1^{15}$: 10.2 $\nu_2^{14}-\nu_2^{15}$: 10.6 $\nu_3^{14}-\nu_3^{15}$: 0.22

Calculated: $\nu_1^{14}-\nu_1^{15}$: 23.0 $\nu_2^{14}-\nu_2^{15}$: 5.4 $\nu_3^{14}-\nu_3^{15}$: 1.30

The following tables provide a comparison between the results, in the two sets of symmetry coordinates, for both molecules.

Table IV

Comparison of NO_2F force constants obtained in the two different coordinate systems, mdyn/Å

$k = 0.10$

		Set I	Set II
F_{11}		12.587±0.036	10.831±0.039
F_{12}		−3.630±0.034	0.973±0.037
F_{13}	(constrained)	0 ± 0	0 ± 0
F_{22}		4.370±0.035	3.724±0.038
F_{23}		−0.437±0.004	−0.373±0.004
F_{33}		0.669±0.014	1.072±0.023
$\sum_i \varepsilon_i^2 W_i$		4.189	5.039

Table V

Comparison of the NO_2Cl force constants obtained in the two different coordinate systems, mdyn/Å

$k = 0.10$

		Set I	Set II
F_{11}		10.057±0.012	9.409±0.015
F_{12}		−2.260±0.011	0.353±0.014
F_{13}	(constrained)	0 ± 0	0 ± 0
F_{22}		7.127±0.012	6.377±0.014
F_{23}		−0.713±0.001	−0.638±0.001
F_{33}		0.270±0.001	0.442±0.003
$\sum_i \varepsilon_i^2 W_i$		0.512	0.725

5. Results in species B_1

The corresponding H.O.F.F. constraint is the following:

$$F_{45} = -\frac{\sqrt{6}}{\sqrt{d_0 D_0}} \left(\frac{\partial d}{\partial \lambda}\right) F_{44} \tag{3}$$

In the tables below the converged force field data are given (the value of the damping parameter is $x = 800$ again).

Table VI

NO_2F force field (mdyn/Å) and frequency errors (exp.—calcd.) (cm^{-1})

F_{44}	7.390 ± 0.006
F_{45}	0.762 ± 0.005
F_{55}	1.095 ± 0.003
$\sum_i \varepsilon_i^2 W_i$	0.032
^{14}N: $\Delta\nu_4 = -2.18$	$\Delta\nu_5 = 0.12$
^{15}N: $\Delta\nu_4 = 2.33$	$\Delta\nu_5 = -0.12$

Table VII

NO_2Cl force field (mdyn/Å) and frequency errors (exp.—calcd.) (cm^{-1})

F_{44}	8.776 ± 0.005
F_{45}	0.040 ± 0.004
F_{55}	0.473 ± 0.001
$\sum_i \varepsilon_i^2 W_i$	0.018
^{14}N: $\Delta\nu_4 = -0.71$	$\Delta\nu_5 - 0.19$
^{15}N: $\Delta\nu_4 = 0.28$	$\Delta\nu_5 = 1.20$

Table VIII

Isotopic frequency shift reproduction (cm^{-1})

	NO_2F	
Experimental:	$\nu_4^{14} - \nu_4^{15}$: 41	$\nu_5^{14} - \nu_5^{15}$: 0.7
Calculated:	$\nu_4^{14} - \nu_4^{15}$: 45.5	$\nu_5^{14} - \nu_5^{15}$: 0.5
	NO_2Cl	
Experimental:	$\nu_4^{14} - \nu_4^{15}$: 37.8	$\nu_5^{14} - \nu_5^{15}$: (0.1)
Calculated:	$\nu_5^{14} - \nu_4^{15}$: 38.8	$\nu_5^{14} - \nu_5^{15}$: 1.5

The datum given in brackets for NO_2Cl was calculated using a frequency value estimated from the overtone.

6. Vibrational forms and Jacobian matrices

In the following the $(L^{-1})'$ matrices and the root-Jacobians are given. (The dash denotes transposition.)

Table IX

NO_2F molecule

Species A_1: ($k = 0.13$)					
$(L^{-1})'$	^{14}N:	2.9546	2.2346	0.9197	
		—0.2728	2.6565	—2.5129	
(a. m. u.)$^{+1/2}$		—0.2418	0.4022	2.1348	
	^{15}N:	3.0351	2.1290	0.9198	
		—0.2399	2.7139	—2.4712	
		—0.2341	0.3995	2.1474	
		λ_1	λ_2	λ_3	
Transpose of the *Jacobian*		0.0852	0.0027	0.0005	F_{11}
matrix		—0.1122	0.0297	—0.0035	F_{12}
	^{14}N	—0.2055	0.0326	0.0172	F_{13}
(a. m. u.)$^{-1}$		0.0370	0.0326	0.0172	F_{22}
		0.1353	0.1788	—0.0558	F_{23}
		0.1239	0.0982	0.1365	F_{33}
Species B_1					
$(L^{-1})'$	^{14}N	1.8178	—2.4755		
(a. m. u.)$^{+1/2}$		0.4739	1.9061		
	^{15}N	1.8677	—2.4587		
		0.4842	1.9126		
		λ_4	λ_5		
Transpose of the *Jacobian*		0.1689	0.0104	F_{44}	
matrix	^{14}N	0.4387	—0.0801	F_{45}	
(a. m. u.)$^{-1}$		0.2849	0.1536	F_{55}	

7. Discussion

One of the interesting results of the calculations is the difference between the NO_2F and NO_2Cl force fields. To facilitate the comparison, the tables below show the optimal H.O.F.F. parameters and the internal force constants calculated therefrom, in mdyn/Å units.

From the value of f_D it is concluded that the order of the bond N—Cl is higher than that of N—F. The same conclusions have been reached in the earlier calculations [2], although the symmetry force constant range calculations

Table X

NO_2Cl molecule

Species A_1: ($k = 0.10$)

$(L^{-1})'$	^{14}N	2.6093	2.6856	0.9149
		—1.1491	3.5305	—2.4977
		—0.0116	—0.1428	2.3255
(a. m. u.)$^{+1/2}$	^{15}N	2.6939	2.6066	0.9056
		—1.1248	3.6023	—2.4428
		—0.0105	—0.1497	2.3317

		λ_1	λ_2	λ_3	
Transpose of the *Jacobian*		0.0790	0.0094	0.0001	F_{11}
matrix		—0.1283	0.0421	0.0002	F_{12}
		—0.2000	0.0378	0.0065	F_{13}
(a. m. u.)$^{-1}$	^{14}N	0.0521	0.0474	0.0001	F_{22}
		0.1624	0.0852	0.0108	F_{23}
		0.1266	0.0383	0.1938	F_{33}
Species B_1					
$(L^{-1})'$	^{14}N	2.2281	—2.1940		
(a. m. u.)$^{+1/2}$		0.1335	2.1239		
	^{15}N	2.2831	—2.1577		
		0.1341	2.1343		

		λ_4	λ_5		
Transpose of the *Jacobian*		0.1786	0.0007	F_{44}	
matrix	^{14}N	0.3691	—0.0236	F_{45}	
(a. m. u.)$^{-1}$		0.1906	0.1966	F_{55}	

gave 4.19 and 3.50 mdyn/Å for the bonds N—Cl and N—X, respectively. According to the data of BERNITT *et al.* [5] the corresponding valence force field values are 2.456 and 2.657 mdyn/Å, so that both of them are definitely below the single bond order level and are practically identical. BERNITT *et al.* also came to similar conclusions in the case of the UREY-BRADLEY model (though they did not regard it as satisfactory for a physically acceptable description of the NO_2X force fields.)

The values for NO_2F obtained in this work, however, show acceptable agreement with those of BURNELLE and DUCHÈSNE [9] who gave the following

Table XI

Optimal hybrid orbital force field parameters in Set II coordinates, mdyn/Å

	NO_2F	NO_2Cl
F_{11}	11.033	9.409
F_{12}	1.088	0.353
F_{13} (constrained)	0	0
F_{22}	4.066	6.377
F_{23}	—0.529	—0.638
F_{33}	0.989	0.442
F_{44}	7.390	8.776
F_{45}	0.762	0.040
F_{55}	1.095	0.473

ranges for f_D, f_d and f_A : 4.3—5.3, 11.0—11.8 and 0.2—0.5 mdyn/Å, resp. The microwave measurements of MILLEN and SINNOTT [10] also suggest a larger N—Cl stretching force constant. They concluded from nuclear quadrupole

Table XII

Optimal internal force constants, mdyn/Å

(Calculated from the data in Table XI)

	NO_2F	NO_2Cl
f_d	9.212	9.093
f_D	4.066	6.377
f_A	0.989	0.442
f_{Dd}	0.769	0.253
f_{DA}	—0.529	—0.638
$(f_{da}—f'_{da})$	0.762	0.040

fine structure studies that the electron distribution of the N—Cl bond does not have axial symmetry, although this would be expected for a pure sigma bond (single bond). In their opinion it is quite possible that the canonical structure III in Fig. 1 contributes to a certain extent to the actual electron distribution of the molecule. Otherwise they calculated 11.6% for the ionic character of the bond. In order to emphasize the problems connected with this point, it is appropriate to note that the N—Cl bond length in NO_2Cl (1.83 Å [11]) is by some 0.10 Å greater than the sum of the covalent atomic radii, although CLAYTON *et al.* [11] do not attribute this to the contribution of canonical

structure III. They concluded from dipole moment measurements (the NO_2Cl dipole moment is 0.53 D) that the contribution of structure II is about 17%. The microwave- and dipole moment data suggest a single bond order in accordance with the results obtained in our studies. Still, it is very likely that the H.O.F.F. values that are significantly higher than those reported by BERNITT *et al.* are related to the assumptions about the rehybridization of nitrogen in the course of the vibration. (BURNELLE and DUCHÈSNE's results were also obtained by considering rehybridization.) It is worth pointing out that the number of valence electrons of NO_2Cl is identical to that of the ion NO_3^- in which all three bonds are equivalent, and their bond order is somewhere between the single and double bond values.

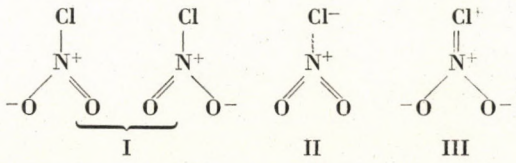

Fig. 1. Canonical structures of NO_2Cl

The N—O stretching force constants in Table XII are somewhat lower than in [2] and also fall much closer. The results of BERNITT *et al.* suggest a larger force constant value (although their UREY-BRADLEY results are similar to those obtained in this work). The empirical correlation curve given by LADD and ORVILLE-THOMAS [12] for the N—O bond length and stretching force constant also supports the conclusions drawn in this work, since the curve predicts a value of 9 mdyn/Å for a bond length of 1.21 Å. (We would like to call attention to a misprint in Eq. 1 in [12], which is a mathematical representation of the correlation curve, since apart from the region 1.15—1.20 Å, the formula gives points which do not fall on the curve.)

The value of the force constant f_A also suggests that the substitution of chlorine into the NO_2 molecule gives rise to a more significant change of the electronic structure than the substitution of fluorine; namely, the NO_2 angle deformation force constant is 1.099 mdyn/Å [13] which falls closer to the corresponding value of NO_2F than to that of NO_2Cl.

A further significant discrepancy can also be found between the two molecules concerning the difference of the two f_{da} type force constants; this can probably be accounted for by assuming that the signs of f_{da} and f'_{da} are identical in NO_2Cl, while opposite in NO_2F.

The force field given in Table XI poorly reproduces the experimentally found nitrogen isotopic shifts in species A_1, especially for NO_2Cl. The reason for this is that the errors of the calculated ν_1 and ν_2 — although relatively small — are of the order of a few wavenumbers. Considering that the number

of species A_1 symmetry force constants is effectively four (two constraints in H.O.F.F.), while the number of frequencies is six (or less, taking into account that there is only a very slight shift of ν_3, and the TELLER-REDLICH product rule allows only five independent values), it cannot be expected that solely on the basis of the present vibrational data any better results can be achieved. For the time being there are no experimental vibration-rotation interaction data available for the molecules discussed.

Tables IX and X contain interesting information about the vibrational assignments. The previous papers [1, 2, 3] already reported a study of the vibrational character of ν_2 and ν_3, and it was established that ν_3 should be assigned to the scissoring NO_2 coordinate. The present results also substantiate this conclusion, and suggest that ν_2 is rather of N—X stretching character than scissoring NO_2. At the same time, it is evident that the symmetry coordinates are strongly mixed in both vibrations. Similar information is yielded by the root-Jacobian matrices, since among the elements referring to λ_3 the last one is the largest in both molecules, *i.e.* F_{33} is most sensitive to λ_3. Further interesting data in this respect are the isotopic shifts themselves, insofar as isotopic substitution leaves ν_3 practically unchanged in both molecules. Clearly, if the latter mode would be dominantly an N—X stretching motion, as it is suggested by BERNITT *et al.*, it ought to be more sensitive to isotope effects. With respect to the vibrational forms in species B_1, Tables IX and X show that ν_4 is mainly of $\nu_{as}NO_2$ character, while S_4 and S_5 are intermingled in ν_5, but F_{55} is the most sensitive to λ_5, thus it can mostly be regarded as an N—X planar deformation mode. Again, according to Table VIII, it can be established that ν_5 hardly involves the motion of the central nitrogen whereas in species B_1 the force field parameters reproduce the experimental isotopic shift quite well.

Contrary to species A_1 iterative calculations, which converged rather slowly, in species B_1 convergence is quicker and definite, and the frequency errors are much smaller.

Finally it is noted with respect to the data in Tables IV and V that Set I and Set II force constants are different first of all in F_{12}. The advantage of Set II coordinates is that in this representation F_{12} has a much smaller value and, furthermore, as it has already been remarked, no redundancy relationships complicate the calculation of the internal force constants.

SUMMARY

Force field calculations were done for ^{14}N and ^{15}N isotope-containing NO_2Cl and NO_2F molecules, in a more simple symmetry coordinate system than the one used previously [1, 2, 3].

The converged force field data suggest that the order of the N—X bond is about unity:

f(N—F) = 4.1 mdyn/Å, f(N—Cl) = 6.4 mdyn/Å; whereas the N—O stretching force constant is practically identical in both molecules: f(N—O) = 9 mdyn/Å.

A study of the vibrational forms has shown, in accordance with previous investigations [1, 2, 3], that ν_3 is the scissoring NO_2 mode. This conclusion is supported by isotopic shift data.

REFERENCES

1. NEMES, L.: Acta chim. Acad. Sci. Hung. **52,** 169 (1967).
2. NEMES, L.: ibid **52,** 179 (1967).
3. NEMES, L.: ibid. **52,** 189 (1967).
4. MILLS, I. M.: Spectrochim. Acta **19,** 1585 (1963).
5. BERNITT, D. L., MILLER, R. H., HISATSUNE, I. C.: Spectrochim. Acta **23A,** 237 (1967).
6. NEMES, L., KÉMÉNCZY, M.: Acta chim. Acad. Sci. Hung. **53,** 359 (1967).
7. Vibrational Spectra of Some Nitrogen Oxyhalides. Ph.D. Thesis, R. H. MILLER, The Pennsylvania State Univ., 1965.
8. CYVIN, S. J.: Acta Scand. **20,** 2616 (1966).
9. BURNELLE, L., DUCHÈSNE, J.: Nature **182,** 653 (1958).
10. MILLEN, D. J., SINNOT, K. M.: J. Chem. Soc. **1958,** 350.
11. CLAYTON, L., WILLIAMS, Q., WEATHERLEY, T. L.: J. Chem. Phys. **30,** 1328 (1959).
12. LADD, J. A., ORVILLE-THOMAS, W. J.: Spectrochim. Acta **22,** 919 (1966).
13. WESTON, R. E.: J. Chem. Phys. **26,** 1248 (1957).
14. BRUNVOLL, J., CYVIN, S. J.: Acta Polytechn. Scand., Mathematics and Computing Machinery Series, No. 11 UDC 539.194:518.5:003.62

László NEMES; Budapest II., Pusztaszeri út 57/69.

Acta Chimica Academiae Scientiarum Hungaricae Tomus 56 (2), pp. 167—173 (1968)

CALCULATION OF FORCE CONSTANTS WITH THE MAXIMUM OVERLAP METHOD. I

TETRAHEDRAL MOLECULES

(SHORT COMMUNICATION)

M. MEZEI* and P. PULAY

Institute for General and Inorganic Chemistry, L. Eötvös University, and Research Group for Inorganic Chemistry, Hungarian Academy of Sciences, Budapest)

Received July 6, 1967

1

It is well known that the molecular force field cannot be determined unambiguously from the vibrational spectrum. Other experimental data depending on the force field are rarely available. A simplified model is assumed then for the force field, which contains less parameters and thus is unambiguously determined by the available data (mostly only the vibrational frequencies). One of the most widely used models is the valence force field, in which it is assumed that the off-diagonal force constants in internal valence coordinate representation are zero. Thus in this model the interaction force constants are neglected.

From the force constants of small molecules determined exactly by means of additional data [3, 9, 10, 14 to 17] we can see that, in general, the interaction force constants cannot be neglected, and that the non-vanishing interaction force constants in molecules of the type XY_k are mainly due to the change in the hybridization of the central atom [6].

On the basis of hybridization force fields have been elaborated by LINNETT and MILLS [7, 8].

In our study we present a more general quantumchemical model with the maximum overlap approximation. In this approximation we assume the bond energy to be proportional with the overlap integral of the bonding orbitals of the two atoms in the bond [4]. Having determined the best hybridization and the corresponding sum of overlap integrals as a function of the internal coordinates (if the molecule is symmetrical, that of the symmetry coordinates), the force constants multiplied with an unknown constant factor are obtained.

Our main goal was to find the signs of the interaction force constants because of the approximative character of the maximum overlap method.

* Present address: *Computational Center of the Hungarian Chemical Industries*, Budapest

Regarding the nature of our approximation, we expect to get meaningful results only for the stretch-bend and bend-bend interaction force constants. The model is not stable for the stretching force constants if we do not take into account the repulsive forces acting between two atoms in a bond. But, in general, the main problem is represented by the interactions containing bending.

The method described in the present paper may be applied for molecules or fragments of a molecule with a central atom that is surrounded by ligands and has no lone pair electrons. If the central atom does possess a lone pair, one cannot expect the maximum of the sum of overlaps to be near the equilibrium of the molecule, because the maximum overlap method does not take the lone pair into account. Detailed investigation of this problem will be made in another publication.

2

Let the state function of the molecule be the linear combination of the atomic orbitals of the atoms in the molecule. Our task is now to obtain the linear combination of the atomic orbitals (hybridization) for which the sum of overlap integrals between the bonding orbitals is maximum.

The problem can generally be solved with the variational method, or with the method of DEL RE [2]. MURREL has described a procedure [11] for the computation of the hybridization in a molecule containing a central atom surrounded by ligands with known bonding orbitals. GOLEBIEWSKI has simplified this procedure [5].

Let the vector of the orbitals of the central atom be $\varphi = (\varphi_1, \varphi_2, \ldots, \varphi_n)$, the vector of the best hybrid orbitals $\psi = (\psi_1, \psi_2, \ldots, \psi_n)$, and that of the ligand orbitals $\Theta = (\Theta_1, \Theta_2, \ldots, \Theta_k)$, $k \leq n$.

The matrix S is defined by the following equation:

$$\mathbf{S}_{ij} = < \Theta_i \mid \varphi_j > \tag{1}$$

MURREL and GOLEBIEWSKI have shown that the maximal value of the sum of the overlap integrals is:

$$s = \mathrm{tr}\,(\mathbf{S}\mathbf{S}^{\mathrm{T}})^{1/2}, \tag{2}$$

and the best hybrid orbitals are determined by the following equation:

$$\psi = (\mathbf{S}\mathbf{S}^{\mathrm{T}})^{-1/2}\,\mathbf{S}\varphi\,. \tag{3}$$

For the determination of $(\mathbf{S}\mathbf{S}^{\mathrm{T}})^{1/2}$ we refer to [12].

It can be shown easily using Eq. (3) that the best hybrid orbitals will possess the same spatial symmetry as the ligand orbitals.

3

The notation of the internal coordinates of a tetrahedral T_d molecule can be seen in Fig. 1: r_1, α_{12} ... denote deviations from the equilibrium values. The symmetry coordinates are presented in Table I.

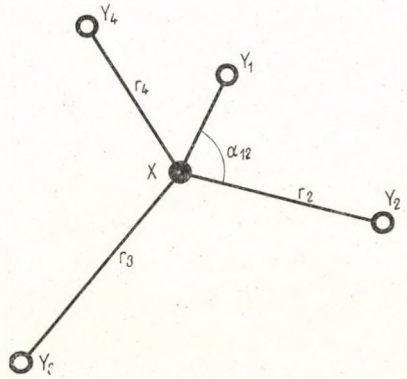

Fig. 1. Internal coordinates of the tetrahedral XY_4 molecule

Table I

The symmetry coordinates of a tetrahedral T_d molecule

Symmetry class	Coordinate	Force constant
A_1	$S_1 = 2^{-1}(r_1 + r_2 + r_3 + r_4)$	F_{11}
E	$S_2 = 12^{-1/2} r_0(2\alpha_{12} - \alpha_{13} - \alpha_{14} - \alpha_{23} - \alpha_{24} + 2\alpha_{34})$	F_{22}
F_2	$S_3 = 2^{-1}(r_1 + r_2 - r_3 - r_4)$ $S_4 = 2^{-1/2} r_0(\alpha_{12} - \alpha_{34})$	F_{33} F_{34} F_{44}

r_0 is the equilibrium bond length

Using the symmetry representation, we will have interaction force constants only in the F_2 species. The interaction of the internal bending coordinates can be calculated from the difference between F_{22} and F_{44}. But the symmetry force constants cannot be converted into internal force constants because the six angle coordinates are redundant.

We have calculated the maximum overlap with the MURREL–GOLEBIEWSKI method at nine values of S_2 and S_4 about the equilibrium state. In both cases α_2 was given the values $-8°$, $-6°$, $-4°$, $-2°$, $0°$, $2°$, $4°$, $6°$, $8°$. The

calculation of S_4 was performed at five different values of S_3 : -0.106 Å; -0.053 Å; 0; 0.053 Å and 0.106 Å.

On the basis of the relation $E = -ks$ (E is the energy of the molecule, s is the sum of overlaps and k is a constant) the force constants are given by the equation:

$$F_{ij} = -k\left(\frac{\delta^2 s}{\delta S_i\, \delta S_j}\right)_0 \quad ij = 22,\ 34,\ 44 \tag{4}$$

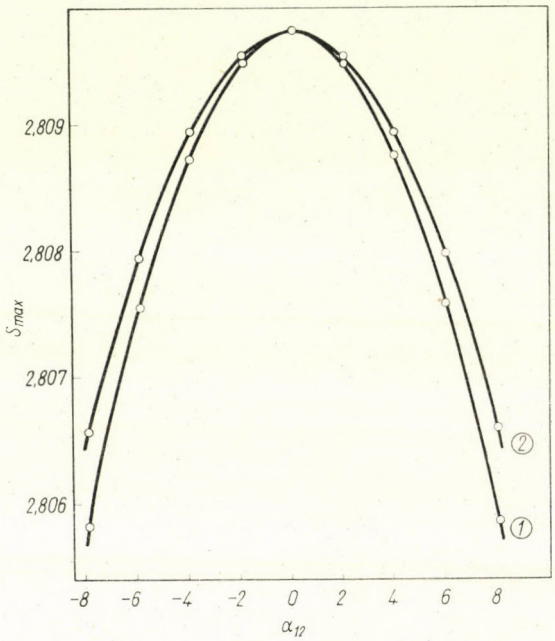

Fig. 2. The change of maximum overlap with the bending vibration of the species E and F_2 of methane at $S_3 = 0$

The functions $s(S_2)$ and $s(S_3, S_4)$ were approximated by polynomials of second degree in S_2 and S_4, respectively. The result hardly changed using polynomials of higher degree. We have got F_{22} and F_{44} as the second derivatives of the polynominals.

F_{34} was determined from the equation

$$F_{34} = -F_{44}\left(\frac{\delta S_4}{\delta S_3}\right) s = \max, \tag{5}$$

which follows from the definition of the force constants. Some typical diagrams are shown in Figs 2 and 3.

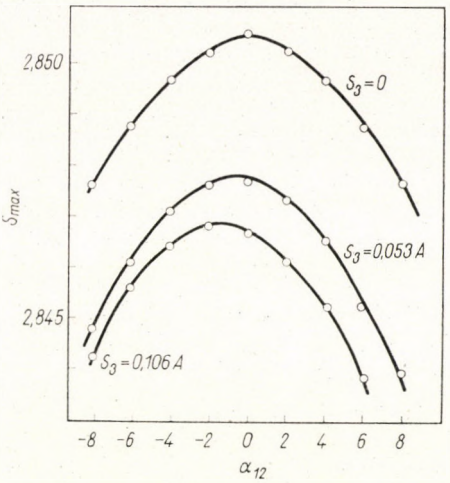

Fig. 3. The change of maximum overlap with the bending vibration of the species F_2 of silane at various values of S_3

4

Our calculations were carried out for the molecules CH_4, SiH_4, CF_4 and CCl_4. The effective nuclear charges used in the Slater type orbitals and the equilibrium geometrical data of the molecules are given in Table II [1, 13]. Fluorine and chlorine atoms were supposed to be *sp*-hybridized, because it produced greater overlap with the atomic orbitals of the central atom than the assumption of pure *s* or *p* orbitals.

Table II

Atomic function and equilibrium bond lengths of the molecules

Atom	Principal quantum number	Effective nuclear charges		
		Z_{ns}	Z_{np}	Z_{nd}
C	2	1.6083	1.5679	
Si	3	1.6344	1.4284	0.3333
H	1	1.0000		
F	2	2.5639	2.5498	
Cl	3	2.3561	2.0387	

	CH_4	SiH_4	CF_4	CCl_4
r_e(Å)	1.093	1.483	1.302	1.778

Table III

The force constants of CH_4, SiH_4 CF_4, and CCl_4 in mdyn/Å

Force constant	CH_4		SiH_4	
	calculated	lit. [9]	calculated	lit. [9]
F_{22}	0.49	0.49	0.188	0.188
F_{34}	—0.262	—0.206	—0.103	—0.023
F_{44}	0.579	0.458	0.196	0.213
Force constant	CF_4		CCl_4	
	calculated	lit. [3]	calculated	lit. [10]
F_{22}	0.71	0.71	0.311	0.311
F_{34}	—0.322	—0.84	—0.210	—0.52
F_{44}	0.733	0.02	0.320	0.38

The calculated force constants are presented in Table III. This table also contains the most realiable data available in the literature [3, 9, 10]. The values of k describing the connection between the energy and the overlap were chosen in such a way that the calculated F_{22} should agree with the experimental value.

It can be seen that the force fields of the molecules investigated are reflected quite well in our results. It is important that the sign of the interaction force constant F_{34} is in agreement with that of the experimental one.

But on the other hand, the results show that our model does not reflect the special characteristics of the force fields of the molecules investigated. So we can conclude from our results calculated so far that our model is fundamentally good, but requires further improvement. We suppose that the most important improvement would be the consideration of the mutual repulsion of the electron pairs on the central atom.

We tried to explain the difference between the force field of methane and silane by allowing the *d* orbitals of silicon to participate in the hybridization. The results, however, were practically the same as those obtained without the use of the *d* orbitals (Table III).

*

We are very much indebted to DR. PAPUSEK *(Czechoslovak Academy of Sciences, Prague)* for directing our attention to the method of maximum overlap.

SUMMARY

Bending and stretching-bending interaction force constants of methane, silane, carbon tetrafluoride and carbon tetrachloride have been determined by the maximum overlap approximation. The results are approaching the experimental data. Using the *d* orbitals of silicon left the results practically unchanged.

REFERENCES

1. CLEMENTI, E., RAIMONDI, D.: J. Chem. Phys. **38,** 2686 (1963).
2. DEL RE, G.: Theoret. Chim. Acta **1,** 188 (1963).
3. DUNCAN, J. L., MILLS, I. M.: Spectrochim. Acta **20,** 1089 (1964).
4. FERREIRA, R.: J. Phys. Chem. **68,** 2240 (1964).
5. GOLEBIEWSKI, A.: Trans. Faraday Soc. **57,** 1849 (1961).
6. HEATH, D. F., LINNETT, J. W.: Trans. Faraday Soc. **44,** 556 (1948).
7. LINNETT, J. W., WHEATLEY, P. J.: Trans. Faraday Soc. **45,** 33 (1949).
8. MILLS, I. M.: Spectrochim. Acta **19,** 1585 (1993).
9. DUNCAN, J. L., MILLS, I. M.: Spectrochim. Acta **20,** 523 (1964).
10. MORINO, Y.: J. Chem. Phys. **32,** 643 (1960).
11. MURREL, J. N.: J. Chem. Phys. **32,** 767 (1960).
12. PULAY, P.: Z. angew. Math. Mech. **46,** 151 (1966).
13. Interatomic Distances. The Chemical Society, London, 1958.
14. ALDOUS, J., MILLS, I. M.: Spectrochim. Acta **19,** 1567 (1963).
15. DUNCAN, J. L.: Spectrochim. Acta **20,** 1197 (1964).
16. DUNCAN, J. K.: Spectrochim. Acta **20,** 1807 (1964).
17. MCKEAN, D. C.: Spectrochim. Acta **20,** 269 (1966).

Mihály MEZEI
Péter PULAY
Budapest VIII., Múzeum krt. s/8.

Acta Chimica Academiae Scientiarum Hungaricae Tomus 56 (2), pp. 175—188 (1968)

ACID-CATALYZED HYDROLYSIS OF ALPHA- AND BETA-METHYLGLUCOPYRANOSIDES

J. SZEJTLI

(Present address: Chinoin Pharmaceutical Works, Budapest)

Received March 21, 1967

Introduction

The acid hydrolysis of the most simple glycosides — α- and β-methylglucosides — is a relatively thoroughly studied reaction. Their hydrolysis is important because, in the investigation of the acid-catalyzed splitting of other glycosidic linkages, the hydrolysis rates are usually compared to that of the corresponding methylglucoside [1].

However, the hydrolysis rate constants published by various authors cannot be compared directly, because they have been determined under various conditions; the values to be compared, the energy and entropy of activation are sometimes quite different. The published values for E_a of α-methylglucoside vary between 31.0 and 38.2 kcal/mole. According to most authors, the apparent E_a of the α-anomer is higher than that for the β-anomer, but a recent investigation [2] showed them to be nearly identical.

The relation of the hydrolysis rates of the anomers is a function of the temperature (see Table I), which proves that the two apparent E_a values may not be identical. However, at the same temperature, *e.g.* at 60 °C, the extreme values of k_β/k_α as calculated from data of various authors are 1.78 and 4.30.

The present paper is a part of a series [3] dealing with the acid-catalyzed hydrolysis of glycosidic linkages. Its aim is to present a reliable average of E_a, ΔS^*, and the rate constants, calculated on basis of both literature and experimental data.

The mechanism and other aspects of the hydrolysis reaction are beyond the scope of this paper. For a detailed summary of the properties of methylglucosides the reader is referred to BOLLENBACK's monograph [4] which contains over 500 references.

Experimental

(a) *Determination of k by measurement of the reducing power*

The hydrolysis and the analysis were carried out in the same way as published in a previous paper [3a]. 414.7 mg of α- and 402.5 mg of β-methylglucopyranoside were dissolved in 31.51 and 31.98 g of water, respectively. To 10-ml aliquots there were added 2-ml portions of

Table I

Ratio of the hydrolysis rates of α- and β-methylglucopyranosides under various conditions

Author	Ref.	t, °C	Acid	mole/l	$k\beta/k_\alpha$
EKENSTEIN	17	—	—	—	3
ARMSTRONG	18	74.1	HCl	0.5	1.79
		74.9			1.93
MOELWYN-HUGHES	10	60	HCl	1.0	2.64
		70			2.17
		80			1.79
		116*			1.00
FREUDENBERG	19	70	H_2SO_4	0.5	2.42
HEIDT, PURVES	6	75	HCl	0.097	1.79
OVEREND *et al.*	2	60	HCl	2.0	1.78
		71.9			1.86
		72.1			1.72
		79.6			1.81
NAKANO, RÅNBY	9	75	H_2SO_4	0.47	1.58
		85			1.51
		40	H_3PO_4	13.6	4.04
		50			3.77
		60			4.30
TIMELL	7a	60	H_2SO_4	0.5	2.16
		80			1.91
		100			1.61
		120			1.17
		132*			1.00
CLANCY, TURVEY	28	65	HCl	0.5	2.14
BUNTON *et al.*	20	72.9	$HC10_4$	0.93	2.03
				1.55	2.04
SZEJTLI	3	65	HCl	1.23	1.89
				0.123	1.90
				0.0123	2.02
		100		1.23	1.36
				0.123	1.70
				0.0123	2.01
		171*		1.0	1.00
		195*		pH = 1.0	1.00

* = extrapolated values

HCl of the appropiate concentration. All measurements were made on an analytical balance. Both glucosides were *Fluka* products of puriss. grade. The hydrolysis was effected in sealed glass tubes (3×100 mm) in an ultrathermostat. The sealed glass tubes containing about 0.5 ml solution were withdrawn at appropriate time intervals, opened with a glass-knife, put in a dry test-tube and cooled abruptly to —18°C. (The glass tubes ruptured in some cases only on touching with a glowing glass-rod.) Into the test tubes 10 ml of $NaHCO_3$ solution of the appropriate concentration was added to dilute and neutralize the acidic reaction mixture, and the reducing power was determined [5].

(b) *Determination of k by measuring the optical activity*

To a 2% glucoside solution an appropriate amount of 10 *N* HCl and water was added to adjust a glucoside concentration of 1%. The reaction mixture was sealed into a glass tube (12×120 mm). At appropriate time intervals samples were withdrawn from the ultrathermostat, cooled in an ice bath, and the rotatory power was measured at 20 °C with a *Schmidth—Haensch* (Berlin) polarimeter.

Results and discussion

The rate constants determined in this work are listed in Table II; the calculated E_a and ΔS^* values, together with those reported in the literature, are shown in Table III. The total number of the collected rate constants is 164, therefore they are not contained in Table III.

The values of $g = \Delta \log k/\Delta \mathrm{pH}$ for the rate constants, determined by reducing power measurements, were for the α- and β-anomers 1.104 ± 0.009 and 1.075 ± 0.006, respectively. The specific rate constants are expressed as a function of the pH as follows:

$$k_r = k/_{(a_{H^+})}g, \textit{ i.e.: } \log k_r = \log k + g.\mathrm{pH}$$

The d values (= limit value of $\log k_r$ versus 1/T when extrapolated to 1/T = 0) calculated on the basis of these specific rate constants [3a] were 17.11 ± 0.11 for the α- and 16.37 ± 0.31 for the β-anomer (k in $1n$ and $\sec^{-1}$). HEIDT and PURVES [6] have defined k_r as follows: $k_r = k/_{[HCl]}$. The calculated d values were 16.86 ± 0.22 and 16.29 ± 0.13 for the α- and β-anomers, respectively.

The role of temperature

The data in Table II cannot be directly compared to those in the literature, because the rates were not determined under identical conditions, *i.e.* at identical temperature, with the same kind and concentration of acid. If only the temperature is different, the extrapolation may easily be performed. Table IV shows an indirect comparison of some rate constants, determined at identical HCl concentration at different temperatures by various authors. Every authors' rate constants have been extrapolated on the basis of their

own E_a value to 100 °C. Taking into consideration the various experimental methods and errors, the agreement is quite good.

Table V contains k_{HCl} data extrapolated to both 100 °C and an acidity of $H_0 = 0.00$. (H_0 = *Hammett* acidity function.) The extrapolated rate con-

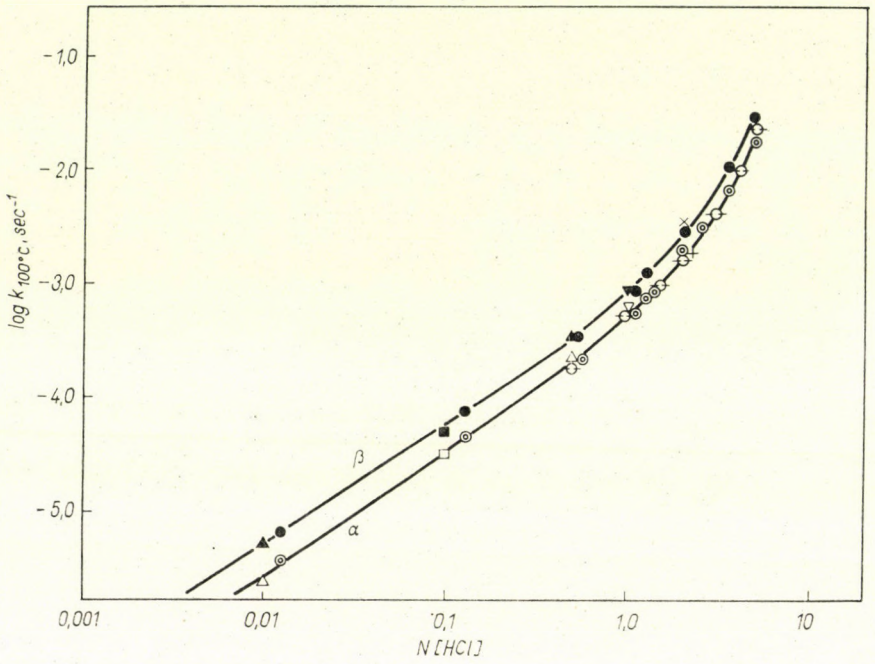

Fig. 1. Rate constants of α- and β-methylglucosides, determined by various authors between 50 and 104 °C and extrapolated to 100 °C, plotted against the hydrochloric acid concentration. The points on the curve represent the average of several rate constants, determined by the same author at identical acidity (see Table V). The authors and the marks for the α- and β-anomers are as follows: ARMSTRONG △ and ▲; HEIDT, PURVES □ and ■; OVEREND *et al.* + and ×; MOELWYN-HUGHES ▽ and ▼; TIMELL ⊖; SZEJTLI ⊙ and ●

stants are plotted against the acid concentration in Fig. 1. As it is seen, the points fall on two curves, one for the α- and one for the β-methylglucoside; scattering is fairly low. As it is shown in Tables IV and V, the value of k does not depend on the analytical method, *i.e.* determination of the reducing power or of the optical activity leads to the same k value.

When the hydrolysis is accomplished with various acids, extrapolation does not give an acceptable accuracy. TIMELL [7a] compared his data obtained with sulphuric acid with those of other authors. The agreement was acceptable only if all the compared values were determined in sulphuric acid; *e.g.*, at 70 °C in 0.5 M H_2SO_4 the rate constants were $2.85 \cdot 10^{-6}$ (TIMELL [7]), $2.96 \cdot 10^{-6}$ (EASTY [8]) and $3.38 \cdot 10^{-6}$ (NAKANO and RÅNBY [9]). The value of $4.64 \cdot 10^{-6}$

Table II

Rate constants of hydrolysis

°C	[HCl], mole/l	$k \cdot 10^5$ sec^{-1}	
		α-methylglucoside	β-methylglucoside
	determined by reducing power measurements		
100.0	1.23	90.4	123.3
	0.123	4.80	8.15
	0.0123	0.345	0.693
75.7	1.23	2.98	4.90
	0.123	0.161	0.292
	0.0123	0.0147	0.0258
65.0	1.23	0.620	1.175
	0.123	0.034	0.0666
	0.0123	0.00305	0.00616
	determined polarimetrically		
104.0	0.5	—	58.3
103.2	0.5	26.8	—
	0.5	29.8	—
	1.0	77.8	—
	1.0	82.6	—
	1.25	132.2	—
	2.0	248.0	—
90.0	0.5	—	9.08
	2.0	39.8	86.3
80.0	1.0	—	7.05
	2.0	13.6	21.5
	3.5	50.0	87.5
60.3	1.0	0.210	0.415
	2.0	0.734	1.43
	2.5	1.28	—
	3.5	2.48	4.65
	5.0	7.55	14.1

determined by OVEREND *et al.* [2] in HCl and extrapolated on basis of the *Hammett* acidity function, is higher by about 60%. The *Hammett* acidity function is not applicable for such purposes, to convert the rate constants determined in various acids to the same acidity [7a].

In calculating the average of apparent E_a (see Table III), the marked extreme values were not taken into consideration; so E_a for the α-anomer is 34.67 kcal/mole and for the β-anomer it is 33.28.

Table III

Literature data on the acid-catalyzed hydrolysis of methylglucosides

Author	Ref.	Temperature range	Range of acid, conc., mole/l	E_a, kcal/mole	ΔS^*, e. u.	Note
			α-methylglucoside HCl			
Bolin	11	70—80	0.05 —0.2			*p*, *c*
Moelwyn-Hughes	10b	60—80	1.0	38.2*		*p*
Overend *et al.*	2	60—79	2.0	34.1	+14.8	*p*
Timell	7a	50—60	0.5 —5.0			*p*
Armstrong	18	75—100	0.01 —0.5			*p*
Heidt, Purves	6a	60—75	0.05 —0.097	34.8	+16.5	*c*
Szejtli		65—100	0.0123—1.23	34.8	+17.6	*c*
Szejtli		60,3—103	0.5 —5.0	34.6	+16.1	*p*
Clancy, Turvey	28	65.0	1.5			
Wang, Hua	29	75.0	0.5			
			H_2SO_4			
Bunton *et al.*	20	72.9	1.13—1.63			*p*
Nakano, Rånby	9	78—85	0.47			*p*
Timell	7a	50—120	0.5 —5.0	35.1	+16.9	*p*
Easty	8	70—90	0.5	35.6	+18.9	*c*
Richards	21	100	0.5			
Freudenberg	19	70	0.25			
			$HClO_4$			
Bunton *et al.*	20	72.9	0.46—3.72			*p*
Armour *et al.*	22	44.6	4.03	33.7	+13.8	*p*
Timell	7a	50.0	0.5 —5.0			*p*
Withey, Whalley	23	100	0.518			**
			H_3PO_4			
Nakano, Rånby	9	40—60	13.6	28.8*		*p*
Timell	7a	50	2.0 —9.0			*p*
			Average	34.67	+16.37	
			β-methylglucoside HCl			
Veibel, Fredericksen	24	60—90	1.0	32.6		
Veibel, Fredericksen	24	70—80	0.5	33.3		
Moelwyn-Hughes	10a	60—80	1.0	33.7		*p*
Heidt, Purves	6b	75	0.097	33.4	+13.7	*c*
Overend *et al.*	2	59.1—79.7	2.0	34.3	+16.5	*p*
Heidt, Purves	6a	60	0.05			*c*
Szejtli		65—100	0.0123—1.23	33.3	+14.3	*c*
Szejtli		60—104	0.5 —5.0	33.2	+13.5	*p*

Table III continued

Author	Ref.	Temperature range	Range of acid conc., mole/l	E_a kcal/mole	ΔS^*, e.u.	Note
BAMFORD *et al.*	25	70	2.0			
ARMSTRONG	18	75—100	0.01—0.5			
CLANCY, TURVEY	28	65	1.5			
			H_2SO_4			
NAKANO, RÅNBY	9	65—85	0.47	31.0*		*p*
TIMELL	7a, 7b	60—120	0.5	32.5	+10.6	*p*
FREUDENBERG *et al.*	19	70	0.25			*p*
THEANDER	30	70—90	0.5	33.6		
			$HClO_4$			
BUNTON *et al.*	20	72.9	0.48—2.69			*p*
			H_3PO_4			
NAKANO, RÅNBY	9	40—60	13.6	29.3*		
			Average	33.28	+13.72	

p = from polarimetric measurements
c = from chemical measurements (determination of reducing power or of the alcohol formed)
* = not taken into consideration when calculating the average
** = hydrolysis under 1000—3000 bar pressure.

Concentration of the glucoside

According to MOELWYN-HUGHES [10], the activity of H^+ ions does not vary appreciably with the carbohydrate concentration if this latter is not higher than 18%. BOLIN's data are in accordance with this, as $k_{80°C}$ for the α-methylglucoside is $2.30 \cdot 10^{-6}$ sec^{-1} in 2% solution, and $2.32 \cdot 10^{-6}$ in 4% solution at pH = 1.00.

The hydrolysis rate of sucrose increases with increasing carbohydrate concentration [12], because the pH decreases, according to DEVILLERS [13], in the following manner:

$$pH = pH_0 - 0.22 \frac{c}{40} \quad pH_0 = pH \text{ in the absence of carbohydrate}$$

c = sucrose concentration, %

This equation is valid if the carbohydrate concentration is not higher than 40%. It means that a 4% solution of sucrose leads to a 0.02% decrease in the pH, which causes about 5% increase in k. It is assumed that these observations are valid also in the case of methylglucosides.

Table IV

Rate constants of the hydrolysis of methylglucosides, determined by various authors at identical HCl concentration and extrapolated to 100 °C on basis of the corresponding apparent E_a values ($k \cdot 10^5$ sec^{-1})

Temperature of hydrolysis, °C	in 0.1 *N* HCl	in 1.0 *N* HCl	in 2.0 *N* HCl
	α-methylglucoside		
50	—	52.0 T, *p*	170 T, *p*
60	—	—	160 T, *p*
	—	63.2 M, *p*	173 O, *p*
60.3	—	54.0 S, *p*	190 S, *p*
61.2	—	—	175 O, *p*
61.4	—	—	153 O, *p*
65	3.33 S, *c*	57.6 S, *c*	167 S, *c*
71.9	—	—	153 O, *p*
75	3.36 H, *c*		—
75.7	3.33 S, *c*	57.3 S, *c*	167 S, *c*
79.6	—	—	175 O, *p*
80	—	63.6 M, *p*	188 S, *p*
90	—	—	143 S, *p*
100	3.46 S, *c*	60.0 S, *c*	150 S, *c*
103.2	—	53.0 S, *p*	170 S, *p*
	—	56.4 S, *p*	
Average:	3.36	57.5	167
	β-methylglucoside		
60	—	78.9 M, *p*	322 O, *p*
60.3	—	85.0 S, *p*	295 S, *p*
61.4	—	—	306 O, *p*
	—	—	320 O, *p*
65	5.26 S, *c*	86.6 S, *c*	290 S, *c*
71.7	—	—	283 O, *c*
75	5.12 H, *c*	—	—
79.7	—	—	316 O, *c*
80	—	91.5 M, *p*	267 S, *p*
	—	87.3 S, *p*	—
75.7	5.26 S, *c*	86.6 S, *c*	290 S, *c*
90	—	—	296 S, *p*
100	5.28 S, *c*	85.0 S, *c*	263 S, *c*
Average:	5.24	86.0	296

p and *c* = polarimetrically or chemically determined rate constants; T = TIMELL [7]; M = MOELWYN-HUGHES [10b]; O = OVEREND *et al.* [2]; H = HEIDT and PURVES [6] (measured in

Table V

Extrapolation of the k_{HCl} values of α- and β-methylglucosides to 100 °C and $H_0 = 0.00$ (k in sec^{-1})

Author		°C	HCl, mole/l	log k_{100} °C		log $k_{100} + H_0$*	
				α	β	α	β
ARMSTRONG		100.0	0.01	—5.596	—5.288	—3.569	—3.251
SZEJTLI	*p*	100.0	0.0123	—5.472	—5.169	—3.523	—3.220
		75.7	0.0123	—5.427	—5.245	—3.478	—3.296
		65.0	0.0123	—5.417	—5.203	—3.468	—3.255
HEIDT, PURVES	*c*	75.0	0.097	—4.524	—4.330	—3.454	—3.260
SZEJTLI	*c*	100.0	0.123	—4.329	—4.099	—3.353	—3.123
		75.7	0.123	—4.387	—4.192	—3.241	—3.216
		65.0	0.123	—4.380	—4.170	—3.404	—3.194
TIMELL	*p*	50.0	0.5	—3.727		—3.527	
ARMSTRONG		75.0	0.5	—3.669	—3.449	—3.469	—3.249
SZEJTLI	*p*	103.2	0.5	—3.746	—3.441	—3.546	—3.241
		103.2	0.5	—3.702		—3.502	
		90.0	0.5		—3.515		—3.315
TIMELL	*p*	50.0	1.0	—3.294		—3.494	
MOELWYN-HUGHES	*p*	60.0	1.0	—3.209	—3.112	—3.409	—3.212
		80.0	1.0	—3.206	—3.046	—3.406	—3.246
SZEJTLI	*p*	103.2	1.0	—3.285		—3.485	
		103.2	1.0	—3.259		—3.459	
		80.0	1.0		—3.067		—3.267
		60.3	1.0	—3.276	—3.079	—3.478	—3.279
	c	100.0	1.23	—3.054	—2.919	—3.374	—3.239
		75.7	1.23	—3.119	—2.967	—3.439	—3.287
		65.0	1.23	—3.109	—2.924	—3.429	—3.234
		103.2	1.25	—3.055		—3.405	
TIMELL	*p*	50.0	1.5	—3.019		—3.489	
		50.0	2.0	—2.781		—3.471	
		60.0	2.0	—2.802		—3.492	
OVEREND *et al.*	*p*	60.0	2.0	—2.567	—2.502	—3.457	—3.192
		71.9	2.0	—2.824	—2.554	—3.154	—3.244
		79.6	2.0	—2.769	—2.506	—3.459	—3.196
		61.2	2.0	—2.766	—2.505	—3.458	—3.195
	c	61.4	2.0	—2.828	—2.522	—3.518	—3.212
SZEJTLI	*p*	103.2	2.0	—2.782		—3.472	

←

0.097 *N* HCl, therefore the k value in the above Table is multiplied by 1.03); S = from own measurements; S, *c* = hydrolysis in 0.123 or in 1.23 *N* HCl; the values in the above Table are interpolated.

Table V continued

Author		°C	HCl, mole/l	log $k_{100\,°C}$		log $k_{100}+H_0$*	
				α	β	α	β
SZEJTLI		90.0	2.0	—2.851	—2.538	—3.541	—3.228
		80.0	2.0	—2.735	—2.584	—3.425	—3.275
		60.3	2.0	—2.732	—2.541	—3.422	—3.231
		60.3	2.5	—2.492		—3.332	
TIMELL	*p*	50.0	3.0	—2.391		—3.441	
SZEJTLI	*p*	80.0	3.5	—2.169	—1.973	—3.399	—3.203
		60.3	3.5	—2.204	—2.029	—3.434	—3.159
TIMELL	*p*	50.0	4.0	—2.006		—3.406	
		50.0	5.0	—1.664		—3.424	
SZEJTLI	*p*	60.3	5.0	—1.720	—1.548	—3.480	—3.308
					Average	—3.457	—3.244

* = according to LONG and PAUL [26], the H_0 values at 0.1 *N* HCl concentration are equal to the pH.

p and *c* = polarimetrically or chemically determined values, respectively.

According to VUKOV [14], in aqueous solutions at low acid concentration, the hydrolysis rate depends on the sucrose concentration as follows:

$$k = k_0 (1 - c)/d_s$$

where

$k_0 = k$ in the absence of carbohydrate;
c = sucrose concentration in g/g of solution;
d_s = density of the solution, g/ml.

With increasing concentration, both d_s and c increase; therefore k increases more slowly than c. It means that the value of k determined in a 4% solution is lower only by about 3% as compared to k_0. The determination of the rate constants is usually done in dilute solutions under 4% carbohydrate concentration, with an accuracy which is not better than ± 3%; therefore, its effect is negligible, and in the present work the influence of the carbohydrate concentration on the rate constant was not taken into account.

Acid concentration

The rate constants determined in various acids cannot be compared with an acceptable accuracy on the basis of the *Hammett* acidity function. Hydrochloric acid is the only acid which does not cause problems. In Fig. 2

the log k_{HCl} values extrapolated to 100 °C are plotted against the H_0 values. The slope of this straight line is 1.00. The relation between log k and the pH up to 1.2 N HCl concentration is also linear; however, the slope is a little greater than unity, similarly to the results obtained for some other investigated neutral

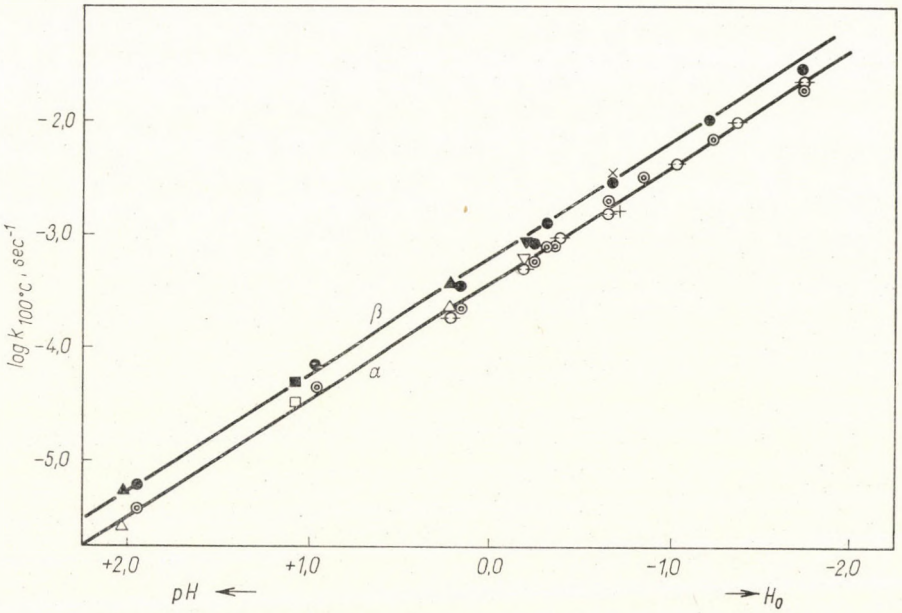

Fig. 2. The $k_{100\,°C}$ values in function of the *Hammett* acidity function for the hydrolysis with hydrochloric acid of α- and β-methylglucosides. (For the legend, see Fig. 1)

Table VI

Rate constants of α-methylglucoside at 50 °C in various acids of identical H_0 values

(From TIMELL's data [7a])

H_0	Acid	mole/l	s**	$k \cdot 10^6$ sec^{-1}
—1.0	HCl	2.85	—1.05	2.52
	$HClO_4$	2.50	—0.85	1.42
	H_2SO_4	2.25	—0.72	1.18
	H_3PO_4	5.90	—0.48	0.33
—2.0	HCl	5.75		26.30
	$HClO_4$	4.55		10.00
	H_2SO_4	4.30		6.33
	H_3PO_4	8.40		0.93

** = s denotes the slope of the log k versus H_0 curve between H_0 = —1.0 and 2.0

glycosides [3, 15]. This slope is denoted as "g". For other acids, the slope of the curve log k versus H_0 is lower than unity, and the rate constants belonging to identical H_0 values are not independent of the acid (see Table VI). Therefore the rate constants determined in various acids cannot be brought to a common basis. The reason for the differences shown in Table VI is not clear.

The relation between log k and H_0 in the case of HCl is in accordance with the ZUCKER — HAMMETT hypothesis, but in other acids the validity of this hypothesis seems to be limited. The value of k_{HCl} is expressed as a function of H_0 and temperature by the following equations:

$$\log k = H_0 + 16.704 - 0.4343 \frac{34670}{RT}$$

$$\log k = H_0 + 16.263 - 0.4343 \frac{33280}{RT}$$

According to LONG and PAUL [26], in acids more dilute than 0.1 N H_0 becomes practically equal to the pH; therefore in such cases, in the above equations H_0 may be substituted by the pH values (the pH may be measured or calculated* as published in a previous paper [3a]).

When sulfuric acid is used as the catalyst of the glycoside hydrolysis, it has to be considered that the catalytic activity of this acid depends not only on its concentration, but also on the temperature [16]. In Table VII the $k_{H_2SO_4}/k_{HCl}$ ratio is illustrated at various temperatures and acid concentrations. At 1 N acid concentration, this activity ratio shows only little change with changing temperature, but at 0.1 normality this variation is considerable. Increasing the temperature from 80 to 103 °C increases the $k_{H_2SO_4}/k_{HCl}$ ratio at 0.1 normality from 0.398 to 0.523. This increase of 12.5% ($k_{HCl} = 100\%$) results in an apparent energy of activation which is higher by about 2.3 kcal/mole than in 1 N acids.

The activity of HCl as a catalyst of the hydrolysis depends on the temperature to a much lesser extent. This is verified by Table V and Fig. 1: the k values within the investigated range of 50—104 °C and 0.01—5.00 N HCl with

* The pH may be calculated by the following equation:

$$pH = 0.091 - 0.973 \cdot \log [HCl] \quad \text{if} \quad [HCl] < 0.2$$

or

$$pH = -0.058 - 1.170 \cdot \log [HCl] \quad \text{if} \quad 1.2 > [HCl] > 0.2$$

In Ref. [3a] in the first equation 0.937 is a misprint; the correct value is 0.973.

acceptable accuracy can be extrapolated to 100 °C. Considering that the relation log k *versus* H_0 is essentially linear with a slope of 1.00, all the k values determined in HCl can be referred to 100 °C and $H_0 = 0.00$. As it is seen in Table V, the agreement is good, and the averages $k = 2.57 \cdot 10^{-4}$ and $k = 5.84 \cdot 10^{-4}$ sec^{-1} for 100 °C and $H_0 = 0.00$ in HCl may be considered as reliable mean values.

Table VII

Dependence of the ratio $k_{H_2SO_4}$ on the temperature and acid concentration

Acid concentration in normality	Hydrolysis of starch*	
	at 103 °C	at 80 °C
0.01	0.659	—
0.1	0.523	0.398
0.5	0.415	0.362
1.0	0.398	0.346
	Hydrolysis of α-methylglucoside**	
	at 100 °C	at 50 °C
1.0	0.336	0.324
2.0	—	0.261
3.0	—	0.205
4.0	—	0.133

* = according to Holló and Szejtli [16]
** = according to Timell [7a]

Hydrochloric acid is, therefore, more appropriate for such investigations than sulfuric acid. Sulfuric acid has a similar catalytic activity only when its concentration is 60—130% higher expressed in normality than that of hydrochloric acid, and the *Hammett* acidity function is applicable to sulfuric acid in special cases only [7].

*

The present paper was made in the *Norsk Institut for Tang og Tareforsking, Trondheim, Norway* (Prof. N. A. Sörensen) and in the *Institut für Ernährung, Potsdam—Rehrücke, German Democratic Republic* (Prof. Dr. H. Haenel). The author is indebted to the *Norges Teknisk Naturvitenskapelige Forskningsråd (Oslo, Norway)* for the award of a postdoctorate fellowship and to the *Deutsche Akademie der Wissenschaften zu Berlin (Berlin, DDR)* for a grant that made this work possible, as well as to Prof. J. N. DeMiller, *Southern Illinios University (Carbondale, U. S. A.)* for his valuable remarks and for correcting the manuscript of this paper.

SUMMARY

Methyl glucosides being the simplest glycosides, play an important role in investigating the acid-catalyzed hydrolysis of glycosidic linkages. Data on the acid hydrolysis of the α- and β-methylglucopyranosides have been compared and averages of the characteristic values calculated. These are, for the α- and β-anomers, respectively, as follows: the rate constants, at 100 °C

and $H_0 = 0.00$, are $3.57 \cdot 10^{-4}$ and $5.84 \cdot 10^{-4}$ sec^{-1} in HCl; the d constants 16.704 and 16.263; the apparent energy of activation 34.67 and 33.28 kcal/mole; the entropy of activation 16.37 and 13.72 kcal/mole x degree. The rate constant may be calculated as follows:

$$\log k = H_0 + d + 0.4343 \frac{E_a}{RT}$$

The agreement of data determined by various authors for the hydrolysis catalyzed by hydrochloric acid is rather good. The catalytic activity of H_2SO_4 strongly depends on the temperature, and does not obey the *Hammett* acidity scale. Therefore, it is suggested that the application of H_2SO_4 in kinetical studies of hydrolysis be avoided. Similar behavior has been observed with $HClO_4$ and H_3PO_4; neither is the hydrolysis-catalyzing activity of these acids proportional to the H_0 value. At identical H_0 values the hydrolysis rate is rather different with the various acids. Hydrochloric acid is the only acid among those investigated which gives a slope of unity on the log k *versus* H_0 diagram.

REFERENCES

1. Shafizadeh, F.: Advances in Carbohydrate Chem. **13,** 9 (1958). Pigman, W.: The Carbohydrates, Academic Press, New York, 1957. p. 290. Feather, M. S., Harris, J. F.: J. Org. Chem. **30,** 153 (1965).
2. Overend, W. G., Rees, C. W., Sequeira, J. S.: J. Chem. Soc. **1962,** 3429.
3. Szejtli, J.: Acta chim. Acad. Sci. Hung. (a) **45,** 141 (1965); (b) **45,** 153 (1965); (c) **45,** 369 (1965); (d) **46,** 77 (1965); (e) **47,** 301 (1966).
4. Bollenback, I. N.: Methylglucosides. Academic Press, New York, 1958.
5. Bamann, R., Myrbäck, K.: Die Methoden der Fermentforschung. Vol. I, Leipzig, 1941, p. 1704.
6. (a) Heidt, L. J., Purves, C. B.: J. Am. Chem. Soc. **66,** 1385 (1944); (b) Capon, B., Overend, W. G.: Advances in Carbohydrate Chem. **15,** 33 (1960).
7. Timell, T. E.: (a) Canadian J. Chem. **42,** 1456 (1964); (b) Chem. Ind. 1208 (1963); (c) Timell, T. E., Enterman, W., Spencer, F., Soltes, E. J.: Canadian J. Chem. **43,** 2296 (1965).
8. Easty, D. B.: J. Org. Chem. **27,** 2102 (1962).
9. Nakano, J., Rånby, B. G.: Svensk Papperstidn. **65,** 29 (1962).
10. Moelwyn-Hughes, E. A.: Trans. Faraday Soc. (a) **25,** 503 (1929); (b) **25,** 81 (1929); (c) **24,** 321 (1928).
11. Bolin, I.: Z. Anorg. u. allgem. Chem. **143,** 201 (1925).
12. Honig, P.: Principles of Sugar Technology. Vol. I, Elsevier, Amsterdam, 1958.
13. Devillers, P. L.: Industr. alim. agr. **75,** 393 (1958).
14. Vukov, K.: Élelmezési Ipar (Budapest), **19,** 13 (1965); Industr. alim. agr. **83,** 113 (1966).
15. Szejtli, J.: Proceedings of the Conference on Some Aspects of Physical Chemistry, Budapest 1966, Vol. I, p. 55; Die Stärke **18,** 274 (1966).
16. (a) Holló, J., Szejtli, J.: Die Stärke **13,** 327 (1961); (b) Die Säurehydrolyse der Stärke. Akademie Verlag, Berlin, 1966.
17. Ekenstein, W. A.: Rec. trav. Pays-Bas **13,** 183 (1894).
18. Armstrong, E. F., Caldwell, R. J.: Proc. Roy, Soc. **74B,** 188, 192 (1904—5); Armstrong, E. F., Glover, W. H.: Proc. Roy. Soc. **80B,** 312 (1908).
19. Freudenberg, K., Dürr, W., Hochstetter, H.: Ber. **61,** 1735 (1928)
20. Bunton, C. A., Lewis, T. A., Llewellyn, D. R., Vernon, C. A.: J. Chem. Soc. **1955,** 4419.
21. Richards, G. N.: Chem. Ind. **1955,** 228.
22. Armour, C., Bunton, C. A., Patai, S., Selman, L. H., Vernon, C. A.: J. Chem. Soc. **1961,** 412.
23. Withey, R. J., Whalley, E.: Canadian J. Chem. **41,** 1849 (1963).
24. Veibel, S., Fredericksen, E.: Kgl. Danske Videnskab, Selskab. Mat.-Fys. Medd. **19,** 1 (1941).
25. Bamford, C., Capon, B., Overend, W. G.: J. Chem. Soc. **1962,** 5138.
26. Long, F. A., Paul, M. A.: Chem. Revs. **57,** 1935 (1957).
27. Meller, A.: J. Polymer Sci. **C2,** 97 (1963).
28. Clancy, M. J., Turvey, J. R.: J. Chem. Soc. **1961,** 2935.
29. Wang, Y., Hua, C.: Hua Hsüeh Hsüel Pao **24,** 413 (1958); C. **54,** 3228b (1960).
30. Theander, O.: Acta Chem. Scand. **18,** 1297 (1964).

József Szejtli; Budapest IV., Tó u. 1—5.

Acta Chimica Academiae Scientiarum Hungaricae Tomus 56 (2), pp. 189—194 (1968)

SYNTHESIS AND REACTION OF ENAMINES, II

SYNTHESIS OF PYRROLENINES

M. A. KIRA, A. BRUCKNER-WILHELMS, F. RUFF and J. BORSY

(Institute of Organic Chemistry, L. Eötvös University Budapest, and Pharmaceutical Research Institute, Budapest)

Received August 16, 1967

In a preceding paper [1], two of the authors have reported on the isolation of 2-dimethylamino-methylenepyrrolenine as the perchlorate salt from a VILSMEIER-aldehyde synthesis with pyrrole. The free base, m. p. 113 °C, was also obtained, although in a low yield, by the neutralization of a methanolic solution of the perchlorate salt with triethylamine.

Now, we describe a direct synthesis for 2-dimethylaminomethylenepyrrolenine, as well as for analogous pyrrolenines, and some reactions of these compounds.

Condensation of pyrrole-2-aldehyde with aqueous dimethylamine at room temperature has now been found to give 2-dimethylaminomethylenepyrrolenine (**Ia**) in about 75% yield. The pyrrolenine prepared by this method was found identical (mixed m. p. and IR spectra) with 2-dimethylaminomethylenepyrrolenine which had been previously isolated from a VILSMEIER-aldehyde synthesis with pyrrole [1]. Similarly,

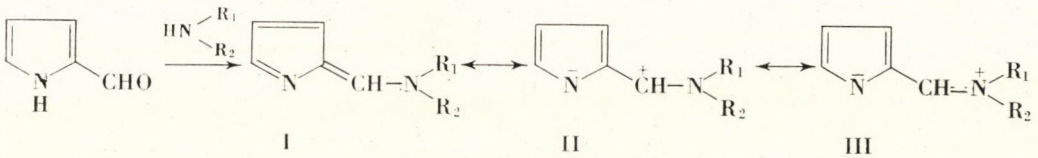

I II III

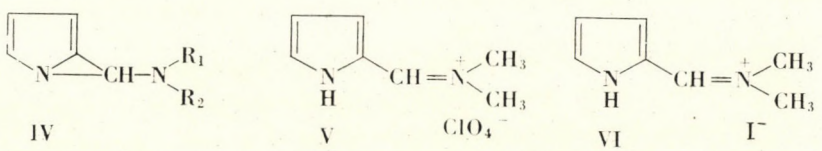

IV V VI

Ia ($R_1 = R_2 = CH_3$)

Ib (NR_1R_2 = morpholino)

Ic (NR_1R_2 = piperidino)

Id (NR_1R_2 = piperazino)

condensation of pyrrole-2-aldehyde with morpholine and/or piperidine in ether solution and with piperazine hydrate in methanolic solution gave, in good yields, the respective pyrrolenines **Ib—d** with decomposition points 195°, 163° and 245 °C.

The structures assigned to these pyrrolenines were inferred from the elemental analyses, from their hydrolysis reactions to pyrrole-2-aldehyde effected by boiling aqueous alkali [2], and from the formation of the phenylhydrazone and/or the oxime of pyrrole-2-aldehyde on treatment with phenylhydrazine or hydroxylamine hydrochloride in pyridine.

The easy formation of these pyrrolenines and their peculiar reactions (see below) are attributed to the possible mesomeric contributions **I—III** together with the valence tautomeric structure **IV** [3]. In favour of this assumption are considerably high melting points. The IR spectra (KBr) with the exception of that of the piperazino derivative **Id** did not show any absorption indicating the presence of a C = N group. The UV spectra of the pyrrolenines **Ia—c** are of particular interest. Compound **Ia** showed in ethanolic solution a maximum absorption at 290 mμ with ε amounting to 12,500 while in chloroform or dioxane solutions the same compound gave an absorption at about the same wavelength but with a much lower extinction coefficient amounting to 112 and 123, respectively. This behaviour is also ahown by the pyrrolenines **Ia—c**.

An explanation for this could be that the pyrrolenines **Ia—c** exist in the valence tautomeric ethyleneimine structure **IV** in nonhydroxylic solvents. In ethanol, however, the unshared pair of electrons on the pyrrole nitrogen, responsible for the formation of the ethyleneimine structure **IV**, is involved in hydrogen bonding, therefore structure **I** is stabilized. Similar postulations have been made during the NMR study of the inversion frequencies for ethyleneimines; the frequencies were found to be substantially decreased in hydroxylic solvents owing to stabilization of the ground state configurations through hydrogen bonding of the solvent with the imino nitrogen [4].

Further evidence for the existence of compounds **Ia/c** in the ethyleneimine structure **IV** in nonhydroxylic solvents, and in the pyrrolenine structure I in hydroxylic solvents, has now been furnished by measuring the IR spectra of both compounds in chloroform and in methanol. In the latter solvent compounds **Ia/c** had absorption bands at 1660 cm^{-1}, and 1655 cm^{-1}, respectively (C = N); these bands were absent in chloroform solution. Since these bands are also absent in the IR spectra of **Ia—c** measured in KBr, it becomes apparent that these compounds exist also in the valence tautomeric form **IV** in the solid state.

The IR spectrum (KBr) of the highly insoluble piperazino derivative **Id** is again in favour of this assumption. Owing to hydrogen between the free NH of piperazine and the pyrrole nitrogen, structure **Id** is stabilized as

indicated by the presence of a band at 1660 cm^{-1} (C = N). The compound is amorphous, insoluble in all solvents, and probably exists in the form of a hydrogen bonded polymer (broad band centered at 3400 cm^{-1}).

The perchlorate salt should possess the immonium structure **V**, and not one of the structures corresponding to **Ia** with the acidic proton linked either to the pyrrole nitrogen or to the nitrogen atom of the side chain. This is inferred from the IR spectra of the perchlorate salt which has bands at 3300 cm^{-1} (NH uncharged), at 1550 cm^{-1} (NH def.), and at 1660 cm^{-1} (C = N).

The UV spectra of 2-pyrrolylmethyleneimines have been recently reported [5], but they do not exist as pyrrolenines.

The pyrrolenines **Ia—d** are characterized by their readiness to polymerization in the presence of any acid and sometimes a nucleophile. Thus, **Ia—d** gave immediately an insoluble, red to brown polymer when treated with either dilute HCl or acetic acid. A brown to black polymer was also formed in quantitative yield when **Ia** was treated with either acetyl chlorid or benzoyl chloride in benzene solution. Phenyl isocyanate effected similar polymerization of **Ia** in benzene or acetone solution. The isolation from the mother liquor of N-phenyl-N'-dimethylurea [6] indicated elimination of dimethylamine in the course of polymerization.

The reaction of **Ia** with methyl iodide, in methanolic or ethanolic solution, is of interest. Instead of N-methylpyrrole-2-dimethylimmonium iodide, the compound expected from a 1.3 addition, the products were tetramethylammonium iodide (in about 50% yield), and a compound of m. p. 149 °C (about 30%). The IR spectrum of the latter (broad band centered at 3000 cm^{-1} NH, 1550 cm^{-1} NH def., 1665 cm^{-1} C = N) indicated an immonium salt structure **VI.** In favour of this assumption is the isolation of the phenylhydrazone of pyrrole-2-aldehyde from the reaction of **VI** phenylhydrazine. The mechanism by which compound **VI** is formed is apparently complicated involving reaction of the pyrrolenine nitrogen with the hydroxylic proton of the solvent, since repetition of the reaction in benzene solution gave only an insoluble brown polymer.

Although these pyrrolenines possess an enamine-like structure, 2-dimethylaminomethylenepyrrolenine did not react with acrylonitrile [7] at temperatures up to 100 °C; the reaction with ethylmagnesium bromide in boiling tetrahydrofuran also failed.

Catalytic hydrogenation of **Ia** in the presence of a platinum catalyst did not proceed smoothly; on the other hand, under the same conditions the perchlorate salt **V** gave quantitatively, after treatment with alkali, 2-dimethylaminomethylpyrrole, which was identical with an authentic sample [8].

It is known that pyrrole-2-aldehyde polymerizes readily in the presence of acids, nitration has been recently achieved at —25 °C [9]. In contrast to the free base, the perchlorate salt of 2-dimethylaminomethylenepyrrolenine (**V**)

is remarkably stable towards the action of hot concentrated acids. Moreover, the positive charge on the side chain nitrogen undoubtedly deactivates the pyrrole ring electrophilic substitution to take place at reasonable temperatures.

Nitration of the perchlorate salt **V** in acetic anhydride at either 10 °C or 20 °C, followed by treatment with alkali, gave in both cases the nitropyrrole-aldehydes with 82% conversion, the yields of the 4- and the 5-nitro derivatives being 57% and 25%, respectively. Almost quantitative separation of the isomers has been achieved by means of the sparingly soluble sodium salt of the 4-isomer.

By reason of the ready polymerization of the pyrrolenines **Ia—d** in acidic media, which is apparently due to the formation of a carbonium ion similar to structure **II** with a hydrogen linked to the pyrrole nitrogen, and considering the possible ethyleneimine structure **IV**, the morpholino derivative **Ib** has been evaluated as a potential biological alkylating agent. Its DL_{50} was found to be about 195 mg/kg for mice *(intraperitoneal)*. Against *Yoshida S. C. sarcoma* (rats) it showed 5% inhibition, and proved inactive against *S/80 S. C. sarcoma* (mice), *Ehrlich ascitis carcinoma* (mice), and *NK/Ly lymphoma* (mice). A single dose of 20% of the LD_{50} was used in all tests.

Experimental*

Synthesis of Pyrrolenines

2-Dimethylaminomethylenepyrrolenine (Ia)

Pyrrole-2-aldehyde (19 g; 0.2 mole) was dissolved at room temperature in 40 ml of aqueous dimethylamine solution (ca. 33%). After 2 hrs the deposited colourless crystalline product (18 g; 75% yield) was filtered off, washed with a little cold methanol and dried in vacuum. It was recrystallized from benzene, to obtain m. p. 113 °C. No melting point depression was observed with a sample prepared from the perchlorate salt [1].
$C_7H_{10}N_2$ (122) Calcd. C 68.85; H 8.20; N 22.93%.
Found C 69.04; H 8.10; N 22.70%.

UV λ_{max} 290 mμ, log ε 4.2 (ethanol),
λ_{max} 283 mμ, log ε 2.05 (chloroform),
λ_{max} 285 mμ, log ε 2.09 (dioxane).

IR spectrum (in methanol): 1650 cm^{-1} (C = N). The morpholino derivative **Ib** was obtained in about 60% yield by dissolving equimolar amounts of pyrrole-2-aldehyde and freshly distilled morpholine in ether. The crude product was recrystallized from a mixture of chloroform–methanol to obtain a decomposition point of 195 °C.
$C_9H_{12}N_2O$ (164) Calcd. C 65.83; H 7.33; N 17.07.
Found C 66.45; H 7.55; N 16.93.

UV λ_{max} 288 mμ, log ε 3.0 (ethanol)

The piperidino derivative **Ic** was prepared in a similar manner in about 66% yield. It was recrystallized from a mixture of chloroform–ether, and had a decomposition point of 163 °C.
$C_{10}H_{14}N_2$ (162) Calcd. C 74.13; H 8.67; N 17.28.

* Melting points are uncorrected.

Found C 74.16; H 8.58; N 16.80.

UV λ_{max} 290 mμ, log ε 3.71 (ethanol)

IR spectrum (methanol): 1660 cm^{-1} (C = N).
The piperazino derivative **Id** was prepared as described above, using methanol instead of ether. The product was obtained in almost quantitative yield and had a decomposition point of 245 °C. It did not dissolve in any solvent.
IR spectrum (KBr): Broad band centered at 3400 cm^{-1} (NH, chelated); 1660 cm^{-1} (C = N); 1550 cm^{-1} (NH def.). Reaction of **Ia** with methyl iodide.

To a solution of **Ia** (2.44 g; 0.2 mole) in 25 ml of methanol, there was added, at room temperature, 1.4 ml (0.22 mole) of methyl iodide. After allowing to stand overnight, the crystalline precipitate (2.5 g) was filtered off and recrystallized from hot water. It did not melt up to 320 °C and was found identical (IR spectra) with an authentic sample of tetramethylammonium iodide [6].

The highly coloured mother liquor, after the isolation of tetramethylammonium iodide, was treated with charcoal, the solvent evaporated in vacuum, and the crystalline residue (one gram) was recrystallized from methanol–ether. The product melted at 149 °C.
$C_7H_{11}N_2I$ (250) Calcd. C 33.58; H 4.47; N 9.77; I 52.18. Found C 33.30; H 4.49; N 10.50; I 52.00.

UV λ_{max} 322 mμ, log ε 4.25; 290 mμ (infl.), log ε 4.1; 220 mμ, log ε 4.20 (ethanol).

R spectrum (KBr): Broad band centered at 3000 cm^{-1} (NH chelated); 1665 cm^{-1} (C = N); 1550 cm^{-1} (NH def.).

2-Dimethylaminomethylpyrrole

A solution of the perchlorate salt **V** (22 g; 0.1 mole) in 300 ml of methanol was hydrogenated using 500 mg of platinum oxide. The hydrogen uptake was ended after 20 minutes. The methanolic solution was filtered from catalyst, evaporated in vacuum, treated with 100 ml of 0.1 *N* sodium hydroxide solution and shaken twice with ether. Evaporation of the dried ether solution gave 12 g of an oil which distilled between 78—79°C (10 mm). It solidified on standing, and the base, m. p. 63 °C, as well as the picrate, m. p. 137 °C *(dec.)*, were found identical with authentic samples prepared according to the literature [8].

Nitration of 2-dimethylaminoethylenepyrrolenine perchlorate

To a well stirred suspension of the perchlorate salt **V** (22.5 g; 0.1 mole) in 35 ml of acetic anhydride, there was added, dropwise, a solution of fuming nitric acid (8 g; 6 ml) in 10 ml of acetic acid, the temperature being kept between 5—8 °C. After the addition had been completed (ca. 50 minutes), the solution was poured on ice (60 g) and neutralized while cooling with 150 ml of a 30% NaOH solution. The mixture was allowed to stand at room temperature for about 1 hr., then chilled in ice, and the precipitated sodium salt of the 4-nitroaldehyde was filtered off. The mother liquor was made just acidic with HCl (1 : 1) and the precipitated crude 5-nitroaldehyde was collected. It was dissolved in ethanol, and treated with charcoal. Evaporation of a part of the solvent gave a yellow crystalline product (1.7 g; 25); m. p. 181 °C (lit. m. p. 182 °C [9]).

The 4-nitroaldehyde (8 g; 57%) was liberated from its sodium salt by acidification with diluted HCl; it had m. p. 141 °C (lit. m. p. 142 °C [9]).

SUMMARY

Pyrrole-2-aldehyde condenses with secondary amines to give the pyrrolenines **Ia–d**. The UV and IR spectra of **Ia–d** indicate that these compounds exist in the pyrrolenine structure **I** in hydroxylic solvents, and in the ethyleneimine valence tautomeric structure **IV** in other solvents as well as in the solid state. Nitration of the perchlorate salt **V** offers an easy route to 4- and 5-nitropyrrole-2-aldehydes.

REFERENCES

1. KIRA, M. A., BRUCKNER-WILHELMS, A.: Acta chim. Acad. Sci. Hung. (1968) in press.
2. SMITH, G. F.: J. Chem. Soc. **1954**, 3842.
3. HUISGEN, R., MIETZSCH, F.: Angew. Chem. **76,** 36 (1964); VOGEL, E., WENDISCH, D., ROTH, W. R.: ibid. **76,** 432 (1964).
4. BOTTINI, T., ROBERTS, J. D.: J. Am. Chem. Soc. **78,** 5126 (1956); ibid. **80,** 5206 (1958).
5. JONES, R. A.: Aust. J. Chem. **17,** 894 (1964).
6. STOLLÉ, R.: J. prakt. Chem. [2] 117, 201 (1927).
7. BRAUNOCK, K. C., BELL, A., BURPITT, R. D.: J. Org. Chem. **29,** 801 (1964).
8. HERZ, W., DITTMAR, K., CRISTOL, S. J.: J. Am. Chem. Soc. **69,** 1698 (1947).
9. TIROUFLET, J., FOURNARI, P.: Bull. soc. chim. France **1963**, 1651.

Mohamed A. KIRA
Adrienne BRUCKNER-WILHELMS
Ferenc RUFF
József BORSY

Budapest VIII., Múzeum krt. 4/b.

Acta Chimica Academiae Scientiarum Hungaricae Tomus 56 (2), pp. 195—197 (1968)

THE EFFECT OF THE AXIAL β-SUBSTITUENT ON THE QUATERNIZATION OF SOME COCAINE DERIVATIVES

(PRELIMINARY COMMUNICATION)

I. Weisz, P. Agócs, M. Halmos and K. Kovács

(Institute for Organic Chemistry, A. József University, Szeged)

Received January 23, 1968

Recently several publications have dealt with the stereochemistry of the quaternization of compounds having tropane skeleton [1], disputing earlier generalized statements [2] concerning the stereoselectivity of the reactions of quaternization. However, in these works the effect of substituents near the nitrogen atom of the tropane skeleton has not been taken into consideration.

An investigation of the reaction rate by the measurements of conductance in methanolic solutions showed that, owing to steric hindrance, the alkylation with methyl iodide of tropane derivatives containing axial β-substituents is much slower than the alkylation of compounds which contain no such substituents.

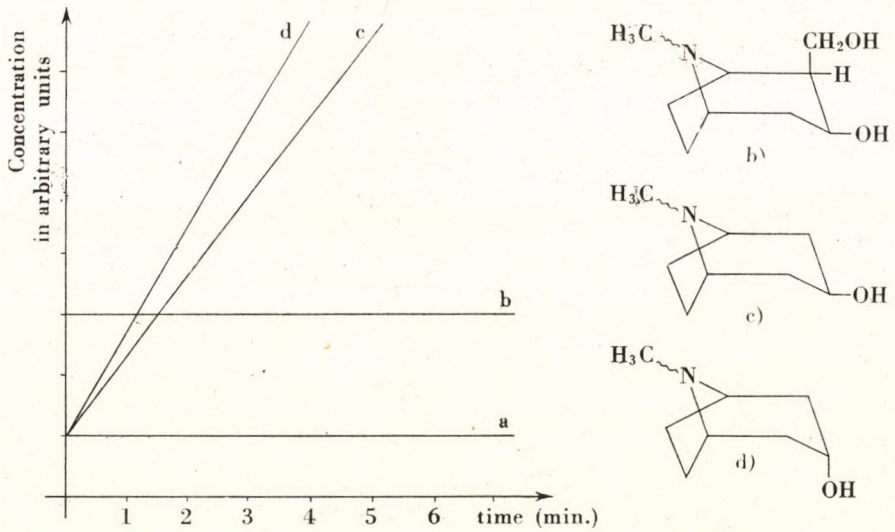

a) Ecgonine methyl ester **(II)**
b) Ecgoninol
c) Pseudo-tropine
d) Tropine

In alkylation experiments with ethyl iodoacetate at room temperature, this steric hindrance prevents a reaction in the case of ecgoninol diacetate (**I**) and ecgonine methyl ester (**II**). As contrary to this, pseudoecgonine methyl ester, containing an equatorial β-substituent (**III**), can be readily alkylated to the quaternary compound **IV**. Under more vigorous conditions, ecgoninol diacetate (**I**) can also be quaternized with ethyl iodoacetate to yield, by stereoselective reaction, a quaternary salt (**V**), which cannot be converted into a compound with lactone ring [3].

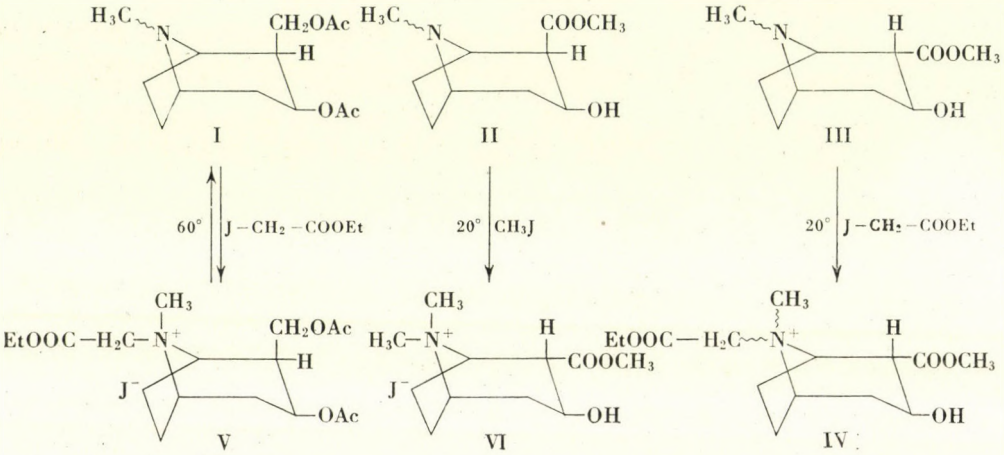

On boiling in toluene, this compound (**V**) decomposes into its initial components. This explains why the heating of N-ethoxycarbonylmethyl-norecgoninol diacetate (**VII**) in toluene in the presence of a great excess of methyl iodide at 120 °C gave ecgoninol diacetate methiodide (**VIII**), as contrary to earlier findings [3, 4].

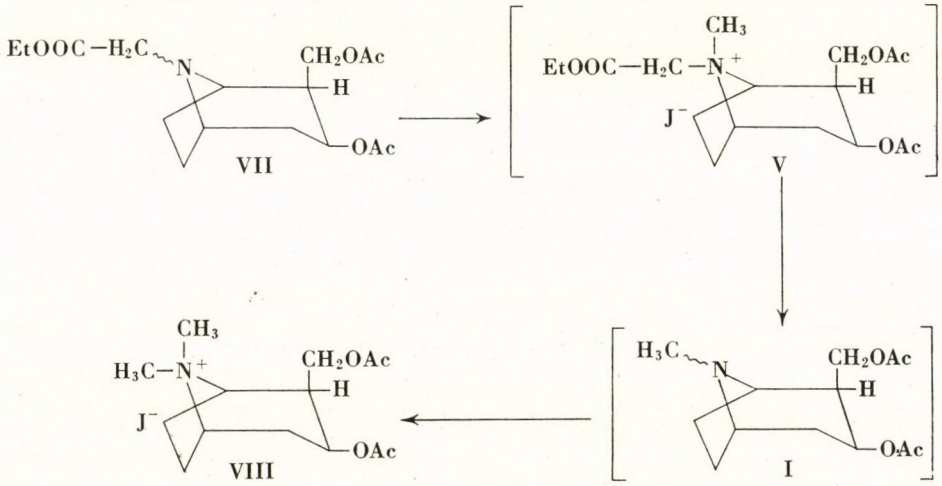

The driving force of the reaction **V**→**I** is 1,3-diaxial non-bonded interaction, in the same way as in the experiments of FINDLAY [5], who methylated ecgonine methyl ester (**II**) to obtain ecgonine methyl ester methiodide (**VI**).

The role of an axial β-substituent in the alkylation of compounds with tropane skeleton is to bring about an extreme assertion of the HAMMETT—CURTIN principle [6]. The alkylation with ethyl iodoacetate proceeds with complete stereoselectivity, since out of the two possible transition states of quaternization (**IX** and **X**) the formation of **IX** is easier.

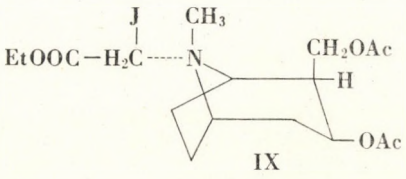

IX

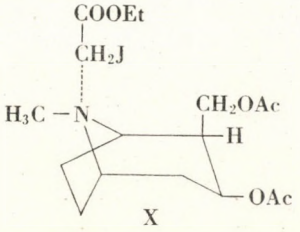

X

It is evident that the different order of introducing the two N-alkyl groups cannot give rise to N-stereoisomers, and consequently, the method of lactone salt formation [2, 4] cannot be used here.

REFERENCES

1. GLOSS, C. L.: J. Am. Chem. Soc. **81,** 5456 (1959); MCKENNA, J., MCKENNA, J. M., TULLEY, A., WHITE, J.: J. Chem. Soc. **1965,** 1711; BROWN, D. R., LYGO, R., MCKENNA, J., MCKENNA, J. M., HUTLEY, B. G.: J. Chem. Soc. **1967,** 1184.
2. FODOR, G.: Chem. and Ind. **1961,** 1500
3. KOVÁCS, Ö., FODOR, G., HALMOS, M.: J. Chem. Soc. **1956,** 873
4. MANSKE, R. H. F., HOLMES, H. L.: The Alkaloids. Vol. 9. FODOR, G.: The Tropan Alkaloids. Academic Press Inc., N.Y. 1967, p. 287
5. FINDLAY, S. P.: J. Am. Chem. Soc. **76,** 2855 (1954).
6. ELIEL, E. L., ALLINGER, N. L., ANGYAL, S. J., MORRISON, G. A.: Conformational Analysis. Interscience Publishers, New York, London, Sidney, 1966, p. 246.

Imre WEISZ
Pál ACÓCS
Miklós HALMOS
Kálmán KOVÁCS

Szeged, Dóm tér 8.

Printed in Hungary

A kiadásért felel az Akadémiai Kiadó igazgatója — Műszaki szerkesztő: Farkas Sándor

A kézirat nyomdába érkezett: 1968. II. 13. — Terjedelem: 10 (A/5) ív, 39 ábra

68.65113 Akadémiai Nyomda, Budapest — Felelős vezető: Bernát György

INDEX

INORGANIC AND ANALYTICAL CHEMISTRY — ANORGANISCHE UND ANALYTISCHE CHEMIE — НЕОРГАНИЧЕСКАЯ И АНАЛИТИЧЕСКАЯ ХИМИЯ

SZAKÁCS-PINTÉR, M. und MAROS, L.: Über eine neuere analytische Anwendung der Oxydation von organischen Verbindungen durch Brom, III. Bestimmung von Furfurol und Furfurylalkohol 87

LENGYEL, B. and CSÁKVÁRI, B.: The Phase Potential between Glass and Liquid Ammonia Solutions of Reduced Vapour Pressure 93

HAHN, G. und DUSDORF, W.: Beitrag zur Mangan-(II)-nitrat-Pyrolyse, I. Die röntgenografische Zusammensetzung und das Widerstandsverhalten von Pyrolysebraunstein .. 99

INCZÉDY, J. and HŐGYE, I.: The Analytical Use of Ion Exchangers in Organic Solvents, II. Swelling and Functioning Properties of Macroporous Ion Exchange Resins 109

HENNING, O.: Derivatographische Untersuchungen an Aluminathydraten (Kurzmitteilung) 117

PHYSICAL CHEMISTRY — PHYSIKALISCHE CHEMIE — ФИЗИЧЕСКАЯ ХИМИЯ

TAMÁS, J. and ÚJSZÁSZY, K.: Mass Spectrum of Tetramethylsilane. Its Decomposition Induced by Electron Bombardment (Preliminary Communication) 125

BILLES, F.: The Quadratic Potential Function of the Cyclopentadienyl Anion 131

TÉTÉNYI, P. and SCHÄCHTER, K.: Catalytic Degradation of Alcohols on Metals 141

NEMES, L.: Harmonic Force Field Refinement Calculations for Polyatomic Molecules, II. Force Field Calculations on NO_2F and NO_2Cl Molecules Containing ^{14}N and ^{15}N Isotopes 153

MEZEI, M. and PULAY, P.: Calculation of Force Constants with the Maximum Overlap Method, I. Tetrahedral Molecules (Short Communication)..... 167

ORGANIC CHEMISTRY — ORGANISCHE CHEMIE — ОРГАНИЧЕСКАЯ ХИМИЯ

SZEJTLI, J.: Acid-Catalyzed Hydrolysis of Alpha- and Beta-Methylglucopyranosides .. 175

KIRA, M. A., BRUCKNER-WILHELMS, A., RUFF, F. and BORSY, J.: Synthesis and Reaction of Enamines, II. Synthesis of Pyrrolenines 189

WEISZ, I., AGÓCS, P., HALMOS, M. and KOVÁCS, K.: The Effect of the Axial β-Substituent on the Quaternization of Some Cocaine Derivatives (Preliminary Communication) 195

ACTA CHIMICA

ТОМ 56 — ВЫПУСК 2

РЕЗЮМЕ

Новое аналитическое использование бромистого окисления органических соединений, III

Определение фурфурола и фурфурилового спирта

М. САКАЧ-ПИНТЕР и Л. МАРОШ

Фурфурол и фурфуриловый спирт быстро, однозначно реагируют с хлористом бромом в водном растворе (эквивалентный вес = молекулярный вес/4). В ходе реакции образуются 3 эквивалента кислоты. Для определения этих соединений авторами был разработан иодометрический метод, а также метод, основанный на измерении кислоты, образующейся в ходе реакции. Авторами изучался механизм окисления с бромом и схлористым бромом. Подробное обсуждение этих исследований приведётся позже.

О фазовом потенциале между стеклом и аммиачным раствором с пониженной упругостью пара

Б. ЛЕНДЕЛ и Б. ЧАКВАРИ

Изучалась поведение стеклянных электродов, изготовленных из стекла типа Мэк-Иннес—Доль, в растворах, приготовленных из жидкого аммиака с пониженной упругостью пара (NaI 3,3 NH_3). В кислой среде стеклянный электрод показывает функцию иона аммония. В основных средах, содержащих амид натрия, определяющая роль иона аммония на величину потенциала прекращается.

О пиролизе нитрата двухвалентного марганца, I

Рентгенографический состав и сопротивление пиролитической двуокиси марганца

Г. ХАН и В. ДУСДОРФ

В связи с рентгенографическим определением фазовой структуры, измерение сопротивления указывает на наличие непосредственной взаимосвязи. Нестехиометрический состав, колеблющийся в широком интервале, в данном случае можно объяснить рентгенографическими данными, указывающими на изменение содержания α-Mn_2O_3, причем оказалось, что 2,0% Mn_2O_3 уже вероятно нельзя обнаружить рентгенографическим путем, и поэтому наименьшие отклонения от стехиометрического состава указывают на наименьшее содержание α-Mn_2O_3. Эти результаты основываются на однозначном появлении во всех образцах рентгеновской интерференции, характерной для α-Mn_2O_3 и β-MnO_2. Причиной отклонения содержания кислорода от стехиометрического значения являются, в первую очередь, примеси α-Mn_2O_3. Поэтому ясно, что недостаток кислорода в пиролитических образцах объясняется не дефектными местами кислорода — как в

случае TiO_2, кристаллизующегося по типу рутила — а тем, что при добавлении малых количеств кислорода к решетке β-MnO_2 происходит распад с образованием α-Mn_2O_3. В дальнейшем поведение сопротивления будет изучаться при других значениях параметров (температура, газовая атмосфера и давление) с целью выяснения механизма разложения при пиролизе.

Аналитическое использование ионообменников в органических растворителях, II

Набухание и работа макропористых ионообменных смол

Я. ИНЦЕДИ и И. ХЁДЬЕ

Изучалось набухание некоторых макропористых ионообменных смол в воде, этаноле, диметилформамиде, диоксане и в ледяной уксусной кислоте.

На основе кинетических исследований и исследований по распределению было проведено хроматографическое разделение бензойной и антраниловой кислот с помощью колонки слабо основной смолы в форме ацетата. В качестве промывной жидкости использовался спиртовый раствор уксусной кислоты.

Квадратичная функция потенциала циклопентадиенилового аниона

Ф. БИЛЛЕШ

Определялась совокупность матриц силовых постоянных для аниона циклопентадиенила. Среди них была выбрана матрица, в которой валентное силовое постоянное связи C—C соответствует плотности π-электронов, большей чем в бензоле. Полученные величины силовых постоянных были анализированы.

Каталитическое разложение спиртов на металлах

П. ТЕТЕНИ и К. ШЕХТЕР

Авторами изучалась возможность параллельной дегидрогенизации и дегидратации изо-пропилового спирта в присутствии Be, Ti, V, Fe, Co, Ni, Cu, Zn, Zr, Mo, Ru, Rh, Pd, Ag, W, Ir, Pt и Au. Установлено, что большинство металлов катализируют обе реакции в интервале температур 230—300 °C, железо является дегидрирующим контактом, а Be, Ti, V, Zr и W — селективными дегидратирующими контактами. Определялись кинетические константы дегидратации трет.-бутилового спирта в присутствии Be, Ti, V, Fn, Zr, Ru, Ir и Au.

В случае обеих реакций наблюдается корреляция между изменением каталитической активности металла и его стандартной энтальпией окисления. Наблюдается также взаимосвязь между дегидрированием изо-пропилового спирта и постоянной решетки металлического катализатора.

Уточнение гармонического силового поля в случае многоатомных молекул, II

Модельные расчеты гибридизированной орбиты молекул NO_2F и NO_2Cl, содержащих изотопы ^{14}N и ^{15}N

Л. НЕМЕШ

Проводились расчеты гибридизированной орбиты молекул NO_2Cl и NO_2F, содержащих изотопы ^{14}N и ^{15}N, с помощью системы симметричных координат более простой, чем использованная ранее [1, 2, 3].

Данные сходящегося силового поля указывают на то, что порядок связи N—X колеблется вокруг значения одинарной связи: f(N—F) = 4,1 мдин/Å, f(N—Cl) = 6,4

мдин/Å, в то время как валентная силовая постоянная N—O является практически одинаковой в обеих молекулах; f(N—O) = 9 мдин/Å.

Изучение форм колебаний, в полном согласии с ранними работами [1, 2, 3], указывает на то, что ν_3 — это частота ножничных колебаний NO_2. Это подтверждается и данными по изотопному смещению.

Расчет силовых постоянных с помощью метода максимального перекрывания, I

Тетраэдрические молекулы

М. МЕЗЕИ и П. ПУЛАИ

С помощью приближенного квантово-химического метода максимального перекрывания были определены поперечные и поперечно-продольные силовые постоянные молекул CH_4, SiH_4, CF_4 и CCl_4 до приближения одного постоянного множителя. Результаты близки к экспериментальным значениям. Принятие в расчет d-орбит в случае SiH_4 практически не изменяет результаты.

Гидролиз α- и β-метилглюкопиранозидов, катализированный кислотами

Й. СЕЙТЛИ

Метилглюкозиды, являющиеся простейшими глюкозидами, играют важную роль в изучении гидролиза глюкозидных связей, катализированного кислотами. Сравнивались данные кислотного гидролиза α- и β-метилглюкопиранозидов, и рассчитывались средние значения характерных величин. Были получены следующие значения: для α- и β-аномеров: при 100°, в соляной кислоте и при $H_0 = 0{,}00$ константы скорости равны $3{,}57.10^{-4}$ и $5{,}84.10^{-4}$ сек$^{-1}$; константа «d» — 16,704 и 16,263; кажущаяся энергия активации — 34,67 и 33,28 ккал/моль; энтропия активации — 16,37 и 13,72 ккал/моль. град., соответственно. Константа скорости рассчитывалась на основе следующего уравнения:

$$\log k = H_0 + d + 04343 \frac{E_a}{RT}$$

Наблюдается хорошая согласуемость с данными, полученными различными авторами, для гидролиза, катализированного соляной кислотой. Активность серной кислоты, как катализатора, сильно зависит от температуры и не может быть отнесена к кислотной шкале Гаммета. Поэтому не применять последнюю в кинетических исследованиях гидролиза является нецелесообразным. Подобное поведение наблюдается и в случае перхлорной и фосфорной кислот, для которых каталитическая активность гидролиза не пропорциональна величине H_0. При одинаковых значениях H_0 скорости гидролиза в различных кислотах значительно различаются. Соляная кислота является единственной среди изученных кислот, дающей линейную зависимость $\log k$ от H_0.

Синтез и реакции энаминов, II

Синтез пирроленинов

М. А. КИРА, А. БРУКНЕР, Ф. РУФФ и Й. БОРШИ

Пиррол-2-альдегид конденсируется со вторичными аминами с образованием пирроленинов **Ia-d.** Ультрафиолетовые и ИК-спектры **Ia-d** указывают на то, что в гидроксильных растворителях они существуют в форме пирроленина **(I),** а в других растворителях и в твердом состоянии — в этилениминовой форме валентного таутомера **(IV).** Нитрование перхлоратной соли **V** представляет легкий путь получения 4- и 5-нитропиррол-2-альдегидов.

The Acta Chimica publish papers on chemistry in English, German, French and Russian.

The Acta Chimica appear in volumes consisting of four parts of varying size, 4 volumes being published a year.

Manuscripts should be addressed to

Acta Chimica
Budapest 502, Postafiók 32.

Correspondence with the editors should be sent to the same address.

The rate of subscription is 165 forints a volume. Orders may be placed with "*Kultúra*" Foreign Trade Company for Books and Newspapers (Budapest I., Fő utca 32. Account No. 43-790-057-181) or with representatives abroad.

Les Acta Chimica paraissent en français, allemand, anglais et russe et publient des mémoires du domaine des sciences chimiques.

Les Acta Chimica sont publiés sous forme de fascicules. Quatre fascicules seront réunis en un volume (4 volumes par an).

On est prié d'envoyer les manuscrits destinés à la rédaction à l'adresse suivante:

Acta Chimica
Budapest 502, Postafiók 32.

Toute correspondance doit être envoyée à cette même adresse.

Le prix de l'abonnement est de 165 forints par volume.

On peut s'abonner à l'Entreprise pour le Commerce Extérieur de Livres et Journaux «*Kultúra*» (Budapest I., Fő utca 32. Compte-courant No. 43-790-057-181) ou à l'étranger chez tous les représentants ou dépositaires.

«*Acta Chimica*» издают трактаты из области химической науки на русском, французском, английском и немецком языках.

«*Acta Chimica*» выходят отдельным выпусками разного объема. 4 выпуска составляют один том. 4 тома публикуются в год.

Предназначенные для публикации рукописи следует направлять по адресу:

Acta Chimica
Budapest 502, Postafiók 32.

По этому же адресу направлять всякую корреспонденцию для редакции.

Подписная цена «*Acta Chimica*» — 165 форинтов за том. Заказы принимает Предприятие по внешней торговле книг и газет «*Kultúra*» (Budapest I., Fő utca 32. Текущий счет № 43-790-057-181) или его заграничные представительства и уполномоченные.

44,— Ft

Reviews of the Hungarian Academy of Sciences are obtainable at the following addresses:

ALBANIA
Ndermarja Shtetnore e Botimeve
Tirana

AUSTRALIA
A. Keesing
Box 4886, GPO
Sydney

AUSTRIA
Globus Buchvertrieb
Salzgries 16
Wien I

BELGIUM
Office International de Librairie
30, Avenue Marnix
Bruxelles 5
Du Monde Entier
5, Place St. Jean
Buxelles

BULGARIA
Raznoiznos
1, Tzar Assen
Sofia

CANADA
Pannonia Books
2, Spadina Road
Toronto 4, Ont.

CHINE
Waiwen Shudian
Peking
P. O. B. 88

CZECHOSLOVAKIA
Artia
Ve Směčkách 30
Praha 2
Poštovná novinová služba
Dovoz tisku
Vinohradská 46
Praha 2
Mad'arská Kultura
Václavské nám. 2
Praha I
Poštová novinová služba
Dovoz tlače
Leningradská 14
Bratislava

DENMARK
Ejnar Munksgaard
Nörregade 6
Copenhagen

FINLAND
Akateeminen Kirjakauppa
Keskuskatu 2
Helsinki

FRANCE
Office International de Documentation et Librairie
48, rue Gay Lussac
Paris 5

GERMAN DEMOCRATIC REPUBLIC
Deutscher Buch-Export und Import
Leninstraße 16
Leipzig 701
Zeitungsvertriebsamt
Clara Zetkin Straße 62
Berlin N. W.

GERMAN FEDERAL REPUBLIC
Kunst und Wissen
Erich Bieber
Postfach 46
7 Stuttgart S.

GREAT BRITAIN
Collet's Holdings Ltd.
Dennington Estate
London Rd.
Wellingborough. Northants.
Robert Maxwell and Co. Ltd.
Waynflete Bldg. The Plain
Oxford

HOLLAND
Swetz and Zeitlinger
Keizersgracht 471—487
Amsterdam C.
Martinus Nijhof
Lange Voorhout 9
The Hague

INDIA
Current Technical Literature
Co. Private Ltd.
India House OPP
GPO Post Box 1374
Bombay I

ITALY
Santo Vanasia
Via M. Macchi 71
Milano
Libreria Commissionaria Sansoni
Via La Marmora 45
Firenze

JAPAN
Nauka Ltd.
92, Ikebukur O-Higashi 1-chome
Toshima-ku
Tokyo
Maruzen and Co. Ltd.
P. O. Box 605
Tokyo-Central
Far Eastern Booksellers
Kanda P. O. Box 72
Tokyo

KOREA
Chulpanmul
Phenjan

NORWAY
Johan Grundt Tanum
Karl Johansgatan 43
Oslo

POLAND
RUCH
ul. Wronia 23
Warszawa

ROUMANIA
Cartimex
Str. Aristide Briand 14—18
Bucureşti

SOVIET UNION
Mezhdunarodnaya Kniga
Moscow G—200

SWEDEN
Almquist and Wiksell
Gamla Brogatan 26
Stockholm

USA
Stechert Hafner Inc.
31, East 10th Street
New York, N. Y. 10003
Walter J. Johnson
111, Fifth Avenue
New York, N. Y. 10003

VIETNAM
Xunhasaba
19, Tran Quoc Toan
Hanoi

YUGOSLAVIA
Forum
Vojvode Mišića broj 1
Novi Sad
Jugoslavenska Knjiga
Terazije 27
Beograd

28. V. 1968. Index : 26.007

ACTA CHIMICA

ACADEMIAE SCIENTIARUM HUNGARICAE

ADIUVANTIBUS

L. ERDEY, K. POLINSZKY, G. SCHAY

AC

R. BOGNÁR, GY. BRUCKNER, Z. CSŰRÖS, T. ERDEY-GRÚZ, Z. FÖLDI, M. FREUND, Á. GERECS, GY. HARDY, J. HOLLÓ, Á. KISS, M. KORACH, F. MÁRTA, F. NAGY, J. PROSZT, E. PUNGOR, Z. SZABÓ, P. TÉTÉNYI, L. VARGHA, K. VAS

REDIGIT

B. LENGYEL

TOMUS 56 FASCICULUS 3

AKADÉMIAI KIADÓ, BUDAPEST

1968

ACTA CHIM. ACAD. SCI. HUNG.

ACTA CHIMICA

A MAGYAR TUDOMÁNYOS AKADÉMIA KÉMIAI TUDOMÁNYOK OSZTÁLYÁNAK IDEGEN NYELVŰ KÖZLEMÉNYEI

SZERKESZTI

LENGYEL BÉLA

TECHNIKAI SZERKESZTŐK

DEÁK GYULA és TAKÁCS VILMOS

Az Acta Chimica német, angol, francia és orosz nyelven közöl értekezéseket a kémiai tudományok köréből.

Az Acta Chimica változó terjedelmű füzetekben jelenik meg, egy-egy kötet négy füzetből áll. Évente átlag négy kötet jelenik meg.

A közlésre szánt kéziratok a szerkesztőség címére (Budapest 502, postafiók 32) küldendők.

Ugyanerre a címre küldendő minden szerkesztőségi levelezés. A szerkesztőség kéziratokat nem ad vissza.

Az Acta Chimica előfizetési ára kötetenként belföldre 120 Ft, külföldre 165 Ft. Megrendelhető a belföld számára az „Akadémiai Kiadó"-nál (Budapest V., Alkotmány utca 21. Bankszámla 05-915-111-46), a külföld számára pedig a „Kultúra" Könyv- és Hírlap Külkereskedelmi Vállalatnál (Budapest I., Fő utca 32. Bankszámla: 43-790-057-181) vagy annak külföldi képviseleteinél és bizományosainál.

Die Acta Chimica veröffentlichen Abhandlungen aus dem Bereiche der chemischen Wissenschaften in deutscher, englischer, französischer und russischer Sprache.

Die Acta Chimica erscheinen in Heften wechselnden Umfanges. Vier Hefte bilden einen Band. Jährlich erscheinen 4 Bände.

Die zur Veröffentlichung bestimmten Manuskripte sind an folgende Adresse zu senden:

Acta Chimica
Budapest 502, Postafiók 32.

An die gleiche Anschrift ist auch jede für die Redaktion bestimmte Korrespondenz zu richten.

Abonnementspreis pro Band: 165 Forint. Bestellbar bei dem Buch- und Zeitungs-Außenhandels-Unternehmen »*Kultúra*« (Budapest I., Fő utca 32. Bankkonto Nr. 43-790-057-181) oder bei seinen Auslandsvertretungen und Kommissionären.

Acta Chimica Academiae Scientiarum Hungaricae Tomus 56 (3), pp. 199—213 (1968)

UNTERSUCHUNG DES MECHANISMUS DER ZWEISTUFIGEN OXYDATION DES FURFUROLS UND FURFURYLALKOHOLS MIT BROM UND BROMCHLOR IN WÄSSRIGER LÖSUNG

M. SZAKÁCS-PINTÉR und L. MAROS

(Institut für Anorganische und Analytische Chemie der L. Eötvös Universität, Budapest)

Eingegangen am 21. Mai 1967

1. Untersuchung der Reaktionsprodukte

Furfurol und Furfurylalkohol reagieren in säurekatalysierten Reaktionen mit einem Molekül Brom nach den folgenden Gleichungen:

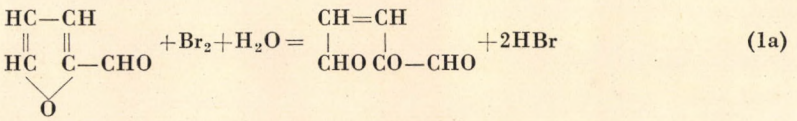

(1a)

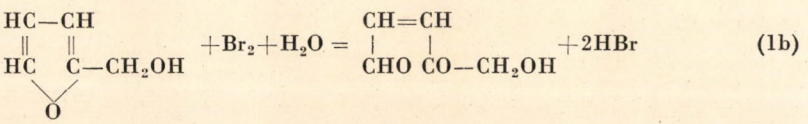

(1b)

Bei der Oxydation bildet sich eine ungesättigte Oxoverbindung. Unsere orientierenden Geschwindigkeitsuntersuchungen haben gezeigt, daß die Reaktionsprodukte mit einem weiteren Molekül Brom — unter sonst gleichen Umständen — um 3—4 Größenordnungen langsamer reagieren. Diese Tatsache hat es möglich gemacht, die Reaktionsprodukte der Oxydation mit einem Molekül Brom eingehend zu untersuchen. Die Bildung des Bromwasserstoffs geht gleichzeitig mit der Oxydation vor sich. Bei den Bestimmungen wurde Bromwasser verwendet. Die Reaktion wurde durch Zugabe von Kaliumjodid gestoppt und das Jod mit Natriumthiosulfat-Meßlösung titriert. Der gebildete Bromwasserstoff wurde bestimmt, indem das Jod nach dem Abstoppen der Reaktion mit Kaliumjodid durch Natriumthiosulfat reduziert und die gebildete Säure mit Natriumhydroxyd-Meßlösung titriert wurde.

Im Zusammenhang mit der Oxydation des Furfurols mit einem Molekül Brom wurde die Reaktion durch HUGHES und ACREE [1] wie folgt beschrieben:

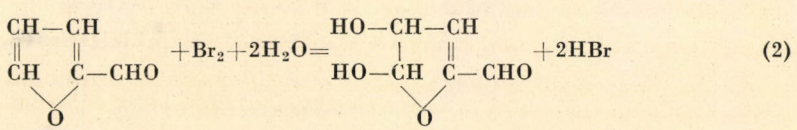

(2)

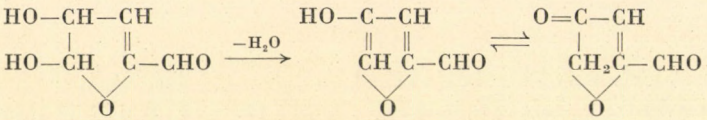

(3)

Ihrer Meinung nach folgt der 2,3-Dihydroxy-Addition Wasseraustritt, und das so gebildete Enol lagert sich in eine Oxoverbindung um. Diese Ansicht beruht darauf, daß das Reaktionsprodukt mit 2 Molekülen Phenylhydrazin ein Phenylhydrazon bildet, das als Niederschlag isoliert werden kann.

Die Tatsache der Ringsprengung konnten wir mit den folgenden Messungen bestätigen. Das Oxydationsprodukt des Furfurols enthält 2 Aldehydgruppen, das des Furfurylalkohols nur eine. Nach der Oxydation mit Brom kann mit dem Bisulfit-Cyanid-Verfahren soviel Aldehyd gemessen werden [2]. Beide Produkte reagierten — der Erwartung entsprechend — mit einem Molekül Perjodat.

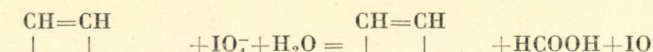

(4a)

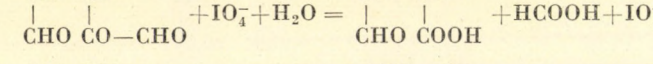

(4b)

Bei der Bestimmung oxydierten wir mit Perjodsäure, der Überschuß des Perjodats wurde mit dem jodometrischen Verfahren nach MÜLLER und WEGELIN [3] bestimmt. Nach der Oxydation mit Brom und Perjodat können beim Furfurol 1 Molekül (Gleichung 4/a), bei Furfurylalkohol 2 Moleküle Aldehyd (Gleichung 4b) mit dem Bisulfit-Cyanid-Verfahren bestimmt werden.

Über die zweite Stufe der Oxydation des Furfurols und des Furfurylalkohols mit Brom sind in der Literatur keine Angaben zu finden. Die zweite Stufe bedeutet eigentlich die Bromierung der ungesättigten Oxoverbindungen. Auch diese Reaktion ist ein säurekatalysierter Vorgang, der mit den folgenden Gleichungen beschrieben werden kann:

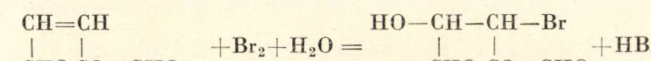

(5a)

(5b)

Bei der Reaktion bildet sich 1 Molekül Bromwasserstoff, der auf die oben beschriebene Weise bestimmt werden kann. Die Aldehydgruppen bleiben bei der Oxydation unverändert, dies wird durch die Bestimmungen mit dem Bisulfit-Cyanid-Verfahren eindeutig bewiesen. Nach der Reaktion des zweiten

Moleküls Brom reagiert die Verbindung — der Erwartung entsprechend — mit 2 Molekülen Perjodat.

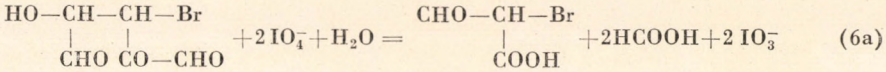

(6a)

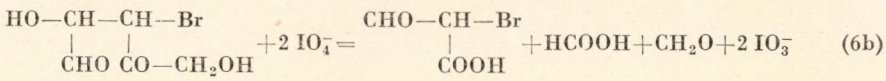

(6b)

Nach der Oxydation mit dem zweiten Molekül Brom und darauffolgend mit Perjodat konnten wir beim Furfurol 1, beim Furfurylalkohol 2 Moleküle Aldehyd mit dem Bisulfit-Cyanid-Verfahren bestimmen. Außer den Ergebnissen der Bestimmung des Bromwasserstoffs und der direkten Aldehydbestimmung, liefern die Oxydationen mit Perjodat die entscheidenden Daten über die in den 5a und 5b Gleichungen beschriebenen Reaktionsprodukte. Ohne diese könnte auch die Bildung des Isomers der α-Bromhydroxy-Verbindung

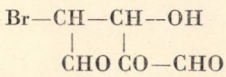

sowie des infolge von Substitution entstehenden Isomerenpaares angenommen werden.

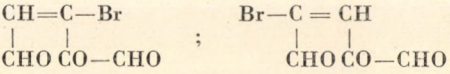

Diese drei Produkte hätten aber nur mit einem Molekül Perjodsäure reagieren können. Im Zusammenhange mit den beiden letzteren Verbindungen ist dies leicht einzusehen, bei der isomeren α-Bromhydroxy-Verbindung aber bedarf es einer näheren Erklärung. Unserer Erfahrung nach reagiert das Produkt in saurer Lösung ($p_H = 2-4$) mit 2 Molekülen Perjodat schnell, die Reaktion läuft in etwa 10 Minuten vollkommen ab. Im Falle des letzteren Isomers ist dies — unserer Meinung nach — nicht möglich. Bei der Reaktion des ersten Moleküls Perjodsäure können nämlich zweierleie Produkte entstehen:

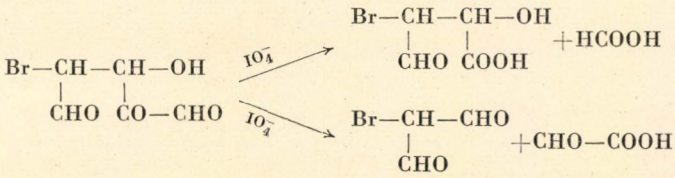

Jedes dieser Produkte könnte nur sehr langsam mit einem weiteren Molekül Perjodat reagieren, und auch die Aldehydmolzahlen könnten mit den erhaltenen Meßergebnissen nicht in Einklang gebracht werden.

2. Mechanismus der ersten Stufe der Oxydation des Furfurols mit Brom und Bromchlor (hypobromiger Säure)

Zur Klärung der einzelnen Phasen der Reaktion wurde der Vorgang kinetisch untersucht. Diese Untersuchungen konnten mit klassischen Methoden nur beim Furfurol vorgenommen werden, der Furfurylalkohol reagiert näm-

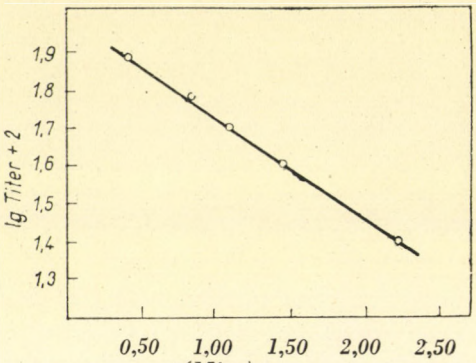

Abb. 1

[Furfurol] = $[Br_2]$ = 5,00 · 10^{-4}; $[H^+]$ = =1,0 · 10^{-2}; 20,0 °C (schwefelsaurige Lösung)

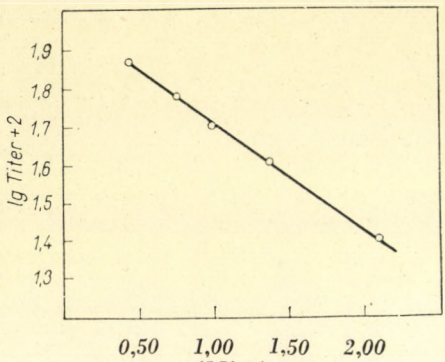

Abb. 2

[Furfurol] = $[Br_2]$ = 5,00 · 10^{-4}; $[H^+]$ = = 1,0 · 10^{-2}; [KBr] = 5 · 10^{-2}; 20,0 °C (salzsaurige Lösung)

lich auch bei 0 °C zu schnell mit 1 Molekül Brom. Bei den Bestimmungen betrug die Konzentration des Furfurols im allgemeinen 5.10^{-4} Mol/Liter. Nachdem festgestellt wurde, daß die Reaktionsgeschwindigkeit durch die Chlorid- bzw. Bromidionen-Konzentration nicht merklich beeinflußt wird, wurde zu den Bestimmungen eine solche wäßrige Bromlösung verwendet, die 5% Kaliumbromid enthielt. Die Reaktionen wurden durch Zugabe von Kaliumjodid gestoppt und das Jod wurde mit 0,01 *n* Natriumthiosulfat-Meßlösung titriert.

Nach unseren Untersuchungen beträgt die globale Ordnung der symmetrischen Reaktion in der ersten Stufe 1 (Abb. 1 und 2) die Teilordnung des Furfurols 1 (Abb. 3) und des Broms 0 (Abb. 4) .

Der Vorgang verläuft bei höherer Wasserstoffionenkonzentration schneller. Die Reaktionsgeschwindigkeit kann mit der Gleichung

$$v = k.\ [\text{Furfurol}]$$

beschrieben werden wenn

$$k = k_{H^+}.\ [H_3O^+]$$

$$\lg k = \lg k_{H^+} + \lg [H_3O^+]$$

Wird lg k als Funktion von lg $[H_3O^+]$ dargestellt, so ergibt sich für die Richtungstangente der Geraden 1 (Abb. 5).

Bei den Untersuchungen der Oxydationen mit Bromchlor bzw. mit hypobromiger Säure, verwendeten wir eine Quecksilber(II)chlorid enthaltende

bromidfreie Bromlösung. Für die globale Ordnung der symmetrischen Reaktion sowie für die Teilordnung des Furfurols ergab sich 1. Die kinetische Identität der Oxydation mit Brom bzw. mit hypobromiger Säure geht aus Abb. 6 hervor.

Auch die Geschwindigkeit der in Gegenwart eines Silberionenüberschusses ausgeführten Oxydationen mit Brom (Oxydation mit hypobromiger Säure) stimmte mit der Geschwindigkeit der in Gegenwart von Bromid ausgeführten Oxydationen mit Brom überein.

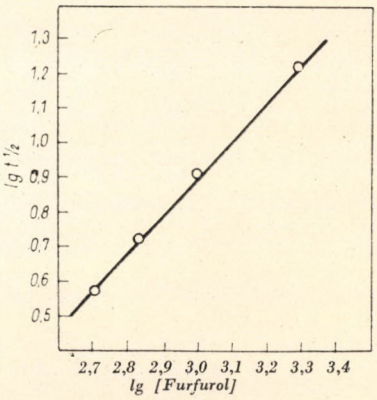

Abb. 3

$[Br_2] = 5{,}00 \cdot 10^{-4}$; 20,0 °C (ungepufferte Lösung)

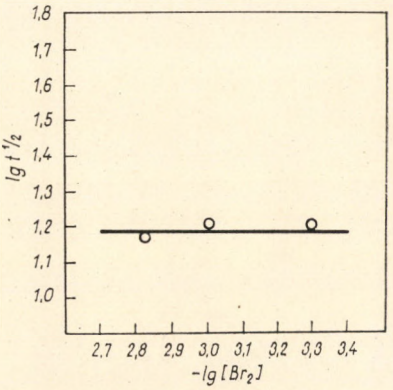

Abb. 4

[Furfurol] = $5{,}00 \cdot 10^{-4}$; 20,0 °C (ungepufferte Lösung)

Die Oxydation mit hypobromiger Säure ist ebenfalls eine säurekatalysierte Reaktion (Abb. 7).

Auf Grund unserer Bestimmungen kann das folgende einfache Reaktionsschema als Grundlage zur Mechanismusuntersuchung dienen:

$$\text{Furfurol} + H_3O^+ \xrightarrow[\text{langsam}]{k_{H^+}} \text{Furfurol}\cdot H^+ + H_2O$$

$$\text{Furfurol}\cdot H^+ + Br_2 + H_2O \xrightarrow[\text{schnell}]{} \text{Produkte} + H_3O^{+*}$$

Ein klassisches Beispiel der säurekatalysierten Halogenierungsvorgänge, nullter Ordnung auf das Halogen bezogen, ist die von LAPWORTH [4] entdeckte Aceton-Halogenierung, die über die Enolform des Acetons verläuft. In diesen Reaktionen ist die Enolbildung der geschwindigkeitsbestimmende Prozeß. Das Enol reagiert mit dem Halogen in jedem Fall schnell.

* Unter den allgemeinen Vorgängen $A \underset{k_2}{\overset{k_1}{\rightleftharpoons}} B \xrightarrow{k_3} C$ besteht in unserem Fall das Verhältnis $k_3 \gg k_2 > k_1$, d. h. die Geschwindigkeit des Vorganges wird durch k_1 bestimmt.

Im Laufe der Geschwindigkeitsuntersuchungen der Oxydationen mit Brom und hypobromiger Säure könnte man daran denken, daß es sich auch in unserem Fall um eine Enolhalogenierung handelt, da die mit einer säurekatalysierten Ringsprengung verbundene Wasseraddition der Furanderivate bekannt ist, wobei sich die entsprechende gesättigte Oxoverbindung bildet.

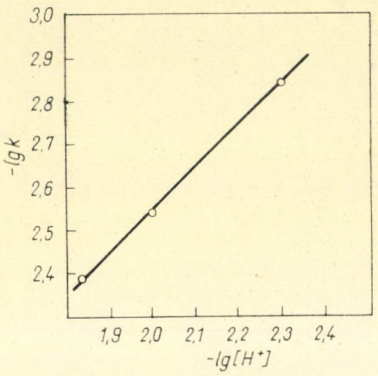

Abb. 5

[Furfurol] = [Br_2] = 5,00 · 10^{-4}; 0,0 °C

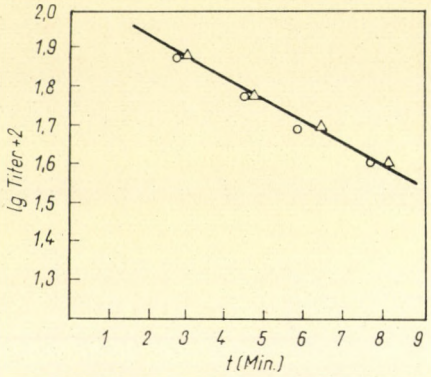

Abb. 6

△ [Furfurol] = [HOBr] = 5,00 · 10^{-4}; [H^+] = 2,0 · 10^{-3}; 22,0 °C

○ [Furfurol] = [Br_2] = 5,00 · 10^{-4}; [H^+] = 2,0 · 10^{-3}; 22,0 °C

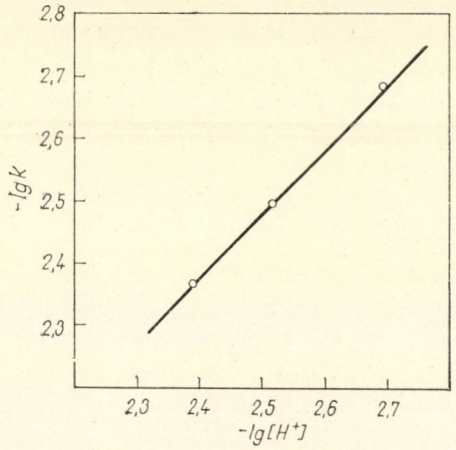

Abb. 7

[Furfurol] = [HOBr] = 5 · 10^{-4}; 14,0 °C

Es kann angenommen werden, daß dieser Vorgang über das Enol verläuft:

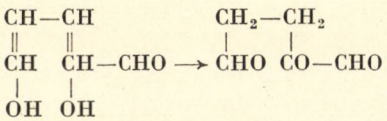

(9)

Die Geschwindigkeit der säurekatalysierten Halogenierung des Acetons ist bei Chlorierung, Bromierung und Jodierung nahezu gleich [5]. Furfurol und Furfuroylalkohol reagieren aber nicht oder nur außerordentlich langsam mit Jod, was gegen den auf der Enolhalogenierung beruhenden Mechanismus spricht; d. h. der Halogenaddition geht keine Wasseraddition und Ringsprengung voran.

Der Furanring wird durch die Protonierung für die Halogenaddition aktiviert. Obwohl wir die Bromierung anderer Furanderivate, außer der des Furfurols bisher noch nicht eingehender untersucht haben, besteht nach unseren orientierenden Untersuchungen in wäßriger Lösung die Reihenfolge Furan $>>$ Furfurilalkohol $>$ Furfurol $>$ 5-Nitrofurfurol für die säurekatalysierten Bromierungsgeschwindigkeiten. Diese Reihenfolge ist auch für die säurekatalysierte nukleophile Wasseraddition und Ringsprengung (Hydrolyse mit Vinyläthercharakter) der Furanderivate gültig [6]. Alle diese Angaben weisen darauf hin, daß die Protonierung in diesen Fällen am Äthersauerstoff eintritt.

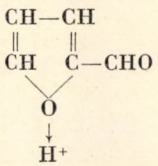

Das so gebildete Oxoniumion bzw. irgendeine seiner polaren Grenzstrukturen reagiert mit Brom. Unsere Untersuchungen haben gezeigt, daß die Reaktion bei den verschiedenen Formen des Broms (Br_2, Br_3^-, HOBr) von gleicher Geschwindigkeit und für Brom von nullter Ordnung ist. Die Tatsache, daß das protonisierte Furanderivat mit Jod (I_3^-) nicht reagiert, macht auf eine Analogie mit den elektrophilen Olefinhalogenierungsmechanismen [7, 8] aufmerksam. Berücksichtigt man auch die Produkte (siehe Gleichung 1), so dürfte der Angriff des Broms auf den Kohlenstoffatomen 2,5 erfolgen. Die Polarisation des Oxoniumions kann auf Grund der obigen Ausführungen bis zur folgenden Grenzstruktur gesteigert werden.

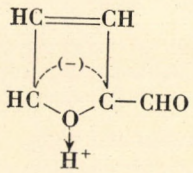

Das Wesen der elektrophilen Bromierung kann durch Bildung entweder von 2,5-Dibromid oder von Bromhydrin erklärt werden. Diesen Übergangszuständen folgen schnelle Hydrolysen.

Für den Mechanismus der säurekatalysierten elektrophilen Bromierung des Furfurols schlagen wir das folgende Schema vor:

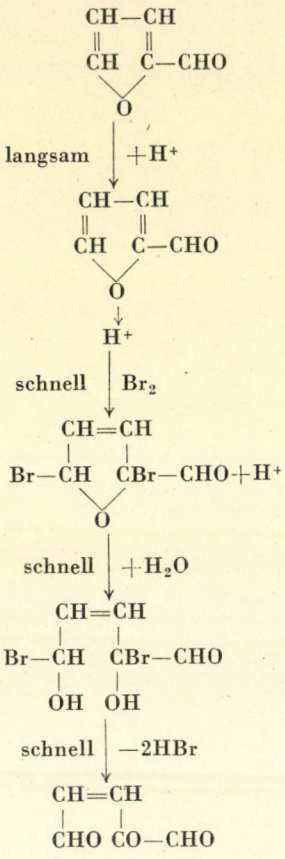

Die relative Stabilität des Produktes gewährleistet die infolge des Effektes der Doppelbindungen zwischen den Oxogruppen bestehende Konjugations-Wechselwirkung.

Tabelle I

Die Arrhenius-Parameter der Oxydation des Furfurols mit Brom

°C	0,0	15,0	19,8
k_{H^+} L/Mol. Sec.	$2{,}9 \cdot 10^{-1}$	$8{,}7 \cdot 10^{-1}$	1,16
E* Kcal/Mol	10,8		
$\Delta S \neq$ cal/Grad. Mol	−23,4		

Die Geschwindigkeitskonstanten und Arrhenius-Parameter der Oxydation des Furfurols mit 1 Molekül Brom und Bromchlor sind in der Tabelle I zusammengefaßt.

3. Mechanismus der zweiten Stufe der Oxydation des Furfurols und Furfurylalkohols mit Brom und Bromchlor (hypobromiger Säure)

Wie schon erwähnt wurde, bedeutet die zweite Stufe der Oxydation dieser Verbindungen die Bromierung der in der ersten Stufe gebildeten ungesättigten Oxoverbindungen (siehe Gleichungen 5a, 5b). Diese Bromierungs-

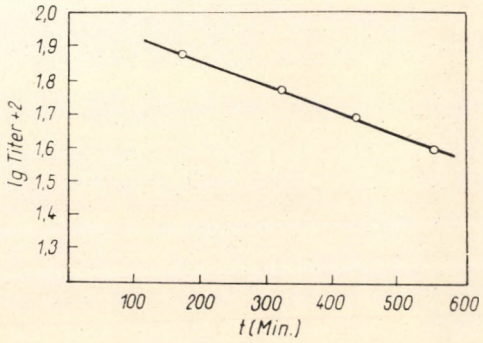

Abb. 8

Furfurol, zweite Stufe: [Ox. Furfurol] = = $[Br_2] = 5{,}00 \cdot 10^{-4}$; $[H^+] = 2{,}7 \cdot 10^{-1}$; 20,0 °C

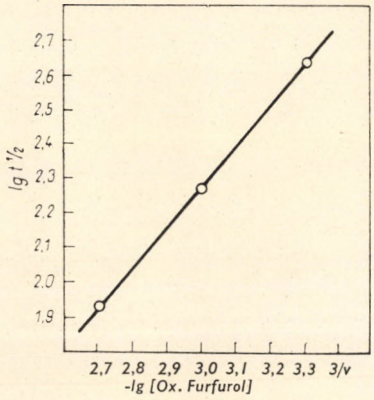

Abb. 9

Furfurol, zweite Stufe: $[Br_2] = 5{,}00 \cdot 10^{-4}$; $[H^+] = 2{,}7 \cdot 10^{-1}$; 20,0 °C

stufen sind bedeutend langsamer, als die ersten Stufen (in Falle von Furfurol bei 20 °C ist $k'_{H^+}/k''_{H^+} = 1{,}2 \cdot 10^4$). Vor diesen Untersuchungen ließen wir das Furfurol und den Furfurylalkohol mit einer nach dem Molverhältnis von 1 : 1 genau berechneten Brommenge reagieren; auf diese Weise erhielten wir nach Beendigung der Reaktion die Lösungen der entsprechenden Oxoverbindungen. Diese Lösungen wurden bei den kinetischen Untersuchungen der zweiten Stufe verwendet. Bei der Untersuchung der Oxydation der ungesättigten Oxoverbindungen mit Brom wurde die Reaktion gleichfalls durch Zugabe von wäßriger Bromlösung eingeleitet, mit Kaliumjodid gestoppt und nachher das ausgeschiedene Jod mit Natriumthiosulfatlösung titriert.

Auf Grund der Messungen der Reaktionsgeschwindigkeit reagierten diese ungesättigten Oxoverbindungen mit Brom (Br_3^-), ebenfalls in einem säurekatalysierten Vorgang, wobei die Teilordnung der Oxoverbindung 1 und die

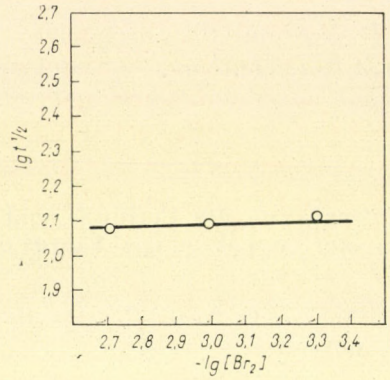

Abb. 10

Furfurol, zweite Stufe: [Ox. Furfurol] = = 5,00 · 10^{-4}; [H^+] = 5,5 · 10^{-1}; 20,0 °C

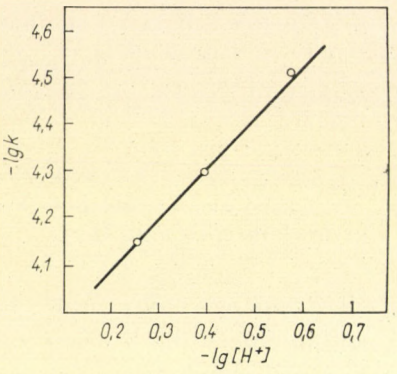

Abb. 11

Furfurol, zweite Stufe: [Ox. Furfurol] = = [Br_2] = 5,00 · 10^{-4}; 20,0 °C

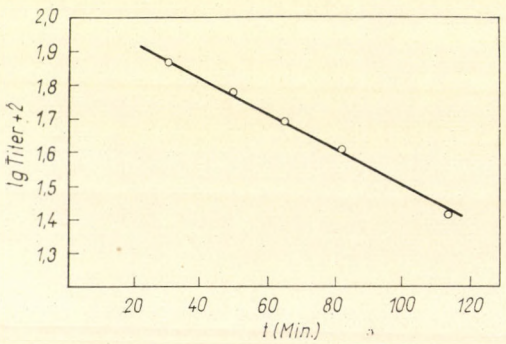

Abb. 12

Furfurylalkohol, zweite Stufe: [Ox. Furfurylalkohol] = [Br_2] = 5,00 · 10^{-4}; [H^+] = = 2,7 · 10^{-1}; 20,0 °C

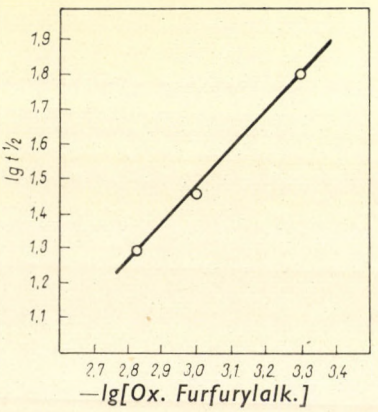

Abb. 13

Furfurylalkohol, zweite Stufe: [Br_2] = 5,00 · · 10^{-4}; [H^+] = 2,7 · 10^{-1}; 20,0 °C

Teilordnung des Broms wieder Null ist. Die Meßergebnisse sind für Furfurol auf Abbildung 8, 9, 10 und 11; für Furfurylalkohol auf Abbildung 12, 13, 14 und 15 dargestellt.

Auf Grund der kinetischen Daten kann ein der ersten Bromierungsstufe ähnliches Reaktionsschema als Basis der Mechanismusuntersuchung betrachtet werden:

$$\text{"Oxo"} + H_3O^+ \xrightarrow[\text{langsam}]{} + \text{"Oxo"} \cdot H^+ + H_2O$$

$$\text{"Oxo"} \cdot H^+ + Br_2 \xrightarrow[\text{schnell}]{} \text{Produkte} + H^+$$

$$\text{"Oxo"} = \begin{matrix} CH{=}CH \\ | \quad | \\ CHO\ CO{-}CHO \end{matrix} \quad ; \quad \begin{matrix} CH{=}CH \\ | \quad | \\ CHO\ CO{-}CH_2OH \end{matrix}$$

$$v = k_{H^+} [\text{"Oxo"}] [H_3O^+]$$

Bezüglich der genaueren Aufdeckung des Mechanismus ist es von entscheidender Bedeutung, daß die säurekatalysierte Halogenierung der Oxoverbindungen auch mit Jod durchgeführt werden kann und die Geschwindigkeit der Jodierung bzw. Bromierung annähernd gleich ist. Die Bromchlorierung bzw. die Oxydation mit hypobromiger Säure aber ist ein vollkommen andersartiger Vorgang. Die Geschwindigkeit der letzteren Reaktion ist von der Wasserstoffionenkonzentration unabhängig, die Teilordnung des Halogens und der Oxo-

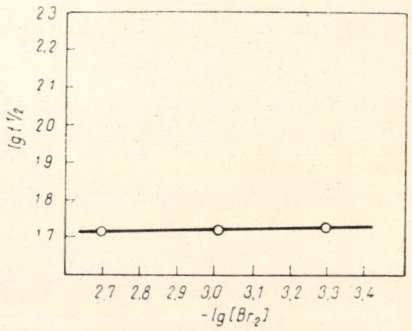

Abb. 14

Furfurylalkohol, zweite Stufe: [Ox. Furfurylalkohol] = $5{,}00 \cdot 10^{-4}$; [H^+] = $2{,}7 \cdot 10^{-1}$; 20,0°C

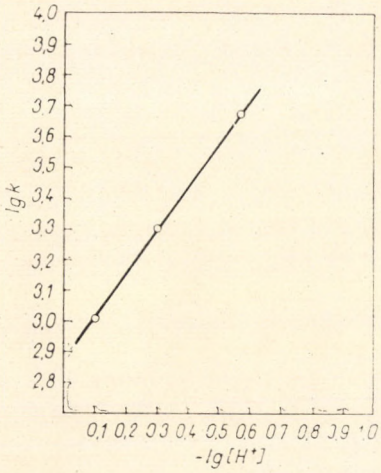

Abb. 15

Furfurylalkohol, zweite Stufe: [Ox. Furfurylalkohol] = [Br_2] = $5{,}00 \cdot 10^{-4}$; 20,0 °C

verbindung ist 1. Dieser Halogenierungsvorgang zweiter Ordnung kann mit dem Mechanismenschema der echten elektrophilen Addition der Olefine charakterisiert werden.*

$$\text{"Oxo"} + \text{BrCl} \rightarrow \text{Produkte}$$

$$v = k_{II}\,[\text{"Oxo"}]\,[\text{BrCl}]$$

Tabelle II

Furfurol, zweite Stufe, Oxydation mit Bromchlor

[Ox. Furfurol] = [BrCl] = $5{,}00 \cdot 10^{-4}$; [H^+] = $5{,}0 \cdot 10^{-3}$; 23,0 °C

Titer %	25	40	50	60	75
t (Sec.)	600	1200	1740	2820	5700
k_{II} (L/Mol. Sec.)	1,11	1,11	1,14	1,10	1,05

*Bei der Reaktion wurde »bromchlorierende« Bromat-Bromid-Lösung [9] bzw., in Gegenwart von Quecksilber(II)Chlorid, bromidfreies Bromwasser benützt.

Die kinetischen Daten der Oxydation mit Bromchlor sind in den Tabellen II, III und IV zusammengestellt.

Tabelle III

Furfurol, zweite Stufe, Oxydation mit Bromchlor
$[H^+] = 5{,}0 \cdot 10^{-3}$; 23,0 °C

[Ox. Furfurol]	[BrCl]	k_{II}(L/Mol. Sec)
$5 \cdot 10^{-4}$	$5 \cdot 10^{-4}$	1,14
$10 \cdot 10^{-4}$	$5 \cdot 10^{-4}$	1,11
$20 \cdot 10^{-4}$	$5 \cdot 10^{-4}$	1,10
$5 \cdot 10^{-4}$	$10 \cdot 10^{-4}$	1,13
$5 \cdot 10^{-4}$	$20 \cdot 10^{-4}$	1,15

Tabelle IV

Furfurol, zweite Stufe, Oxydation mit Bromchlor
[Ox. Furfurol] = [BrCl] = $5{,}00 \cdot 10^{-4}$; 23,0 °C

$[H^+]$	k_{II}(L/Mol. Sec)
$5 \cdot 10^{-3}$	1,11
10^{-2}	1,11
$3 \cdot 10^{-1}$	1,08

Unter Berücksichtigung der bekannten Mechanismen der elektrophilen Addition der Doppelbindung [10] schlagen wir für den Bromchlorierungsprozeß folgenden Reaktionsmechanismus vor:

$$\mathrm{CHO{-}CH{=}CH{-}CO{-}CHO}$$

langsam $\downarrow$ $+\mathrm{Br^+(H_2OBr^+)}$

$$\mathrm{CHO{-}\overset{+}{C}H{-}CHBr{-}CO{-}CHO}$$

schnell $\downarrow$ $+\mathrm{H_2O}$

$$\mathrm{CHO{-}CH(OH){-}CHBr{-}CO{-}CHO + H^+}$$

Die Bromierung (Br_2, Br_3^-) liefert die gleichen Endprodukte, wenn auch nach einem abweichenden Mechanismus. Die Säurekatalyse und die nullte Ordnung des Broms weisen auf einen Enol-Bromierungs-Mechanismus hin. Diese Annahme wird auch durch jene Tatsache unterstützt, daß die Oxoverbindungen mit Jod (I_3^-) jodiert werden können, und dieser Prozeß ist, der Jodierung des Acetons ähnlich, in stark saurer Lösung reversibel. Die gleichen kinetischen Eigenschaften können auch bei der Bromierung und Jodierung des Crotonaldehyds beobachtet werden, obwohl die Reaktion in diesem Fall um Größenordnungen schneller verläuft. Über den Mechanismus der Halogenierung des Crotonaldehyds in wäßriger Lösung fanden wir keine Daten in der Literatur, seine säurekatalysierte Wasseraddition (und ebenso die säurekatalysierte Wasseraddition von 2,2-Dimethylacrolein) ist von LUCAS und Mitarbeitern [11, 12] untersucht worden. Nach der Deutung von TAFT [13], beschrieb HINE [14] den wahrscheinlichsten Mechanismus, wie folgt:

$$CH_3-CH=CH-CHO+H_3O^+ \underset{k_{-1}}{\overset{k_1}{\rightleftharpoons}} [CH_3-CH=CH-CHOH]^+ + H_2O$$

I II

$$[CH_3-CH=CH-CHOH]^+ + H_2O \underset{k_{-2}}{\overset{k_2}{\rightleftharpoons}} CH_3-\underset{\displaystyle OH_2^+}{\underset{|}{CH}}-CH=CHOH$$

II III

$$CH_3-\underset{\displaystyle OH_2^+}{\underset{|}{CH}}-CH=CHOH \xrightarrow[H_2O]{k_3} CH_3-\underset{\displaystyle OH}{\underset{|}{CH}}-CH_2-CHO+H_3O^+$$

III IV

$$k_3 \text{ und } k_{-1} \gg k_2$$

Wäre das hydratisierte und protonierte (oder deprotonierte) Enol jene Form, die mit dem Brom reagiert, so wären prinzipiell auch die Geschwindigkeiten der Hydration and Bromierung des Crotonaldehyds gleich. Die Bromierung nullter Halogen-Teilordnung ist aber ein etwa um 2 Größenordnungen schneller Vorgang ($k_{H+\text{Bromierung}} : k_{H+\text{Hydration}} \sim 200 : 1$). Diese Tatsache weist darauf hin, daß die dem Übergangszustand entsprechende Form II bzw. ihr carboniumionisches tautomeres Enol mit Brom schneller reagiert als mit Wasser.

$$[CH_3-CH=CH-CHOH]^+ \rightleftharpoons [CH_3-CH-CH=CHOH]^+$$

Bezüglich des Mechanismus der eingehend untersuchten zweiten Stufe der säurekatalysierten Bromierung des Furfurols und Furfurylalkohols nehmen wir analoge Reaktionen und Reaktionsfähigkeit von analogen Formen an. Dementsprechend schlagen wir für die säurekatalysierte Bromierung den folgenden Mechanismus vor:

$$CHO-CH=CH-CO-A+H_3O^+ \qquad -A=-CHO;\ -CH_2OH$$

langsam $\downarrow$ $-H_2O$

$$[CHO-CH=CH-\underset{\displaystyle OH}{\underset{|}{C}}-A]^+$$

$$\uparrow\downarrow$$

$$[CHO-CH-CH=\underset{\displaystyle OH}{\underset{|}{C}}-A]^+$$

schnell $\downarrow$ $+Br_2$

$$[CHO-CH-\underset{\displaystyle Br}{\underset{|}{CH}}-\underset{\displaystyle OH}{\underset{|}{CBr}}-A]^+$$

$\downarrow$

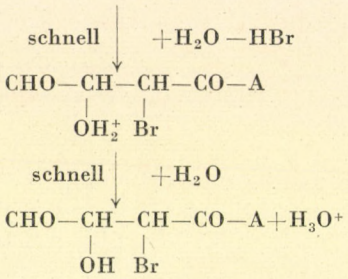

Tabelle V

Furfurol, zweite Stufe

t °C	20,0	24,9
k_{H^+} (L/Mol. Sec.)	$1{,}00 \cdot 10^{-4}$	$1{,}73 \cdot 10^{-4}$
E^* (Kcal/Mol.)	19	
$\Delta S^{\neq}$ (cal/Grad. Mol.)	−16	

Tabelle VI

Furfurylalkohol, zweite Stufe

t °C	15,0	20,1
k_{H^+} (L/Mol. Sec.)	$3{,}44 \cdot 10^{-4}$	$5{,}96 \cdot 10^{-4}$
E^* (Kcal/Mol.)	18	
$\Delta S^{\neq}$ (cal/Grad. Mol.)	−16	

Tabelle VII

Furfurol, zweite Stufe der Oxydation mit Bromchlor

t °C	14,0	20,0	23,0
k_{II} (L/Mol. Sec.)	0,45	0,81	1,14
E^* (Kcal/Mol.)	35		
$\Delta S^{\neq}$ (cal/Grad. Mol.)	52		

Die Arrhenius-Parameter der zweiten Stufe der Oxydation mit Brom und Bromchlor sind in den Tabellen V, VI und VII zusammengestellt.

Die Aktivierungsenergie der Hydration des Crotonaldehyds beträgt 18,2, die der Hydration des Dimethylacroleins 19,1, die der säurekatalysierten Bromierung des Crotonaldehyds 20,5 Kcal/Mol.

Die zweistufige Oxydation des Furfurols und des Furfurylalkohols mit Bromchlor wurde von uns für analytische Zwecke benützt [15].

ZUSAMMENFASSUNG

Das Furfurol sowie der Furfurylalkohol reagiert in einem säurekatalysierten Vorgang mit 1 Molekül Brom, wobei die Teilordnung des Furanderivates 1, die des Halogens Null ist. Bei der Reaktion entstehen (in wäßriger Lösung) 2 Moleküle Bromwasserstoff, und das Furanderivat liefert infolge von Ringsprengung die entsprechende ungesättigte Oxoverbindung. Die Geschwindigkeit des Vorganges wird — auch bei der Bromchlorierung — durch die Protonierungsgeschwindigkeit des Äthersauerstoffes bestimmt. Nach dem angenommenen Mechanismus folgt diesem eine schnelle 2,5-Halogenaddition und eine schnelle Hydrolyse.

Furfurol und Furfurylalkohol reagieren mit dem zweiten Molekül Brom um 3—4 Größenordnungen langsamer. Diese Reaktion bedeutet eigentlich die Bromierung der ungesättigten Oxoverbindungen, auf Grund des angenommenen Mechanismus einen säurekatalysierten Enolhalogenierungsvorgang, bei dem die Teilordnung des Broms Null ist.

Die ungesättigten Oxoverbindungen reagieren nach einem echten elektrophilen Additionsmechanismus mit Bromchlor. Eine Säurekatalyse ist in diesem Fall nicht zu beobachten, die Teilordnung der ungesättigten Oxoverbindung und des Bromchlors ist 1.

Bei der Reaktion des zweiten Brom- und Bromchlor- Moleküls bildet sich Bromhydrin sowie ein Molekül Wasserstoffhalogenid.

LITERATUR

1. Hughes, E. E., Acree, S. F.: J. Research Nat. Bur. Standards **24,** 172 (1940); Ch. Z.: **1,** 40 (1941).
2. Schulek, E., Maros, L.: Acta Chim. Acad. Sci. Hung. **17,** 369 (1958).
3. Müller, E., Wegelin, G.: Z. anal. Chem. **52,** 755 (1913).
4. Lapworth, A.: J. Chem. Soc. **85,** 30 (1904).
5. Bell, R. P., Yates, K.: J. Chem. Soc. 1927 **1962.**
6. Dunlop, A. P., Peters, F. N.: The Furans. Reinhold, New York, 1953, p. 640.
7. Atkinson, J. T., Bell, R. P.: J. Chem. Soc. 3860 **1963.**
8. Bell, R. P., Pring, M.: J. Chem. Soc. B. 1199. **1966.**
9. Schulek, E., Burger, K.: Magyar Tud. Akad. Oszt. Közl. **12,** 9 (1959).
10. Hine, J.: Physical Organic Chemistry. McGraw-Hill, 1956, p. 213.
11. Winstein, S., Lucas, H. J.: J. Am. Chem. Soc. **59,** 1461 (1937).
12. Lucas, H. J., Stewart, U. T., Pressmann, D. P.: J. Am. Chem. Soc. **66,** 1818 (1944).
13. Taft, R. W. jr.: J. Am. Chem. Soc. **74,** 5372 (1952).
14. Hine, J.: Physical Organic Chemistry. McGraw-Hill 1956, p. 216.
15. Szakács-Pintér, M., Maros, L.: Acta Chim. Acad. Sci. Hung. **56,** 87 (1968).

Margit Szakács-Pintér
László Maros
Budapest VIII., Múzeum körút 4/b.

Acta Chimica Academiae Scientiarum Hungaricae Tomus 56 (3), pp. 215—219 (1968)

THEORIE DER LICHTABSORPTION DER CYCLOPENTADIENYL-KOMPLEXE DER ÜBERGANGSELEMENTE

Á. KISS

(Institut für Allgemeine und Physikalische Chemie der Universität Szeged)

Eingegangen am 5. Juni 1967

1. Bindungsmodelle der Komplexe

Bei Ferrocen haben FISCHER und Mitarbeiter [1, 2, 3] mit dem Bindungsmodell 12 bei C_{5v}-Symmetrie des Ligandfeldes und bei *cis*-Anordnung der zwei Cyclopentadienyl-Ringe gerechnet. Bei der Komplexbindung gehen die zwei Elektronen von C_5H_5- zum Fe(11)-Ion über. Außerdem werden die zwei Ringe mit 10 Sandwichbindungen festgehalten.

Durch Röntgenuntersuchungen [4] wurden die zehn Sandwichbindungen bestätigt. Aber mit dem Modell können die magnetischen Momente der Komplexe und ihre Lichtabsorption nicht interpretiert werden. Außerdem haben die zwei Ringe *trans*- und nicht die angenommene *cis*-Anordnung, bzw. werden die Komplexe vorwiegend mit Metallionen und nicht mit Metallatomen gebildet.

KEALEY und PAUSON [5] haben mit dem Bindungsmodell 12 gerechnet.

Bei Benützung der SCF-LCO-MO Methode erhält YAMASAKY [11] 33% kovalente Bindung beim Ferrocen. Nach den Berechnungen sind 10 Anregungen möglich, von denen die wichtigsten ${}^1A_{lg} \rightarrow {}^1A_{lg} \rightarrow {}^1E_u$ sind.

ORGEL [6, 7] hat die Berechnungen mit dem Bindungsmodell 10 bei *trans*-Stellung der zwei Cyclopentadienyl-Ringe und bei der richtigen D_{5d}-Symmetrie des Ligandfeldes ausgeführt.

Bei der Berechnung der Termenergien der Komplexe benützen LIEHR und BALLHAUSEN [8] die Ligandfeldtheorie. Bei elektrovalenten Komplexen können diese Berechnunsresultate gut verwertet werden.

Nach MOFITT [9] kann man in normalen Fällen das paramagnetische Moment der Komplexe zur Entscheidung dessen benützen, ob diese mit Metallionen oder mit Metallatomen gebildet werden. Bei anomal paramagnetischen Komplexen versagt diese Methode, aber mit der Arbeitshypothese (vgl. 2) kann das anomale magnetische Verhalten und ihre Lichtabsorption gut erklärt werden.

COTTON und WILLKINSON [10] verwerfen das Bindungsmodell von FISCHER [2—3], da mit diesem das magnetische Verhalten und die Lichtabsorption der Komplexe nicht interpretiert werden kann. Außerdem werden

die Komplexe vorwiegend mit Metallionen und nicht mit Metallatomen gebildet.

Mit der LCAO-MO Methode berechnen BALLHAUSEN und DAHL [12] die Energie der Sandwich-Bahnen und behaupten, daß durch die schwache Verdrehung der zwei Ringe die Bindungsenergie der Komplexe kaum geändert wird.

Nach den mit der MO-LCAO Methode ausgeführten Berechnungen von WOODWARD, ROSENBLUM und WITTIG [13] können sich die zwei Cyclopentadienyl Ringe um das Metallatom bzw. Metallion drehen.

2. Grundlinien einer neuen Arbeitshypothese

DUNITZ und ORGEL [14, 15] haben die Überlappungsintegrale berechnet. Da der Komplex durch das $C_5H_5^-$-Ion gebildet wird, gehen die zwei Elektronen zum Fe(II)-Ion über, somit wurde das Bindungsmodell 12 von FISCHER [2, 3] interpretiert.

Neuerdings deuten einige Forscher die Resultate dieser Berechnungen damit, daß die Cyclopentadienyl-Komplexe durch die zwei lokalisierten Bindungen gebildet werden. Dabei werden die 10 Sandwich-Bindungen nicht berücksichtigt. Aber mit diesem Modell kann man die Lichtabsorption der Komplexe nicht interpretieren. Deshalb soll hier mit einer neuen, auch die Sandwich-Bindung in Betracht ziehenden Arbeitshypothese gearbeitet werden, deren Grundlinien die folgenden sind:

Mit zwei Cyclopentadienyl-Anionen werden die Komplexe in der Mehrzahl der Fälle mit dsp^3-Bahnhybridisation und D_{5d}-Symmetrie durch p-Elektronen der fünf Kohlenstoffatome gebildet. Demzufolge entstehen 10 Sandwich-Bindungen.

Durch die Bindungselektronen wird eine d-Bahn des Metallions bzw. Metallatoms besetzt. Somit stehen vier d-Bahnen der d^n-Elektronen der Metallionen zur Verfügung. Unter systematischer Benützung dieser Annahme wird das Versuchsmaterial kritisch besprochen. Aber erst durch die genaue Ausmessung der fehlenden Absorptionskurven, weiterhin durch Herstellung neuer Komplexe kann man die Arbeitshypothese eiwandfrei begründen. Diesbezügliche Versuche sind im Gange.

In normalen Fällen bei $d^1(1)$, $d^2(2)$, $d^3(3)$, $d^4(4)$, $d^5(3)$, $d^6(2)$, $d^7(1)$ Elektronen, mit den in Klammern gesetzten Zahlen, ist der Komplex paramagnetisch und bei d^8 Elektronen wird er diamagnetisch. Bei d^9 Elektronen kann keine Sandwichbindung vorliegen.

Wenn der Komplex nach der Ausbildung der Bindungsbahnen noch freie d-Elektronen besitzt, so werden die symmetrie- und spinverbotenen Banden von der Zahl der ungepaarten d-Elektronen abhängen.

Im Folgenden wird gezeigt, inwieweit mit der Arbeitshypothese die Lichtabsorption der Komplexe erklärt werden kann. Außerdem werden die Ursachen des anomalen Verhaltens angegeben. Die Richtigkeit dieses Verfahrens kann man nur mit Versuchsdaten entscheiden.

3. Besprechung der Versuchsdaten

Mit Hilfe der Resultate von quantenmechanischen Berechnungen werden die zur Verfügung stehenden Lösungsspektren kritisch besprochen. Beim Fehlen dieser Daten wird die theoretisch erwartete Lichtabsorption erwähnt.

Ti(IV) $(C_5H_5^-)_2$ Komplex besitzt kein d-Elektron, somit treten nur die Ligand- und Elektronenüberführungbanden auf.

Ti(III) $(C_5H_5^-)_2$ Komplex ist mit d^1-Elektron paramagnetisch [16a], somit wird das Auftreten der symmetrieverbotenen Banden erwartet.

Ti(XI) $(C_5H_5^-)_2$ Komplex [8] ist mit d^2-Elektronen diamagnetisch, welches Verhalten durch Spinpaarung verursacht wird. Demzufolge erwarten wir nur die Ligandabsorption.

Cr(XI) $(C_5H_5^-)_2$ Komplex besitzt d^4 Elektronen. Nach Berechnungen von JAFFE [17] soll das gemessene magnetische Moment des Komplexes unrichtig sein. Mit unserer Arbeitshypothese kann dieses Verhalten so erklärt werden, daß der Komplex wegen Spinpaarung nur d^2-Elektronen entsprechend paramagnetisch ist. Bei d^2 Elektronen wird das Auftreten der symmetrie- und spinverbotenen Banden erwartet.

Cr(CXI) $(C_5H_5^-)_2$ Komplex besitzt d^3 Elektronen und ist diesen entsprechend paramagnetisch. Somit wird das Auftreten der symmetrie- und spinverbotenen Banden erwartet.

Mn(XI) $(C_5H_5^-)_2$ Komplex [19] besitzt d^5 Elektronen und ist diesen entsprechend paramagnetisch, somit kann seine Bindung nur elektrovalent sein. Mit der Temperatur ändert sich sein paramagnetisches Moment [20]. Wegen der halbaufgefüllten d-Schale erwartet man die niedrigen spinverbotenen Banden, außerdem die Ligand- und Elektronenüberführungsbanden.

Fe(CXI) $(C_5H_5^-)_2$ Komplex ist mit d^5 Elektronen anomal (2,26 BM) paramagnetisch. Sein magnetisches Moment ändert sich mit der Temperatur [21]. In 1,0 mol. $HClO_4$-Lösung tritt eine niedrige bzw. eine hohe Bande bei 610 mμ ($\varepsilon = 360$) bzw. bei 235 mμ ($\varepsilon = 13\,300$) auf. Die niedrige bzw. hohe Bande kann eine symmetrieverbotene bzw. Elektronenüberführungsbande sein. Unserer Meinung nach hat man die Absorptionskurve nicht vollständig gemessen.

Fe(XI) $(C_5H_5^-)_2$ Komplex ist mit d^6 Elektronen diamagnetisch, welches Verhalten durch Spinpaarung verursacht werden kann. Normalerweise sollte der Komplex d^2 Elektronen entsprechend paramagnetisch sein. Nach unseren

Messungen [22] liegen die wichtigsten Banden bei 455 mμ und 323 mμ. Außerdem tritt eine Elektronenüberführungsbande bei 240 mμ auf.

Bei Polyferrocenen sind die Anregungsvorgänge die gleichen wie beim Ferrocen. Demzufolge liegen die Banden beinahe an gleicher Stelle wie beim Ferrocen, nur die Bandenintensitäten sind größer [23].

Os(XI) $(C_5H_5^-)_2$ und Ru(XI) $(C_5H_5^-)_2$ Komplexe [24] mit d^3 Elektronen sind diamagnetisch, somit erwarten wir die gleichen Anregungsvorgänge wie beim Ferrocen.

Co(XI) $(C_5H_5^-)_2$ mit d^7-Elektronenkonfiguration soll nach der Ausbildung der 10 Sandwichbindungen ein ungepaartes d-Elektron besitzen. Demzufolge erwartet man das Auftreten der symmetriverbotenen Banden.

Ni(XI) $(C_5H_5^-)_2$ Komplex mit d^8 Elektronen soll nach der Ausbildung der 10 Sandwichbindungen diamagnetisch sein. Demgegenüber ist er zwei ungepaarten d-Elektronen entsprechend paramagnetisch [23]. Somit liegt eine elektrovalente Bindung vor. Beim Grundterm ^3F erwartet man die symmetrie- und spinverbotenen Banden.

3.1. Lichtabsorption der Cyclopentadienyl-Derivate

$C_6H_6 \cdot$ Ti(I) $(C_5H_5^-)$ Komplex besitzt kein Symmetriezentrum [25, 26]. Nach der Ausbildung der Sandwichbahnen ist der Komplex mit d^3-Elektronenkonfiguration paramagnetisch. Somit erwartet man das Auftreten der symmetrie- und spinverbotenen Banden.

C_6H_6Mn(I) $(C_5H_5^-)$ Komplex mit d^6-Elektronenkonfiguration besitzt kein Symmetriezentrum. Nach der Ausbildung der Sandwichbahnen ist der Komplex diamagnetisch. Demzufoge treten nur die Ligandbanden auf.

C_9H_{11}Fe(XI) $(C_5H_5^-)$ Komplex mit d^6-Elektronenkonfiguration besitzt kein Symmetriezentrum und der Benzolring ist hydratisiert. So werden die Cyclopentadienyl-Ringe an das Fe(XI)—Ion mit dsp^3 Bahnhybridisation gebunden. In seinem Elektronenanregungsspektrum liegt eine symmetrieverbotene Bande bei 510 mμ ($\varepsilon = 269$) [27]. Die übrigen Banden hat man nicht gemessen.

$C_5H_5^-$Fe(XI)C_5NH_5 Komplex besitzt d^6-Elektronenkonfiguration. In dem Komplex wird ein $C_5H_5^-$ Anion durch ein Pyrrolmolekül ersetzt. Mit 10 Sandwichbindungen werden die zwei Liganden festgehalten. Man hat sein Infrarot- und magnetisches Resonanzspektrum gemessen [28]. Im Elektronenanregungsspektrum liegen zwei Banden bei 442 mμ ($\varepsilon = 102$) und bei 330 mμ ($\varepsilon = 175$).

$C_5H_5^-$Mn(XI) $(CO)_2$ Komplex mit d^5 Elektronen besitzt die folgende Bindungsart: $C_5H_5^-$ wird mit fünf Sandwichbindungen und CO mit kovalenter Bindung festgehalten. Nach der Ausbildung der Bindungsbahnen besitzt der Komplex noch ungepaarte d-Elektronen. Demzufolge erwartet man das Auftreten der symmetrieverbotenen Banden.

ZUSAMMENFASSUNG

Es wurde die Lichtabsorption der Cyclopentadienyl-Komplexe unter Berüchsichtigung der ungepaarten *d*-Elektronen des Metallions bzw. Atoms mit einer neuen Arbeitshypothese kritisch besprochen. Dabei wurde die durch ein starkes Ligandfeld verursachte Spinpaarung und das anomale magnetische Verhalten der Komplexe berücksichtigt. Auf dieser Grundlage wurde die erwartete Zahl der Symmetrie- und spinverbotenen Banden vorausgesagt. Wegen des Fehlens von zuverlässigen Versuchsdaten konnte die Arbeitshypothese nicht in allen Fällen einwandfrei bekräftigt werden. Zur weiteren Begründung der Arbeitshypothese sind experimentelle Untersuchungen und quantenmechanische Berechnungen geplant.

LITERATUR

1. RUCH, E. O.: Rec. Trav. Chim. Pays-Bas **75**, 638 (1950).
2. RUCH, E. O., FISCHER, E. O.: Z. Naturforsch. **7B**, 1 (1953).
3. FISCHER, E. O.: Z. Naturforsch. **7B**, 1 (1953).
4. SCHOTT, D. B., BECKER, R. S.: J. Chem. Phys. **35**, 516 (1961).
5. KEALEY, T. S., PAUSON, P. R.: Nature **168**, 1039 (1951).
6. ORGEL, L. E.: Ligand Field Theorie (1961).
7. ORGEL, L. E.: Z. Naturforsch. **171**, 121 (1953).
8. LIEHR, A. D., BALLHAUSEN, C. J.: Acta Chem. Scand. **11**, 207 (1957).
9. MOFITT, W.: J. Am. Chem. Soc. **76**, 3386 (1954).
10. COTTON, F. A., WILLKINSON, G.: Z. Naturforsch. **9B**, 453 (1963).
11. YAMASAKY, J. J.: Chem. Phys. **24**, 1260 (1956).
12. BALLHAUSEN, C. J., DAHL, J.: Acta Chem. Scand. **15**, 1333 (1961).
13. WOODWARD, R. B., ROSENBLUM, M., WITTIG, M. C.: J. Am. Chem. Soc. **74**, 3458 (1952).
14. DUNITZ, F. D., ORGEL, L. E.: J. Chem. Phys. **23**, 954 (1955).
15. DUNITZ, J. D., ORGEL, L. E.: Z. Naturforsch. **171**, 121 (1953).
16. WILLKINSON, G., PAUSON, P. L., BIRMINGHAM, J. M., COTTON, F. A.: J. Am. Chem. Soc. **75**, 1011 (1953).

16a. MOFITT, W.: J. Am. Chem. Soc. **76**, 156 (1954).

17. JAFFE, H. G.: J. Chem. Phys. **21**, 156 (1953).
18. KEALEY, V. J., PAUSON, P. L.: Nature **168**, 103 (1954).
19. WILLKINSON, G., COTTON, F. A., BIRMINGHAM, J. M.: Inorg. Nucl. Chem. **2**, 95 (1956).
20. WILLKINSON, G., ROSENBLUM, M., WITTIG, M. C., WOODWARD, R. B.: J. Am. Chem. Soc. **74**, 2125 (1956).
21. FISCHER, E. O., LEIPFINGER, H.: Z. Naturforsch. **9B** (1955).
22. KISS, Á.: Lichtabsorption des Ferrocens. Nicht publizierte Daten.
23. WATANABE, H., MATOYAMA, I., HATA, H.: Bull. Chem. Soc. Japan **34**, 780 (1966).

23a. PFAB, W., FISCHER, E. O.: Z. anorg. Allg. Chem. **274**, 316 (1963).

24. MARCK, V., RUCH, M. D.: Inorg. Chem. **3**, 116 (1963).
25. KIMBALL, G. E.: J. Chem. Phys. **8**, 188 (1940).
26. SANDELL, V., CLOSSON, R. D.: J. Am. Chem. Soc. **74**, 5826 (1957).
27. KING, R. D., BISNETH, M. B.: Inorg. Chem. **3**, 796 (1964).
28. KING, R. D., BISNETH, M. B.: Inorg. Chem. **3**, 790 (1964).
29. FISCHER, E. O.: J. Inorg. Nucl. Chem. **8**, 268 (1958).
30. ORGEL, L. E.: J. Inorg. Nucl. Chem. **8**, 315 (1956).

Árpád KISS; Szeged, III., Menhely u. 7.

Acta Chimica Academiae Scientiarum Hungaricae Tomus 56 (3), pp. 221—227 (1968)

BEITRÄGE ZUR QUANTITATIVEN DIFFERENTIALTHERMOANALYSE

UNTERSUCHUNG DES ZUSAMMENHANGES ZWISCHEN DER SPITZENFLÄCHE UND DER PROBEMENGE UNTER DEN VERSUCHSBEDINGUNGEN DER DERIVATOGRAPHISCHEN MESSUNG

A. Rokosz,* J. Paulik,** F. Paulik** und L. Erdey**

(Universytet Jagiellonska Katedra Chemii Nieorg., Kraków. ** Institut für Allgemeine und Analytische Chemie der Technischen Universität, Budapest)*

Eingegangen am 15. September 1967

Das Problem der quantitativen Auswertung der Spitzenfläche der differential-thermoanalytischen Kurve ist so alt wie die DTA-Methode selbst. Die anfangs auf grober Schätzung beruhende Auswertung verwandelte sich mit der Entwicklung der Meßverfahren in eine immer verläßlichere Ergebmisse liefernde Methode. Trotz dieses Fortschritts betrug ihre Genauigkeit bis zu den letzten Jahren nicht mehr als $\pm 5-10\%$.

Das Problem der quantitativen Auswertung kann in zwei Formen erscheinen. Es kann gefragt werden, wieviel von einer Komponente in der aus einem Gemenge bestehenden Probe in Prozenten enthalten ist, oder wieviel Wärme bei einer Umwandlung frei wird bzw. verschwindet.

Wird die Menge einer Komponente gesucht, so reicht die Genauigkeit von $\pm 5-10\%$ meistens aus, wenn auch nicht behauptet werden kann, sie sei befriedigend. Ein solches Problem läßt sich mit Hilfe der klassischen DTA-Geräte im allgemeinen lösen, wenn auch der Zusammenhang zwischen der Fläche unter der DTA-Kurve und der Menge der Analysensubstanz kein linearer ist [1]. Die in verschiedenen Höhen liegenden Schichten der Probe üben nämlich keine einheitliche Wirkung auf das Thermoelement aus. Dieser Umstand erschwert in entscheidendem Maße die weitere Erhöhung der Genauigkeit der klassischen differential-thermoanalytischen Einrichtungen.

Die Entwicklung der Methode der dynamischen Differentialkalorimetrie (DDK) [2] brachte einen wesentlichen Fortschritt auf dem Gebiete der quantitativen Differentialthermoanalyse. Sie machte die genauere Bestimmung der freigesetzten Wärmemenge möglich, und ist somit auch zur Beantwortung der zweiten Frage geeignet.

Der Unterschied zwischen der DDK- und der klassischen DTA-Methode besteht im folgenden: Bei der DTA-Methode steht das Thermoelement mit der Analysensubstanz in Berührung, so daß die Temperatur des Thermoelements nur durch die in der Nähe der Lötstelle befindliche Substanz unmittelbar beeinflußt wird. Bei der dynamischen Differentialkalorimetrie hingegen über-

nimmt die Wärmeeffekte der Substanz ein gut leitender Metalltiegel, dessen Temperatur mit dem Thermoelement gemessen wird.

Bei den dynamischen differential-kalorimetrischen Messungen stellt das aus Probe und Probebehälter bestehende System von thermischem Gesichtspunkte eine Einheit, deren durch Erhitzung oder Kühlung hervorgerufene gleichmäßige Temperaturänderung durch die in der Probe auftretenden Wärmeeffekte modifiziert wird. Die Größe dieses Einflusses ist der frei werdenden oder aufgenommenen Wärmemenge proportional, was so viel bedeutet, daß zwischen der Menge der Probe und der Größe der Fläche unter der DDK-Kurve im allgemeinen ein linearer Zusammenhang besteht.

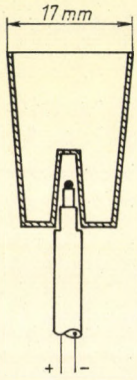

Abb. 1. Querschnitt des derivatographischen Probebehälter-Tiegels

Unsere Versuche bezweckten die Feststellung dessen, wie sich dieser Zusammenhang unter den Versuchsbedingungen der derivatographischen Messung gestaltet.

Versuchsbedingungen

1. Analysensubstanz

Die Analysensubstanz war Kaliumnitrat, das bei 129 °C einer polymorphen Umwandlung unterliegt und bei 334 °C schmilzt. Beide Vorgänge können im DTA-Verfahren in Form von endothermen Spitzen registriert werden. Diese beiden Vorgänge wurden untersucht. Das analysenreine Präparat wurde aus Wasser umkristallisiert und im Vakuum bei 100 °C getrocknet, dann im Achatmörser gepulvert und in Fraktionen von 0,5—0,3, 0,3—0,25, 0,25—0,1 und < 0,1 mm Korngröße zerlegt. Als Interstoff diente ausgeglühtes Aluminiumoxyd.

2. Gerät

Die Einrichtung bestand aus einem Röhrenofen, dessen Heizung mit einem Toroidtransformator geregelt werden konnte. Zwei in jeder Hinsicht gleiche Öfen wurden benutzt (mit 1 und 2 bezeichnet). Probe und Interstoff wurden im Ofen so untergebracht, wie es beim Derivatographen üblich ist [3]. Jeder Versuch wurde im gleichen Platintiegel ausgeführt. Der Querschnitt des derivatographischen Tiegels ist in Abb. 1 gezeigt. Wie man sieht, ist im Tiegelboden eine röhrenförmige Einbuchtung zu finden, in welche die Lötstelle des Thermoelements hineinreicht. Es wurde dafür gesorgt, daß bei den Messungen alle Versuchsbedingungen konstant blieben.

3. Auswertung der Thermogramme

Die Größe der Fläche unter der Spitze wurde mit Hilfe eines Planimeters bestimmt. Jedes Endresultat ist der Mittelwert von drei parallelen Messungen. Fünfmal wurde die zu messende Fläche bei der Bestimmung mit dem Planimeter umkreist. Bei der DTA-Spitze der polymorphen Umwandlung bereitete die Eintragung der Grundlinie keine Schwierigkeit, da keine Grundlinienverschiebung auftritt. Beim Schmelzen hingegen trat infolge der wesentlichen Veränderung der thermischen Eigenschaften der Substanz eine erhebliche Verschiebung der Grundlinie auf. In diesem Falle wurde von dem den Anfang des Schmelzens anzeigenden eindeutigen Knickpunkt zum Ende der Spitze eine Tangente gezogen (Abb. 2, 3).

4. Aufheizgeschwindigkeit

Die Aufheizgeschwindigkeit betrug bei jedem Versuch 7 °C/Min.

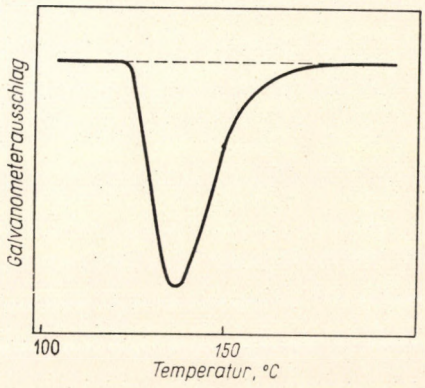

Abb. 2. DTA-Kurve der polymorphen Umwandlung von Kaliumnitrat

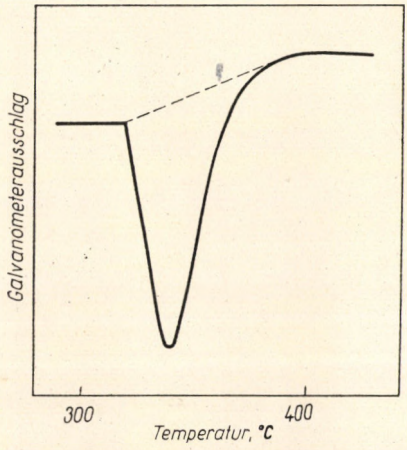

Abb. 3. DTA-Kurve des Schmelzvorganges von Kaliumnitrat

5. Einfluß der Korngröße

Es wurde der Einfluß der Korngröße auf die Größe der Spitzenfläche untersucht. Die Ergebnisse sind in Tab. I zusammengestellt. Wie zu sehen ist, war die Korngröße praktisch ohne Einfluß auf die Spitzenfläche.

Tabelle I

Flächengröße (mm^2) in Abhängigkeit von der Korngröße

Einwaage: 0,9970 g

Korngröße Ø mm	Polymorphe Umwandlung			Schmelzvorgang		
	Ofen 1	Ofen 2	Mittelwert	Ofen 1	Ofen 2	Mittelwert
0,5—0,3	752,0	746,6	749,3	894,	891,4	893,0
0,3—0,25	764,6	747,2	755,9	910,6	884,6	897,6
0,25—0,1	764,6	758,0	761,0	893,2	868,6	880,9
< 0,1	737,4	746,6	742,0	862,6	884,6	873,6

6. Einfluß der Probemenge auf die Größe der Spitzenfläche

Das Gewicht des bei den Versuchen angewandten Platintiegels betrug 8,1 g. Die Menge des Interstoffes betrug bei jedem Versuch 1,62 g.* Die Menge der Analysensubstanz bewegte sich zwischen 0,2 und 3,2 g. Die Daten der Tabelle II. sind in Abb. 4 und 5 gezeigt.

Tabelle II

Flächengröße (mm^2) als Funktion der Menge der Probe (KNO_3). *Korngröße:* 0,25—0,1 *mm*

Einwaage, g	Polymorphe Umwandlung			Schmelzvorgang		
	Ofen 1	Ofen 2	Mittelwert	Ofen 1	Ofen 2	Mittelwert
0,2	143	141	142	212	199	205
0,4	280	293	286	402	403	402
0,8	619	603	611	771	747	759
1,2	893	854	873	1038	1036	1037
1,4	1052	1072	1062	1148	1169	1158
1,6	1251, 1217	1273, 1252 1231	1245	1386, 1283	1383, 1325 1308	1337
1,7	1278, 1297 1351	1309, 1263	1300	1355, 1367 1386	1387, 1347	1368
1,75	1372	1331	1351	1406	1410	1408
1,8	1401, 1381	1382, 1365	1382	1526, 1438	1496, 1449	1477
1,9	1498, 1484	1403, 1521	1476	1555, 1491	1509, 1503	1515
2,0	1575, 1568	1535, 1540	1554	1563, 1558	1521, 1560	1550
2,1	1676, 1638	1691, 1587	1648	1625, 1581	1593	1600
2,3	1798	1741	1769	1715	1739	1727
2,6	2009	1926	1967	1932	1920	1926
2,9	2209	2203	2206	2135	2171	2153
3,0	2392, 2301 2298	2359, 2344	2348	2300, 2078 2103	2312, 2228	2204
3,2	2509	2472	2490	2324	2374	2349

* Bei quantitativen DTA-Untersuchungen sollten die Wärmekapazität und Wärmeleitfähigkeit sowie die Größe der den Musterträger berührenden, die Wärme zuführenden Oberfläche des Inertstoffes mit der Probe übereinstimmen. Das genaue Abstimmen dieser Faktoren stößt aber auf unüberwindliche Schwierigkeiten. Ist aber die Wärmesymmetrie nicht gesichert, so wird sich die Grundlinie der DTA-Kurve verschieben und sich außerdem die Größe der Spitzenoberflächen auf unkontrollierbare Weise ändern [4]. Demzufolge geht man in der Praxis meistens so vor, daß man die Menge und somit die Wärmekapazität des Inertstoffes so lange ändert, bis sich die Grundlinie der DTA-Kurve nicht mehr verschiebt. Man kann jedoch unter Umständen auch so verfahren — wie z. B. im vorliegenden Falle —, daß die Menge des Inertstoffes sowohl bei der Kalibration als auch bei der Untersuchung des unbekannten Materials unverändert gelassen wird. Verfährt man auf diese Weise, so bleiben die aus der Wärmeassymmetrie stammenden Fehler der Kalibration und der Untersuchung gleich. Dementsprechend wird nicht nur das Verfahren einfacher, sondern es lassen sich auch die Fehler beseitigen.

Nach Tab. II und Abb. 4 besteht zwischen der Menge der Probe und der Größe der DTA-Spitzenfläche im Falle der Umwandlung von Kaliumnitrat ein streng linearer Zusammenhang. Beim Schmelzen des Kaliumnitrats wurden hingegen etwas abweichende Ergebnisse erhalten (Abb. 5), die sich in Kenntnis der Form des Tiegels (Abb. 1) deuten lassen.

Abb. 5 zeigt, daß die spezifische Zunahme der Größe der Spitzenfläche bei kleinen Einwaagen größer, bei mittleren Einwaagen hingegen kleiner war als bei der Prüfung von großer Einwaagen. Zur Deutung dieser merkwürdigen Erscheinung wurde die Kurve auf drei Abschnitte aufgeteilt. Als Punkt *A* wurde jene Stelle betrachtet, wo die Einwaage den Tiegel zu Beginn des Ver-

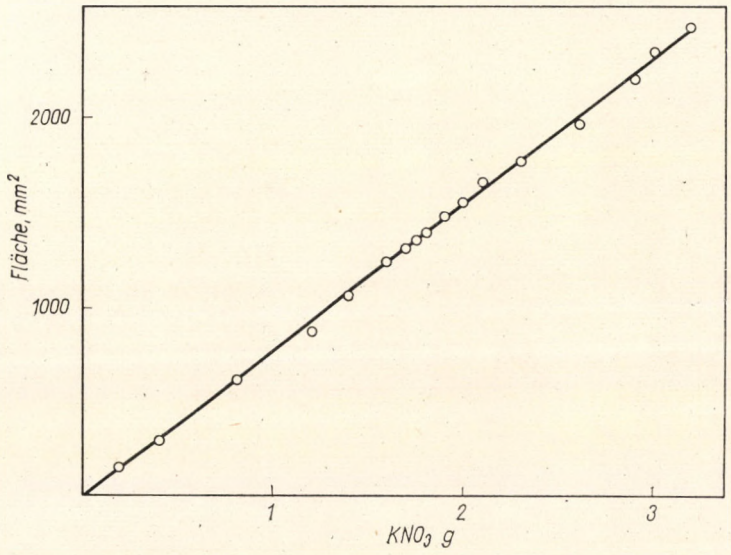

Abb. 4. Spitzenflächengröße der DTA-Kurve der polymorphen Umwandung von Kaliumnitrat in Abhängigkeit von der Probemenge

suchs so ausfüllte, daß die Einbuchtung des Tiegelbodens durch die Analysensubstanz eben noch überdeckt war.

Beim Umwandlungspunkt ändert sich das Probevolumen nicht, nimmt jedoch beim Schmelzen erheblich ab. Der Punkt *B* wurde so gewählt, daß nach dem Schmelzen die Höhe der Schmelze gerademit der Höhe der Einbuchtung übereinstimmte.

Die auf diese Weise erhaltenen drei Kurvenabschnitte wurden separat analysiert, und es wurde gefunden, daß die Meßpunkte mit befriedigender Genauigkeit auch mit Geraden verbunden werden können (gestrichelte Linie in der Abbildung), was so viel bedeutet, daß innerhalb eines Abschnittes ein linearer Zusammenhang zwischen der Probemenge und der Größe der Spitzen-

fläche besteht. Die Meßpunkte zeigen in der mittleren Strecke die größte Abweichung von der der gestrichelt gezogenen Linien.

Aus diesen Beobachtungen wurde gefolgert, daß das sonderbare Verhalten mit der Form des Tiegels und dem Schmelzvorgang verbunden ist. Wäre die Erscheinung nur durch die Tiegelform bedingt, so hätte bei der Umwandlung des Kaliumnitrats bei Einwaagen um 1,2 g auch in Abb. 4 ein Knickpunkt erscheinen müssen.

Man darf auf Grund der Versuche feststellen, daß der quantitativen DTA-Untersuchung solcher Vorgänge, bei denen der Aggregatzustand der Probe unverändert bleibt, Einwaagen von beliebigen Größen gestattet sind. Ist jedoch die Größe der Schmelzwärme zu bestimmen, so ist von den erwähnten

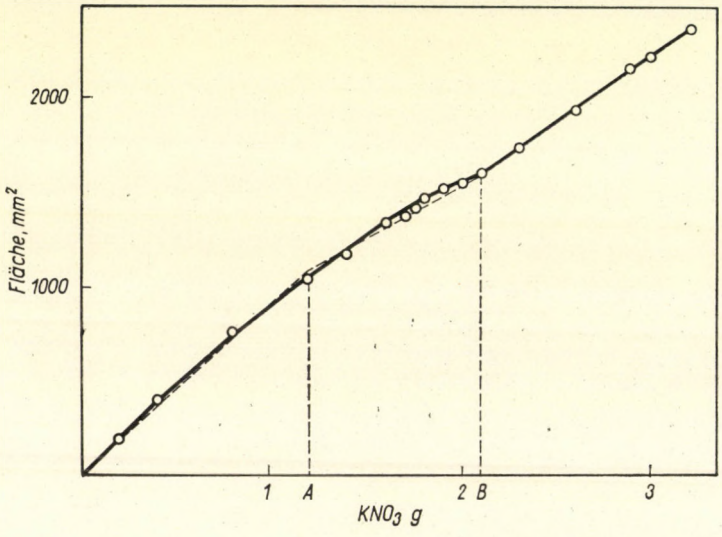

Abb. 5. Spitzenflächengröße der DTA-Schmelzkurve in Abhängigkeit von der Probemenge

drei Abschnitten der Kurve die erste oder die dritte zu wählen, innerhalb dieser die Kalibration auszuführen und dann eine solche Einwaage zu nehmen, deren Größe nicht nahe der Grenze des ausgesuchten Gebietes liegt.

ZUSAMMENFASSUNG

Es wurde untersucht, welcher Zusammenhang zwischen der Menge der Einwaage und der DTA-Spitzenfläche unter derivatographischen Versuchsbedingungen besteht. Es wurden jene Umstände bestimmt, bei denen eine quantitative Untersuchung ausgeführt werden kann.

LITERATUR

1. De Jong, J.: Am. Ceram. Soc. **40,** 42 (1957).
2. Schwiete, H. E., Ziegler, G.: Ber. Deutschen Keram. Gesellsch. **35,** 193 (1958).
3. Paulik, F., Paulik, J., Erdey, L.: Z. anal. Chem. **160,** 241 (1958).
4. Barrall, E. M., Rogerns, L. B.: Anal. Chem. **34,** 1101 (1962).

Andrej Rokosz Kraków, Polen
Jenő Paulik, Ferenc Paulik, László Erdey Budapest XI., Gellért tér 4.

Acta Chimica Academiae Scientiarum Hungaricae Tomus 56 (3), pp. 229—250 (1968)

ULTRAVIOLET SPECTROSCOPIC STUDY OF THE ACID-BASE EQUILIBRIA OF PYRIMIDINE DERIVATIVES, I

URACIL DERIVATIVES

A. TÓTH and F. BILLES

(Department of Physical Chemistry, Polytechnical University, Budapest)

Received March 5, 1967

1. Introduction

The acid-base equilibrium of a number of pyrimidine derivatives have been investigated by various authors by measuring the pH dependence of the ultraviolet absorption spectra. For the derivatives to be treated in the present paper, these measurements were either incomplete or entirely lacking. In the first case the authors generally omitted to offer an interpretation of the observed substituent effects.

Besides reporting the pH-dependence of the spectra and the equilibrium constants, we wish to present here also the structures of the forms in equilibrium and to point out the causes producing the changes in the equilibrium constants and the spectra.

For the sake of a more convenient treatment the conception of the protonization state has been introduced. The protonization state (P) of the "basic" or "acidic" form of a compound is given by the number of protons taken up or given off compared to the neutral (non-ionic) form. Thus, for basic forms P is greater and for acidic forms it is less than zero. In the following, the equilibrium will be characterized by the protonization state of that of the two forms in equilibrium for which the absolute value of P is higher. It may occur that the electron distributions of two or several forms with identical P values differ to such an extent that the pertaining equilibria can be distinguished on the basis of the UV spectra. These forms and the corresponding equilibria are denoted by capital letters after the protonated state.

For all equilibria the negative logarithm of the acidic dissociation constant will be given (pK_a). The value of pK_a is always characteristic of the proton affinity of the form in the lower protonization state. The lower the value of pK_a, the more the equilibrium is shifted to the lower protonated state, *i.e.* the lower is the value of proton affinity. This proton affinity is, of course, a function of the electron distribution in the ring. This latter affects the electron spectrum, thus there will be a close correlation between the substituent effect manifest in the values of the equilibrium constants, and in the values of spectral maxima.

The equilibrium constant was not determined for cases in which the equilibrium was markedly shifted toward the state of lower (P) value, as this would have required special methods [1].

The investigations started with pyridine, followed by an examination of uracil. In the other compounds the substituent effect was compared with the case of uracil. This was necessitated by the fact that several forms of uracil (and of its derivatives) are cyclic amides while no such form occurs in the case of pyridine. On the other hand, the forms of uracil and of its derivatives with the highest negative P values contain a pyridine ring, thus also the spectrum of pyridine had to be investigated.

A UNICAM Type SP 500 spectrophotometer was used for the measurements. The media of various pH values were prepared with Robinson's buffer.

2. Pyrimidine

Spectrum. Two bands appear in the UV spectrum of the aqueous solution of pyrimidine, the more intense at 242 nm, the less intense at 274 nm.

The band at 274 nm completely disappears at sufficiently low pH

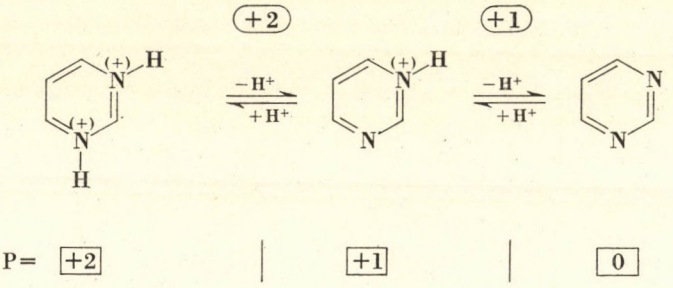

Fig. 1. Acid-base equilibria of pyrimidine

values (Table I), and it is shifted in non-polar solvents to longer wavelengths (to 298 nm in cyclohexane [3]), indicating that the band can be assigned to the excitation of the non-bonding electrons of nitrogen to unoccupied π orbitals of the ring [2]. This $n \rightarrow \pi^*$ transition is hindered by proton uptake which binds the unshared electron pair, and thus reduces the energy of the ground state, with a consequent increase of the energy of the transition process. In polar solvents hydrogen bonds are formed which also engage part of the non-bonding electrons, thereby again reducing the energy of the ground state, *i.e.* raising the energy of the transition process. In this latter case the shift toward shorter wavelengths of the band is slight, but in the first case it may reach an extent when the band is shifted into the vacuum-UV region.

Table I

Influence of the pH on the UV spectrum of pyrimidine
(λ values in nm)

Present work			Literature values [2, 3]	
pH of medium	Band λ_{max} (lg ε)	Shoulder λ(lg ε)	pH of medium	λ_{max} (lg ε)
1.45				242 (3.60)
1.98	242 (3.57)	275 (2.40)	H_2O	244 (3.50)
3.50				272 (2.46)
				274 (3.60)
H_2O	242 (3.47)			
	274 (2.53)			
7.45				
10.00	242 (3.40)			
11.20	272 (2.55)			
12.50				

The position of the 242 nm band is not sensitive to pH changes, though its intensity increases at lower pH values (Table I). This band corresponds to a $\pi \rightarrow \pi^*$ transition (E band).

Substituent effect. In case of an $n \rightarrow \pi^*$ transition, the position of the maximum is shifted to longer or shorter wavelengths depending on whether the substituent decreases or increases the electron density on the nitrogen atoms of the ring [3].

Most substituents cause a reduction of the $\pi \rightarrow \pi^*$ transition energy. The position and intensity of the maximum are characteristic of the substituent [4].

For monosubstituted pyrimidines the conditions are fairly simple; in polysubstituted pyrimidines the effects are superimposed. The effects are in good approximation additive, provided there is no conjugation between the substituent and the ring; in the case of conjugation, additivity is only a rough approximation. Nevertheless, it may serve to distinguish isomers, since the substituent effects of the spectrum greatly depend on the position of the substituent.

Equilibria. The acid-base equilibria of pyrimidine are shown in Fig. 1. As the proton affinity of the +1 protonated form is very low, it was not possible to determine the +2 equilibrium constant.

The measured and literature values of the equilibrium constants are summed up in Table VII. A comparison of the pK_a value of the +1 equilibrium with the corresponding pK_a value of pyridine (Table VII) shows a considerably

lower proton affinity for the $P = 0$ form of pyrimidine than for pyridine. This may be ascribed to the strong $-M$ effect of the second nitrogen, which greatly reduces electron density on the nitrogens of pyrimidine.

3. Uracil

Spectrum. There are two pH-dependent bands in the UV spectrum of uracil (Table II). Both in acid and neutral media an intense band appears at 259 nm. With increasing pH the intensity of this band decreases, and its position is somewhat shifted to longer wavelengths; finally the band merges with the other band and completely disappears in strongly alkaline media. The second band appears in strongly alkaline media at 284 nm, and as the pH is decreased it merges with the 259 nm band, and completely disappears in neutral medium.

Table II

Influence of the pH on the UV spectrum of uracil
(λ values in nm)

Present work			Literature values [5, 6]	
pH of medium	Band λ_{max} (lg ε)	Shoulder λ (lg ε)	pH of medium	λ_{max} (lg ε)
3*N* HCl			1*N* HCl	
2.20			3.00	259 (3.92)
3.50			H_2O	
4.80	259 (3.92)		7.00	258 (3.93)
6.00			11.00	282 (3.81)
H_2O				
7.15				
7.85	259 (3.90)	2.77 (3.50)		
8.40				
9.00	259 (3.82)	2.79 (3.52)		
9.50	264 (3.74)	282 (3.56)		
11.20				
12.06	283 (3.76)			
12.60				
2*N* NaOH	284 (3.89)			

In weakly acid and neutral media uracil is present as a cyclic amide or cyclic amide ion (Fig. 2). This is indicated by the *K*-band at 259 nm ($\pi \rightarrow \pi^*$ transition). Shifting of the latter to longer wavelengths indicates that, in the

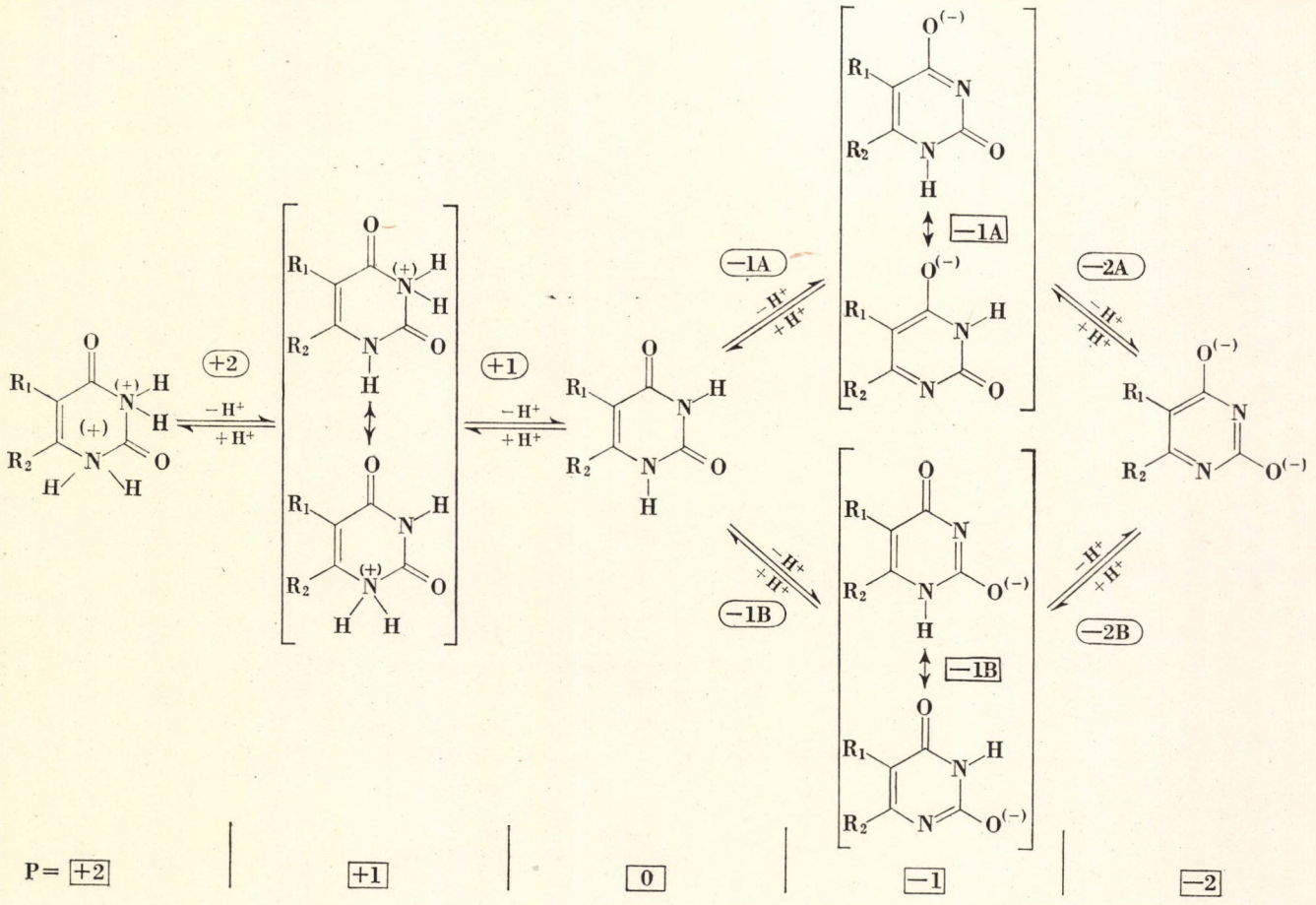

Fig. 2. Acid-base equilibria of uracil and of some uracil derivatives

	R_1	R_2
Uracil	H	H
5-Methyluracil	CH_3	H
6-Methyluracil	H	CH_3
5-Nitrouracil	NO_2	H

case of uracil, the transition energy is somewhat reduced with decreasing P values. This corresponds to the observation with pyrimidine, namely that substitution reduces the energy of the $\pi \rightarrow \pi^*$ transition.

The $P = 2$ protonated form gradually appears in strongly alkaline media as indicated by the 284 nm band of a $n \rightarrow \pi^*$ transition. There is a 10-nm wavelength shift as compared with the $n \rightarrow \pi^*$ band of pyrimidine, which

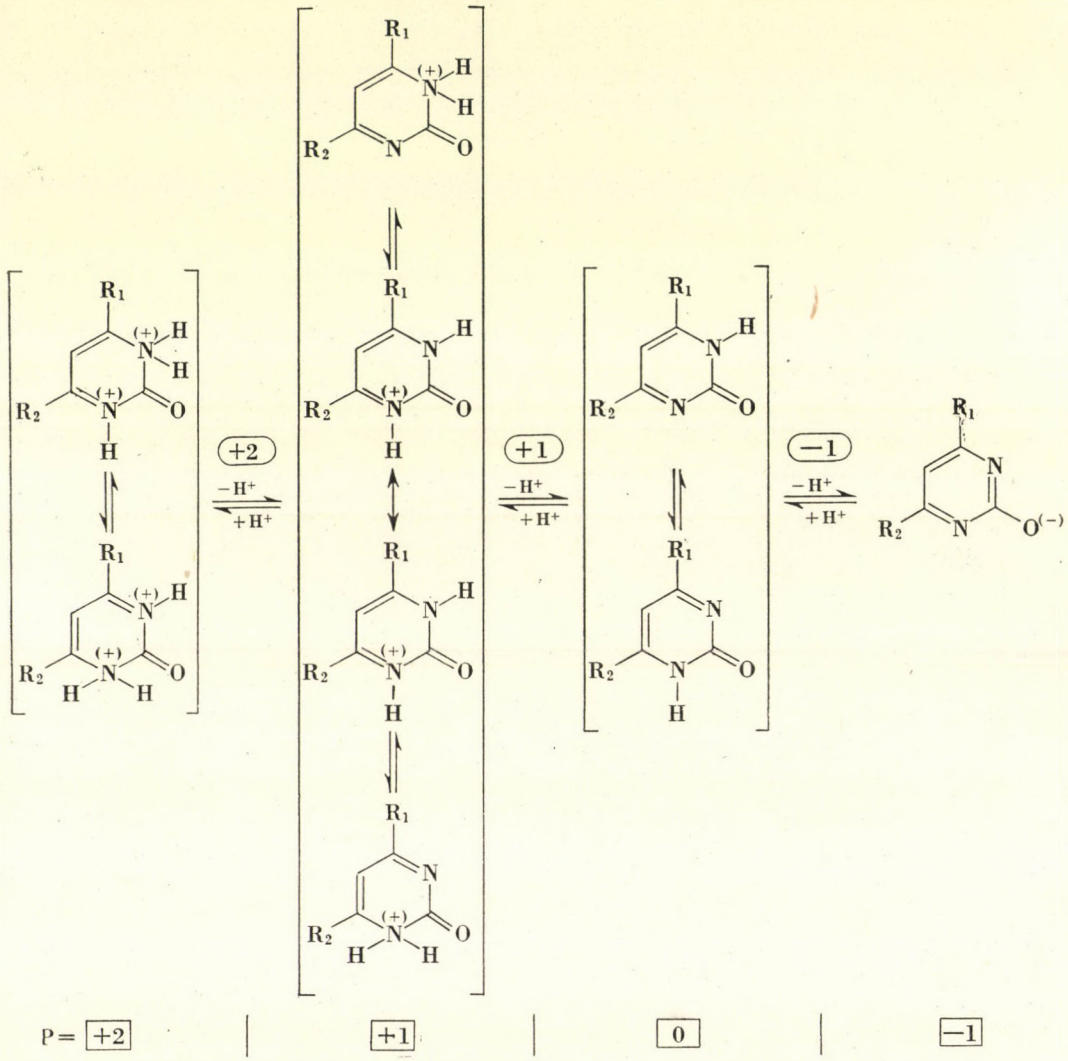

Fig. 3. Acid-base equilibria of 2-hydroxypyrimidine and of some

2-hydroxypyrimidine derivatives	R_1	R_2
2-Hydroxypyrimidine	H	H
2-Hydroxy-4-methylpyrimidine	CH_3	H
2-Hydroxy-6-methylpyrimidine	H	CH_3

can be ascribed to the extremely strong $+I$ and $+M$ effects of the O^- substituents that give rise to an increase of the electron density on positions 1 and 3 of the ring.

Equilibria. The pK_a values of the $+1$ and $+2$ equilibrium are extremely low, and thus escaped measurement. As it may be seen from Table VII, only the value of pK_a of the $+1$ equilibrium has been reported in the literature, and this is considerably lower than that of pyrimidine because of the electron-withdrawing effect ($-I$, $-M$) of the carbonyl groups leading to an increased electron density on the nitrogens and a corresponding decrease of proton affinity.

From the spectrum pK_a values pertaining to two -1 equilibria were obtained.

It can be seen in Fig. 2 that the —NH group is in position 3 in one tautomeric form. In position 2 the electron-donor effects of the —NH and —N= groups jointly assert themselves, while in position 4 only the effect of the —NH group prevails, and consequently the electron distribution is nearer to the upper mesomeric structure.

In the other tautomeric form, in position 2 again the electron-donor effects of the —NH and —N= groups, while in positions 4 the effect of the —N= group are asserted. Since the effect of —N= is considerably stronger than that of an —NH group, a shift similar to the one observed above in the direction of one of the mesomeric forms cannot be ascertained. In order to find the assignation of the acidic equilibria $-1A$ and $-1B$ (Fig. 2), the acid-base equilibria of 2-hydroxypyrimidine (Fig. 3) and of 4-hydroxypyrimidine (Fig. 4) have also been investigated. As the pK_a value is lower in the latter case, in accordance with the above theoretical considerations, the lower pK_a value belongs to the equilibrium $-1A$ (Table VII). It can be further established that the electron distribution in form $-1B$ is nearer to the upper mesomeric structure. It was not possible to separate the equilibria $-2A$ and $-2B$, as a single pK_a value was obtained (Table VII).

4. 5-Methyluracil

Spectrum. The $+I$ effect of the 5-methyl group appears primarily in positions 4 and 6 and less markedly in positions 2. In the protonization states -1, 0, $+1$ and $+2$ (Fig. 2) the electronic ground states are more polar than the corresponding ground states of uracil, thus, compared to uracil, the *K*-bands in the 5-methyl derivative will be shifted to longer wavelengths.

The energy of the $n \rightarrow \pi^*$ transition pertaining to the protonated state -2 must also decrease because of the reduced possibility of proton uptake

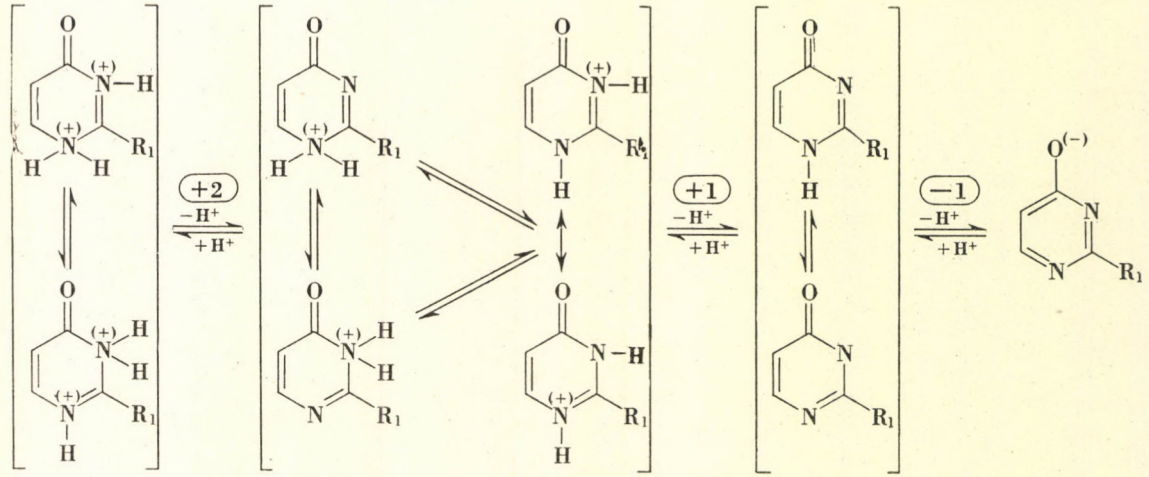

Fig. 4. Acid-base equilibria of 4-hydroxypyrimidine and of its 2-methyl derivative

	R_1
4-Hydroxypyrimidine	H
4-Hydroxy-2-methylpyrimidine	CH_3

under the $+I$ effect of the methyl group (the nitrogen-containing part of the ring will be more negative).

Band shifts of a direction corresponding to the above considerations have been found in the spectrum of 5-methyluracil as compared to the spectrum of uracil. The position of the K-band was at 264 nm (5-nm shift to longer wavelengths), while in weakly alkaline media the band was shifted to the region of shorter wavelengths. The $n \rightarrow \pi^*$ band at 290 nm was shifted by 6 nm to longer wavelengths (Table III).

Table III

Influence of the pH on the UV spectrum of 5-methyluracil
(λ values in nm)

Present work		Literature values [8]	
pH of medium	Band λ_{max} (lg ε)	pH of medium	λ_{max} (lg ε)
3*N* HCl	262 (3.88)	4.40	
1.90		H_2O	264 (3.90)
3.10		7.20	
4.50	264 (3.89)	10.00	267 (3.78)
6.90		11.00	290 (3.71)
H_2O		12.00	291 (3.74)
8.00		13.00	
8.90	266 (3.86)		
9.60	272 (3.82)		
10.70	274 (3.72)		
11.50	290 (3.70)		
12.00	290 (3.72)		
2*N* NaOH	290 (3.96)		

Equilibria. The $+I$ effect of the 5-methyl group enhances electron density more markedly in position 4 than in position 2. Therefore, the electron distributions in forms $-1A$ and $-1B$ (Fig. 2) are much more similar than in the case of uracil; this hindered the separation of the equilibria $-1A$ and $-1B$ (Table VII). Increase in the electron density in positions 2 and 4 hinders the formation of the anionic forms, resulting in higher acidic pK_a values than the corresponding values of uracil. In agreement with the above, proton affinity should decrease in the protonization states $+1$ and 0, leading to smaller basic pK_a values.

5. 5-Aminouracil

Spectrum. The $+M > -I$ effect of the 5-amino group asserts itself primarily in positions 4 and 6, and less markedly in position 2. As the electron-donor effect of the amino group is much stronger than that of the methyl group, there should be a greater shift of the bands in the spectrum to longer wavelengths than in the case of 5-methyluracil, when both are compared to uracil.

The spectrum has two bands; the *K*-band at 264 nm (its long-wavelength shift, as compared to uracil, is 5 nm) which shifts to shorter wavelengths with decreasing pH. The $n \rightarrow \pi^*$ band at 295 nm (whose long-wavelength shift compared to uracil is 11 nm) shifts to the short wavelength region with decreasing pH, and contrary to the case of uracil and 5-methyluracil, this band appears even in moderately acidic media as a shoulder (Table IV).

Table IV

Influence of the pH on the UV spectrum of 5-aminouracil
(λ values in nm)

Present work			Literature values [7]	
pH of medium	Band λ_{max} (lg ε)	Shoulder λ (lg ε)	pH of medium	λ_{max} (lg ε)
3*N* HCl			3.00	260 (4.09)
2.00	262 (3.86)		7.00	290 (3.93)
			11.00	290 (3.83)
2.30	262 (3.82)	290 (3.02)		
2.70	264 (3.78)	290 (3.24)		
3.35	264 (3.67)	290 (3.57)		
3.60	285 (3.63)			
3.80	285 (3.68)			
H_2O	290 (3.70)			
7.10				
9.00				
10.20	292 (3.72)			
11.10				
12.45				
2*N* NaOH	295 (3.88)			

Equilibria. The 5-amino group, similarly to an 5-methyl group, has but a slight reducing effect on the pK_a values of basic uracil (Fig. 5; equilibria $+1$, $+2AA$ and $+3A$). The amino group in position 5 is, as compared to the

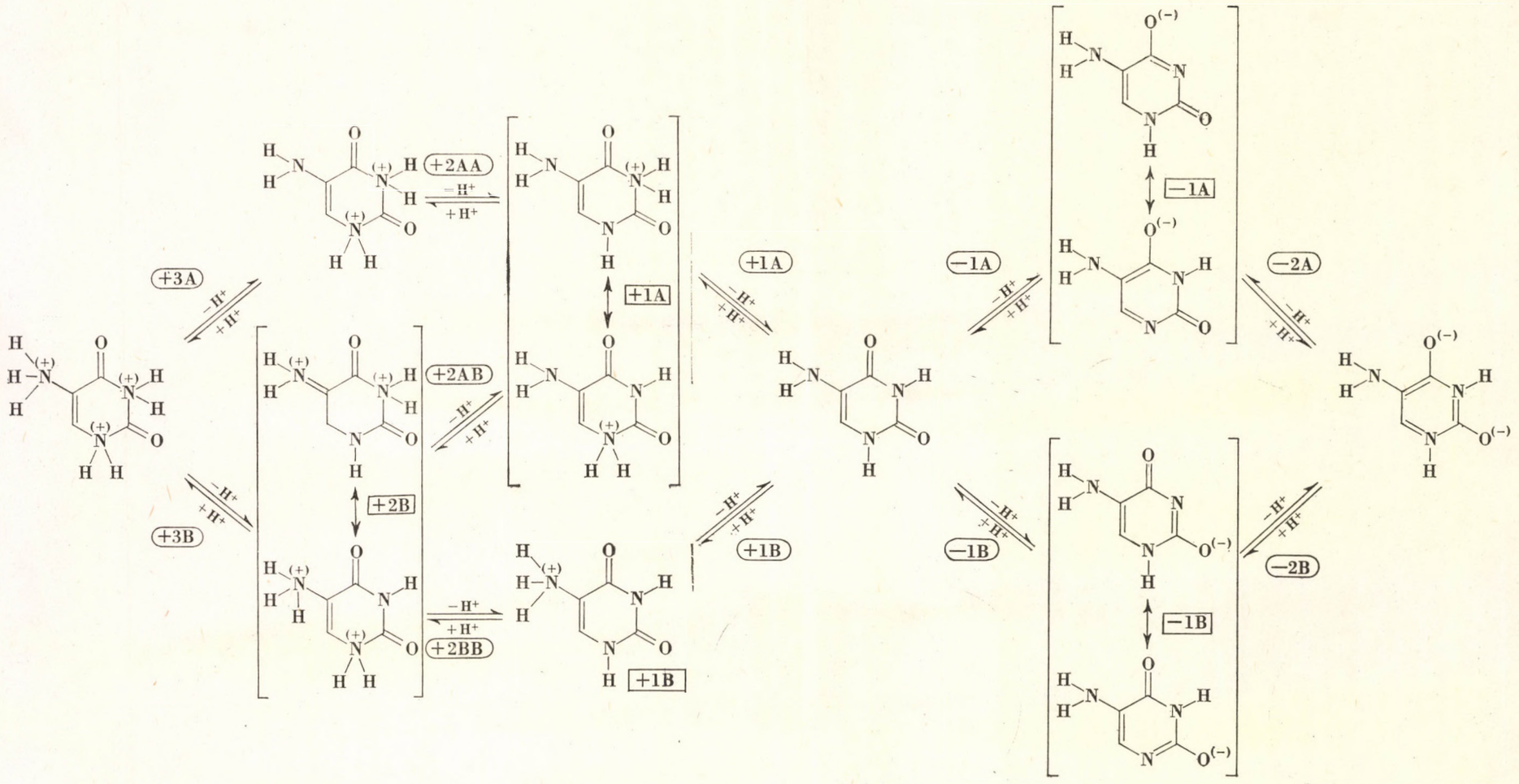

Fig. 5. Acid-base equilibria of 5-aminouracil

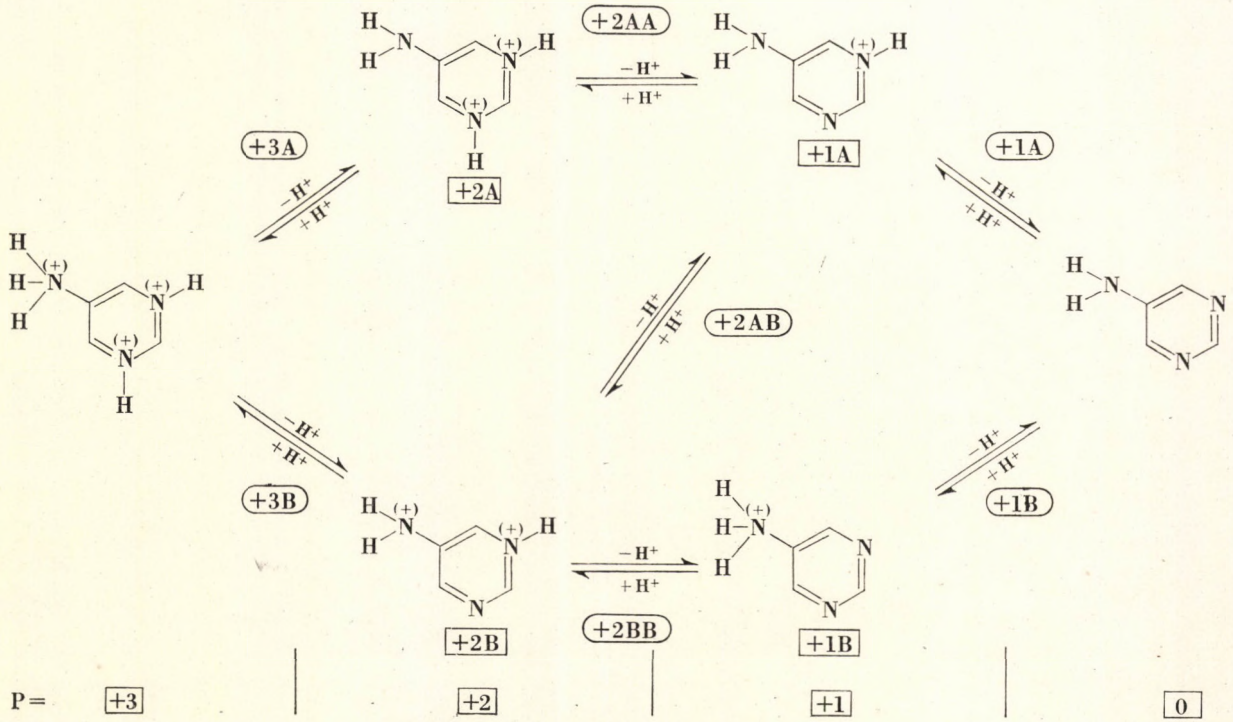

Fig. 6. Acid-base equilibria of 5-aminopyrimidine

nitrogens of the ring, a very strong proton acceptor, as the electron density is here considerably higher [8]. Consequently, in the case of 5-aminouracil, out of the basic equilibria the sequence $+1B$, $+2BB$, $+3B$ will predominate. An examination of the equilibrium constants of pyrimidine (Fig. 1) and of 5-aminopyrimidine (Fig. 6) shows [6, 9], that the basic pK_a values of 5-aminopyrimidine are considerably higher than those of pyrimidine (Table VII).

In the case of the acidic equilibria, $-1A$ and $-1B$ cannot be separated

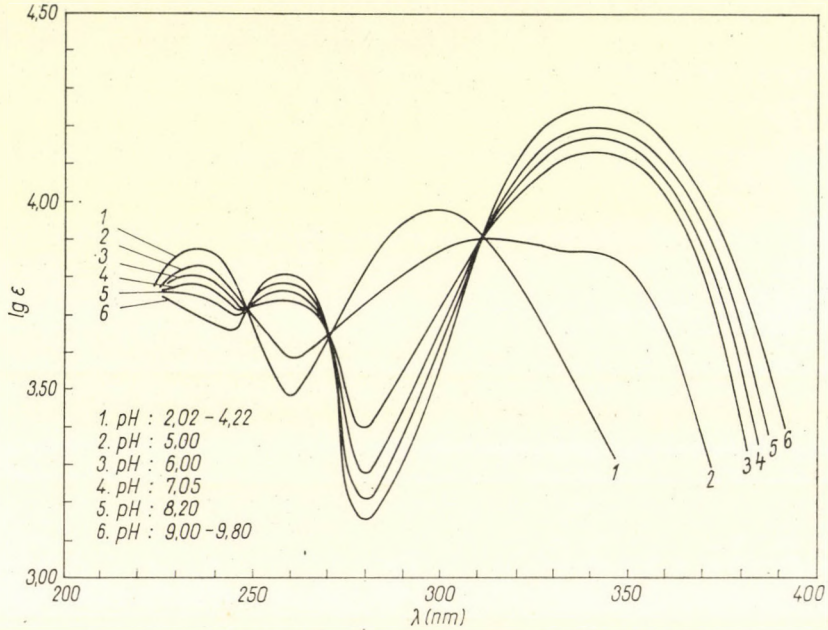

Fig. 7. Influence of the pH on the spectrum of 5-nitrouracil

owing to the electron-donor effect of the 5-amino group, similarly to the case of 5-methyluracil. All acidic pK_a values are higher owing to the effect which has been described for 5-methyluracil. The values of the equilibrium constants are given in Table VII.

6. 5-Nitrouracil

Spectrum. The strong $-I$ and $-M$ effects of the 5-nitro group reduces the electron density mainly in the positions 4 and 6, and less markedly in position 2, leading decreased electron density primarly in the positions in which it was the highest in uracil. In other words, the molecule is less polarized in the ground state than uracil (in excited states this difference is obviously smaller). Consequently, as compared to uracil, the energy of the transition is increased and the maximum of the corresponding band is shifted by 23 nm, to 236 nm.

On the other hand, the electron densities are considerably higher in positions 1 and 3, resulting in an increased $n \rightarrow \pi^*$ transition energy, with a corresponding decrease of the maximum of the respective band by 26 nm as compared to uracil, to 258 nm (Table V).

Besides these two bands, some charge transfer (*CT*) bands also appear. The gradual disappearance of the 300 nm *CT* band and the formation of a 312 nm *CT* band with increasing pH, and the accompanying decrease of the intensity of the *K*-band, are clearly visible, followed by the disappearance of the 312 nm *CT* band and the appearance of a new *CT* band at 340 nm, together with the gradual formation of the $n \rightarrow \pi^*$ band (Fig. 7).

Table V

Influence of the pH on the UV spectrum of 5-nitrouracil

(λ values in nm)

Present work		Literature values [10, 11]	
pH of medium	Band λ_{max} (lg ε)	pH of medium	λ_{max} (lg ε)
1.10		1.00	
2.20	236 (3.87)	3.00	237 (3.86)
3.20	300 (3.98)		
		5.00	236 (3.83)
4.22		5.60	233 (3.80)
5.00	236 (3.83)		260 (3.68)
	312 (3.90)	7.00	235 (3.90)
	234 (3.80)		338 (4.02)
6.00	260 (3.73)	7.20	230 (3.78)
	336 (4.20)		
	234 (3.86)	10.00	258 (3.74)
H_2O	312 (3.90)		342 (4.20)
	338 (3.86)		
	234 (3.78)		
7.05	258 (3.76)		
	340 (4.17)		
	258 (3.78)		
8.20	340 (4.20)		
9.00	256 (3.80)		
9.40	340 (4.25)		
9.80			

The protonated states of 5-nitrouracil are shown in Fig. 2. From the above considerations and from the determined values of the equilibrium constants (Table VII) it follows that in strongly acidic media the $P = 0$, in mildly acidic media the $P = -1$, and in alkaline media the $P = -2$ forms predominate. The *CT* bands are assigned to the various forms in the following order: $P = 0$ (300 nm), $P = -1$ (312 nm) and $P = -2$ (340 nm). Electron transfer occurs probably from ring (in the case of the $P = -2$ form perhaps from the negatively charged O^- in position 4 to the nitro group. The more extensive the conjugated system of the ring (which is increasingly fulfilled for states of higher negative *P*), the lower the deepest unoccupied π electron level. This explains the decrease in *CT* transition energy with increasing negative values of *P*. (The lowering of the π level is also considerable when the role of the ring is limited to charge transfer only.)

Equilibrium. The effect of a nitro group in position 5 is just the opposite to that of an amino group in the same position. The difference between the electron distributions of forms $-1A$ and $-1B$ is even greater than in the case of uracil, resulting in a greater difference between the two acidic pK_a values (Table VII). Decreased electron densities in positions 2 and 4 further the formation of anionic forms, therefore all acidic pK_a values are lower than those of uracil (Table VII). At the same time, there is an increase in the electron densities in positions 1 and 3, with a consequent increase in proton affinity leading to higher values of the basic pK_a's than in the case of uracil.

As compared to 2-aminopyrimidine, the basic pK_a values of 2-amino-5-nitropyrimidine are lower (Table VII), which fact appears to be in contradiction with the aforesaid. If, however, Fig. 8 is compared with the equilibria of 5-aminouracil (Fig. 5) and of 5-aminopyrimidine (Fig. 6), it becomes obvious that also here the equilibrium sequence $+1B$, $+2BB$, $+3B$ is predominating, but the nitro group has exactly the opposite effect on position 2 as compared with positions 1 and 3. Consequently, the basic values of 2-amino-5-nitropyrimidine should indeed be lower than the corresponding values of 2-aminopyrimidine.

7. 6-Methyluracil

Spectrum. The methyl group in position 6 causes an essentially similar, but substantially smaller electron shift in the pyrimidine ring of uracil than the nitro group in position 5. This difference is due to the fact that the changes of electron density caused by the $+I$ effect of the methyl group are different on the two ring-nitrogens. Therefore, the polarity of the molecule in the ground state is increased, resulting in a shift of the *K*-band (by 3 nm), as compared with uracil to the longer wavelength region (to 262 nm).

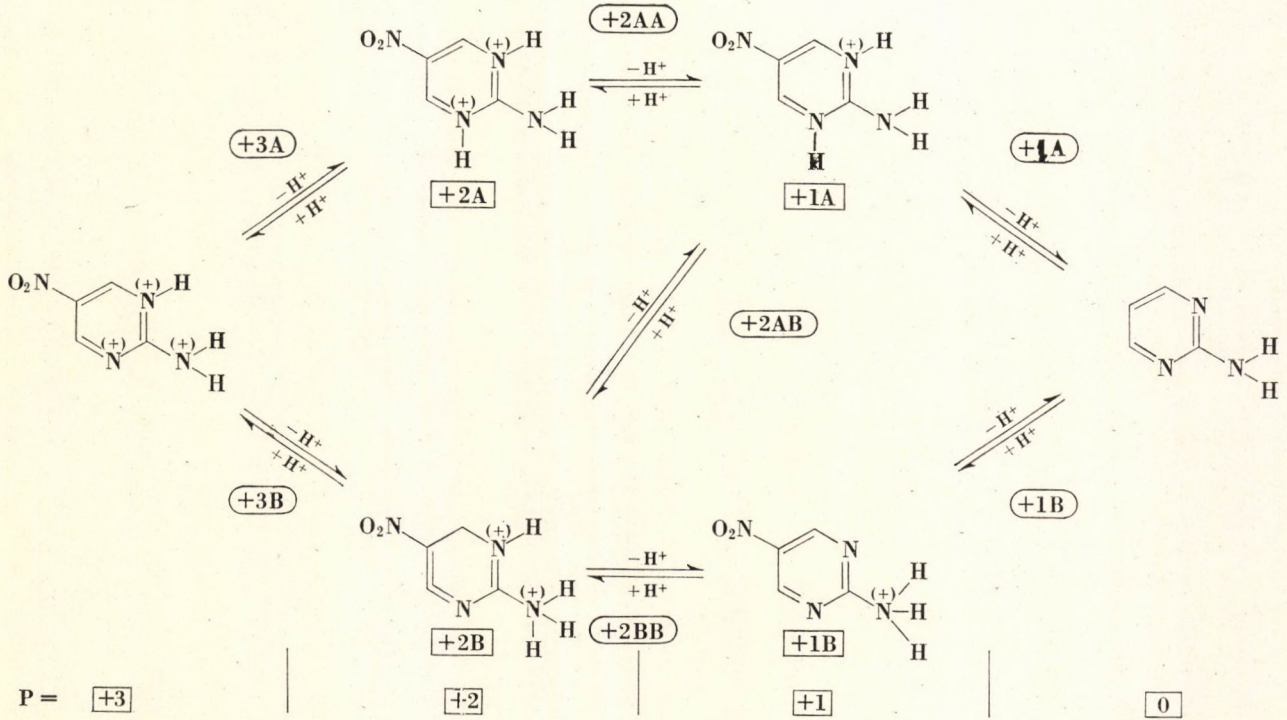

Fig. 8. Acid-base equilibria of 2-amino-5-nitropyrimidine

Similarly to 5-nitrouracil, the electron densities in positions 1 and 3 are higher with a simultaneous increase in proton affinity; therefore, as compared with uracil, the maximum of the $n \rightarrow \pi^*$ band is shifted to shorter wavelength (by 9 nm, to 275 nm; see Table VI).

Equilibria. According to ALBERT and PHILLIPS [8] the methyl group in position 6 behaves contrary to exception. This, however, cannot be agreed with, since the shift of the corresponding pK_a values, as compared with uracil, agrees with that found for 5-nitrouracil (Table VII). There is a decrease in the acidic pK_a values here too, but the equilibria $-1A$ and $-1B$ can be separated better than those of uracil, and less than those of 5-nitrouracil (Fig. 2). The basic pK_a values are higher than those of uracil.

The 6-methyl group has a similar effect also in 6-methylpyrimidine (Table VII).

Table VI

Influence of the pH on the UV spectrum of 6-methyluracil
(λ values in nm)

Present work		Literature values [6, 12]	
pH of medium	Band λ_{max} (lg ε)	pH of medium	λ_{max} (lg ε)
3*N* HCl	262 (4.01)	1.03	260 (3.97)
1.90		5.60	260 (4.01)
2.60		10.20	271 (3.81)
3.50		12.90	275 (3.84)
4.70	262 (3.99)	1*N* NaOH	277 (3.83)
5.80			
6.50			
H_2O			
7.05			
8.22	262 (3.96)		
8.82	262 (3.93)		
9.50	262 (3.89)		
9.70			
10.12	270 (3.85)		
10.70			
11.50	274 (3.86)		
12.50			
2*N* NaOH	275 (3.90)		

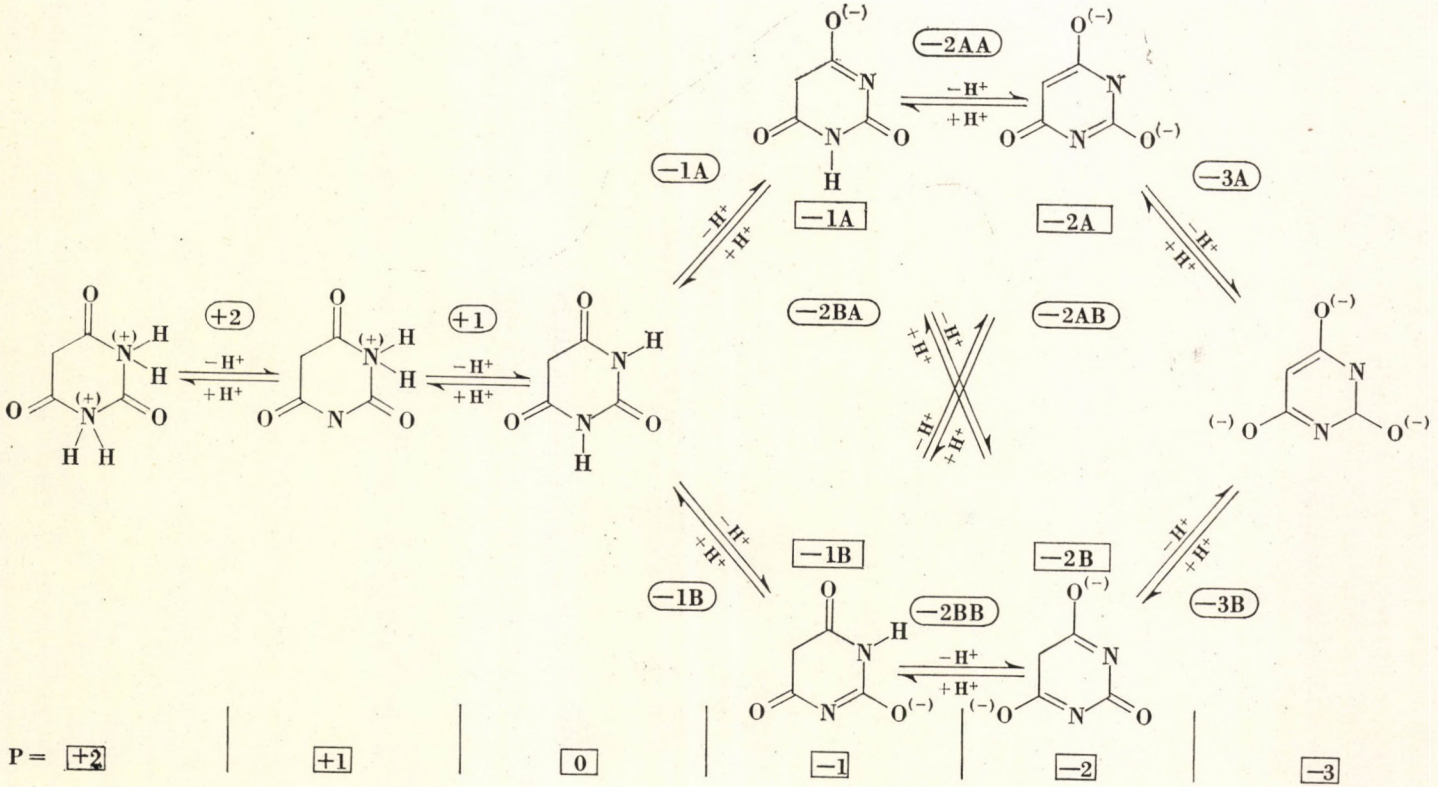

Fig. 9. Acid-base equilibria of barbituric acid

Table VII

pK_a values of acid-base equilibria

(∅ = no equilibrium; — = no literature data available;

Compound	+1A		+1B	
	present work	lit.	present work	lit.
Pyridine	5.20	5.23 [8]	∅	∅
Pyrimidine	1.31	1.30 [3, 12]	∅	∅
4-Methylpyrimidine	*	1.98 [8, 15]	∅	∅
2-Hydroxypyrimidine	*	2.24 [8, 12, 15]	∅	∅
4-Hydroxypyrimidine	*	1.85 [12, 14]	∅	∅
2-Amino-pyrimidine	*	~	*	3.54 [17]
5-Aminopyrimidine	*	~	*	2.60 [6, 9]
2-Hydroxy-4-methylpyrimidine	*	3.15 [15]	∅	∅
4-Hydroxy-6-methylpyrimidine	*	2.15 [15]	∅	∅
4,6-Dihydroxypyrimidine	*	~	∅	∅
2-Amino-5-nitropyrimidine	*	~	*	0.39 [17]
2,4-Dihydroxypyrimidine (uracil)	~	0.50 [8]	∅	∅
2,4-Dyhidroxy-5-methylpyrimidine (5-methyluracil)	~	~	∅	∅
2,4-Dihydroxy-5-aminopyrimidine (5-aminouracil)	~	—	3.30	—
2,4-Dihydroxy-5-nitropyrimidine (5-nitrouracil)	~	~	∅	∅
2,4-Dihydroxy-6-methylpyrimidine (6-methyluracil)	~	1.20 [15, 19]	∅	∅
2,4,6-Trihydroxypyrimidine (6-hydroxyuracil, barbituric acid)	~	~	∅	∅

8. 6-Hydroxyuracil (barbituric acid)

Spectrum. The pH-dependence of the UV spectrum of barbituric acid has been extensively studied [10, 12], so that this spectrum and its evaluation will not be discussed here (Table VIII).

Equilibria. The hydroxyl group in position 6 may have a twofold effect. If present in the keto form, it may act as an electron acceptor reducing the electron densities in positions 1, 3 and 5 and increasing the same in positions 2, 4 and 6. If present in the anionic form, it has the opposite, but considerably stronger effect.

Contrary to expectation, only one pK_a value of both -1 and -2 type equilibria could be determined, indicating that in the corresponding protonization states only one form predominate, the concentrations of the other forms being negligible.

Another evidence for the overwhelming presence of the form $-1A$ (Fig. 9) is that dissociation occurs unequivocally in position 4, while in the tautomeric form $-1B$ some average electron distribution is obtained. The

of pyrimidine derivatives

$\sim$ = special method required for measuring the equilibrium [1]; * = not measured)

Character of the equilibrium							
$-1A$		$-1B$		$-2A$		$-2B$	
present work	lit.	present work	lit.	present work	lit.	present work	lit.
∅	∅	∅	∅	∅	∅	∅	∅
∅	∅	∅	∅	∅	∅	∅	∅
∅	∅	∅	∅	∅	∅	∅	∅
∅	∅	*	9.17 [12, 14, 8]	∅	∅	∅	∅
*	8.59 [12, 14, 15, 8]	∅	∅	∅	∅	∅	∅
∅	∅	∅	∅	∅	∅	∅	∅
∅	∅	∅	∅	∅	∅	∅	∅
∅	∅	∅	9.80 [15]	∅	∅	∅	∅
*	9.00 [15]	∅	∅	∅	∅	∅	∅
*	{5.40 [8] / 5.35 [13]}	*	—	*	—	*	—
∅	∅	∅	∅	∅	∅	∅	∅
8.95	9.38 [16]	9.35	9.38 [16]	12.30	12.0 [8, 16]	12.30	12.00 [10]
10.00	9.90 [11]	10.00	9.90 [11]	12.90	13.0 [11]	12.90	13.00 [11]
11.60	—	11.60	—	13.20	—	13.20	—
5.40	5.55 [18]	7.40	5.55 [18]	11.00	11.30 [18]	11.00	11.30 [18]
8.00	—	9.10	—	9.70	9.70 [8, 15]	9.70	9.70 [8]
3.86	3.90 [8]	$\sim$	$\sim$	12.10	12.50 [8]	$\sim$	$\sim$

presence of form $-1A$ is further supported by the fact that — as already observed in the comparison of the equilibria of 4-hydroxypyrimidine and of 2-hydroxypyrimidine — dissociation proceeds more readily in position 4.

The slight change in the value of the equilibrium constant as compared with that of uracil shows the presence of the form $-2A$. This can be explained by the fact that the carbonyl group in position 6 has hardly any influence on the electron density in position 2.

The strongly acidic character of the hydroxyl groups in positions 2 and 4 is also manifest in the case of 4,6-dihydroxypyrimidine (Fig. 10; Table VII) [6, 13].

9. Notes

These investigations had the purpose to account for the substituent effects in the case of uracil and pyrimidine derivatives, on the basis of the theory of electronic spectra. The effects on the electronic spectra are illustrated

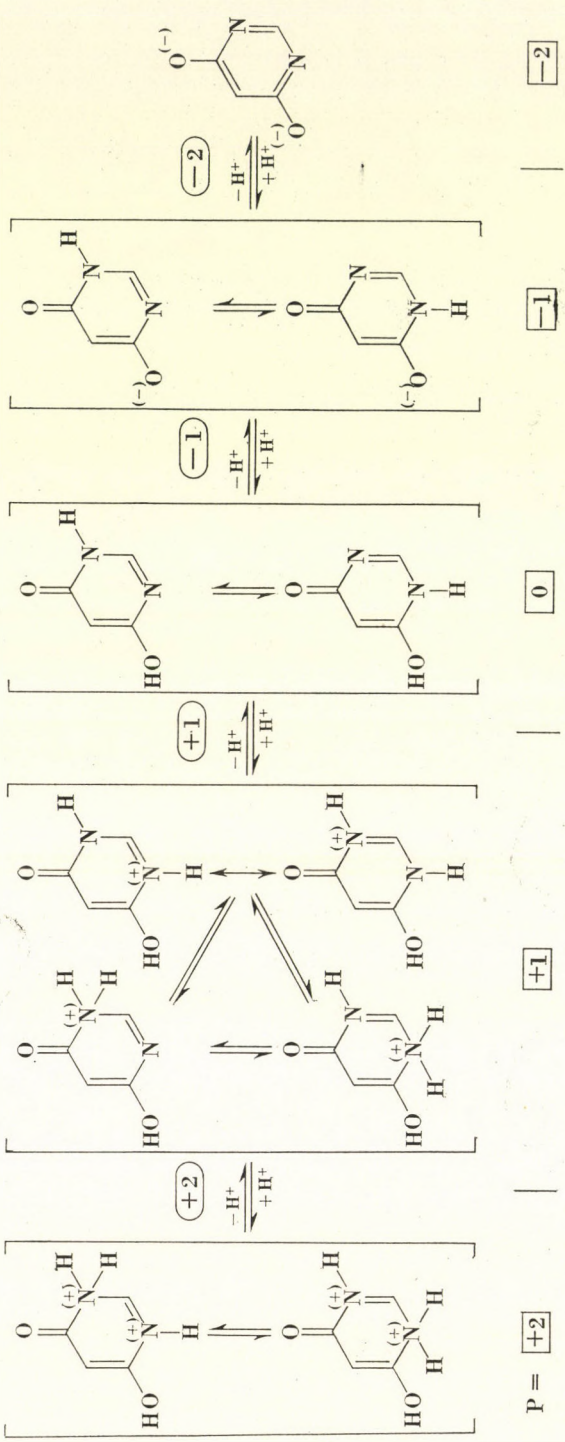

Fig. 10. Acid-base equilibria of 2,4-dihydroxypyrimidine

by our own data in Table VIII. Table VII shows the pK_a values of the various equilibria (both our own measurements and literature data) according to a system developed by us.

The effects mentioned earlier appear quite distinctly. These include, *e.g.*, the identical tendencies of the 5-nitro and 6-methyl groups on the equilibria of uracil, and the opposite effects of the 5-amino and 5-methyl groups.

Table VIII

Position of the characteristic bands of uracil derivatives for the states with the highest ($\pi \rightarrow \pi^*$) and lowest ($n \rightarrow \pi^*$) measurable P values

Compound	$\pi \rightarrow \pi^*$ band (λ max., nm)	$n \rightarrow \pi^*$ band (λ max., nm)
Pyrimidine	242	272
Uracil	259	284
5-Methyluracil	263	290
5-Aminouracil	262	295
5-Nitrouracil	236	256
6-Methyluracil	262	275
6-Hydroxyuracil	221*	259

*pH = 4,50

SUMMARY

The acidic and basic equilibria of uracil and several of its 5- and 6-substituted derivatives have been studied by examining the pH-dependence of their electronic spectra. The equilibria are interpreted on basis of the substituent effects. For a systematization of the various equilibria, the conception of protonization state has been introduced to characterize the forms in equilibrium. The separation of the equilibria of the two types of monovalent anions could be achieved.

REFERENCES

1. McBryde, W. A. E.: Can. J. Chem. **43,** 3472 (1965)
2. Mason, S. F.: J. Chem. Soc. **1959,** 1240
3. Mason, S. F.: J. Chem. Soc. **1959,** 1247
4. Boarland, M. P. V., McOmie, F. W.: J. Chem. Soc. **1952,** 3716
5. Halverson, F., Hirt, R. C.: J. Chem. Phys. **19,** 711 (1951)
6. Boarland, M. P. V., McOmie, F. W.: J. Chem. Soc. **1952,** 3722
7. Wyatt, G. R.: Biochem. J. **48,** 584 (1951)
8. Albert, A., Phillips, J. N.: J. Chem. Soc. **1956,** 1294
9. Whittaker, N.: J. Chem. Soc. **1951,** 1565
10. Stimson, M. M.: J. Am. Chem. Soc. **71,** 1470 (1949)
11. Shugar, D., Fox, J. J.: Biochim. Biophys. Acta **3,** 199 (1960)
12. Albert, A., Brown, O. J., Cheeseman, G.: J. Chem. Soc. **1951,** 474
13. Davoll, J., Laney, D. H.: J. Chem. Soc. **1956,** 2124

14. BROWN, D. J., MASON, S. F.: J. Chem. Soc. **1955,** 211
15. MARSHAL, J. R., WALKER, J. : J. Chem. Soc. **1951,** 1004
16. BROWN, D. J., MASON, S. F.: J. Chem. Soc. **1955,** 4035
17. BROWN, D. J., JACOBSEN, N. W.: J. Chem. Soc. **1960,** 1978
18. BROWN, D. J.: J. Chem. Soc. **1959,** 3647
19. MARSHAL, R., WOLKER, J.: J. Chem. Soc. **1951,** 1012

Antal TÓTH
Ferenc BILLES } Budapest XI., Műegyetem rkp. 3.

Acta Chimica Academiae Scientiarum Hungaricae Tomus 56 (3), pp. 251—270 (1968)

THERMAL STABILITY OF CHLORINE OXY-SALTS IN THE SOLID STATE, I

KINETIC STUDY OF THE DISPROPORTIONATION AND EXPLOSION OF SOME CHLORITES

F. SOLYMOSI and T. BÁNSÁGI

(Reaction Kinetical Research Group of the Hungarian Academy of Sciences, Szeged)

Received May 22, 1967

Introduction

Our knowledge of the behaviour of salts with oxygen-containing anions at high temperature is relatively slight. Despite the fact that the decomposition products of oxy-anions have been satisfactorily explored, we know very little about the kinetics and mechanism of the decomposition. Particularly little information can be found in the literature about the factors influencing the thermal stability of the compounds belonging to the same group. The possible reason for this is that the investigations involved only one or two members of a group which was not enough to draw a general conclusion.

From among the salts of oxygen-containing anions the study of chlorine oxy-salts promised to be interesting for various reasons:

(*a*) Owing to the different valency states of chlorine, oxy-anions with different oxygen contents are formed, which gives a good opportunity to carry out some comparative experiments, and to get more general conclusions.

(*b*) There are very few data on the thermal behaviour and decomposition mechanism of the salts of chlorine oxy-acids.

(*c*) The compounds, primarily perchlorates, are technically important substances as a source of oxygen in propellants.

(*d*) The stability of the compounds sensitively depends on the presence of different foreign substances; this fact makes possible to study catalytic reactions in the solid phase.

Earlier study of the compounds showed that they transform into each other at higher temperatures. Chlorites and chlorates, besides decomposition or explosion, undergo a considerable disproportionation, resulting in chloride and chlorate, or chloride and perchlorate, respectively. The decomposition of perchlorates occurs in steps through the formation of chlorate. All this indicates that the learning of the nature and mechanism of the reactions of any salt of a chlorine-acid is possible only by systematic studies, extending the experiments to all members of the system. As the stability of the substances and the direction of their reactions depend on the cations attached to them, to

complete the picture, the effect of different cations should also be clarified.

In the following series we give an account of the thermal stabilities of chlorites, chlorates and perchlorates of different cations. Besides kinetic investigations, we determined some important physical properties of the compounds relating to the type of bonding and the electronic structures of the substances. This program made it possible to compare the thermal stabilities and other properties of the chlorite, chlorate, and perchlorate of the same cation, and to study the effect of various cations in the groups of chlorite, chlorate and perchlorate. In the present paper we describe the behaviour of sodium, barium, and lead chlorites.

The physical and chemical properties of chlorites have been studied mainly by LEVI *et al.* They described the methods of preparation of the compounds, their characteristic reactions, and in some cases they determined the crystal structures of the substance as well [1, 2]. In connexion with the thermal stability of chlorites, it has been pointed out that they are extremely sensitive even to very weak mechanical effects, and explode very easily. Of sodium chlorite it has been stated that it explodes when it is struck, but on the effect of heat it is converted only into sodium chlorate [3]. TAYLOR *et al.* [4] later observed that sodium chlorite exploded only if the surface of the metal performing the striking contained grease. These authors found the substance stable below 150 °C, however, a considerable chlorate formation was experienced above 200 °C. Of lead and barium chlorites it has been stated that the explosion takes place above 100 °C [4].

Experimental

Materials

Sodium chlorite was prepared from a BDH product by fractional crystallization. The substance containing two molecules of water of crystallization, was dried in vacuum over potassium hydroxyde. By iodometric analysis it contained 99% sodium chlorite. For the preparation of barium chlorite the reaction

$$2\ ClO_2 + Ba(OH)_2 + H_2O_2 = Ba(ClO_2)_2 + 2\ H_2O + O_2,$$

was used [5]. Chlorine dioxide was obtained by BODENSTEIN's method [6]. Lead chlorite was prepared by mixing the solutions of lead nitrate and sodium chlorite. The yellow precipitate was filtered, washed and recrystallized. The lead chlorite content of the substance was 99.4%.

Methods

The disproportionation reaction of chlorites was studied as follows; known quantities of the substances were weighed into crucibles which were then placed into an oven heated to the reaction temperature. After given periods the loss of weight was determined, then the substance was dissolved in water. In the first test chlorite was determined by iodometric analysis in acetic acid solution. In the next aliquot the chlorite and chlorate contents were measured together also by iodometric analysis, but in strong hydrochloric acid solution [7]. In a new test the amount of chloride was measured by argentometric titration.

The explosion of chlorites was investigated at the atmospheric pressure of air, as in the case of ammonium perchlorate [8]. Differential thermal analysis (DTA, DTG) was carried out in a PAULIK—PAULIK—ERDEY derivatograph. The refractive indices were determined by the BECKE line method using a LEITZ microrefractometer. Reflexion spectra of the compounds were taken by a UNICAM SP instrument adapted for this purpose. Magnesium carbonate served as standard material. The low frequency dielectric constants were measured in a MARCONI apparatus, using pellets of 20 mm in diameter and 2 mm in thickness.

Results

1. Sodium chlorite

(a) *Derivatographic investigations.* The derivatograms of sodium chlorite are plotted in Fig. 1a. There are three exothermic peaks on the DTA curve, at 191 °C, 273 C° and 557 °C. An endothermic change appeared at 260 °C. From the first two exotherms only the second one was connected with a very slight,

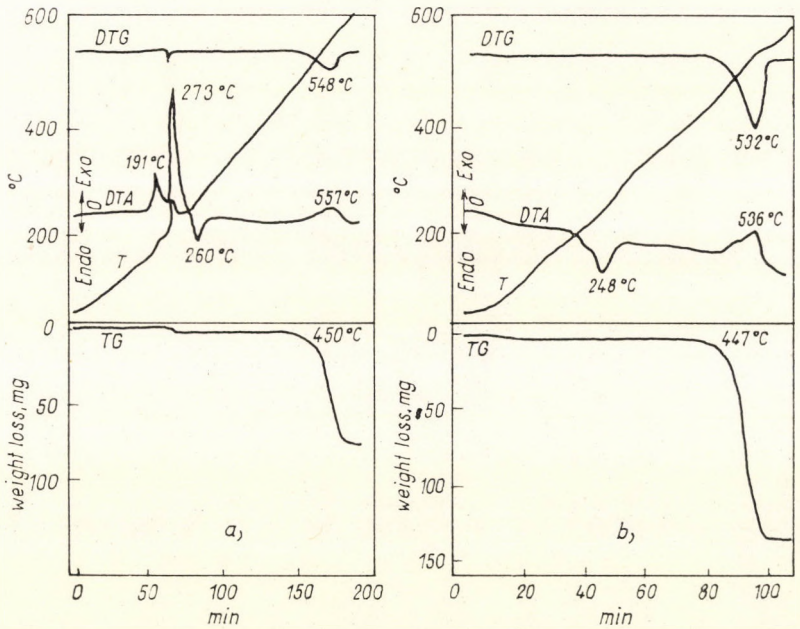

Fig. 1. Derivatogram of sodium chlorite. (a) After the interruption at 280 °C (b) Weight of substance: 210 mg; heating rate: 6 °C/min.

but reproducible, weight loss (about 1%). The decomposition of the substance started at 440—450 °C. On increasing the heating rate (from 3 °C/min. to 18 °C/min.) the exothermic peaks and also the onset of the loss of weight were shifted towards the higher temperature. Using a heating rate of 6 °C/min. or 18 °C/min. endothermic peaks did not appaear at all.

Interrupting the measurements after the second exothermic process, at 280 °C and 320 °C, and cooling down the sample, in a repeated experiment the substance did not exhibit the exothermic peaks previously observed (Fig. 1*b*).

The solid residue obtained at the interruption did not contain any sodium chlorite; it had the composition 73.7 weight-% sodium chlorate and 24.3 weight-% sodium chloride. We also attempted making interruptions after the first exotherm at 210 °C. The chemical composition and thermal behaviour of the residue were essentially similar to that of the previous one. Nevertheless, we noticed, however quickly the interruption of the measurement and the cooling down of the sample (by lifting up the furnace) was performed, we could not hinder the start of the second exothermic process.

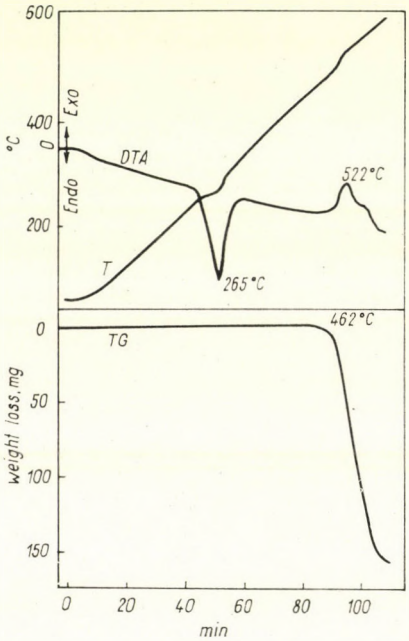

Fig. 2. Derivatogram of sodium chlorate. Weight of substance: 460 mg; heating rate: 6 °C/min

The derivatogram of sodium chlorate is plotted in Fig. 2. A comparison of the two figures clearly shows that above 250 °C the derivatograms of sodium chlorite and sodium chlorate are practically the same. This result indicates that under the experimental conditions applied, sodium chlorite is transformed into sodium chlorate and sodium chloride, according to the equation:

$$3\ NaClO_2 = 2\ NaClO_3 + NaCl.$$

The exothermic character of the reaction is in accordance with the reaction

heat calculated from the heats of formation of the substances (Table VI). The endothermic change experienced at 260 °C, as well as the decomposition which started above 448 °C, was due to the melting and decomposition of sodium chlorate. The latter process is characterized on the DTA curves by an exothermic peak. The above results indicate that sodium chlorite is completely transformed into sodium chlorate without any decomposition. If the interruption occurred at 160 °C, *i.e.* before the appearance of the first exothermic peak, only 5% sodium chlorate was found in the sample.

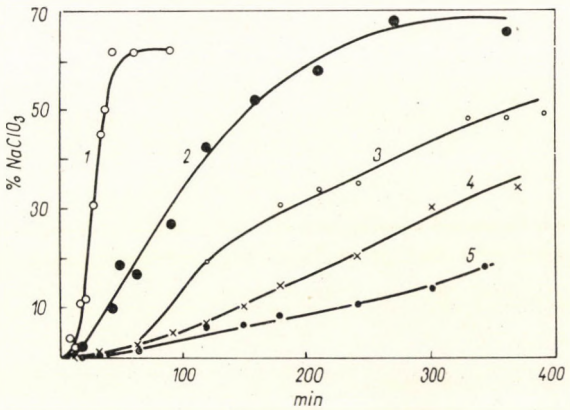

Fig. 3. The amount of sodium chlorate formed during the disproportionation of sodium chlorite. 1. 160 °C; 2. 155 °C; 3. 150 °C; 4. 145 °C; 5. 140 °C

The derivatogram of sodium chlorite was taken in the presence of sodium chlorate and sodium chloride, resp. (molar ratio 1 : 1). It appeared that the products of the disproportionation reaction did not essentially influence the characteristics of the transformation of sodium chlorite.

(b) *Kinetic investigations.* Considering that a significant evolution of heat occurs in the substance above 170 °C, kinetic investigations were performed below this temperature. The percentages of sodium chlorate formed at different temperatures are plotted in Fig. 3.

The reaction starts without an induction period, and the rate increases with the increase of temperature.

The half-time of the reaction at 150 °C is 222 minutes. Table I contains data obtained at 145 °C. The quantities of sodium chlorite, sodium chlorate, and sodium chloride are expressed in mole fractions. In the kinetic analysis, the first order equation was found to fit the results the best (Fig. 4).

This equation described the reaction at a higher temperature up to 50—70 percentage transformation, and at a lower temperature to a 30—40 percentage conversion. The rate constants as functions of 1/T well satisfied the

Disproportionation of sodium chlorite at 145 °C

Time (min.)	X_1	X_2	X_3
10	0.9675	0.0325	—
30	0.9201	0.0157	0.0642
60	0.8658	0.0322	0.1020
90	0.8401	0.0437	0.1162
120	0.8138	0.0628	0.1234
150	0.7834	0.0889	0.1277
180	0.7362	0.1231	0.1407
240	0.6739	0.1839	0.1422
300	0.5502	0.2694	0.1804
370	0.5103	0.2891	0.2006

X_1 = mole fraction of sodium chlorite
X_2 = mole fraction of sodium chlorate
X_3 = mole fraction of sodium chloride

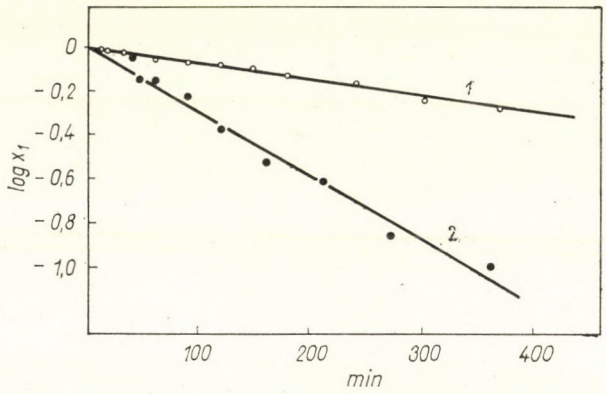

Fig. 4. Kinetic analysis of the disproportionation of sodium chlorite by the first order equation. 1. 145 °C; 2. 155 °C

Arrhenius law. The value of activation energy was 54.3 kcal/mole. Calculating the activation energy from the dependence on temperature of the time required for 25% disproportionation, we got 51.0 kcal/mole. Kinetic data are listed in Table II.

The thermal stability of sodium chlorite has also been investigated at a higher temperature. It was thought that when sodium chlorite is dropped in a reaction vessel heated up to high temperature, in addition to the disproportionation reaction, the decomposition of sodium chlorite

$$NaClO_2 = NaCl + O_2$$

might also take place. Experiments were performed at 200, 300 and 350 °C. The gas formation found, however, did not exceed the value corresponding to 1% decomposition. This value conforms to the loss of weight observed in

Table II

Kinetic data of the disproportionation of sodium chlorite

Temperature, °C	$k_1 \cdot 10^3$	$\tau_{1/4}$ min.
140	0.396	270
145	0.751	188
150	1.27	90
155	2.97	45
160	—	18
Activation energy, kcal/mole	54.2	51
Frequency factor (min.$^{-1}$)	$1.85 \cdot 10^{25}$	

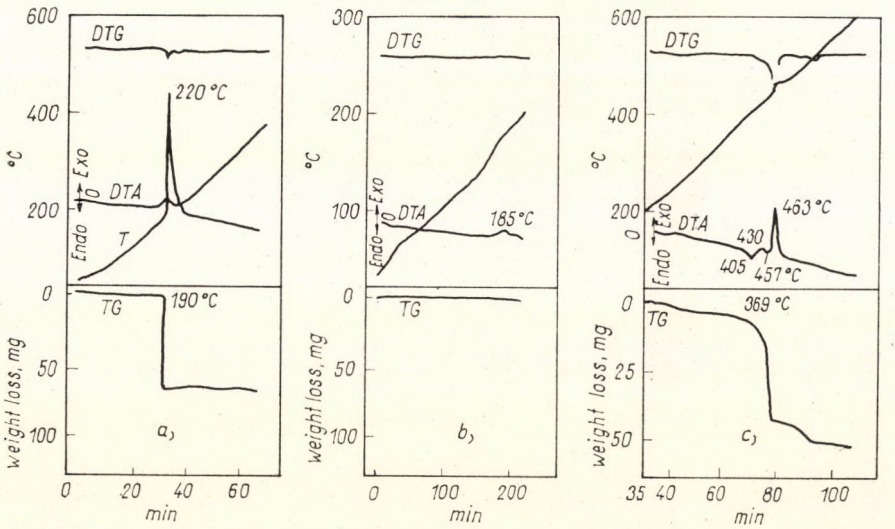

Fig. 5. Derivatogram of barium chlorite. Weight of substance: 160 mg; heating rate (a) 6 °C/min.; (b) 1 °C/min.; (c) continuation of the former measurement with 6 °C/min.

the derivatographic experiments at the appearence of the second exothermic peak. A considerable gas evolution occurred only above 400 °C, which is very likely the result of the decomposition of the formed sodium chlorate.

2. *Barium chlorite*

(a) *Derivatographic investigation.* On the DTA curve of barium chlorite (Fig. 5*a*) an exothermic heat effect started to develop at 180 °C. Contrary to sodium chlorite, an extremely fast decomposition appeared on the TG curve darallel to the heat evolution. The extent of the loss of weight depended sensitively on the heating rate, and in the case of a fast heating up it corresponded to the reaction:

$$Ba(ClO_2)_2 = BaCl_2 + 2\ O_2.$$

The decreasing of the heating rate lowered both the height of the exothermic peak and the extent of decomposition. At 1 °C/min. there was no decomposition at the above temperature (Fig. 5*b*). In this case — as a chemical analysis

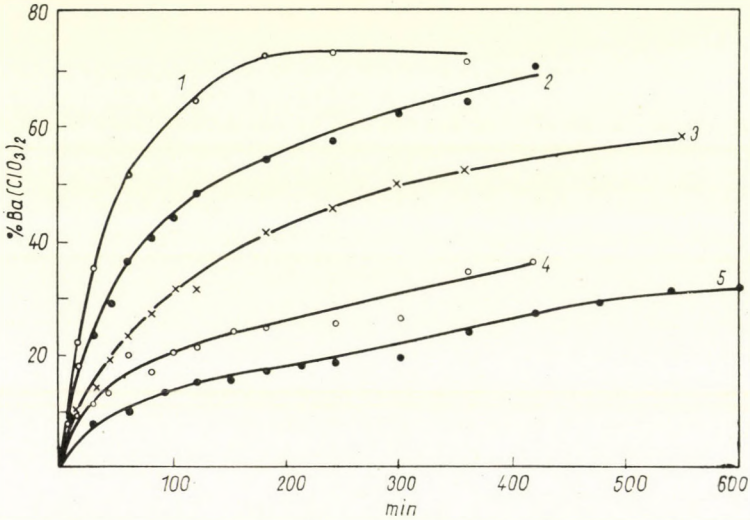

Fig. 6. Amount of barium chlorate formed during the disproportionation of barium chlorite. 1. 170 °C; 2. 160 °C; 3. 150 °C; 4. 140 °C; 5. 130 °C

of the sample revealed — the disproportionation of barium chlorite took place. In accordance with it, on further heating at a rate of 6 °C/min. (Fig. 5*c*) the behaviour of the sample corresponded to that of barium chlorate [9].

When barium chlorite was mixed in 1 : 1 molar ratio with aluminium oxide sintered at 1100 °C, the exothermic change starting at 175 °C—180 °C also took place, but this was connected — even at a heating rate of 6° C/min. — with a loss in weight of not more than 2 mg. The slow decomposition of the substance began at 380 °C. The same behaviour was observed in the presence of nickel oxide, barium chlorate and barium chloride (molar ratio, 1 : 1): barium chlorite was completely transformed into barium chlorate without

decomposition. This process was indicated by an exothermic peak at 180 °C.

Reducing the quantity of aluminium oxide (molar ratio, 3 : 1), however, the fast decomposition of barium chlorite already occurred at 192.5 °C, as in the absence of aluminium oxide.

(b) *Kinetic investigations.* Kinetic measurements of the transformation barium chlorite → barium chlorate were carried out between 130—170 °C. The quantities of barium chlorate formed at different temperatures are plotted in Fig. 6.

The relation between the barium chlorite transformed and barium chlorate produced corresponds to the following equation:

$$3\ Ba(ClO_2)_2 = 2\ Ba(ClO_3)_2 + BaCl_2.$$

The mathematical analysis of the curves was done by the first order equation (Fig. 7).

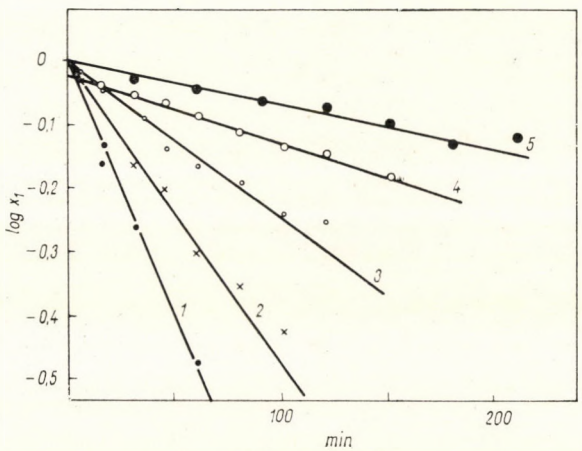

Fig. 7. Kinetic analysis of the disproportionation of barium chlorite by the first order equation. 1. 170 °C; 2. 160 °C; 3. 150 °C; 4. 140 °C; 5. 130 °C

From the 1/T-dependence of the rate constants we got an activation energy of 23.5 kcal/mole. Somewhat higher activation energy was obtained from the temperature dependence of the half-times and quarter-times.

(c) *Explosion of barium chlorite.* Barium chlorite — unlike sodium chlorite — explodes above 190 °C even in pure state. Using 50 mg substance, the lowest temperature of the explosion was 190 °C. The substance kept below 190 °C did not decompose (suffering only disproportionation) even after several hours, so the slow decomposition of barium chlorite could not be studied. In the explosion about 10 ml of gas evolved, which consisted of oxygen and did not contain any chlorine or chlorine dioxide. Accordingly, the solid residue of the explosion was barium chloride. As there was no noticeable gas formation

Table III

Kinetic data of the disproportionation of barium chlorite

Temperature, °C	$k_1 \cdot 10^3$	$\tau_{1/2}$min.	$\tau_{1/4}$min.
130	0.71	—	300
140	1.18	453	125
150	2.50	174	53
160	5.20	75	27
170	8.19	43	15
Activation energy, kcal/mole	23.5	28.5	28.0
Frequency factor (min.$^{-1}$)	$3.88 \cdot 10^9$		

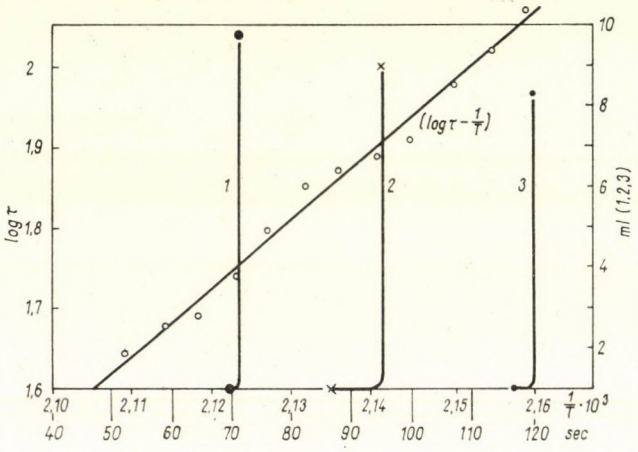

Fig. 8. Explosion of barium chlorite and the Arrhenius diagram of the induction periods, τ = induction period before the explosion, ml = the amount of gases formed during the explosion. 1. 196 °C; 2. 192 °C; 3. 190 °C

during the induction period, only the time lapse until the explosion was measured. These are shown in dependence of 1/T in Fig. 8. In the Figure some explosion curves are also plotted. The value of activation energy is 38.8 kcal/mole. By means of a small thermocouple placed into the barium chlorite sample, a very slight self-heating was detected before the explosion. At the moment of explosion, however, a 40 °C temperature rise was registered.

3. Lead chlorite

(a) *Derivatographic investigations.* The derivatogram of lead chlorite is shown in Fig. 9. The exothermic change started at 103 °C. At the same time a very fast decomposition of the substance occurred (Fig. 9a). Even when the

measurement was interrupted before the decomposition took place, the substance already contained 8.9% lead chlorate. This indicates that a slight disproportionation of lead chlorite has occurred before the explosion-like reaction. Since the decomposition of lead chlorite begins only above 200 °C [9], the foregoing change in weight is due to the decomposition of lead chlorite. Decreas-

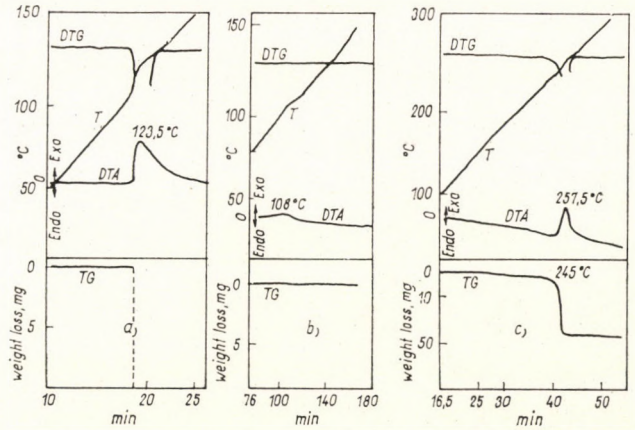

Fig. 9. Derivatogram of lead chlorite. Weight of substance: 100 mg; (a) heating rate: 6 °C/min.; (b) heating rate: 1 °C/min.; (c) continuation of the former measurement interrupted at 150 °C/at a heating rate of 6 °C/min.

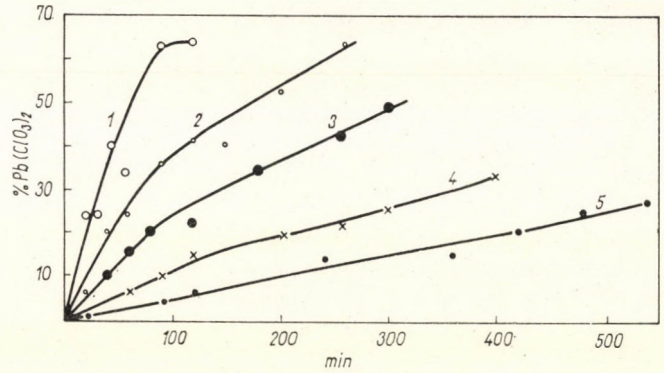

Fig. 10. The amount of lead chlorate formed during the disproportionation of lead chlorite 1. 95 °C; 2. 90 °C; 3. 85 °C; 4. 80 °C; 5. 75 °C

ing the heating rate of the sample from 6 °C to 1 °C per minute, the extent of the former exothermic heat change decreased, and it was not accompanied by any loss in weight (Fig. 9*b*). Analysis of the sample obtained after interruption at 205 °C revealed a composition of 66 mole-% chlorate and 33 mole-% chloride. This shows that the disproportionation of lead chlorite was complete in this case. On further heating at a rate of 6 °C/min., a new exothermic peak appeared,

and decomposition of the substance set in at 240 °C (Fig. 9*c*). This latter corresponds to the decomposition of lead chlorate formed in the disproportionation reaction.

It is to be mentioned that when a heating rate of 6° C/min. is used, the fast decomposition of lead chlorite at about 110 °C cannot be prevented even by the addition of a relatively large quantity of aluminium oxide to the sample [$Pb(ClO_2)_2 : Al_2O_3$ molar ratio 1 : 5].

(b) *Kinetic investigations.* The disproportionation of lead chlorite was studied between 70—95 °C in detail. The amounts of lead chlorate formed are plotted in Fig. 10. The rate constants of the reaction have been determined by the first order equation here, too. The value of activation energy was 39.4 kcal/mole.

Activation energies of 37.9—36.9 kcal/mole were obtained from the temperature dependence of the quarter- and half-times of the reaction. The kinetic data are listed in Table IV.

Table IV

Kinetic data of the disproportionation of lead chlorite

Temperature, °C	$k_1 \cdot 10^3$	$\tau_{1/4}$min.	$\tau_{1/2}$min.
75.5	0.28	359	—
80	0.69	162	424
85	1.75	80	182
90	3	42	101
95	6.07	14	44
Activation energy, kcal/mole	39.4	37.9	36.9
Frequency factor (min.$^{-1}$)	$1.62 \cdot 10^{21}$		

(c) *Explosion of lead chlorite.* In this case again the slow decomposition of the compound could not be studied kinetically. The substance exploded at 112 °C; below this temperature, gas formation was negligible. In vacuum we noticed a small pressure rise, but this was too fast to be followed in time. The explosion of lead chlorite was investigated between 112 °C and 125 °C. Before the explosion, a very slight gas formation was observed. At higher temperatures the induction period of the explosion decreased. From 50 mg substance about 7.5 ml of gas evolved in the explosion, which, in contrast to the former case, contained about 20% chlorine, too. Some explosion curves and the 1/T dependence of induction periods are plotted in Fig. 11.

The value of the activation energy is 28 kcal/mole.

We determined also here the temperature rise in the substance at the moment of its explosion; it amounted to 40 °C.

4. The structure and physical characteristics of chlorites

From among the chlorites studied, we have found crystallographic data merely for lead chlorite. According to LEVI [10] lead chlorite has a pseudo-teragonal structure, $a : c = 1 : 1.51$, $a = 4.14$ Å. In order to characterize the

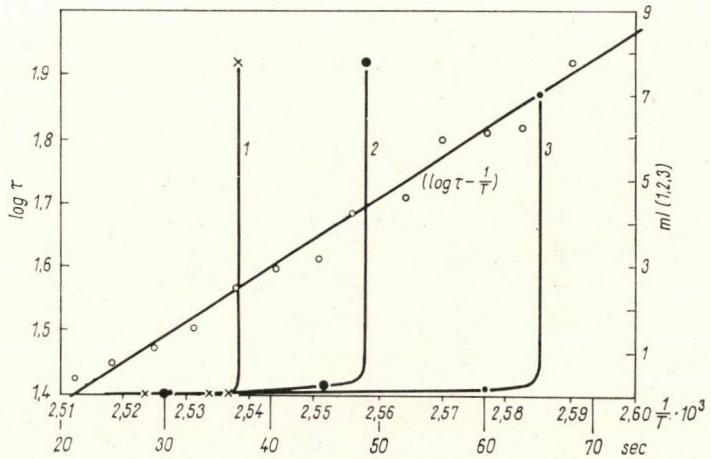

Fig. 11. Explosion of lead chlorite and the Arrhenius diagram of the induction periods (for τ and ml, see Fig. 8). 1. 121 °C; 2. 118 °C; 3. 114 °C

type of bonding and to get acquainted with the electronic structure of chlorites, we have determined some electric and optical properties of the compounds. The reflection spectra of the substances are shown in Fig. 12.

The reflection spectrum of the chlorites shows relatively little dependence on the cation, and the position of the absorption edge shifts towards the longer wavelengths in the order: sodium, barium, lead. From the absorption edges of the compounds the following optical activation energies (E_0) were calculated: sodium chlorite 4.66 eV, barium chlorite 4.28 eV, lead chlorite 3.10 eV. The refractive index of each compound was also determined, and we obtained 1.547 for sodium chlorite, and 1.645 for barium chlorite. The refractive index of lead chlorite was higher than measurable by the refractometer at our disposal. Since the refractive indices of chlorides and chlorites do not differ very much, we have taken the value of 2.1 as the possible refractive index of lead chlorite. The low frequency dielectric constants of the compounds

(K) were 6.535, 4.215 and 5.417 for sodium, barium and lead chlorites, respectively. The high frequency dielectric constants (K_0) were calculated from the values of the refractive indices by the equation

$$K_0 = n^2 \quad (n = \text{refractive index}).$$

The ratio of the two dielectric constants, which gives some information about the nature of the bond, is near to the unit in case of lead chlorite, but there is a significant deviation from it in barium chlorite and still more in sodium chlorite.

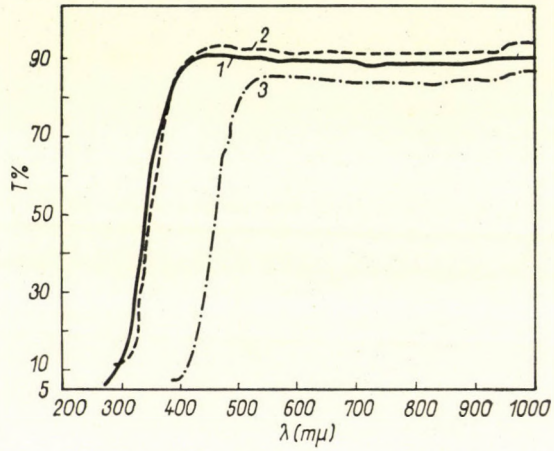

Fig. 12. Reflection spectra of chlorites. 1. $NaClO_2$; 2. $Ba(ClO_2)_2$; 3. $Pb(ClO_2)_2$

From the above data the thermal activation energies (E_T) of the compounds were calculated using the relation

$$E_T = E_0 \frac{K_0}{K}.$$

Table V contains data concerning the physical properties and the electric structures of the compounds.

On the basis of these results (refractive index, absorption edge and the ratio of low and high frequency dielectric constants, or E_0/E_T), it can be assumed that the ionic character of the compounds is decreasing in the order: sodium, barium silver and lead chlorite. This assumption is supported by calculating the percentage ionic character of the bond according to SANDERSON's method [12] (Table V).

Table V

Some physical constants of chlorites

Compound	Radius of cation, Å	Ionization potential, eV	F^*	Refractive index, n_D^{22}	K Dielectric constant, at 350 Kc/s	Absorption edge, Å	Optical activation, eV E_0	Thermal activation energy, eV E_T	K_0/K	Ionic character of bond, %
$NaClO_2$	0.88	5.138	2.915	1.547	6.535	2660	4.66	1.70	0.366	68.5
$Ba(ClO_2)_2$	1.35	10.00	*	1.645	4.215	2900	4.28	2.75	0.642	44.95
$AgClO_2$	1.13	7.56	3.394	~2.1	5.282	4050	3.06	2.55	0.835	35.8
$Pb(ClO_2)_2$	1.25	15.03	3.876	~2.1	5.417	4000	3.10	2.52	0.814	16.99

$F^* = \frac{Z^* \cdot e}{r^2}$; F^* = effective electric field strength of cation

r = radius of cation

Z^* = effective nuclear charge number, $Z^* \cdot e = (Z—S)e$

Z = nuclear charge, S = screening number

* The effective electric field strength of barium cannot be calculated owing to the lack of data for the determination of its screening number. The Table contains the data concerning the properties of silver chlorite, the decomposition of which has been studied earlier by us [11].

Discussion

It has been shown that on the effect of heat, metal chlorites transform in two directions. At lower temperatures they disproportionate to chlorate and chloride, and at a higher temperature — with the exception of sodium chlorite — they explode, giving rise to different solids and gaseous produets.

Let us deal first with the disproportionation reaction. The disproportionation of chlorine oxy-salts has been known for a long time. Detailed measurements, however, were carried out only with the alkali chlorates, but even these were done not from the kinetic point of view. The possible reason for it is that, besides disproportionation, the decomposition of chlorates also occur, so the investigations were mainly restricted to establishing the ratio of the two reactions and the influence of different experimental conditions on this ratio.

In connection with the mechanism of the disproportionation of chlorine oxy-anions two opinions have been voiced. According to GLASNER and WEIDENFELD [13] the atomic oxygen formed during the decomposition of potassium chlorate reacts with the chloride, *i.e.*, with the solid product of the decomposition of chlorate:

$$KCl + 4\,O = KClO_4.$$

BOSCH and ATEN's [14] isotopic investigations, however, did not prove this conception. According to the calculations of MARKOVITZ, BORYTA and

STEWART [15, 16], thermodynamicaly it is possible that the perchlorate is produced by the oxidation of chlorate with molecular oxygen. DODÉ and BASSET's [17] former experiments, however, in the case of sodium chlorate did not give rise to perchlorate even under 1200 atm. of oxygen at 475 °C. The result was the same when MARKOVITZ *et al.* kept the mixture of lithium chlorate and lithium chloride for several days under 100 atm. pressure of oxygen at 150 °C. Therefore they described the formation of perchlorate by assuming a reaction between atomic oxygen and chlorate:

$$MClO_3 + O = MClO_4.$$

As we can see in Table VI, the oxidation of chlorites by molecular oxygen is thermodynamically also possible. Kinetically, however, in no case of chlorites was it experienced. It may be assumed here, too, that the oxidation proceeds with the assistance of the atomic oxygen formed during the decomposition of chlorite. In this case we should take as the first step the reaction

$$MClO_2 \overset{w_1}{\rightleftharpoons} MClO + O$$

which is followed by the processes:

$$MClO \overset{w_2}{\rightleftharpoons} MCl + O$$

$$O + MClO_2 \overset{w_3}{\rightleftharpoons} MClO_3$$

$$S + O + O \overset{w_4}{\rightleftharpoons} O_2 + S.$$

(S = solid surface promoting the recombination of oxygen atoms.) However, the facts that the disproportionation of chlorites at a lower temperature occurs without gas formation, and what is more, that sodium chlorite does not decompose at all, raise some doubt about this internal oxidation mechanism.

It is true that the concentration of oxygen atoms is initially very small and so the recombination reaction is negligible. But it is difficult to explain the absence of oxygen evolution at higher temperatures when, due to the very high value of w_1, the concentration of oxygen atoms is increased. In the case of sodium chlorite, oxygen evolution was less than 1% even at such a high temperature when the disproportionation reaction occurred instantaneously. If we accept the formation of, and oxidation by, atomic oxygen, when sodium chlorite is heated up to an elevated temperature, but still below the disproportionation temperature of sodium chlorate, the oxygen atom should oxidize not only the remaining chlorite, but — to a smaller extent — the formed

chlorate, too. From pure sodium chlorite, however, even at 200, 300, 350 and 400 °C no sodium perchlorate did form. In these experiments, sodium chlorite was dropped in a pre-heated reaction tube. It is true that below 400 °C the transformation of pure sodium chlorate into perchlorate proceeds extremely slowly. The possible reason for this, according to the internal oxidation mechanism, would be that the breaking of the Cl—O bond in sodium chlorate, *i.e.* the formation of atomic oxygen, is extremely slow at this temperature. In addition, we did not find any perchlorate in the mixture of sodium chlorite and sodium chlorate (molar ratio 1 : 1) at this temperature, either.

On the basis of the above considerations it seems more acceptable that chlorate is the result of a rearrangement taking place inside the lattice without the formation of atomic oxygen. This is connected with a release of 13—30 kcal/mole heat of reaction. The transformation of chlorites can happen so that by the effect of heat, simultaneously with the vibration and the weakening of the Cl—O bond, an interaction is taking place between the oxygen and the chlorine ions of two neighbouring chlorite molecules. This state, owing to the greater thermodynamic stability of chlorate, becomes rearranged so that chlorate and chloride are formed.

Whichever mechanism is accepted, the step to be activated in the disproportionation of chlorites is obviously the rupture of the original Cl—O bond. According to the oxidation mechanism, the activation energy of the reaction should be consistent with the value of the dissociation energy of this chlorine—oxygen bond. The approximate value of it is about 60 kcal [18]. In the decomposition of chlorates and perchlorates, where this step proved to be the rate determining reaction, nearly the same activation energies were obtained [9, 11, 19]. In the present case the activation energies of the reactions were significantly smaller. In our opinion, the values of activation energy are in better agreement with a rearrangement process taking place between the chlorite ions. In this case, owing to the formation of a new Cl—O bond, evidently a smaller energy is needed for the breaking of the original Cl—O linkage. In the most favourable case ($\alpha = 1$), the value of activation energy will be equivalent to the difference between the dissociation energies of the chlorine—oxygen bonds in the two compounds.

$$E = D_{\text{dissociating}} \quad -\alpha D_{\text{forming}} \quad (\alpha = \text{constant})$$

The temperature of dispropotionation of the chlorites and the activation energy of the reaction depend to a great extent on the cation connected to the chlorite ion. To establish the stability order of the compounds, we have taken into account the value of the temperature, where the rate constant of the reaction is 1.10^{-3} (min.$^{-1}$). In this way the following order has been obtained:

$NaClO_2$ 147.4 °C; $Ba(ClO_2)_2$ 136.2 °C; $AgClO_2$ 91 °C;$Pb(ClO_2)_2$ 79.9 °C.

Considering the data in Table VI about the nature of the cations, and about the bonding and physical properties of the listed compounds, we can state that the less the ionic character of the compounds, or the greater the polarization power of the cation present, the lower is their stability.

We may deal now with the explosion of chlorites. In the case of silver chlorite it was assumed that the reaction preceding the explosion takes place according to an electron transfer process which gives rise to metallic silver and chlorine dioxide [11]. The explosion would be the result of the fast decomposition of chlorine dioxide on the surface of the solid. However, the reaction products and the activation energy calculated from the temperature dependence of the induction periods do not support this mechanism in the present case.

It should be mentioned that prior to the explosion of chlorites only an extremely small decomposition could be observed. We assumed that the absence of gas formation was due to disproportionation occurring during the induction period. The chemical analysis of the solid products obtained by interrupting the experiments immediately before the explosion proved this idea, as in barium chlorite 3—5%, and in lead chlorite about 2.5—5.5% chlorate was found. Considering that the disproportionation of chlorites is an exothermic reaction, it seems very probable that the heat developed in this process plays a significant part in the occurrence of the explosion of chlorites. Accordingly, on heating the chlorites quickly to a high temperature, the formation of chlorate sets in immediately, but because of the resulting reaction heat the rate of the disruption of the Cl—O bonds will increase to such an extent that there will be no possibility for the formation of the new Cl—O bonds, *i.e.* for the stabilization of chlorite in form of chlorate. As the reaction

$$MClO_2 = MCl + O_2$$

is much more exothermic (Table VI) than the disproportionation reaction, this may result in further acceleration of the reaction, and finally in explosion. This conception is proved by the thermal behaviour of barium chlorite and lead chlorite at a slow heating rate (1 °C/min.) (Figs 5 and 9). In these cases explosion did not occur because the dissipation of the heat of disproportionation was ensured, so the chlorite was completely transformed into chlorate. Further evidence is furnished by the measurements carried out in the presence of different inert substances. In 1 : 1 molar mixtures of barium chlorite with aluminium oxide, barium chlorate, or barium chloride, we observed no explosion, even at a heating rate of 6 °C/min. The inert substances absorbed and dissipated the heat produced by the disproportionation.

In this respect sodium chlorite is an exception, for here the disproportionation did not go into explosion even at a higher temperature when the

Table VI

Heat of reaction of different transformations of chlorites

Compound	Heat of formation, kcal/mole	ΔH_1 kcal/mole	ΔH_2 kcal/mole	ΔH_3 kcal/mole	ΔH_4 kcal/mole
$NaClO_2$	−76.65	−9.08	−13.25	−21.58	+25.19
$Ba(ClO_2)_2$	−158.2	−23.5	−31.45	−47.36	+25.2
$AgClO_2$	0.0	−5.73	−13.9	−30.36	+3.26
$Pb(ClO_2)_2$	—	—	—	—	—

$$\Delta H_1,\ MClO_2 + \frac{1}{2} O_2 = MClO_3$$

$$\Delta H_2,\ MClO_2 = \frac{2}{3} MClO_3 + \frac{1}{3} MCl$$

$$\Delta H_3,\ MClO_2 = MCl + O_2$$

$$\Delta H_4,\ 2MClO_2 = M_2O + Cl_2 + \frac{3}{2} O_2$$

reaction, and so the release of the reaction heat, occurred very quickly. The possible reason is the greater stability of sodium chlorate as compared with other chlorates. According to our recent investigations, however, the presence of certain oxides changes the direction of the reaction of sodium chlorite, and instead of the disproportionation, the explosion-like decomposition occurs [20]. The proneness to explosion of the compounds increases in the following order:

$NaClO_2$ (no explosion); $Ba(ClO_2)_2$(190° C); $AgClO_2$ (145° C); $Pb(ClO_2)_2$(112° C).

The numbers in brackets denote the lowest temperature of the explosion. This order coincides with the above-mentioned one which shows that the factors previously regarded as decisive for the stability of substances, are here also valid.

The authors wish to express their thanks to Miss Éva Berényi for her helpful assistance in the experiments.

SUMMARY

It has been shown that at lower temperatures chlorites undergo disproportionation into chlorate and chloride without any measurable decomposition. A kinetic analysis of the disproportionation reaction has been made by the first order equation, and the activation energies have been calculated. On the basis of kinetic data and some observations it was assumed that the disproportionation of chlorites occurs by rearrangement inside the lattice. At higher temperatures sodium chlorite still suffers only disproportionation, even at 400 °C, while the other compounds explode violently to give mainly chloride and oxygen. Before the explosion of the compounds only a very slight decomposition could be observed, but disproportiona-

tion occurred to some extent. The stability of the compounds depended on the cation and followed the order: Na, Ba, Ag, Pb. It is assumed that in determining the order of stability, the effective electric field strength of the cation and the ionic character of the substances play an important role.

REFERENCES

1. Levi, G. R.: Gazz. chim. ital. **45,** 177 (1915); Selecta Chimica **13,** 97 (1953)
2. Artini, E.: Atti accad. Lincei [5] 31. II. 65/1922
3. Levi, G. R.: Gazz. chim. ital. **52,** 417 (1922)
   Riolo, C.: Gazz. chim. ital. **84,** 884 (1954)
4. Taylor, M. C., White, J. F., Vincent, C. P., Cunningham, G. L.: Ind. Chem. Eng. **32,** 900 (1940)
5. Levi, G. R.: Gazz. chim. ital. **52,** 418 (1922)
6. Bodenstein, M., Harteck, P., Padelt, E.: Z. anorg. allg. Chem. **147,** 233 (1925)
7. Ditz, H.: Chem. Ztg. **25,** 727 (1901). Rupp, E.: Z. anal. Chem. **56,** 580 (1917)
8. Solymosi, F., Krix, E.: J. Catalysis **1,** 468 (1962) Solymosi, F., Révész, L.: Z. anorg. allg. Chem. **322,** 861 (1963)
9. Solymosi, F., Bánsági, T.: Acta. Chim. Hung. (In the press)
10. Levi, G. R.: Selecta Chimica **13,** 1091 (1953)
11. Solymosi, F.: Z. phys. Chem. N. F. **57,** 1 (1968)
12. Sanderson, R. T.: J. Chem. Educ. **31,** 138 (1954); **32,** 140 (1955)
13. Glasner, A., Weidenfeld, L.: J. Am. Chem. Soc. **74,** 2467 (1952)
14. Bosch, A. V., Aten, A. H. W.: J. Am. Chem. Soc. **75,** 3835 (1953)
15. Markovitz, M. M., Boryta, D. A., Stewart, H.: J. Phys. Chem. **68,** 2282 (1964)
16. Markovitz, M. M., Boryta, D. A., Stewart, H.: J. Chem. Eng. Data **9,** 573 (1964)
17. Dodé, M., Basset, J. Bull. soc. chim. [5] **2,** 344 (1935)
18. Wells, A. F.: Structural Inorganic Chemistry. p 236. (Clarendon) Oxford, 1962 Cottrell, R. L.: The Strengths of Chemical Bonds. (Butterworths) London, 1958
19. Solymosi, F.: Acta. Chim. Hung. (In the press)
20. Unpublished results

Frigyes Solymosi
Tamás Bánsági
Szeged, Rerrich tér

Acta Chimica Academiae Scientiarum Hungaricae Tomus 56 (3), pp. 271—284 (1968)

ISOTOPIC EFFECTS ON VAPOUR PRESSURE, III

DEUTERATION EFFECT ON THE VAPOUR PRESSURE OF ALCOHOLS

I. KISS, GY. JÁKLI, G. JANCSÓ and H. ILLY

(Central Research Institute for Physics, Budapest)

Received May 23, 1967

Introduction

In two earlier papers [1, 2] the results of vapour pressure measurements, first, on heavy water, second, on deuteromethanol and deuteroethanol have been reported. The vapour pressures of various deuterated alcohols, such as propanol-1 and -2, butanol-1 and -2 and 2-methyl-propanol-1, have been measured, for the propanols in the temperature range from 20° to 70 °C, and for the butanols from 20° to 80 °C, by RABINOVICH [3, 4]. The separation factor α has been determined for propanol-2 at temperatures from 40° to 82.5 °C also by EFREMOV and ZEL'VENSKII [5] who used RAYLEIGH distillation technique taking the separation factor to be equal to the vapour pressure ratio of the isotopic compounds. The values measured by the latter authors are by 7—25% lower than those reported by RABINOVICH. The narrow range of temperatures, as well as the given accuracy of these measurements, seems to be insufficient for establishing any definite features in the temperature behaviour of the isotopic effects on the vapour pressure of deuterated alcohols. In the following the results of the vapour pressure measurements on deuterated alcohols (other than methanol and ethanol) which have been already reported in brief communications [6, 7, 8] will be discussed in detail, completing the data with the results of the repeated and more recent measurements.

Experimental technique

Two methods, differing in principle, were used for the production of deuteroalcohols in order to ascertain the purity of the products in this way, too. In one of the procedures metal alcoholates prepared from alcohols purified by distillation are first hydrolyzed in 99.9 atomic % heavy water, then processed in a semi-micro rectifier (see [2, 9]). In the alternative method the alcohols are deuterated on a preparative gas chromatograph by isotope exchange technique [10, 11]. The column of the gas chromatograph is filled first with a compound containing mobile hydrogen atoms (*e.g.* diglycerol) which are exchanged with the deuterium atoms of D_2O passed through the column. These deuterium atoms are then exchanged with the hydrogen atoms of the hydroxyl groups of the alcohols passed through the column in the next step. By this procedure the OH group in each alcohol can be deuterated to 99.0 atomic %. The method, which has been described elsewhere [12] in greater detail, proved to be a simple technique for the deuteration of any organic compound with mobile hydrogen atoms. The products are of gas chromatographic purity and can be obtained in appreciable quantities (0.2—2 ml).

The deuterium content in the OD groups of the deuteroalcohols used in the experiments as evaluated from the measured refractive index of the water obtained on the combustion of the products [13, 14] or/and from mass spectrometry, was found to be higher than 99%. The data of the deuteroalcohols produced for use in the experiments are listed in Table I

Table I

Data of compounds used in the experiments

Alcohol	Refractive index, $n_D^{30°}$		Boiling point of the non-deuterated alcohol, °C
	R—OH	R—OD	
Propanol-1	1.3854	1.3843	97.8
Propanol-2	1.3776	1.3766	82.5
Butanol-1	1.3991	1.3980	117.5
Butanol-2	1.3975	1.3969	99.5
2-Methyl-propanol-2	1.3850*	1.3848*	82.9
Pentanol-3	1.4107	1.4101	116.1

*$n_D^{25°}$

The method described already in the earlier reports was used for measuring the vapour pressure difference between the deuteroalcohols and the alcohols with natural isotopic abundance. At lower temperatures and smaller pressure differences the measurements were performed with a membrane manometer [1], at higher pressure differences with a liquid differential manometer [2].

Results

The results of the comparative vapour pressure measurements are summarized in Tables II—VII. The vapour pressure data of the natural alcohols were taken from the manual of STULL [15]. No data having been reported on pentanol-3, the vapour pressure *versus* temperature curve for this compound was determined in a special run. The separation factor α which must be known for the fit to BIGELEISEN's equation [16, 17] was evaluated in each case from the natural to deuterated vapour pressure ratio by making use of the known virial coefficients in the manner described in the earlier report [2].

For propanol-2 the separation factor was evaluated from the equation

$$\ln \alpha \approx \ln \frac{P_H}{P_D} + B_0 (P_H - P_D) + 1/3\, D_0 (P_H^3 - P_D^3) \qquad (1)$$

Table II

Results for $CH_3(CH_2)_2OH$ *and* $CH_3(CH_2)_2OD$

t °C	P_H^* mm Hg	ΔP mm Hg	$10^2 \ln \frac{P_H}{P_D}$	$10^2 \ln \alpha$
4.6	5.0	0.410	8.555	
7.3	6.0	0.465	8.067	
9.3	7.0	0.560	8.344	
9.3	7.0	0.543	8.077	
11.2	8.0	0.605	7.865	
11.2	8.0	0.615	8.003	
12.9	9.0	0.665	7.697	
12.9	9.0	0.670	7.733	
14.4	10.0	0.727	7.549	
14.4	10.0	0.733	7.614	
15.8	11.0	0.790	7.485	
17.2	12.0	0.850	7.344	
18.3	13.0	0.897	7.148	
19.4	14.0	0.963	7.130	
20.4	15.0	1.020	7.047	
21.4	16.0	1.060	6.860	
21.5	16.05	1.050	6.766	
22.3	17.0	1.123	6.833	
23.2	18.0	1.183	6.796	
24.1	19.0	1.20	6.524	
24.7	20.0	1.25	6.458	
30.6	28.0	1.65	5.902	
35.4	38.7	2.10	5.582	
43.5	61.3	2.95	4.938	
44.5	65.0	3.15	4.965	
45.0	66.8	3.30	4.668	
49.0	83.2	3.70	4.546	
50.0	88.0	3.85	4.477	
51.5	95.3	4.00	4.288	
52.0	98.0	4.15	4.325	
52.1	98.5	4.20	4.355	
53.0	102.8	4.30	4.279	
55.0	113.0	4.55	4.115	
56.5	122.5	4.70	3.913	
58.0	131.5	5.10	3.952	
60.0	146.0	5.35	3.731	
60.4	148.5	5.40	3.701	

Table II (continued)

t °C	P_H* mm Hg	ΔP mm Hg	$10^2 \ln \frac{P_H}{P_D}$	$10^2 \ln \alpha$
63.0	169.0	5.95	3.586	3.546
65.1	186.5	6.55	3.576	3.534
67.0	204.0	6.95	3.470	3.426
69.4	227.0	7.20	3.228	3.185
72.0	256.0	7.90	3.034	2.960
74.0	282.0	8.05	2.898	2.853
75.0	294.0	8.70	3.005	2.957
76.0	308.0	8.80	2.898	2.850
83.4	422.0	10.95	2.626	2.571
84.7	445.0	11.00	2.499	2.445
85.0	452.0	11.10	2.489	2.435
87.0	492.0	11.30	2.323	2.269
88.2	515.0	11.80	2.313	2.257
88.6	523.0	12.10	2.343	2.286
89.4	541.0	12.35	2.313	2.256
89.5	545.0	12.75	2.372	2.313
98.0	765.0	14.30	1.882	1.823
98.0	765.0	14.65	1.932	1.871
98.2	771.0	14.75	1.931	1.870
98.3	773.0	15.20	1.990	1.927
98.3	773.0	15.00	1.961	1.899

*P_H is the vapour pressure of the non-deuterated alcohol

For the rest of the alcohols the accuracy of the reported data did not permit but the use of the equation containing only the second virial coefficient in the form

$$\ln \alpha \approx \ln \frac{P_H}{P_D} + B_0(P_H - P_D) . \qquad (2)$$

The virial coefficient of propanol-2 has been studied by several authors [18, 19, 20, 21]. The second virial coefficient was determined by Foz *et al.* [18, 19] and by Cox [21] in the temperature ranges 77 °C—125 °C and 105 °C—150 °C, respectively, while both the second and fourth virial coefficients were used by KRETSCHMER and WIEBE [20] to describe the vapour densities measured from 60 °C to 120 °C.

The data on propanol-1 and butanol-1 are known from the measurements of Foz *et al.* [18, 19] covering the temperature ranges, 77 °C—125 °C and 98 °C—125 °C, and from the experiments of Cox [21] performed in the tem-

Table III

Results for $CH_3CH(OH)CH_3$ *and* $CH_3CH(OD)CH_3$

t °C	P_H mm Hg	ΔP mm Hg	$10^2 \ln \frac{P_H}{P_D}$	$10^2 \ln \alpha$
−10.3	3.58	0.271	7.874	
−2.8	6.50	0.470	7.503	
+1.0	8.65	0.601	7.206	
2.6	9.90	0.666	6.962	
3.8	10.8	0.717	6.870	
5.2	12.1	0.785	6.711	
6.2	13.0	0.831	6.607	
8.0	15.0	0.917	6.308	
9.5	16.2	0.988	6.290	
11.2	18.2	1.070	6.062	
12.6	19.8	1.143	5.951	
15.8	24.4	1.349	5.686	
20.0	31.5	1.60	5.212	
25.0	43.0	2.00	4.767	
29.0	54.5	2.50	4.698	
34.0	73.0	3.05	4.267	
39.0	96.0	3.90	4.414	4.070
44.0	127.0	4.82	3.864	3.781
48.0	153.0	5.60	3.731	3.645
53.0	199.0	6.85	3.498	3.407
57.0	240.0	7.90	3.374	3.273
61.0	296.0	9.07	3.111	3.010
65.0	350.0	10.30	2.987	2.882
69.0	430.0	11.52	2.713	2.610
73.0	502.0	13.00	2.625	2.512
76.0	580.0	14.00	2.439	2.328
80.0	680.0	15.50	2.305	2.189
82.0	745.0	16.30	2.215	2.102
85.0	840.0	17.60	2.119	2.006
87.0	900.0	18.45	2.070	1.954
90.0	1010	19.80	1.981	1.862
93.0	1120	21.10	1.902	1.784
97.0	1305	22.50	1.736	1.617
101.0	1510	24.05	1.603	1.486

Table III (continued)

t °C	P_H mm Hg	ΔP mm Hg	$10^2 \ln \frac{P_H}{P_D}$	$10^2 \ln \alpha$
105.0	1740	25.60	1.481	1.478
109.0	1980	27.03	1.373	1.258
113.0	2250	28.35	1.271	1.158
117.0	2545	29.62	1.172	1.062
121.0	2885	30.78	1.073	0.966
125.0	3270	31.72	0.974	0.871
129.0	3665	32.58	0.896	0.797
133.0	4100	33.40	0.818	0.724

Table IV

Results for $CH_3(CH_2)_3OH$ *and* $CH_3(CH_2)_3OD$

t °C	P_H mm Hg	ΔP mm Hg	$10^2 \ln \frac{P_H}{P_D}$	$10^2 \ln \alpha$
2.1	1.134	0.101	9.986	
4.0	1.321	0.113	9.624	
6.15	1.65	0.147	9.350	
35.0	13.4	0.82	6.299	
40.0	18.3	1.05	5.923	
45.0	24.7	1.32	5.449	
50.0	33.0	1.65	5.166	
55.0	44.0	2.10	4.880	
60.0	59.0	2.60	4.498	
65.0	77.0	3.20	4.210	
70.0	99.0	3.80	3.828	3.822
75.0	128.0	4.45	3.537	3.499
80.0	164.0	5.05	3.247	3.207
85.0	207.0	6.00	2.957	2.913
90.0	258.0	6.50	2.665	2.620
95.0	318.0	7.40	2.469	2.422
97.5	350.0	7.90	2.372	2.324

Table V

Results for $CH_3CH(OH)CH_2CH_3$ *and* $CH_3CH(OD)CH_2CH_3$

t °C	P_H mm Hg	ΔP mm Hg	$10^2 \ln \frac{P_H}{P_D}$	$10^3 \ln \alpha$
+0.7	3.00	0.197	6.727	
6.0	4.30	0.267	6.412	
8.4	5.42	0.363	6.200	
10.5	6.27	0.394	6.061	
11.8	6.90	0.387	5.804	
13.1	7.60	0.420	5.688	
14.9	8.65	0.470	5.596	
15.4	9.00	0.486	5.543	
17.0	10.0	0.536	5.504	
18.6	11.2	0.580	5.343	
25.0	16.9	0.800	4.480	
30.0	23.7	1.10	4.786	
35.0	32.2	1.40	4.498	
40.0	44.0	1.70	3.922	
45.0	58.0	2.00	3.537	
50.0	77.0	2.40	3.151	
55.0	100.0	3.00	3.054	3.021
60.0	128.0	3.65	2.960	2.923
65.0	165.0	4.40	2.664	2.623
70.0	212.0	5.15	2.469	2.491
75.0	267.0	5.90	2.275	2.228
80.0	333.0	6.75	2.079	2.029
85.0	415.0	7.65	1.882	1.830
90.0	510.0	8.60	1.686	1.631
95.0	620.0	9.70	1.577	1.520
100.0	790.0	10.60	1.347	1.289
105.0	940.0	11.75	1.273	1.214
110.0	1120	12.65	1.140	1.080
115.0	1360	13.50	0.995	0.936
120.0	1620	14.10	0.868	0.811
125.0	1900	14.60	0.769	0.713
130.0	2240	15.00	0.670	0.617
135.0	2600	15.20	0.571	0.520
140.0	3000	15.00	0.500	0.454
145.0	3500	14.60	0.428	0.386
150.0	4100	13.50	0.329	0.292

Table VI

Results for $(CH_3)_3COH$ *and* $(CH_3)_3COD$

t °C	P_H mm Hg	ΔP mm Hg	$10^2 \ln \frac{P_H}{P_D}$	$10^2 \ln \alpha$
30.7	58.0	2.75	4.859	4.819
35.5	78.0	3.40	4.449	4.408
41.0	107.0	4.30	4.104	4.052
43.0	120.0	4.70	3.995	3.940
45.0	133.0	5.10	3.903	3.846
49.0	164.0	5.85	3.634	3.573
51.5	188.0	6.35	3.436	3.373
54.0	210.0	6.95	3.362	3.296
56.9	243.0	7.70	3.217	3.147
60.1	280.0	8.60	3.111	3.038
61.5	300.0	8.90	3.015	2.941
65.0	348.0	9.80	2.860	2.783
68.4	410.0	10.95	2.704	2.623
72.3	480.0	11.90	2.508	2.425
75.6	550.0	12.75	2.344	2.260
77.6	600.0	13.50	2.275	2.190
81.2	700.0	14.60	2.107	2.014
84.4	800.0	15.60	1.941	1.852
88.9	955.0	16.90	1.785	1.696
91.6	1050	17.60	1.686	1.596
95.0	1190	18.45	1.559	1.461
99.0	1360	19.50	1.442	1.356
103.6	1600	20.50	1.283	1.197
107.6	1820	21.30	1.184	1.100
110.2	2000	22.00	1.103	1.019
110.6	2030	21.60	1.016	0.934
116.0	2420	22.00	0.917	0.840
122.6	2950	20.70	0.698	0.633
125.2	3250	20.50	0.629	0.566
128.0	3550	18.65	0.518	0.464

perature ranges 105 °C—150 °C and 120 °C—166°, respectively. The latter determined the second virial coefficient also for butanol-2 and 2-methylpropanol-2 at temperatures between 105 °C and 150 °C. For lack of literary data on pentanol-3, the values obtained for other alcohols were extrapolated, and it was found that the correction could not be more than 1% of the value of $\ln P_H/P_D$, thus α was taken to be equal to the vapour pressure

Table VII

Results for $CH_3CH_2CH(OH)CH_2CH_3$ *and* $CH_3CH_2CH(OD)CH_2CH_3$

t °C	P_H mm Hg	ΔP mm Hg	$10^2 \ln \frac{P_H}{P_D} = 10^2 \ln \alpha$
24.8	6.50	0.22	3.441
24.8	6.50	0.28	4.403
29.8	9.80	0.33	3.422
29.8	9.80	0.39	4.058
34.8	13.8	0.50	3.692
34.8	13.8	0.45	3.314
39.8	19.6	0.61	3.160
44.8	27.2	0.78	2.909
49.8	37.0	1.00	2.743
54.8	49.9	1.22	2.480
59.8	65.0	1.44	2.245
64.8	85.0	1.67	1.981
69.8	110.0	1.94	1.785
74.8	140.0	2.22	1.598
79.8	175.0	2.55	1.469
84.8	220.0	2.89	1.301
89.8	282.0	3.27	1.163
94.8	350.0	3.77	1.085

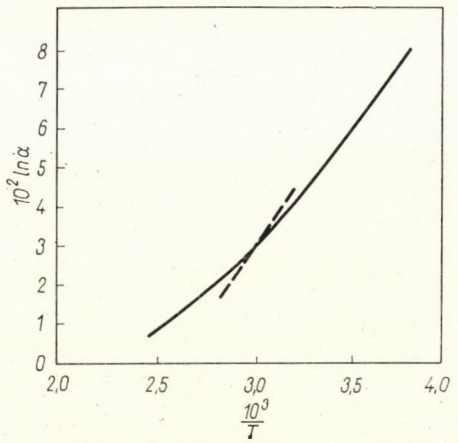

Fig. 1. Comparison of vapour pressure data for the isotopic pair $CH_3CH(OH)CH_3$–$CH_3CH(OD)CH_3$: ——— Efremov and Zel'venskii [5]; —— present authors

ratio of the isotopic compounds. The values of the virial coefficients used in the calculations are listed in Table VIII, while those of $\ln \alpha$ calculated from

Table VIII

The virial coefficients of alcohols

Alcohols	log (—RTB$_0$)*	References
Propanol-1	12.491—3.7 log T	[21]
Butanol-1	14.711—4.5 log T	[21]
Butanol-2	14.678—4.5 log T	[21]
2-Methyl-propanol-2	15.359—4.8 log T	[21]
Propanol-2	log [300 + 0.755 exp (2483/T)] log (—RTD$_0$) = log [—2.70×10^{-5} + + 3.16×10^{-15} exp (9215/T)]	[20]

* The equation of state is: $PV/RT = 1 + B_0P + D_0P^3$

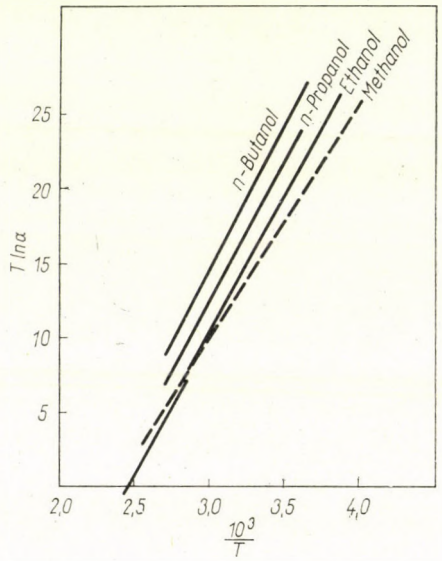

Fig. 2. Effect of deuterium substitution on the vapour pressure of primary alcohols

the measured vapour pressure differences with the use of Eqs (1) and (2) are to be seen in Tables II—VII. (No correction was applied at lower temperatures, where the correction is known to be less than 1% of ln P_H/P_D.) Our results could not be compared with those of RABINOVICH, because of the discrepancy between the data in the figure and the equations formulated for the description of the results [3, 4]. The comparison with the results of EFREMOV and ZEL'VENSKII [5] for propanol-2 in Fig. 1 shows a satisfactory agreement considering the different measuring techniques used.

Discussion

The values of the separation factor obtained from the measured data were fitted by least squares to BIGELEISEN's equation [16, 17] (see [2])

$$\ln \alpha = \frac{A}{T^2} - \frac{B}{T} . \qquad (3)$$

The values of the constants A and B in Eq. (3) for each of the alcohols investigated are given in Table IX. To illustrate the variation of the isotopic effect with the order of the alcohol, the diagrams plotted in the form T ln α *vs.* reciprocal temperature are shown separately for each order of alcohol in Figs 2, 3 and 4.

Fig. 2 shows that for primary alcohols, with the exception of methanol, the isotopic effects yield nearly parallel straight lines. Though the values of A in Eq. (3) exhibit a slight variation with the alcohol (molecular weight), as it is apparent from Table IX, those of B remain unaltered within the experimental error.

Table IX

Values of the constants A and B in Eq. (3) for the alcohols investigated

Alcohols		$A \cdot 10^{-2}$	$\sigma_A \cdot 10^{-2}$*	B	σ_B*
Ethanol**	between −15 and +78 °C	183.43	0.49	44.45	0.12
	between 78 and 140 °C	179.6	5.9	43.96	0.22
n-Propanol		190.15	0.99	44.39	0.22
n-Butanol		198.4	3.3	44.80	0.40
Isopropanol		138.3	1.7	31.33	0.26
sec-Butanol		138.6	2.1	31.94	0.29
Pentanol-3		128.5	3.2	31.15	0.39
Methanol**		160.39	0.48	38.03	0.17
t-Butanol		157.1	2.4	37.19	0.30

* σ_A and σ_B denote the standard errors in the values of A and B
** see the previous publication [2]

In Fig. 3 the vapour pressures of three types of secondary alcohol isotope pairs are compared. The slope of the curves characterizing the secondary alcohols is seen to be different from that of the primary alcohols. The values

of A show again some dependence on the molecular weight, while those of B arising from the zero-point energy shift of the internal frequencies on condensation, do not change and thus, like in the case of primary alcohols, B is a characteristic value of secondary alcohols.

The curves plotted for the isotopic effects on the vapour pressure of methanol and tertiary butanol are shown in Fig. 4. It is apparent that they are similar in shape, as can be inferred also from data in Table IX. This seems to be due to the similar molecular symmetries of these compounds.

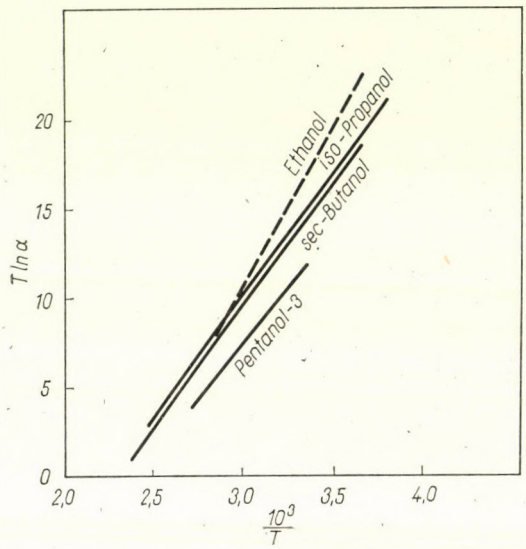

Fig. 3. Effect of deuterium substitution on the vapour pressure of secondary alcohols

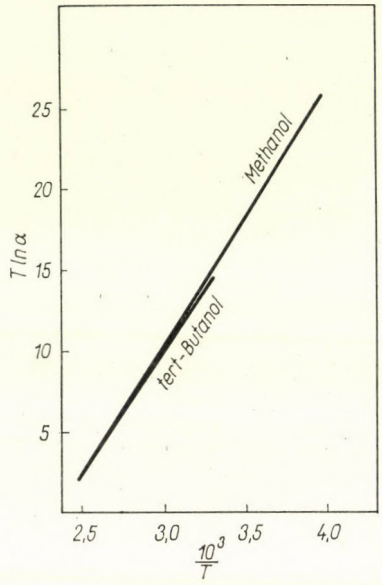

Fig. 4. Effect of deuterium substitution on the vapour pressure of methanol and *t*-butanol

The results definitely show that there is a close relationship between the molecular structure of the compound and the extent to which the temperature behaviour of the isotopic effect on vapour pressure is affected by the hindered molecular translation and rotation of the liquid molecules and by the shift of the internal vibrational frequencies. In the case of alcohols the isotopic effect is above all a function of the order of the alcohol pair involved, while for methanol and tertiary butanol it seems to be determined by the molecular symmetry.

Making use of our knowledge of the molecular physics of alcohols and, in particular, of their IR spectra, an attempt was made at the interpretation of the data obtained by the comparative vapour pressure measurements. It turned out, however, that the minimum necessary data for the calculations we wanted to perform were available only for methanol and ethanol [22—30];

even those were uncertain as it could be seen from the calculations of the heats of vaporization made by us for ethanol and deuteroethanol [31], and by RABINOVICH for methanol and deuteromethanol [4]. For the other alcohols the problem is not only the lack of some data (particulary, on the hindered translation and rotation of the alcohol molecules in the liquid phase), but also the not yet unambiguous interpretation of the various bands appearing in the spectra of these compounds (see [22—30] and [32—41]).

Nevertheless, at least some qualitative analogy can be established between the observed isotopic effect on vapour pressure and the differences between the IR spectra of the alcohols of different orders and those of their derivatives deuterated at the hydroxyl group.

The hindered rotation of the OH-group in the vapour phase of alcohol is reflected by the factor A in Eq. (3). It is of interest to note here that in the case of primary and secondary alcohols the potential field of the hindered rotation of the OH group is asymmetric, while for methanol and tertiary butanol, for which the isotopic effect was observed to be of similar magnitude, this potential field is symmetric [42, 43, 44]. The spectra also show that the isotopic shifts of the OH in-plane deformation frequencies in methanol and tertiary butanol differ from that observed in other alcohols. Moreover, the doublet appearing for the OH in-plane deformation frequencies (in the liquid phase) for primary and secondary alcohols, does not show up in the spectra of methanol and tertiary butanol. Similarly, the coupling of the C—O and C—C vibrations is almost negligible in the primary, much stronger in the secondary and the most apparent in the tertiary alcohols.

The evaluation of the constants in Eq. (3) and a satisfactory explanation of the order-dependence of the vapour pressure differences in the case of alcohols require the knowledge of more data. It is mainly a better understanding of the molecular motions of the alcohols in the liquid phase which is expected to be of help in the quantitative interpretation of the vapour pressure differences.

SUMMARY

The differences between the vapour pressures of propanol-1, propanol-2, butanol-1, butanol-2, 2-methyl-propanol-2, pentanol-3 and their derivatives deuterated at the hydroxyl group have been determined over a wide range of temperatures. Using the experimental data and the virial equation for alcohol vapours, the distillation separation factor α was evaluated for each pair of isotopic compounds and fitted by the method of least squares to BIGELEISEN's equation, $\ln \alpha = \frac{A}{T^2} - \frac{B}{T}$ Considering both the present and the earlier [2] data, it seems that the value of constant B, determined by the zero-point energy shift of the internal vibrations on condensation, depends either on the order of the alcohol or on the molecular symmetry.

REFERENCES

1. KISS, I., JÁKLI, GY., ILLY, H.: Acta Chim. Acad. Sci. Hung. **47,** 379 (1966)
2. KISS, I., JÁKLI, GY., JANCSÓ, G.: Acta Chim. Acad. Sci. Hung. **51,** 65 (1967)
3. RABINOVICH, I. B.: Usp. Khim. **31,** 101 (1962)

4. RABINOVICH, I. B.: Vodorodnaja svyaz. Ed. Sokolov and Chulanovskii, Moscow, 1964
5. EFREMOV, A. A., ZEL'VENSKII, YA. D.: Zhur. Vsesoyuz. Khim. Obshchestva im. D. I. Mendeleeva, **6**, 359 (1961)
6. KISS, I., JÁKLI, GY.: Dritte Arbeitstagung über stabile Isotope, Leipzig, 1963. Abh. d. D. Akademie d. Wissenschaften Kl. für Chemie, Geologie und Biologie 1964, No. 7. 107
7. KISS, I., JANCSÓ, G., JÁKLI, GY., ILLY, H.: Vierte Arbeitstagung über stabile Isotope, Leipzig, 1965
8. KISS, I., JÁKLI, GY., JANCSÓ, G., ILLY, H.: Conference on Some Aspects of Physical Chemistry, No. 1. Vol. IV. p. 567. Budapest, 1966
9. JÁKLI, GY., JANCSÓ, G., ILLY, H.: KFKI Közlemények **13**, 235 (1965)
10. KISS, I., JANCSÓ, G., JÁKLI, GY., ILLY, H., POROS, K.: Vierte Arbeitstagung über stabile Isotope, Leipzig, 1965
11. JANCSÓ, G., JÁKLI, GY., ILLY, H., KISS, I., POROS, K.: I. Magkémiai Szimpozium, Debrecen, 1965
12. KISS, I., JANCSÓ, G., JÁKLI, GY., ILLY, H., POROS, K.: J. of Labelled Compounds **3**, 411 (1967)
13. KIRSHENBAUM, J.: Physical Properties of Heavy Water. McGraw-Hill Co., New York, 1951
14. ROLLE, W.: see [6] p. 447
15. STULL, D. R.: Ind. Eng. Chem. **39**, 517 (1947)
16. BIGELEISEN, J.: J. Chem. Phys. **34**, 1485 (1961)
17. BIGELEISEN, J.: J. chim. Phys. **60**, 35 (1963)
18. FOZ, MARCILLO, MENDEZ: Anal. Fis. Quim. **50**, 17 (1954)
19. FOZ, MARCILLO, MASIÁ, MENDEZ: Anal. Fis. Quim. **50**, 23 (1954)
20. KRETSCHMER, C. B., WIEBE, R.: J. Am. Chem. Soc. **76**, 2579 (1954)
21. COX, J. D.: Trans. Far. Soc. **67**, 1674 (1961)
22. FALK, M., WHALLEY, E.: J. Chem. Phys. **34**, 1554 (1961)
23. PIMENTAL, G. C., MCCLELLAN, A. L.: The Hydrogen Bond. (Freeman and Co.) San Francisco—London, 1960
24. MACLOU, M., HENRY, M. L.: Compt. rend. **244**, 1494 (1965)
25. MACLOU, M., CORVAL, M.: J. chim. Phys. **60**, 1044 (1963)
26. STUART, A. V., SUTHERLAND, G. B. B. M.: J. Chem. Phys. **24**, 559 (1956)
27. QUINAN, J. R., WIBERLEY, S. E.: Anal. Chem. **26**, 1762 (1954)
28. STUART, A. V., SUTHERLAND, G. B. B. M.: J. Chem. Phys. **20**, 1977 (1952)
29. TARTE, P., DEPONTHIERE, R.: Bull. soc. chim. Belg. **66**, 525 (1957)
30. PLYLER, E. K.: J. Res. Natl. Bur. Standards **48**, 281 (1952)
31. JANCSÓ, G.: KFKI Közlemények **14**, 219 (1966)
32. NORTHER, H. D.: J. Chem. Phys. **10**, 693 (1942)
33. DAVIES, M. M.: J. Chem. Phys. **16**, 267 (1948)
34. BORDEN, A., BARKER, E. F.: J. Chem. Phys. **6**, 553 (1938)
35. QUINAN, J. R., WIBERLEY, S. E.: J. Chem. Phys. **21**, 1896 (1953)
36. THOMPSON: J. Chem. Soc. **1948**, 328
37. TANAKA, C., KURATANI, K., MIZUSHIMA, S. I.: Spectrochim. Acta **9**, 265 (1957)
38. TARTE, P., DEPONTHIÈRE, R.: J. Chem. Phys. **26**, 962 (1957)
39. SMITH, F. A., CREITZ, E. C.: J. Res. Natl. Bur. Standards **46**, 145 (1951)
40. TANAKA, C.: Nippon Kagaku Zasshi **81**, 1042 (1960); **83**, 398, 521, 792 (1962)
41. HERZBERG, G.: Molecular spectra and molecular structure, II. D. van Nostrand Company, Inc., Toronto—New York—London, 1954
42. BARROW, G. M.: J. Chem. Phys. **20**, 1739 (1952)
43. ASTON, J. G., ISSEROW, S., SZASZ, G. J., KENNEDY, R. M.: J. Chem. Phys. **12**, 336 (1944)
44. HALFORD, J. O.: J. Chem. Phys. **17**, 111 (1949)

István KISS
György JÁKLI
Gábor JANCSÓ
Hedy ILLY

Budapest XII., Konkoly Thege-út

Acta Chimica Academiae Scientiarum Hungaricae Tomus 56 (3), pp. 285—296 (1968)

ON THE PARAMETER FORM OF FORCE CONSTANT MATRIX, V*

THE MAXIMUM AND MINIMUM VALUES OF FORCE CONSTANTS

F. TÖRÖK and P. PULAY

(Institute of General and Inorganic Chemistry. L. Eötvös University, Research Group for Inorganic Chemistry of the Hungarian Academy of Sciences, Budapest)

Received June 17, 1967

The number of spectroscopical data available is usually not sufficient for the determination of force constants of molecules. In most cases it is only in the knowledge of the normal frequencies that the force field has to be determined. Although, in this case, the elements of force constant matrices F [1] cannot be determined unambiguously, it does not mean that they can possess any arbitrary value.

Useful information concerning the force field of molecules can be obtained by investigating the minimum and maximum values (*i.e.* the extreme values) of the elements of force constant matrices, reproducing normal frequencies. To solve this problem, a method based on an analogue computer has been elaborated, applicable only for small molecules [2]. For the extreme values a rather rough estimation can be easily obtained by FADINI's method [3], but with a similarly restricted sphere of applicability.

In our previous papers [4, 5, 6, 7] we have dealt with a parametrical representation of matrices F reproducing the normal frequencies. By this method, in principle, it is possible to determine analytically the parameters giving maximum or minimum values to a prescribed element of F. It is, however, a very clumsy way of solving this problem, since in order to find the extreme values it is necessary to solve a non-linear equation system which consists of $\binom{n}{2}$ equations constructed by making the partial derivatives of the considered force constant with respect to the parameters equal to zero.

Another possibility of finding the extreme values is "mapping" of the force field with the help of the parameter method, *i.e.* the calculation of force constant matrices by a digital computer, with some systematically varied parameter values. It is, however, obviously impractical to examine all the possible F matrices, and it is sufficient to content ourselves with examining the force constants belonging to a given assignment. In a previous work [7] we have shown that the assignment belonging to the zero point of the parameter space is defined by the sequence of the rows of matrices G and A. When

* Part IV: Acta Chim. Acad. Sci. Hung. 52, 49 (1967)

investigating the matrices F belonging to a fixed assignment, we choose the parameters from the $\frac{\pi}{4}$ region of zero point, *i.e.*

$$-\frac{\pi}{4} \leq \alpha_{ij} \leq \frac{\pi}{4} \qquad (i < j = 2, \ldots, n).$$

In Table I the map of the E_g species of ethane is shown. The normal frequencies, with the approximative assignments in brackets, are as follows:

$$\nu_1 = 2950 \text{ cm}^{-1} \text{ (CH asym. stretch.)}$$
$$\nu_2 = 1469 \text{ cm}^{-1} \text{ (CH asym. bend.)}$$
$$\nu_3 = 1190 \text{ cm}^{-1} \text{ (CH}_3 \text{ rock.)}$$

The data are from DUNCAN's paper [8]. The values of parameters from the $\left[-\frac{\pi}{4}, \frac{\pi}{4}\right]$ region have been modified in each step by adding 0.1π. In Table I the parameter values are given in π radian units, hence, *e.g.*, $0.25 = \pi/4$. Considering the difficulties of the theoretical analysis of the distribution of local minimum and maximum values, this method gives a reliable, and at same time, an illustrative picture of the force field of the molecule, and of the distribution of the extreme values of force constants. Nevertheless, it is obvious that this process is also unapplicable to a problem of higher order. For, if we are to solve a problem of order n and to determine the force constants at 10 values of each parameter, we ought to calculate $10^{\binom{n}{2}}$ F matrices.

For solving the problem we have found an iteration method the most convenient, when starting from a point of the parameter space, the parameters giving the nearest local maximum or minimum value to the given force constant can be reached. As it can be seen from Table I containing the force constants of ethane, highly improbable values may also occur among the elements of F matrices of a given assignment. So a further restriction of the region to be examined is desirable. This is possible in most cases, since some force constants are known to have their value in a fairly narrow range, leaving only those of the others uncertain. Therefore, with the help of the parameter representation, a method has been developed enabling us to find the extreme values of some of the force constants, on the condition that the others remain within prescribed limits. The essential features of our method can be summarized as follows.

Let the independent elements of the force constant matrix and the parameters be the components of a vector f of order $\binom{n+1}{2}$ and the elements of a vector a of order $\binom{n}{2}$, respectively. Because of their advantages in

numerical calculations, the antisymmetric parameters described in [6] were used. The parameter form of force constants can be written briefly $f = f(a)$. Our task is to find the extreme value of one of the elements of f on the condition that

$$l_j \leq f_j \leq u_j \quad j = 1, 2 \ldots, \binom{n+1}{2} \tag{1}$$

where l_j and u_j are the lower and upper limits for f_j, respectively.

For the sake of simplicity it has been assumed that for each element of f, minimum and maximum values are known. If such limits are not at our disposal, we can take for example, $l = -100$ and $u = 100$, as it is certain that the absolute value of no force constant can be greater than 100.

To be more definite, let us suppose that the maximum of f_i is to be found. For this a slightly simplified version of the gradient projection method elaborated by ROSEN [9] was applied. The essence of this method is to change the parameters in small steps, starting from a point of parameter space in such a way that f_i should increase at the highest possible rate, with the inequality system (1) remaining valid. The choice of the starting point has been discussed in detail in another paper [6].

Let the vector d be the gradient of f_i, *i.e.*

$$d_k = \frac{\partial f_i}{\partial a_k} .$$

The calculation of the derivatives has also been given elsewhere [6]. The increase of f_i is the greatest if the next step is made in the direction of vector d, *i.e.*

$$a = Nd \tag{2}$$

where the normalization constant N is necessary since, because of the non-linearity of the function $f_i(a)$, small steps only can be made. In our program, N was chosen so that $|a| = 0.01$ to 0.05.

By changing the parameters in the direction defined by Eq. (2), some of the inequalities may be violated. Let the force constants for which the prescribed restrictions have been violated be

$$f_{k_1}, f_{k_2}, \cdots, f_{k_m}$$

Let us build matrix M having the $\mu\nu$ element

$$M_{\mu\nu} = \pm \frac{\partial f_{k\mu}}{\partial a_\nu} \qquad \begin{matrix} \mu = 1, 2, \ldots, m \\ \nu = 1, 2 \ldots, \binom{n}{2} \end{matrix} \tag{3}$$

Table I

The map of the E_g species of ethane

The force constants belong to the simmetry coordinates defined in [8] with the difference that the bending coordinates are scaled by bond length $r_{CH} = 1.102$Å consequently the dimension of all the force constants is mdyn/Å

Parameters			f (11)	f (12)	f (13)	f (22)	f (23)	f (33)
—.25	—.25	—.25	1.642	— .606	— .935	821	.535	2.011
—.25	—.25	—.15	1.687	— .547	— .962	.814	.578	1.954
—.25	—.25	—.05	1.777	— .510	— .941	.785	.627	1.923
—.25	—.25	.05	1.877	— .511	— .879	.746	.663	1.928
—.25	—.25	.15	1.948	— .549	— .800	.711	.671	1.968
—.25	—.25	.25	1.964	— .609	— .735	.695	.650	2.027
—.25	—.15	—.25	2.334	—1.024	— .721	1.071	.361	1.185
—.25	—.15	—.15	2.391	— .977	— .737	1.075	.401	1.102
—.25	—.15	—.05	2.470	— .948	— .702	1.062	.453	1.055
—.25	—.15	.05	2.540	— .949	— .629	1.035	.497	1.061
—.25	—.15	.15	2.575	— .978	— .545	1.004	.515	1.118
—.25	—.15	.25	2.562	—1.025	— .484	.983	.501	1.204
—.25	—.05	—.25	2.883	—1.335	— .100	1.244	— .057	.793
—.25	—.05	—.15	2.944	—1.298	— .095	1.259	— .029	.698
—.25	—.05	—.05	3.002	—1.275	— .044	1.261	.017	.644
—.25	—.05	.05	3.037	—1.275	.033	1.249	.064	.651
—.25	—.05	.15	3.033	—1.297	.107	1.226	.094	.716
—.25	—.05	.25	2.993	—1.334	.150	1.203	.094	.814
—.25	.05	—.25	3.094	—1.422	.688	1.268	— .563	.985
—.25	.05	—.15	3.147	—1.388	.717	1.290	— .551	.897
—.25	.05	—.05	3.177	—1.366	.780	1.305	— .514	.846
—.25	.05	.05	3.172	—1.365	.855	1.309	— .468	.852
—.25	.05	.15	3.133	—1.385	.911	1.298	— .430	.913
—.25	.05	.25	3.076	—1.419	.929	1.278	— .414	1.005
—.25	.15	—.25	2.906	—1.252	1.345	1.126	— .962	1.688
—.25	.15	—.15	2.939	—1.212	1.391	1.149	— .964	1.621
—.25	.15	—.05	2.932	—1.186	1.458	1.175	— .940	1.584
—.25	.15	.05	2.888	—1.184	1.522	1.194	— .899	1.589
—.25	.15	.15	2.823	—1.208	1.558	1.198	— .857	1.636
—.25	.15	.25	2.762	—1.247	1.552	1.187	— .830	1.706
—.25	.25	—.25	2.408	— .889	1.625	.866	—1.098	2.633
—.25	.25	—.15	2.413	— .837	1.673	.886	—1.108	2.596
—.25	.25	—.05	2.368	— .804	1.732	.918	—1.095	2.576
—.25	.25	.05	2.289	— .802	1.778	.950	—1.064	2.580
—.25	.25	.15	2.206	— .832	1.796	.971	—1.026	2.607
—.25	.25	.25	2.152	— .883	1.776	.971	— .997	2.647

Table I (cont.)

Parameters			f (11)	f (12)	f (13)	f (22)	f (23)	f (33)
—.15	—.25	—.25	2.171	— .567	—1.153	.608	.278	2.006
—.15	—.25	—.15	2.156	— .507	—1.200	.624	.315	1.947
—.15	—.25	—.05	2.192	— .448	—1.207	.612	.367	1.911
—.15	—.25	.05	2.266	— .413	—1.170	.576	.416	1.911
—.15	—.25	.15	2.350	— .416	—1.104	.530	.441	1.947
—.15	—.25	.25	2.412	— .454	—1.033	.491	.434	2.005
—.15	—.15	—.25	3.184	— .901	— .853	.718	.165	1.185
—.15	—.15	—.15	3.192	— .855	— .889	.741	.201	1.100
—.15	—.15	—.05	3.229	— .812	— .884	.740	260	1.048
—.15	—.15	.05	3.281	— .788	— .839	.714	.318	1.048
—.15	—.15	.15	3.327	— .792	— .773	.674	.353	1.100
—.15	—.15	.25	3.351	— .823	— .710	.634	.352	1.184
—.15	—.05	—.25	3.944	—1.146	— .068	.796	— .115	.802
—.15	—.05	—.15	3.967	—1.112	— .078	.827	— .086	.705
—.15	—.05	—.05	3.995	—1.085	— .055	.838	— .030	.645
—.15	—.05	.05	4.019	—1.075	— .008	.825	.031	.645
—.15	—.05	.15	4.029	—1.084	.045	.793	.075	.705
—.15	—.05	.25	4.022	—1.111	.084	.754	.084	.802
—.15	.05	—.25	4.175	—1.202	.900	.807	— .458	1.003
—.15	.05	—.15	4.194	—1.176	.920	.843	— .441	.913
—.15	.05	—.05	4.201	—1.162	.961	.866	— .393	.857
—.15	.05	.05	4.195	—1.165	1.007	.867	— .333	.857
—.15	.05	.15	4.178	—1.185	1.040	.846	— .284	.913
—.15	.05	.25	4.155	—1.214	1.048	.810	— .265	1.003
—.15	.15	—.25	3.802	—1.042	1.684	.740	— .732	1.712
—.15	.15	—.15	3.798	—1.016	1.727	.779	— .725	1.644
—.15	.15	—.05	3.774	—1.010	1.778	.812	— .689	1.602
—.15	.15	.05	3.738	—1.028	1.817	.827	— .637	1.602
—.15	.15	.15	3.705	—1.062	1.831	.818	— .589	1.643
—.15	.15	.25	3.686	—1.099	1.813	.788	— .564	1.711
—.15	.25	—.25	2.980	— .720	1.986	.614	— .827	2.657
—.15	.25	—.15	2.941	— .688	2.035	.654	— .828	2.619
—.15	.25	—.05	2.879	— .687	2.083	.695	— .805	2.595
—.15	.25	.05	2.818	— .716	2.113	.723	— .766	2.595
—.15	.25	.15	2.780	— .766	2.113	.726	— .726	2.619
—.15	.25	.25	2.781	— .817	2.083	.703	— .701	2.657

Table I (cont.)

Parameters			f (11)	f (12)	f (13)	f (22)	f (23)	f (33)
—.05	—.25	—.25	2.535	— .329	—1.242	.450	— .012	2.029
—.05	—.25	—.15	2.473	— .291	—1.304	.488	.013	1.969
—.05	—.25	—.05	2.449	— .231	—1.338	.499	.063	1.929
—.05	—.25	.05	2.471	— .173	—1.330	.478	.118	1.924
—.05	—.25	.15	2.532	— .139	—1.285	.435	.157	1.956
—.05	—.25	.25	2.607	— .142	—1.218	.384	.165	2.012
—.05	—.15	—.25	3.707	— .472	— .904	.467	— .047	1.206
—.05	—.15	—.15	3.680	— .444	— .955	.507	— .018	1.120
—.05	—.15	—.05	3.673	— .403	— .979	.522	.039	1.063
—.05	—.15	.05	3.688	— .363	— .969	.506	.105	1.056
—.05	—.15	.15	3.721	— .340	— .928	.465	.154	1.103
—.05	—.15	.25	3.757	— .343	— .871	.415	.166	1.185
—.05	—.05	—.25	4.562	— .583	— .044	.482	— .158	.815
—.05	—.05	—.15	4.558	— .567	— .066	.524	— .132	.716
—.05	—.05	—.05	4.561	— .546	— .073	.544	— .072	.651
—.05	—.05	.05	4.568	— .528	— .060	.534	— .001	.644
—.05	—.05	.15	4.577	— .520	— .034	.497	.052	.698
—.05	—.05	. 25	4.584	— .525	— .004	.449	.069	.792
—.05	.05	—.25	4.775	— .610	1.009	.485	— .306	1.005
—.05	.05	—.15	4.776	— .603	1.020	.530	— .285	.913
—.05	.05	—.05	4.775	— .603	1.035	.556	— .230	.852
—.05	.05	.05	4.772	— .609	1.048	.553	— .162	.845
—.05	.05	.15	4.770	— .619	1.054	.521	— .107	.895
—.05	.05	.25	4.768	— .629	1.051	.474	— .086	.984
—.05	.15	—.25	4.271	— .532	1.854	.473	— .433	1.705
—.05	.15	—.15	4.252	— .531	1.891	.520	— .419	1.635
—.05	.15	—.05	4.234	— .549	1.922	.552	— .374	1.588
—.05	.15	.05	4.223	— .578	1.934	.556	— .315	1.582
—.05	.15	.15	4.223	— .607	1.924	.530	— .264	1.620
—.05	.15	.25	4.235	— .626	1.894	.485	— .242	1.686
—.05	.25	—.25	3.245	— .368	2.166	.447	— .485	2.646
—.05	.25	—15	3.191	— .369	2.213	.496	— .479	2.606
—.05	.25	—.05	3.146	— .400	2.248	.533	— .447	2.578
—.05	.25	.05	3.128	— .450	2.259	.543	— .403	2.574
—.05	.25	.15	3.142	— .498	2.241	.524	— .363	2.594
—.05	.25	.25	3.184	— .528	2.201	.481	— .342	2.632

Table I (cont.)

Parameters			f (11)	f (12)	f (13)	f (22)	f (23)	f (33)
.05	—.25	—.25	2.587	.008	—1.197	.417	— .318	2.079
.05	—.25	—.15	2.512	.011	—1.265	.466	— .306	2.020
.05	—.25	—.05	2.442	.049	—1.321	.497	— .265	1.977
.05	—.25	.05	2.405	.109	—1.343	.498	— .210	1.967
.05	—.25	.15	2.414	.168	—1.324	.470	— .162	1.994
.05	—.25	.25	2.466	.202	—1.270	.422	— .140	2.047
.05	—.15	—.25	3.701	.092	— .873	.423	— .270	1.246
.05	—.15	—.15	3.665	.091	— .931	.470	— .252	1.159
.05	—.15	—.05	3.626	.116	— .982	.498	— .200	1.099
.05	—.15	.05	3.600	.158	—1.007	.496	— .134	1.087
.05	—.15	.15	3.597	.201	— .995	.465	— .078	1.128
.05	—.15	.25	3.617	.228	— .952	.416	— .054	1.207
.05	—.05	—.25	4.499	.134	— .032	.424	— .201	.830
.05	—.05	—.15	4.493	.126	— .064	.471	— .179	.731
.05	—.05	—.05	4.482	.133	— .098	.496	— .122	.661
.05	—.05	.05	4.470	.153	— .122	.490	— .050	.648
.05	—.05	.15	4.462	.178	— .127	.456	.007	.697
.05	—.05	.25	4.461	.198	— .110	.407	.030	.789
.05	.05	—.25	4.671	.128	1.002	.423	— .140	.992
.05	.05	—.15	4.676	.111	1.004	.468	— .118	.897
.05	.05	—.05	4.681	.098	.993	.491	— .060	.831
.05	.05	.05	4.684	.094	.971	.483	.009	.819
.05	.05	.15	4.685	.100	.949	.446	.065	.865
.05	.05	.25	4.682	.114	.934	.396	.085	.951
.05	.15	—.25	4.143	.087	1.836	.421	— .110	1.668
.05	.15	—.15	4.137	.061	1.866	.465	— .089	1.596
.05	.15	—.05	4.145	.027	1.875	.486	— .039	1.544
.05	.15	.05	4.163	— .000	1.859	.475	.022	1.533
.05	.15	.15	4.185	— .012	1.824	.437	.070	1.567
.05	.15	.25	4.203	— .002	1.783	.386	.087	1.633
.05	.25	—.25	3.111	.038	2.147	.419	— .118	2.601
.05	.25	—.15	3.077	.003	2.190	.463	— .103	2.558
.05	.25	—.05	3.076	— .048	2.210	.483	— .064	2.527
.05	.25	.05	3.107	— .097	2.200	.471	— .018	2.519
.05	.25	.15	3.160	— .124	2.164	.432	.019	2.537
.05	.25	.25	3.213	— .119	2.116	.381	.032	2.574

Table I (cont.)

Parameters			f (11)	f (12)	f (13)	f (23)	f (23)	f (33)
.15	—.25	—.25	2.313	.307	—1.018	.531	— .618	2.151
.15	—.25	—.15	2.261	.273	—1.083	.576	— .621	2.094
.15	—.25	—.05	2.176	.278	—1.153	.617	— .593	2.050
.15	—.25	.05	2.092	.319	—1.201	.639	— .545	2.037
.15	—.25	.15	2.041	.380	—1.210	.633	— .495	2.060
.15	—.25	.25	2.041	.439	—1.174	.601	— .463	2.109
.15	—.15	—.25	3.170	.568	— .752	.609	— .497	1.303
.15	—.15	—.15	3.155	.539	— .811	.652	— .491	1.217
.15	—.15	—.05	3.109	.539	— .882	.686	— .451	1.155
.15	—.15	.05	3.050	.569	— .937	.697	— .391	1.139
.15	—.15	.15	3.001	.618	— .956	.681	— .335	1.175
.15	—.15	.25	2.981	.666	— .931	.644	— .303	1.250
.15	—.05	—.25	3.784	.728	— .020	.649	— .258	.850
.15	—.05	—.15	3.798	.699	— .057	.690	— .243	.750
.15	—.05	—.05	3.790	.691	— .115	.714	— .193	.677
.15	—.05	.05	3.763	.708	— .173	.714	— .127	.659
.15	—.05	.15	3.727	.742	— .207	.688	— .070	.704
.15	—.05	.25	3.695	.782	— .206	.647	— .045	.793
.15	.05	—.25	3.903	.733	.896	.641	.003	.966
.15	.05	—.15	3.934	.698	.890	.678	.027	.870
.15	.05	—.05	3.957	.678	.852	.693	.082	.800
.15	.05	.05	3.964	.679	.799	.681	.147	.783
.15	.05	.15	3.951	.702	.749	.646	.198	.825
.15	.05	.25	3.925	.737	.722	.602	.215	.911
.15	.15	—.25	3.469	.587	1.647	.595	.189	1.608
.15	.15	—.15	3.498	.542	1.668	.626	.216	1.532
.15	.15	—.05	3.540	.506	1.653	.631	.269	1.477
.15	.15	.05	3.580	.492	1.608	.609	.327	1.461
.15	.15	.15	3.602	.505	1.551	.567	.369	1.493
.15	.15	.25	3.597	.541	1.503	.522	.378	1.559
.15	.25	—.25	2.630	.354	1.942	.531	.231	2.528
.15	.25	—.15	2.643	.297	1.976	.558	.254	2.483
.15	.25	—.05	2.694	.244	1.978	.555	.297	2.448
.15	.25	.05	2.763	.216	1.947	.524	.343	2.436
.15	.25	.15	2.824	.223	1.895	.477	.374	2.453
.15	.25	.25	2.854	.263	1.841	.432	.379	2.490

Table I (cont.)

Parameters			f (11)	f (12)	f (13)	f (22)	f (23)	f (33)
.25	—.25	—.25	1.828	.441	— .708	.757	— .891	2.241
.25	—.25	—.15	1.827	.384	— .763	.786	— .906	2.187
.25	—.25	—.05	1.764	.354	— .838	.824	— .893	2.143
.25	—.25	.05	1.664	.362	— .905	.856	— .857	2.128
.25	—.25	.15	1.564	.405	— .938	.870	— .811	2.147
.25	—.25	.25	1.503	.467	— .925	.861	— .774	2.193
.25	—.15	—.25	2.330	.764	— .529	.961	— .715	1.374
.25	—.15	—.15	2.355	.718	— .583	.991	— .721	1.290
.25	—.15	—.05	2.327	.695	— .666	1.021	— .695	1.227
.25	—.15	.05	2.256	.704	— .745	1.040	— .648	1.208
.25	—.15	.15	2.168	.742	— .792	1.039	— .597	1.241
.25	—.15	.25	2.099	.794	— .787	1.020	— .563	1.313
.25	—.05	—.25	2.695	.969	.019	1.072	— .334	.874
.25	—.05	—.15	2.745	.929	— .019	1.100	— .325	.774
.25	—.05	—.05	2.754	.910	— .095	1.119	— .287	.700
.25	—.05	.05	2.719	.920	— .179	1.122	— .233	.680
.25	—.05	.15	2.652	.954	— .240	1.107	— .186	.721
.25	—.05	.25	2.581	.999	— .254	1.080	— .161	.808
.25	.05	—.25	2.767	.977	.730	1.054	.103	.935
.25	.05	—.15	2.833	.937	.715	1.076	.126	.837
.25	.05	—.05	2.877	.918	.655	1.081	.174	.764
.25	.05	.05	2.881	.926	.574	1.068	.228	.744
.25	.05	.15	2.844	.960	.502	1.041	.268	.784
.25	.05	.25	2.780	1.005	.466	1.011	.279	.869
.25	.15	—.25	2.500	.785	1.330	.922	.431	1.532
.25	.15	—.15	2.572	.738	1.338	.934	.462	1.454
.25	.15	—.05	2.643	.714	1.300	.925	.513	1.394
.25	.15	.05	2.686	.722	1.230	.897	.563	1.376
.25	.15	.15	2.685	.758	1.155	.861	.593	1.406
.25	.15	.25	2.640	.809	1.103	.832	.592	1.473
.25	.25	—.25	1.978	.467	1.585	.732	.524	2.437
.25	.25	—.15	2.046	.410	1.608	.735	.555	2.388
.25	.25	—.05	2.137	.378	1.590	.712	.600	2.350
.25	.25	.05	2.215	.383	1.538	.672	.640	2.336
.25	.25	.15	2.251	.424	1.472	.631	.662	2.352
.25	.25	.25	2.231	.484	1.417	.604	.655	2.391

In Eq. (3) the positive sign is valid, if $f_k \leq u_k$ has been violated, and the minus sign if it is the inequality $f_k \geq l_k$. Let I be the unit matrix of order $\binom{n}{2}$. ROSEN defines the direction

$$a' = N/I - M' \, (MM')^{-1} M/d. \tag{4}$$

He has shown that when making a small step in this direction ("small" means that the functions f_i(a) may be considered linear), the values of $f_{k_1}, f_{k_2}, \ldots f_{k_m}$ do not change, while that of f_i increases at the highest possible rate allowed by this condition. Geometrically, this means that a step is made on the surface of the region defined by (1).

The demand that the value of $f_{k_1}, f_{k_2}, \ldots f_{k_m}$ should remain unchanged is sometimes unnecessarily rigorous. ROSEN proved that if the vector $(MM')^{-1} M/d$ has negative components, one row corresponding to the index of one of the negative components (*e.g.*, to the index of the negative one with the greatest absolute value) can be omitted from matrix M. The inequality system (1) remains valid moving in the direction

$$a^* = N/I - M^{*\prime}(M^* M^{*\prime})^{-1} M^*/d \tag{5}$$

defined by matrix M^* formed from M as described above. In this case, the force constant belonging to the omitted row will change, but within the prescribed limits.

It is to be noted that because the inequality system (1) is non-linear in the function of the parameters, by stepping in directions (4) or (5) the conditions (1) may be violated to a slight extent. To overcome this a special correctional method has been elaborated by ROSEN. As only small steps are allowed in our program, the error originating from the non-linearity is negligible.

This process may end in three ways:

(*i*) It may lead to a local maximum, which is indicated by the decrease of f_i as compared to the previous steps.

(*ii*) The number of rows of matrix M^* equals $\binom{n}{2}$. Then $a^* = 0$, and the extreme value belongs to the parameters which are in a vertex of the region allowed.

(*iii*) The upper limit u_i prescribed for f_i has been reached. Naturally, in this case no further information is obtained.

To illustrate our method, again the E_g species of ethane was chosen, for which reliable force constants were given by DUNCAN on the basis of the *Hybrid Orbital Force Field* method. For the sake of comparison his results are included in Table II. It is to be noted that in our work the bending internal coordinates were scaled with the bond length $r_{CH} = 1.102$ Å, and therefore DUNCAN's original data were converted correspondingly.

Table II

Minimum and maximum values of force constants in the E_g species of ethane
(All values in mdyn/Å)

	Duncan	A				B			
		l	*u*	min.	max.	*l*	*u*	min.	max.
F_{11}	4.714	4.6	5.0	4.60	4.81	4.6	5.0	4.60	4.84
F_{12}	−0.069	−0.5	0.0	−0.50	0.00	−1.0	1.0	−0.94	0.30
F_{13}	0.069	0.0	0.5	0.00	0.50	−1.0	1.0	−0.11	1.00
F_{22}	0.456	0.0	0.8	0.32	0.53	0.0	0.8	0.32	0.70
F_{23}	0.010	−0.2	0.2	−0.20	0.05	−0.6	0.6	−0.38	0.11
F_{33}	0.675	0.0	1.0	0.63	0.99	0.0	1.0	0.63	1.00

Two condition systems, designated by A and B, were used. In both cases the diagonal force constants were restricted in the same way, but in case A the signs of F_{12} and F_{13} were constrained according to the prescriptions of Hoff, and it was assumed that $|F_{23}| \leq 0.2$. In case B only the milder restrictions $|F_{12}| \leq 1$, $|F_{13}| \leq 1$ and $|F_{23}| \leq 0.6$ were made.

The upper and lower limits as well as the results are summarized in Table II. It can be seen from the Table that for a considerable number of force constants, *e.g.*, for F_{22}, F_{23} and F_{33}, a fairly narrow range can be found on the basis of plausible restrictions alone. It is very significant that even with the very mild restrictions B, F_{12} is negative or slightly positive, while F_{13} may have only positive or slightly negative values, confirming the validity of the Hoff model, according to which F_{12} is negative and F_{13} is positive.

SUMMARY

By the parameter representation, described earlier, all the force constant matrices, compatible with the experimental frequencies, can be built. When the experimental data are insufficient to determine the force field unambiguously, an iterattion method has been worked out, which permits the finding of the maximum and minimum values of force constants in agreement with the experimental data. According to our experience, if the frequencies are the only experimental data, very improbable maximum or minimum values may occur, even in a prescribed assignment. In practice, however, the probable limits of a number of force constants are known, and only the maximum and minimum values of the others are to be determined. Our computer program, based on the parameter method, makes it possible to find the maximum and minimum values of the latter constants, with the values of the former ones being kept within the prescribed limits.

REFERENCES

1. Wilson, E. B., Decius, J. C., Cross, P. C.: Molecular Vibrations. McGraw-Hill Book Company, New York, 1955
2. Lehmann, W. J., Beckmann, L., Gutjahr, L., Mecke, R.: Spectroscopia Molecular **14**, 160 1965)

3. FADINI, A.: Z. für Naturforsch. **21a,** 425 (1966)
4. PULAY, P., TÖRÖK, F.: Acta Chim. Acad. Sci. Hung. **44,** 287 (1965)
5. PULAY, P., TÖRÖK, F.: Acta Chim. Acad. Sci. Hung. **47,** 273 (1965)
6. PULAY, P.: Acta Chim. Acad. Sci. Hung. **52,** 49 (1967)
7. TÖRÖK, F.: Acta Chim. Acad. Sci. Hung. **52,** 205 (1967)
8. DUNCAN, J. L.: Spectrochim. Acta **20,** 1197 (1964)
9. ROSEN, J. B.: J. Soc. Industrial and Applied Mathematics **8,** 181 (1960); **9,** 514 (1961)

Ferenc TÖRÖK
Péter PULAY
Budapest VIII., Múzeum krt. 6/8.

Acta Chimica Academiae Scientiarum Hungaricae Tomus 56 (3), pp. 297—301 (1968)

SIMULTANEOUS POSITIVE AND NEGATIVE DEVIATIONS FROM THE IDEAL BEHAVIOUR IN THE SYSTEM OF TWO VOLATILE COMPONENTS

(SHORT COMMUNICATION)

Gy. VARSÁNYI

(Department of Physical Chemistry, Technical University, Budapest)

Received November 21, 1967

The relation of positive and negative deviations from the ideal behaviour of two volatile components is usually discussed on thermodynamic basis. The relation is furnished by the DUHEM-MARGULES equation. A modified form of this equation is as follows:

$$x_1 \frac{\partial \ln \gamma_1}{\partial x_1} = -x_2 \frac{\partial \ln \gamma_2}{\partial x_1} \tag{1}$$

If the activity coefficients have no extreme value in the whole concentration range, then, in case of a positive deviation of component 1, $\partial \ln \gamma_1 / \partial x_1$ must be negative and consequently, $\partial \ln \gamma_2 / \partial x_1$ must be positive over the whole concentration range. When rational activity coefficients are used, γ_1 has to equal 1 when $x_1 = 1$; at other values of x it has to be greater than 1 in case of a positive deviation. On the other hand, if $\partial \ln \gamma_2 / \partial x_1$ is positive and γ_2 equals 1 in case of $x_1 = 0$, component 2 can also show positive deviation only. As a matter of fact, a similar reasoning may be applied in the case of mutual negative deviations.

However, all this proves the simultaneous positive and negative deviations of the two components only if the activity coefficients have no extreme value in the whole concentration range. On the other hand, it is a well-known fact that, at a given concentration, the activity coefficients of dilute electrolytes have a minimum, as it can also be concluded from the DEBYE-HÜCKEL theory. According to equation (1), this means that at this concentration the activity coefficient of the solvent must have a maximum. As the differently defined activity coefficients are proportional to each other, in dilute solutions, this statement has to be valid for the rational activity coefficients. This means that in dilute solutions of the electrolytes, which show a negative deviation from the ideal behaviour nearly over the whole concentration range, the solvent must be of positive deviation, contrarily to the solute. The rational activity coefficient of the solvent equals 1 when $x_0 = 1$ (x_0 is the molar fraction of the solvent); afterwards it increases when x_0 begins to decrease. This is also con-

firmed by the DUHEM-MARGULES equation: the activity coefficient of the solute decreases with the increase of the molar fraction in this range.

Fig. 1 shows the vapour pressure diagram of aqueous hydrochloric acid within the limits of solubility at 25 °C [1]. The straight line representing ideal behaviour is also shown in the diagram. Measured vapour pressure data are available only for hydrochloric acid solutions more concentrated than 3 mole-%. The

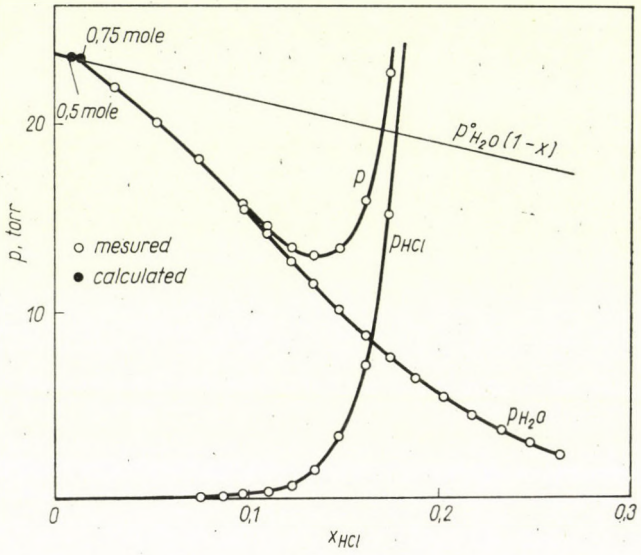

Fig. 1

minimum of the activity coefficient of HCl is found at 0.9 mole-%; consequently, the maximum of the activity coefficient of H_2O must be assumed at this concentration. The rational activity coefficients of water can be calculated from the concentration-dependence of the mean activity coefficient of hydrochloric acid. (Fig. 2). As maximal activity coefficient 1.0003 is obtained in 0.5 *M* solution which means, however, an unmeasurably low deviation from the ideal behaviour. The partial vapour pressure curve of water intersects the ideal straight line at 0.75 molality. In the case of polyvalent electrolytes the positive deviation of water becomes more significant. For example in sulfuric acid [2] (Fig. 3) the maximum of the activity coefficient of water is found at 1.75 molality, with a value of 1.0065.

In connection with the experimental observability of the phenomenon it has to be pointed out that the boiling point elevation, freezing point depression, and osmotic pressure measured in dilute solutions of strong electrolytes are lower than may be expected for complete dissociation in the case of ideal solutions, — this being a time-honoured empirical fact. The osmotic coefficient

f_0 defined in connection with this phenomenon is generally lower than 1 [3]. As

$$f_0 \equiv 1 + \frac{\ln \gamma_0}{\ln x_0} \tag{2}$$

when $f_0 < 1$, then necessarily $\gamma_0 > 1$.

A descriptive explanation has been given, for deviations equally positive for both components. (The case of mutual negative deviations is obvious.) For example, the positive deviation for both components in a dilute aqueous

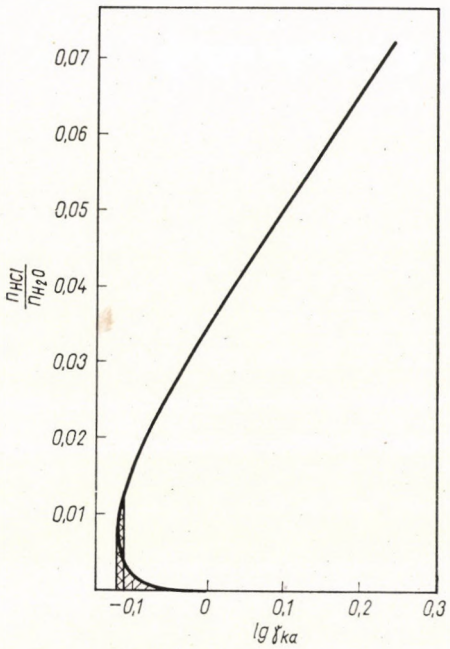

Fig. 2

solution of alcohol can be interpreted, as for the alcohol, with the fact that the strongly associating molecules of water quasi "crowd out" the alcohol molecules. The deviation has to be positive at the same time with regard to the water, since the association is decreased by the alcohol molecules inserted in between the strongly associating water molecules. In the case of dilute electrolyte solutions, the positive deviation of water from the ideal behaviour can be interpreted by the hydrated ions similarly "crowding out" the water molecules. The negative deviation of the solute can readily be explained by the hydration itself. The difference between the two "crowding-out" effects in dilute solution is as follows: in the case of mutual positive deviations the solute is "crowded-out" by the solvent, in the case of simultaneous positive and negative deviation this is done inversely.

At certain concentrations the positive deviation of the solvent turns into negative; for example, the partial vapour pressure curve intersects the ideal straight line. At this point, the two opposite effects, the "crowding out" Coulomb forces and the ion—dipole forces producing solvation, compensate each other. With the decrease of the inter-ionic distance, the latter forces prevail, as they increase more rapidly than the Columb forces. In the case of multiple charged ions, the intersection shifts towards more concentrated solutions. This is expressed in the DEBYE-HÜCKEL theory and it is congruent with the experience according to which the minimum of the activity coefficient of polyvalent electrolytes appears in more concentrated solutions, than that of

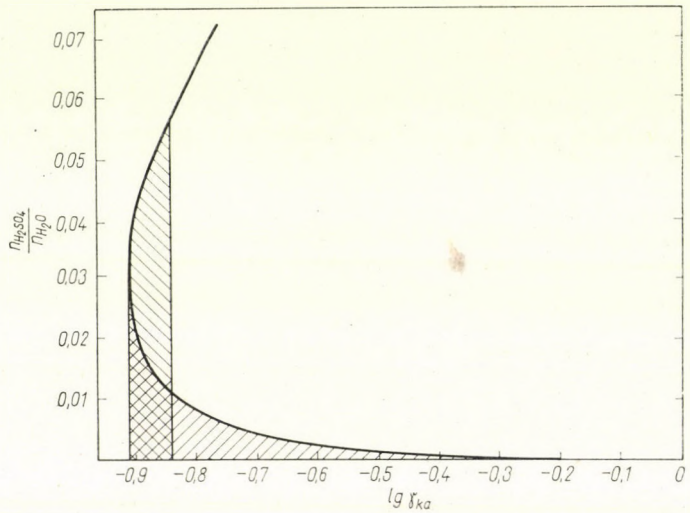

Fig. 3

univalent ions. In the case of hydrochloric acid, at the critical 0.75 molal concentration the average interionic distance amounts approximately to 10 Å. If the ions were positioned in an ideal cubic lattice, at most two water molecules could be located along the imaginary axis between the Cl^-, and H_3O^+ ions, and considering a deformed lattice, even less. Thus, at this concentration no regular ionic spheres can be expected. In other words, the ions cannot be surrounded by so many water molecules as they could be in regular hydrates.

At the same concentration of polyvalent ions the lattice is obviously even more deformed, as a consequence of stronger ion—ion interaction, therefore the hydrate spheres are even less complete. This is the reason why it is only at concentrations higher than the former that the ion—dipole interaction leading to negative deviation, can compensate the ion—ion interaction, which causes a positive deviation by crowding out the solvent. One may calculate for example that in 3 *M* sulfuric acid solution, corresponding to

the intersection of the partial vapour pressure of water with the ideal straight line, the average distance between the SO_4^{2-} and H_3O^+ ions in an undeformed lattice amounts approximately to 6Å, of which more than 4Å are occupied by the ions themselves. This means that at such a concentration there is no longer room for a water molecule in the axis of the ions.

REFERENCES

1. PERRY, S. H.: Chemical Engineers' Handbook. McGraw-Hill, New York, 1950
2. CONWAY, B. E.: Electrochemical Data. Elsevier, Amsterdam, 1952
3. HARNED, H. S., OWEN, B. B.: The Physical Chemistry of Electrolytic Solutions. Reinhold, New York, 1958. p. 259

György VARSÁNYI; Budapest XI., Műegyetem rkp. 3.

Acta Chimica Academiae Scientiarum Hungaricae Tomus 56 (3), pp. 303—306 (1968)

HERSTELLUNG VON 7-KETO-STEROIDVERBINDUNGEN

G. MAGYAR und P. BITE

(Institut für Arzneimittelforschung, Budapest)

Eingegangen am 29. Mai 1967

KLYNE [1] hat aus 3 beta-Acetoxy-delta-5-pregnen-20-on die entsprechende 7-Keto-Verbindung durch Oxydation in Eisessig hergestellt. Da die 7-Keto-steroidverbindungen mannigfaltige biologische Wirkungen aufweisen [2], schien es uns zweckmäßig zu sein, aus der Schlüsselsubstanz der Stereoidindustrie, dem 3 beta-Acetoxy-delta-5,16-pregnadien-20-on (**I**) auch die 7-Keto-Verbindung herzustellen, um diese zu weiterem chemischem Umbau zu benützen.

Das Derivat 3 beta-Acetoxy-delta-5,16-pregnadien-7,20-dion wurde mit der aus der Steroidliteratur bekannten Methode unmittelbar aus 3 beta-Acetoxy-delta-5,16-pregnadien-20-on durch warme Eisessig-Chromsäureoxydation gewonnen.

Wir stellten es jedoch auch her, indem wir beim Abbau von *Solasodin* [3] die Oxydation bei Siedetemperatur und in Anwesenheit eines erheblich größeren Überschusses von Chromsäureanhydrid durchführten. Im letzteren Fall läßt sich das Rohprodukt umständlicher und mit niedrigerer Ausbeute gewinnen.

Aus I konnten wir, nach einer von uns früher mitgeteilten Methode [4], die Verbindung delta 3,5,16-Pregnatrien-7,20-dion herstellen (**IV**).

Aus **I** und aus durch Desacetylierung von **I** gewonnenem **II** wurden die salpetersauren Salze der 20-Guanylhydrazone (**V** und **VI**) hergestellt.

Das aus der Verbindung **II** hergestellte salpetersaure Salz (**VI**) von 20-Guanylhydrazon weist nach den Untersuchungen unserer Pharmakologischen Abteilung eine cytostatische Wirkung auf.

Beschreibung der Versuche

(Schmelzpunkte unkorrigiert)

3-beta-Acetoxy-delta-5,16-pregnadien-7,20-dion (I)

a) Aus 3 beta-Acetoxy-delta-5,16-pregnadien-20-on

5 g (0,014 Mol) 3 beta-Acetoxy-delta-5,16-pregnadien-20-on wurden nach KLYNE [1] in 200 ml Eisessig gelöst, die Lösung wurde auf 55 °C erwärmt und mit einem aus 4 g (0,04 Mol) Chromsäureanhydrid, 4 ml Wasser und 40 ml Eisessig bestehenden Gemisch während 40

Minuten unter ständigem Rühren tropfenweise versetzt und noch eine weitere Stunde bei 55 °C gehalten. Nach dem Abkühlen wurde der Überschuß von Chromsäure mit Natriumhydrogensulfit zerstört, und dann das erkaltete Gemisch mit Wasser auf das vierfache Volumen gebracht. Das ausgeschiedene Öl wurde in Benzol aufgenommen, die Lösung mit Natriumhydrogencarbonat-Lösung behandelt, mit Wasser gewaschen und danach mit Natriumsulfat getrocknet. Nach Filtrieren und Eindampfen der Lösung wog das Rohprodukt 2,7 g, Schmp. 190—200 °C. Nach dreimaligem Umkristallisieren aus Methanol erhielten wir das analysenreine Produkt vom Schmp. 219—222 °C. $[\alpha]_D = -101°$ (c = 1, Chloroform), λ max 236 mμ (log ε: 6,41). Im IR-Spektrum der Verbindung liegt die Bande $\nu_{C=O\ (Ester)}$ bei 1740 cm^{-1}, das konjugierte $\nu_{C=O}$ ist bei 1670 cm^{-1}, während die konjugierten Banden $\nu_{C=C}$ bei 1635 bzw. 1600 cm^{-1} sind.

$C_{23}H_{30}O_4$ (370,44) Ber. C 74,56; H 8,15%
Gef. C 74,48; H 8,33%

b) Aus Solasodin

10 g (0,033 Mol) *Solasodin* wurden in 45 ml wasserfreiem Triäthylamin und 5 ml (0,05 Mol) Essigsäureanhydrid gelöst und eine halbe Stunde lang bis zum Sieden erhitzt. Danach wurde die Lösung im Vakuum zur Trockne eingedampft, der Rückstand kalt in 100 ml Eisessig gelöst und die Lösung eine halbe Stunde lang gekocht. Nach Abkühlung wurde die Lösung bei 16—25 °C mit einem aus 4,8 g (0,048 Mol) Chromsäureanhydrid, 4 ml Wasser und 40 ml Eisessig bestehenden Gemisch während 10 Minuten tropfenweise versetzt, danach eine Stunde bei Raumtemperatur stehen gelassen. Nach Ablauf dieser Zeit wurde die einmal kalt oxydierte Lösung unter Rückfluß gekocht und mit einem zweiten Oxydationsgemisch, bestehend aus 8 g Chromsäureanhydrid, 6 ml Wasser und 60 ml Eisessig, nachoxydiert. Danach wurde die Lösung noch eine Stunde gekocht. Das erkaltete Gemisch wurde in Wasser von dreifachem Volumen gegossen und mit Benzol durchgeschüttelt. Die benzolische Lösung wurde mit Wasser, Natriumhydrogencarbonat-Lösung und wieder mit Wasser neutral gewaschen, getrocknet, dann filtriert. Das Rohprodukt wog 5,65 g; es wurde aus 15 ml Methanol umkristallisiert: Ausbeute 1,85 g, Schmp. 198—203 °C. Hierauf wurde das Produkt viermal aus Methanol umkristallisiert. So erhielten wir 0,6 g Reinprodukt vom Schmp. 219—222 °C. Die Verbindung erwies sich mit dem aus 3-beta-Acetoxy-delta-5,16-pregnadien-20-on hergestellten, 7,20-Dion als vollständig identisch. Sie zeigte mit letzterem keine Schmelzpunktdepression und auch die IR-Spektren waren identisch.

$C_{23}H_{30}O_4$ (370,44) Ber. C 74,56; H 8,15%
C 74,6; H 8,05%

3 beta-Oxy-delta-5,16-pregnadien-7,20-dion (II)

10 g (0,027 Mol) 3 beta-Acetoxy-delta-5,16-pregnadien-7,20-dion wurden in 660 ml Methanol gelöst und mit einer Lösung von 9 g (0,09 Mol) Kaliumhydrogencarbonat in 56 ml Wasser versetzt. Das Gemisch wurde zwei Stunden lang gekocht, dann auf das halbe Volumen eingedampft und nach dem Erkalten bei Raumtemperatur stehen gelassen, wobei sich bald ein kristalliner Niederschlag bildete. Dieser wurde abgesaugt und das Rohprodukt aus Methanol kristallisiert. Das 3,22 g wiegende Reinprodukt hatte einen Schmp. von 238—242 °C. Im IR-Spektrum der Verbindung erscheint die Bande von $\nu_{C=O\ (Ester)}$ erwartungsgemäß nicht bei 1740 cm^{-1}, statt dessen liegt die Bande von ν OH bei 3450 cm^{-1}.

$C_{21}H_{28}O_3$ (328,4) Ber. C 76,88; H 8,6%
Gef. C 76,58; H 8,55%

3 beta-Tosyloxy-delta-5,16-pregnadien-7,20-dion (III)

Es wurden 2,15 g (0,0065 Mol) 3 beta-Oxy-delta-5,16-pregnadien-7,20-dion in 10 ml abs. Pyridin warm gelöst. Die klare Lösung wurde mit 2,15 g (0,012 Mol) p-Toluolsulfonsäurechlorid versetzt und das Gemisch einen Tag lang bei Zimmertemperatur stehengelassen. Dann wurde die Lösung in Wasser gegossen und der entstandene Niederschlag nach kurzem Stehen

filtriert. Die Substanz wurde mit Wasser neutral gewaschen und getrocknet. Das Rohprodukt wurde dreimal aus Aceton umkristallisiert. Das Reinprodukt schmolz bei 154—156 °C.

$C_{28}H_{34}O_5$ (482,52) Ber. C 69,69; H 7,09; S 6,63%
Gef. C 69,72; H 7,16; S 6,39%

delta-3,5,16-Pregnatrien-7,20-dion (IV)

2,11 g (0,0045 Mol) 3 beta-Tosyloxy-delta-5,16-pregnadien-7,20-dion (Schmp. 154—156 °C) wurden in 40 ml Dimethylformamid gelöst, das 2 g Kaliumjodid enthielt, dann 5 Stunden lang auf 100—110 °C erwärmt. Nach dem Erkalten wurde die Lösung in Wasser gegossen, der entstandene Niederschlag abgesaugt, mit Wasser neutral gewaschen und getrocknet. Das Rohprodukt wog 1,25 g und schmolz bei 140—152 °C. Es wurde durch dreimaliges Umkristallisieren aus Methanol gereinigt, worauf der Schmp. des Reinproduktes auf 196—198 °C stieg.

$C_{21}H_{26}O_2$ (310,4) Ber. C 81,25; H 8,4%
Gef. C 81,14; H 8,66%

Salpetersaures Salz des Guanidylhydrazons des 3 beta-Acetoxy-delta-5,16-pregnadien-7,20-dions (V)

1,6 g (0,004 Mol) 3 beta-Acetoxy-delta-5,16-pregnadien-7,20-dion (Schmp. 216—220 °C) wurden in 50 ml Methanol warm gelöst, und mit einer Lösung von 1,6 g (0,0011 Mol) Aminoguanidinnitrat in 25 ml warmem Methanol versetzt. Hierauf wurden noch 25 ml Methanol zugegeben und das Gemisch wurde rasch zum Sieden erhitzt. Nach kurzer Zeit setzte in der klaren Lösung Kristallisation ein. Nach dreitägigem Stehen bei Zimmertemperatur wurde der entstandene Niederschlag abgesaugt; er wog 1,26 g, Schmp. 210—217 °C. Das Produkt erwies sich als Ausgangsmaterial. Die Mutterlauge wurde auf das halbe Volumen eingedampft und bei 0 °C aufbewahrt. Es entstand ein 0,35 g wiegendes, weißes, kristallines Produkt, das unter Zersetzung bei 255—260 °C schmolz. Dieses Rohprodukt wurde aus 7 ml Äthanol und 7 ml Wasser umkristallisiert. Das analytisch reine Produkt wog 0,15 g, Schmp. (unter Zersetzung) 258—263 °C. Das IR-Spektrum der Verbindung zeigte die Banden von νNH bei 3500 und 3000 cm^{-1}, die Bande von $\nu_{C=O\ (Ester)}$ bei 1740 cm^{-1}, während die Banden von $\nu_{C=O}$ und Guanidyl zusammenfallend bei 1680 und 1630 cm^{-1} erschienen.

$C_{24}H_{35}O_6N_5$ (489,5) Ber. C 58,88; H 7,2; N 14,4%
Gef. C 59,3; H 7,5; N 14,5%

Salpetersaures Salz des Guanidylhydrazons des 3 beta-Oxy-delta-5,16-pregnadien-7,20-dions (VI)

Es wurden 1,4 g (0,0042 Mol) 3 beta-Oxy-delta-5,16-pregnadien-7,20-dion in 50 ml Methanol gelöst und mit der Lösung von 1,8 g (0,013 Mol) Aminoguanidinnitrat in 25 ml Methanol versetzt. Die Lösung wurde drei Tage lang bei 0 °C aufbewahrt. Der entstandene Niederschlag wurde abgesaugt und die Mutterlauge auf das halbe Volumen eingedampft, dann einige Tage lang stehen gelassen. Die ausgeschiedenen Kristalle wurden filtriert und getrocknet. Das Rohprodukt schmolz (unter Zersetzung) bei 254—256 °C. Nach dreimaligem Umkristallisieren aus Methanol-Wasser (2 : 1) schmolz das Reinprodukt (unter Zersetzung) bei 269—272 °C. Im IR-Spektrum erschienen die Banden von ν OH und ν NH bei 3500 und 3000 cm^{-1}, die Banden von νC = O und Guanidyl zusammenfallend bei 1680 und 1630 cm^{-1}.

$C_{22}H_{35}O_5N_5$ (447,5) Ber. C 59,04; H 7,5; N 15,66%
Gef. C 58,44; H 8,2; N 15,23%

Die IR-Spektren (in KBr) wurden mit einem »Zeiss« UR-10 Spektrometer aufgenommen.

Verfasser sind der *Analytischen Abteilung* (Leiter: A. Mizsei) und *Pharmakologischen Abteilung* (Leiter: Dr. J. Borsy) des Institutes für die ausgeführten Untersuchungen, Frau Dr. G. Villányi-Barsi für ihre wertvolle Hilfe bei der Aufarbeitung der Literatur und Frau L. Balázs-Nagy für ihre technische Hilfe bei den Versuchen zu besonderem Dank verpflichtet.

ZUSAMMENFASSUNG

Durch Oxydation von 3 beta-Acetoxy-delta-5,16-pregnadien-20-on bzw. durch eine warme Nachoxydation des kalt oxydierten, beim Abbau von Solasodin entstandenen pseudo-Diacetylsolasodins wurde das 3 beta-Acetoxy-delta-5,16-pregnadien-7,20-dion hergestellt. Aus diesem konnten die folgenden Derivative erhalten werden: 3 beta-Oxy-delta-5,16-pregnadien-7,20-dion, 3 beta-Tosyloxy-delta-5,16-pregnadien-7,20-dion und delta-3,5,16-Pregnatrien-7,20-dion. Es wurden außerdem die salpetersauren Salze der 3 beta-Acetoxy- und 3 beta-Oxy-delta-5,16-pregnadien-7,20-dion-guanidylhydrazone hergestellt.

LITERATUR

1. KLYNE, W.: J. Chem. Soc. (London) **1951,** 3450.
2. MARSHALL, C. W., RAY, R. E., LAOS, I., RIEGEL, B.: J. Am. Chem. Soc. **79,** 6303 (1957), J. Am. Chem. Soc. **79,** 6308 (1957).
3. MAGYAR, GY.: Acta Chim. Acad. Sci. Hung. **25,** 321 (1960).
4. BITE, P., MAGYAR, GY.: Acta Chim. Acad. Sci. Hung. **48,** 255 (1966).

György MAGYAR
Pál BITE
} Budapest IV., Újpest, P.O.Box 82.

Acta Chimica Academiae Scientiarum Hungaricae Tomus 56 (3), pp. 307—310 (1968)

BROMINE ADDITION TO SOME UNSATURATED SULPHONES

SP. SHANMUGANATHAN and D. SRI RAMA RAO

(Department of Chemistry, Pachaiyappa's College, Madras-30, India)

Received July 10, 1967

A systematic study of the addition of bromine to several α, β- and β, γ-unsaturated sulphones in carbon tetrachloride was made by BALIAH and SHANMUGANATHAN [1]. The slight increase in the value of $k_{\beta,\gamma}$ over $k_{\alpha,\beta}$ was attributed to the weaker inductive effect of the sulphonyl group on the ethylenic bond in β, γ-unsaturated sulphones due to the intervening methylene group. Enough evidence has been accumulated [2—7] to show that there is no significant conjugation of the sulphonyl group with the ethylenic linkage in the ground state of α, β-unsaturated sulphones.

The study of halogen addition in strongly polar media, particularly in aqueous solution, involves much faster reactions; the results obtained with less polar solvents are less reproducible, many details are anomalous and not well understood. Hence, a systematic study of the kinetics of bromine addition to unsaturated sulphones in polar solvents will be necessary to understand the mechanism of the reaction, since it is in such circumstances that some knowledge of the heterolytic mechanism is most easily obtained. With this object in view, the present investigation has been undertaken with acetic acid as the solvent.

Experimental

Materials. Phenyl vinyl sulphone and *p*-tolyl vinyl sulphone were prepared according to the method of SMITH and DAVIS [8]. Allyl phenyl sulphone and allyl *p*-tolyl sulphone were obtained according to the method of OTTO [9]. Cinnamyl phenyl sulphone and cinnamyl *p*-tolyl sulphone were prepared according to the method of RUPE and BURGAIN [10]. The method of BALIAH and SHANMUGANATHAN [11] was used for the preparation of *p*-nitrostyryl *p*-tolyl sulphone and *m*-nitrostyryl *p*-tolyl sulphone. *p*-Chlorostyryl *p*-tolyl sulphone, *p*-chlorostyryl phenyl sulphone, *m*-nitrostyryl *p*-tolyl sulphone, *m*-nitrostyryl phenyl sulphone, *p*-nitrostyryl phenyl sulphone,* phenyl styryl sulphone and styryl *p*-tolyl sulphone were obtained following the method of BALASUBRAMANIAN and BALIAH [12].

Acetic acid and bromine were purified by conventional methods, and were free from moisture.

The kinetics of bromine addition to unsaturated sulphones was studied in the usual manner at 30 °C. The following second-order rate constants at a total concentration of *M*/240 were obtained (Table I).

* Prepared for the first time in 75% yield. Recrystallized from ethanol, yellow needles, m. p. 174—175.5 °C. Anal: Calcd. for $C_{14}H_{11}O_4NS$; C 58.11; H 3.83; N 4.84; S 11.09. Found: C. 57.93; H 3.90; N 4.88; S 11.28%.

Table I

Rate constants for the bimolecular addition of bromine in acetic acid at 30 °C

Sulphone	$*k_2 \cdot 10^2$ (mole/l)$^{-1}$/sec.$^{-1}$	$k_{\beta,\gamma}/k_{\alpha,\beta}$
$CH_3SO_2CH = CH_2$	0.12	2.80
$CH_3SO_2CH_2CH = CH_2$	0.34	
$C_6H_5SO_2CH = CH_2$	0.27	1.96
$C_6H_5SO_2CH_2CH = CH_2$	0.53	
p-$CH_3C_6H_4SO_2CH = CH_2$	0.29	1.86
p-$CH_3C_6H_4SO_2CH_2CH = CH_2$	0.54	
$C_6H_5SO_2CH = CHC_6H_5$	0.63	7.60
$C_6H_5SO_2CH_2CH = CHC_6H_5$	4.80	
p-$CH_3C_6H_4SO_2CH = CHC_6H_5$	0.83	6.60
p-$CH_3C_6H_4SO_2CH_2CH = CHC_6H_5$	5.50	
$C_6H_5SO_2CH = CHC_6H_4NO_2$-$m$	0.13	
p-$CH_3C_6H_4SO_2CH = CHC_6H_4NO_2$-$m$	0.35	
$C_6H_5SO_2CH = CHC_6H_4NO_2$-p	0.19	
p-$CH_3C_6H_4SO_2CH = CHC_6H_4NO_2$-$p$	0.43	
$C_6H_5SO_2CH = CHC_6H_4Cl$-$p$	0.56	
p-$CH_3C_6H_4SO_2CH = CHC_6H_4Cl$-$p$	0.61	

* McDONALD, MILBURN and ROBERTSON [2] report $k_2 = 0.0011$, 1 mole^{-1} min.$^{-1}$, using $M/40$ solutions of sulphones and bromine. It has been observed by the author that the rate constant varies considerably with the concentrations of sulphones and bromine (cf. ROBERTSON [13]). Hence comparison of the two rate constants may be misleading.

In all cases the rates of bromine addition to β, γ-unsaturated sulphones are consistently higher than those to the corresponding α, β-unsaturated sulphones, though the difference is not much except in the case of the styryl and cinnamyl sulphones. This small difference only is to be expected from the fact that *(a)* the sulphur-oxygen bond in the sulphone group is semipolar, and *(b)* the sulphur function is not efficiently conjugated with the ethylenic linkage in the ground state of α, β-unsaturated sulphones. Therefore, the slight increase in the value of $k_{\beta,\gamma}$ over $k_{\alpha,\beta}$ is to be attributed to the weakening of the inductive effect of the sulphonyl group on the ethylenic linkage in β γ-unsaturated sulphones due to the intervening methylene group. This conclusion is essentially the same as that reported for the addition of bromine to these sulphones in carbon tetrachloride as solvent. The higher difference between the values of the styryl and cinnamyl sulphones is probably due to the increased polarization of the system.

However, one striking difference is evident. The rate constants in the solvent acetic acid for the ten sulphones for which data in carbon tetrachloride are available fall into two categories (Table II).

The vinyl and allyl sulphones have lesser rate constants in acetic acid, whereas the styryl and cinnamyl sulphones have higher rate constants in carbon tetrachloride. Thus, in the solvent acetic acid the nature of R′ in $RSO_2CH = CHR'$ or $RSO_2CH_2CH = CHR'$ seems to influence the rate considerably. This may be due to not only the increased polarization of the unsaturated system when R′ = phenyl as compared to R′ = H, but also to the fact that a less polar system will be favoured to a greater extent in a non-polar solvent such as carbon tetrachloride, whereas a polar medium like acetic acid would favour a more polar system. This would possibly mean that the polarization of the double bond at the time of halogen attack is controlled to an almost equal extent by both R and R′. When R′ is phenyl, the deactivation of the ethylenic double bond due to the R—SO_2 group seems to be counteracted.

Table II

Sulphone	$k_2(CCl_4)$	k_2(HOAc)	k_{CCl_4}/k_{HOAc}
$CH_3SO_2CH = CH_2$	0.0061	0.0012	5.1
$CH_3SO_2CH_2CH = CH_2$	0.0271	0.0034	8.0
$C_6H_5SO_2CH = CH_2$	0.0065	0.0027	2.4
$C_6H_5SO_2CH_2CH = CH_2$	0.0083	0.0053	1.6
p-$CH_3C_6H_4SO_2CH = CH_2$	0.0068	0.0029	2.3
p-$CH_3C_6H_4SO_2CH_2CH = CH_2$	0.0084	0.0054	1.6
	k_2(HOAc)	$k_{2(CCl_4)}$	k_{HOAc/CCl_4}
$C_6H_5SO_2CH = CHC_6H_5$	0.0063	0.0033	1.9
$C_6H_5SO_2CH_2CH = CHC_6H_5$	0.0480	0.0054	8.9
p-$CH_3C_6H_4SO_2CH = CHC_6H_5$	0.0083	0.0035	2.4
p-$CH_3C_6H_4SO_2CH_2CH = CHC_6H_5$	0.0550	0.0054	10.2

at least partly, by the phenyl group. Hence the sulphones $RSO_2CH = CHR'$ and $RSO_2CH_2CH = CHR'$ (R′ = phenyl) add bromine at a faster rate in acetic acid than in carbon tetrachloride. In the absence of this additional polarization, the sulphones $RSO_2CH = CH_2$ and $RSO_2CH_2CH = CH_2$ add bromine more slowly in acetic acid solvent than in carbon tetrachloride. It is also probable that in a non-polar solvent like carbon tetrachloride subtle differences between the polarization of the reacting systems may not be seen, whereas they may be very much in evidence in a polar solvent such as acetic acid.

Further, the greater dipole moments [14] of $C_6H_5SO_2CH = CHC_6H_5$ (μ = 5.93 D) and $C_6H_5SO_2CH_2CH = CHC_6H_5$ (μ = 5.69 D) when compared with those of $C_5H_5SO_2CH = = CH_2$ (μ = 5.29 D) and $C_6H_5SO_2CH_2CH = CH_2$ (μ = 5.24 D) are responsible for the increased polarization of the systems. This increase facilitates dipole—dipole interactions between these sulphones and the solvent acetic acid. Such interactions will occur to a lesser extent in carbon tetrachloride as solvent.

Regarding the effect of substituents on the rate of bromine addition, the p-tolyl sulphones have higher rates than the corresponding phenyl sulphones; the difference, however, is very small (Table I). This is to be expected because the p-tolyl group is slightly more electron-releasing than the phenyl group, and this results in the phenylsulphonyl group exerting a relatively greater inductive effect on the ethylenic bond than p-tolylsulphonyl. It may be noted that even here the differences are more significant with **I** $RSO_2CH = CHR'$ and **II** $RSO_2CH_2CH = CHR'$ (R′ = phenyl, m-nitrophenyl, p-nitrophenyl, or p-chlorophenyl in **I** and R′ = phenyl in **II**) than with $RSO_2CH = CH_2$ and $RSO_2CH_2CH = CH_2$ (R = phenyl. p-tolyl).

In all cases the rate constants for $RSO_2CH = CHC_6H_4X$ (R = phenyl or p-tolyl; X = m-NO_2, p-NO_2 or p-Cl) are less than those for the corresponding unsubstituted sulphones $RSO_2CH = CHC_6H_5$ (R = phenyl or p-tolyl). The decrease seems to be due only to the inductive effect of the substituent. The relatively greater inductive effect of the nitro group reduces the rate to a greater extent than that of chlorine. Therefore, it seems that electron accession to the double is the dominant factor controlling the addition, at any rate in the absence of suitable catalysts and at the concentrations of the sulphones and bromine employed in the present study.

SUMMARY

The kinetics of bromine addition to α, β-and β, γ-unsaturated sulphones in acetic acid at 30 °C has been studied. The addition follows second order kinetics. However, the sulphones $RSO_2CH = CHR'$ and $RSO_2CH_2CH = CHR'$ (R′ = phenyl) add bromine at a faster rate in acetic acid than in carbon tetrachloride, whereas the sulphones $RSO_2CH = CH_2$ and

$RSO_2CH_2CH = CH_2$ add bromine more slowly in acetic acid than in carbon tetrachloride. This observation has been tentatively explained on the basis of the difference in the polarization of the systems in acetic acid. The effect of substituents on the rates of bromine addition has also been studied. The results have been interpreted in terms of the polar effects of the substituents.

REFERENCES

1. Baliah, V., Shanmuganathan, Sp.: J. Phys. Chem. **63,** 2016 (1959).
2. McDonald, I. R. C., Milburn, R. M., Robertson, P. W.: J. Chem. Soc. **1950,** 2836.
3. Koch, H. P.: J. Chem. Soc. **1949,** 409.
4. Barnard, D., Fabian, J. M., Koch, H. P.: J. Chem. Soc. **1949,** 2442.
5. De La Mare, P. B. D., Robertson, P. W.: J. Chem. Soc. **1950,** 2838.
6. Baliah, V., Shanmuganathan, Sp.: Trans. Faraday Soc. **55,** 232 (1959).
7. Shanmuganathan, Sp.: Ph. D. Thesis, Annamalai University.
8. Smith, L. I., Davis, H. R.: J. org. Chem. **15,** 824 (1950).
9. Otto, R.: Ann. **283,** 184 (1894).
10. Rupe, Burgain,: Ber. **43,** 173 (1910).
11. Baliah, V., Shanmuganathan, Sp.: J. Ind. Chem. Soc. **35,** 31 (1958).
12. Balasubramanian, M., Baliah, V.: J. Chem. Soc. **1954,** 1844.
13. Robertson, P. W.: Rev. Pure and Appl. Chem. **7,** 155—64 (1957).
14. Baliah, V., Seshapathirao, M.: Unpublished work.

Sp. Shanmuganathan
D. Sri Rama Rao
Department of Chemistry, Pachaiyappa's College, Madras — 30, India

Acta Chimica Academiae Scientiarum Hungaricae Tomus 56 (3), pp. 311—313 (1968)

INDOL UND INDOLDERIVATE, III*

DIE SYNTHESE VON 6-RO-INDOL- UND INDOLIN-DERIVATEN

Á. GERECS, M. BARTA, T. TÓTH und A. LAY

(Lehrstuhl für Chemische Technologie der L.-Eötvös-Universität, Budapest)

Eingegangen am 21. Juli, 1967

6-Hydroxy- und 6-Benzyloxy-indol wurden bereits von BEER u. Mitarb [1] und von STOLL u. Mitarb. [2] dargestellt. Diese Synthese beruht auf der reduktiven Cyclisierung von 2-Nitro-4-benzyloxy-phenyl-brenztraubensäure und darauffolgender Decarboxylierung. Das so erhaltene 6-Benzyloxy-indol wurde durch Hydrogenolyse in 6-Hydroxy-indol umgewandelt.

Die Ausgangsverbindung der von uns entwickelten Synthese bildet das *via* Indol→ Indolin→ 6-Nitro-indolin→ 1-Benzoyl-6-nitro-indolin bequem zugängliche 1-Benzoyl-6-amino-indolin [3]. Aus letzterem wurden folgende Indolderivate dargestellt: 1-Benzoyl-6-hydroxy-indolin (**I**), 1-Benzoyl-6-methoxy-indolin (**IIa**), 6-Methoxy-indolin (**IIIa**), 1-Benzoyl-6-benzyloxy-indolin (**IIb**), 6-Benzyloxy-indolin (**IIIb**), 6-Hydroxy-indolin (**IV**) und 6-Hydroxy-indol (**V**).

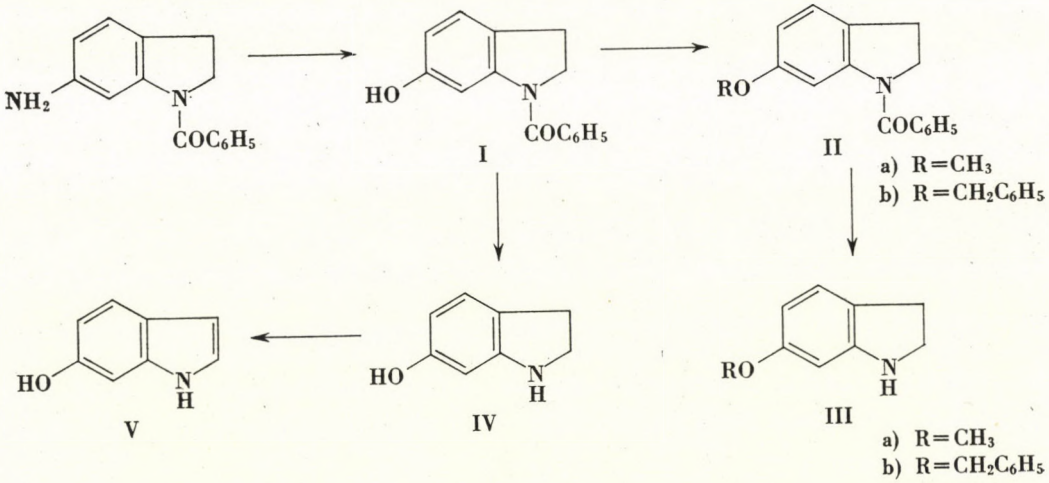

* »Die hier zusammengefaßten Untersuchungen wurden im Jahre 1965 durchgeführt. Diesbezüglich wurden zwei ungarische Patentanmeldungen (3. VI. 1965 und 29. XI. 1965) eingereicht. Inzwischen haben R. R. HUNT und R. C. RICKARD im J. Chem. Soc. (C) 1966 S. 344 im wesentlichen den gleichen Weg zur Darstellung von 6-Hydroxy- und 6-Methoxy-indol beschrieben.«

Die über Diazotierung von 1-Acyl-6-amino-indolinen erfolgende Einführung der Hydroxylgruppe konnte mit der 1-Acetyl-Verbindung nicht durchgeführt werden, da die Acetylgruppe auch unter den mildesten Reaktionsumständen abgespalten und dadurch nur teeriges Reaktionsprodukt erhalten wurde.

Wir danken Frau M. BALOGH für die Mikroanalysen.

Beschreibung der Versuche

6-Nitro-indolin. Diese Verbindung wurde nach TERENTJEW und Mitarb. [4] dargestellt. Schm. 65—66 °C (Lit. 66,5—67,5 °C).

1-Benzoyl-6-nitro-indolin [3]. Aus 6-Nitro-indolin mit Benzoylchlorid und Pyridin bei 0 °C: Ausb. 92%, Schmp. 166—168 °C (Lit. 166—167 °C).

1-Benzoyl-6-amino-indolin [3]. Das 1-Benzoyl-6-nitro-indolin (14,6 g) wurde in einem Gemisch von Methanol (700 ml) und *n* Salzsäure (200 ml) mit Pd-Kohle bei 20 °C und atmosphärischem Druck hydriert. Nach Filtrieren und Abdestillieren des Methanols wurde die wäßrige Lösung mit 2 *n* Natronlauge versetzt, worauf die 6-Amino-Verbindung in 96,2%iger Ausbeute (12,5 g) erhalten wurde. Schmp. 183 °C.

1-Benzoyl-6-hydroxy-indolin (I). 4,76 g 1-Benzoyl-6-amino-indolin (20 Mmol) wurden in 60 ml *n* H_2SO_4 gelöst und bei 0 °C mit 20 ml *n* $NaNO_2$ diazotiert. Die erhaltene Lösung wurde 2 1/2 Stunden bei 70—75 °C gehalten, worauf sich 4,0 g eines rotbraunen kristallinen Produktes ausschieden; Schmp. 223 °C. Aus Chloroform umkristallisiert; 2,7 g (56,5%), Schmp. 228—230 °C.
$C_{15}H_{13}NO_2$ (239,28). Ber. N: 5,86%. Gef. N: 6,05%.

1-Benzoyl-6-methoxy-indolin (IIa). 23,9 g **I** (0,1 Mol) wurden in einem Gemisch von 150 ml Methanol und 10 ml 10 *n* NaOH gelöst und bei 25—30 °C portionsweise mit 15 ml (0,15 Mol) Dimethylsulfat versetzt, wobei das Reaktionsgemisch durch Zugabe von jeweils 0,5 ml 10 *n* NaOH alkalisch gehalten wurde. Nach 3stündigem Rühren wurde mit Wasser auf 1 Liter verdünnt und das ausgeschiedene pulverförmige Produkt nach einer Stunde filtriert: 25,1 g (99%) 12,6 g aus 400 ml Petroläther umkristallisiert: 10,5 g (84%); Schmp. 78—79 °C.
$C_{16}H_{15}NO_2$ (253,27). Ber. CH_3O: 12,25%; N: 5,53%. Gef. CH_3O: 12,20%, 12,27%; N: 5,56%, 5,54%.

6-Methoxy-indolin (IIIa). Das Reaktionsgemisch von 12,7 g **IIa** (Rohprodukt, 0,05 Mol), 100 ml Äthanol und 30 ml 10 *n* NaOH wurde 4 Stunden unter Rückfluß gekocht und nach Abkühlen mit 20 ml 2 *n* HCl versetzt. Der größte Teil des Äthanols wurde abdestilliert, der Rückstand mit 100 ml Wasser verdünnt und das ausgeschiedene Öl mit Benzol extrahiert. Der Rückstand der benzolischen Lösung wurde destilliert: Kp_{15} = 145—146 °C, 5,8 g (78%) farbloses Öl; n_D^{20} = 1,5878.
$C_9H_{11}NO$ (149,19). Ber. CH_3O: 20,80%, N: 9,39%. Gef. CH_3O: 20,71%, N: 9,50%, 9,51%.
Hydrochlorid: Aus äthanolischer Lösung durch Sättigung mit trockenem Chlorwasserstoffgas. Farblose Nadeln, Schmp. 227—228 °C.
$C_9H_{12}ClNO$ (185,66). Ber. CH_3O: 16,72%, N: 7,55%. Gef. CH_3O: 16,82%, N: 7,80%, 7,86%.

1-Benzoyl-6-benzyloxy-indolin (IIb). 0,116 g Natrium (5 Mmol) wurden in 25 ml *n*-Propanol gelöst, die Lösung wurde mit 1,20 g (5 Mmol) **I** und 0,75 ml (6,5 Mmol) Benzylchlorid versetzt und 3 Stunden unter Rückfluß gekocht. Der Rückstand des Reaktionsgemisches wurde mit Wasser und Äthylacetat verrührt, die organische Phase abgetrennt und das Lösungsmittel abdestilliert. Der Rückstand kristallisierte nach Verrühren mit 5—6 ml Methanol: 1,375 g (83,6%), Schmp. 110—113 °C.
$C_{22}H_{19}NO_2$ (329,40). Ber. N: 4,25%. Gef. N: 4,50%, 4,52%.

6-Benzyloxy-indolin (IIIb). Das Reaktionsgemisch von 1,8 g **IIb** (5,47 Mmol), 15 ml abs. Äthanol und 5,5 ml 20%iger Natronlauge wurde 3 1/2 Stunden unter Rückfluß gekocht. Dann wurde in Kohlendioxydatmosphäre das Äthanol abdestilliert, der Rückstand abgekühlt, mit 30 ml Wasser versetzt und nach einer halben Stunden das ausgeschiedene

kristalline Produkt filtriert: 1,2 g (95,2%) Rohprodukt. Aus Benzin (Kp. 60—80 °C) umkristallisiert: 0,73 g, Schmp. 67—69 °C.
$C_{15}H_{15}NO$ (225,30). Ber. N: 6,22%. Gef. N: 6,24%, 6,21%.

6-Hydroxy-indolin (IV). Das Reaktionsgemisch von 5 g (20,9 Mmol) **I** und 25 ml 65%iger Schwefelsäure wurde 30 Minuten unter Rückfluß gekocht. Das abgekühlte, von der Benzoesäure durch Filtrieren getrennte Reaktionsgemisch wurde mit Na_2CO_3 neutralisiert und aus dem entstandenem Kristallbrei das 6-Hydroxy-indolin mit Äthylacetat (3×50 ml) extrahiert. Diese Lösung wurde mit 3×50 ml 2 *n* HCl ausgeschüttelt und die wäßrige Lösung eingetrocknet: 2,7 g kristallines, rohes 6-Hydroxy-indolin-hydrochlorid (75,2%). Dieses wurde in Methanol gelöst, die Lösung mit Aktivkohle behandelt, filtriert und eingetrocknet: 2,3 g farbloses kristallines Hydrochlorid.
$C_8H_9NO \cdot HCl$ (171,63). Ber. Cl^-: 20,60%. Gef. Cl^-: 20,69%.

Freie Base: 1,71 g (0,01 Mol) Hydrochlorid wurden in 10 ml Wasser gelöst, die Lösung mit 10 ml Äthylacetat bedeckt und dann portionsweise mit 0,88 g $NaHCO_3$ versetzt. Die organische Phase wurde abgetrennt, die wäßrige Lösung mit 5 ml Äthylacetat ausgeschüttelt. Die vereinigte äthylacetatische Lösung wurde mit Aktivkohle behandelt und eingedampft: 1,18 g hellgelber kristalliner Rückstand (87,5%), Schmp. 118—119 °C. Reinheit auf Grund der potentiometrischen Titration 99,5%.
C_8H_9NO (135,17). Ber. N: 10,36%. Gef. N: 10,38%, 10,36%.

N-Nitroso-Derivat: Aus **IV**-Hydrochlorid mit der äquivalenten Menge $NaNO_2$ bei 0 °C: Kristalline Substanz, Ausb. 94,5%, Schmp. 157—159 °C.

N-Nitroso-O-acetyl-Derivat: Aus der Nitroso-Verbindung mit Essigsäureanhydrid und Pyridin bei 0 °C: Hellgelbe Kristalle, Schmp. 130—132 °C.

6-Hydroxy-indol (V). 6,40 g feuchtes Raney-Nickel wurden mit 200 ml Butylacetat versetzt und durch Abdestillieren von 120 ml entwässert. Es wurden 5,40 g (40 Mmol) 6-Hydroxy-indolin zugegeben und 1 1/2 Stunden unter Rückfluß gekocht. Die filtrierte Lösung wurde mit *n* HCl, dann mit Wasser ausgeschüttelt, getrocknet und unter vermindertem Druck eingedampft. Der hellgraue kristalline Rückstand wurde mit 20 ml Chloroform versetzt, das Gemisch wurde 15 Minuten gekocht, abgekühlt und filtriert: 3,22 g farblose kristalline Substanz (60,5%), Schmp. 125—127 °C. (Lit. 124—126 °C).

ZUSAMMENFASSUNG

Es wurde eine neue Synthese für 6-RO-Indol- und Indolin-Verbindungen entwickelt. Im Laufe dieser Untersuchungen wurden folgende Verbindungen dargestellt: 1-Benzoyl-6-hydroxy-, 1-Benzoyl-6-Methoxy-, 6-Methoxy-, 1-Benzoyl-6-benzyloxy-, 6-Benzyloxy-, 6-Hydroxy-indolin und 6-Hydroxy-indol.

LITERATUR

1. Beer, R. J. S., Clarke, K., Khorana, H. G., Robertson, A.: J. Chem. Soc. **1948,** 1605.
2. Stoll, A., Troxler, F., Peyer, I., Hofmann, A.: Helv. Chim. Acta **38,** 1452 (1955).
3. Kinoshita, T., Inone, H., Imoto, E.: J. Chem. Soc. Japan, **78,** 1372, (1957); Z. **1958,** 13226.
4. Terentjew, A. P., Preobrashenskaja, M. N., Bobkow, A. S., Sorokina, G. M.: J. Obsch. Chim. **1959,** XXIX, 2541.

Árpád Gerecs
Margit Barta-Bukovecz
Tibor Tóth
Aranka Lay-Kónya

Budapest VIII., Múzeum krt. 6/8.

Acta Chimica Academiae Scientiarum Hungaricae Tomus 56 (3), pp. 315—323 (1968)

ON THE EXTENDED DAMKÖHLER EQUATION

L. FÁY

(Technical University of Chemical Engineering, Veszprém)

Received February 20, 1967

1. Importance of the Damköhler equation in describing chemical engineering processes

1.1. Concepts and definitions

Describing a chemical engineering operational unit is equivalent to determining, by means of the operating parameters of the operational unit in question, the transformation transferring the input stream vector into the output one [19, 20].

The exact description of the operational unit can be achieved on the basis of the laws of conservation. In chemical engineering processes, the laws of energy, momentum, and mass are primarily considered [2].

It was DAMKÖHLER [1] who established, in terms of vector analysis, these laws of conservation (the so-called balance equations) in the particular case of chemical reactors. In the equations set up by Damköhler, however, the transfer phenomenon, which is of extraordinary importance in chemical engineering, was not accounted for. The Damköhler equation, therefore, became suitable to describe chemical engineering processes only after having been completed with a transfer term by BENEDEK and LÁSZLÓ [3]. Now, the Damköhler equation extended in this way is suitable to determine all the processes in chemical engineering; hence, with some exaggeration, it may be said that this equation is of the same importance in chemical engineering science as the SCHRÖDINGER equation in quantum mechanics (the two equations are similar in their forms as well).

Let Ψ denote the quantity that the conservation law refers to. The derivatives of Ψ with respect to the time and volume, respectively are called stream and density, designated by J and Γ, respectively; the derivative of the stream with regard to the volume is called source, designated by G. Further, let v denote the vector of the flow rate, so we have

$$J = \frac{\partial \Psi}{\partial t}$$

$$\Gamma = \frac{\partial \Psi}{\partial V} \tag{1}$$

$$G = \frac{\partial J}{\partial V}$$

and the extended Damköhler equation expressing the conservation of Ψ becomes:

$$\text{div}\,(\Gamma v) - \text{div}\,(\delta\ \text{grad}\ \Gamma) + \omega\varepsilon\Delta\Gamma + G = -\frac{\partial\Gamma}{\partial t} \tag{2}$$

where ω, ε and δ are parameters dependent on material quality, $\Delta\Gamma$ being the transfer term [3]. It can be seen that Eq. (2) is a partial differential equation of the second order and not necessarily linear. The transfer, source, and other terms therein are only exceptionally linear in practice, consequently the solution of this equation cannot be achieved with the known methods.

1.2. An example of applying the Damköhler equation in chemical engineering processes

In this section, we will shortly illustrate how to apply the Damköhler equation in describing industrial chemical processes. To this end let us consider the following recirculation process (Fig. 1).

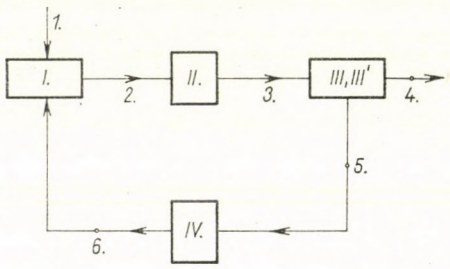

Fig. 1

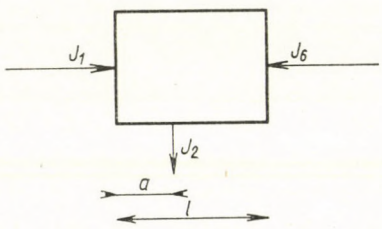

Fig. 2

Mathematically, the operational units (designated by Roman numbers) mean such transformations as transfer the input stream vector into the output one. It is not the aim of the present paper to set up and to solve the Damköhler equations for each operational unit. We shall come back to this question, here only touched upon, in a later publication.

Let us denote the transformations belonging to the individual blocks with T_{I}, T_{II}, T_{III}, and T_{IV}, further, the input and output streams with $J_1(t)$ and $J_4(t)$, respectively. In this case the following equations can be written:

$$\begin{gathered} J_2 = T_{\text{I}}(J_1, J_6),\ J_3 = T_{\text{II}}(J_2) \\ J_4 = T_{\text{III}}(J_3),\ J_5 = T'_{\text{III}}(J_3) \\ J_6 = T_{\text{IV}}(J_5) \end{gathered} \tag{3}$$

Our task being to determine J_4 with given J_1 and with given transformations, and J_6 being also needed to this end, let us write J_6 by means of the other streams:

$$J_6 = T_{IV}(J_5) = T_{IV}\,T_{III}\,(J_3) = T_{IV}\,T'_{III}\,T_{II}\,(J_2) = T_{IV}\,T'_{III}\,T_{II}\,T_I\,(J_1, J_6)\,. \quad (4)$$

Introducing the notation $T = T_{IV}\ T'_{III}\ T_{II}\ T_I$ and considering that J_1 has the meaning of an initial parameter, we have:

$$J_6 = T(J_6). \quad (5)$$

This equation can be solved by iteration if the conditions of BANACH's fixed point theorem are fulfilled: J_6 has to be an element of a complete metric space and T has to be a contractive operator. (Regarding these definitions, see the relevant literature [6, 8].) According to the foregoing, iteration is generally needed in order to calculate recirculation processes. Since conservation laws are valid for the individual blocks, *i.e.* balance equations can be established for them, the transformations corresponding to the blocks are connected, in mathematical terms, with performing the solution of the Damköhler equations. Now we will not be concerned in detail with computing the individual blocks, *i.e.* with applying the Damköhler equation to the individual operational units. Only in the case of a single operational unit, namely of the blender, shall we show how to use the Damköhler equation so as to compute this operational unit.

1.2.1. Application of the Damköhler equation to a blender

Let us consider the I-block of Fig. 1 where there are two input streams and an output one denoted with J_1, J_6, and J_2, respectively. The corresponding velocity of these liquid streams are designated with V_1, V_6 and V_2, respectively, assuming them, for the sake of simplicity, to be a constant. The concentrations of the input liquid streams J_1 and J_6 should be $\Gamma_1(t)$ and $\Gamma_6(t)$, *i.e.* we allow them to change in the time.

Let us now start from a one-dimensional model, *i.e.* let us take into account only the axial concentration change. Further, δ is supposed to be a constant. In this case Eq. (2) reads as follows:

$$D\frac{\partial^2 \Gamma}{\partial x^2} - \frac{\partial}{\partial x}(\Gamma v) - G(x, a, t) = \frac{\partial \Gamma}{\partial t} \quad (6)$$

$$\text{where } v(0,t) = v_1(t)$$
$$v(l,t) = -v_6(t)$$

$$G(x, a, t) = \lim_{u \to 0} \frac{\Gamma(x, t)}{\sqrt{\pi u}}\, v_2(t)\, e^{-\frac{(x-a)^2}{u}} \quad (6a)$$

On Fig. 2 l denotes the length of the interval in which the concentration change occurs, whereas by a the output place of the stirred liquid is designated. According to the nature of the problem, the initial and boundary conditions are the following:

$$\begin{aligned} \Gamma(0,t) &= \Gamma_1(t) \\ \Gamma(l,t) &= \Gamma_6(t) \\ \Gamma(x,0) &= \varphi(x) \end{aligned} \tag{7}$$

where $\varphi(x)$ denotes the initial concentration distribution which is, in general' identically zero: $\varphi(x) \equiv 0$. The output concentration is now given by the function $\Gamma(a,t)$:

$$\Gamma_2(t) = \Gamma(a,t)$$

Since v_1, v_2, v_6, Γ_1, Γ_5, and $\varphi(x)$ have been given, the problem can be solved as the first boundary value problem for the Damköhler equation. It should be further mentioned that in Eq. (6) D denotes the effective diffusivity.

Eqs (6) and (7) can easily be checked. Let us consider the case of perfect mixing. For the sake of simplicity we also suppose the concentrations of the input materials to be a constant in time and no volume change to occur during the mixing. In this case, the mixture being homogeneous because of the perfect agitation, *i.e.* $\frac{\partial \Gamma}{\partial t} = 0$ being valid, $\frac{\partial^2 \Gamma}{\partial x^2} = 0$ follows. The concentration may not change in time either: $\frac{\partial \Gamma}{\partial t} = 0$, further $v_2 = v_1 + v_6$ when the inlet and outlet areas are equal. Inserting these quantities into Eq. (6), integrating both sides from 0 to l and with respect to Eq. (6a) we have for the concentration of the output material:

$$\Gamma = \Gamma_2 = \frac{v_1 \Gamma_1 + v_6 \Gamma_6}{v_1 + v_6}$$

which is the well-known mixing rule. So the correctness of Eq. (6) has been checked.

1.3. On the boundary value problems of second-order partial differential equations

A second-order partial differential equation with constant coefficients

$$a_{11} u_{xx} + 2 a_{12} u_{xy} + a_{22} u_{yy} + b_2 u_x + b_2 u_y + cu + f = 0 \tag{8}$$

is called hyperbolic, parabolic or elliptic depending on whether the expression $a_{12}^2 - a_{11} a_{22}$ is positive, negative, or zero. The Damköhler equation being

parabolic, we shall be concerned with this type only. The first boundary value problem for parabolic equations reads as follows: determine the function of two variables satisfying the differential equation given and the following conditions:

$$\begin{aligned} u(0,y) &= \mu_1(y) \\ u(l,y) &= \mu_2(y) \\ u(x,0) &= \varphi(x). \end{aligned} \tag{9}$$

Here the first two equations are called boundary conditions, whereas the last one is the initial condition. Should we have to do with a non-linear partial differential equation, the above classification would change somewhat.

In this case with the equation

$$F(x_1, x_2, u, u_{x_1}, u_{x_2}, u_{x_1x_1}, u_{x_2x_2}\, u_{x_1x_2}) = 0$$

an equation with constant coefficients will be adjuncted as follows:

$$\sum_{i,k=1}^{2} a_{ik} \frac{\partial^2 u}{\partial x_1\, \partial x_k} = 0 \tag{10}$$

where

$$a_{ik} = \frac{\partial F}{\partial \left\{ \dfrac{\partial^2 u}{\partial x_i\, \partial x_k} \right\}} .$$

Depending on whether this equation is hyperbolic, parabolic or elliptic, so is the original equation, too [6]. It can be seen that by Eq. (6) with the conditions (7) the first boundary value problem of the Damköhler equation is defined.

There are general methods to solve the boundary value problems of partial differential equations only in the linear case. Two basic methods should be mentioned: that of FOURIER [4] and CAUCHY [5], respectively.

In the non-linear case we do not know any procedure by means of which, similarly to the RUNGE-KUTTA method for solving ordinary differential equations, boundary value problem of partial differential equations could be solved automatically [7]. The advantage of such a method would be the possibility of computer programming, independently of the form of the equation and the initial and boundary conditions.

The aim of the present paper is to show such a method. By its use the mathematical modelling of a chemical plant is reduced to solving the Damköhler equation with different initial and boundary conditions, naturally with the help of computer.

2. Iterative solution of the first boundary value problem of the one-dimensional Damköhler equation

The method to be outlined in the following is based upon the method named successive approximation or iteration [8]. This approach can be used to solve problems of different types, such as non-linear equations and systems of equations with one or many unknowns, ordinary, differential equations (approach of PICARD-LINDELÖF), etc.

To solve the initial value problems of hyperbolic partial differential equations, a method was elaborated by COURANT and HILBERT [9], while to the boundary value problem of elliptic equations (without initial conditions) iteration procedures were applied by POGGI [10], CAPLAN [11], and SAUER [12]. CRANK and NICHOLSON [15] as well as HOPKINS [14] also used iterative methods to solve the differential equations of diffusion.

2.1. Explanation of the method

Let us rearrange the one-dimensional Damköhler equations as follows:

$$D\frac{\partial^2 \Gamma}{\partial x^2} - \frac{\partial \Gamma}{\partial t} = \varrho(x, t, \Gamma, \Gamma_x, \Gamma_t, \Gamma_{xx}). \tag{11}$$

In the case of the first boundary value problem the initial and boundary conditions are:

$$\begin{aligned} \Gamma(0,t) &= \mu_1(t) \\ \Gamma(l,t) &= \mu_2(t) \\ \Gamma(x,0) &= \varphi(x). \end{aligned} \tag{12}$$

Let us insert $\varrho = 0$ into Eq. (11) and solve the new equation obtained with conditions (12). Now let the solution (which can be obtained, for example, with the FOURIER method) be inserted into Eq. (11) and let the new equation be solved with conditions (12). Repeating this procedure, we have after m steps [16]:

$$\begin{aligned} \Gamma_m(x,t) = \mu_1(t) + \frac{x}{l}[\mu_2(t) - \mu_1(t)] + \\ + \frac{2}{1}\int_0^l \left\{\varphi(\xi) - \mu_1(0) - \frac{\xi}{l}[\mu_2(0) - \mu_1(0)]\right\} \cdot \\ \cdot \sum_{n=1}^{\infty} e^{-\frac{n^2\pi^2 Dt}{l^2}} \cdot \sin\frac{n\pi\xi}{l} \sin\frac{n\pi x}{l}\, d\xi + \end{aligned} \tag{13}$$

$$+\frac{2}{1}\int_0^t\int_0^l \sum_{n=1}^{\infty} e^{-\frac{n^2\pi^2 D}{l^2}(t-\tau)} \cdot \sin\frac{n\pi x}{l}$$

$$\sin\frac{n\pi\xi}{l}\left[\frac{\partial\mu_2}{\partial t} - \frac{\partial\mu_1}{\partial t} + \varrho_{m-1}(\xi, t)\right] d\xi\, d\tau\ .$$

By direct substitution we can convince ourselves that the initial and boundary conditions (12) are satisfied in every case. Convergence and uniqueness of the method can also be proved on the basis of BANACH's theorem [17], provided the conditions mentioned in 1.2 are fulfilled (which is generally the case in practice). Error estimation can also be obtained for a differential equation given with initial and boundary conditions, to be solved by iteration [16]. The method outlined may be generalized for the second and third boundary value problem [21] as well as for multi-dimensional cases. The method can also be applied to systems of equations of non-independent components [3], to which we will return in a later communication.

2.2. Computing method for the solution of the first boundary value problem of the one-dimensional Damköhler equation

Eq. (13) can easily be used by a computer. As against the stepwise integration method generally used to solve partial differential equations it has the advantage of being adaptable automatically for a computer after the function ϱ as well as the initial and boundary conditions have been given.

An ALGOL-60 program has been made for a GIER computer. The following input data have to be given:

the x—t parallelogram as well as the step length in which the computation must be carried out;

the number of iterations;

the number of the terms in the Fourier series in Eq. (13);

the number of subintervals needed for the integration;

the expression of the Damköhler equation on giving function ϱ;

the initial and boundary conditions on giving the corresponding functions.

The integration is performed by means of the trapezoidal rule. As the result of the program, we have values of x, t, and Γ satisfying Eqs (11) and (12), and existing in the parallelogram x—t given before.

The program described was checked in connection with the model problem of component transfer on a rotating disk [18]. The computation to be carried out is the following.

The differential equation of the problem reads [18]:

$$D\frac{\partial^2\Gamma}{\partial x^2} - \frac{\partial\Gamma}{\partial t} = kx^2\frac{\partial\Gamma}{\partial x} \qquad (14)$$

with the initial and boundary conditions:

$$\Gamma(0, t) = 0$$

$$\Gamma(l, t) = 0$$

$$\Gamma(x, 0) = \begin{cases} 0 & \text{if } x = 0 \\ 1 & \text{if } x \neq 0 \end{cases}$$

The constants are:

$$D = 0.1$$

$$k = 1$$

With the program outlined above, we have computed the values of Γ for $t = 3$ from $x = 0$ to $x = 1$, choosing 0.1 as step length.

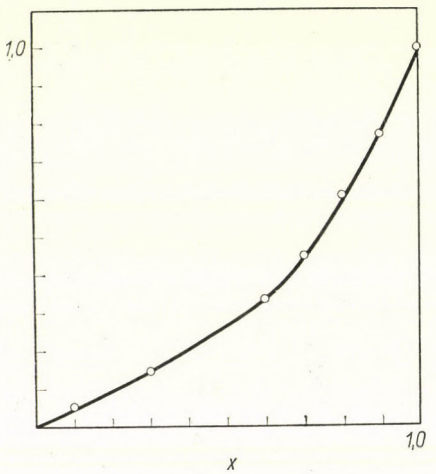

Fig. 3

The results of the computation are to be seen in Fig. 3. The integration was carried out with the trapezoidal rule, the interval of integration being divided into 21 subintervals. Applying two iteration steps, the error remains inside 3%. Wanting to check this, we also made a three-iteration computation, which showed the results obtained in the second and third iterations to agree to 8 digits. From this the sufficiency of only two iteration steps in practice can be concluded. It is worth-while remarking that the time of the calculation strongly depends on the number of the subintervals of integration, this time increasing proportionally to about the fourth power of the number of subintervals.

From all these facts it can be concluded that, when modelling chemical engineering processes, instead of using empirical formulae, it is worthwhile starting from the exact Damköhler equation and describing the individual operational units with it. To this end, for example, the solving procedure

outlined and its computer program, respectively, may be used. On the basis of the method presented, at least in principle, the mathematical modelling of a plant can be achieved by means of the Damköhler equation set up for the individual operational units.

The author is deeply indebted to Professor A. László for his guidance and valuable suggestions while writing this paper, and to Miss M. Farkas for taking part in solving some of the problems.

SUMMARY

The mathematical description of chemical engineering processes is possible with the use of conservation laws. Some authors call the corresponding mathematical expressions Damköhler equations. These are non-linear partial differential equations with initial and boundary conditions. This circumstance is illustrated in the case of a recirculation process. An illustration of the application of the Damköhler equation to an operational unit is given on the example of the blender.

An iterative method is described to solve the first boundary value problem in the case of the one-dimensional equation.

The method is well suitable for use on a computer. This is shown by describing an ALGOL program made to solve the model problem of component transfer on a rotating disk. The program is applicable to solve the first boundary value problem of the one-dimensional equation in the most general case.

In order to carry out the program, the terms of the equation and its initial and boundary conditions must be given in algebraic form. In this case all problems concerning the first boundary value problem of the one-dimensional Damköhler equation can be solved.

REFERENCES

1. Damköhler, G.: Z. Elektrochem. **42,** 846 (1936)
2. van Krevelen, D. W.: Brennstoff-Chem. **37,** 65 (1956)
3. Benedek, P., László, A.: A vegyészmérnöki tudomány alapjai. Műszaki Könyvkiadó, Budapest, 1964. (In Hungarian)
4. Fourier, J.: Théorie analytique de la chaleur. Paris, 1822
5. Cauchy, A.: Résumé des leçons à l'École polytechnique données sur le calcul infinitésimal. Paris, 1823
6. Naas, J., Schmid, H. L.: Mathematisches Wörterbuch. Teubner, Berlin, 1962.
7. Kjaer, J.: Programming of Chemical Calculations, Vol. 3. Numerical Methods for Integration and Solution of Differential Equations. Haldor Topsøe, Vedbaek, Denmark, 1965, p. 60
8. Weissinger, J.: Math. Nachr. **8,** 193 (1952)
9. Courant, R., Hilbert, D.: Mathematische Physik. Springer, Berlin, 1937
10. Poggi, L.: Aerotechnica **12,** 1579 (1932); **14,** 532 (1934)
11. Caplan, C.: NACA Rep. 621, (1938), 671, (1939)
12. Sauer, R.: Math. Nachr. **8,** 193 (1952)
13. Knighting, J. W. in L. Fox: Numerical Solution of Ordinary and Partial Differential Equations. Pergamon, 1962. p. 492
14. Hopkins, M. R.: Proc. Phys. Soc. **50,** 703 (1938)
15. Crank, J.: The Mathematics of Diffusion. Clarendon Press, Oxford, 1956
16. Fáy, L.: Vegyipari műveleti egységek leírása a kibővített Damköhler egyenletek alapján. (Description of Operational Units of Chemical Engineering on the Basis of the Extended Damköhler Equation.) (In Hungarian) Dissertation, Veszprém, 1967
17. Natanson, I. P.: Theorie der Funktionen einer reellen Veränderlichen. 2. Ausgabe, Akademie Verlag, Berlin, 1962
18. Levics, V. G.: Fizikai kémiai hidrodinamika. Akadémiai Kiadó, Budapest, 1958
19. Vegyipari üzemek matematikai modellezése (Mathematical Modelling of Chemical Plants). 1. Közl. Vegyipari Tröszt, Budapest, 1966. (In Hungarian)
20. Vegyipari üzemek matematikai modellezése (Mathematical Modelling of Chemical Plants). 2. Közl. Vegyipari Tröszt, Budapest, 1966. (In Hungarian)
21. Tihonov—Samarski: Equation in the Mathematical Physics. (Russian) Moscow, 1953

László Fáy; Veszprém, Csermák Antal u. 7.

Acta Chimica Academiae Scientiarum Hungaricae Tomus 56 (3), pp. 325—327 (1968)

PREPARATION AND INVESTIGATION OF LEWIS ACID COMPLEXES, III*

THE MECHANISM OF THE PREPARATION OF α-ACETOCHLOROGLUCOSE FROM β-PENTAACETYLGLUCOSE

(PRELIMINARY COMMUNICATION)

Z. CSŰRÖS, GY. DEÁK, L. FENICHEL, S. HOLLY and J. PÁLINKÁS

(Institute of Organic Chemical Technology, Technical University, Budapest, and Central Research Institute of Chemistry of the Hungarian Academy of Sciences, Budapest)

Received November 15, 1967.

An interesting example of the reactions catalyzed by LEWIS acids is the conversion of carbohydrates when the LEWIS acid plays the part of a reaction partner, in addition to its action as the catalyst. PACSU [1] was the first to find that α-acetochloroglucose could be prepared from β-pentaacetylglucose with titanium tetrachloride in excellent yields. Later on the reaction was studied by LEMIEUX [2], who suggested a mechanism. LEWIS acid complexes are formed from the starting material and from the product in this case, too; we thought that elucidation of the structures of these complexes may be helpful in a further investigation of the reaction mechanism.

The complex of 1 : 1 ratio was prepared from β-pentaacetylglucose with titanium tetrachloride as described previously [3]. Its infrared spectrum showed a new band at about 1540 cm^{-1}, in addition to the changes due to complex formation, described in [4]. This band is missing in the spectrum of the similar complex of 1 : 1 ratio of the α-anomer. LEMIEUX [2] ascribed the sole reactivity of the β-anomer to the loosening effect of the *trans* acetyl group at C—2. Under the conditions of the reaction — according to him — this group influences the acetyl group at C—1 so that it rapidly dissociates, and the sugar moiety is converted into a carbonium ion of temporary stability. We supposed — taking into account LEMIEUX's conception — that the titanium tetrachloride is attached first to the carbonyl oxygen of the acetyl group at C—1, in the complex, and the joint effect of complex formation and of the C—2 acetyl group results in splitting of the $C_1—O_{(Ac)}$ bond to give a compound which

* Part II: Z. CSŰRÖS, GY. DEÁK, I. GYURKOVICS, S. HOLLY, M. HARASZTHY-PAPP, A. TÖRÖK-KALMÁR and E. ZÁRA-KACZIÁN: Acta Chim. Acad. Sci. Hung. **55**, 347 (1968).

consists of an acetoxytitanium tetrachloride anion and a carbonium cation.

When preparing [3] the complex, a chloroform solution of the starting compound was mixed with a solution of titanium tetrachloride in petroleum ether and chloroform; the yellow complex was separated as a solid. When carrying out the reaction for preparative purposes, only chloroform was used as the solvent. In this case, mixing of the solutions of β-pentaacetylglucose and titanium tetrachloride gave first a yellow oily material, which dissolved after a few minutes of stirring. The addition of petroleum ether to the solution caused the separation of a yellow, solid complex consisting of 1 mole of β-pentaacetylglucose and 1 mole of titanium tetrachloride, as shown by analysis. The complex was decomposed with water and the organic component extracted with chloroform. Measurement of its optical rotatory power showed that it was acetochloroglucose, largely in the β-configuration. Accordingly, the isolated complex should be a complex of β-acetochloroglucose and acetoxytitanium trichloride. The other possibility is that the complex has ionic structure and the carbon—chlorine bond is formed during the process of work-up. In order to clarify this point, further experiments were made in solution without isolating the complex.

The infrared spectrum of the solution was taken a few minutes after mixing equimolar solutions of β-pentaacetylglucose and titanium tetrachloride. It was found that chlorination had been completed within this short period, and the spectrum was that of the β-acetochloroglucose complex. The conversion of the β-anomer into α-anomer was also examined; at room temperature, this reaction was completed in 4—5 hours after its beginning.

The spectra of both the solution and the Nujol suspension of the prepared substance had a new band at about 1550 cm^{-1}. This band can be found in the spectrum of the model compound, acetoxytitanium trichloride in Nujol. On the basis of this evidence, it can be supposed that the complex is formed from the β- or α-anomer and acetoxytitanium trichloride, produced during the reaction.

To verify this conception, the complex of β-acetochloroglucose and acetoxytitanium trichloride was prepared, and its infrared spectrum was compared with that of the end product from the reaction of β-pentaacetylglucose and titanium tetrachloride. The spectra were found to be essentially identical.

Since acetoxytitanium trichloride is also a LEWIS acid, it is not only a by-product of the reaction, but a catalyst of the conversion of the β-chloro derivative into the α-anomer. This fact has been proved by our kinetic measurements showing a relatively slow conversion of the β-chloro derivative into the α-anomer in chloroform solution; this process was significantly accelerated in the presence of acetoxytitanium trichloride.

REFERENCES

1. PACSU, E.: Ber. **61**, 1508 (1928).
2. LEMIEUX, R. V., BRICE, C.: Can. J. Chem. **30**, 295 (1952).
3. CSŰRÖS, Z., DEÁK, GY., FENICHEL, L.: Acta Chim. Acad. Sci. Hung. **21**, 169 (1960).
4. CSŰRÖS, Z., DEÁK, GY., GYURKOVICS, I., HOLLY, S., HARASZTHY-PAPP, M., ZÁRA-KACZIÁN, E.: Periodica Polytechnica, in press.

Zoltán CSŰRÖS
Gyula DEÁK
László FENICHEL
Sándor HOLLY
János PÁLINKÁS
Budapest XI., Műegyetem rakpart 3.

INDEX

INORGANIC AND ANALYTICAL CHEMISTRY — ANORGANISCHE UND ANALYTISCHE CHEMIE — НЕОРГАНИЧЕСКАЯ И АНАЛИТИЧЕСКАЯ ХИМИЯ

SZAKÁCS-PINTÉR, M. und MAROS, L.: Untersuchung des Mechanismus der zweistufigen Oxydation des Furfurols und Furfurylalkohols mit Brom und Bromchlor in wäßriger Lösung 199

KISS, Á.: Theorie der Lichtabsorption der Cyclopentadienyl-Komplexe der Übergangselemente 215

ROKOSZ, A., PAULIK, J., PAULIK, F. und ERDEY, L.: Beiträge zur quantitativen Differentialthermoanalyse. Untersuchung des Zusammenhanges zwischen der Spitzenfläche und der Probemenge unter den Versuchsbedingungen der derivatographischen Messung 221

PHYSICAL CHEMISTRY — PHYSIKALISCHE CHEMIE — ФИЗИЧЕСКАЯ ХИМИЯ

TÓTH, A. and BILLES, F.: Ultraviolet Spectroscopic Study of the Acid-Base Equilibria of Pyrimidine Derivatives, I Uracil Derivatives 229

SOLYMOSI, F. and BÁNSÁGI, T.: Thermal Stability of Chlorine Oxy-Salts in the Solid State, I. Kinetic Study of the Disproportionation and Explosion of Some Chlorites 251

KISS, I., JÁKLI, GY., JANCSÓ, G. and ILLY, H.: Isotopic Effects on Vapour Pressure, III. Deuteration Effect on the Vapour Pressure of Alcohols 271

TÖRÖK, F. and PULAY, P.: On the Parameter Form of Force Constant Matrix, V. The Maximum and Minimum Values of Force Constants 285

VARSÁNYI, GY.: Simultaneous Positive and Negative Deviations from the Ideal Behaviour in the System of Two Volatile Components (Short Communication) .. 297

ORGANIC CHEMISTRY — ORGANISCHE CHEMIE — ОРГАНИЧЕСКАЯ ХИМИЯ

MAGYAR G. und BITE, P.: Herstellung von 7-Keto-Steroidverbindungen 303

SHANMUGANATHAN, SP. and SRI RAMA RAO, D.: Bromine Addition to Some Unsaturated Sulphones 307

GERECS, Á., BARTA, M., TÓTH, T. und LAY, A.: Indol und Indolderivate, III. Die Synthese von 6-RO-Indol- und Indolin-Derivaten 311

CHEMICAL TECHNOLOGY — CHEMISCHE TECHNOLOGIE — ХИМИЧЕСКАЯ ТЕХНОЛОГИЯ

FÁY, L.: On the Extended Damköhler Equation 315

CSŰRÖS, Z., DEÁK, GY., FENICHEL, L., HOLLY, S. and PÁLINKÁS, J.: Preparation and Investigation of Lewis Acid Complexes, III. The Mechanism of the Preparation of α-acetochloroglucose from β-pentaacetylglucose (Preliminary Communication) 325

Printed in Hungary

A kiadásért felel az Akadémiai Kiadó igazgatója — Műszaki szerkesztő: Farkas Sándor

A kézirat nyomdába érkezett: 1968. III. 12. — Terjedelem: 11,50 (A/5) ív 54 ábra, 1 melléklet

68.65280 Akadémiai Nyomda, Budapest — Felelős vezető: Bernát György

ACTA CHIMICA

ТОМ 56 — ВЫП. 3

РЕЗЮМЕ

Изучение механизма двухступенчатого окисления фурфурола и фурфурильных спиртов с бромом и хлористым бромом в водных средах

М. ПИНТЕР-САҚАЧ и Л. МАРОШ

Фурфурол и фурфуриловый спирт реагируют в присутствии кислоты, как катализатора, с 1 молем брома. Процесс имеет 1-ый порядок по производным фурана и 0-вой — по галогену. В ходе реакции (водная среда) образуется 2 моля бромистого водорода, и производное фурана через разрыв кольца дает соответствующее ненасыщенное оксо-соединение. Скорость процесса — также и с применением хлористого брома — лимитируется скоростью протонирования кислорода эфира. Согласно предложенному механизму, за этим следует присоединение галогена в положение 2,5 с последующим быстрым гидролизом.

Скорость реакции фурфурола и фурфурилового спирта со вторым молем брома является меньшей на 3—4 порядка. Эта реакция, собственно, представляет собой бромирование ненасыщенных оксо-соединений, которое, согласно предложенному механизму, является процессом галогенирования энолов, катализируемым кислотой; причем порядок по брому равен нулю.

Ненасыщенные оксо-соединения реагируют с хлористым бромом по механизму обыкновенного электрофильного присоединения. Катализ с кислотой не наблюдается в данном случае. Порядок по ненасыщенному оксо-соединению и хлористому брому равен 1.

При реакции со 2-ым молем брома и хлористого брома образуется бром-гидрин, а также 1 моль галогенистого водорода.

Теория поглощения света комплексов переходных металлов с циклопентадиенилом

А. КИШ

Принимая во внимание количество неспаренных d-электронов, поглощение света комплексов переходных металлов с циклопентадиенилом обсуждается критически с помощью новой рабочей гипотезы. Принимались во внимание спаривание спинов, вследствие сильного лигандного поля и магнитные моменты комплексов. На основе этого задавались предлагаемые числа симметрии и спино-запрещенных полос. Т. к. данные по светопоглощению некоторых соединений являются неполными, то в этих случаях рабочую гипотезу спекулятивно нельзя безупречно доказать. Поэтому для последних планируются экспериментальные исследования и квантово-механические расчеты.

Количественный дифференциальный термоанализ

А. РОКОС, Й. ПАУЛИК, Ф. ПАУЛИК и Л. ЭРДЕИ

Изучалась зависимость между количеством образца и площадью под пиками в дериватографии. Были установлены наиболее благоприятные условия для количественного анализа.

Изучение кислотно-основных равновесий производных пиримидина с помощью метода ультрафиолетовой спектроскопии

А. ТОТ и Ф. БИЛЛЕШ

Изучались кислотные и основные равновесия урацила и его некоторых 5- и 6-замещенных производных на основе зависимости их электронного спектра от pH. Равновесия интерпретировались на основе влияний заместителей. Для систематизирования разнообразных равновесий вводилось понятие состояния протонирования для видов, принимающих участие в равновесиях. Удалось разделить равновесия однозаряженных анионов двух различных типов.

Термическая стабильность солей с анионами, содержащими кислород и хлор, в твердом состоянии, I. Кинетическое изучение диспропорционирования и взрыва некоторых хлоритов

Ф. ШОЙМОШИ и Т. БАНШАГИ

Было показано, что при низких температурах хлориты диспропорционируются в хлораты и хлориды без какого-либо измеряемого разложения. Кинетический анализ реакции диспропорционирования был проведен по уравнению первого порядка, и рассчитывалась энергия активации. На основе кинетических данных и некоторых наблюдений полагалось, что диспропорционирование хлоритов происходит за счет перегруппировки внутри решетки. При повышенных температурах хлорит натрия все еще только диспропорционируется, даже при 400 °C, в то время как другие соединения интенсивно взрываются, давая в основном хлориды и кислород. Перед взрывом наблюдалось лишь слабое разложение веществ, а реакция диспропорционирования протекала лишь до известной степени. Стабильность соединений зависит от катиона и изменяется в следующем порядке: Na, Ba, Ag, Pb. Полагалось, что в определении порядка стабильности играют важную роль сила эффективного электрического поля катиона и ионность веществ.

Изотопные эффекты в давлениях паров, III Изотопный эффект дейтерия в давлении паров спиртов

Й. КИШ, ДЬ. ЯКЛИ, Г. ЯНЧО и Х. ИЛЛИ

В широком интервале температур определялась разность в давлении паров пропанола-(1), пропанола-(2), бутанола-(1), бутанола-(2), 2-метил-пропанола-(2), пентанола-(3) и их дейтерированных в гидроксильной группе производных. С использованием экспериментальных данных были рассчитаны значения факторов разделения при перегонке (α) для этих пар соединений на основе уравнения состояния для спиртовых паров. Величины с помощью метода наименьших квадратов приводились к зависимости Бигелейсена ($\ln \alpha = A/T^2 - B/T$). При сравнении настоящих и более ранних результатов [2] было установлено, что величина постоянной B, связанной со смещением нулевой энергии внутримолекулярных колебаний, зависит от порядка спирта, а также от симметрии молекулы

Параметрическое получение матрицы силовых постоянных, V Крайние значения силовых постоянных

Ф. ТЁРЁК и П. ПУЛАИ

С помощью параметрического метода, описанного в предыдущих сообщениях. могут быть составлены все матрицы силовых постоянных F, находящиеся в согласии с частотами, определенными экспериментальным путем. Для случая, когда для однознач-

ного установления силовых постоянных не хватает экспериментальных данных, был разработан метод итерации, который позволяет определить максимальные и минимальные значения отдельных силовых постоянных, находящиеся еще в согласии с экспериментальными данными. Согласно наблюдениям, если в распоряжении находятся только частоты, то могут быть получены почти весьма невероятные крайние значения даже и в том случае, если ограничиваемся одним заданным отнесением. Однако на практике в большинстве случаев, некоторая часть силовых постоянных известна с хорошим приближением, и, таким образом, необходимо определить крайние значения только остальных силовых постоянных. С помощью разработанной нами программы для вычислительной машины крайние значения последних силовых постоянных могут быть определены при условии, если первые остаются в пределах, заданных заранее.

Получение 7-кэто-стероидных соединений

ДЬ. МАДЯР и П. БИТЭ

3-β-ацетокси-Δ-5,16-прегнадиен-7,20-дион получился окислением 3-β-ацетокси-Δ-5,16-прегнадиен-20-она и из получившегося при деградации соласодина псеудо-диацетил соласодина путем низкотемпературного окисления и последующего высокотемпературного окисления образовавшейся реакционной смеси.

Из 3-β-ацетокси-Δ-5,16-прегнадиен-7,20-диона приготовился 3-β-окси-Δ-5,16-прегнадиен-7,20-дион, 3-β-тозилокси-Δ-5,16-прегнадиен-7,20-дион и Δ-3,5,16-прегнатриен-7,20-дион, а также азотнокислые соли 3-β-ацетокси и 3-β-окси-Δ-5,16-прег-надиен-7,20-дион-20-гуанидилхидразонов.

Присоединение брома к некоторым ненасыщенным сульфонам

СП. ШАНМУГАНАТАН и Д. СРИ РАМА РАО

Изучалась кинетика присоединения брома к α, β- и β, γ-ненасыщенным сульфонам в растворе уксусной кислоты при 30 °C. Присоединение протекает по реакции второго порядка. Присоединение брома к сульфонам типа $RSO_2CH{=}CHR'$ и $RSO_2CH_2CH{=}CHR'$ (R' = фенил) протекает быстрее в уксусной кислоте, чем в четыреххлористом углероде, в то время как присоединение брома к сульфонам типа $RSO_2CH{=}CH_2$ и $RSO_2CH_2CH{=}CH_2$ в уксусной кислоте протекает медленнее, чем в четыреххлористом углероде. Это наблюдение пытались объяснять на основе различия в поляризации систем в уксусной кислоте. Изучалось также влияние заместителей на скорость присоединения брома. Результаты интерпретировались на основе полярных эффектов заместителей.

Индол и его производные, III
Синтез производных 6-RO-индола и 6-RO-индолина

А. ГЕРЕЧ, М. БАРТА, Т. ТОТ и А. ЛАЙ

Был разработан новый синтез производных 6-RO-индола и 6-RO-индолина. В ходе этих исследований были получены следующие соединения: 1-бензоил-6-гидрокси-, 1-бензоил-6-метокси-, 6-метокси-, 1-бензоил-6-бензилокси-, 6-бензилокси-, 6-гидрокси-индолин и 6-гидрокси-индол.

О распространении уравнения Дамкьёлера

Л. ФАЙ

Процессы химической промышленности математически описываются с помощью законов сохранения. Некоторые авторы называют математические выражения этих законов уравнениями Дамкьёлера. Они являются дифференциальными уравнениями в

частных производных, дополненными соответствующими начальными и граничными условиями. В настоящей работе рассматривается это условие в связи с процессами рециркуляции. Применение уравнения Дамкьёлера демонстрируется на примере конкретного аппарата, смесителя.

Для решения проблемы первого граничного значения одноразмерного уравнения был разработан итерационный метод, описываемый в настоящем сообщении.

Метод легко применяется для машинных расчетов. Для иллюстрации этого описывается программа ALGOL, составленная для расчета передачи компонентов на вращающемся диске. Программа пригодна для решения проблемы первого граничного значения одноразмерного уравнения Дамкьёлера и в наиболее общем случае.

Для выполнения расчета граничное условие и форма уравнения должны быть заданы в алгебраической форме, что позволяет решение всех проблем, связанных с первым граничным значением одноразмерного уравнения Дамкьёлера.

The Acta Chimica publish papers on chemistry in English, German, French and Russian.

The Acta Chimica appear in volumes consisting of four parts of varying size, 4 volumes being published a year.

Manuscripts should be addressed to

Acta Chimica
Budapest 502, Postafiók 32.

Correspondence with the editors should be sent to the same address.

The rate of subscription is 165 forints a volume. Orders may be placed with "*Kultúra*" Foreign Trade Company for Books and Newspapers (Budapest I., Fő utca 32. Account No. 43-790-057-181) or with representatives abroad.

Les Acta Chimica paraissent en français, allemand, anglais et russe et publient des mémoires du domaine des sciences chimiques.

Les Acta Chimica sont publiés sous forme de fascicules. Quatre fascicules seront réunis en un volume (4 volumes par an).

On est prié d'envoyer les manuscrits destinés à la rédaction à l'adresse suivante:

Acta Chimica
Budapest 502, Postafiók 32.

Toute correspondance doit être envoyée à cette même adresse.

Le prix de l'abonnement est de 165 forints par volume.

On peut s'abonner à l'Entreprise pour le Commerce Extérieur de Livres et Journaux «*Kultúra*» (Budapest I., Fő utca 32. Compte-courant No. 43-790-057-181) ou à l'étranger chez tous les représentants ou dépositaires.

«*Acta Chimica*» издают трактаты из области химической науки на русском, французском, английском и немецком языках.

«*Acta Chimica*» выходят отдельными выпусками разного объема. 4 выпуска составляют один том. 4 тома публикуются в год.

Предназначенные для публикации рукописи следует направлять по адресу:

Acta Chimica
Budapest 502, Postafiók 32.

По этому же адресу направлять всякую корреспонденцию для редакции.

Подписная цена «*Acta Chimica*» — 165 форинтов за том. Заказы принимает предприятие по внешней торговле книг и газет «*Kultúra*» (Budapest I., Fő utca 32. Текущий счет № 43-790-057-181) или его заграничные представительства и уполномоченные.

Reviews of the Hungarian Academy of Sciences are obtainable at the following addresses:

ALBANIA

Ndermarja Shtetnore e Botimeve
Tirana

AUSTRALIA

A. Keesing
Box 4886, GPO
Sydney

AUSTRIA

Globus Buchvertrieb
Salzgries 16
Wien I

BELGIUM

Office International de Librairie
30, Avenue Marnix
Bruxelles 5
Du Monde Entier
5, Place St. Jean
Bruxelles

BULGARIA

Raznoiznos
1, Tzar Assen
Sofia

CANADA

Pannonia Books
2, Spadina Road
Toronto 4, Ont.

CHINA

Waiwen Shudian
Peking
P. O. B. 88

CZECHOSLOVAKIA

Artia
Ve Směčkách 30
Praha 2
Poštovná Novinová Služba
Dovoz tisku
Vinohradská 46
Praha 2
Mad'arská Kultura
Václavské nám. 2
Praha I
Poštová Novinová Služba
Dovoz tlače
Leningradská 14
Bratislava

DENMARK

Ejnar Munksgaard
Nörregade 6
Copenhagen

FINLAND

Akateeminen Kirjakauppa
Keskuskatu 2
Helsinki

FRANCE

Office International de Documentation et Librairie
48, rue Gay Lussac
Paris 5

GERMAN DEMOCRATIC REPUBLIC

Deutscher Buch-Export und Import
Leninstraße 16
Leipzig 701
Zeitungsvertriebsamt
Clara Zetkin Straße 62
Berlin N. W.

GERMAN FEDERAL REPUBLIC

Kunst und Wissen
Erich Bieber
Postfach 46
7 Stuttgart S.

GREAT BRITAIN

Collet's Holdings Ltd.
Dennington Estate
London Rd.
Wellingborough. Northants.
Robert Maxwell and Co. Ltd.
Waynflete Bldg. The Plain
Oxford

HOLLAND

Swetz and Zeitlinger
Keizersgracht 471—487
Amsterdam C
Martinus Nijhof
Lange Voorhout 9
The Hague

INDIA

Current Technical Literature
Co. Private Ltd.
India House OPP
GPO Post Box 1374
Bombay I

ITALY

Santo Vanasia
Via M. Macchi 71
Milano
Libreria Commissionaria Sansoni
Via La Marmora 45
Firenze

JAPAN

Nauka Ltd.
92, Ikebukur O-Higashi 1-chome
Toshima-ku
Tokyo
Maruzen and Co. Ltd.
P. O. Box 605
Tokyo-Central
Far Eastern Booksellers
Kanda P. O. Box 72
Tokyo

KOREA

Chulpanmul
Phenjan

NORWAY

Johan Grundt Tanum
Karl Johansgatan 43
Oslo

POLAND

RUCH
ul Wronia 23
Warszawa

ROUMANIA

Cartimex
Str. Aristide Briand 14—18.
București

SOVIET UNION

Mezhdunarodnaya Kniga
Moscow G—200

SWEDEN

Almquist and Wiksell
Gamla Brogatan 26
Stockholm

USA

Stechert Hafner Inc.
31, East 10th Street
New York, N. Y. 10003
Walter J. Johnson
111, Fifth Avenue
New York, N. Y. 10003

VIETNAM

Xunhasaba
19, Tran Quoc Toan
Hanoi

YUGOSLAVIA

Forum
Vojvode Mišića broj 1
Novi Sad
Jugoslovenska Knjiga
Terazije 27
Beograd

28. VI. 1968 Index: 26.027

ACTA CHIMICA

ACADEMIAE SCIENTIARUM HUNGARICAE

ADIUVANTIBUS

L. ERDEY, K. POLINSZKY, G. SCHAY

AC

R. BOGNÁR, GY. BRUCKNER, Z. CSŰRÖS, T. ERDEY-GRÚZ, Z. FÖLDI, M. FREUND, Á. GERECS, GY. HARDY, J. HOLLÓ, Á. KISS, M. KORACH, F. MÁRTA, F. NAGY, J. PROSZT, E. PUNGOR, Z. SZABÓ, P. TÉTÉNYI, L. VARGHA, K. VAS

REDIGIT

B. LENGYEL

TOMUS 56 FASCICULUS 4

AKADÉMIAI KIADÓ, BUDAPEST

1968

ACTA CHIM. ACAD. SCI. HUNG.

ACTA CHIMICA

A MAGYAR TUDOMÁNYOS AKADÉMIA KÉMIAI TUDOMÁNYOK OSZTÁLYÁNAK IDEGEN NYELVŰ KÖZLEMÉNYEI

SZERKESZTI

LENGYEL BÉLA

TECHNIKAI SZERKESZTŐK

DEÁK GYULA és TAKÁCS VILMOS

Az Acta Chimica német, angol, francia és orosz nyelven közöl értekezéseket a kémiai tudományok köréből.

Az Acta Chimica változó terjedelmű füzetekben jelenik meg, egy-egy kötet négy füzetből áll. Évente átlag négy kötet jelenik meg.

A közlésre szánt kéziratok a szerkesztőség címére (Budapest 502, postafiók 32) küldendők.

Ugyanerre a címre küldendő minden szerkesztőségi levelezés. A szerkesztőség kéziratokat nem ad vissza.

Az Acta Chimica előfizetési ára kötetenként belföldre 120 Ft, külföldre 165 Ft. Megrendelhető a belföld számára az „Akadémiai Kiadó"-nál (Budapest V., Alkotmány utca 21. Bankszámla 05-915-111-46), a külföld számára pedig a „Kultúra" Könyv- és Hírlap Külkereskedelmi Vállalatnál (Budapest I., Fő utca 32. Bankszámla: 43-790-057-181) vagy annak külföldi képviseleteinél és bizományosainál.

Die Acta Chimica veröffentlichen Abhandlungen aus dem Bereiche der chemischen Wissenschaften in deutscher, englischer, französischer und russischer Sprache.

Die Acta Chimica erscheinen in Heften wechselnden Umfanges. Vier Hefte bilden einen Band. Jährlich erscheinen 4 Bände.

Die zur Veröffentlichung bestimmten Manuskripte sind an folgende Adresse zu senden:

Acta Chimica
Budapest 502, Postafiók 32.

An die gleiche Anschrift ist auch jede für die Redaktion bestimmte Korrespondenz zu richten.

Abonnementspreis pro Band: 165 Forint. Bestellbar bei dem Buch- und Zeitungs-Außenhandels-Unternehmen »*Kultúra*« (Budapest I., Fő utca 32. Bankkonto No. 43-790-057-181) oder bei seinen Auslandsvertretungen und Kommissionären.

Acta Chimica Academiae Scientiarum Hungaricae Tomus 56 (4), pp. 329—330 (1968)

REACTION OF XENON DIFLUORIDE WITH WATER

(SHORT COMMUNICATION)

I. FEHÉR and M. LŐRINC

(Central Research Institute for Physics of the Hungarian Academy of Sciences, Budapest)

Received August 7, 1967

It was found by MALM *et al.* [1] that xenon difluoride reacts with water according to the equation:

$$XeF_2 + H_2O = Xe + 0.5\ O_2 + 2\,HF\,.$$

The half-life of the reaction was evaluated by iodometric measurements by APPELMAN and MALM [2] and found to be about 7 hr. at 0°C.

This reaction has been investigated in the experiments now reported by evaluating the rate constant for the homogeneous reaction with three different methods, namely, tracer technique with ^{133}Xe, ^{133m}Xe tracer, volumetry of the Xe and O_2 gas products, and electric conductivity measurement of the HF yield at 0° and 25°.

Experimental

Material: High purity XeF_2, prepared in the *Central Research Institute for Physics* [3].

Radioactive tracer method. The rate constant of the reaction was evaluated from the time behaviour of the activity measured on the labelled XeF_2 solution by gamma spectrometry. XeF_2 was labelled by irradiation in a reactor for 3 hrs. with a $2 \cdot 10^{13}$n cm^{-2} sec^{-1} thermal neutron flux. During this irradiation time no appreciable decomposition of XeF_2 could be observed. The activity measurements covering the radiations from ^{133}Xe ($t_{1/2} = 5{,}2$ days) and ^{133m}Xe ($t_{1/2} = 2{,}1$ days) were performed 10 to 20 days after irradiation of the solution of the labelled XeF_2, having first driven out the xenon gas formed during the reaction by an argon gas current passed through the reaction vessel.

Volumetry of the gas yield. The reaction kinetics were determined from the measured volumes of the Xe and O_2 gas products. The measurement was performed in a thermostated, polyethylene-lined glass vessel using a mercury burette as gas recipient.

Electrical conductivity measurement. The rate constant was evaluated from the measured electrical conductivity of the solution that was observed to increase with the rate of HF formation. The measurement was performed in the thermostated polyethylene vessel, using an OK-12 type conductometer and Pt electrodes on teflon support.

Results and discussion

The range of initial concentrations covered by the measurements was 640 to 2547 mg XeF_2/100 ml of solution.

XeF_2 dissolved in the reagent at 0° in 20—25, and at 25° in 6—8 minutes. The loss of less than 5% of the measured XeF_2 during dissolution has not been taken into account in the evaluation of the rate constant.

The reaction of XeF_2 with H_2O was found to be an essentially homogeneous process. In the presence of air or argon current, XeF_2 rapidly escapes from the homogeneous aqueous solution. This possibility was reduced to minimum by the experimental conditions used.

The electrical conductivity of XeF_2 solutions in water over the concentration range from 640 to 2547 mg/100 ml was found to be determined by the amount of HF produced in the reaction.

The reaction, as measured by any of the three methods, seems to be a first-order process in the investigated range of concentrations. The rate constant as evaluated by different methods was found to be the same within the experimental error.

The investigations confirm the validity of the stoichiometric equation formulated by MALM *et al.* [1].

The mean values of the rate constant were found to be at 0° $(1.7 \pm \pm 0.1) \cdot 10^{-3}$ min.$^{-1}$; at 25° $(1.51 \pm 0.04) \cdot 10^{-2}$ min.$^{-1}$.

The value obtained at 0° is in good agreement with the result of APPELMAN and MALM [2].

These additional data on the mechanism of the XeF_2-H_2O reaction are expected to be useful for an interpretation of the toxicologic effect of XeF_2 on intake by a living organism.

REFERENCES

1. MALM, I. G., HATT, B. D., BAUE, R. W.: "Noble-Gas Compounds". University of Chicago Press, Chicago, Ill. 1963, p. 169.
2. APPELMAN, E. M., MALM, J. G.: J. Am. Chem. Soc. **86,** 2297 (1964).
3. GRÓZ, P., KISS, I., RÉVÉSZ, A., SIPOS, T.: KFKI Közlemények **13,** 5 (1965).

István FEHÉR
Mária LŐRINC
Budapest 114, Postafiók 49.

Acta Chimica Academiae Scientiarum Hungaricae Tomus 56 (4), pp. 331—335 (1968)

CALCULATION OF FORCE CONSTANTS WITH THE MAXIMUM OVERLAP METHOD, II

MOLECULES WITH LONE PAIR ELECTRONS OR EMPTY ORBITALS

(SHORT COMMUNICATION)

M. MEZEI* and P. PULAY

(Institute for General and Inorganic Chemistry, L. Eötvös University, Budapest, and Research Group for Inorganic Chemistry, Hungarian Academy of Sciences, Budapest)

Received October 6, 1967

Introduction

In a previous paper [5] the force constants of tetrahedral molecules were computed on the assumption that the energy of the molecules was proportional to the sum of overlap integrals between the bonding orbitals. The sum of overlap integrals was computed with the *maximum overlap method* [6, 1]. In that case the number of bonding orbitals of the central atom was identical with the number of ligands.

The *maximum overlap method* can also be used in cases, where there are fewer ligands than bonding orbitals on the central atom, but the result does not depend on the non-bonding orbital being empty or occupied by a lone pair. The two cases clearly differ from each other physically. So we must first decide, which of the two possible cases is represented by the hybrid orbitals, obtained by the *maximum overlap method.*

1.

If the geometry of the above-mentioned two types of molecules is taken into account, it can be seen that the difference is not only quantitative but also qualitative, *i.e.* the symmetry of the molecules is different. (For example, BF_3 belongs to the D_{3h} group, while NH_3 to the C_{3v} group.) On the basis of this qualitative difference it will be shown that the hybrids obtained with the *maximum overlap method* correspond to the case of empty orbitals.

XY_2 and XY_3 type molecules were examined in a general form. We used only *s* and *p* orbitals, and consequently the XY_i distances and the $Y_i—X—Y_j$ angles were equal in the same molecule. In the following we will vary only the bond angle.

If the overlap integrals between the atomic orbitals are known, the overlap matrix can be computed (**S**), and the maximal sum of overlaps between

* Present address: *Computational Centre of the Hungarian Chemical Industries, Budapest.*

the bonding orbitals (MAX) can be obtained in the following way [1, 6]:

$$\mathrm{MAX} = \mathrm{tr}\,(\mathbf{S}\mathbf{S}^{\mathrm{T}})^{1/2}, \tag{1}$$

where $\mathbf{S}^{\mathrm{T}}$ is the transposed of S. The elements of S depend only on the geometrical data of the molecule, namely in our case the Y_i-X-Y_j angle, denoted in the following by α, and the atomic overlap integrals between the ligand orbitals and the *s* and *p* orbitals of the central atom, denoted by *S* and *P*, respectively. Using Eq. (1), the maximal sum of overlaps, MAX, can be obtained as a function of these three parameters. We succeeded in expressing the maximal overlap with a relatively simple formula in both cases:

$$XY_2\text{: } \mathrm{MAX} = \sqrt{2S^2 + P^2(1 + \cos\alpha)} + \sqrt{p^2(1 - \cos\alpha)} \tag{2}$$

$$XY_3\text{: } \mathrm{MAX} = 2\sqrt{2}P\sin\alpha + \sqrt{3}\sqrt{S^2 + P^2}\sqrt{1 - 1.33\sin^2\alpha} \tag{3}$$

Having obtained Eqs. (2) and (3), the maximal value of MAX was searched with respect to the angle α. It is clear that the *maximum overlap method* predicts this configuration to be the most stable. In this way we derived an equation from which the equilibrium bond angle could be expressed explicitly. We obtained the same formula for both cases:

$$\cos\alpha_0 = S^2/P^2 \tag{4}$$

We found, moreover, that if $S/P > 1$ for XY_2 molecules and if $S/P > 2^{-1/2}$ for XY_3 molecules, the equilibrium bond angle would be 180° and 120°, respectively. In the case of common molecules S/P is always greater than 1. It follows that the hybrid orbitals obtained by the *maximum overlap method* correspond to the case of empty non-bonding orbitals.

2.

Papers in the literature dealing with the problem of lone pair electrons conclude that the experimental equilibrium data in the case of molecules with lone pair electrons cannot be reproduced with the *maximum overlap method*, unless an empirical parameter is introduced.

Del Re *et al.* [2] reproduced the experimental bond angle of water by introducing a parameter which represented the interaction of the lone pair electrons with the others. This parameter was chosen in such a way as to fit the experimental data.

The works of Volkov [8] have shown that no serious mistake is made if the lone pair electrons are considered to be on the *s* orbital, and treated as an inert pair.

According to our calculation, we ought to decrease the value of S to obtain results, in accordance with the former procedures. But if there is no theoretical reason for doing so, it must be considered an arbitrary action.

It appears that for the consideration of the lone pair, further effects must be taken into account. We refer primarily to the electrostatic interaction of the electrons. If the central atom does not possess a lone pair, the electrostatic repulsions of the electrons are almost compensated, because the bonding electrons are equivalent or nearly equivalent. If the central atom does possess a lone pair, the electrostatic repulsions no longer be considered to be compensated. This problem requires further detailed investigation.

3.

Before speaking about the numerical calculations, a theoretical problem will be discussed with the aid of Eq. (4). We know from experimental results that if a bond distance increases, there is a decrease in the s content of the bonding orbital [7]. This phenomenon can be interpreted in the case of XY_2 and XY_3 type molecules with the *maximum overlap method.*

The connection between the equilibrium bond and the s content of the hybrid orbital has to be investigated first. On the basis of the geometry of the s and p orbitals, it is clear that the angle between the hybrid orbitals decreases when there is a decrease in the s content of the hybrid. Moreover, it can be seen that the hybrid orbital always points to the direction of the ligand, because we are dealing with the maximum overlap configuration. In this way the angle between the hybrids is the same as the angle between the bonds.

Next, we investigate the connection between the ratio S/P and the bond length. On the basis of the geometry of the s and p orbitals it can be seen that S/P is a monotonically decreasing function of the bond length. Thus it can be seen using Eq. (4) that the experimental facts are in accordance with the results of the *maximum overlap method.*

4.

In order to show that the *maximum overlap method* can be used if the non-bonding orbital is empty, the force constants of BF_3 were calculated. In our calculations the same method was used as in the case of tetrahedral molecule [5]. The bonding orbital of fluorine was taken to be sp hybrid. Only the bending and the stretching — bending force constants were computed, because the model is unstable to stretching.

The symmetry coordinates are shown in Table I. r_i is the distance between the i-th F atom and the B atom, α_{ij} is the $F_i - B - F_j$ angle and β_i is the

Table I

Symmetry coordinates and force constants of planar XY_3 molecules

Symmetry class	Symmetry coordinate	Force constant
A_1'	$S_1 = 3^{-1/2}(\delta r_1 + \delta r_2 + \delta r_3)$	F_{11}
A_2''	$S_2 = 3^{-1/2} r_0(\delta\beta_1 + \delta\beta_2 + \delta\beta_3)$	F_{22}
E'	$S_3 = 2^{-1/2}(\delta r_2 - \delta r_3)$	F_{33} F_{34}
	$S_4 = 2^{-1/2} r_0(\delta\alpha_{13} - \delta\alpha_{12})$	F_{44}

r_0 is the equilibrium bond length.

angle between the threefold symmetry axis and the i-th bond. The effective nuclear charges are shown in Table II.

Table II

The effective nuclear charge of the Slater orbitals

	2s	2p
B	1.608	1.569
F	2.564	2.550

Table III

The calculated and the experimental force constants of BF_3

	Reference [4]	Reference [3]	Calculated
F_{22}	—	0.865	0.865
F_{34}	−0.268	−0.313	−0.311
F_{44}	0.525	0.515	0.323

Table III contains the calculated and the experimental values of the force constants. The constant factor was chosen so that the calculated F_{22} should agree with the experimental one.

The results are qualitatively in agreement with the experimental values, as in the case of the tetrahedral molecules. The sign of the non-diagonal force constant is correct, but its numerical agreement must be considered accidental.

SUMMARY

We have shown that the *maximum overlap method* can be used, provided the central atom does not possess any lone pair electrons.

The stretching and stretching—bending force constants of BF_3 were computed up to a constant factor with our previously applied method. The sign of the non-diagonal force constant was obtained correctly in this case, too.

REFERENCES

1. Golebiewski, A.: Trans. Faraday Soc. **57,** 1849 (1961).
2. Del Re, G., Esposito, U., Carpentieri, M.: Th. Chim. Acta **6,** 36 (1966).
3. Duncan, J. L.: J. Mol. Spectrosc. **13,** 338 (1964).
4. McKean, D. C.: J. Chem. Phys. **24,** 1002 (1956).
5. Mezei, M., Pulay, P.: Acta Chim. Acad. Sci. Hung. (In press.)
6. Murrel, J. N.: J. Chem. Phys. **32,** 767 (1960).
7. Orville-Thomas: The structure of small molecules. Elsevier, New York, 1966.
8. Volkov, V. M.: Zhur. Neorg. Khim. **8,** 1820 (1963).

Mihály Mezei Budapest XIV., Hungária krt. 178
Péter Pulay Budapest VIII., Múzeum krt. 6/8

Acta Chimica Academiae Scientiarum Hungaricae Tomus 56 (4), pp. 337—355 (1968)

THE THERMAL STABILITY OF CHLORINE OXY-SALTS IN THE SOLID STATE, II*

KINETIC AND DERIVATOGRAPHIC STUDY OF THE THERMAL DECOMPOSITION OF SOME METAL CHLORATES

F. SOLYMOSI and T. BÁNSÁGI

(Reaction Kinetical Research Group of the Hungarian Academy of Sciences, Szeged)

Received May 22, 1967

Introduction

From among metal chlorates only the thermal stabilities of alkali chlorates have been studied in detail so far [1, 2, 3, 4]. It appeared that at higher temperatures they disproportionate into perchlorate and chloride, and on the other hand, they decompose to chloride and oxygen. The ratio of these two reactions was found to depend sensitively on the experimental conditions and the contaminations present. No kinetic analysis of the reactions has been successfully performed so far. The purpose of the present paper is to give a better understanding of the nature of the reactions occurring in chlorates, to establish the properties which control their stability and to elucidate the probable mechanism of the decomposition.

The investigations included the study of the thermal behaviour of sodium, barium and lead chlorates.

Experimental

1. Methods

The thermal decomposition of chlorates was followed in vacuum by measuring the pressure of oxygen formed. Chlorine and chlorine dioxide, resp., were frozen out by a liquid air trap placed between the reaction vessel and the manometer. Detailed methods are described elsewhere [5].

Besides these methods, the decomposition of chlorates was also investigated by chemical analysis. In this case anhydrous chlorate was measured in a crucible, and placed in an oven previously heated up to the required temperature. After different reaction times the crucible was removed from the oven, rapidly cooled, and the loss of weight of the substance was registered. The chloride content of the sample was determined by argentometric, and the chlorate content by iodometric, methods. The amount of perchlorate formed during the reaction was measured by titanometric methods [6] or, whenever it was possible, was calculated in the knowledge of previous data. The solid residue of the decomposition of chlorates was analyzed in a similar manner.

Differential thermal analyses of the compounds were performed with a *Paulik—Paulik—Erdey* derivatograph.

* Part I: Acta Chim. Acad. Sci. Hung. **56**, 251 (1968)

2. Reagents

Sodium chlorate was commercial c.p. substance. Barium chlorate was prepared by mixing sodium chlorate and barium chloride. Since the solubility of barium chlorate is less than that of sodium chlorate, first the crystals of barium chlorate separate from the solution. The procedure was as follows: 48.8 g of $BaCl_2 \cdot 2\ H_2O$ was dissolved in 136 ml of twice-distilled water, and 80 ml of a hot (80°) solution containing 76 g of sodium chlorate was added dropwise to the previous solution heated up to 70—80°. Barium chlorate was allowed to crystallize at 10—15°. The composition of the substance obtained in this way was $Ba(ClO_3)_2 \cdot H_2O$. Dehydration was effected in vacuum over potassium hydroxide.

Lead chlorate was obtained by a reaction between *Merck* c.p. lead(II) oxide and 20% chloric acid solution. The substance was twice recrystallized and dried in vacuum. The product contained 99.8% lead chlorate.

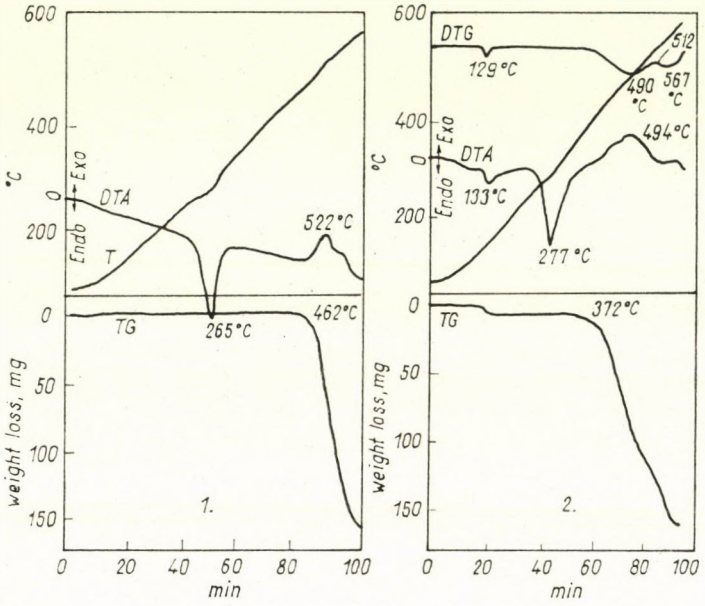

Fig. 1. 1. Derivatogram of sodium chlorate. 2. Derivatogram of a mixture of sodium chlorate and sodium chloride (molar ratio 1 : 1). Heating rate: 6°/min.

Results

1. Sodium chlorate

(a) Derivatographic investigations

In Fig. 1 we show the derivatogram of pure sodium chlorate. The first important change is shown by an endothermic peak at 265° which corresponds to the melting of sodium chlorate. The decrease in weight begins at about 430°, and following this, at 460° it accelerates so much that the substance overflows the platinum crucible. The exothermic heat change, characterizing the decom-

position, begins at 475°. In the presence of sodium chloride (sodium chlorate — sodium chloride molar ratio 5 : 1) the endothermic peak appears at 277°, while the loss of weight at 415°. The exothermic peak starts to develop at 440°. In a mixture of 1 : 1 molar ratio the melting point remains unchanged, but the decomposition of sodium chlorate already begins at 370° (Fig. 1).

(b) Kinetic measurements

The decomposition of sodium chlorate is described by the equation:

$$NaClO_3 = NaCl + 1.5\,O_2 \qquad (1)$$

In the reaction product neither chlorine nor chlorine dioxide were found even in traces. Kinetical measurements were made in the range 450—480°. The $\alpha - t$ curves are plotted in Fig. 2.

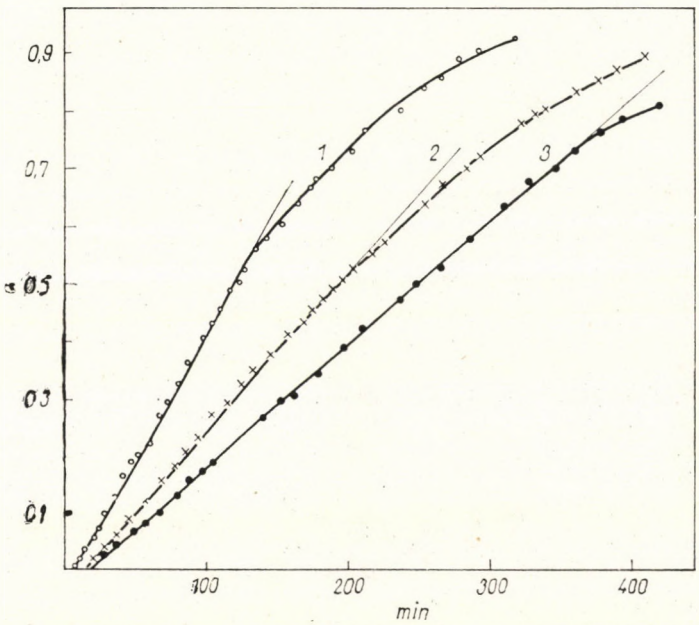

Fig. 2. α-time curves of the decomposition of sodium chlorate, (1) 466°C; (2) 462°C; (3) 457°C

$$\alpha = \frac{p_t}{p_f},\ p_t, \text{ the pressure of gases at time } t,$$

$$p_f = \text{final pressure.}$$

The reaction is preceded by a time lag lasting only for a few minutes. The reaction rate slightly increases to about $\alpha = 0.02$. Rate constants of the decomposition were determined from the initial straight line of the $\alpha - t$ curves. The value of the energy of activation is 68 kcal/mole. The same values were

obtained from the temperature dependence of times elapsed till different values of the decomposition. Kinetical data are summarized in Table I.

Table I

Kinetic data of the thermal decomposition of sodium chlorate

Temperature, °C	$k_1 \cdot 10^3/\text{min}^{-1}$
457	2.09
462	2.81
466	4.31
466	4.04
472	6.31
478	6.02
Activation energy kcal/mole	68.6
Frequency factor (min.$^{-1}$)	$8.6 \cdot 10^{17}$
k_1; 0.0—0.55 α (α — t plots)	

After the gas evolution had ceased, non-decomposed chlorate could not be detected in the solid residue. Besides sodium chloride, however, the solid residue contained a considerable amount of perchlorate. This indicates that in the above temperature range, in addition to Reaction 1, the disproportionation of sodium chlorate also occurs:

$$4\,NaClO_3 = 3\,NaClO_4 + NaCl \qquad (2)$$

The formation of sodium perchlorate was studied at some temperatures as a function of time. At 390°, where the decomposition of sodium chlorate is negligible, disproportionation is also extremely slow. After 5 hours only 2.5% of sodium perchlorate was formed. On increasing temperature the perchlorate content increased, and above 450° it ran parallel to the decomposition.

Some results are given in Table II.

2. Barium chlorate

(a) Derivatographic investigations

The derivatogram of barium chlorate can be seen in Fig. 3.

The initial loss of weight starting at 146°, and the endothermic peak at 170° belonging to this process, are due to the loss of the water of crystallization. The endothermic heat change indicating the melting of barium chlorate starts at 396°, and the peak can be found at 404°. Simultaneously the decom-

position of the substance occurs, which on increasing the temperature becomes extremely rapid, but later — in spite of the higher temperature — becomes slower. The decomposition of barium chlorate is an exothermic process.

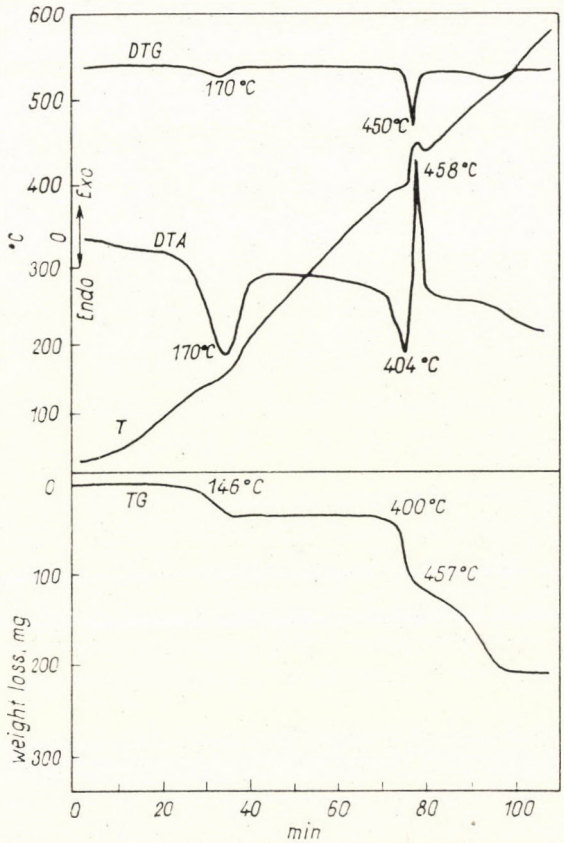

Fig. 3. Derivatogram of barium chlorate. Heating rate: 6°/min.

Table II

Disproportionation of sodium chlorate (44—45 mg samples)

Temperature °C	Time of reaction, (min.)	$NaClO_4$ formed	
		mg	% weight
390	300	1.1	2.50
400	120	2.1	4.51
410	120	2.7	6.20
420	120	5.0	11.44
430	120	10.2	23.65
440	120	21.7	50.80
450	120	25.7	66.20
460	10	6.1	9.91
460	20	10.4	20.10
460	60	19.4	45.20

(b) Kinetic measurements

The slow decomposition of barium chlorate under isothermal conditions begins at about 380°. The reaction starts without a time lag, and proceeds extremely slowly. The reaction rate at first slightly increases, reaches a maximum, and then falls to a very low value. The behaviour of the substance practically does not change up to 395°. The stopping of gas evolution cannot be reached in this temperature range even after eight hours. On account of the relatively small amount of gas evolved it was thought that, instead of the decomposition, barium chlorate suffered disproportionation:

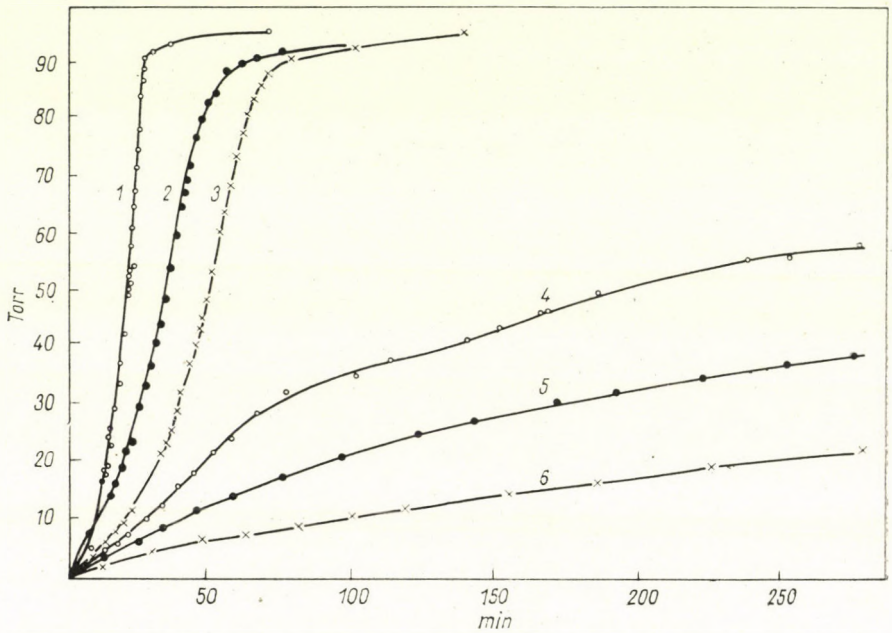

Fig. 4. Pressure-time curves of the decomposition of barium chlorate (1) 405°C; (2) 401°C; (3) 396°C; (4) 392°C; (5) 384°C; (6) 380°C

$$4\,Ba(ClO_3)_2 = 3\,Ba(ClO_4)_2 + BaCl_2 \qquad (3)$$

This was justified by the chemical analysis of the solid residue, however, depending on the temperature and time of the reaction, 20—30% of non-decomposed barium chlorate was also found.

Above 396° the run of decomposition suddenly changed and the reaction occurred at a high rate (Fig. 4). In Fig. 5 the rate-time curves of the rapid decomposition are plotted. On increasing the temperature, the time required to reach the rate maximum, τ_{max}, decreases, while the rate, w_{max}, increases.

Nevertheless, it should be mentioned that disproportionation took place above 396° too. It is also interesting that after the final pressure has developed

besides barium perchlorate, non-decomposed barium chlorate was also found in the solid substance. The gaseous product of the decomposition was oxygen containing no chlorine or chlorine dioxide. The reaction equation is:

$$Ba(ClO_3)_2 = BaCl_2 + 3\,O_2 \qquad (4)$$

It was observed that below 395° the decomposition occurred completely in the solid phase, however, above this temperature barium chlorate melted. Thus the marked increase in the reactivity of barium chlorate as experienced above 395°, is a result of the melting of the compound. It was also found that barium chlorate solidified again as the reaction proceeded which was

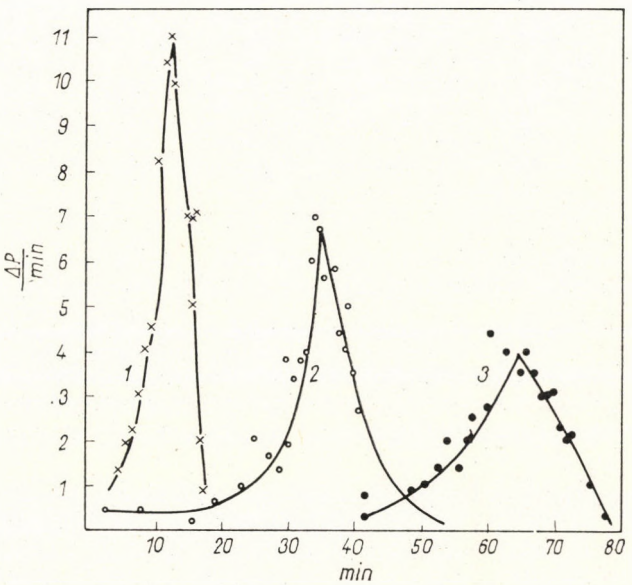

Fig. 5. Rate-time curves of the decomposition of barium chlorate (1) 410°C; (2) 403°C; (3) 400°C

Table III

Disproportionation of barium chlorate

(90—100 mg samples)

Temperature °C	Time of reaction (min.)	$Ba(ClO_4)_2$ formed	
		mg	% weight
350	120	1.6	1.45
360	120	6.3	1.67
370	120	6.3	6.60
380	120	22.0	22.15
390	30	25.1	25.88
390	200	30.0	31.48
390	305	31.6	33.44

accompanied by the decrease and cessation of gas evolution. For the kinetical analysis of the time-pressure curves, the *Prout—Tompkins* equation proved to be relatively the best. Owing to a considerable scattering of the rate constants, the activation energy of the decomposition could not be satisfactorily determined. It can be stated, at least, that it is a relatively large value, higher than 75 kcal/mole.

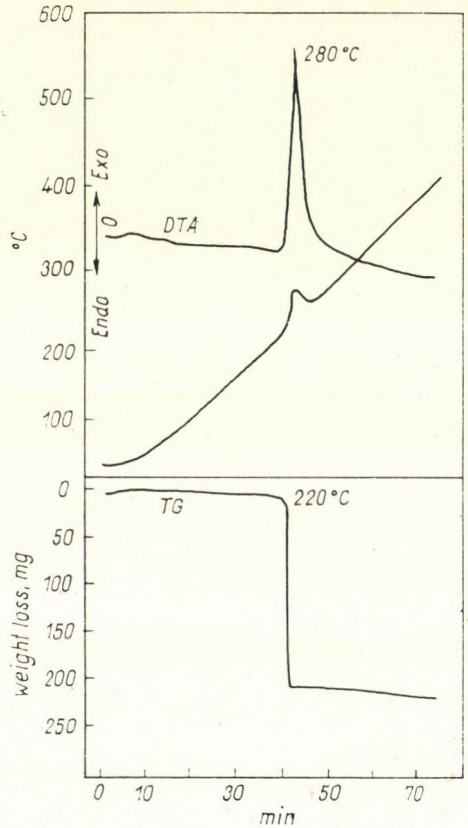

Fig. 6. Derivatogram of lead chlorate. Heating rate: 6°/min.

In Table III data concerning the disproportionation of barium chlorate are collected. It should be noted that even at 350—370°, *i.e.* below the temperature of the decomposition of barium chlorate, the very slow formation of barium perchlorate can be detected.

3. Lead chlorate

(a) Derivatographic investigations

The derivatogram of lead chlorate is shown in Fig. 6. The decomposition begins at 220° and takes place instantaneously, accompanied by the liberation

of a large amount of heat. The substance remains solid during the decomposition. The residue is a brownish-black solid. The percentage weight-loss is 37.7%.

(b) Kinetic measurements

Kinetic measurements were made between 194 and 216°. The decomposition was followed by measuring the pressure of the gases evolved by a sensitive silicon oil manometer, without using a liquid air trap. The pressure-time curves are shown in Fig. 7. The weight of lead chlorate was 24.2 mg.

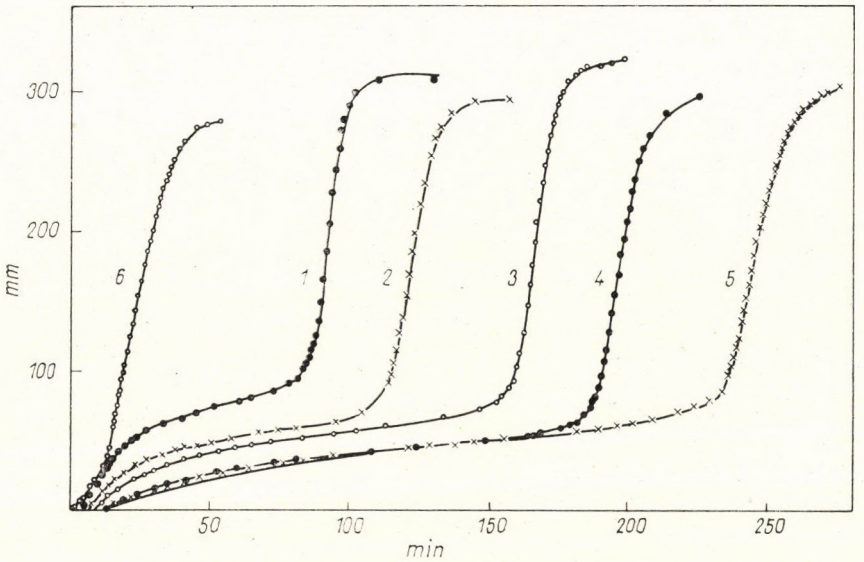

Fig. 7. Pressure-time curves of the decomposition of lead chlorate
1) 216°C; (2) 212°C; (3) 207°C; (4) 203°C; (5) 199.5°C; (6) $Pb(ClO_3)_2$ + reaction products, weight ratio 5 : 1, 207.5°C

The reaction started with a short time lag (after some minutes of warming up) and could be divided into the following phases:

1. an initial rapid decomposition of deceleratory character;
2. a subsequent slow reaction;
3. an extremely rapid decomposition in which about 2/3 part of the substance reacted;
4. a short, slow decay period.

The above phases are well distinguishable in the curves of rate *vs.* time. (The rate maximum observed in some cases at the beginning of the reaction is only apparent, and can be ascribed to the warming-up of the sample.) (Fig. 8.)

The kinetic analysis of the first phase was carried out by means of the monomolecular decay equation:

$$\log \frac{1}{1-\alpha} = k_{2.3}\, t + c \qquad (5)$$

(the pressure value preceding the start of the rapid decomposition was taken as the final pressure). From the start of the decomposition up to about $\alpha=0.4$ we got straight lines. The temperature dependence of the rate constants satisfied the *Arrhenius* function.

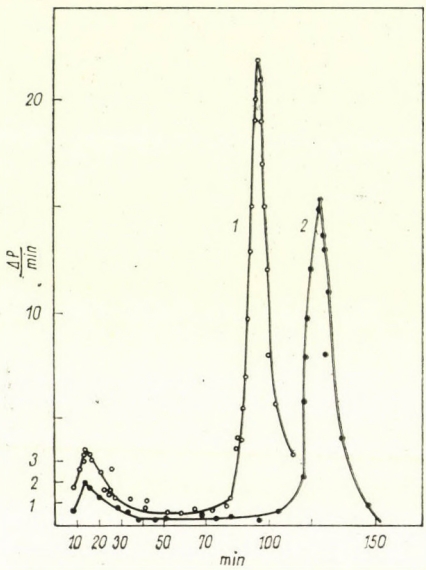

Fig. 8. Rate-time curves of the decomposition of lead chlorate (1) 216°C; (2) 211°C

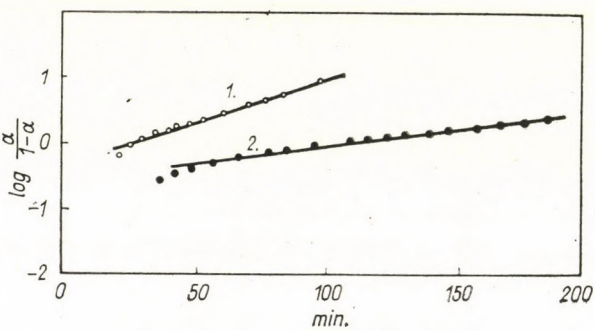

Fig. 9. Kinetical analysis of the decomposition of lead chlorate by the *Prout—Tompkins* equation. (1) 212°C; (2) 200°C

The analysis of the slowly accelerating decomposition has been done by the *Prout—Tompkins* equation:

$$\log \frac{\alpha}{1-\alpha} = k_4 . t + c \qquad (6)$$

and by means of the *Avrami—Erofeev* equations (Fig. 9):

$$[-(\log 1 - \alpha)^{1/3}] = k_6 t + c. \tag{7}$$

The *Prout—Tompkins* equation gave better straight lines and described the reaction from $\alpha = 0.35$ to the sudden increase of pressure ($\alpha = 0.85$). The activation energy is 43 kcal/mole. From the times required to reach the rate maxima, τ_{max}, as the function of 1/T, an activation energy of 36.4 kcal was obtained.

Table IV

Kinetic data of the thermal decomposition of lead chlorate

Temperature °C	$k_2 \cdot 10^3$(min.$^{-1}$)	$k_4 \cdot 10^3$(min.$^{-1}$)	τ_{max} (min.)	W max., $\frac{\Delta p}{\Delta t}$	tg α
195	1.6	2.91	397.5	11	8.7
200	3.7	5.31	224	11	9.4
203.2	5.1	8.81	201	14	11.2
207	7.9	7.84	167	18	14.1
212	15.9	12.7	123	15.3	13.5
216	21.2	21.9	93.5	22	14.3
Activation energy, kcal/mole	51.2	43.1	36.4	—	—
Frequency factor (min.$^{-1}$)	$1.81 \cdot 10^{21}$	$4.14 \cdot 10^{17}$	—	—	—

k_2; 0.0—0.4 α (first-order)
k_4; 0.35—0.85 α (Prout—Tompkins)
tg α = the slope of the third fast decomposition

The rate of decomposition of lead chlorate in the third phase depends only to small extent on temperature (Table IV).

Kinetic data are shown in Table IV.

The loss of weight until the rapid decomposition sets in is about 15.8% and after the completion of the reaction 35.3%. According to the chemical analysis of the solid residue, it consisted of 84.39% lead dioxide and 14.9% lead chloride, the molar ratio being 6.58. No lead perchlorate or non-decomposed lead chlorate was found. For the sake of completeness, we attempted to detect perchlorate at different phases of the decomposition, and also below the decomposition temperature of lead chlorate. In neither case was any perchlorate found even by means of the sensitive strychnine sulphate test. The decomposition of lead chlorate can be characterized by the following overall equation:

$$8\,Pb(ClO_3)_2 = 7\,PbO_2 + PbCl_2 + 5.5\,Cl_2 + 3\,ClO_2 + 14\,O_2 \tag{8}$$

Accordingly, the percentage loss of weight is 34.8 and the molar ratio of lead dioxide to lead chloride is 7. The experimentally found chlorine/chlorine dioxide molar ratio was also in good agreement with the above reaction equation.

As chlorine dioxide decomposes at the experimental temperature, it could be expected that with the progress of the reaction the sudden increase of the pressure can be partly ascribed to the decomposition of chlorine dioxide. When a trap, placed between the reaction vessel and the manometer, was continuously cooled with liquid air from the start of the experiment, the shape of the pressure curve agreed with the former one with the only difference that the values of pressure were smaller. The sudden pressure increase occurred at the same time here, too.

The decomposition of lead chlorate was also studied by simultaneous measurement of the pressure of the gases and the loss of weight of the samples. The $\alpha - t$ curves, determined by the two different methods, are essentially the same. All these experiments indicate that the sudden pressure increase during the decomposition cannot be attributed to the decomposition of chlorine dioxide, or to any other reaction in the gaseous phase, but it is a characteristic of the decomposition of lead chlorate in the solid phase.

The decomposition of lead chlorate was studied at higher temperatures, too. The explosion of 50 mg substance compressed under 2700 atm/cm^2 first occurred at 246°. Before explosion, a well-measurable decomposition was observed. The composition of the gaseous product was 84.5% oxygen and 15.2% chlorine. The induction periods before the explosion were reproducible. Their dependence on temperature resulted in an activation energy of 64.9 kcal/mole.

4. Structure and physical properties of chlorates

There are very few data in the literature concerning the structure and physical properties of chlorates. The structures of sodium chlorate and barium chlorate are known. Sodium chlorate is of cubic structure [7]. The chlorate ions form a flat trigonal pyramid. The Cl—O distance is 1.48 Å, that of O—O is 2.39 Å. Barium chlorate, containing one molecule water of crystallization, is of monoclinal structure [8]. The Cl—O and O—O distances are larger than in sodium chlorate, 1.57 and 2.60 Å, respectively.

By differential thermal analysis and visual observation, sodium chlorate melts at 262°, while the melting point of barium chlorate is 404°. The melting point of lead chlorate cannot be determined, since this compound is decomposed before reaching the melting point.

Of the refractive indices of the compounds only those of sodium chlorate and barium chlorate are known. We attempted to determine the refractive index of other chlorates by the Becke-line method. However, the experiments only showed that the refractive index of lead chlorate was larger than 1.78.

The low-frequency dielectric constants of the compounds were measured at 350 Kc/s frequency. To determine the absorption edge of the compounds,

their reflection spectra were taken. In the case of sodium chlorate and barium chlorate no change was experienced up to 2800 Å. The reflection spectrum of lead chlorate is given in Fig. 10. The absorption edge of lead chlorate can be located at 2380 Å. The substance shows an absorption band at about 3600 Å. A similar behaviour was experienced earlier in the reflection spectra of silver chlorate [9]. Data on the structure and physical properties of chlorates are summarized in Table V.

Discussion

Depending on the cation, the thermal properties of chlorates differ largely from one another. There are considerable differences in the temperature of the onset of decompositions, their kinetics and the direction of the reactions.

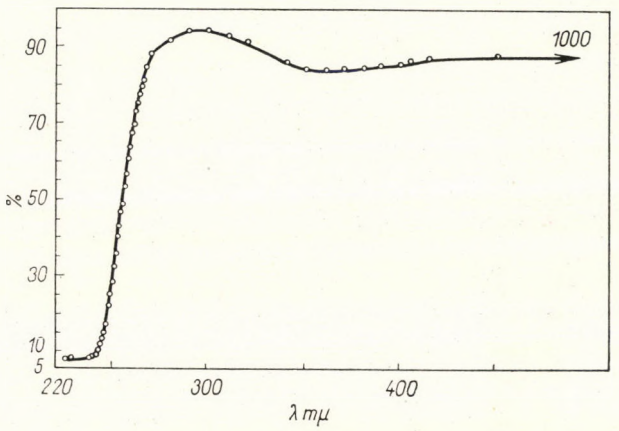

Fig. 10. Reflexion spectrum of lead chlorate

Sodium chlorate decomposes at 450°, at a temperature almost 200° higher than the melting point.

In the case of barium chlorate a very slow gas evolution is observed to begin in the solid phase. A marked increase in the rate of decomposition is apparent at 396°, when the melting of the substance commences. It is an interesting characteristic that after a period of high velocity, the decomposition practically stops, in spite of the fact that the residue still contains non-decomposed barium chlorate. A possible reason for this behaviour is the solidification of the substance. But this alone does not seem to be a sufficient explanation, since the solid material undergoes decomposition even at 380°. It is more

Table V*

Some data of structure and physical properties of chlorates

Compound	M.p., °C	Cl—O distance, Å	O—O distance, Å	Density	Refractive index	Dielectric constant, at 350 kc/s	K_o/K	Absorption edge, Å	Optical activation energy, E_o, eV	Thermal activation energy, E_T, eV
$NaClO_3$	250	1.48	2.39	2.490	1.515	5.9	0.389	—	—	—
$Ba(ClO_3)_2$	404	1.57	2.60	3.179	1.577	4.34	0.573	—	—	—
$AgClO_3$	232	1.48	2.39	4.430	1.83	5.81	0.575	2.550	4.86	2.79
$TlClO_3$	decomp.	—	—	4.037	—	7.78	—	2.420	5.12	—
$Pb(ClO_3)_2$	decomp.	—	—	5.047	—	11.78	—	2.380	5.21	—

* In order to compare the properties of the compounds studied in this paper with that of other chlorates, the data for silver [9] and thallium chlorate [J4] are also included.

Table VI

Equivalent heats of reaction of the different reactions of chlorates
(kcal/mole,* at 25°C)*

	ΔH_1	ΔF_1	ΔH_2	ΔF_2	ΔH_3	ΔF_3	ΔH_4	ΔF_4	ΔH_5	ΔF_5	ΔH_6
$NaClO_3$	−12.5	−32.7	+34.27	+14.2	−7.96	−8.6	− 9.08	—	−6.45	−0.5	+1.31
$Ba(ClO_3)_2$	−11.93		+24.35		−7.14		+11.75		−5.55		+3.1
$AgClO_3$	−24.57		+ 2.47		−7.67		+ 5.73		−2.02		+1.86
$Pb(ClO_3)_2$	—		—		—		—		—		—
$TlClO_3$	—		—		—		—		—		—

1. $MClO_3 = MCl + 1.5\ O_2$
2. $MClO_3 = 1/2\ M_2O + 5/4\ O_2 + 1/2\ Cl_2$
3. $MClO_3 = 3/4\ MClO_4 + 1/4\ MCl$
4. $MClO_3 = MClO_2 + 1/2\ O_2$
5. $MClO_3 + 1/2\ O_2 = MClO_4$
6. $MClO_3 = 1/2\ MClO_4 + 1/2\ MClO_2$

* Unfortunately ΔF values were available only in the case of sodium chlorate, which show some parallelism with the values of ΔH. It is very likely that the same is valid in the case of other chlorates, too.

probable that the glass-like state of the substance also has a part in the higher stability of the solidified melt; its surface and porosity markedly differ from the initial solid substance. The gaseous product of the decomposition of both compounds consist only of oxygen. The disproportionation of both chlorates was already observable below the decomposition temperature of the compounds. At higher temperature disproportionation occurs parallel to the decomposition.

In contrast to the above compounds, lead chlorate suffers complete decomposition in the solid state at a much lower temperature, between 190 and 216°. The gaseous products of the decomposition of lead chlorate are chlorine, chlorine dioxide and oxygen.

The $p - t$ curve of the decomposition of lead chlorate is markedly different from that of the other compounds. Similar decomposition curves were obtained in the investigation of the decomposition of lithium aluminium hydride [10] and potassium azide [11], with the difference that in these cases the initial fast reaction was less than in the present case. It is likely, that the initial rapid decomposition is a surface reaction, which penetrates into the interior of the crystal to some depth. The decomposition in the mass actually occurs in the third very fast reaction, which is preceded by a long constant-rate process. This can be regarded as an induction period of the former reaction. We assume that the decomposition in the third stage takes place at the interface between the salt and the products. This idea is supported by investigating the effect of the reaction products (Fig. 7). In this case the slow constant-rate process between the initial and later rapid reactions is practically eliminated.

In contrast to the sodium and barium compounds, no disproportionation of lead chlorate could be detected. However, at higher temperatures the substance exploded. A similar behaviour was observed in the case of thallium chlorate [14].

Let us first deal with the decomposition mechanism of sodium chlorate and barium chlorate. Although we did not succeed in detecting chlorite during the decomposition of the chlorates, it can be assumed on the analogy of the decomposition of perchlorates [5] that the decomposition takes place also here in steps and chlorite is formed as a transient intermediate:

$$MClO_3 = MClO_2 + O\,. \qquad (1)$$

In the next step chlorite either decomposes into oxygen and sodium chloride

$$MClO_2 = MCl + O_2 \qquad (2)$$

or it gives chlorate and chloride by disproportionation:

$$MClO_2 = \frac{2}{3} MClO_3 + \frac{1}{3} MCl. \qquad (3)$$

From our former experiments concerning the stability of chlorites it appeared that sodium chlorite transforms only according to Reaction 3, while barium chlorite decomposes above 100° mainly by Equation (2) [12]. Both reactions are very fast at the temperatures of chlorate decomposition, so it is understandable why chlorite formation could not be detected during the decomposition of chlorates. The rate-determining step of the decomposition of these chlorates is very likely Reaction (1) that involves the rupture of the Cl—O bond. The value of activation energy experimentally found for the decomposition of sodium chlorate is about the same as the dissociation energy of the chlorine-oxygen bond (60 kcal), and as it will be seen later, it agrees very well with the endothermic heat of the reaction, too.

Different views concerning the disproportionation of chlorine oxy-anions have been expressed previously. According to the data listed in Table VI, the oxidation of chlorate with molecular oxygen is thermodynamically possible, for kinetic reasons the reaction does not take place even at high oxygen pressures and temperatures [13]. Therefore MARKOVITZ *et al.* [2, 3] postulated that the formation of perchlorate was the result of a reaction between chlorate and atomic oxygen formed during the decomposition of chlorate:

$$MClO_3 + O = MClO_4 \qquad (4)$$

From detailed kinetical measurements carried out in the case of chlorites and from some other observations we have concluded that the disproportionation of chlorites is the result of the rearrangement of molecules inside the lattice [5,12]. In the present case it is very difficult to find decisive proof for the mechanism since decomposition of chlorates prevents kinetic measurements concerning the disproportionation. Nevertheless, it can be assumed that the disproportionation reactions of chlorites and chlorates are due to the same causes and occur in an essentially similar way. It was observed also in this work that the disproportionation of both sodium chlorate and barium chlorate — although only to a small extent — occurred below their decomposition temperatures. The absence of oxygen evolution, however, does not exclude the internal oxygenation mechanism [2, 3], since owing to the low concentration of atomic oxygen, its recombination

$$O + O + \text{Solid} = O_2 + \text{Solid}, \qquad (5)$$

can be practically neglected.

The mechanism of molecular rearrangement may be supposed by energetic considerations. The simplest case of the molecular rearrangement is the interaction of two molecules of chlorate of which one molecule perchlorate

and one molecule chlorite are formed:

$$2\,MClO_3 = MClO_4 + MClO_2 \tag{6}$$

The formed chlorite undergoes rapidly disproportionation into chlorate and chloride. If D_1 means the dissociation energy of the Cl—O bond in the chlorate and D_2 that in the perchlorate, we get:

$$E = \alpha D_1 + \beta D_2 \tag{7}$$

(α and β are constants). This means that in the optimal case ($\alpha = 1$ and $\beta = 1$) the activation energy of the disproportionation is equal to the difference between the two dissociation energies, *i.e.* to the reaction heat. This, as it appears from Table VI, is endothermic only by a few kcal. Naturally, this optimal case is far from the real one.

The rate determining step in the oxidation mechanism of perchlorate formation should be the rupture of the Cl—O bond, just as well as in the decomposition reaction. These reactions are endothermic (9.08 kcal for sodium chlorate and 11.75 kcal for barium chlorate). Considering, however, that atomic oxygen should be formed to accomplish the oxidation of chlorate, the heat of formation of the oxygen atoms (59.2 kcal) must also be considered. Thus for the reaction

$$MClO_3 = MClO_2 + O \tag{8}$$

the endothermic heats of reaction of 68.3 and 70.91 are obtained. While these values agree well with the activation energy values found for the decomposition reactions they also indicate that this route of disproportionation is energetically less favourable than the other one.

The decomposition of lead chlorate is much more complicated than that of the previous compounds. The overall reaction equation found in the case of lead chlorate

$$8\,Pb(ClO_3)_2 = 7\,PbO_2 + PbCl_2 + 5.5\,Cl_2 + 3\,ClO_2 + 14\,O_2 \tag{9}$$

is composed of at least two other ones:

$$Pb(ClO_3)_2 = PbCl_2 + 3\,O_2 \tag{10}$$

$$Pb(ClO_3)_2 = PbO_2 + 2\,ClO_2\,(Cl_2 + 2\,O_2) \tag{11}$$

It is probable that these reactions take place independently of each other, but the rate of the first one, considering the experimentally found $PbO_2/PbCl_2$ ratio, is about 6.5 times lower than the second one.

It is very likely that in the decomposition of lead chlorate the breaking of the Cl—O bond is the slowest process. The lower values of the activation energy can be attributed to the high polarizing power of the lead ion and to the great catalytic effect of the solid decomposition products. The probable reason for the absence of perchlorate formation is that the formation of lead(IV) oxide involves considerably larger decrease of the free energy than that of perchlorate formation. Unfortunately, no thermodynamic data are available for these compounds, thus this explanation cannot be justified thermodynamically.

In the experiments some physical characteristics of the compounds have also been determined (Table V). Although we did not succeed in every case to measure the absorption edge and refractive indices of the substances, the physical properties of the compounds indicate that the bond between the metal ion and the complex anion has greatest ionic character in the case of sodium and barium, and the least in lead and thallium [14] chlorates. This is shown by the smaller values of the refractive indices, the large difference between the low and high frequency dielectric constants, and the position of the absorption edge (< 2300 Å). The percentage ionic character of the bond between the metal ion and the complex anion was calculated from SANDERSON's electronegativity data; the following values were obtained:

$NaClO_3$	68.75;	$Ba(ClO_3)_2$	45.17;	$AgClO_3$	36.04,
$TlClO_3$	25.21;	$Pb(ClO_3)_2$	17.15.		

Taking into account the above results and the stability of the compounds studied in this paper and in some others [9, 14], we may come to the same conclusion as in the case of chlorites [12], namely, that in determining the stability of chlorates, the effective electric field strength of the cation present and the ionic character of the salt play a decisive role.

SUMMARY

The kinetics and the mechanism of the thermal decomposition of sodium, barium, and lead chlorates have been studied. The thermal behaviour of these chlorates (the temperature, products and the kinetics of decomposition) depends very sensitively on the nature of the cation. The stabilities decrease in the above order. Parallel to the decomposition — and to a very small extent before the decomposition — the disproportionation of sodium and barium chlorates also occurs. In the case of lead chlorate, perchlorate formation cannot be detected, but the compound explodes at higher temperatures. On the basis of kinetic data and the physical properties of the substances, the mechanisms of the decomposition and disproportionation reaction are discussed.

REFERENCES

1. GLASNER, A., WEIDENFELD, L.: J. Am. Chem. Soc. **74,** 2464 (1952).
2. MARKOVITZ, M. M., BORYTA, D. A., STEWART, H.: J. Chem. Eng. Data **9,** 573 (1964). MARKOVITZ, M. M., BORYTA, D. D., STEWART, H.: J. Phys. Chem. **68,** 2282 (1964).
3. TOBISAWA, S.: Bull. Chem. Soc. Japan **34,** 89 (1961).
4. SOLYMOSI, F., KRIX, E.: Acta Chim. Acad. Sci. Hung. **34,** 241 (1962).
5. SOLYMOSI, F.: Acta Chim. Acad. Sci. Hung. (To be published.)
6. EAGLES, D. C.: Chem. and Ing. **1954,** 1002.
7. DICKINSON, R. G., GOODLUNE, E. A.: J. Am. Chem. Soc. **43,** 2045 (1921). ARAVINDAKSHAN, C.: Z. Krist. **111,** 241 (1958).
8. KARTHA, G.: Acta Cryst. **5,** 845 (1952).
9. SOLYMOSI, F.: Z. phys. Chem. N. F. **57,**1 (1968).
10. HAYCOCK, K.: Proc. Roy. Soc. **A211,** 335 (1952).
11. GARNER, W. E., MARKE, K.: J. Chem. Soc. **1936,** 657.
12. SOLYMOSI, F., BÁNSÁGI, T.: Acta Chim. Acad. Sci. Hung. **56,** 251 (1968)
13. DODÉ, M., BASSET, J.: Bull. soc. chim. France, [5] **2,** 344 (1935).
14. SOLYMOSI, F., BÁNSÁGI, T.: Magyar Kém. Foly. **74,** 32 (1968).

Frigyes SOLYMOSI
Tamás BÁNSÁGI
Szeged, Rerrich tér, Hungary

Acta Chimica Academiae Scientiarum Hungaricae Tomus 56 (4), pp. 357—360 (1968)

ON SOME PROPERTIES OF URANIUM TRIOXIDE DIHYDRATE

(SHORT COMMUNICATION)

Z. Pokó, M. Fodor and E. Szabó

(Central Research Institute for Physics, Budapest)

Received August 7, 1967

The compound produced by the hydration at room temperature different types of uranium trioxide, described as $UO_3 \cdot 2H_2O$, has been thoroughly studied by several authors using various physico-chemical methods. The results, however, are discrepant as to both the actual composition and the molecular structure of this dihydrate. Thus, it is described as uranic acid monohydrate [1—3], or uranyl hydroxide monohydrate [4—7], but also more complex dimeric [8—9], and even polymeric [10—12] molecular structures have been suggested.

Vier [13] was the first to infer, from an analysis of the system, $UO_3—H_2O$, the existence of two crystallographically distinct forms, namely α- and β-$UO_3 \cdot 2H_2O$. From the X-ray diffraction patterns of the $UO_3 \cdot 2H_2O$ products of different origins, most authors [3, 4, 7, 14—16] except Porte *et al.* [8] were not able to identify distinctly the two modifications. The reason for this is probably that the X-ray diffraction technique is considerably impeded in the case of this compound. The scattering power of the uranium atoms being much higher than those of the considerably lighter oxygen atoms, this, combined with large absorption of the radiation and poor crystallization, renders it very difficult to determine the actual positions of the oxygen atoms. For this reason it was thought to be of interest to obtain additional information concerning the existence and the properties of the two modifications of $UO_3 \cdot 2H_2O$ with the use of other experimental methods.

Experimental results and discussion

The investigations were performed on hydration products of different modifications of uranium trioxide. The thermal decomposition of the hydration products and the hydrolytic products in uranyl salt solutions were also studied. Parallel with the thermogravimetric experiments, the hydrated and hydrolyzed forms, as well as the products of their thermal decomposition, were analyzed by IR spectroscopy.

For thermogravimetry a derivatograph developed by F. PAULIK, J. PAULIK and L. ERDEY [17] was used. Simultaneous plotting of the differential thermogravimetric (DTG), the thermogravimetric (TG) and differential thermoanalytical (DTA) curves, possible by this method, permits to evaluate separately even overlapping processes, and to obtain a more accurate picture of the thermal decomposition of the uranium trioxides and their hydrates. The IR absorption spectra were obtained with a Zeiss UR-10 spectrometer.

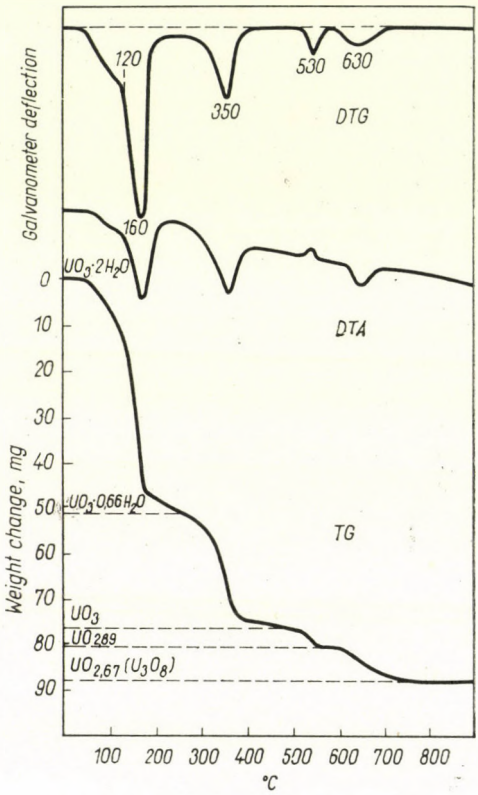

Fig. 1. Derivatogram of α-$UO_3 \cdot 2\,H_2O$

Preparation, analysis, identification of samples and the measuring technique were the same as described in the earlier reports [11, 12].

It has been established as a result of these investigations that the hydration or hydrolysis of amorphous and all crystalline UO_3 forms, with the only exception of γ-UO_3, result in the same type of dihydrate with properties corresponding to the α-variety described by VIER, while the β-$UO_3 \cdot 2H_2O$ can be produced exclusively from γ-UO_3. α-$UO_3 \cdot 2H_2O$ forms also on the hydrolysis of uranyl salt solutions [12], if it takes place in the presence of

an anion exchange resin in the hydroxyl form, without the addition of alkaline solution.

A comparison of the derivatograms obtained for the two modifications of $UO_3 \cdot 2H_2O$ (Figs 1 and 2) definitely reveals the difference between their thermal properties, and a detailed study suggests it to be due to structural differences. It can be established from the graphical analysis of the derivatograms that in both types the two water molecules are lost identically in three

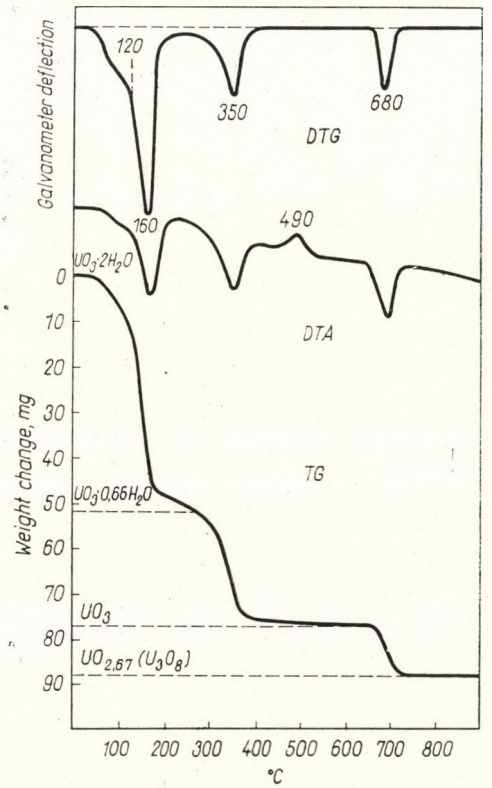

Fig. 2. Derivatogram of β-$UO_3 \cdot 2\ H_2O$

steps. The first water loss is manifested by the DTG curve at 120° by an inflexion, while at 160° and at 350° the removal of water produces each time a definite DTG peak. These dehydration processes are seen to be endothermic. In the earlier report on the analysis of the derivatograms and infrared spectra of α-$UO_3 \cdot 2H_2O$ samples [12], it was shown that the two first steps in the thermal decomposition correspond to the removal of differently bonded water molecules, while the third indicates the presence of hydroxyl groups. All this suggests that the compound α-$UO_3 \cdot 2H_2O$ can be described by the formula $[U_3O_7(OH)_4 \cdot 2H_2O] \cdot 2H_2O$.

It is upon complete dehydration that the difference between the two dihydrates becomes apparent from their thermal behaviour.

The thermal decomposition of dehydrated α-$UO_3 \cdot 2H_2O$ proceeds correspondingly to that observed for amorphous UO_3. The first oxygen loss occurs at 530° with the formation of a $UO_{2.89}$ phase in an exothermic process, the second at 630° in an endothermic one, involving 1/3 and 2/3 parts of the total oxygen loss, respectively.

Dehydrated β-$UO_3 \cdot 2H_2O$, on the other hand, as seen from the derivatogram, retains its composition unaltered up to 650°. The DTA curve, however, shows at 490° the onset of a characteristic exothermic process which does not cause any change in weight. As a results of this exothermic process, the UO_3-type product which is originally red, turns into olive-green. The UO_3 produced in this way by the thermal decomposition of β-$UO_3 \cdot 2H_2O$ is thought to undergo at 490° a phase transformation before its conversion into U_3O_8 in a single step at 680°.

Derivatographic analysis proves to be a convenient method for the identification of the α- and β-types of uranium trioxide dihydrate. The nature of the observed differences indicates that they originate from the unlike properties of the uranium-oxygen bonds.

REFERENCES

1. HÜTTIG, G. F., VON SCHROEDER, E.: Z. anorg. Chem. **121,** 243 (1922).
2. GENTILE, P. S., TALLEY, L. H., COLLOPY, T. J.: J. Inorg. Nucl. Chem. **10,** 114 (1959).
3. DEBETS, P. C., LOOPSTRA, B. O.: J. Inorg. Nucl. Chem. **25,** 945 (1963).
4. CHRIST, C. L., CLARK, J. R.: Amer. Mineral. **45,** 1026 (1960).
5. DEANE, A. M.: J. Inorg. Nucl. Chem. **21,** 238 (1961).
6. SCHWARZMANN, E., GLEMSER, O.: Z. anorg. Chem. **315,** 305 (1962).
7. RODE, E. A., GOLOVLEVA, Z. S., KUZNETSOV, V. G., KOZMIN, P. A.: Zh. Neorgan. Khim. **8,** 2751 (1963).
8. PORTE, A. L., GUTOWSKY, H. S., BOGGS, J. E.: J. Chem. Phys. **36,** 1695 (1962).
9. LONADIER, F. D., BOGGS, J. E.: J. Less-Common Metals **5,** 112 (1963).
10. PROTAS, J.: Bull. Soc. France Miner. Crist. **82,** 239 (1959).
11. FODOR, M., POKÓ, Z., SZABÓ, E.: Magyar Kém. Foly. **71,** 104 (1965).
12. FODOR, M., POKÓ, Z., MINK, J.: Mikrochimica Acta **1966,** 865.
13. VIER, D. T.: U.S. AEC. Report, A-1277 (1944).
14. DAWSON, J. K., WAIT, E., ALCOCK, K., CHILTON, D. R.: J. Chem. Soc. **1956,** 3531.
15. DELL, R. M., WHEELER, V. J.: Trans. Faraday Soc. **59,** 485 (1963).
16. WHEELER, V. J., DELL, R. M., WAIT, E.: J. Inorg. Nucl. Chem. **86,** 1829 (1964).
17. PAULIK, F., PAULIK, J., ERDEY, L.: Z. anal. Chem. **160,** 241 (1958).

Zoltán POKÓ
Miklós FODOR
Elek SZABÓ
Budapest XII., Konkoly Thege út

Acta Chimica Academiae Scientiarum Hungaricae Tomus 56 (4), pp. 361—367 (1968)

STEROIDS, VIII

SYNTHESES OF 2- AND 4-CH_2-X SUBSTITUTED ESTRONE-3-ALKYL ETHERS

B. MATKOVICS, A. F. ABOULEZZ, F. KATONA and Ö. K. J. KOVÁCS

(Institute of Organic Chemistry, A. József University, Szeged)

Received February 1, 1967

For pharmaceutical investigations, 2- and 4-methoxymethyl, generally 2- and 4-CH_2—X substituted estrone-3-alkyl ethers were needed. It is known [1] that substitution at various positions on the aromatic ring of the estrone molecule significantly modifies the biological effect of the parent substance.

Recently, PATTON [2] synthesized 2-dimethylaminomethylestrone by the Mannich reaction of estrone. This product was converted with acetic anhydride into the corresponding diacetate. We repeated the experiment described by PATTON, and the diacetate was subjected to alkaline hydrolysis. Treatment of the resulting diol with dimethyl sulphate or with methyl iodide, however, equally failed to give the dimethoxy derivative in satisfactory quantity and purity. The synthesis of the compound from the corresponding estrone-3-alkyl ether by Mannich reaction is not feasible, because the activating effect of the carbonyl group at position 17 towards the 3-alkoxy group is much stronger, and so a 16-dialkylaminomethyl derivative will result [3, 4]. On the other hand, PATTON [2] reported that, owing to their crypto-phenolic character, subsequent methylation of the Mannich compounds could not be effected [2]. For this reason, and in ignorance of the successful efforts since published by KANEKO, HASHIMOTO and KOBAYASHI [5], we did not consider this approach suitable for the synthesis of methoxymethylestrone-3-alkyl ether derivatives.

Thus, following the suggestion of one of us (A.F.A.), for a starting step we selected the reaction of estrone-3-alkyl ethers with chloromethylmethyl ether, on the analogy of the similar reactions of phenols and phenol ethers. For the use of this reagent in the domain of steroid chemistry only a few examples are known [6—9].

When estrone-3-methyl ether (**Ia**) was allowed to react in acetic acid with chloromethylmethyl ether, processing and purification by chromatography gave a derivative shown by analysis to be a chloromethyl compound; however, TLC revealed that it was a mixture of two substances. This mixture (**IIa**) was treated with dimethylamine and piperidine. The crude reaction product was found again by TLC to consist of a mixture; at this phase the preponderance of one of the isomers was clearly perceptible. The nitrogen-con-

taining isomers could be separated by fractional crystallization. The elemental analyses showed that the two substances (**IIIa** and **IVa**, further **IIIb** and **IVb**) were isomers. The IR spectra made it highly probable that the isomers **IVa** and **IVb**, present in small quantities and having the lower melting points, are unsubstituted at position 16 [2]. For further modification, and also in order to elucidate the structures, an attempt was made to convert the isomers **IIIa**, **IIIb** and **IVa**, **IVb** into the corresponding methoxymethyl-3-methyl ether

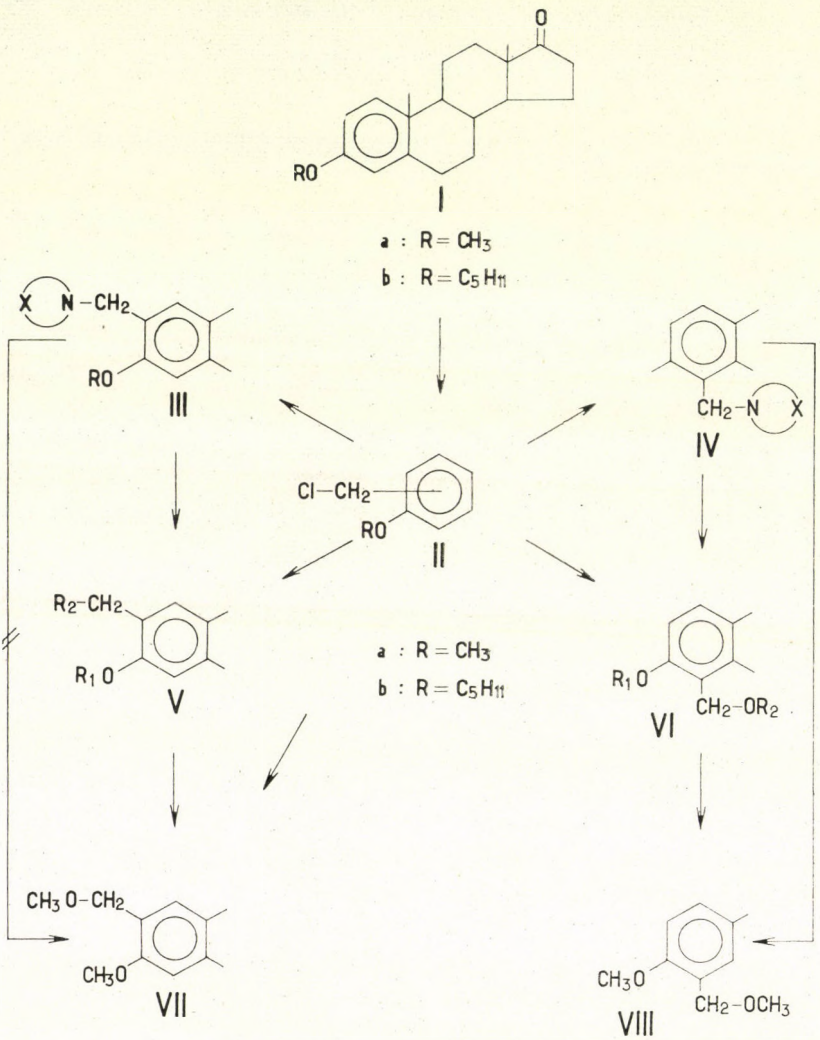

Fig. 1. Legend for III and IV
a: $R = CH_3$; $X = (CH_3)_2$
b: $R = CH_3$; $X = (-CH_2)_5$
c: $R = C_5H_{11}$; $X = (-CH_2)_5$
d: $R = C_5H_{11}$; $X = -(CH_2)_2 - O - (CH_2)_2-$

derivatives (**VII**) and (**VIII**), according to the method (use of dimethyl sulphate in hot methanolic potassium hydroxide) evolved by the Japanese authors [5], since it was at about this stage that their method became known to us. Unfortunately, only the initial compound could be recovered from this experiment. Treatment of the isomers **IIa, IIb** and **IVa, IVb** with methyl iodide similarly failed to give the desired products.

Similar results were obtained in the chloromethylation of estrone-3-cyclopentyl ether. The mixture (**IIb**) of the chloromethyl compounds was treated with piperidine and morpholine, and the isomers were then separated by fractional crystallization to **IIIc, IVc** and **IIId, IVd.** Here again, attempts to effect a reaction with dimethyl sulphate or with methyl iodide proved unsuccessful. The isomers **IIIc** and **IIId,** obtained in higher yields, and the isomers **IVc** and **IVd,** formed in lower yields, were treated separately with acetic anhydride; this converted them into the same acetoxymethyl derivatives **Vb** and **VIb.** The results of this experiment support the view that substitution occurs on the aromatic ring during chloromethylation in both cases.

In possession of this information, we carried out the solvolysis of the chloromethylestrone-3-methyl ether isomeric mixture (**IIa**) in acetic acid, in the presence of sodium acetate. In this case no adequate separation could be achieved (the two isomers were detected by TLC only), therefore, the mixture of the acetoxymethyl isomers was hydrolyzed with sodium carbonate in dioxane, and the two isomers were separated by preparative TLC. The two isomers (**Va** and **VIa**) were found, according to the physical constants and IR spectra, to be the 2- and 4-hydroxymethylestrone-3-methyl ethers, respectively, prepared recently by JOHNS [10]. The 2- and 4-methoxymethylestrone-3-methyl ethers (**VII** and **VIII**) could be synthesized in low yields by the methylation of the two isomers. The 2-methoxymethyl derivative (**VII**) was also prepared [10] by the methanolysis of the chloromethyl mixture (**IIa**).

KANEKO *et al.* explain [5] the conversion of 2- and 4-dimethylaminomethylestrone into the corresponding dimethoxy derivatives (**VII** and **VIII**) by the amine exchange reaction of the Mannich bases [11]. They suppose that the secondary base (cf. Fig. 2) is quaternized in the first step and, in an alkaline medium is then converted into a methylene quinone. This intermediate reacts with the nucleophilic alkoxide ion present, and finally the reaction sequence is closed by the alkylation of the phenolate ion. On the basis of this explanation it is clear why the method of KANEKO *et al.* proved unsuccessful in our case: the 3-hydroxyl group is already alkylated (presence of a 3-methoxyl group), so it cannot give rise to the intermediary methylene quinone structure; therefore, the exchange of the tertiary amino group does not occur in a manner utilizable for a preparative process.

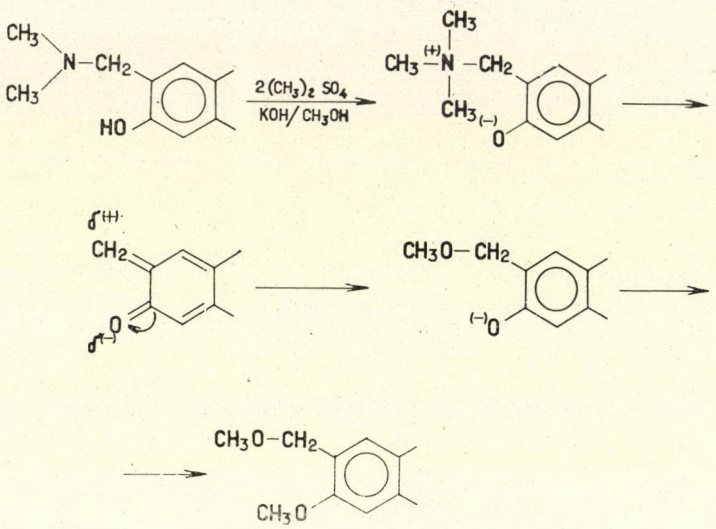

Fig. 2.

Legend for V and VI
a: $R_1 = CH_3$; $R_2 = OH$
b: $R_1 = C_5H_{11}$; $R_2 = OAc$

Experimental

Chloromethylation of estrone-3-methyl ether (Ia)

Estrone-3-methyl ether [3] (**Ia**; 2.84 g; 0.01 mole) was dissolved in glacial acetic acid (60 ml); chloromethylmethyl ether (10 ml) was added, and the solution was allowed to stand at room temperature for 24 hours. The mixture was poured on ice, extracted with chloroform, and the extract was washed with 5% $NaHCO_3$ solution, then with water, and dried over anhydrous $CaCl_2$. The residue (2.75 g) obtained after evaporating the solvent, was chromatographed on 100 g of alumina (neutral, activity III/IV). From the middle fraction (petroleum ether/ether 4 : 6) a yellow, amorphous substance (**IIa**; 2.45 g) was obtained.

$C_{20}H_{25}O_2Cl$ (332.87) Calcd. C 72.17; H 7.57; Cl 10.65. Found: C 72.92; H 8.22; Cl 9.88%.

Chloromethylation of estrone-3-cyclopentyl ether (Ib)

Estrone-3-cyclopentyl ether [12] (**Ib**; 3.38 g; 0.1 mole) was treated as described for **Ia**. When poured on ice, a slightly yellow solid separated (2.92 g) which was washed with water, and dried.

$C_{24}H_{31}O_2Cl$ (386.97) Calcd. C 74.49; H 8.07; Cl 9.16. Found: C 72.24; H 9.10; Cl 8.72%.

2- and 4-Dimethylaminomethylestrone-3-methyl ether (IIIa and IVa)

Crude chloromethylestrone-3-methyl ether (**IIa**; 1.66 g; 5 mmoles) was refluxed for a few hours in benzene (18 ml) with dimethylamine (1.12 g; 25 mmoles). The mixture was allowed to cool and the benzene phase was extracted with 2 *N* HCl (150 ml, in two portions), clarified with activated carbon, and treated with a solution of Na_2CO_3. The precipitate that separated was filtered off next day; after washing and drying a product (1.48 g) was obtained which was recrystallized from acetone, and fractionated by recrystallization from methanol. The main product (0.82 g; m.p. 195—205°), 2-dimethylaminomethylestrone-3-methyl ether (**IIIa**), had m.p. 205—207°; $[\alpha]_D^{20}$ + 142° (chloroform); ν_{max}^{KBr} 825, 235 (ether), 1410, 1500, 1600 (ar.), 1720 (ketone) cm^{-1}.

$C_{22}H_{31}O_2N$ (341.50) Calcd. C 77.83; H 9.15; N 4.01. Found C 77.42; H 9.42; N 3.85%.

After recrystallization, the 4-dimethylaminomethyl isomer (**IVa**) obtained in a small quantity (0.21 g; m.p. 164—170°) had the following constants: m.p. 170—172°; $[\alpha]_D^{20}$ + 119° (chloroform); ν_{max}^{KBr} 1260 (ether), 1502, 1605 (ar.), 1720 (ketone) cm^{-1}.

$C_{22}H_{31}O_2N$ (341.50) Calcd. C 77.83; H 9.15; N 4.01. Found: C 77.68; H 9.24; N 3.68%.

2- and 4-Piperidinomethylestrone-3-methyl ether (IIIb and IVb)

The preparation of these compounds was carried out as described for **IIIa** and **IVa**, starting with crude chloromethylestrone-3-methyl ether (**IIa**; 1.66 g; 5 mmoles) and using piperidine (2.13 g; 25 mmoles) as the amino component. Processing and fractional crystallization gave 2-piperidinomethylestrone-3-methyl ether (**IIIb**) (0.92 g), m.p. 166—170°. After repeated recrystallizations from methanol the m.p. rose to 173—175°; $[\alpha]_D^{20}$ + 106° (chloroform); ν_{max}^{KBr} 1260 (ether), 1560, 1580, 1620 (ar.) 1715, 1718 (ketone) cm^{-1}.

$C_{25}H_{35}O_2N$ (381.56) Calcd. C 78.70; H 9.25; N 3.67. Found C 78.52; H 8.94; N 3.90%.

The m.p. (150—155°) of the crude 4-piperidinomethyl isomer rose to 154—155° after recrystallizations. $[\alpha]_D^{20}$ + 82.6° (chloroform); ν_{max}^{KBr} 1260 (ether), 1575, 1460, 1467 (ar.), 1715...1718 (ketone) cm^{-1}.

$C_{25}H_{35}O_2N$ (381.56) Calcd. C 78.70; H 9.25; N 3.67. Found. C 78.52; H 8.94; N 3.90%.

The m.p. (150—155°) of the crude 4-piperidinomethylisomer rose to 154—155° after recrystallizations. $[\alpha]_D^{20}$ + 82.6° (chloroform); ν_{max}^{KBr} 1260 (ether), 1575, 1460, 1467 (ar.), 1715...1718 (ketone) cm^{-1}.

$C_{25}H_{35}O_2N$ (381.56) Calcd. C 78.70; H 9.25; N 3.67. Found C 78.62; H 9.02; N 3.83%.

2- and 4-Piperidinomethylestrone-3-cyclopentyl ether (IIIc and IVc)

Crude chloromethylestrone-3-cyclopentyl ether (**IIb**; 1.94 g; 5 mmoles) was treated with piperidine (213 g; 25 mmoles) in benzene (20 ml) at the boiling point. Processing, as above, gave two products on fractional crystallization. The main product (**IIIc**; 0.92 g) had m.p. 172—174°; $[\alpha]_D^{20}$ + 128° (chloroform); ν_{max}^{KBr}. 1260 (ether), 1560, 1575, 1605 (ar.), 1725 (ketone) cm^{-1}.

$C_{29}H_{41}O_2N$ (435.65). Calcd. C 79.96; H 9.45; N 3.21. Found C 79. 62; H 9.31; N 3.45%.

The substance (**IVc**) isolated in a smaller quantity (0.18 g) had m.p. 153—155°; $[\alpha]_D^{20}$ + + 104° (chloroform); ν_{max}^{KBr} 1260 (ether), 1490, 1590 (ar.), 1728 (ketone) cm^{-1}.

$C_{29}H_{41}O_2N$ (435.65) Calcd. C 79.96; H 9.45; N 3.21. Found C 79.74; H 9.65; N 3.55%.

2- and 4-Morpholinomethylestrone-3-cyclopentyl ether (IIId and IVd)

These compounds were prepared as described for **IIIc** and **IVc**, using morpholine (2.18 g; 25 mmoles) as the amino component. Processing and fractional crystallization produced two substances; the one (**IIId**) isolated in greater quantity (0.84 g) had m.p. 142—144°; $[\alpha]_D^{20}$ + + 106° (chloroform); ν_{max}^{KBr} 1120, 1260 (ether), 1505, 1579, 1609 (ar.), 1730 (ketone) cm^{-1}.

$C_{28}H_{39}O_3N$ (437.62) Calcd. C 76.85; H 8.98; N 3.20. Found C 76.56; H 8.80; N 3.45%.

The other isomer (**IVd**; 0.09 g) had m.p. 128—129°; $[\alpha]_D^{20}$ + 75° (chloroform); ν_{max}^{KBr} 1118, 1260 (ether), 1480, 1590 (ar.), 1730 (ketone) cm^{-1}.

$C_{28}H_{39}O_3N$ (437.62) Calcd. C 76.85; H 8.98; N 3.20. Found C 76.90; H 8.99; N 3.36%.

2- and 4-Hydroxymethylestrone-3-methyl ether (Va and VIa)

Crude chloromethylestrone-3-methyl ether (**IIa**; 0.67 g; 2 mmoles) was dissolved in acetic acid (8 ml) containing some acetic anhydride. Dry sodium acetate (0.41 g; 5 mmoles) was added, and the mixture was gently boiled for 7 hours. The cooled mixture was diluted

with water, treated with $NaHCO_3$, and extracted with chloroform. Drying over magnesium sulphate and removal of the solvent left a thick oil in which the presence of two substances could be detected by TLC, though separation was not sharp enough. Therefore, the oily mixture was hydrolyzed (30 min., 100°) in 1 : 1 aqueous dioxane (8 ml) in the presence of Na_2CO_3 (0.8 g). The reaction mixture was evaporated to dryness in vacuum, the residue taken up in water and extracted with five portions of chloroform. Repeated thin-layer chromatography (20 by 20 cm plate, a 2-mm layer of Silica Gel, G. Merck; benzine: ethyl acetate 4 : 1) of the substance obtained after working up of the organic phase achieved the separation of the two isomers. Crystallization from a mixture of methylethylketone and hexane gave **Va**, m.p. 162—163° and **VIa**, m.p. 199—200°; ν_{max}^{KBr} 833 (ar.), 1748 (ketone), 3663 (alk.) cm^{-1}, and 813 (ar.), 1730 (ketone), 3521 (alk.) cm^{-1}, respectively.

$C_{20}H_{26}O_3$ (314.42). Calcd. C 76.40; H 8.33. Found C 76.24; H 8.14, and C 76.14; H 8.22, respectively.

2-Acetoxymethylestrone-3-cyclopentylether (Vb)

2-piperidinomethylestrone-3-cyclopentyl ether (**IIIc**; 0.44 g; 1 mmole) was refluxed in acetic anhydride (5 ml) for 2 hours, and the mixture was poured on ice. Next day the precipitate was collected by filtration, and dried (0.31 g). Recrystallization from methanol water gave **Vb**, m.p. 136—137°; $[\alpha]_D^{20}$ + 108° (chloroform); ν_{max}^{KBr} 1260 (ether), 1238 (acetate), 1590 (ar.), 1715, 1730 (ketone) cm^{-1}.

$C_{26}H_{34}O_4$ (410.56) Calcd. C 76.06; H 8.52. Found C 75.88; H 8.20%.

With the product, m.p. 135—137°, of a similar experiment with 2-morpholinomethylestrone-3-cyclopentyl ether (**IIId**), no depression of the mixed m.p. was observed. $[\alpha]_D^{20}$ + 107° (chloroform); ν_{max}^{KBr} 1120, 1260 (ether), 1238 (acetate), 1590 (ar.), 1715, 1730 (ketone) cm^{-1}.

$C_{26}H_{34}C_4$ (410.56). Calcd. C 76.06; H 8.52. Found C 75.97; H 8.45%.

4-Acetoxymethylestrone-3-cyclopentyl ether (VIb)

Starting with 4-piperidinomethyl- (**IVc**), or with 4-morpholinomethylestrone-3-cyclopentyl ether (**IVd**) and proceeding as in the preparation of **Vb**, the same acetoxymethyl compound (**VIb**) was obtained from both starting materials. This product crystallized with difficulty (methanol-water); the semi-crystalline compound had m.p. 56—59°; $[\alpha]_D^{20}$ + 92 ± 2° (chloroform); ν_{max}^{KBr} 1120, 1242 (ether acetate), 1572, 1605 (ar.), 1710, 1725 (ketone) cm^{-1}

$C_{26}H_{34}O_4$ (410.56) Calcd. C 76.06; H 8.52. Found C 75.12; H 8.08 and C 75.42; H 8.16% respectively.

2-Methoxymethylestrone-3-methyl ether (VII)

(a) *From the chloromethylation product of estrone-3-methyl ether* (**IIa**)

Crude chloromethylestrone-3-methyl ether (**IIa**; 3.32 g; 10 mmoles) was dissolved in abs. methanol (70 ml) containing sodium methoxide (30 mmoles; prepared from 0.70 g of sodium metal), and refluxed for 2 hours. Water (70 ml) was added to the mixture, and it was saturated with carbon dioxide. The methanol was evaporated and the residue extracted with chloroform. Drying and evaporation yielded a yellow oil (2.54 g) which was chromatographed on an alumina column (neutral, activity III/IV). The fraction, extracted with benzene containing 30% of ether, gave a crystalline substance (0.84 g; m.p. 112—120°) which was twice recrystallized from methanol, mp. 123—124° [5, 10]; $[\alpha]_D^{20}$ + 139° (chloroform); ν_{max}^{KBr} 1240 (ether), 1580, 1615 (ar.), 1725 (ketone) cm^{-1}.

$C_{21}H_{28}O_3$ (328.45). Calcd. C 76.80; H 8.59. Found C 76.64; H 8.48%.

(b) *From 2-hydroxymethylestrone-3-methyl ether* (**Va**)

Abs. ether (2 ml) was poured on sodium hydride (0.05 g; 2.2 mmoles) and 2-hydroxymethylestrone-3-methyl ether (**Va**) (0.64 g; 2 mmoles) was added in portions. This mixture was stirred for 24 hours (with interruptions) and admixed with methyl iodide (0.57 g; 0.38 ml; 4 mmoles), then it was refluxed, with stirring, for 5 hours, cooled, and diluted with ether (20 ml).

After treatment with water, the organic phase was washed with water, dried, and evaporated. The residue, a brown oil (0.52 g), was chromatographed on alumina (neutral, III/IV activity). From the fraction, obtained by extraction with benzene containing 10% of ether, 2-methoxymethylestrone-3-methyl ether (**VII**; 0.11 g m.p. 114—119°) could be isolated. After recrystallization from methanol the product had m.p. 122—124° [5, 10]. Mixed m.p. with the substance prepared according to (a) was 122—123°; $[\alpha]_D^{20}$ + 139° (chloroform); ν_{max}^{KBr} 1241 (ether), 1625 (ar.), 1720 (ketone) cm^{-1}.

$C_{21}H_{28}O_3$ (328.45) Calcd. C 76.80; H 8.59. Found C 76.52; H 8.28%.

4-Methoxymethylestrone-3-methyl ether (VIII)

From 4-hydroxymethylestrone-3-methyl ether (**VIa;** 0.64 g; 2 mmoles) the pure 4-methoxymethyl compound (0.04 g) could be obtained by the operations just described, m.p. 150—152° [5]; $[\alpha]_D^{20}$ + 133° (chloroform); ν_{max}^{KBr} 1120, 1260 (ether), 1582 (ar.), 1728 (ketone) cm^{-1}.

$C_{21}H_{28}O_3$ (328.45) Calcd. C 76.80; H 8.59. Found C 76.64; H 8.18%.

*

The authors are indebted to Dr. HIDEHIKO KANEKO *(Research Laboratory, Dainippon Pharmaceutical Co. Ltd.)* for the samples of 2- and 4-methoxymethylestrone kindly sent for comparison. Thanks are due to Mrs. K. L. LÁNG and Mrs. B. G. BOZÓKI for the microanalyses, and to Mr. J. SZABÓ for recording and evaluating the infrared spectra.

One of the authors (A.F.A.) wishes to thank the *National Research Centre of Cairo* and the *Hungarian Government* for a fellowship and the opportunity to carry out this work.

The substances used in this work were supplied by the courtesy of *Chemical Works Gedeon Richter, Budapest, Hungary*. Thanks are due for this help.

SUMMARY

Isomers substituted at positions 2 and 4 have been isolated in the form of the dimethylaminomethyl, piperidinomethyl, morpholinomethyl, acetoxymethyl, hydroxymethyl, and methoxymethyl derivatives from mixtures obtained by the chloromethylation of estrone-3-methyl ether, and estrone-3-cyclopentyl ether.

REFERENCES

1. APPLEZWEIG, A. N.: "Steroid Drugs" Vol. I., MacGraw-Hill Book Co., New York, 1962; Vol. II., Holden-Day Inc., San Francisco, 1964.
2. PATTON, T. L.: J. Org. Chem. **25,** 2148 (1960).
3. KINCL, F. A., GARCIA, M.: Ber. **92,** 595 (1959).
4. VINCZE, W. I., SCHNEIDER, GY., KŐVÁRI, I.: Acta Chim. Acad. Sci. Hung. (to be published).
5. KANEKO, H., HASHIMOTO, M., KOBAYASHI, A.: Chem. Pharm. Bull. **12,** 196 (1964).
6. QUELET, R.: Bull. soc. chim. France **1953,** 46.
7. QUELET, R., ABOULEZZ, A. F.: Compt. rend. **240,** 1439 (1955).
8. ABOULEZZ, A. F., ZAYED, S. M. A. D., ELHAMOULY, W. S.: Acta Chim. Acad. Sci. Hung. **42,** 41 (1964).
9. FRIED, J. H., NUTILE, A. N., ARTH, G. E.: J. Org. Chem. **26,** 976 (1964).
10. JOHNS, W. F.: J. Org. Chem. **30,** 3993 (1965).
11. SNYDER, H. R., BREWSTER, J. H.: J. Amer. Chem. Soc. **70,** 4230 (1949).
12. ERCOLI, A., GARDI, R.: Chem. Ind. **1961,** 1037.

Béla MATKOVICS; Szeged, Dóm tér 8.
A. F. ABOULEZZ; National Research Center of Cairo, U.A.R.
Ferenc KATONA; Szeged, Dóm tér 8.
Ödön K. J. KOVÁCS; Budapest. II., Pusztaszeri út 57—59.

Acta Chimica Academiae Scientiarum Hungaricae Tomus 56 (4), pp. 369—384 (1968)

CHEMICAL TRANSFORMATIONS OF DIOLS AND CYCLIC ETHERS, XXIV*

INVESTIGATION OF THE CONVERSION OF 2-MONOSUBSTITUTED OXETANES IN THE PRESENCE OF PLATINUM CATALYSTS BY THE MICROREACTOR TECHNIQUE

M. BARTÓK and K. KOVÁCS

(Institute for Organic Chemistry, A. József University, Szeged)

Received February 20, 1967

The conversions in the presence of contact catalysts of 2-monosubstituted derivatives of four-membered cyclic ethers have not been studied systematically. In a few papers attempt has been made to approach this field of research, calling attention to the theoretical interest and to the necessity of such investigations. According to a remark of BARBOT [1], in the semi-pinacol type conversion of oxetanes both isomeric aldehydes and ketones are formed:

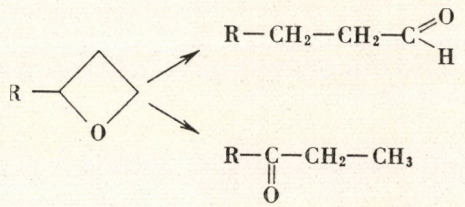

The author doesnot mention the preparation of the oxetanes, the conditions of the conversion, or the nature of the radical R; only the possibility of the process is reported. This same communication [1] and a later work [2] described that in the dehydratation of 1-R-propanediol-1,3 derivatives, in the presence of dilute sulphuric acid at 130°—180°, the formation of considerable quantities of isomeric aldehydes and ketones can be observed besides that of insubstantial amounts of oxetanes. The formation of the oxo compounds is explained by the semipinacol-type rearrangement of the oxetanes. These findings are very important, but have to be substantiated by modern research techniques.

COPENHAVER and BIGELOW, in their investigations on the conversion of butanediol-1,3 to butadiene in the presence of a catalyst containing phosphate and sulphuric acid on a coke carrier, observed the formation of 2-methyloxetane, and, as was assumed by them, that of its decomposition and isomeri-

* Part XXIII: Acta Chim. Acad. Sci. Hung. **55**, 61 (1968).

zation products [3]:

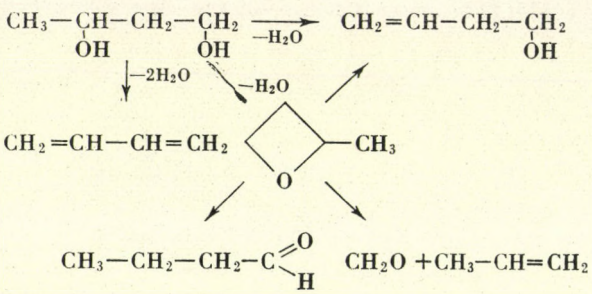

Initial results of our study on preparative scale of the conversion of 2-monosubstituted oxetanes, over a platinum catalyst on carbon carrier, were reported in 1962 [4]. Besides isomerization to aldehyde, thermal decomposition was observed. SUJKIN and AN [5, 6] studied the conversion of 2-ethyloxetane in the presence of a $TiO_2—Al_2O_3$ catalyst. The main process was found to be the splitting of the investigated compound into butene and formaldehyde. At the same time, particularly at lower temperatures, the isomerization of the four-membered cyclic ether into a five-membered one was also observed:

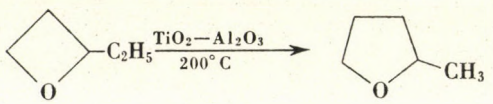

The mechanism of the occurring processes has not been discussed.

Our present communication reports on the investigation of the conversion of 2-monosubstituted oxetanes in the presence of Pt/T and Pt/C* catalysts. The object of the work was to prove the isomerization to carbonyl compounds, and to determine the effect on the nature of the α-substituent on the rate and direction of the processes proceeding on the catalyst.

Our experimental work involved a study of the conversion of 2-methyl-, 2-*n*-propyl-, 2-i-propyl, 2-*n*-butyl-, 2-cyclohexyl- and 2-phenyloxetanes over Pt/T and Pt/C catalysts in the presence of the carrier gases hydrogen helium. A simple method of microreactor techniques, the so-called "pulse" feeding was chosen. The microreactor was connected directly to the feed inlet of a *Willy—Giede* gas chromatograph Type GCHF 18/2.**

* T = thermolite carrier; C = activated carbon carrier.

** Experimental methods for the investigation of the heterogeneous catalytic conversion of oxetanes (microreactor techniques, analysis) have been described in detail in Part XV [7], XVI [8], and XIX [9] of this series. The synthesis of 2-monoalkyl- and -aryloxetanes has been reported in an earlier work [11].

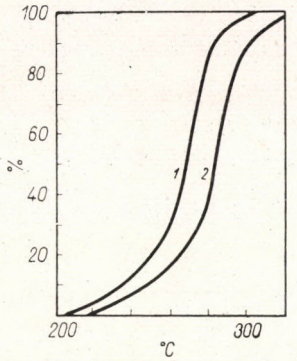

Fig. 1. The conversion of 2-methyloxetane in the presence of Pt/T catalyst as a function of the temperature and the nature of the carrier gas *1.** 1.1 Pt/T; *2.* 1 TCP; *3.* 140; *4.* 50 H_2 (Curve 1), 50 He (Curve 2); *5.* 140; *6.* 1/8, 1/4; *7.* 0.01

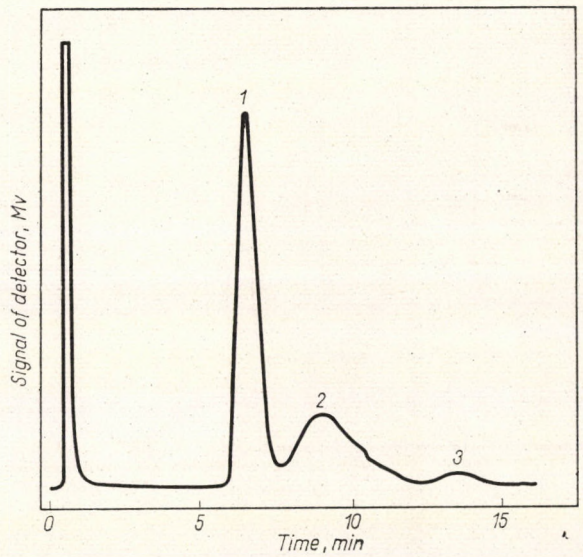

Fig. 2. Chromatogram of the products formed in the conversion of 2-methyloxetane on Pt/T catalyst *1.** 1.1 Pt/T, 280; *2.* 1 ODP; *3.* 60; *4.* 50 H_2; *5.* 140; *6.* 1; *7.* 0.01. Notation of peaks: *1* 2-methyloxetane, *2* butyraldehyde, *3* methyl ethyl ketone

* Notations: *1* is the quantity (ml) of the microreactor packing (particle diameter 0.2—0.4 mm), and its temperature (°C). Q — quartz, T — thermolite, C — activated carbon;

2 is the length (m) and the composition of the chromatographic column of 5 mm internal diameter: 20% of the partition liquid deposited on thermolite having the particle size of 0.02—0.4 mm, and alumina (Al_2O_3), resp.;

3 is the thermostat temperature of the chromatograph (°C);

4 is the flow rate (ml/min) of the carrier gases helium (He) and hydrogen (H_2), respectively;

5 is the detector current (mA);

6 is the sensitivity of the *Willy—Giede* gas chromatograph Type GCHF 18/2 (1 — compensograph final amplitude: 2 mV; 1/2 — compensograph final amplitude; 4 mV; 1/4—, etc.);

7 is the volume of substance injected into the microreactor (ml). TCP: tricresyl phosphate; ODP: β,β'-dipropionitrile ether. AG: *Apiezon* grease "L".

The majority of the experiments was made using a Pt/T catalyst in the presence of hydrogen. For comparison — similarly to the case of 3-monosubstituted oxetanes — the effect of a Pt/C catalyst on the rate and the direction of the processes has also been investigated.

Conversion of 2-monosubstituted oxetanes on Pt/T catalyst

Our first aim was to study the effect of temperature and the nature of the carrier gas on the rate of decomposition of the oxetanes. For this purpose, the conversion of 2-methyloxetane in the presence of a Pt/T catalyst was studied in the temperature range between 200 and 320° (Fig. 1).

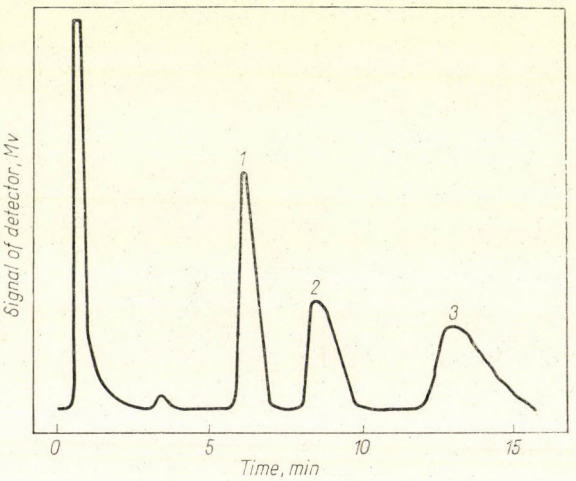

Fig. 3. Chromatogram of the products formed in the conversion of 2-methyloxetane on Pt/T catalyst *1.* 1.1 Pt/T, 320; *2.* 1 ODP; *3.* 60; *4.* 50 H_2; *5.* 140; *6.* 1/2; *7.* 0.01. Notation of peaks: *1* 2-methyloxetane, *2* butyraldehyde, *3* methyl ethyl ketone

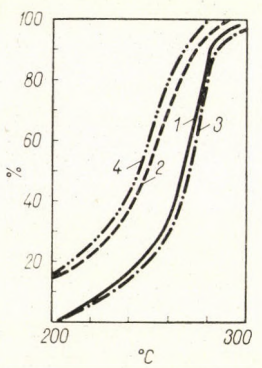

Fig. 4. The conversion of 2-monoalkyloxetanes on Pt/T catalyst as a function of temperature
1. 2-methyl-, *2.* 2-*n*-propyl-, *3.* 2-i-propyl-, *4.* 2-*n*-butyloxetane
1. 1.1 Pt/T; *2.* 1 AG; *3.* 100—200; *4.* 50 H_2; *5.* 140; *6.* 1.1/2, 1/2; *7.* 0.01

The presence of hydrogen accelerated the process, however, it had no substantial effect on the direction of the conversion. Figs 2 and 3 show the chromatograms of the two experiments carried out at 280 and 320°, respectively.

On the basis of the experimental results, the conversion of 2-methyloxetane in the presence of Pt/T catalyst can be represented by the following reaction scheme:

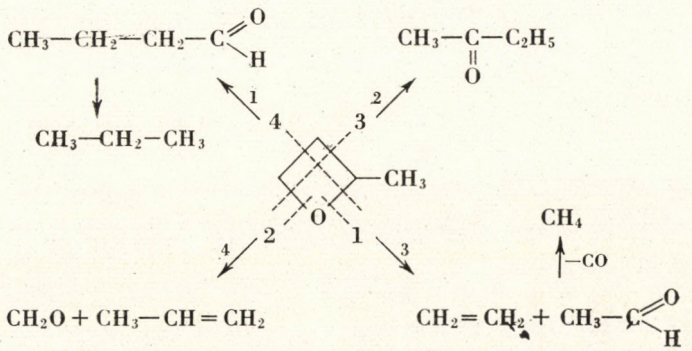

It may be seen that the presence of the methyl group in the ring exerts an important effect on the direction of the processes taking place. At lower temperatures the isomerizations *1* and *2* are the main directions of the reaction. Their ratio is 4—5 : 1. A raise in temperature is favourable for conversions *3* and *4*, and for the secondary processes. At 330 to 340°, the quantity of propylene becomes equal to that of propane, formed by the decarbonylation of butyraldehyde. Conversion *3* proceeds only to a very slight degree.

In Fig. 4, the percentage conversions of 2-methyl-, 2-*n*-propyl-, 2-i-propyl and 2-*n*-butyloxetanes on Pt/T catalyst in the presence of hydrogen are plotted as a function of the temperature.

The diagram shows that an increase in the $+I$ effect of the substituent accelerates the conversion rate. 2-i-propyloxetane, the conversion of which is the slowest, is an exception. This experimental finding, similarly to the case of 3-i-propyloxetane, can be explained by the place of the i-propyl group in the *Baker—Nathan* series. The conversion of 2-*n*-propyl- and 2-*n*-butyloxetanes begins already below 200°, and it is complete at 280°. Figs 5—15, presenting some characteristic chromatograms, afford information about the directions of the conversions of these oxetanes.

On the basis of the experimental results, the conversion of 2-monoalkyloxetanes on Pt/T catalyst can be represented by the following reaction scheme:

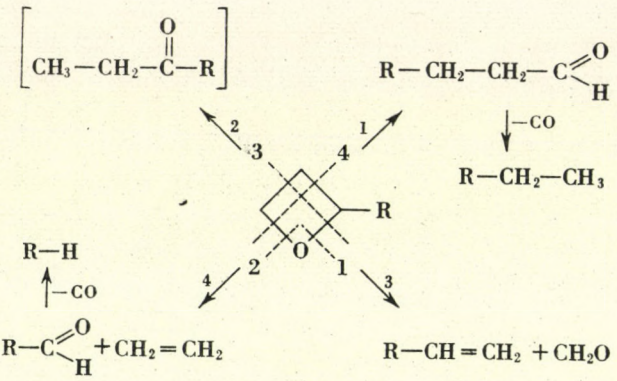

where R is *n*-propyl, i-propyl, and *n*-butyl.

Thus, it has been experimentally proved that isomerization to carbonyl compounds (*1* and *2*), which, at lower temperatures (below 260°), is the main direction of the conversion, proceeds also with this type of oxetanes. This may be readily seen in Figs 5 and 10, where the isomerization of oxetanes occurs to about 30—40%, and owing to the low temperature, the rate of conversions *3* and *4*, as well as that of the secondary processes is negligibly low. In some of the experiments also the formation of unsaturated alcohols isomeric with the oxetanes could be observed. At higher temperatures, evidently, the quantity of unsaturated hydrocarbons formed by thermal decomposition, increases considerably. This may be clearly seen in Figs 13—15; the experiments conducted at 340° yielded substantially more olefins than saturated hydrocarbons.

Evaluated on the basis of Figs 5—8, the ratio of the isomerization processes *1* and *2* is 5 : 1. No quantitative evaluation has been attempted yet to determine the influence of the temperature and of the nature of the substituent on the processes shown in the former scheme. As it is seen from the chromatograms, besides the secondary conversions shown in the scheme, the isomerization of both saturated hydrocarbons and olefins takes place on the Pt catalyst. Conversion *4* proceeds only to a very slight degree.

Figs 5 to 8. Chromatograms of the products formed in the conversion of 2-*n*-propyloxetane on Pt/T catalyst as a function of the temperature *1.* 1.1 Pt/T, 215, 280, 340 and 380, resp.; *2.* 1 AG; *3.* 180; *4.* 50 H_2; *5.* 140; *6.* 1/2; *7.* 0.01*

* Note to Figs 5—15. The peaks marked by numbers denote the following substances: *1:* CO; *2:* saturated hydrocarbon containing one carbon atom less than the corresponding oxetane; *3:* olefin containing the same number of carbon atoms as *2; 4* and *5:* aldehyde or ketone isomeric with the oxetane homologue, resp.; *4'*: hydrocarbon having the same number of carbon atoms as the oxetane homologue; *6:* the starting oxetane; *7:* α,β-unsaturated alcohol isomeric with the oxetane homologue.

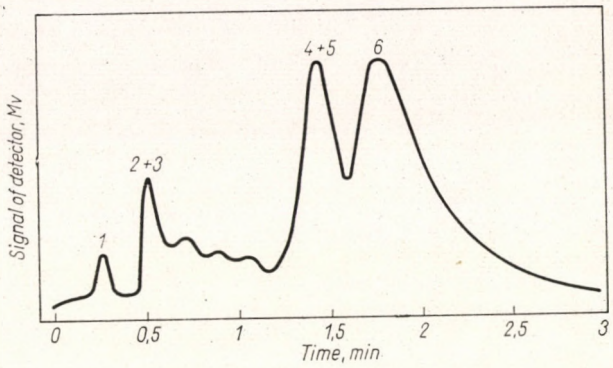

Fig. 5

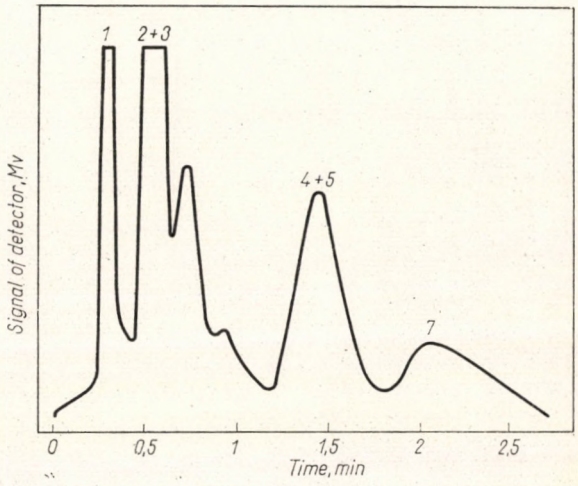

Fig. 6

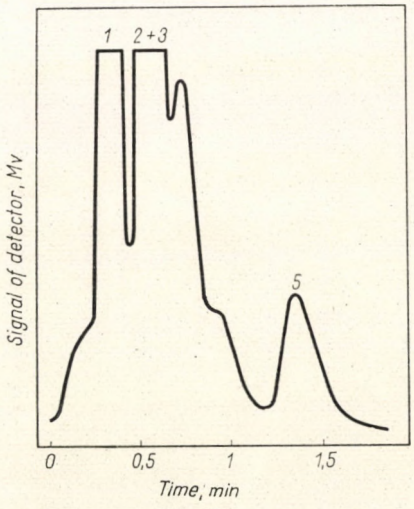

Fig. 7

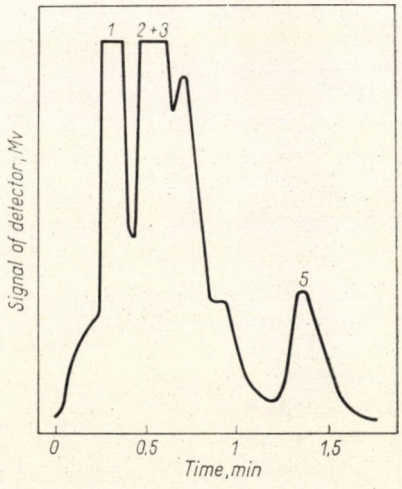

Fig. 8

Summing up, it may be stated that isomerization to aldehydes takes place also with this type of oxetanes, and even at a higher rate than in the case of the 3-monosubstituted analogues. Simultaneously, owing to the substituent in position *2*, also the isomerization to ketone, though to a lesser degree, takes place. On the evidence of these experiments, it can be stated that 2-monosubstituted oxetanes, as contrary to five-membered cyclic ethers

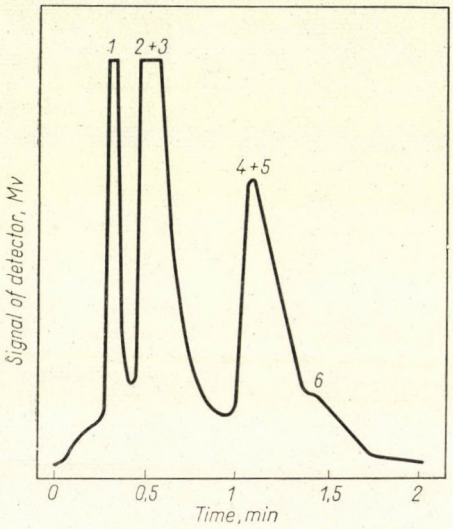

Fig. 9. Chromatogram of the products formed in the conversion of 2-i-propyl oxetane on Pt/T catalyst *1.* 1.1 Pt/T, 240; *2.* 1 AG; *3.* 180; *4.* 50 H_2; *5.* 140; *6.* 1/2; *7.* 0.01*



Fig. 10. Chromatogram of the products formed in the conversion of 2-*n*-butyloxetane on Pt/T catalyst. *1.* 1.1 Pt/T, 240; *2.* 1 AG; *3.* 180; *4.* 50 H_2; *5.* 140; *6.* 1; *7.* 0.01*

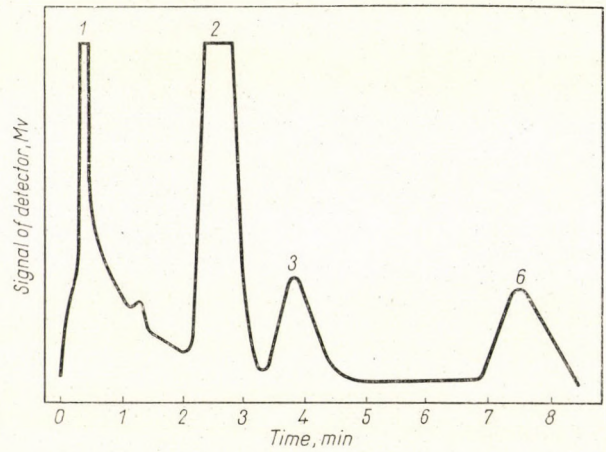

Fig. 11. Chromatogram of the products formed in the conversion of 2-cyclohexyloxetane on Pt/T catalyst. *1.* 1.1 Pt/T, 280; *2.* 1 AG; *3.* 200; *4.* 50 H_2; *5.* 140; *6.* 1; *7.* 0.01*

[10], are split under the given conditions most readily along the C—O linkage next to the substituent. The aldehydes formed undergo decarbonylation at higher temperatures to yield saturated hydrocarbons. Above 280—300°, the rate of thermal decomposition increases considerably, and this process leads to the formation of unsaturated hydrocarbons and formaldehyde. The decarbonylation of the latter yields hydrogen.

Figs 11 and 12 show the chromatograms of the conversion of 2-cyclohexyl- and 2-phenyloxetane, respectively, on Pt/T catalyst in the presence

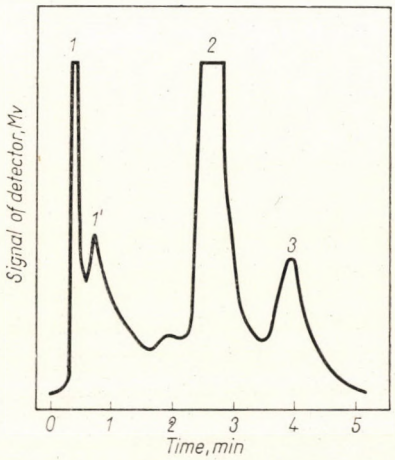

Fig. 12. Chromatogram of the products formed in the conversion of 2-phenyloxetanes on Pt/T catalyst. *1.* 1.1 Pt/T, 240; *2.* 1 AG; *3.* 200; *4.* 50 H_2; *5.* 140; *6.* 1; *7.* 0.01*

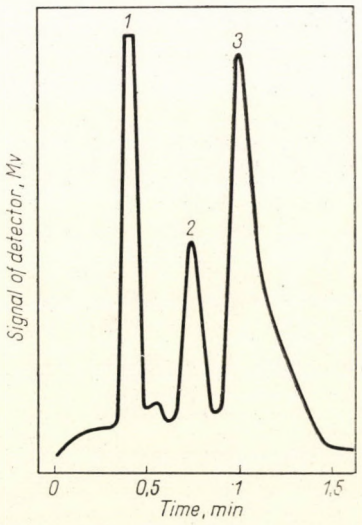

Fig. 13

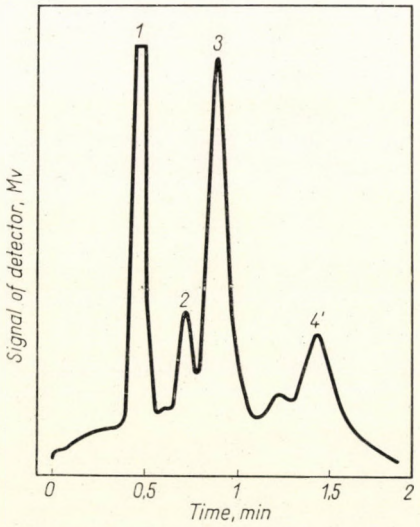

Fig. 14

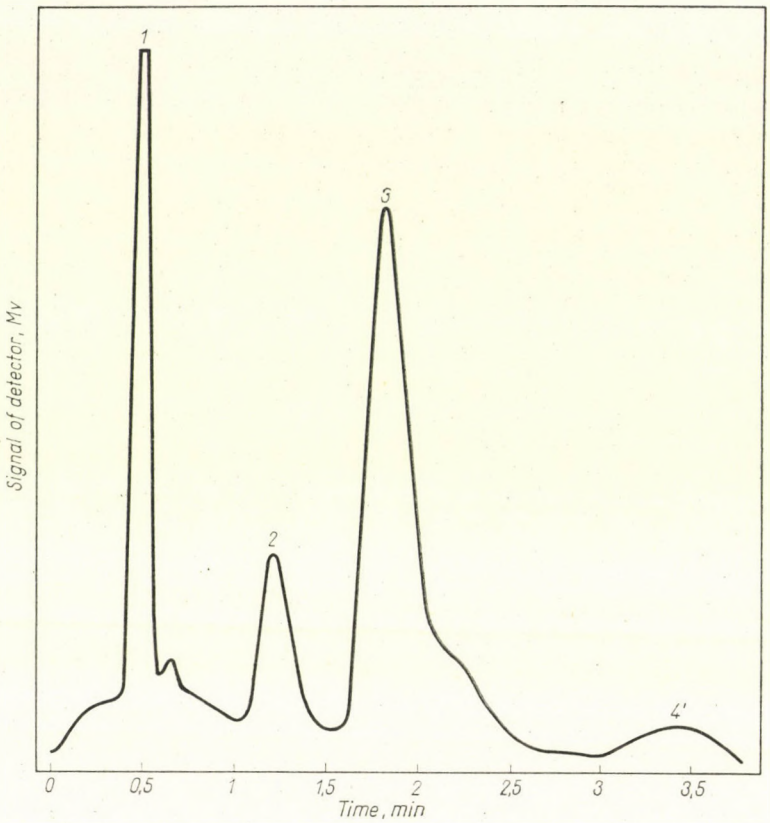

Fig. 15

Figs 13 to 15. Chromatograms of the hydrocarbons formed in the conversion of 2-*n*-propyl, 2-i-propyl- and 2-*n*-butyloxetanes on Pt/T catalyst. *1.* Pt/T, 340; *2.* 1 ODP; *3.* 30; *4.* 50 H_2; *5.* 140; *6.* 1/4, 1/4, 1/2; *7.* 0.01*

of hydrogen. As it can be seen from the chromatograms, substances of aromatic character (ethylbenzene, styrene) are formed in both cases, the rate of formation being much higher for the cyclic ether with phenyl substituent:

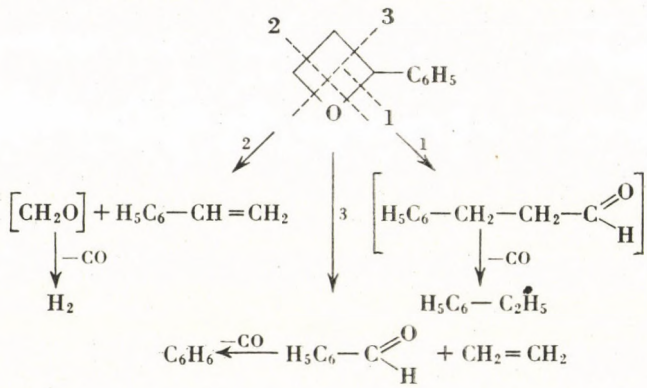

The presence of phenylpropionaldehyde, formed as an intermediate during the isomerization could not be verified experimentally, because it undergoes rapid decarbonylation as soon as it is formed. As it may be seen from the chromatogram, ethylbenzene is the main product in the conversion of 2-phenyltrimethylene oxide (peak *2*). Moreover, as shown by the scheme, small amounts of benzene and styrene are formed (peaks *1'* and *3*, respectively). All these conversions are to be observed already at 240°, and the formation of relatively great quantities of ethylbenzene — as compared to styrene — is due to the low temperature.

With 2-cyclohexyloxetane — as is to be expected — these processes proceed at a slower rate, since the formation of the aromatic skeleton is possible only by means of dehydrogenation and this reaction requires higher temperatures. The primary process is isomerization, and this is followed by aromatization:

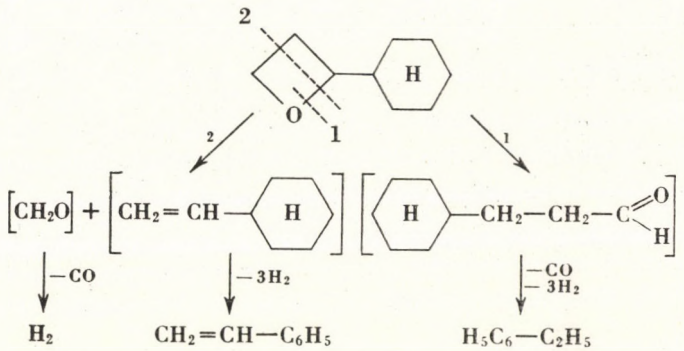

Ketone formation could not be observed in any of the cases.

Conversion of 2-monosubstituted oxetanes on Pt/C catalyst

The conversion of 2-monoalkyloxetanes in the presence of Pt/C catalyst — in accordance with other types of oxetanes — proceeds at a higher rate than on platinum catalyst on thermolite carrier. Figs 16—22 show some characteristic chromatograms of the products.

The processes to be expected on Pt/C catalyst in the presence of hydrogen are summarized in the following scheme:

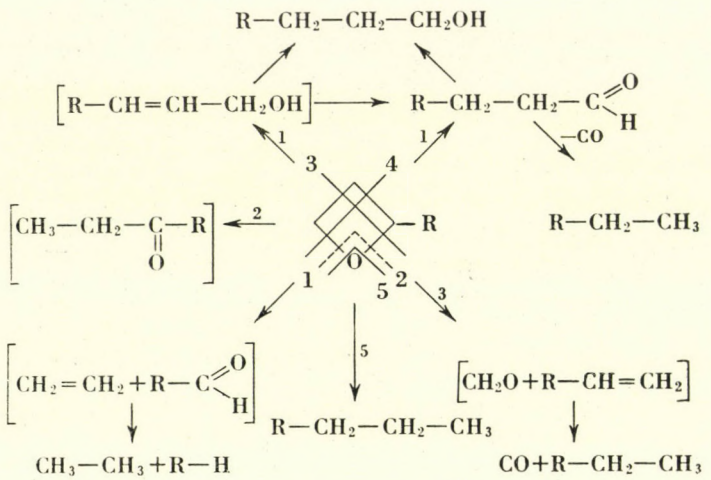

where R is methyl, ethyl, *n*-propyl, i-propyl, *n*-butyl.

The main direction of the conversion is the formation of saturated hydrocarbons having one carbon atom less than the corresponding oxetanes (peaks *3*). These saturated hydrocarbons are formed by the decarbonylation of the alde-

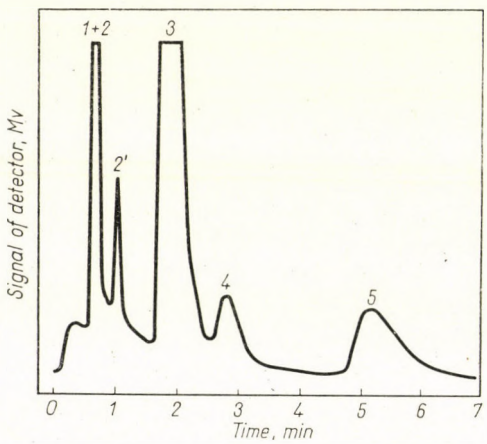

Fig. 16. Chromatogram of the products formed in the conversion of 2-methyloxetane on Pt/C catalyst. *1.* 0.3 Pt/C, 320; *2.* 1 Al_2O_3; *3.* 140; *4.* 50 H_2; *5.* 140; *6.* 1/2; *7.* 0.01*

hydes produced by isomerization (*1*). Below 300°, the Pt/C catalyst is selective; practically, only process *1* takes place. With this type of oxetanes, another way of formation of the said saturated hydrocarbon is also conceivable, *i.e.* the dehydrohydrogenation of the formaldehyde and the olefins formed during decomposition (reaction course 3). The formation of ketones could not be observed in the presence of Pt/C catalyst. Owing to the simultaneous hydro-

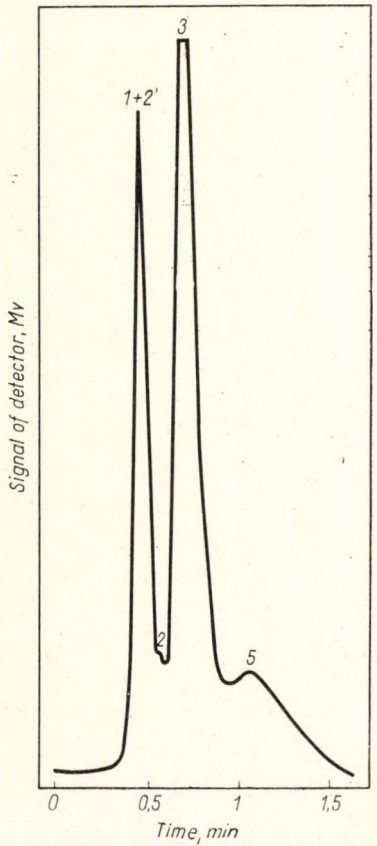

Fig. 17. Chromatogram of the products formed in the conversion of 2i-propyloxetane on Pt/C catalyst. *1.* 0.3 Pt/C, 295; *2.* 1 ODP; *3.* 30; *4.* 50 H_2; *5.* 140; *6.* 1/2; *7.* 0.01*

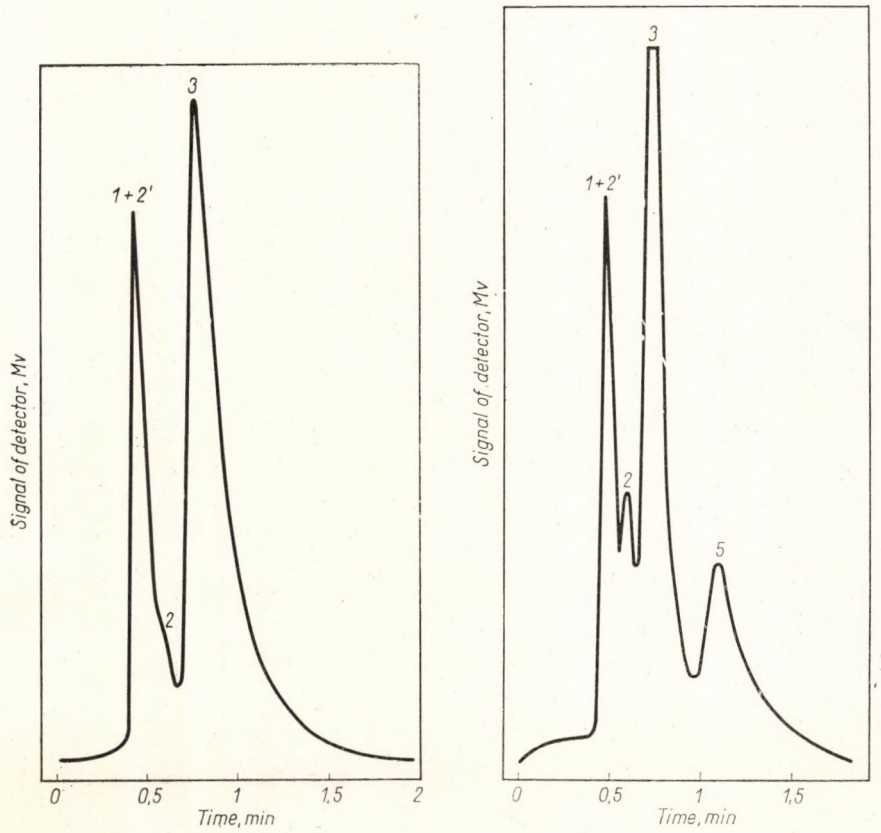

Fig. 18—19. Chromatograms of the products formed in the conversion of 2-*n*-propyloxetane on Pt/C catalyst. *1.* 0.3 Pt/C, 265 and 340, resp.; *2.* 1 ODP; *3.* 30 and 40, resp.; *4.* 50 H_2; *5.* 140; *6.*1/2; *7.* 0.005*

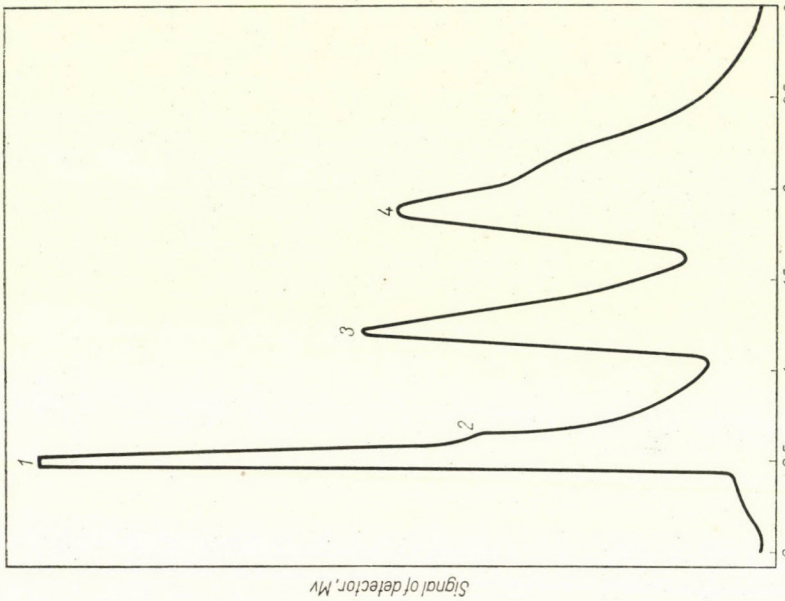
Signal of detector, Mv
Time, min
0
0.5
1
1.5
2
2.5
3
1
2
3
4

Fig. 21

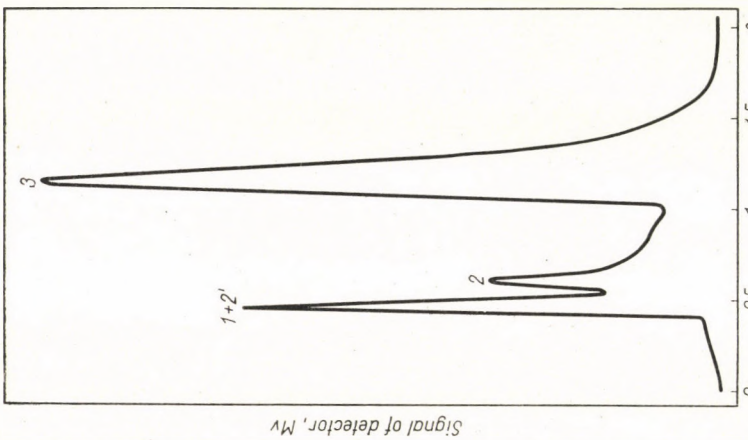
Signal of detector, Mv
Time, min
0
0.5
1
1.5
2
1+2'
2
3

Fig. 20

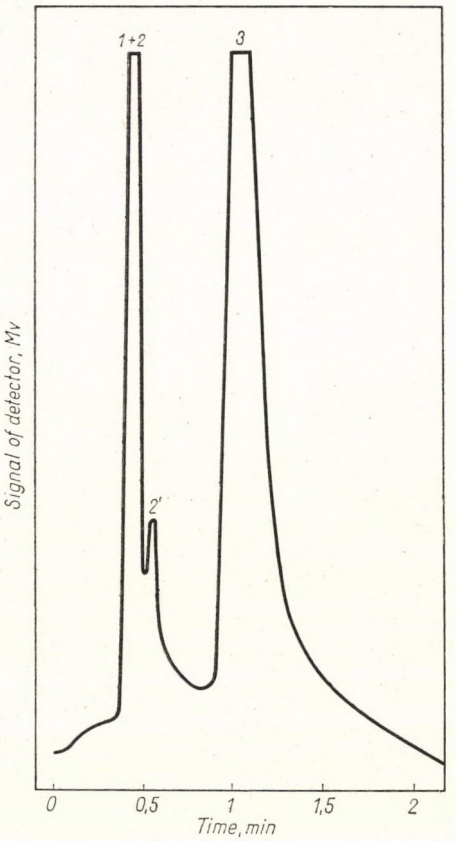

Fig. 22

Figs 20 to 22. Chromatograms of the products formed in the conversion of 2-*n*-butyloxetane on Pt/C catalyst. *1.* 0.3 Pt/C, 320, 310, 307; *2.* 1 ODP; *3.* 30; *4.* 50 H_2, 50 He, 50 H_2; *5.* 140; *6.* 1/2; *7.* 0.005, 0.01, 0.01*

genolysis of the two C—O linkages of the oxetane molecule, also the formation of saturated hydrocarbons having the same number of carbon atoms as the starting cyclic ether can be observed (peaks marked by *5*). The decomposition processes marked by *3* and *4* occur primarily on a deactivated catalyst at higher temperatures, when conditions are unfavourable for hydrogenation. The degree of hydrogenolysis increases with the decrease in weight of the substituting radical (Figs 16—18) and with increasing temperature. These two experimental findings are closely related, as indeed opposite conditions favour isomerization. Otherwise, the decomposition process marked by *3*, starting

* Note to Figs 16—22. The peaks marked by numbers represent the following substances: *1* CO; *2* and *2'* ethane formed in the conversion marked by the number *4* on the scheme, and a saturated hydrocarbon having three carbon atoms less than the starting oxetane homologue; *3* saturated hydrocarbon formed from the aldehyde isomer of the oxetane homologue; *4* olefin having one carbon atom less than the starting oxetane; *5* saturated hydrocarbon with the same number of carbon atoms as the starting oxetane.

with the splitting of the C—O linkage next to the substituent, proceeds to a considerably higher degree than conversion *4*, which latter results in the formation of ethylene. The formation of the end-products of these processes can be explained also by the direct hydrogenolysis of the C—C linkages, besides the route described above.

In the absence of hydrogen, process *3* proceeds to a very high degree on Pt/C catalyst, with helium as the carrier gas (Fig. 21). When immediately after this experiment the same is repeated under practically identical experimental conditions but in the presence of hydrogen, the difference both in the direction and the rate of the reaction is conspicuous (Figs 21 and 22).

SUMMARY

The conversions of 2-monosubstituted oxetanes (methyl-, *n*-propyl-, i-propyl-, *n*-butyl-, cyclohexyl- and phenyloxetane) over platinum catalyst on thermolite and carbon carrier in the presence of hydrogen or helium carrier gases have been studied by microreactor techniques in the temperature range 200—400°C. Under the studied conditions the principal directions of the conversion of these oxetanes were found to be isomerization yielding aldehydes and ketones, and decomposition leading to the formation of olefins and formaldehyde. The ratio of aldehydes and ketones is 5 : 1. The primary processes are accompanied by several secondary reactions. Conclusions have been drawn concerning the influence of various parameters, such as the catalyst carrier, temperature, carrier gas and the nature of the substituent, on the extent and course of the conversions of oxetanes.

REFERENCES

1. BARBOT, A.: Bull. soc. chim. France **1936,** 1438.
2. BARBOT, A.: Ann. chim. **11,** 519 (1939).
3. COPENHAVER, J., BIGELOW, M.: Khimija acetilena. Ed. I. L. Moskow, 1954, p. 156.
4. SUJKIN, N. I., BARTÓK, M., KOVÁCS, Ö., BELYSKIJ, I. F.: Izvest. Akad. Nauk. SSSR Ser. Khim. **1962,** 1653.
5. SUJKIN, N. I., AN, V. V.: Izvest. Akad. Nauk. SSSR Ser. Khim. **1962,** 1476.
6. SUJKIN, N. I., AN, V. V.: Izvest. Akad. Nauk. SSSR Ser. Khim. **1963,** 1478.
7. BARTÓK, M., FÉNYI, SZ.: Acta Phys. et Chem. Szeged **12,** 157 (1966).
8. BARTÓK, M.: Acta Phys. et Chem. Szeged **13,** 59 (1967).
9. BARTÓK, M.: Acta Chim. Acad. Sci. Hung. **51,** 403 (1967).
10. SUJKIN, N. I., BELYSKIJ, I. F.: Dokl. Akad. Nauk. SSSR. **120,** 548 (1958).
11. BARTÓK, M., GILDE, A. S.: Acta Phys. et Chem. Szeged **9,** 25 (1963).

Mihály BARTÓK
Kálmán KOVÁCS
Szeged, Dóm tér 8.

Acta Chimica Academiae Scientiarum Hungaricae Tomus 56 (4), pp. 385—392 (1968)

CHEMICAL TRANSFORMATIONS OF DIOLS AND CYCLIC ETHERS, XXV*

INVESTIGATION OF THE CONVERSION OF 3,3-DIALKYLOXETANES IN THE PRESENCE OF PLATINUM CATALYSTS BY THE MICROREACTOR TECHNIQUE

M. BARTÓK and B. KOZMA

(Institute for Organic Chemistry, A. József University, Szeged)

Received February 20, 1967

Our investigations into the chemistry of cyclic ethers included the study of the conversions of oxetanes in the presence of platinum catalysts. The results obtained with triethylene oxide and its 3- and 2-monosubstituted homologues have been reported [1, 2, 3].

There is only one work published on the heterogeneous catalytic conversion of 3,3-disubstituted derivatives of trimethylene oxide. NIENBURG and ELSCHNIG [4] obtained β,β'-dimethyl-γ-butyrolactone in 55—60% yield from 3,3-dimethyltrimethylene oxide by reacting it with carbon monoxide at 200° and 200—250 atm pressure, in the presence of cobalt octacarbonyl catalyst.

In our recent investigations, experiments were carried out to study the conversion of 3,3-dialkyl-substituted oxetanes over a platinum catalyst on thermolite (T) and activated carbon (C) carriers (Pt/T and Pt/C), in the temperature range from 220 to 350° using hydrogen as the carrier gas. A simple method of microreactor techniques, employing the "pulse" feeding was chosen for these investigations. The microreactor was connected directly to the feed inlet of a *Willy Giede* Type GCHF 18/2 gas chromatograph.**

The effect of the catalyst carriers on the decomposition of trimethylene oxide was discussed in detail in our previous paper [1]. These experimental results prompted us to study the conversion of 3,3-dialkyloxetanes mainly on Pt/T catalyst. However, in certain cases, reactions proceeding in the presence of Pt/C catalyst were also investigated.

* Part XXIV: Acta Chim. Acad. Sci. Hung. (in this volume).

** Methods (microreactor techniques, analysis of the products) for the investigation of the thermal and heterogeneous catalytic conversion of oxetanes have been described in detail in earlier publications [5—7].

The conversion of 3,3-dialkyloxetanes on Pt/T catalyst

Our experiments comprised the investigation of the conversion of 3,3-dimethyl-, 3,3-diethyl-, 3-methyl-3-*n*-propyl- and 3-ethyl-3-*n*-butyloxetanes* on Pt/T catalyst, at temperatures between 220 and 350°.

Before the evaluation of the conversions, a few chromatograms, characteristic of the heterogeneous catalytic conversion of the investigated oxetanes

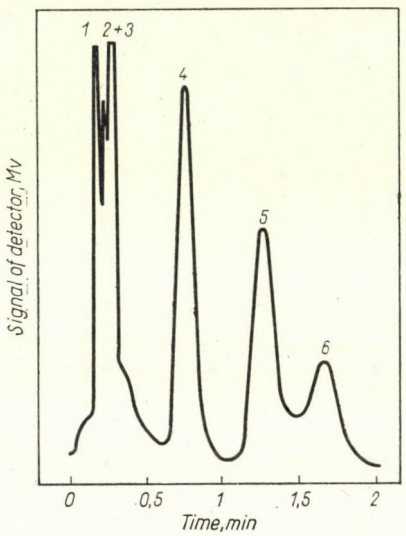

Fig. 1. Chromatogram of the products formed in the conversion of 3,3-dimethyloxetane on Pt/T catalyst. *1.*** 1.1 Pt/T, 314; *2.* 1 TCP; *3.* 150; *4.* 50 H_2; *5.* 140; *6.* 1/2; *7.* 0.01***

will be presented. From these chromatograms, conclusions may be drawn concerning the process of the decomposition of the oxetanes.

* The synthesis of 3,3-dialkyloxetanes has been described in an earlier paper [8].

** Notations: *1* is the quantity (ml) of the microreactor packing (particle size of 0.2—0.4 mm), and its temperature (°C) Q — quartz, T — thermolite, C — activated carbon;

2 is the length (m) and the composition of the chromatographic column of 5 mm internal diameter: 20% of the partition liquid deposited on thermolite having the particle size of 0.2—0.4 mm, and alumina (Al_2O_3), respectively;

3 is the thermostat temperature of the chromatograph (°C);

4 is the flow rate (ml/min) of the hydrogen (H_2) carrier gas;

5 is the detector current (mA);

6 is the sensitivity of the *Willy Giede* gas chromatograph Type GCHF 18/2 (1 — compensograph final amplitude: 2 mV; 1/2 — compensograph final amplitude: 4 mV; 1/4—, etc.);

7 is the volume of the substance injected into the microreactor (ml). TCP: tricresyl phosphate; ODP: β,β'-oxydipropionitrile ether; AG: *Apiezon* grease "L".

*** The peaks marked by numbers on the graphs denote the following substances: *1* — carbon monoxide; *2* — saturated hydrocarbon containing one carbon atom less than the starting oxetane; *3* — as *2*, but unsaturated hydrocarbon; *4* — aldehyde isomeric with the oxetane homologue: *5* — oxetane; *6* — ketone isomeric with the oxetane homologue (see reaction scheme).

Comparison of the conversion degree (rate) of 3,3-dialkyloxetanes with the conversion rates of the oxetanes studied earlier under identical conditions, shows that the rate of decomposition of the 3,3-disubstituted oxetanes is the

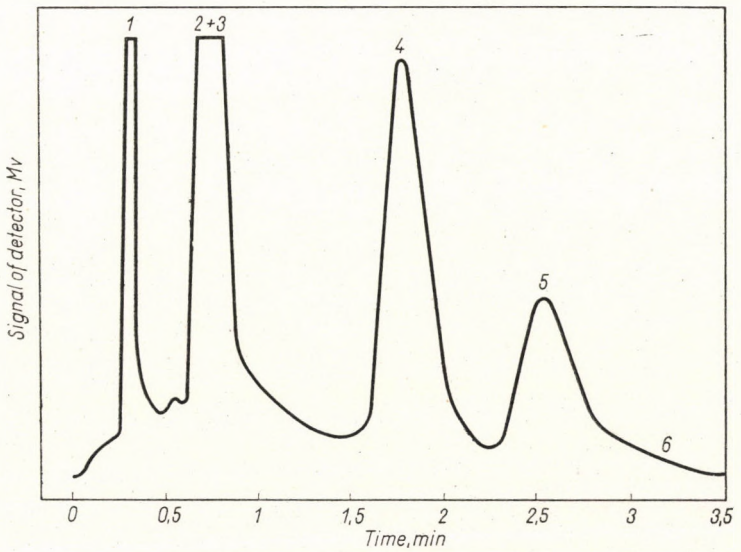

Fig. 2. Chromatogram of the products formed in the conversion of 3,3-diethyloxetane on Pt/T catalyst. *1.* 1.1 Pt/T, 350; *2.* 1 AG; *3.* 200; *4.* 50 H_2; *5.* 140; *6.* 1/2;7. 0.01

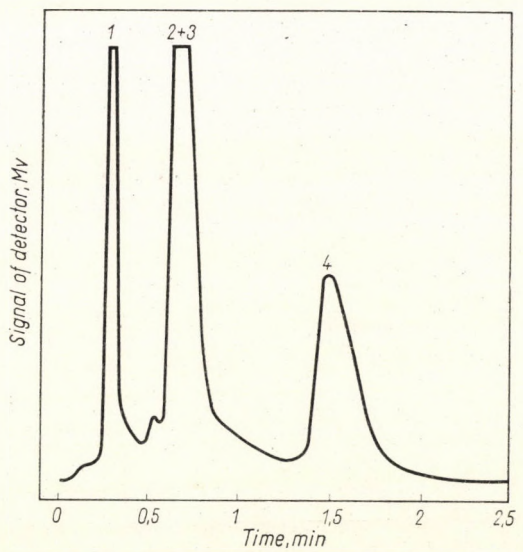

Fig. 3. Chromatogram of the products formed in the conversion of 3-methyl-3-*n*-propyloxetane. *1.* 1.1 Pt/T, 350; *2.* 1 AG; *3.* 200; *4.* 50 H_2; *5.* 140; *6.* 1/2; 7. 0.01*

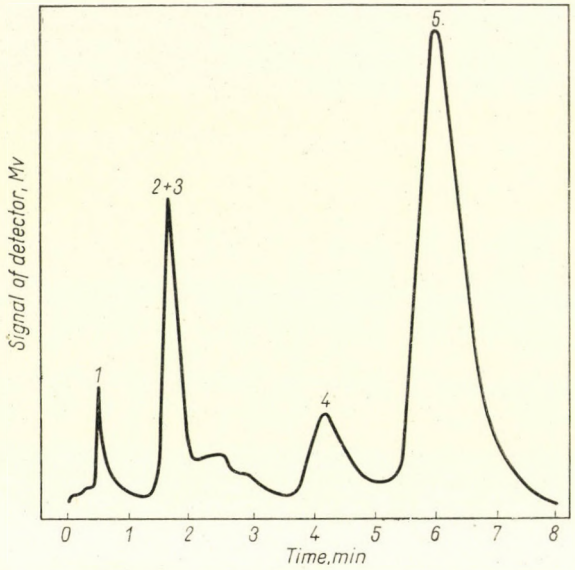

Fig. 4. Chromatogram of the products formed in the conversion of 3-ethyl-3-*n*-butyloxetane. *1.* 1.1 Pt/T, 270; *2.* AG; *3.* 200; *4.* 50 H_2; *5.* 140; *6.* 1; *7.* 0.01*

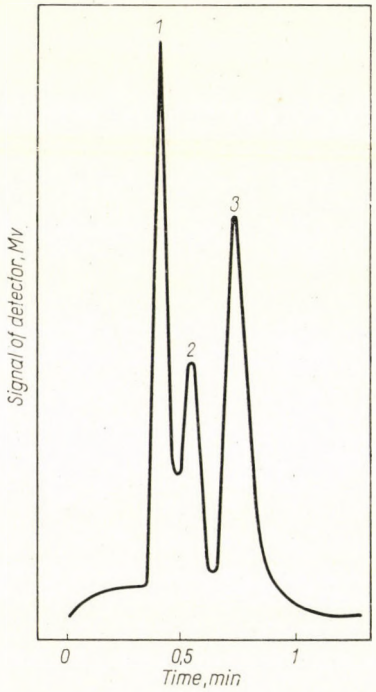

Fig. 5



Fig. 6

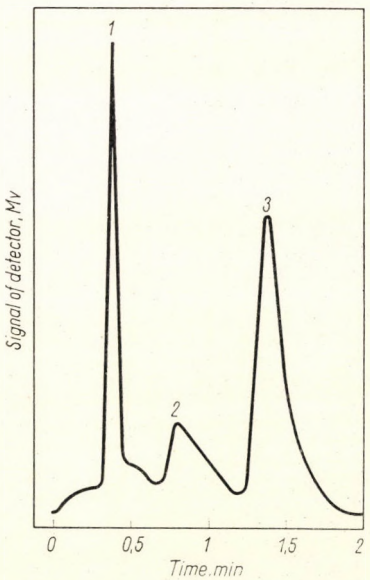

Fig. 7

Figs 5 to 7. Chromatograms of the hydrocarbons formed in the conversion of 3,3-dimethyl-, 3,3-diethyl and 3-methyl-3-*n*-propyloxetanes. *1.* 1.1 Pt/T; 345, 340 and 330, respectively; *2.* 1 ODP; *3.* 30; *4.* 50 H_2; *5.* 140; *6.* 1/4, 1/2 and 1/2, respectively; *7.* 0.01*

slowest. Thus, *e.g.*, at 270°, when the conversion of 2-butyloxetane on Pt/T catalyst has already reached 80% [3], the conversion of 3-ethyl-3-*n*-butyloxetane is only beginning (Fig. 4).

Of the 3,3-dialkyl-substituted oxetanes, the decomposition of 3-methyl-3-*n*-propyloxetane was found to proceed at a higher rate than that of the isomeric 3,3-diethyloxetane (Figs 2 and 3).

On the basis of the experimental results the conversion of 3,3-dialkyloxetanes in the presence of a Pt/T catalyst is described by the following reaction scheme:

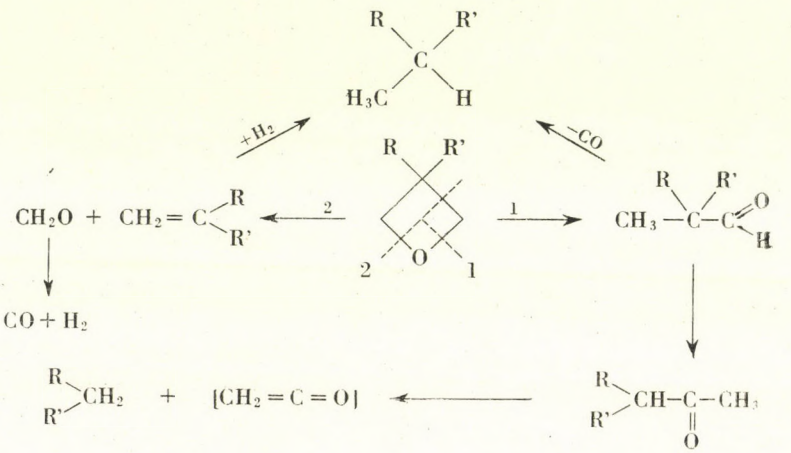

where R,R′ is methyl, methyl; ethyl, ethyl; methyl, *n*-propyl; or ethyl, *n*-butyl.

The course of the conversions in the presence of a Pt/T catalyst is highly dependent on temperature. Thus, at lower temperatures, the isomerization to aldehydes can be observed. However, since the conversion of 3,3-disubstituted oxetanes begins at higher temperatures than that of other oxetane homologues, the decarbonylation rate of the aldehydes formed, resulting in saturated hydrocarbons, is relatively high. For the same reason, the thermolysis of these oxetanes which yields unsaturated hydrocarbons, is already taking place together with the isomerization at the initial stage of decomposition. The evaluation of the chromatograms (*e.g.*, Figs 2 and 6) 3,3-dialkyl-substituted oxetanes are converted in about 60% by isomerization to yield aldehydes, and in about 40% by thermal decomposition leading to the formation of unsaturated hydrocarbons. With these oxetanes, the formation of isomeric ketones and unsaturated alcohols, or of unsaturated aldehydes is not possible without a change in the carbon skeleton [1].

However, in the case of 3,3-dimethyloxetane the rearrangement aldehyde → ketone, involving a change in the structure of the carbon skeleton, was observed (peak *6* in Fig. 1). At higher temperatures, the primary con-

versions are followed by secondary processes (isomerization of saturated and unsaturated hydrocarbons accompanied by the change of the carbon skeleton, or by the migration of the double bond; dehydrogenation of saturated hydrocarbons).

The conversion of 3,3-dialkyloxetanes on Pt/C catalyst

Figs 8—10 show a few characteristic chromatograms of experiments made in the presence of Pt/C catalyst.

On comparing the chromatograms in Figs 6 and 9 with those in Figs 7 and 10, respectively, the effect of the Pt/C catalyst, both on the rate and the direction of the conversion of 3,3-dialkyloxetanes becomes obvious. It can be seen that, as compared to their conversion on Pt/T catalyst, the compounds are rapidly converted into saturated hydrocarbons by way of decarbonylation of the aldehydes, which have been formed as primary products by isomerization. Since olefins, under the given experimental conditions, may be hydrogenated to saturated hydrocarbons, the possibility of this reaction, marked *2* on the scheme, cannot be excluded, either.

In the reaction of 3,3-dimethyloxetane, the formation of relatively high quantities of propane (peak *2′* in Fig. 8) can be explained by the decomposition of the ketone, produced by the rearrangement of aldehyde, as indicated in the scheme.

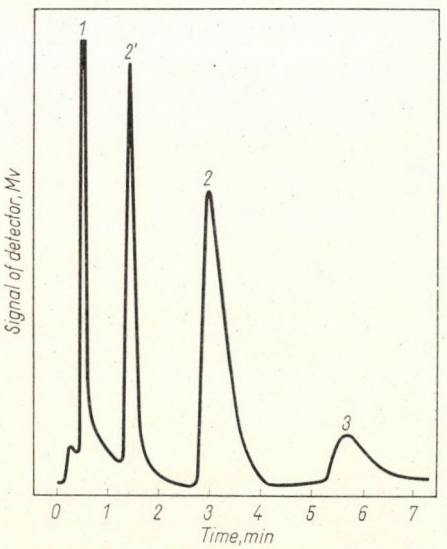

Fig. 8

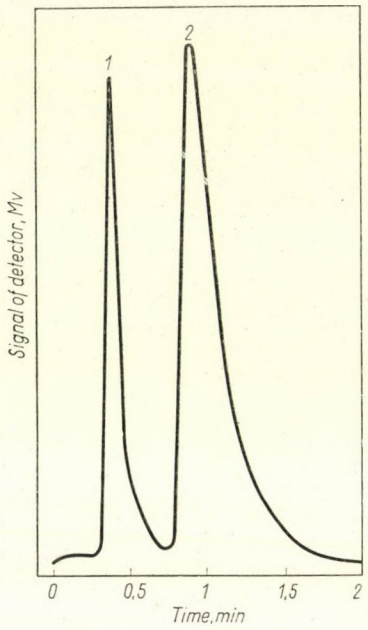

Fig. 9

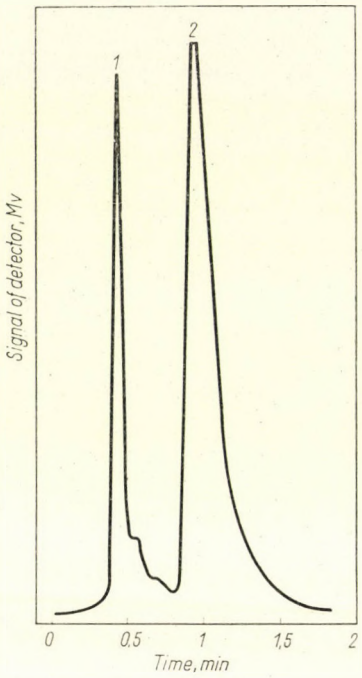

Fig. 10

Figs 8 to 10. Chromatograms of the hydrocarbons formed in the conversion of 3,3-dimethyl-, 3,3-diethyl- and 3-methyl-3-*n*-propyloxetanes on Pt/C catalyst. *1.* 0.3 Pt/C, 330, 303, 320; *2.* 1 Al_2O_3, 1 ODP, 1 ODP; *3.* 140, 30, 30; *4.* 50 H_2; *5.* 140; *6.* 1, 1/2, 1/2; *7.* 0.01, 0.005, 0.005 The marking of the peaks is the same as in Fig. 1 (*2'* — propane)

SUMMARY

The conversions of 3,3-dialkyloxetanes (dimethyl, diethyl, methyl-*n*-propyl, ethyl-*n*-butyl) have been studied by the microreactor technique over platinum catalysts on thermolite and carbon carriers in the presence of hydrogen between 220 and 350°C. Under these conditions, the principal conversion processes of the oxetanes are isomerization, yielding aldehydes, and decomposition, yielding olefins and formaldehyde. These primary processes are accompanied by several secondary reactions. Conclusions have been drawn concerning the influence of the experimental conditions on the extent and course of the conversions of 3,3-dialkyloxetanes.

REFERENCES

1. BARTÓK, M., KOVÁCS, K.: Acta Chim. Acad. Sci. Hung. **55,** 49 (1968).
2. BARTÓK, M., KOZMA, B.: Acta Chim. Acad. Sci. Hung. **55,** 61 (1968).
3. BARTÓK, M., KOVÁCS, K.: Acta Chim. Acad. Sci. Hung. (in this volume).
4. German Pat. 1.066.572; C.A. **55,** 10323 (1961).
5. BARTÓK, M., FÉNYI, SZ.: Acta Phys. et Chem. Szeged **12,** 157 (1966).
6. BARTÓK, M.: Acta Phys. et Chem. Szeged **13,** 59 (1967).
7. BARTÓK, M.: Acta Chim. Acad. Sci. Hung. **51,** 403 (1967).
8. SUJKIN, N. I., BARTÓK, M., KOZMA, B.: Izvest. Akad. Nauk SSSR **1967,** 153.

Mihály BARTÓK
Béla KOZMA
Szeged, Dóm tér 8, Hungary

Acta Chimica Academiae Scientiarum Hungaricae Tomus 56 (4), pp. 393—404 (1968)

CHEMICAL TRANSFORMATIONS OF DIOLS AND CYCLIC ETHERS, XXVI*

INVESTIGATION OF THE CONVERSION OF 2,4-DIALKYL-SUBSTITUTED OXETANES IN THE PRESENCE OF PLATINUM CATALYST BY THE MICROREACTOR TECHNIQUE

M. BARTÓK, K. KOVÁCS and N. I. SHUIKIN**

(Institute for Organic Chemistry, A. József University, Szeged)

Received February 20, 1967

In our earlier papers the results of investigations into the conversions of trimethylene oxide and its 3-mono-, 2-mono- and 3,3-dialkyl-substituted homologues over platinum catalysts were reported [1].

In our investigations on the heterogeneous catalytic reactions of oxetanes, experiments were carried out to study the conversion of cis- and trans-isomeric mixtures of 2,4-dialkyloxetanes, over platinum catalysts on thermolite (T) or activated carbon (C) carrier (Pt/T and Pt/C), in the temperature range from 200 to 350°C, in the presence of hydrogen or helium gas. A simple method of the microreactor technique, involving "pulse" feeding, was chosen. The microreactor was connected directly to the feed inlet of a *Willy—Giede* Gas Chromatograph Type 18/2.*** Previous experience [1] guided us in selecting the experimental parameters. Concerning the method of evaluation of the experimental results we refer to our previous paper [1].

Conversion of 2,4-dialkyloxetanes on Pt/T catalyst

In these experiments we investigated the conversion of 2-methyl-4-ethyl-, 2-methyl-4-*n*-butyl- and 2-methyl-4-cyclohexyloxetanes**** on Pt/T catalyst, at temperatures between 200 and 320°.

Owing to structural factors, the decomposition of these oxetanes can proceed in more directions than that of the analogues previously investigated. This becomes evident from the following figures, where the chromatograms indicate the formation of a considerably greater number of substances.

Fig. 5 shows the rate of conversion of 2-methyl-4-ethyl- and 2-methyl-4-*n*-butyloxetanes on Pt/T catalyst as a function of the temperature.

* Part, XXV: Acta Chim. Acad. Sci. Hung. (in this volume).

** *Institute for Organic Chemistry*, Moscow, SSSR.

*** Methods (microreactor techniques, product analysis) for the investigation of the thermal and heterogeneous catalytic conversions of oxetanes have been described in detail in earlier communications [2—4].

**** Communiction XIV of this series deals with the synthesis of the oxetanes.

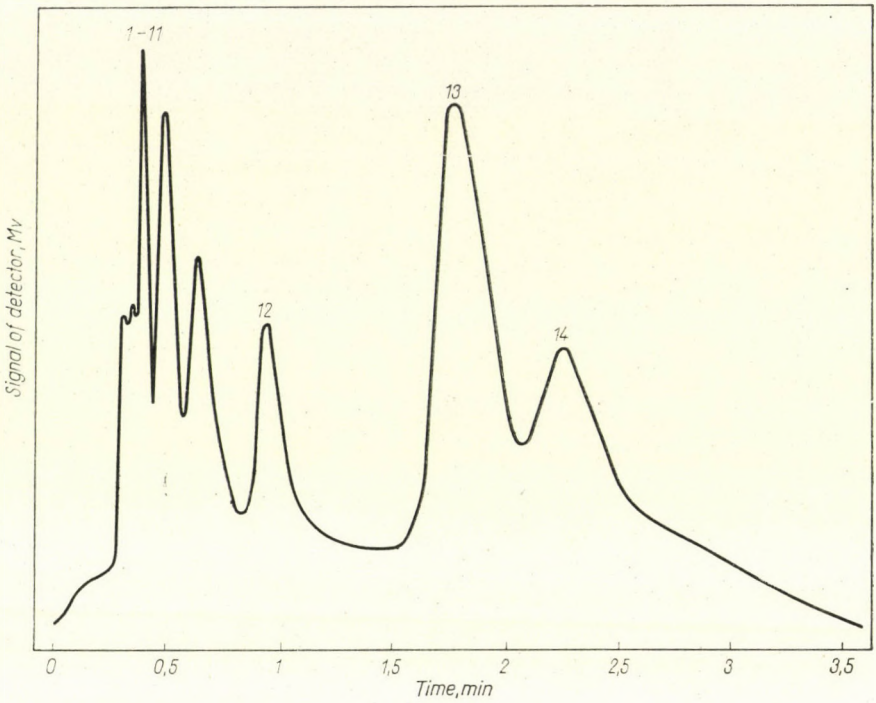

Fig. 1

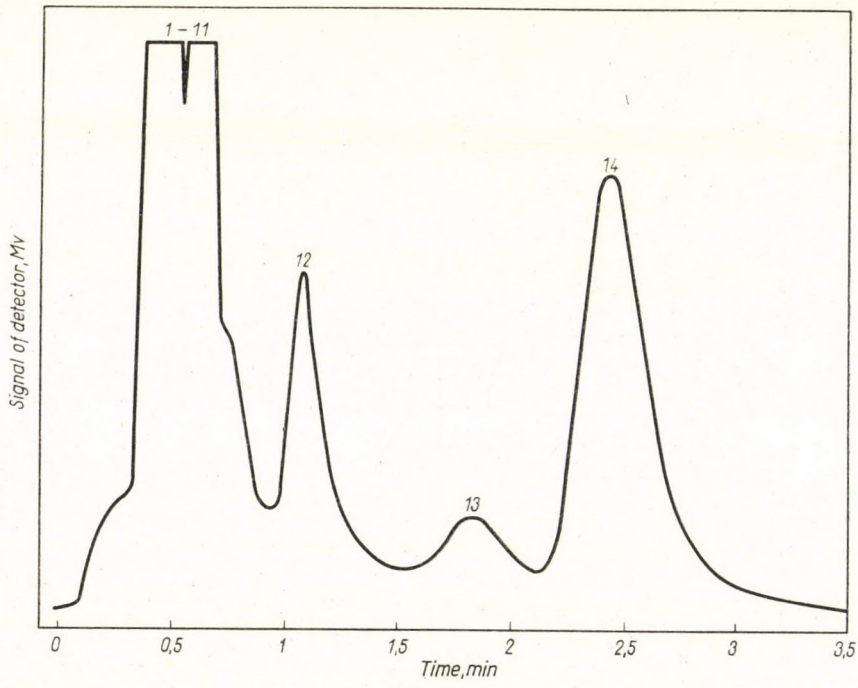

Fig. 2

Figs 1—2. Chromatograms of the products formed in the conversion of 2-methyl-4-ethyl-oxetane. *1.** 1.1 Pt/T, 280, 330; *2.* 1 AG; *3.* 160; *4.* 50 H_2; *5.* 140; *6.* 1/2; *7.* 0.01**

These experiments show the increase of the reaction rate with an increase of the positive inductive effect of the substituents.

On the basis of the experimental results, the conversion of 2,4-dialkyloxetanes in the presence of Pt/T catalyst can be described by the following reaction scheme:

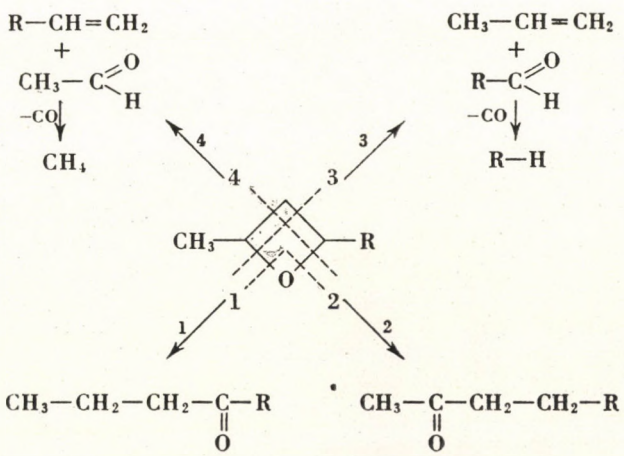

where R is ethyl or *n*-butyl.

Owing to the low selectivity of the column, the chromatograms (Figs 1—4) do not allow to draw exact conclusions about the direction of the conversions actually taking place. The separation of the ketones, formed by the isomerizations *1* and *2*, could not be realized. From the chromatograms presented in Figs 6 and 8, a quantitative though indirect evaluation can be made of the isomerization processes *1* and *2*. This is based on the fact that the reactions involving splitting (marked by *3* and *4*) and the subsequent secondary

---

*Notations: *1* is the quantity (ml) of the microreactor packing (particle size 0.2 to 0.4 mm), and its temperature (°C). Q — quartz, T — thermolite, C — activated carbon;

2 is the length (m) and the composition of the chromatographic column of 5 mm internal diameter [20% of the partition liquid deposited on thermolite having the particle size of 0.2—0.4 mm, and alumina (Al_2O_3), respectively];

3 is the thermostat temperature (°C) of the chromatograph;

4 is the flow rate (ml/min) of the helium (He) and hydrogen (H_2) carrier gas, respectively;

5 is the detector current (mA);

6 is the sensitivity of the *Willy—Giede* Type GCHF 18/2 gas chromatograph (1 — compensograph final amplitude: 2 mV; 1/2 — compensograph final amplitude: 4 mV; 1/4 — etc.);

7 is the volume of the substance (ml) injected into the reactor. TCP: tricresyl phosphate; ODP: β,β'-oxydipropionitrile ether; AG: *Apiezon* grease "L".

** Marking of peaks: *1*: carbon monoxide; *2—10*: saturated and unsaturated hydrocarbons; *11—12*: aldehydes; *13*: the starting oxetane homologue; *14*: ketone isomers of the oxetane homologue.

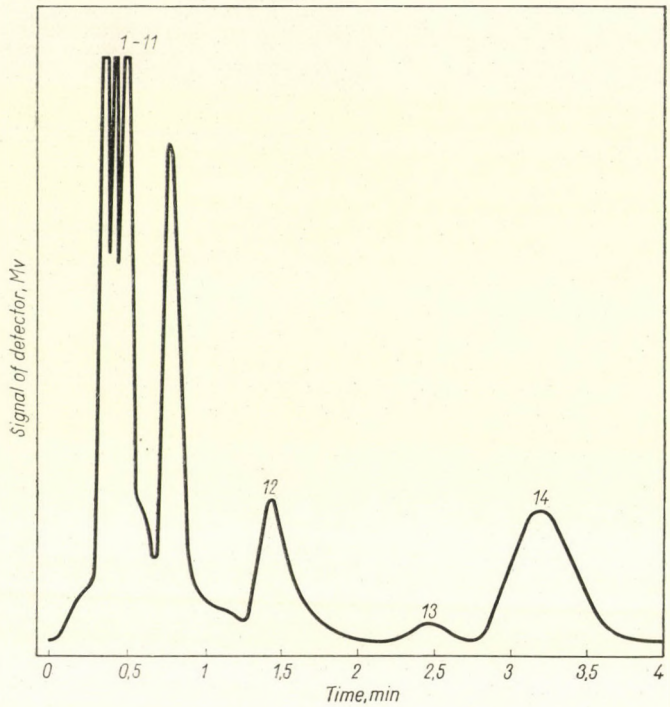

Fig. 3

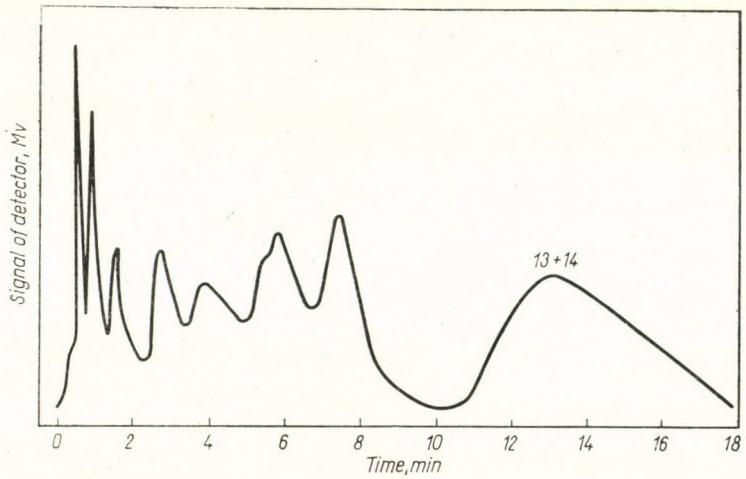

Fig. 4

Figs 3—4. Chromatograms of the products formed in the conversion of 2-methyl-4-*n*-butyl- and 2-methyl-4-cyclohexaloxetanes. *1.* 1.1 Pt/T, 330, 245; *2.* AG; *3.* 200; *4.* 50 H_2; *5.* 140; *6.* 1; 7. 0.01

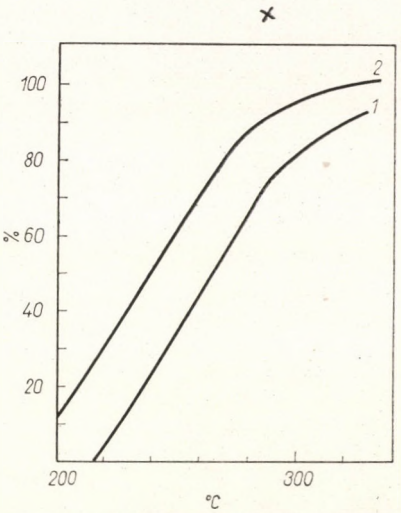

Fig. 5. The rate of conversion of 2,4-dialkyl-substituted oxetanes on Pt/T catalyst as a function of the temperature. *1.* 2-methyl-4-ethyloxetane; *2.* 2-methyl-4-*n*-butyloxetane

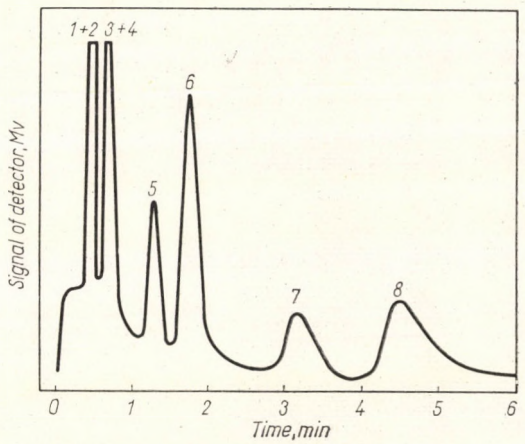

Fig. 6. Chromatogram of the hydrocarbons formed in the conversion of 2-methyl-4-ethyloxetane on Pt/T catalyst. *1.* 1.1 Pt/T, 325; *2.* 1 Al_2O_3; *3.* 160; *4.* 50 H_2; *5.* 140; *6.* 1; *7.* 0.01

process yield saturated hydrocarbons and olefins of lower molecular weight, which are easier to separate. The ratio of the processes *3* and *4* gives approximately the relative ratio of process *1* and *2*.

Summarizing the above experimental results and considerations, the following statements can be made concerning the conversions of 2,4-dialkyloxetanes in the presence of a Pt/T catalyst. The four primary processes (1, 2, 3, 4) proceed simultaneously, even at low temperatures. Their relative ratio largely depends on the activity of the catalyst, on temperature, and on

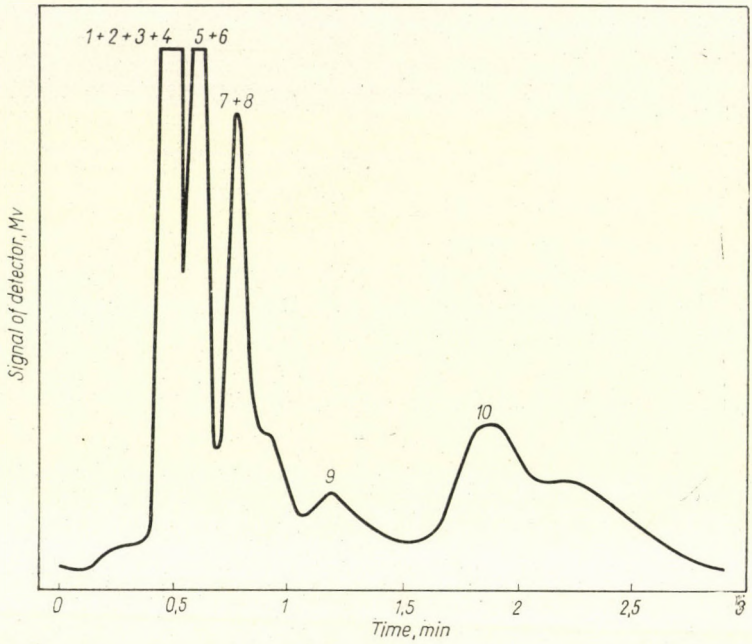

Fig. 7. Chromatogram of the hydrocarbons formed in the conversion of 2-methyl-4-ethyloxetane on Pt/T catalyst. *1.* 1.1 Pt/T, 340; *2.* 1 ODP; *3.* 30; *4.* 50 H_2; *5.* 140; *6.* 1/2; *7.* 0.01. Marking of the peaks: *1*: CO; *2*: methane; *3*: ethane; *4*: ethylene; *5*: propane; *6*: propylene; *7*: butane; *8*: butene-1; *9*: hexane; *10*: hexenes

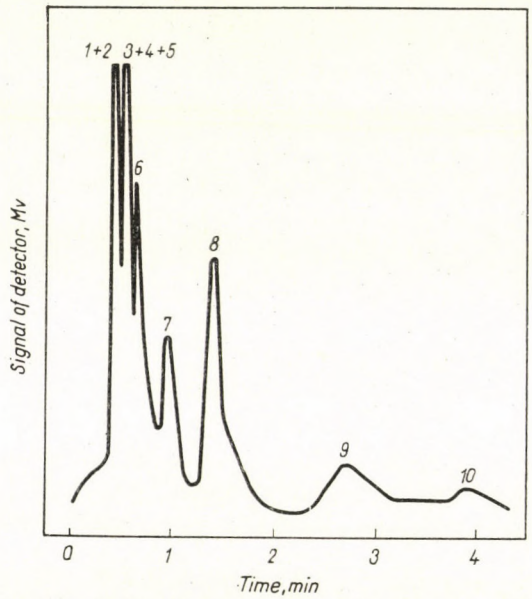

Fig. 8. Chromatogram of the hydrocarbons formed in the conversion of 2-methyl-4-*n*-butyloxetane on Pt/T catalyst. *1.* 1.1 Pt/T, 330; *2.* ODP; *3.* 30; *4.* 50 H_2; *5.* 140; *6.* 1/2; *7.* 0.01.Marking of the peaks: *1*: CO; *2*: methane; *3*: propane; *4*: propylene; *5*: butane; *6*: butene-1; *7*: hexane; *8*: hexenes; *9*: octane; *10*: octene

the inductive effect of the substituent. Higher catalyst activity and lower temperatures favour the isomerization processes (*1* and *2*), while lower catalyst activity and at higher temperatures the thermal decomposition will be the predominant process. Conversions *3* and *4* yield by way of the decarbonylation of the corresponding olefins and aldehydes saturated hydrocarbons. Generally, isomerization occurs in 60—70%, and thermal decomposition in 30—40%. The relative ratio of the processes *1* and *2*, *3* and *4*, respectively, is a function of the $+I$ effect of the substituent. Since the C—O linkage adjacent to the substituent of the higher $+I$ effect is split more readily, processes *4* and *2* will proceed at a rate one and a half to two times quicker than reactions *3* and *1*, respectively. The partial hydrogenation of the olefins also takes place on activated Pt/T catalyst (*e.g.*, peaks *5* and *7* in Fig. 5, and peak *7* in Fig. 7). At higher temperatures, saturated and unsaturated hydrocarbons with the same carbon atom number as the oxetane homologue are formed by the hydrogenolysis of the oxetanes (*e.g.*, peaks *9* and *10* in Figs 7 and 8).

It is therefore apparent that the conversion of 2,4-dialkyloxetanes in the presence Pt/T catalyst and hydrogen is a complex process, which is undoubtedly brought about in part by the simultaneous presence of two oxetane isomers. Having accomplished the resolution of the *cis* and *trans* isomers of the oxetanes investigated we intend to study their chemical conversions separately in detail, with a view to elucidate the mechanism of the various processes.

The conversions of 2,4-dialkyloxetanes in the presence of Pt/C catalyst

The conversions of 2,4-dialkyloxetanes were studied over Pt/C catalyst in helium and hydrogen carrier gas streams. A few characteristic chromatograms of these experiments are shown in Figs 9—15.

Owing to the substantially higher activity of the Pt/C catalyst, there are some processes taking place here which do not occur in the presence of Pt/T. The principal processes are again isomerization, yielding oxo-compounds, and the accompanying thermal decomposition. The conversion of the 2,4-dialkyloxetanes proceeds at lower temperatures, and consequently, the rate of the pyrolytic processes is substantially reduced.

When the conversions were carried out in helium using dehydrogenized Pt/C catalyst, it was observed that 2-methyl-4-ethyloxetane gave propane (peak *5* in Fig. 9) and hexene (peak *10* in Fig. 10), while 2-methyl-4-*n*-butyloxetane yielded hexane (peak *7* in Fig. 11), in addition to the main products. The formation of these hydrocarbons can be explained only by intermolecular dehydrogenation—hydrogenation processes proceeding on the catalyst. Their formation is furthered by increasing temperature.

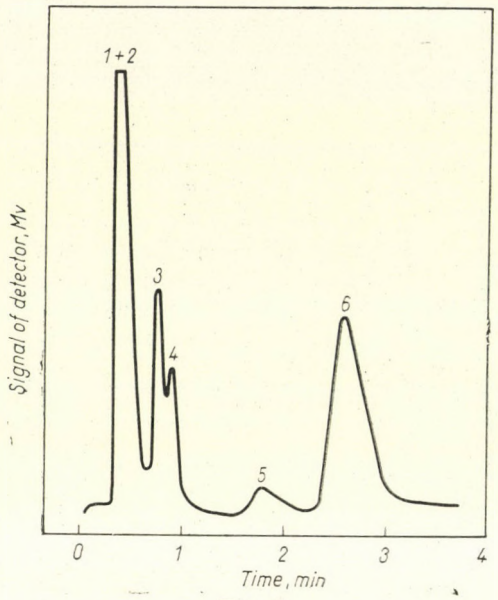

Fig. 9

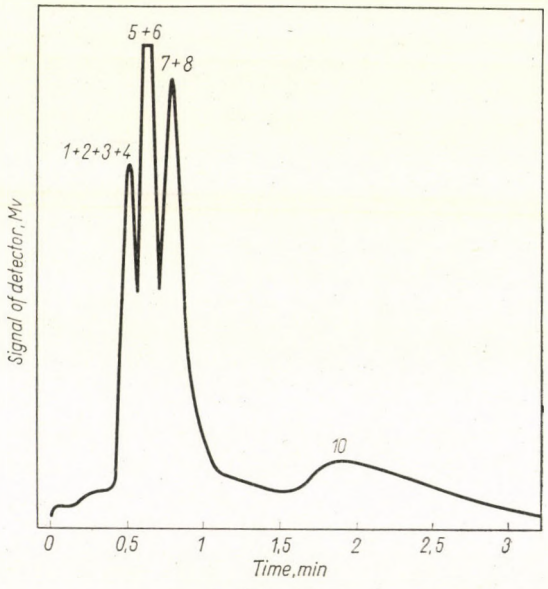

Fig. 10

Figs 9—10. Chromatograms of the hydrocarbons formed in the conversion of 2-methyl-4-ethyloxetane over Pt/C catalyst in helium. *1.* 0.3 Pt/C, 310 and 305, resp.; *2.* 1 Al_3O_3 and 1 ODP, resp.; *3.* 120 and 30, resp.; *4.* 50 He; *5.* 140; *6.* 1/2; *7.* 0.01*

* In Figs 9—15, the marking of the peaks is the same as that of peaks in Figs 6 and 8.

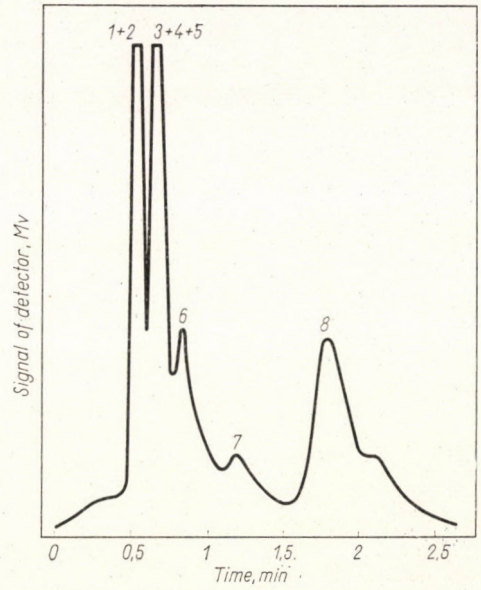

Fig. 11. Chromatogram of the hydrocarbons formed in the conversion of 2-methyl-4-*n*-butyloxetane over Pt/C catalyst in helium. *1.* 0.3 Pt/C, 370; *2.* ODP; *3.* 30; *4.* 50 He; *5.* 140; *6.* 1/2; *7.* 0.01

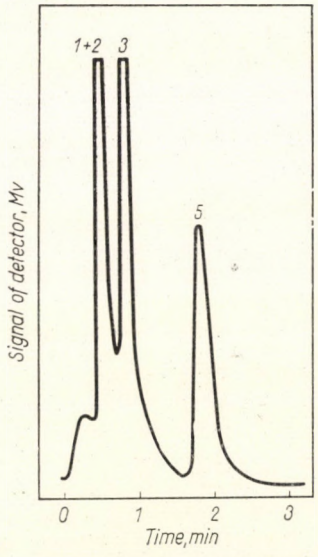

Fig. 12

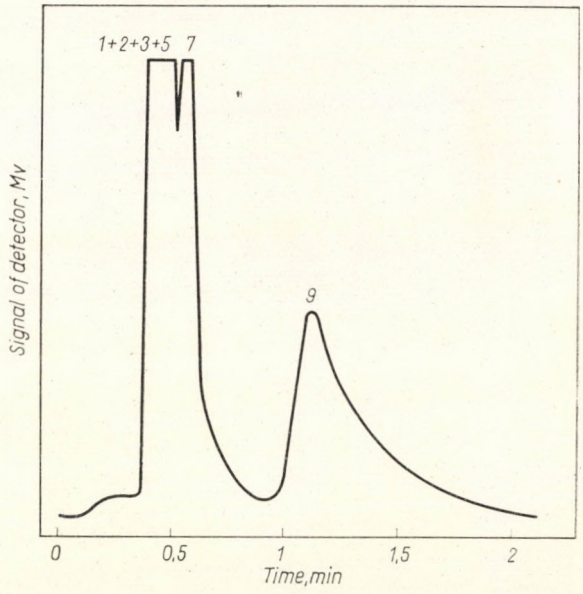

Fig. 13

Figs 12—13. Chromatograms of the hydrocarbons formed in the conversion of 2-methyl-4-ethyloxetane on Pt/C catalyst in hydrogen. *1.* 0.3 Pt/C, 325 and 300, resp.; *2.* 1 Al_2O_3 and 1 ODP, resp.; *3.* 120 and 30, resp.; *4.* 50 H_2; *5.* 140; *6.* 1 and 1/2, resp.; *7.* 0.01

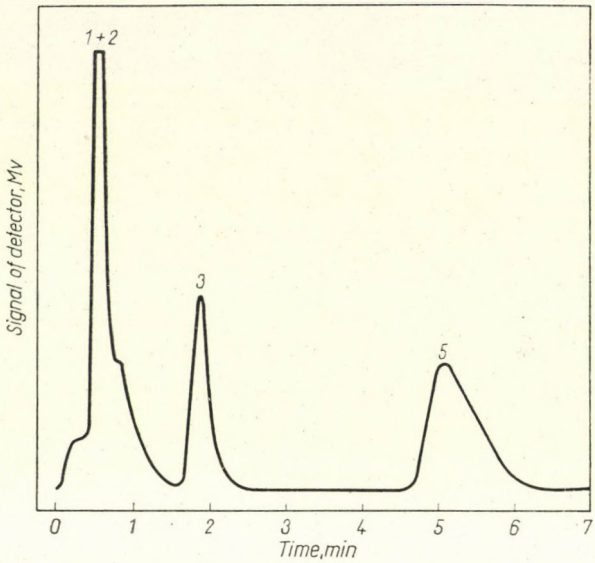

Fig. 14

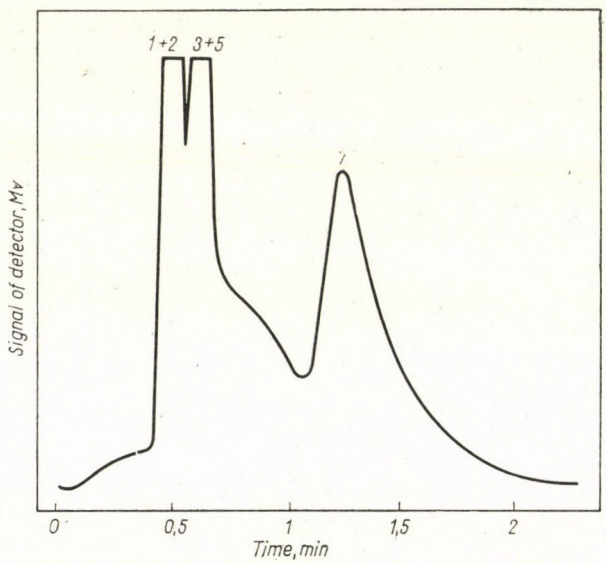

Fig. 15

Figs 14—15. Chromatograms of the hydrocarbons formed in the conversion of 2-methyl-4-*n*-butyloxetane over Pt/C catalyst in hydrogen. *1.* 0.3 Pt/C, 350 and 310, resp.; *2* 1 Al_2O_3 and 1 ODP, resp.; *3.* 120 and 30, resp.; *4.* 50 H_2; *5.* 140; *6.* 1 and 1/2, resp.; *7.* 0.01 and 0.005, resp.

The processes observed on Pt/C catalyst in the presence of hydrogen are summarized in the following scheme:

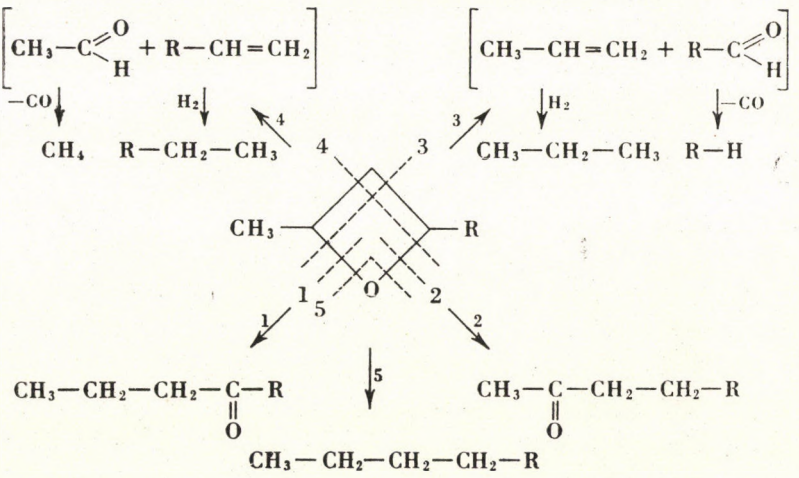

where: R is ethyl, or *n*-butyl.

Figs 12—15 show that no olefins are formed. However, the formation of considerable quantities of saturated hydrocarbons can be observed. This proves directly our earlier finding that saturated hydrocarbons are formed by two routes in the conversion of various types of oxetanes on Pt/C catalyst in the presence of hydrogen: by decarbonylation of the aldehydes, and by hydrogenation of the olefins which latter are formed by simultaneous thermal decomposition. It depends on the given molecular structure, on the nature of the catalyst and on the temperature, which of the two processes is predominant.

The conversion of 2,4-dialkyloxetanes proceeds at a considerably higher rate on Pt/C catalyst in the presence of hydrogen, than on Pt/T catalyst. This can be clearly seen by comparing the corresponding figures (*e.g.* Figs 7 and 13). The degree of formation of saturated hydrocarbons having the same number of carbon atoms as the starting oxetane homologue, by the simultaneous hydrolysis of the two C—O linkages of the cyclic ether, was found to be the highest with 2,4-dialkyloxetanes.

SUMMARY

The conversions of mixtures of the *cis* and *trans* isomers of 2,4-dialkyloxetanes (methyl-ethyl, methyl-*n*-butyl, methyl-cyclohexyl) over platinum catalysts on thermolite and carbon carriers have been studied by the microreactor technique in the presence of hydrogen and helium carrier gases, in the temperature range from 200 to 350°C. The rate of conversion of the oxetanes and the direction of the processes were studied as a function of the experimental parameters, *i.e.* the catalyst, the temperature, the carrier gas and the structure of the oxetanes.

The principal directions of the conversion of 2,4-dialkyloxetanes, under the given conditions, were the formation of isomeric ketones by the splitting of the two C—O linkages (60—70%), and thermal decomposition yielding olefins and the corresponding aldehydes (30—40%). The primary processes are accompanied by secondary reactions, and the nature of these is dependent on the experimental conditions.

REFERENCES

1. BARTÓK, M., KOVÁCS, K., KOZMA, B.: Acta Chim. Acad. Sci. Hung. (in press).
2. BARTÓK, M., FÉNYI, SZ.: Acta Phys. et Chem. Szeged **12,** 157 (1966).
3. BARTÓK, M.: Acta Phys. et Chem. Szeged **13,** 59 (1967).
4. BARTÓK, M.: Acta Chim. Acad. Sci. Hung. **51,** 403 (1967).

Mihály BARTÓK
Kálmán KOVÁCS
Szeged, Dóm tér 8.
Nikoláj Ivanovics SHUIKIN; Moscow, SSSR

Acta Chimica Academiae Scientiarum Hungaricae Tomus 56 (4), pp. 405—411 (1968)

BENZAZEPINES, II

PREPARATION AND REACTIONS OF 2,3-DIHYDRO-6,7-BENZO-(1,5)-THIAZEPINES

K. HIDEG and H. O. HANKOVSZKY

(Institute of Pharmacology, University Medical School, Pécs)

Received February 24, 1967

As it has been reported in an earlier communication [1], β-piperidinopropiophenone, obtained in the known way from acetophenone by *Mannich* reaction, does not react with *o*-aminothiophenol in the same way, as is usual for ketones [2—6]. The reaction to yield the expected 2-(aminoethyl)-2-phenylbenzthiazoline hydrochloride did not take place either in polar or in non-polar solvents, but a product which proved to be 2,3-dihydro-4-phenyl-6,7-benzo-(1,5)-thiazepine was obtained.

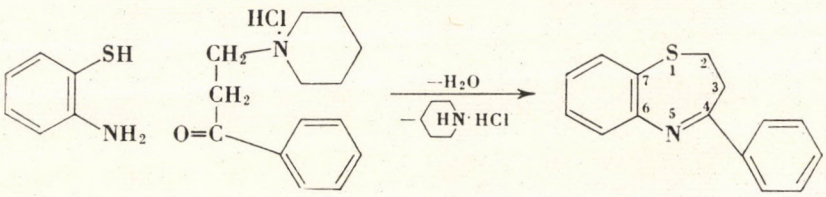

As by-products, piperidine hydrochloride and water were formed in stoichiometric amounts.

Starting with this reaction, a general method of preparation of new 1,5-benzthiazepines has been developed, and some of their reactions studied. The reaction gives with open-chain *Mannich* ketones 4-substituted 2,3-dihydro-6,7-benzo-(1,5)-thiazepines; with alicyclic *Mannich* ketones 2,3-dihydro-3,4-polymethylene-6,7-benzo-(1,5)-thiazepines are obtained. In the latter case, the number of the members in ring C depends on the size of the alicyclic ring used. The reaction may apparently be generalized:

(a) The amino group can be other than piperidine, *e.g.* morpholine, diethylamine, dimethylamine, methylpiperazine, and, in general, an open-chain or alicycic amine.

(b) The aminoketone can be used as the base or the salt (the salt being more advantageous) to effect the ring closure.

(c) The phenyl group can be substituted or unsubstituted. The presence of substituents does not exclude the possibility of the ring closure.

(d) The phenyl group may be linked directly or indirectly, for example through a methylene group, to the carbonyl group.

(e) Of the methylene groups, the one in alpha position can be substituted, *e.g.*, with a methyl group.

(f) Instead of open-chain ketones, alicyclic ketones — or rather their *Mannich* salts — can be used to effect the ring closure.

The above generalization may be represented by the reaction scheme given below. The reaction is thought to proceed as follows: The carbonyl group of the *Mannich* ketone salt undergoes a condensation reaction with the primary amine: subsequently the tertiary amine group in beta-position is eliminated, a secondary amine salt is split off, and a vinyl group is formed at the end of the chain; addition to this group of the nucleophilic sulfhydryl group, being in favourable steric position, results in the closure of the ring:

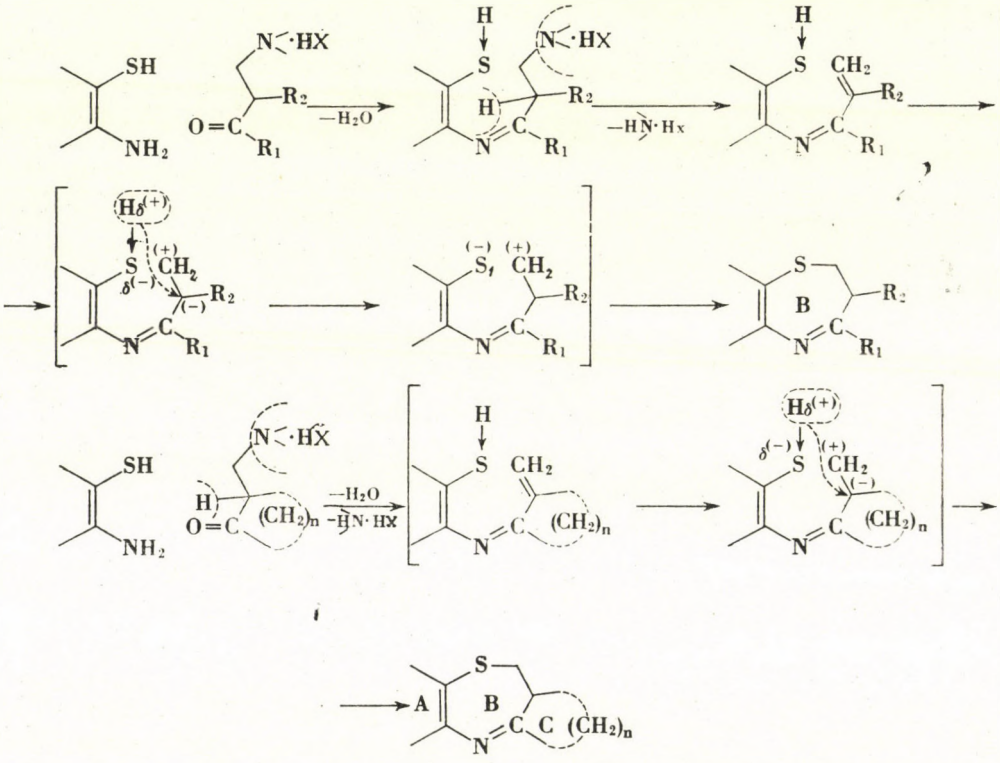

The reactions of the tertiary N atom contained in ring *B* of the 2,3-dihydro-6,7-benzo-(1,5)-thiazepines formed by the above syntheses have been investigated. This N atom, which has formed by a *Schiff* reaction, can be regarded as a cyclic azomethine group, and accordingly, the study of its

behaviour in a few reactions was reasonable.

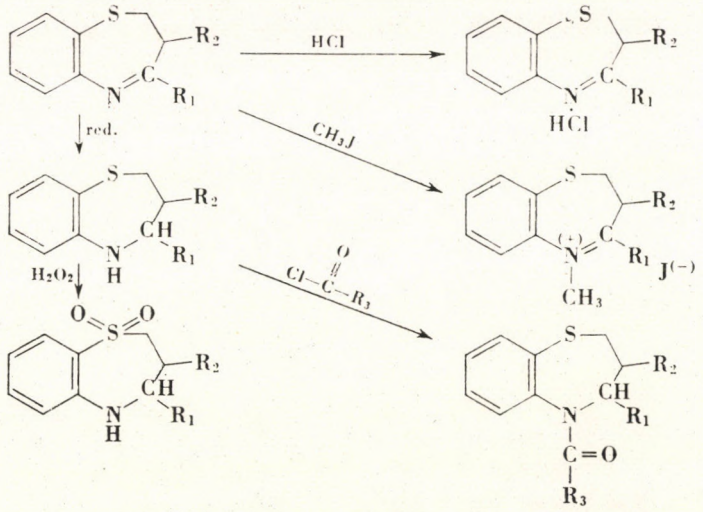

The linkage shows only partly the properties characteristic of *Schiff* bases. Thus, it is not hydrolyzed to carbonyl and amine when boiled with an aqueous acid it forms a stable hydrochloride which, as a salt of a weak base and a strong acid, undergoes hydrolysis in aqueous medium to give the base, but the ring is not cleaved at the azomethine group.

With alkyl iodides, *e.g.* with methyl iodide, it can be converted into a thiazepinium salt.

The C=N bond, as that of a *Schiff*-base, can be saturated with reducing agents ($NaBH_4$, $LiAlH_4$) to give a 2,3,4,5-tetrahydrobenzothiazepine in good yield; the product can be acylated in the presence of an acid binding agent both with aliphatic and aromatic acid chlorides to a 5-acyl-2,3,4,5-tetrahydro-4-substituted-6,7-benzo-(1,5)-thiazepine.

The sulphur atom of the tetrahydro derivative is oxidized in glacial acetic acid by hydrogen peroxide to sulphone.

The compounds prepared are listed in Tables I and II.

Experimental

2,3-Dihydro-4-phenyl-6,7-benzo-(1,5)-thiazepine (No. 1)

37.5 g (0.3 mole) of *o*-aminothiophenol and 76.1 g (0.3 mole) of *β*-piperidinopropiophenone hydrochloride were refluxed for 2 hrs. with 500 ml of xylene in an apparatus equipped with a water separator.

During this time, 5.4 ml (0.3 mole) of water was collected in the water separator. The reaction mixture was filtered to isolate the separated white crystals (35 g), m.p. 245°. This substance was shown on analysis to be piperidine hydrochloride. The filtrate was subjected to fractional distillation in vacuum. After the evaporation of xylene, the product, 2,3-dihydro-4-phenyl-6,7-benzo-(1,5)-thiazepine, distilled as a viscous, yellow oil (51.0 g; 35%), b.p.: 224—230°/2.5 mm.

Table I

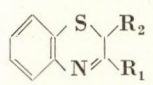

No.	R_1	R_2	M.p., °C or B.p., °C/mm	Formula (molecular weight)	Analysis, %				Ref.
					C	H	N	S	
					Calcd. Found				
1	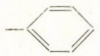	H	224—230/2.5	$C_{15}H_{13}NS$ (239.35)					[1]
2		H	170—172	$C_{15}H_{12}N_2O_2S$ (284.35)					[1]
3		CH_3	63— 66 220—226/0.4	$C_{17}H_{17}NS$ (267.40)	76.36 76.40	6.41 6.26	5.24 5.35	11.99 12.08	
4	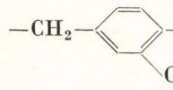	H	30— 32	$C_{18}H_{19}NO_2S$ (313.43)	68.99 68.80	6.11 6.30	4.47 4.50	10.22 10.89	
5	$-CH_2-CH_2-CH_2-CH_2-$		220/0.4	$C_{13}H_{15}NS$ (217.33)	71.85 71.98	6.96 7.26	6.44 6.03	14.75 14.32	
6	$-CH_2-CH_2-CH_2-CH_2-CH_2-$		180—186/0.05	$C_{11}H_{17}NS$ (231.36)	72.68 72.78	7.41 7.51	6.05 6.04	13.86 13.78	

Table II

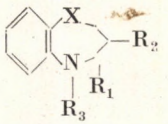

No.	R_1	R_2	R_3	X	M.p., °C or B.p., °C/mm	Formula (Molecular weight)	Analysis, %			
							C	H	N	S
							Calcd / Found			
7		H	H	S	186—190/0.4	$C_{15}H_{15}NS$ (241.36)	74.65 74.85	6.26 6.47	5.80 5.61	13.29 13.31
8	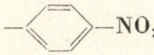	H	H	S	138—140	$C_{15}H_{14}N_2O_2S$ (286.36)	62.92 63.35	4.93 4.89	9.78 10.14	11.19 11.05
9	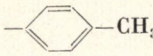	CH_3	H	S	60— 62 240—250/0.5	$C_{17}H_{19}NS$ (269.42)	75.79 75.74	7.11 6.63	5.20 5.21	11.90 12.04
10	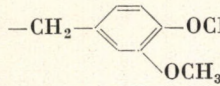	H	H	S	48— 51	$C_{18}H_{21}NO_2S$ (315.44)	68.54 68.07	6.71 7.11	4.44 4.60	10.17 9.79
11	$-CH_2-CH_2-CH_2-CH_2-$		H	S	170—174/0.1	$C_{13}H_{17}NS$ (219.35)	71.18 71.71	7.81 8.42	6.39 5.95	14.62 14.87
12		H	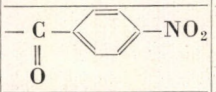	S	146—147	$C_{22}H_{18}N_2O_3S$ (390.48)	67.67 67.20	4.65 4.96	7.18 7.18	8.21 8.10
13		H	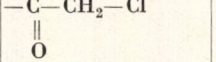	S	106—107	$C_{17}H_{16}ClNOS$ (317.85)	64.24 64.30	5.07 5.20	4.41 4.51	10.09 9.87
14		H	H		165—166	$C_{15}H_{15}NO_2S$ (273.36)	65.91 65.50	5.53 5.58	5.12 5.20	11.73 12.28
15	$-CH_2-CH_2-CH_2-CH_2-$		H		150—152	$C_{13}H_{17}NO_2S$ (251.35)	62.13 62.13	6.81 6.03	5.57 5.34	12.76 12.66

2,3-Dihydro-4-phenyl-6,7-benzo-(1,5)-thiazepine hydrochloride

Gaseous hydrogen chloride was introduced into a solution of 2,3-dihydro-4-phenyl-6,7-benzo-(1,5)-thiazepine in acetone; the hydrochloride precipitated almost quantitatively as white crystals, m.p. 107—109°. $C_{15}H_{13}NS \cdot HCl$ (275.81), Calcd. N 5.08; S 11.63; Cl 12.86. Found N 4.91; S 11.82; Cl 12.68%.

2,3-Dihydro-4-phenyl-6,7-benzo-(1,5)-thiazepine methiodide

An alcoholic solution of 2,3-dihydro-4-phenyl-6,7-benzo-(1,5)-thiazepine was refluxed with an equivalent quantity of methyl iodide. Clarification and dilution with ether gave the monomethiodide as a precipitate in a yield of 65%, m.p. 176—178°. $C_{16}H_{16}INS$ (381.29). Calcd. I 33.29; N 3.67; S 8.41. Found I 32.86; N 3.50; S 8.90%.

2,3-Dihydro-4-(4′-nitrophenyl)-6,7-benzo-(1,5)-thiazepine (No. 2)

28.6 g (0.1 mole) of β-diethylamino-*p*-nitropropiophenone hydrochloride and 12.5 g (0.1 mole) of *o*-aminothiophenol were refluxed for 2 hrs. in 250 ml of xylene. 1.6 ml of water collected in the water separator. After the separation of the precipitated diethylamine hydrochloride by filtration, the filtrate was cooled to precipitate 21.6 g of the product in the form of orange-yellow crystal needles (76%), m.p. 170—172° (after recrystallization from xylene).

$$\lambda_{max}^{EtOH,\ c = 0.25 \cdot 10^{-4}\ mole} \quad 256,\ 278\ nm$$

2,3-Dihydro-3,4-tetramethylene-6,7-benzo-(1,5)-thiazepine (No. 5)

12.5 g (0.1 mole) of *o*-aminothiophenol was refluxed in 100 ml of benzene with 24.8 g (0.1 mole) of 2-(piperidinomethyl)-cyclohexanone. First, the water formed in the condensation began to collect in the separator, then piperidine hydrochloride precipitated in the xylene solution. A reaction time of 8 hrs. gave 1.6 ml of water and 12.0 g of piperidine hydrochloride. The filtrate was evaporated in vacuum, and the residue distilled under reduced pressure to give 16.4 g (80%) of a yellow, viscous oil, b.p. 220°/0.4 mm-Hg.

Reduction

(a) *With* $NaBH_4$

2,3,4,5-Tetrahydro-4-phenyl-6,7-(1,5)-thiazepine (No. 7)

12.0 g (0.05 mole) of 2,3-dihydro-4-phenyl-6,7-benzo-(1,5)-thiazepine was dissolved in 200 ml of anhydrous ethyl alcohol, and after cooling, a suspension of 2.5 g (0.066 mole) of $NaBH_4$ in anhydrous ethyl alcohol was added. The reduction started with the evolution of heat and gas, and the dark yellow colour of the solution disappeared. The mixture was refluxed for 1 hr., and the complex decomposed by dilution with water. The alcohol was evaporated, and the aqueous solution extracted with ether. The ether extract was dried over anhydrous Na_2SO_4, evaporated, and the residue distilled, b.p. 186—190°/0.4 mm to obtain, 10.8 g (90%) of a viscous oil.

(b) $LiAlH_4$

2,3,4,5-Tetrahydro-3-methyl-4-(4′-methylphenyl)-6,7-benzo-(1,5)-thiazepine (No. 9)

26.7 g (0.01 mole) of 2,3-dihydro-3-methyl-4-(4′-methylphenyl)-6,7-benzo-(1,5)-thiazepine was dissolved in 100 ml of abs. ether, and a suspension of 5 g of $LiAlH_4$ in ether was added to the solution. The reaction mixture was refluxed for 2 hrs., and the complex decomposed with water. The ether extract was dried and evaporated, and the residue fractionated, b.p. 240—250°/0.5 mm. The yield was almost quantitative.

Acylation

2,3,4,5-Tetrahydro-4-phenyl-5-chloroacetyl-6,7-benzo-(1,5)-thiazepine (No. 13)

24.1 g (0.1 mole) of 2,3,4,5-tetrahydro-4-phenyl-6,7-benzo-(1,5)-thiazepine was dissolved in 300 ml of hot benzene. After cooling, 10 g of K_2CO_3 was added, and a solution of 13.6 g (9.3 ml; 0.12 mole) of chloroacetyl chloride in 50 ml of benzene was introduced dropwise. The reaction mixture was refluxed for 2 hrs., filtered, and the solvent evaporated. The residue was crystallized from alcohol to obtain the white, crystalline chloroacetyl derivative (24.8 g; 78%), m.p. 106—107°.

$\lambda_{max.}$ EtOH, $c = 0.25 \cdot 10^{-5}$ mole 248 nm.

2,3,4,5-Tetrahydro-4-phenyl-5-(4′-nitrobenzoyl)-6,7-benzo-(1,5)-thiazepine (No. 12)

A solution of 2.4 g (0.01 mole) of 2,3,4,5-tetrahydro-4-phenyl-6,7-benzo-(1,5)-thiazepine and 1.85 g (0.01 mole) of *p*-nitrobenzoyl chloride in 100 ml of xylene was refluxed for 2 hrs. while 1 g of K_2CO_3 was added. The hot mixture was filtered, cooled and the yellow crystals collected by filtration (2.5 g; 65%), m.p. 146—147°.

$\lambda_{max.}$ EtOH, $c = 0.25 \cdot 10^{-4}$ mole 248 nm.

Oxidation with H_2O_2

1,1-Dioxy-2,3,4,5-tetrahydro-4-phenyl-6,7-benzo-(1,5)-thiazepine (No. 16)

2.4 g (0.01 mole) of 2,3,4,5-tetrahydro-4-phenyl-6,7-benzo-(1,5)-thiazepine was dissolved in 50 ml of acetic acid, and 10 ml of 30% H_2O_2 was added to the solution.

The cherry-red solution was allowed to stand for a day, then diluted with water. Standing and cooling gave the product as a white crystalline substance in a yield of 25%, m.p. 165—166°.

*

The authors wish to thank Mrs. M. Ott for the microanalyses.

SUMMARY

A general method for the preparation of 2,3-dihydro-6,7-benzo-(1,5)-thiazepines is described. The reaction consists in the cyclization of *o*-aminothiophenol with an open-chain or alicyclic aminoketone which can be obtained in good yields by the Mannich reaction. The dihydroderivatives may be reduced ($NaBH_4$, $LiAlH_4$) to the 2,3,4,5-tetrahydro derivatives. The reduced products are acylated with acid chlorides to the 5-acyl derivatives. Tetrahydrobenzthiazepine is oxidized with H_2O_2 to 1,1-dihydroxy-2,3,4,5-tetrahydrobenzthiazepine.

REFERENCES

1. Hideg, K., Hankovszky, H. O.: Acta Chim. Acad. Sci. Hung. **50,** 403 (1966).
2. Bogert, M., Stull, A.: J. Am. Chem. Soc. **47,** 3078 (1925).
3. Bogert, M., Naimen, G.: J. Am. Chem. Soc. **57,** 1529 (1935).
4. Kiprianov, A. M., Portnyagina: Zh. Obsch. Khim. **25,** 2257 (1955).
5. Kiprianov, A. J., Portnyagina: Zh. Obsch. Khim. **25,** 2261 (1955).
6. Hromatka, O., Augl, J., Flieder, E., Kirchmayr, R., Klink, R.: Monatsh, Chem. **92,** 88 (1961).

Kálmán Hideg
Olga H.-Hankovszky
Pécs, Rákóczi út 2.

Acta Chimica Academiae Scientiarum Hungaricae Tomus 56 (4), pp. 413—422 (1968)

OXIDATION OF ALDEHYDES BY AQUEOUS CERIC IONS IN PERCHLORIC ACID

M. RANGASWAMY and M. SANTAPPA

(Department of Physical Chemistry, University of Madras, Madras-25, India)

Received March 4, 1967

Introduction

SHORTER [1], who studied the oxidation of acetaldehyde by ceric sulphate, did not give kinetic data or mechanism for the oxidation, but concluded that the possible enolization of acetaldehyde was low compared to that of acetone, methyl ethyl ketone, etc. Acetic acid and formic acid were the major products in the oxidation of acetaldehyde ($\sim 0.005\ M$) with ceric sulphate ($\sim 0.05\ M$) in H_2SO_4 ($\sim 2\ N$) at 70°. From SHORTER's work it can be concluded that enolization of acetaldehyde, *i.e.* $CH_2 = CH.\ OH$, did not precede its oxidation, — the rate of oxidation being much higher than the rate of enolization. However, more recently BELL and CLUNIE [2] showed that acetaldehyde was hydrated to ~58% in aqueous solution at 20° and that hydration was catalyzed by acids and bases. HARGREAVES and SUTCLIFFE [3], from their study on the oxidation of formaldehyde by Ce^{4+} in $HClO_4$ concluded that the reaction occurred between Ce^{4+} and the diol of the aldehyde, $HCH(OH)_2$, and the formation of the latter was assumed to be complete. The reaction was found to be second order, — first order each with respect to $[Ce^{4+}]$ and [HCHO]. A stoichiometry, $\Delta Ce^{4+}/\Delta$ formaldehyde ≈ 2, was also observed. The present study refers to the kinetics of the oxidation of acetaldehyde and chloral hydrate by ceric perchlorate in $HClO_4$ medium at 20° and 45°, respectively. Work on formaldehyde [3] was extended with the purpose to evaluate the thermodynamic parameters. DUKE's theory [4] of complex formation between oxidant and reductant, common to many homogeneous oxidation reactions of organic compounds by metal ions, was not applicable to the aldehydes used, since no evidence for complex formation between Ce^{4+} and the aldehydes could be obtained, either from kinetics or by an independent spectrophotometric method [5] at least under our experimental conditions. The main purport of the present investigation has been to give evidence for the reaction between Ce^{4+} and the diol form of aldehydes; the differences in the rates of oxidation are interpreted in terms of the structures. The various rates and thermodynamic parameters for the system Ce^{4+}–aldehyde, are evaluated and discussed.

Experimental

All solutions for the kinetic studies were prepared in doubly distilled and deionized water. The ceric perchlorate solution used *(G. Frederick Smith Chemical Co.*, USA; 0.5 *M* in 5.0 *M* perchloric acid) was over 99.9% pure as tested from its ε at $\lambda = 290$ mμ [15] being $1.89 \cdot 10^3$ M^{-1} cm^{-1}. The acetaldehyde, chloral hydrate and formaldehyde (A.R., B.D.H.) were pure samples and were used as such without further purification. The perchloric acid *(E. Merck;* 70%) and sulphuric acid *(Basynth A. R., India;* sp. gr. 1.8) were not further purified. The sodium perchlorate ($\approx$ 4.0 *M*) was prepared by neutralization of $HClO_4$ ($\approx$ 8.0 *M*) with NaOH ($\approx$ 8.0 *M*) and assayed by ion exchange method [16]. Cerous perchlorate was prepared by dissolving pure cerous carbonate *(Atomic Energy Establishment, India)* in $HClO_4$, and the cerous content was estimated, after precipitation and weighing as cerous oxalate, and the free acid in the cerous solution was then estimated by ion exchange method [16]. The organic acids, formic, acetic and trichloroacetic acids, used for product studies were pure BDH samples.

The reaction vessel was a three-necked pyrex flask (250 ml; one B24 middle and two B19 side necks), the middle neck being fitted with a mercury-sealed stirrer; one side neck was used for bubbling nitrogen gas through the system, while the second neck was used for the exit of the gas, and for withdrawing aliquots of the reaction mixture in the kinetic runs. The reaction system consisted of ceric perchlorate ($\sim 3.5 \cdot 10^{-3}$ *M*); aldehyde ($\sim$ formaldehyde, 0.01 *M*; acetaldehyde, 0.01 *M*; and chloral hydrate, 0.12 *M*); H^+ (1.0 *M*) with a total volume of 100 ml and at an ionic strength 1.2. All the components, except Ce^{4+}, were placed in the reaction flask, which was thermostated (controlled by a toluene regulator and a hot wire vacuum switch relay). The ceric solution was also thermostated in a separate flask at the same temperature. The ceric solution was added to the aldehyde solution, the beginning of the reaction being taken as the time when half of the solution had been transferred. The reaction was followed (for the system formaldehyde–Ce^{4+} for 15 min. and to $\sim$80% conversion of Ce^{4+}; for Ce^{4+}–acetaldehyde for 30 min. and to $\sim$60% conversion, and for the system chloral hydrate–Ce^{4+} for 40 min. and to $\sim$30% conversion) by measuring the rates of ceric disappearance at 5-minute intervals, aliquots (10 ml) being withdrawn and added to a known excess of Fe^{2+} sulphate solution ($\sim 3.5 \cdot 10^{-3}$ *M*), using ferroin indicator. The photochemical oxidation of water by ceric perchlorate is a well established fact [17]; therefore, all reactions were conducted with the reaction vessel covered with a black cloth, and the thermostat was painted black inside. Absorption measurements in order to detect complex formation were carried out using a *Hilger* and *Watts* H 700 ultraviolet spectrophotometer.

Results

Experimental results

(1) *Orders with respect to [Ce^{4+}] and [aldehyde]*

At constant [aldehyde] ($\approx$ 0.1 *M* for acetaldehyde and 0.12 *M* for chloral hydrate), [$HClO_4$], (=1.0 *M*) μ ($\approx$ 1.2), and temperature (20° for acetaldehyde and 45° for chloral hydrate), and varying the [Ce^{4+}] ($2.5 \cdot 10^{-3}$ *M* — $5.0 \cdot 10^{-3}$ *M*), a first-order dependence with respect to [Ce^{4+}] was observed (Fig. 1; A and B). From the linear plots of log [Ce^{4+}] *vs.* time, the pseudounimolecular rate constants, $k_{obs.}$, were evaluated. At constant [Ce^{4+}] ($3.5 \cdot 10^{-3}$ *M*), [$HClO_4$] (1.0 *M*), μ (1.2) and temperature, variations of the excess aldehyde ($7.7 \cdot 10^{-3}$ *M* — $1.15 \cdot 10^{-2}$ *M* for acetaldehyde; 0.12 *M* — 0.35 *M* for chloral hydrate) gave increasing rates with increasing [aldehyde]. Plots of $k_{obs.}$ *vs.* [aldehyde] (Fig. 1; C and D), being linear and passing through the origin, indicated that the reaction with respect to [aldehyde] followed first order kinetics. A total order of two for the Ce^{4+}–aldehyde (acetaldehyde) reaction was also realized from the 1/[Ce^{4+}] *vs.* time plot (Fig. 2; C) under conditions [Ce^{4+}] = [acetaldehyde] = $3.5 \cdot 10^{-3}$ in 1.0 *M* perchloric acid.

(2) *Effect of* [H^+]

At constant μ, the rate of oxidation increased with increasing [H^+] (0.1 *M* — 1.0 *M*), but at higher [H^+] (> 1.5 *M*) the rate reached a limiting value. Plots of $1/k_{obs.}$ *vs.* 1/[H^+] were linear with intercepts for the aldehydes studied (Fig. 2; D and E).

(3) *Effect of the ionic strength (μ)*

Keeping $[H^+]$ constant and varying μ (between 1.1 and 2.0) increased rates (2% for acetaldehyde; 9% for chloral hydrate and 14% for formaldehyde) due to normal salt effects were observed.

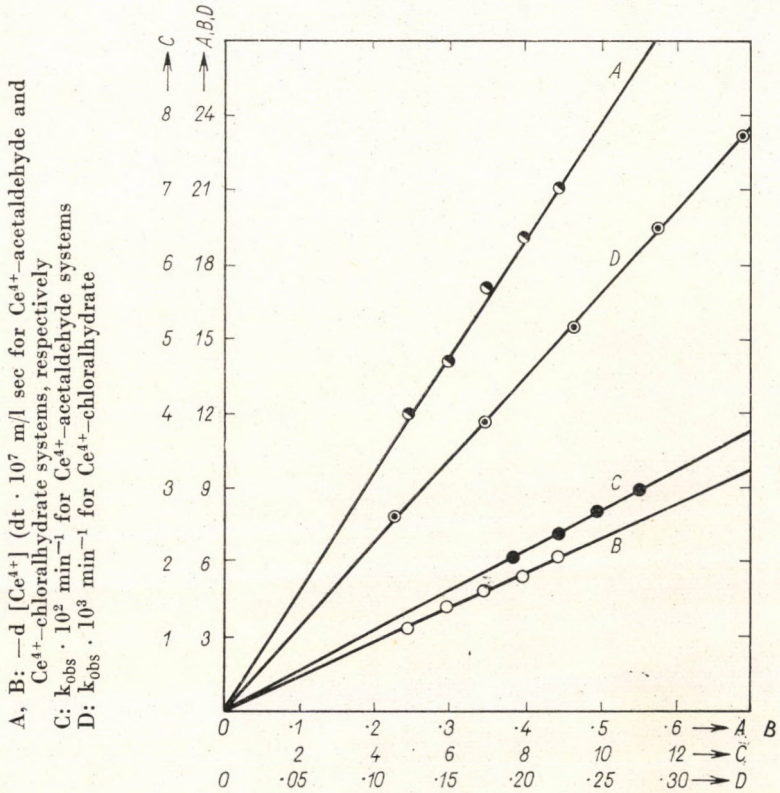

Fig. 1. Order of $[Ce^{4+}]$ and [aldehyde].
A, B: Plots of $\left(\frac{-d\,[Ce^{4+}]}{dt}\right) \cdot 10^7$ (m/l/sec) *vs.* $[Ce^{4+}] \cdot 10^3$ (moles/litre) for the systems ceric ion–acetaldehyde and ceric ion–chloralhydrate, respectively.
C: Plot of $k_{obs.} \cdot 10^2$ (min.$^{-1}$) *vs.* [acetaldehyde] $\cdot 10^3$ mole/litre.
D: Plot of $k_{obs.} \cdot 10^3$ (min.$^{-1}$) *vs.* [chloralhydrate] (mole/litre)

(4) *Effect of initially added products*

(*a*) Ce^{3+}: *At* constant $[Ce^{4+}]$, [aldehyde], $[H^+]$ μ, temperature, etc., the initial addition of $[Ce^{3+}]([Ce^{3+}]/[Ce^{4+}] \geq 2)$ did not affect the rate of oxidation of the aldehydes studied.

(*b*) Formic, acetic and trichloroacetic acids

In the cases of formaldehyde and chloral hydrate, the corresponding acids formed were not further oxidized under our experimental conditions. This was also proved by the rate of

the Ce^{4+}–aldehyde reaction which was slightly decreased by the initial addition of the corresponding acids (formic, or acetic, or trichloroacetic acids under conditions $[Ce^{4+}] = [\text{organic acid}] \approx 3.5 \cdot 10^{-3}\ M$).

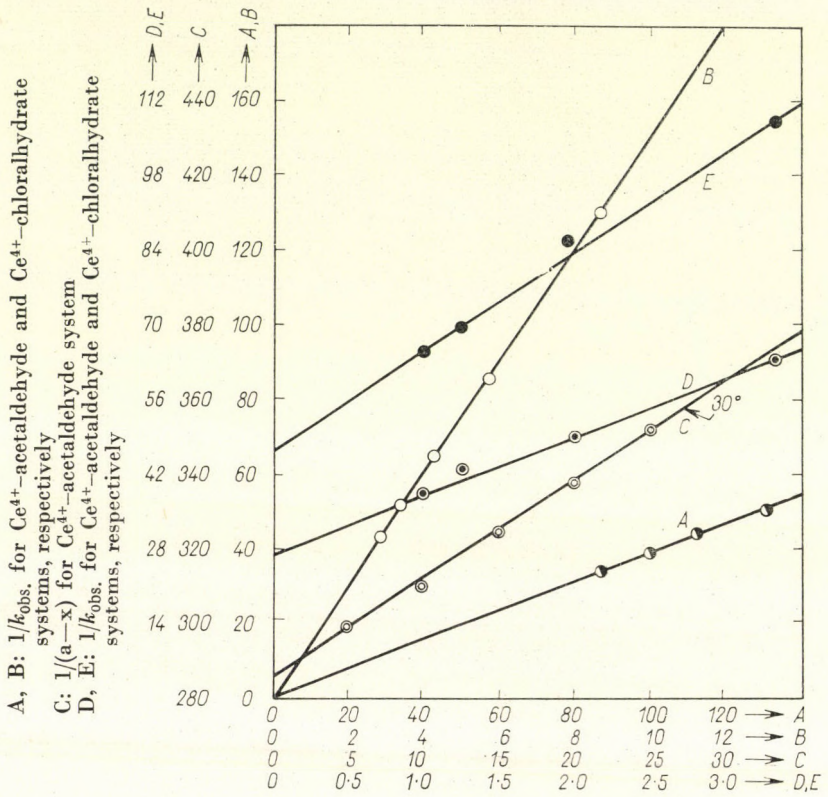

A: 1/[acetaldehyde]. B: 1/[chloral hydrate].
C: Time (min.) for the system Ce^{4+}–acetaldehyde.
D, E: Plots of $\frac{1}{k_{obs}}$ *vs.* $\frac{1}{[H^+]}$ for the systems Ce^{4+}–acetaldehyde and Ce^{4+}–chloral hydrate, respectively.

Fig. 2. A, B: Plots of $\frac{1}{k_{obs.}}$ *vs.* $\frac{1}{[\text{aldehyde}]}$ for the systems ceric ion–acetaldehyde and Ce^{4+}–chloralhydrate, respectively.

C: Bimolecular plot of $\frac{1}{[Ce^{4+}]}$ *vs.* time (minutes) for the system Ce^{4+}–acetaldehyde (total order).

D, E: Plots of $\frac{1}{k_{obs.}}$ $\frac{1}{[H]^+}$ for the systems Ce^{4+}–acetaldehyde and Ce^{4+}–chloralhydrate, respectively.

(5) *Stoichiometry*

The stoichiometry, $\Delta\, Ce^{4+}/\Delta$ acetaldehyde ≈ 2 (under conditions of initial $[Ce^{4+}] = 2 \cdot 10^{-3}\ M$; $3.5 \cdot 10^{-3}\ M$ and $5 \cdot 10^{-3}\ M$ and initial [aldehyde] $= 3 \cdot 10^{-2}\ M$; $[HClO_4] = 1.0\ M$; temperature 30°) was established by precipitating the unreacted aldehyde as hydrazone (conversion of acetaldehyde: $\sim 99.5\%$) with 2,4-dinitrophenylhydrazine, and weighing the hydrazone.

Search for complex formation between Ce^{4+} and aldehydes

Aldehydes are known to react with oxidants like Ce^{4+}, Co^{3+}, $S_2O_8^{2-}$, UO_2^{2+}, etc. [3, 6—8] in their diol forms, *i.e.* $H_2C(OH)_2$, $CH_3CH(OH)_2$, etc., and therefore a mechanism involving complex formation between Ce^{4+} and the diol forms (*cf.* Ce^{4+} and 2,3-butanediol [9]) was anticipated. But in the present study, as well as in the oxidation of formaldehyde [3] by Ce^{4+}, no kinetic or absorptiometric evidence was obtained for such complex formation under our experimental conditions. At higher [Ce^{4+}] and [aldehyde], a colour change (possible complex formation) was observed, but the reaction under these conditions was too fast to be followed. Absence of kinetic evidence for complex formation in our experiments was obvious from plots of $1/k_{obs}$. *vs.* 1/[Aldehyde] (Fig. 2; A and B) passing through the origin; had there been complex formation, such plots would have left intercepts on the ordinates (*cf.* MICHAELIS and MENTEN [10] and others [5, 11, 12]). Further, no shift of the absorption peak of the ceric ion from the near ultraviolet region ($\lambda = 320$ mμ), and no change in the optical density of the ceric perchlorate ($\sim 3.5 \cdot 10^{-3}$ *M* in 0.5 *M* $HClO_4$ were observed on the addition of excess aldehyde; ([chloral hydrate] $\approx 4 \cdot 10^{-2}$ *M*), suggesting the absence of complex formation between Ce^{4+} and the aldehydes under consideration.

Discussion

Mechanism of oxidation

The rates of oxidation of aldehydes by Ce^{4+} in $HClO_4$ were unaffected by the initial addition of Ce^{3+} to the system and, therefore, the possibility of oxidation by OH radicals produced in a possible equilibrium

$$Ce^{4+} + H_2O \rightleftharpoons Ce^{3+} + H^+ + OH \qquad (1)$$

might be ruled out. The forward reaction of (1), *i.e.* the oxidation of water by Ce^{4+} was, in fact, negligible under our experimental conditions, as shown by blank experiments. In all systems consisting of aqueous perchloric acid and Ce^{4+}, the hydrolytic equilibrium:

$$Ce^{4+} + H_2O \overset{K_h}{\rightleftharpoons} Ce^{4+}OH^- + H^+ \qquad (2)$$

and dimerization of the hydrolyzed species:

$$2\,CeOH^{3+} \rightleftharpoons (Ce—O—Ce)^{6+} + H_2O \qquad (3)$$

should occur, high acidities (< 4.0 *M* [H^+]) favouring the predominance of unhydrolyzed Ce^{4+}; low [Ce^{4+}] and low [H^+] contributing to $Ce^{4+}OH^-$, and very high [Ce^{4+}] favouring dimeric species [13]. Since [Ce^{4+}] $\approx 10^{-3}$ *M* and an acidity of 1.0 *M* was used, dimers may be neglected, and Ce^{4+} as well as $Ce^{4+}OH^-$ would be present in our systems. Our experimental observation that the rates increased with increasing [H^+] (Fig. 2; D and E), together with Equilibrium (2) operating to the left at high [H^+], would mean that the unhydrolyzed species, Ce^{4+}, is the active species in our systems. Our results in the reaction of Ce^{4+} with acetaldehyde in $HClO_4$ may be explained on the

basis of a possible mechanism involving Ce^{4+} (aq) and the diol of the aldehyde:

$$Ce^{4+} + H_2O \overset{K_h}{\rightleftharpoons} Ce^{4+}OH^- + H^+ \tag{4}$$

$$CH_3CHO + H_2O \overset{K'}{\rightleftharpoons} CH_3CH(OH)_2 \tag{5}$$

$$CH_3CH(OH)_2 + H^+ \overset{K''}{\rightleftharpoons} CH_3\overset{+}{C}H(OH) + H_2O \tag{6}$$

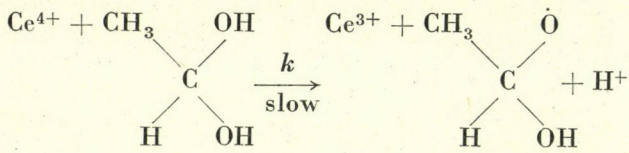

(7)

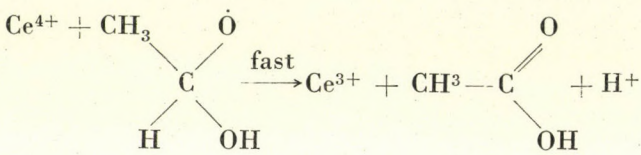

(8)

Among other possible mechanisms two more may be mentioned:

A possible mechanism, taking into consideration unhydrated acetaldehyde (48.2% at 20°) as the active species, cannot be totally disregarded:

$$Ce^{4+} + CH_3CHO \xrightarrow{\text{slow}} CH_3\dot{C}O + Ce^{3+} + H^+$$

$$CH_3\dot{C}O + Ce^{4+} + H_2O \xrightarrow{\text{fast}} CH_3COOH + Ce^{3+} + H^+$$

This mechanism, however, does not explain the observed kinetics of inverse dependence of the rate on $[H^+]$.

Recently TRAHANOVSKY and YOUNG [12a] suggested a mechanism for the oxidation of substituted toluenes to benzyl alcohols by monomeric Ce^{4+} involving a two-electron transfer with a possible Ce^{2+} intermediate. Therefore, yet another possible mechanism for the reaction of Ce^{4+} with aldehydes would be:

$$RCHO + Ce^{4+} \longrightarrow R^+CO + Ce^{2+} + H^+ \tag{8a}$$

$$R\overset{+}{C}O + H_2O \xrightarrow{\text{fast}} RCOOH + H^+ \tag{8b}$$

$$Ce^{2+} + Ce^{4+} \xrightarrow{\text{fast}} 2\,Ce^{3+} \tag{8c}$$

This mechanism, however, seems to be unlikely, because of the absence of any experimental evidence for a Ce^{2+} intermediate, and since the ceric ion-aldehyde redox system initiating vinyl polymerization [12b] must involve free radicals and not ionic intermediates. At constant $[H^+]$, the state lawwould be

$$-\,d\,[Ce^{4+}]/dt = k\,[Ce^{4+}]\,[CH_3CH(OH)_2] = k_1\,[Ce^{4+}]_T\,[CH_3CHO]_T \tag{9}$$

where k and k_1 are the theoretical and observed rate constants, while $[Ce^{4+}]_T$ and $[CH_3CHO]_T$ denote the total $[Ce^{4+}]$ and $[CH_3CHO]$. Taking into consideration the following equalities $[Ce^{4+}]_T = [Ce^{4+}] + K_h\,[Ce^{4+}]/[H^+]$ and $[CH_3CHO]_T = [CH_3CH(OH)_2] + K''\,[CH_3CH(OH)_2]\,[H^+] + K'\,[CH_3CH(OH)_2]$ derived from the mechanism, the rate equation (9) can be expressed in the form of equation (10):

$$\frac{[H^+]}{k_1} = \frac{K_h}{k}\left[1+\frac{1}{K'}\right] + \frac{[H^+]}{k}\left[1+\frac{1}{K'}+K''\,K_h\right] + \frac{K''[H^+]^2}{k} \qquad (10)$$

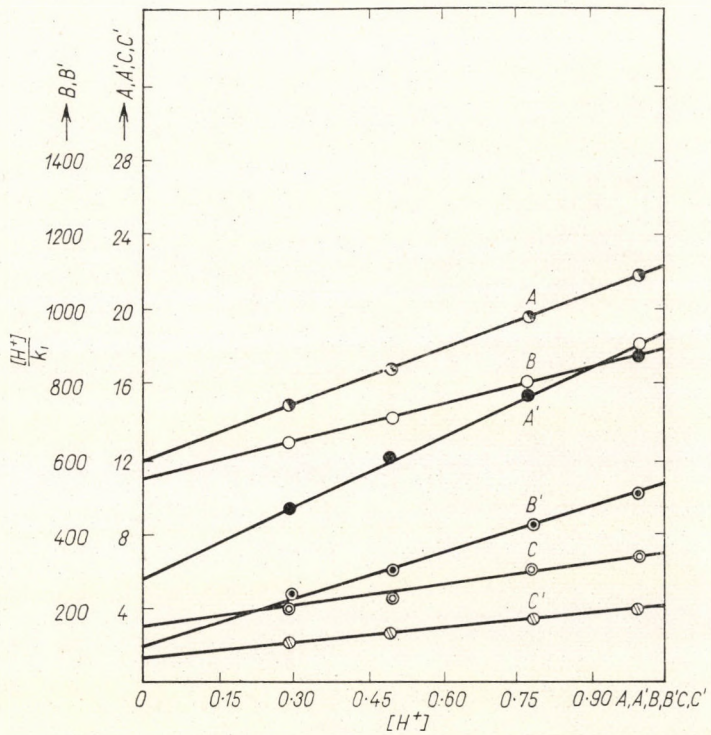

A. A′: Ce^{4+}–acetaldehyde system at 20° and 25° C, respectively
B. B′: Ce^{4+}–chloral hydrate system at 45° and 50° C, respectively
C. C′: Ce^{4+}–formaldehyde system at 15° and 20° C, respectively

Fig. 3. A, A′; B, B′ and C, C′ represent plots of $[H^+]/k$, *vs.* $[H^+]$ for the systems Ce^{4+}–acetaldehyde, Ce^{4+}–chloralhydrate and Ce^{4+}–formaldehyde, respectively

Eq. (10) may also be recast with no $[H^+]$ on the *L.H.S.*, and k_1 would then be directly as well as inversely proportional to $[H^+]$, the latter arising from equilibrium (6) above. Plots of $\frac{[H^+]}{k_1}$ *vs.* $[H^+]$ (Fig. 3; A and A′) were per-

fectly linear with no curvature ($[H^+] \approx 0.1$ to $1.0\ M$). From the intercept on the ordinate, and taking [13] $K_h \approx 3.4$ at 20° and 5.2 at 25° and $K' \approx 0.99$ at 20° and 0.88 at 25° (calculated by us on the basis [2] that 58.2% and 55.3% of acetaldehyde are present as diol at 20° and 25°, respectively) the theoretical rate constant $k \approx 0.6$ at 20° and 1.01 at 25° were obtained. We wish to state this value must be taken with caution because it is based on an approximate computation of the value of K'. From the slope of the plot, and with known values of K_h and K', $K'' \approx 0.77$ at 20° and 1.33 at 25° were evaluated, and for K'' $\Delta H \approx 19$ kcal/mole was calculated.

Chloral hydrate

Chloral hydrate is hydrated even in the solid state [14]; therefore, a solution of chloral hydrate in water is fully hydrated, and hence no equilibrium for diol formation need be assumed. The sequence of reactions (4) to (8) suggested for acetaldehyde would then apply except (5), and equations (11) and (12) (cf. HARGREAVES and SUTCLIFFE for formaldehyde oxidation [3]) hold for the chloral hydrate oxidation:

$$\frac{1}{k_1} = \frac{1}{k} + \frac{K_h}{k[H^+]} + \frac{K''K_h}{k} + \frac{K''[H^+]}{k} \tag{11}$$

and

$$\frac{[H^+]}{k_1} = \frac{K_h}{k} + \frac{[H^+]}{k}(1 + K''K_h) + \frac{K''[H^+]^2}{k} \tag{12}$$

Plots of $[H^+]/k^1$ *vs.* $[H^+]$ were linear (Fig. 3; B and B′) with no tendency for curvature for $[H^+] \approx 0.1-1.0\ M$ used in our experiments. From the intercept on the ordinate and $K_h \approx 28.41$ at 45° and 42.02 at 50° (calculated from $K_h = 5.2$ at 25° and $\Delta H \approx 16$ kcal/mole [13]), $k \sim 0.105$ at 45° and 0.42 at 50° were calculated. From the slope of the plot and with known values of k and K_h, $K'' \approx 2.35$ at 45° and 4.08 at 50° and for K'' $\Delta H \approx 22.5$ kcal/mole were obtained.

Formaldehyde

Plots of $\frac{[H^+]}{k_1}$ *vs.* $[H^+]$, being linear with an intercept and with no tendency for curvature, were also obtained for formaldehyde (Fig. 3; C and C′). $k \sim 0.8$ at 15° and 2.43 at 20°; $K'' \sim 0.71$ at 15° and 1.52 at 20°, and for K'' $\Delta H \approx 25.6$ kcal/mole were calculated.

Rate and thermodynamic data and their interpretation

From kinetic experiments carried out at three temperatures (10°, 15° and 20° for formaldehyde; 13°, 20° and 25° for acetaldehyde; 40°, 45° and

50° for chloral hydrate) the ΔE, $\Delta S^{\ddagger}$ and $\Delta F^{\ddagger}$ values for k_1 and k have been computed for the aldehydes under consideration (Table I).

Table I

Rate and thermodynamic parameters

Aldehyde	Temperature, °C	k_1 l·moles^{-1} sec^{-1}, at 1 M [H$^+$]	k	ΔE, kcal/mole		$\Delta S^{\ddagger}$, e.u.		$\Delta F^{\ddagger}$, kcal/mole	
				k_1	k	k_1	k	k_1	k
HCHO	20°	0.2700	2.43	15.3	37.3	−11.1	68.4	18.6	17.3
CH_3CHO	20°	0.0450	0.60	9.65	18.1	−33.8	0.1	19.6	18.04
CCl_3CHO (hydrate)	45°	0.0011	0.105	24.72	56.6	5.31	113	23.03	20.63

No rational explanation is possible for the $\Delta S^{\ddagger}$ values which are negative for HCHO and CH_3CHO. But the change in the $\Delta S^{\ddagger}$ values for chloral hydrate as compared to formaldehyde or acetaldehyde shows drastic differences in the structures of their activated states.

Structure and reactivity

The low rate of oxidation of chloral hydrate may be explained on the basis of the greater stability of this compound. Owing to the strong electron-withdrawing character of chlorine $CCl_3\overset{+}{C}\begin{matrix}O^-\\H\end{matrix}$, chloral is polarized as $CCl_3\overset{+}{C}\begin{matrix}O^-\\H\end{matrix}$ and by the addition of water the hydrate $CCl_3C\begin{matrix}OH\\-OH\\H\end{matrix}$ is formed to 100%, while acetaldehyde is only ~58% hydrated. Hence in chloral hydrate the OH groups are tightly bound to the aldehydic carbon atom.

Further, by virtue of rotation about the C—C bond, chloral hydrate can have two conformations, gauche and staggered. The gauche form could be represented in *Newman* projection as follows:

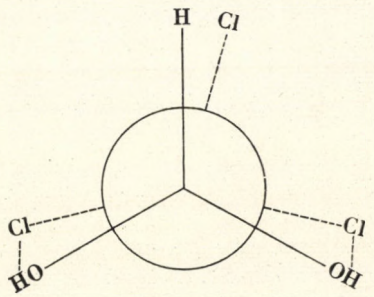

where the H, OH and Cl groups are coplanar, while in the staggered form they are not coplanar. The strong electron-withdrawing character of chlorine makes the aldehydic carbon atom highly positive, while the three Cl atoms acquire fractional negative charges leading to intramolecular hydrogen bonding, as shown in the *Newman* projection. This gives greater stability for chloral hydrate, reducing its reactivity with Ce^{4+}. This tendency of relative stabilization may not be seen in the staggered form (non-coplanarity of the functional groups were assumed). The stabilization due to the formation of intramolecular hydrogen bonding in acetaldehyde may not be predominant, since the methyl group in acetaldehyde is electron-releasing, and hence the reaction with Ce^{4+} is fast.

SUMMARY

The kinetics of oxidation of acetaldehyde (at 13°, 20° and 25°) and chloral hydrate (at 40°, 45° and 50°) by ceric perchlorate in perchloric acid medium ($[H^+]$ 0.1—1.0 *M*) were studied. The reactions were followed by determining rates of disappearance of the ceric ion for variations in $[Ce^{4+}]$, [aldehyde], $[H^+]$, ionic strength (μ), temperature, etc. Product analyses were made, and the stoichiometry $\Delta Ce^{4+}/\Delta$ acetaldehyde ≈ 2 was established. The reactions were found to be second order,— first order each with respect to $[Ce^{4+}]$ and [aldehyde]. No evidence for complex formation between Ce^{4+} and the aldehydes was observed. Ce^{4+} (aq) and the diol forms of the aldehydes are assumed to be the active species. The rates of oxidation were correlated with the structures of the aldehydes. The rate constants and their thermodynamic parameters were calculated and discussed. An extension of the work on the oxidation of formaldehyde by Ce^{4+} in $HClO_4$ by HARGREAVES and SUTCLIFFE was made, particularly with the purpose to evaluate the kinetical and thermodynamic data.

REFERENCES

1. SHORTER, J.: J. Chem. Soc. **1950,** 3425.
2. BELL, CLUNIE: Trans. Faraday Soc. **48,** 439 (1952); see also BELL, and DARVENT, B. DEB.: Trans. Faraday Soc. **46,** 34 (1950); **52,** 1093 (1956).
3. HARGREAVES, G., SUTCLIFFE, L. H.: Trans. Faraday Soc. **51,** 1105 (1955).
4. DUKE, F. R.: J. Am. Chem. Soc. **69,** 2855 (1947).
5. ARDON, M.: J. Chem. Soc. **1957,** 1811.
6. HARGREAVES, G., SUTCLIFFE, L. H.: Trans. Faraday Soc. **51,** 786 (1955).
7. VENKATA RAO, K., SANTAPPA, M.: Unpublished results.
8. SUBBRAMAN, L. R., SANTAPPA, M.: Z. Physik. Chem. (Frankfurt) **48,** 172 (1966).
9. DUKE, F. R., BREMER, R. F.: J. Am. Chem. Soc. **73,** 5179 (1951).
10. MICHAELIS, L., MENTEN, M.: Biochem Zeit. **49,** 333 (1913).
11. LINEWEAVER, H., BURKE, D.: J. Am. Chem. Soc. **56,** 81 (1934).
12. RANGASWAMY, M., SANTAPPA, M.: Unpublished results.
12a. TRAHANOVSKY, S., YOUNG, L. B.: J. Org. Chem. **31,** 2033 (1966).
12b. SUBRAMANIAN, S. V., SANTAPPA, M.: Unpublished results.
13. HARDWICK, T. J., ROBERTSON, E.: Canad. J. Chem. **29,** 818 (1951); see also KING, E. L., PANDOW, M. L.: J. Am. Chem. Soc. **74,** 1966 (1952).
14. HINE, J.: "Physical Organic Chemistry", 2nd ed., McGraw-Hill Book Co., Inc., N. Y.— Kogaksuha Co., Ltd., Tokyo, p. 250.
15. BAKER, F. B., NEWTON, T. W., KHAN, M.: J. Phys. Chem. **64,** 109 (1960).
16. BHATNAGAR, D. W.: J. Sci. Ind. Res. (India), **B 16,** 23 (1957).
17. HEIDT, L. J., SMITH, M. E.: J. Am. Chem. Soc. **70,** 2476 (1948).

M. RANGASWAMY
M. SANTAPPA
Department of Physical Chemistry, University of Madras, A.C. College of Technology Building, Madras-25. India

John D. ROBERTS and Marjorie C. CASERIO: *Modern Organic Chemistry*. W. A. Benjamin Inc., New York—Amsterdam, 1967. XII + 844 S.

Vor drei Jahren sind die »*Basic Principles of Organic Chemistry*« aus der Feder der Autoren des vorliegenden Werkes erschienen und haben in der Zwischenzeit in den Fachkreisen überall gute Aufnahme gefunden.

Die »*Modern Organic Chemistry*« ist eine um etwa 35% des Gesamtumfanges verkürzte Version der »*Basic Principles*« und als elementares Lehrbuch der organischen Chemie gedacht. Jeder Lehrer der organischen Chemie weiß, wie schwer est ist, die Forderungen der Modernität, und der elementaren Darstellung in einem Lehrbuch (oder Lehrgang) so zu vereinigen, daß hierbei auch der Umfang ein vernünftiges Maß nicht überschreiten soll. Um dieses Ziel zu erreichen, ist es unumgänglich, gewisse Teile der klassischen Lehrbücher der organischen Chemie bzw. der klassischen Vorlesungen über diese aufzuopfern und auf ihre Wiedergabe zu verzichten. Nach Ansicht des Rezensenten haben Professor ROBERTS und Professor CASERIO in der »*Modern Organic Chemistry*« das Problem »was ja und was nicht?« sehr gut gelöst, indem sie sich in erster Linie auf die Darstellung allgemeiner Eigenschaften (allgemeiner Bildungs- und Reaktionsweisen usw.) der einzelnen Stoffklassen, nebst der zugehörigen Theorie beschränkten und auf die Wiedergabe von Einzeltatsachen verzichteten. Das will aber nicht bedeuten, daß wichtige Vertreter einzelner Stoffklassen wenigstens in Tabellenform oder sogar etwas ausführlicher im Text nicht erwähnt werden. So z. B. findet man bei den Äthern die Erklärung, was unter Trivialnamen wie »Cellosolve«, »Carbitol«, »Diglyme« zu verstehen ist. Beispiele ließen sich auch weiter häufen, dies erscheint aber unnötig. Gegenbeispiele ließen sich ebenfalls anführen, aber schließlich ist doch ein Lehrbuch kein Lexikon!

Was dem Leser in der »*Modern Organic Chemistry*« am meisten auffällt, und was er zugleich mit großer Freude begrüßt, ist das große Gewicht, das auf die Anwendung und Besprechung der spektroskopischen (IR, UV, KMR, MS) Methoden gelegt wird — was in Kenntnis des Hauptinteressengebietes der Autoren den Leser natürlich nicht verwundert.

Ein 25 Seiten starkes Kapitel (das zweite des Bandes) ist einer allgemeinen Einführung in die spektroskopischen Methoden, ihrer allgemeinen Beschreibung gewidmet, dann aber ist in jedes Kapitel über eine neue Stoffklasse ein besonderer Abschnitt über die spektroskopischen Eigenschaften der betreffenden Stoffklasse eingebaut. So findet man im Bande wertvolle Hinweise auf die Spektren der Alkane, Cycloalkane, Alkene, Alkine, Alkohole, Carbonylverbindungen, Carbonsäuren, Amine, Amide und Arene. Im Zusammenhange mit gewissen aromatischen Verbindungen wird auch die ESR-Spektroskopie kurz erwähnt.

Die meisten amerikanischen Lehrbücher der organischen Chemie legen bekanntlich großen Wert darauf, den Hintergrund der Erscheinungen und Experimentalbefunde von der Strukturtheorie und der Kinetik aus aufzurollen. Dieses Bestreben zeigt sich auch in dem vorliegenden Lehrbuch, wie man sich an Hand der folgenden, keinen Anspruch auf Vollständigkeit erhebenden Aufzählung der behandelten theoretischen Probleme—Rotationsisomerie, Bindungsenergien, Ringspannung, Cis-Trans-Isomerie, Atomorbitale, gerichtete Kovalenzen, Hybridisierung, Resonanz- und MO-Methode (wobei, sehr richtig, für keine der beiden gegenüber der anderen Stellung genommen wird), nucleophile Substitutions- und Eliminierungsreaktionen, Carbonylreaktionen, Elektronenverschiebungen und Säurenstärke, optische Isomerie, Stereochemie der Amine, elektrophile aromatische Substitution, nichtbenzoide Aromaten, organische Photochemie etc. — vergewissern kann.

In ihrem Lehrbuch konnten die Autoren auch für ganz spezielle Gebiete, die gegenwärtig im Mittelpunkt des Interesses vieler Forscher stehen und sich daher in rascher Entwicklung befinden, teils aber seit jeher wichtige Spezialgebiete sind (wie z. B. Protein- und DNS-Struktur, genetischer Code, Kohlenhydrate, Naturprodukte, Farbstoffe, Polymere,

Isoprenoide, Steroide, Biogenese, Silizium-, Phosphor- und bororganische Verbindungen) einen Platz finden, obwohl natürlich die Behandlung dieser Gebiete nicht sehr eingehend sein kann. Dies wäre jedoch auch nicht Aufgabe eines elementaren Lehrbuches.

Eine Reihe von Übungsaufgaben ist teils in den Text der einzelnen Kapitel eingearbeitet, teils einfach an ihr Ende angeschlossen. Es handelt sich nicht um Aufgaben, die einfach das Rezitieren des Gelernten erforden, sondern um solche, die zum Denken und zur *Anwendung* des Gelernten zwingen. Mit manchen der Fragen ist von den Schülern (teils auch von den Lehrern !) etwas zu viel verlangt — dies geben auch die Verfasser zu —, aber sie werden dafür wohl zu nützlichen Diskussionen etwa in Seminaren anregen.

Der Druck und das Papier des Buches sind ausgezeichnet, die Formeln gut lesbar und leicht überblickbar, die Figuren und Abbildungen sehr lehrreich und einleuchtend. Das Durchblättern des Buches wird auch dem Fortgeschrittenen viel Nutzen bringen.

Der Student, der die Elementarvorlesungen über organische Chemie bei Professor ROBERTS erleben darf oder sie nach dem Plan der »*Modern Organic Chemistry*« bekommt, wird es nicht leicht haben. Wenn er aber den gebotenen Stoff meistert, ihn versteht und auch anwenden kann, so ist gewährleistet, daß aus ihm später ein guter Organiker wird.

K. LEMPERT

A. R. KATRITZKY and J. M. LAGOWSKI: *The Principles of Heterocyclic Chemistry*. Methuen & Co. Ltd., London, 1967, XVI + 183 S.

Es ist allgemein bekannt, daß unter allen Zweigen der organischen Chemie wohl das Studium der Heterocyclenchemie — in ihrer stürmischen Entwicklung und der Fülle ihres Tatsachenmaterials — sowohl für Lehrer als auch für Studierende das größte Problem darstellt. Schätzungsweise soll etwa ein Drittel der heute bekannten Kohlenstoffverbindungen heterocyclisch sein und, zumindest prinzipiell, läßt sich ausgehend von jeder einzelnen heterocyclischen Grundverbindung eine ganze »Chemie«, vergleichbar etwa mit der Chemie der Benzolderivate, ableiten. Es ist klar, daß die verschiedenen Kollegien und Kurse an Universitäten und Hochschulen, sowie auch die für die Studenten gedachten Lehrbücher der Heterocyclenchemie nur eine ganz bescheidene Auswahl des Materials bringen können — und das große Problem besteht eben in der Beantwortung der Frage, was gebracht werden soll und wie.

Bereits vor einigen Jahren haben A. R. KATRITZKY und J. M. LAGOWSKI mit ihrer »*Heterocyclic Chemistry*« eine ganz neuartige — und recht gut gelungene — Antwort auf diese Frage gegeben und das jetzt vorliegende Bändchen, »*The Principles of Heterocyclic Chemistry*« ist eigentlich nichts anderes als eine konsequente Weiterführung der Grundgedanken des früheren Werkes, wobei in erster Linie auf die weitere Reduktion des reinen Tatsachenmaterials und die Erleichterung der »Verdaulichkeit« des Textes geachtet wurde.

Bei der Auswahl des Stoffes konnten die Autoren die altbewährte Tradition der Lehrbücher übernehmen und sich in erster Linie auf die Besprechung der fünf- und sechsgliedrigen O-, N- und S-Heterocyclen beschränken, da auch heute noch Vertreter dieser Klassen als die auch von praktischen Gesichtspunkten aus wichtigsten Repräsentanten der heterocyclischen Verbindungen bezeichnet werden können. Hierbei wurde das Hauptgewicht auf die Besprechung der Heteroaromaten gelegt, da — ebenso wie bei den Homocyclen — auch bei den Heterocyclen das Auftreten grundsätzlich neuer Eigenschaften mit der Ausbildung des aromatischen Sextetts, Decetts usw. auf das Engste verbunden ist. Entsprechend der zunehmenden Bedeutung der kleineren Ringe enthält das Buch außerdem ein kurzes Kapitel über drei- und viergliedrige Heterocyclen.

Es ist ebenfalls alter Brauch, den Stoff nach Ringgröße und Anzahl der Heteroatome zu ordnen, und auch die Autoren des vorliegenden Bandes sind so vorgegangen. Während aber in anderen Werken über denselben Gegenstand die heterocyclischen Systeme gleicher Ringgröße und Heteroatomzahl — wie z. B. Oxazole, Thiazole und Imidazole — meistens einfach nacheinander behandelt werden, erfolgt im vorliegenden Bändchen die Behandlung nebeneinander, und es geht den Autoren in erster Linie darum, das Allgemeine an diesen Systemen herauszuarbeiten. Hierzu stützen sie sich sehr stark auf die Elektronentheorie der chemischen Struktur und Reaktivität, wodurch das große Tatsachenmaterial nicht nur fast von selbst geordnet, sondern auch sein Verständnis und seine Einprägbarkeit sehr erleichtert wird.

Es sei hervorgehoben, daß — entsprechend dem auf dem ganzen Heterocyclengebiet herrschenden Trend — die Autoren großes Gewicht auf die Besprechung der physikalischen Eigenschaften (als heute unentbehrliches Hilfsmittel der Strukturaufklärung) sowie des Tautomerieproblems legen. Letzteres ist besonders zu begrüßen, da einerseits — wegen des häufigen

Verwechselns des Tautomeriebegriffs mit dem der doppelten Reaktionsfähigkeit — hier noch ziemlich viel Unrichtiges in der Literatur zu finden ist, und da andererseits die Autoren bekannte Spezialisten eben dieses Gebietes sind.

Das Buch enthält keine Hinweise auf primäre Literaturquellen: dies wäre, da es sich ja um ein Lehrbuch handelt, auch nicht nötig. Anstatt dessen enthält es jedoch einen Abschnitt »Die Literatur der Heterocyclen-Chemie«, in dem die wichtigsten sekundären Quellen — Handbücher, Serien, Fortschrittsberichte — mit einem Hinweis auf eine leicht zugängliche Zusammenstellung über Monographien und Übersichtsarbeiten dieses Gebietes für Leser, die sich im Stoff vertiefen möchten, zusammengestellt sind.

Es ist zwar auch Geschmackssache, welches Symbol man in den Strukturformeln für die Kennzeichnung des aromatischen Zustandes anwendet, der Rezensent möchte es aber dennoch nicht unerwähnt lassen, daß er mit der im vorliegenden Werke benutzten Symbolik, nämlich der Verwendung von Kekuleschen Doppelbindungsformeln nicht zufrieden ist.

Davon abgesehen hält er die »*Principles of Heterocyclic Chemistry*« aber für ein sehr gut gelungenes Werk, das sich seiner Meinung nach auch als Lehrbuch sehr gut bewähren und sich im Kreise der Chemiestudenten großer Beliebtheit und Verbreitung erfreuen wird.

K. LEMPERT

Méthodes d'analyse CETAMA 1966, Recueil No 3, Presses universitaires de France

Der Band ist die dritte Sammlung der Normvorschriften der Französischen Atomenergiekommission zur Analyse von bei der Atomforschung benutzten verschiedenen Stoffen. Über die zweite Sammlung wurde in dieser Zeitschrift — **45**, 383 (1965) — bereits berichtet. Der vorliegende Band ist den vorangehenden ähnlich und zeichnet sich gleichfalls durch die Klarheit und Eindeutigkeit der analytischen Vorschriften aus. In dieser Sammlung sind Vorschriften für die Fluorbestimmung in Wasser, für die Bestimmung von Eisen, Aluminium, Indium, Cadmium, Phosphor, Molybdän, Silicium in Uran, Vorschriften zur Bestimmung verschiedener Spuren von Verunreinigungen in Urantetrafluorid, verschiedener radioaktiver Substanzen in biologischen Flüssigkeiten und zur Prüfung von Spaltungsprodukten zu finden. Es sind auch mehrere Verfahren zur Bestimmung von Elementen durch Aktivierungsanalyse angegeben, die auch dem nicht in der Atomforschung tätigen Chemiker von Nutzen sein können. Zumeist werden keine besonderen Geräte zur Ausführung der Bestimmungen empfohlen.

F. SZABADVÁRY

Walter RUSKE: *100 Jahre Deutsche Chemische Gesellschaft.* Verlag Chemie, Weinheim, 1967, 259 S., 54 Bilder

Es ist üblich, daß Institutionen, Firmen, Gesellschaften, Universitäten usw. anläßlich ihres hundertjährigen Bestehens eine Festschrift herausgeben. Es sind dies meistens Bücher, die von vielem Nutzen für jemanden sein können, der einmal eine bestimmte Information über den Gegenstand haben möchte oder für den Historiker, der nach bestimmten Angaben sucht, sind jedoch in der Regel Bücher, die im allgemeinen langweilig sind und kaum gelesen werden. Das zu besprechende Buch unterscheidet sich angenehmer Weise von den übrigen seiner Art. In diesem Buch, das W. RUSKE im Auftrag der ruhmreichen *Deutschen Chemischen Gesellschaft* anläßlich des hundertjährigen Bestehens dieser Gesellschaft verfaßte, findet man zwar keine komplette Aufzählung aller Funktionäre der Gesellschaft samt ihren Verdiensten und Lebensdaten, aber es ist ein Buch, in das man anfangs nur hineinblättert, man es dann aber interessiert, wie eine Lektüre, von der ersten bis zur letzten Seite durchliest. Man überblickt die Geschichte der Gesellschaft im Spiegel der jeweiligen wirtschaftlichen, industriellen und politischen Geschehnisse und in Abhängigkeit von diesen. Viele weitere, für die verschiedenen Zeitalter charakteristische Bemerkungen findet man außerdem erwähnt, wie z. B. die Verdienste von Firmeninhabern und Arbeitern oder die Studienmöglichkeiten der Frauen. Nicht Persönlichkeiten — charakterisiert in entsprechendem Nekrologstyl — sondern Menschen lernen wir hier kennen, die mit zeitgenössischen oder ihren eigenen Zitaten oder durch Bemerkungen des Verfassers lebhaft und lebendig beschrieben werden. Selbst August Wilhelm HOFFMANN wurde aus dem chemischen Halbgott deutscher Biographien zu einem Professor mit Tatkraft, Talent und menschlichen Eigenschaften. Der gemütliche und lebenslustige HOFFMANN und der düstere

und arbeitsbesessene E. FISCHER scheinen den Teil über die Epoche der Kaiserzeit zu beherrschen, während anderen Persönlichkeiten vielleicht etwas wenig Raum gewidmet wurde, dagegen findet man in dem Teil vom ersten Weltkrieg bis zum »Dritten Reich« verhältnissmäßig wenig über die Gesellschaft selbst, um so mehr aber über *Duisberg* und *Bosch* und die chemische Industrie. Man könnte aus diesem Umstand folgern, daß während vor dem ersten Weltkrieg die Wissenschaftler in erster Linie in der Deutschen Chemischen Gesellschaft maßgebend waren, nachher die Industriellen zu größerem Einfluß gelangten. Zu anerkennen ist, daß der Autor auch nicht vor der kritischen Schilderung der Vorgegenwart zurückscheute. Ruske unterdrückt seine persönliche Meinung und Einstellung nicht. Dazu hat und soll auch immer jeder Autor sein Recht haben. Seine persönlichen Bemerkungen — ob man ihnen zustimmt oder nicht — machen den Stil frisch. Hier möchte ich bemerken, daß ich z. B. nicht verstehe, warum er gereizt ist, daß man einigen Chemikern in Deutschland Standbilder errichtet hat. Ich glaube RUSKE irrt, wenn er schreibt: »Auch diese Denkmäler sind als Zeugnisse der etwa bis zum ersten Weltkrieg übertonten nationalen Tendenzen in Deutschland zu werten und damit Ausdruck einer Zeit die in der Errichtung von Standbildern die dauerhafteste Form der Erinnerung an deutsche Größe sah.« Standbilder zu errichten ist seit ältester Zeit und bis heute, unabhängig von Land, Volk und gesellschaftlicher Form, üblich. Ob nun in der Welt immer jene Standbilder bekamen, die es verdient hatten, ist wohl mit Recht zu bezweifeln. Man sollte sich daher also eher freuen, daß neben so vielen Herrschern, Politikern und Feldherrn auch einige Wissenschaftler ihre Standbilder haben. Die Menschheit verdankt ihnen ja viel mehr als den ersteren!

Zusammenfassend: W. RUSKE wurde beauftragt eine Festschrift zu verfassen und er hat statt dieser ein interessantes Buch, eine kleine chemische Zeitgeschichte geschrieben, wofür der Leser ihm dankbar ist.

F. SZABADVÁRY

P. ZAKAR: *Bitumen.* (Kleine Erdöl-Bibliothek, 2. überarbeitete Auflage.) VEB Deutscher Verlag für Grundstoffindustrie, Leipzig, 1967, 180 S.

Bitumen ist ein vielseitig verwendbarer und billiger Rohstoff, der heute in mehreren Industriezweigen zu einer immer wachsenden Bedeutung gelangt.

Das vorliegende Handbuch stellt eine Monographie dar, in welcher sämtliche Aspekte der Herstellung, Eigenschaften, Prüfung und Verwendung des Bitumens gründlich behandelt werden.

Der erste Teil des Buches befaßt sich mit der Gewinnung und den Eigenschaften des Bitumens. Der Verfasser war bestrebt alle Unklarheiten, die auf dem Gebiete der Bezeichnung von Bitumina, Asphalten, Pechen, Harzen und anderen verwandten Produkten früher bestanden, sorgfältig zu klären. Besondere Beachtung wird in diesem Teil den Untersuchungsmethoden gewidmet mit denen die vielerlei Bitumenqualitäten beurteilt werden können.

Im zweiten Teil werden die Fragen der Bitumenherstellung besprochen. Die wichtigsten Verfahren, Destillation, Extraktion, Verblasen und Cracken werden unter Berücksichtigung der neuesten Ergebnisse beschrieben. Im weiteren werden den Betriebsfachleuten nützliche Hinweise für die Manipulation (Mischen, Verschneiden, Emulgieren, Abfüllung, Konfektionierung, Versand) des Bitumens gegeben. Man merkt, daß der Verfasser das größte Gewicht auf diesen Teil seines Buches gelegt hat. Dieser Umstand kann nicht nur damit erklärt werden, daß dieses Gebiet zu seinem engeren Interessenkreis gehört, sondern auch damit, daß die Herstellungs- und Manipulationsprozesse des Bitumens in den letzten Zeiten einen bedeutenden Aufschwung genommen haben.

Der dritte Teil ist ein Überblick der wichtigsten Einsatzmöglichkeiten des Bitumens im Straßenbau, in der Bauindustrie, im Korrosionsschutz und auf anderen Gebieten der Industrie. Dieser Abschnitt enthält über die jeweils erforderlichen Bitumenqualitäten wertvolle Auskünfte, welche besonders den Praktikern gute Dienste leisten. Schließlich gibt der Verfasser eine Liste der gültigen DDR-Normen auf dem Bitumensektor und ein Quellenverzeichnis mit über 300 Literaturangaben.

In die völlig umgearbeitete zweite Auflage wurden einige neue Kapitel aufgenommen. Besonders die Probleme des Bitumenblasens wurden detaillierter behandelt, weil auf diesem Gebiet der Bitumentechnologie im Weltmaßstab intensive theoretische und praktische Arbeiten durchgeführt wurden.

Zusammenfassend kann festgestellt werden, daß dieses gut übersichtliche, bequem behandelbare Büchlein nicht nur ein nützliches Handbuch für die Praktiker, sondern auch als Lehrbuch für die Ausbildung der Bitumenfachleute verwendbar ist.

V. TAKÁCS

H. B. GRAY and G. B. HAIGHT: *Basic Principles of Chemistry*. W. A. Benjamin, Inc. New York, 1967, xvii + pp. 595

It is rather difficult to compile in a single volume all that we know about the basic principles of chemistry, even at introductory level. This interesting and expressive text-book is an approach to solving of this problem.

In the Preface the authors outline the distinguishing characteristics of their new chemistry text. They point out that "the old categories of physical, organic, inorganic and analytical chemistry have steadily merged so that we have an assortment of combination names, such as physical organic, physical inorganic, organometallic, electroanalytical, and so on. The challenge today is to reclassify the fields of chemistry along the natural borders of contemporary research". Therefore, they based their train of thought on the development of structural chemistry and chemical reactivity, neglecting the old categories of classification into inorganic and organic structures and reactions.

Another novel feature of the text-book is an endeavour to integration in the treatment of problems from different points of view of physical, analytical, organic and inorganic chemistry: *i.e.* the book aims at giving a continuous pattern instead of treating the various individual aspects of the matter separately. This helps the reader to evolve an integral chemical view, but it may cause some difficulties for students, who need more basic knowledge of the individual disciplines.

After a brief introduction on the patterns of scientific investigation, Chapters 1 to 7 are devoted to the "classical" ideas of chemical structure: properties of substances, elements and compounds, quantities of mass and energy, classical atomic theory and its modern interpretation, kinetic gas theory, changes of state, physical equilibria, electrolysis and ionization, the periodic system, classical views of molecular structure, and stoichiometry.

The book then turns to the modern description of chemical structure by beginning with the Bohr model of the atom and working through the modern interpretation of atomic properties to the atomic and molecular orbitals and their application to the elucidation of chemical structures both for simple molecules and for condensed systems. This part of the book incorporates Chapters 8 to 13.

In the last six chapters the topic of reactivity is discussed; chemical dynamics, rates, equilibria and mechanisms, acid–base equilibria, coordination chemistry, heterogeneous equilibria involving aqueous solutions, precipitation, solvent extraction, vaporization, oxidation-reduction equilibria. The book concludes with a comprehensive chapter on the chemistry of some non-metallic elements: hydrogen, oxygen, nitrogen, boron, etc. This latter is the only chapter which treats the material in the sense of classical "descriptive chemistry".

The appearance of the book, its form, printing, and the quality of paper are excellent. The illustrations are expressive: the whole book is easy to survey.

In conclusion, this text-book can be considered a successful attempt for a modern interpretation of the basic principles of chemistry. It can be recommended to all those concerned with the problems of introductory chemistry teaching.

V. TAKÁCS

Organosilicon Chemistry. Special Lectures Presented at the International Symposium on Organosilicon Chemistry, held in Prague, Czechoslovakia, 6—9 September, 1965. Butterworths, London, 1966, pp. 327

This book is a selection of lectures presented at the first "*International Symposium on Organosilicon Chemistry*" which was held under the auspices of IUPAC in Prague, in September, 1965. The five plenary and sixteen main lectures survey recent developments in organosilicon chemistry. The presentation of the latest results is one of the most valuable features of the book, as for some years no concise handbook has been published on this subject. The papers were read by prominent authorities in the field, whose choice of subject and working methods faithfully reflect the trend of development and the preparative and instrument demands of up-to-date research methods.

R. WEST (USA) deals with two classical problems of organosilicon chemistry. He reports on the successful preparation of the pentacoordinated organosiliconium ion $[Ph_3Si(bipy)]^+$. The stable existence of such a compound might be the proof and at the same time the model of the pentacoordinated intermediates which are often presumed in the reactions of organosilicon compounds. West studied the role of the *d*-orbitals of Si on a model containing neither lone electron pairs nor π-electrons. The anion-radical $[Si(CH_3)_2]_6^-$ was prepared by the reduc-

tion of dodecamethylcyclohexasilane $[Si(CH_3)_2]_6$. The e.s.r. spectrum of the anion-radical indicates that the unpaired electron is deloca'ized in a molecular orbital extended equally over all six silicon atoms, just as the unpaired electron in aromatic anion-radicals, with the difference that, because of the nature of the *d*-orbitals in the silicon compound, it is not essential for the ring to be planar.

M. SCHMIDT (Germany) compares the organic chemistry of the elements in Group IV/b, and follows up changes in the properties on the hand of many examples. He establishes correlations between these changes and the characteristic parameters of the elements, such as atomic radius, ionization potential, electronegativity, polarizability, electron donor or acceptor nature, and other related characteristics. The author presents a survey of the analogies and differences between the behaviours of the organic compounds of silicon and germanium from which he draws the conclusion that the polarity of the metal-oxygen bond increases in the order Si—Ge—Sn—Pb while the stability of the bond decreases in the same order. Schmidt also mentions the sulphur, selenium, tellurium and nitrogen derivatives and the preparation of many new compounds.

M. G. VORONKOV (USSR) gives a report on a new family of compounds containing pentacoordinated silicon atom for which he suggests the name "silatranes". The "atrane" skeleton consists of three five-membered rings with two common atoms and is an intracomplex heterocyclic inorganic ester and alcoholate of triethanolamine, with the general formula; $R_{n-3}M(OCH_2CH_2)_3N$, where R is an organic radical, hydrogen or any other substituent, *n* is the valency of the central atom M, and M might be B, Al, Si, Ti, Zr, Bi, V, Fe. The silatranes can be prepared by a simple method. The author describes a large number of compounds belonging into this group, and discusses the structure of the silatrane skeleton on the basis of dipole moment, infrared and proton magnetic resonance spectrum data. He also presents some data on the physiological activity of this interesting group of compounds.

R. CALAS (France) deals with some possibilities of using hydrosilanes in organic chemistry. He gives an example of asymmetric synthesis by the addition of hydrosilane to the olefin bond, and sums up the new preparative possibilities implicit in the reactions of ketones and aldehydes, acetals, nitriles, lactones and lactams with hydrosilanes.

J. GOUBEAU (Germany) reviews the preparation and properties of heterocyclic organosilicon compounds containing either phosphorus or arsenic, including a number of new compounds such as bicyclic spirane-type derivatives. The investigation of silicon-containing amines extends to their preparation and to the nature of their complex-forming properties.

Some very interesting new possibilities of preparing organosilicon halides by using a fused salt as the reaction medium are described by W. SUNDERMEYER (Germany). These melts are good solvents for gases and highly suitable as media for catalytic processes. By using molten alkali pseudo-halides the cyanides, isocyanates and isothiocyanates of silicon, and even the hitherto unknown azidosilanes can be prepared starting from chlorosilanes. Combined with an electrolytic process, this method is suitable for the preparation of SiH_4, of chlorosilanes containing Si—H bonds, and of alkyl chlorosilanes. Direct synthesis in the salt melt has many advantages. The author gives the details of a new continuous method for the preparation of tetramethylsilane starting with silicon tetrachloride and methyl chloride. By this method the methyl derivatives of Ge, Sn, B, As, Sb and Hg can also be prepared.

W. NOLL (Germany) investigates the dependence of the properties of the siloxane bond on the donor—acceptor nature of the substituents. Alteration of the electron density at the siloxane oxygen influences in a very sensitive manner the physical and chemical behaviour of the siloxanes. The author has worked out a method for the continuous recording of the *F*/*A*-isotherms of siloxane films spread on the surface of water. From the specific behaviour of the two-dimensional silicone–water system, the results can be brought into correlation with the electron density at the siloxane oxygen and the donor—acceptor influence of the substituents. It appears that the spreading power of methyl and methyl hydrogen siloxanes is the highest, while alkyl substituents with higher C numbers or phenyl groups very quickly reduce the spreading power. The measurements seem to indicate the acceptor character of the hydrogen in methyl hydrogen siloxanes, *i.e.* the hydrogen reduces electron density at the oxygen. Noll investigated the acidolysis of siloxanes by titrating with Karl Fischer's reagent and he noted a very marked effect of the substituents.

R. C. MEHROTRA (India) sums up the recent results achieved in the preparation of alkoxy- and acyloxysilanes and the properties of these compounds. He also describes new preparative methods and several new compounds.

R. A. BENKESER (USA) deals with the stereochemistry of silane addition reactions and the governing effect of various catalysts on additions to systems with triple —C≡C— bonds. This addition can be used in the synthesis of silicon-containing heterocyclic compounds. The author also discusses the problem of the mechanism of silane addition.

The problem of silane addition is the subject also of the paper by R. N. MEALS (USA) who characterizes the reaction from the point of view of the preparation of organosilanes. Certain side-reactions (polymerization, isomerization of the olefins) will interfere with the addition, and the preparation of the Si—H compound is also cumbersome. In uncatalyzed thermal reactions mainly anti-Markownikoff addition takes place. Meals also discusses the addition-promoting catalysts and the reaction mechanisms. It appears that the easily polarizable silicon-hydrogen bond can be cleaved either homolytically or heterolytically depending on the catalyst. The author gives a brief survey of the addition of other hydrides (B, Ge, Sn, P).

In their comparative investigation of the organic chemistry of carbon and silicon, D. SEYFERT, G. SINGH and R. SUZUKI (USA) emphasize the importance of the steric effect beside the assumed C → Si π bond.

M. KUMADA (Japan) surveys recent results in the study of organopolysilanes. Starting from the so-called disilane fraction, which is obtained as a by-product in the direct synthesis, disilanes with different silicon functions can be prepared whose hydrolysis leads to cyclic and cubic products containing siloxane and disilane bonds. These latter can be equilibrated similarly to cyclic siloxanes. The author reviews the new preparative possibilities of linear, permethylated polysiloxanes, the electrophilic and oxidative cleavage of the Si—Si bond, the new ferrocene-silicon derivatives, and the ultraviolet activity of organopolysilanes.

E. A. V. EBSWORTH (UK) discusses the structural chemistry of Si—H compounds and emphasizes the advantages of the SiH_3 models over the $-SiR_3$ groups in structure research, as the former are easier to study whether by electron diffraction, microwave spectroscopy or vibrational spectroscopy. He gives a detailed account of the application possibilities of proton resonance spectra.

Recent results achieved in the spectroscopic investigations of organosilicon compounds are reviewed by H. KRIEGSMANN (Germany), who discusses the influence of substituents and solvents on the infrared and Raman wavenumbers and intensities, and analyzes the structure of cyclic siloxanes. Hydrogen as a substituent has an inductive strengthening effect on the siloxane bond.

A. G. BROOK (Canada) deals with the rearrangement of α-silylcarbinols to the isomeric silyl ethers. This rearrangement can be made use of in the investigation of optically active silicon compounds and can be easily followed by nuclear magnetic resonance spectroscopy. The rearrangement of α-silylketones also lends itself to stereochemical studies.

V. CHVALOVSKY (Czechoslovakia) has investigated the role of the *d*-orbitals of silicon. Using the spectroscopic data of the stretching frequencies of the Si—H bond, he has studied the formation of the $(p \rightarrow d)_\pi$ bond for substituents with free electron pair, and with π bond. He arrives at the conclusion that neither the vinyl nor the phenyl group induces any significant $(p \rightarrow d)_\pi$ bond in the case of R_3SiH type compounds, contrary to oxygen-containing substituents, where in the case of a single ethoxy group considerable $(p \rightarrow d)_\pi$ interaction seems probable. The conclusions are supported by the evidence of nuclear magnetic resonance spectroscopy, the Hammet σ constant and dipole moment measurements.

E. G. ROCHOW (USA) presents an excellent survey of the properties of methylsilazanes and of recent preparative methods. He discusses in detail the problem of equilibration of silazanes and the surprising fact that the preparation of linear silazanes can be solved by equilibration in NH_3 atmosphere. The behaviour of the polymers as a function of temperature can be satisfactorily followed by special broad-line methyl proton resonance spectroscopy.

U. WANNAGAT (Austria) is in a position to treat the preparation and properties of cyclic silicon-nitrogen compounds on the basis of his huge experimental material.

G. FRITZ (Germany) sums up the chemistry of carbosilanes which are linear and cyclic compounds with alternate Si and C atoms. The author suggests for their preparation from alkyl silanes a special pyrolysis technology. The products can be separated chromatographically. Fritz also lists the data of the compounds which have been identified so far. The formation of the products can be interpreted by the radical mechanism.

R. A. SHAW (UK) surveys the radiation chemistry of silicon compounds, their formation by silent electrical discharge, in the electric arc and under the influence of gamma-radiation and the probable mechanism of the processes.

V. BAŽANT (Czechoslovakia) reports on his latest results in the direct synthesis of organo-halosilanes. He gives an empirical correlation for the reaction rate and quotes some of his results with *p* and *n* type silicon and with respect to the side-reactions of direct synthesis. Bažant pays great attention to the examination of the contact mass, measures its bulk density, specific surface area and the adsorption isotherms, and examines its structure by infrared spectroscopy, electron microscope, and X-ray phase analysis. He has also investigated the solid condensation products formed by side-reactions and the surface inactivation of the copper catalyst.

P. GÖMÖRY

S. T. IOFFE, and A. N. NESMEYANOV: *Methods of Elemento-Organic Chemistry. Vol. 2. The Organic Compounds of Magnesium, Beryllium, Calcium, Strontium and Barium.* North-Holland Publishing Co., Amsterdam, 1967. 747 pages, 42 tables, 15 figures

The reviewer has already opportunity of giving review of the first volume of the English version of this excellent series edited by NESMEYANOV and KOCHESKOV, and published by the firm *North-Holland.* As mentioned at that time, this version is no simple translation of the Russian original. Instead, it comprises all the important results obtained in this field since the appearance of the first Russian edition. Thus, a significant completion of the work became necessary. When now reviewing the second volume, without repeating the statements referring to the series as a whole, we must emphasize the excellent choice and abstracting work done by the authors. They did not aim at bibliographic completeness, as it is also seen from the size of the book. However, as regards the essential achievements of the field, the book is quite complete, *i.e.* the reader obtains the results of a well designed and logical selection. Obviously, a careful and critical choice was required only in the case of organomagnesium compounds, the metallo-organic chemistry of other elements being of a small volume, as interest turned to them only in the last few years. This interest, which has brought important new achievements mainly in the field of metalation reactions, may be appreciably increased by the present, long-needed book.

The essential part of the work, 659 pages, is mainly devoted to the organic chemistry of magnesium, to the Grignard reagents that have developed for more than half a century, and to their reactions. Naturally, the authors made use of the literature on Grignard reagents and Grignard reactions published so far, a part of which has already become classic knowledge; however, the completion of the fundamental data with aspects of up-to-date, mainly synthetic, chemistry, and the rearrangement and refreshing of knowledge fill up a gap which has long been apparent. In this respect, the reviewer would like to emphasize that, in accordance with the title of the series, synthesis and chemical practice always play the leading role in the treatment of the subject. Structural problems are discussed only tangentially and to such a depth as is necessitated by the synthetic material. The authors attribute great significance, and accordingly, they devote large space, to the discussion of reaction mechanisms. By this feature, the book emerges from the simple level of encyclopedic describing literature, and becomes really modern. Some chapters dealing with current problems of chemistry, such as those discussing the reactions of Grignard reagents with epoxides (Chapter 15), the rearrangement reactions connected with Grignard reaction (Chapter 18), and the mechanism of free-radical reactions and their practical significance (Chapter 19) are particularly interesting and pleasant to read.

In nearly all chapters, the authors frequently take the opportunity of presenting structure proofs obtainable by means of Grignard reactions (such as in the case of steroids), and of demonstrating the interrelations of synthesis, reaction mechanisms, and the elucidation of structure.

The reader may experience some disappointment finding that at certain places in the text (*e.g.*, in Chapter 3, in connection with the structure of Grignard compounds), when reviewing contradictory data of literature, the authors omit to express their personal opinion as to which view is to be taken as correct. It would have been worth-while to summarize and to compare, in a short chapter at the beginning of the book, the similarities and differences of the organic derivatives of the discussed elements. The chapter beginning on page 651 does not appear to be sufficient in that respect.

However, weighing up all the merits and criticisms concerning the book, one must state that the recently published Volume 2 represents an excellent source and aid for readers engaged both in practical syntheses and in the theory of reactions. As compared to earlier books of similar nature, the book of IOFFE and NESMEYANOV offers another great advantage: besides the results attained in Western countries, it summarizes also the vast work done in the Soviet Union in this field, mainly under the personal supervision of the authors of the book.

T. SZÉKELY

B. LENGYEL, Z. BOKSAY and B. CSÁKVÁRI: *A szilikátüvegek elektromos tulajdonságai.* (The electric properties of silicate glasses.) (In Hungarian.) Monographs of Silicate Chemistry, No. VII. Akadémiai Kiadó (Publishing House of the Hungarian Academy of Sciences). Budapest, 1966. 197 pages, with many figures and tables

The present volume VII of the *Monographs of Silicate Chemistry* initiated by the *Committee for Silicate Chemistry* of the *Hungarian Academy of Sciences* is a worthy continuation of the series. Current problems of prominent importance are discussed at international level: these problems, which have been investigated since as long ago as 1800, are the subject of active research even at the present time.

The monograph is divided into four chapters. *Chapter I*, as an introduction, describes in an extremely interesting manner the basic phenomena of glass electrolysis. It is clearly seen from this presentation that the flow of electric current in glass is mediated by the migration of ions. This is followed by a brief discussion of the diffusion of ions. Electric conduction is treated in detail in *Chapter II*. The mechanism of conduction and the effect of external factors on conductance are closely correlated with the structure of glass, which even today is still not perfectly known. For a discussion of conductance the only suitable basis is afforded by the model where alkali, alkali-earth and other modifying cations are located in the cavities of the irregular tetrahedral network. The so-called crystallite theory does not reveal anything in this. The conductance of glass is fundamentally affected by the composition of the glass (obviously this effect is different for inner conductance and surface conductance).

The dielectric properties of glass are also treated in detail. For that purpose, rather complicated though not too difficult mathematical deductions are required. Dielectric loss, a value of technical importance, depends again on the structure and chemical composition of the glass. These properties are treated in *Chapter III*. Lastly, *Chapter IV* is devoted to a detailed and thorough discussion of phase boundary potentials occurring on glass surfaces. The research of B. LENGYEL conducted in this field for more than three decades with the co-operation of Z. BOKSAY, B. CSÁKVÁRI and others has obtained general recognition in the international world of science. They made possible the precise treatment of some extremely complicated problems, such as that of the behaviour and the so-called alkaline error of glass electrodes frequently used in practice. The final paragraphs of the book deal with the problems of phase boundary potentials formed between silica glass and electrolyte solutions, and of phase boundary potentials occurring in glass melts. A list of 340 references to literature, author and subject indexes usefully complement the book.

Some remarks appear to be necessary concerning silicate chemistry or glass structure. Monosilicates are mentioned on page 58, whereas today only the expression "metasilicate" is used. The compounds containing the radical Si_2O_7, that were denoted earlier as pyrosilicates, are known today as disilicates, instead of the silicates based on layers of the composition Si_4O_{10}, which latter are usually called now dimetasilicates. — The Mg^{2+} ions do not occupy the centre of the tetrahedrons forming the skeleton; the distance between the ion forming the network and the O^{2-}-ion does not exceed 1.82 to 1.84 Å, while the distance Mg—O is, even in a tetrahedral coordination, 1.96 Å (*e.g.*, in $MgAl_2O_4$). Thus, the Mg—O bond is of medium strength (55 kcal). Of course, there are some cases when glass is built up with weaker bonds *e.g.*, the independent SiO_4 tetrahedrons in a glass of high lead content are linked by Pb atoms of trigonal (pyramidal) coordination. Since the bond strength Pb—O is only 48 kcal, a lead glass of this type has lower stress and strain values than for example silica glass constructed solely with Si—O bonds, the bond strength Si—O being 106 kcal. These comments do not lessen the value of the book.

The Hungarian style is excellent, and explanations are readily understandable. The book is based on a careful collection of literature data and on extensive original experimental work: the references include, in addition to earlier classical titles, a number of works published since 1960.

The reviewed book of LENGYEL, BOKSAY and CSÁKVÁRI is a valuable contribution to the increasing comprehensive Hungarian chemical literature. In the reviewer's opinion, the international group of glass scientists would certainly welcome a translation of the book; this should be made as soon as possible.

I. NÁRAY-SZABÓ

P. KARLSON: *Kurzes Lehrbuch der Biochemie für Mediziner und Naturwissenschaftler.* G. Thieme, Stuttgart, 1966, Fifth German edition, pp. 371.

There is no doubt that "*the Karlson*" is one of the most successful biochemistry textbooks of this decade. This newest and substantially revised book is now the fifth German edition discounting the unchanged reprintings since the first publication in 1960. It has been translated into five languages and there are now 12 foreign editions altogether including two English ones. The great popularity of this book is due primarily to its excellent structure, which has enabled the author to make an amazingly appropriate selection of topics. An illustration of the unparalleled conciseness of this work is that the index of this 371-page volume comprises nearly 2000 entries. The reviewer, active in biochemistry teaching for two decades, was unable to discover any topic of the slightest general importance not represented, at least in the form of some short reference. But even the shortest remarks are chosen with proper consideration. This makes it possible, for example, to treat the biochemistry of organs (alimentary tract, liver, blood, kidney and urine, other processes of excretion, muscle and nerve) in 11 pages!

Obviously this conciseness in the case of unsolved problems leads to some inevitable rounding-offs and simplified presentations. These simplifications, however, are based on correct didactic reflections and result only in exceptional cases in perfunctory wording, as in the case of allosteric inhibition. It is quite understandable that in a biochemistry text of this size which aims at completeness, hardly any space is given to the presentation of the methods, all being reserved to the description of results. This is a policy deliberately chosen by the author as he states in the foreword.

This book is ideal for the public for which it was intended as stated in the title. It is, however, not quite certain that it is the very best of introductions for prospective biochemists. One feels this doubt especially when reading the chapters on protein structure and foundations of enzymology. But by a more prejudiced selection the well-balanced economy of the book would certainly be upset. And for those who read it as a foundation of studies in other fields, it would hardly be possible to give a better synopsis of the biochemistry of our days.

A special reference should be made to the quite exceptionally immaculate get-up of this book. Besides the 65 figures, among them many excellently reproduced electronmicroscope pictures, there are countless schemes to illustrate reaction chains and metabolic pathways. A supplement in the form of a big folder presents an imposing all-round metabolic map printed in two colours, and on the reverse side of it we find the sequences of the pituitary hormones of several species, of the human hemoglobins, and as a "stop-press news" the nucleotide sequence of the first transfer-RNA solved by HOLLAY *et al.* hardly six months before this book could have been out of press.

N. A. BIRÓ

Reinstoffprobleme. Herausgegeben von Prof. E. REXER. Band III. *Realstruktur und Eigenschaften von Reinststoffen.* Akademie-Verlag Berlin, 1967, XIII, 1052 Seiten, 594 Abbildungen, davon 226 auf 129 Tafeln — 49 Tabellen

Dem von der Chemischen Gesellschaft in der Deutschen Demokratischen Republik, der Gesellschaft Deutscher Berg- und Hüttenleute und der Physikalischen Gesellschaft in der Deutschen Demokratischen Republik vom 28. September bis zum 2. Oktober 1965 in Dresden veranstalteten 2. Internationalen Symposium »*Reinststoffe in Wissenschaft und Technik*« wurde gegenüber dem ersten Symposium im Jahre 1961 ein viel größeres Interesse entgegengebracht. Der gesamte Tagungsbericht, der 174 Vorträge aus allen Gebieten der Reinststofforschung enthält, erschien in drei Bänden; I. *Reinststoffdarstellung*, II. *Reinststoffanalytik*, III. *Realstruktur und Eigenschaften von Reinststoffen.* Alle Vorträge sind in der Vortragssprache (deutsch, englisch, französisch, russisch) gedruckt, die russischen Texte aber wurden auch ins Deutsche übersetzt. Jedem Vortrag ist eine dreisprachige Zusammenfassung vorangestellt.

Band III enthält die Plenarvorträge von Prof. E. REXER über »Die Bedeutung reinster Metalle für Grundlagenuntersuchungen technischer Probleme« sowie von Prof. A. SEEGER und Dr. M. WILKENS über »Die Versetzungen und ihre Rolle bei der plastischen Verformung reiner Metalle«. Es schließen sich 74 Haupt- und Kurzvorträge an, die die Gebiete »Realstruktur und Einkristallzüchtung«, »Störungsempfindliche Eigenschaften«, »Versetzungsstheorie« und »Spezielle Halbleiterprobleme« behandeln. Am Schluß steht noch der Plenarvortrag von E. BILLIG über »*Some recent developments in solid state*«.

Der Plenarvortrag von Prof. REXER behandelt die elektrische Leitfähigkeit und mechanischen Eigenschaften von hexagonalen und kubisch-flächenzentrierten Metallen in Abhängig-

keit von der Reinheit sowie die Problematik der Rekristallisation. Durch die Verunreinigungen in Reinstmetallen werden die freien Weglängen der Elektronen bei tiefen Temperaturen (z. B. bei 4,2°K) sehr stark und charakteristisch beeinflußt. Die mechanischen Eigenschaften der kubisch-flächenzentrierten Metalle werden in der Regel weniger, in Beryllium, das hexagonal ist, stärker vom Reinheitsgrad geändert. Beim Prozeß der Rekristallisation entstehen und bewegen sich Korngrenzen, die starke Abhängigkeit von Verunreinigungen zeigen in Beziehung der Orientierung benachbarter Körner.

Im Plenarvortrag von Prof. A. SEEGER und Dr. M. WILKENS findet man einen Überblick über die experimentellen Verfahren zur Untersuchung der Bewegung und der Anordnung von Versetzungen in plastisch verformten reinen Metallkristallen. Die Vorzüge und Nachteile sowie die möglichen Fehlerquellen der verschiedenen Methoden wurden erörtert, besonders in Hinblick auf das Studium der Versetzungsanordnung in massiven plastisch verformten Metallkristallen. Die Anwendung der elektronenmikroskopischen Durchstrahlung, der Röntgenabbildung und der Ätzgrübchenmethode wird anhand zahlreicher Beispiele besprochen.

Nach dem Hauptvortrag von J. M. STEEDS: »*The application of transmission electron microscopy in metal physics*« der neben dem Überblick und der Anwendbarkeit der Elektronenmikroskopie auch spezielle Ergebnisse behandelt, befinden sich noch 23 Vorträge in dieser Gruppe, die neue Forschungsergebnisse über Elektronmikroskopie, Röntgen- und Neutronenbeugung sowie Ätzfigurentechnik der Metallphysik behandeln.

Der 2. Teil »Störungsempfindliche Eigenschaften« wird vom Hauptvortrag von P. HAASEN über »*Versetzungen und die Verformung der kubisch-raumzentrierten Metalle*« eingeleitet und von 30 Kurzvorträgen gefolgt, die einzelnen Problemen der Plastitizität, Diffusion, inneren Reibung, Erholung und Rekristallisation behandeln. In dieser Gruppe befinden sich noch drei größere Vorträge; H. BROSS: »*Einige Bemerkungen zur Theorie der elektrischen Leitungserscheinungen in idealen und gestörten Metallen*«; G. J. VAN DEN BER: »*Über den Einfluß kleiner Mengen von Übergangsmetallen auf verschiedene Eigenschaften der normalen Metalle bei niedrigen Temperaturen*« und Prof. N. E. ALEKSEEVSKIJ: »*Galvanomagnetische Eigenschaften von Metallen.*« Es folgen noch drei Vorträge über den Einfluß der Verunreinigungen auf die Streuprozesse.

Der 3. Teil (eigentlich theoretisches Seminar) beginnt mit zwei Hauptvorträgen: B. PEGEL: »*Zur thermisch aktivierten Verzetzungsbewegung*« und G. SAADA: »*Stacking faults in body centred cubic metals.*« Diesen folgen 7 Vorträge, die hauptsächlich die Eigenschaften von kubisch-raumzentrierten Metallen behandeln.

Den Band schließen 5 Vorträge aus dem Gebiet »Spezielle Halbleiterprobleme«, die sich mit der Dünnschichtproblematik von Galliumarsenid und Verwendung von Ätzverfahren beschäftigen.

Es soll bemerkt werden, daß der Band *Realstruktur und Eigenschaften von Reinststoffen* nicht als ein Nachschlagwerk betrachtet werden kann, sondern als ein Querschnitt der Problematik hauptsächlich der Metallphysik und Metallographie, der Fachleuten die auf diesem speziellen Gebiet arbeiten, einen guten Überlick über den Stand der Forschung vor zwei Jahren geben kann.

F. J. KEDVES

Kurt MISLOW: *Einführung in die Stereochemie.* Verlag Chemie G.m.b.H. 1967, 172 S.

Das Buch ist die deutsche Übersetzung der im Jahre 1965 erschienenen amerikanischen Publikation »*Introduction to Stereochemistry*«. Von der Originalausgabe weicht es insoweit ab, als der Verfasser diese Gelegenheit zur Abänderung einiger Fachausdrücke benutzte. So werden z. B. im ganzen Werk statt der unbequemen Ausdrücke »dissymmetrisch« und »nicht-dissymmetrisch« die Bezeichungen »chiral« und »achiral« geprägt. Außerdem werden die Ausdrücke »enantiomer« und »diastereomer« in Fällen, wo es sich um die Stereochemie der Umgebung eines Atoms handelt, durch die Ausdrücke »enantiotop« und »diastereotop« ersetzt.

Der erste Abschnitt (S. 1—42) trägt den Titel »*Struktur und Symmetrie*«. In diesem Teil wird die Geometrie der in Kohlenstoff-Verbindungen vorliegenden Bindungen behandelt, und es werden die Symmetrieelemente, die in den Molekülen auftretenden Spannungsenergien und die Molekül-Modelle dieser Verbindungen besprochen. Die Schwierigkeiten der Konstruktion dieser Modelle werden klar betont, und es wird festgestellt, daß stets nach der gewünschten Information diese oder jene Modellsätze zu verwenden sind.

Der zweite Abschnitt (S. 47—104) beschäftigt sich mit Fragen der Stereoisomerie. Hier werden die verschiedenen Arten der Strukturisomerie, die optische Aktivität, die Diastereomerie und die Torsions-Stereoisomerie sowie die mit dem asymmetrischen Kohlenstoffatom

zusammenhängenden Konfigurationsprobleme diskutiert. Makromoleküle werden besprochen, und ganz kurz die topologische Isomerie.

Der dritte Abschnitt des Werkes (S. 111—149) beschäftigt sich mit der Trennung und Konfiguration der Stereoisomeren. Dieser Themenkreis umfaßt die Trennung der Enantiomeren und Diastereoisomeren, die asymmetrische Synthese und die kinetische Racemat-Trennungsmethode sowie die absolute Konfiguration und die chemischen und physikalischen Methoden der Konfigurationsbestimmung.

Über die moderne Behandlungsweise und den Begriffreichtum hinaus ist es eines der Hauptverdienste des Buches, daß nach jedem Abschnitt eine Beispielsammlung gegeben wird. Die Lösung dieser Aufgaben vermittelt zweifelsohne ein tieferes Verständnis der Probleme. Am Ende des Buches liegen die Lösungen dieser Aufgaben vor, so daß der Leser seine eigenen Resultate kontrollieren kann.

Das vom didaktischen Standpunkt ausgezeichnet aufgebaute Buch ist eine wertvolle Hilfe zur Aneignung der stereochemischen Anschauungsweise.

Cs. SZÁNTAY

Fortschritte der Arzneimittelforschung (Herausgeber: E. JUCKER, Basel). Band 10. Birkhauser Verlag, Basel und Stuttgart, 1966

Der vor kurzem erschienene Band 10 der einen bedeutenden wissenschaftlichen Ruf erzielten Serie »*Fortschritte der Arzneimittelforschung*« entspricht wieder den nun schon ganz selbstverständlich gewordenen Erwartungen. Der Band bringt 9 ausgezeichnete Kapitel über die neuesten Ergebnisse der Arzneimittelforschung. Die ersten zwei von R. G. DENKEWALTER und M. TISCHLER bzw. von G. EHRHART verfaßten Abschnitte behandeln im wesentlichen die Geschichte und die Gesichtspunkte der Arzneimittelforschung, und die Fortschritte in ihrer Entwicklung. Beide sind interessante Lektüren, auch hinsichtlich des Rückblicks im Besitze unserer gegenwärtigen Kenntnisse auf frühere Ergebnisse der Arzneimittelforschung. J. H. BIEL und B. K. B. BLUM verfaßten einen der interessantesten pharmazeutisch-chemischen Abschnitte des Bandes: eine zeitgemäße Diskussion über die Chemie und Pharmakologie der Beta-Rezeptorblocker. Ein besonderes Verdienst des Abschnittes ist, daß darin die chemischen und pharmakologischen Gesichtspunkte, der Zusammenhang zwischen Wirkung und Struktur in einer geschlossenen Einheit, nach modernen Prinzipien behandelt werden. Der von C. A. WINTER verfaßte Abschnitt behandelt ein großes Gebiet der nicht zu den Steroiden gehörenden Antiphlogistika. In diesem Kapitel wird nur wenig über neue Arzneimittel berichtet, umso interessanter ist jedoch der Teil über die Biochemie der Entzündungen und über die Wertbestimmung der entzündunghemmenden Verbindungen. J. BÜCHI beschäftigt sich mit der Auswertung und der Wertbestimmung von Arzneimitteln, wobei auch die staatliche Arzneimittelkontrolle in einigen Ländern beschrieben wird. Dieser Abschnitt dürfte vor allem für Apotheker von großem Interesse sein. Diesem Thema schließt sich die kleine, 150 Seiten umfassende Monographie von K. MÜNZEL an, die einen ausgezeichneten, modern abgefaßten Überblick über die wichtige Rolle gibt, die der Formgebung zukommt, um aus der wirksamen Verbindung ein verwendbares Arzneimittel zu schaffen. Dies wird besonders für jene eine lohnende Lektüre sein, die sich mit der Synthese und Pharmakologie neuer Arzneimittel befassen, denn sie zeigt jene erhebliche Arbeit, die geleistet werden muß, um Chemikalien in Arzneimittel umzuwandeln. W. KUNZ gibt auch in diesem Band eine klar zu überblickende Beschreibung neuer Arzneimittel. Dieser Abschnitt ist den ähnlichen früher erschienenen insoweit wesentlich überlegen, daß hier solche neue Arzneimittel behandelt werden, die tatsächlich auch in den Verkehr gebracht wurden. Eine eingehende Analyse der zur selben Wirkungsgruppe gehörenden Verbindungen trägt viel dazu bei, um diesen regelmäßig erscheinenden Abschnitt der Fortschritte der Arzneimittelforschung noch anregender zu machen. Für die auf dem Gebiete der theoretischen Arzneimittelforschung tätigen wird gewiß der von E. J. ARIENS unter dem Titel »*Molekulare Pharmakologie als Grundlage der Arzneimittelplanung*« verfaßte Abschnitt einen der wertvollsten Kapitel des Buches darstellen. Die ausgezeichneten Beispiele, die leicht übersichtliche Einteilung, sowie die moderne Behandlungsweise tragen dazu bei, daß dieses Werk des auch international allgemein anerkannten Autors eine äußerst interessante und nützliche Lektüre bildet. Der von F. LABHARDT geschriebene Abschnitt über die klinische Verwendung der Psychopharmaka spricht vor allem die in der klinischen Pharmakologie tätigen an, doch wird dieser Abschnitt auch für Arzneimittelchemiker und Pharmakologen von großem Nutzen sein, da er zu einer guten praktischen Beurteilung der sich auch in der klinischen Praxis gut bewährten Psychopharmaka verhilft.

Wie stets, befriedigt die Ausstattung des Buches jeden Anspruch. Das Sachregister ist reichhaltig obzwar es noch erweitert werden könnte. Die Bände der Serie »*Fortschritte der Arzneimittelforschung*« befriedigen in jeder Hinsicht die Anforderungen der in der theoretischen oder praktischen Forschung tätigen Fachleute, sind zeitgemäß abgefaßt und sollten daher aus der Handbibliothek keines Arzneimittelforschers fehlen.

K. NÁDOR

S. HAUPTMANN: *Über den Ablauf organisch-chemischer Reaktionen.* Akademie-Verlag, Berlin 1967. 208 S. »Paperback«

Die erste Auflage dieses Buches von HAUPTMANN wurde bereits früher in unserer Zeitschrift besprochen [Acta Chim. Acad. Sci. Hung. 41, 471 (1964)]. Die zweite Auflage weicht von der ersten vor allem insoweit ab, daß in der Diskussion der Struktur von ungesättigten und aromatischen Verbindungen außer der Mesomerie-Theorie auch die Grundprinzipien der Molekülbahn- (MO) Theorie behandelt werden. Auch dieser neue Abschnitt enthält zahlreiche anschauliche Zeichnungen, die dem praktischen organischen Chemiker die Aneignung der Grundprinzipien der Theorie erleichtern. Diese Ergänzung ist mit Freude zu registrieren, da die Bedeutung der MO-Methode in den letzten Jahren stets stärker in den Vordergrund rückt, und ihre Diskussion selbst in einem Buch kleineren Umfangs heute nicht fehlen darf. Zum Abschluss bringt die neue Auflage ein ausführliches Literaturverzeichnis, welches den Lesern, die sich mit diesem Themenkreis eingehender befassen wollen, eine wertvolle Hilfe bietet.

Gy. DEÁK

INDEX

INORGANIC AND ANALYTICAL CHEMISTRY — ANORGANISCHE UND ANALYTISCHE CHEMIE — — НЕОРГАНИЧЕСКАЯ И АНАЛИТИЧЕСКАЯ ХИМИЯ

FEHÉR, I. and LŐRINC, M.: Reaction of Xenon Difluoride with Water (Short Communication) 329

MEZEI, M. and PULAY, P.: Calculation of Force Constants with the Maximum Overlap Method, II. Molecules with Lone Pair Electrons or Empty Orbitals (Short Communication) 331

PHYSICAL CHEMISTRY — PHYSIKALISCHE CHEMIE — ФИЗИЧЕСКАЯ ХИМИЯ

SOLYMOSI, F. and BÁNSÁGI, T.: The Thermal Stability of Chlorine Oxy-salts in the Solid State, II. Kinetic and Derivatographic Study of the Thermal Decomposition of Some Metal Chlorates 337

POKÓ, Z., FODOR, M. and SZABÓ, E.: On Some Properties of Uranium Trioxide Dihydrate (Short Communication) 357

ORGANIC CHEMISTRY — ORGANISCHE CHEMIE — ОРГАНИЧЕСКАЯ ХИМИЯ

MATKOVICS, B., ABOULEZZ, A. F., KATONA, F. and KOVÁCS, Ö. K. J.: Steroids, VIII. Syntheses of 2- and 4-CH_2-X Substituted Estrone-3-Alkyl Ethers 361

BARTÓK, M. and KOVÁCS, K.: Chemical Transformations of Diols and Cyclic Ethers, XXIV. Investigation of the Conversion of 2-monosubstituted Oxetanes in the Presence of Platinum Catalysts by the Microreactor Technique 369

BARTÓK, M. and KOZMA, B.: Chemical Transformations of Diols and Cyclic Ethers, XXV. Investigation of the Conversion of 3,3-dialkyloxetanes in the Presence of Platinum Catalysts by the Microreactor Technique 385

BARTÓK, M., KOVÁCS, K. and SHUIKIN, N. I.: Chemical Transformations of Diols and Cyclic Ethers, XXVI. Investigation of the Conversion of 2,4-Dialkyl-substituted Oxetanes in the Presence of Platinum Catalyst by the Microreactor Technique 395

HIDEG, K. and HIDEG-HANKOVSZKY, O.: Benzazepines, II. Preparation and Reactions of 2,3-dihydro-6,7-benzo-(1,5)-thiazepines 405

RANGASWAMY, M. and SANTAPPA, M.: Oxidation of Aldehydes by Aqueous Ceric Ions in Perchloric Acid 413

Book Reviews — Buchbesprechungen — Рецензии книг 423

Printed in Hungary

A kiadásért felel az Akadémiai Kiadó igazgatója — Műszaki szerkesztő: Farkas Sándor

A kézirat nyomdába érkezett: 1968. III. 26. — Terjedelem: 9,75 (A/5) ív, 79 ábra

68.65357 Akadémiai Nyomda, Budapest — Felelős vezető: Bernát György

ACTA CHIMICA

ТОМ. LVI — ВЫП 4

РЕЗЮМЕ

Термическая стабильность солей с анионами, содержащими кислород и хлор, в твердом состоянии, II. Кинетическое и дериватографическое изучение термического разложения хлоратов некоторых металлов

Ф. ШОЙМОШИ и Т. БАНШАГИ

Изучались кинетика и механизм термического разложения хлоратов натрия, бария и свинца. Термическое поведение этих хлоратов (температура, продукты и кинетика разложения) сильно зависит от природы катиона. Их стабильность уменьшается в вышеупомянутом порядке. Параллельно с разложением протекает — уже в малой степени и до разложения — диспропорционирование хлоратов натрия и бария. В случае хлората свинца, образование перхлората не было обнаружено, а вещество взрывалось при повышенных температурах. На основе кинетических данных и физических свойства веществ обсуждается механизм разложения и диспропорционирования.

Стероиды, VIII. Синтезы 3-алкильных эфиров 2- и 4-CH_2-X — замещенных эстрона

Б. МАТКОВИЧ, А. Ф. АБУЛЕЗ, Ф. КАТОНА и Э. К. Й. КОВАЧ

Из смеси, полученной при хлорметилировании 3-метилового и 3-циклопентилового эфиров эстрона удалось выделить его замещенные 2- и 4-изомеры в виде различных производных, а именно диметиламинометил-, пиперидинометил-, морфолинометил-, ацетоксиметил-, гидроксиметил- и метоксиметил-производных.

Изучение химических превращений диолов и циклических эфиров, XXIV. Исследование превращений 2-монозамещенных оксетанов на платиновом катализаторе с помощью микрореакторной техники

М. БАРТОК и К. КОВАЧ

С помощью микрореакторной техники исследовались превращения 2-монозамещенных (метил, *н.* пропил-, изопропил-, *н.* бутил-, циклогексил-, фенил-) оксетанов на платиновом катализаторе, нанесенном на термолит и углерод, в присутствии водорода и гелия, в интервале температур 200—400° С. В изученных условиях главными направлениями превращений оксетанов являются изомеризация, приводящая к образованию альдегидов и кетонов, и разложение, приводящее к образованию олефинов и формальдегида. Отношение альдегидов к кетонам равно 5:1. Первичные процессы сопровождаются различными вторичными превращениями. Определялась зависимость степени превращения оксетанов и направления протекающих процессов от различных параметров: носитель, температура, газ-носитель, природа заместителя.

Исследование химических превращений диолов и циклических эфиров, XXV. Исследование превращений 3,3-диалкил-оксетанов на платиновых катализаторах с помощью микрореакторной техники

М. БАРТОК и Б. КОЗМА

С помощью микрореакторной техники изучались превращения 3,3-диалкилоксетанов (диметил, диэтил, метил-*н.* пропил, этил-*н.* бутил) на платиновом катализаторе, нанесенном на термолит или углерод, в присутствии водорода, в интервале температур 220—350° С. При изученных условиях оксетаны претерпевают следующие главные превращения: изомеризация, приводящая к образованию альдегидов, и разложение, приводящее к образованию олефинов и формальдегида. Эти первичные процессы сопровождаются некоторыми вторичными превращениями. Были сделаны заключения о влиянии экспери ментальных условий на степень превращения и на направление протекающих процессов.

Изучение химических превращений диолов и циклических эфиров, XXVI. Изучение превращений 2,4-диалкилзамещенных оксетанов на платиновых катализаторах с помощью микрореакторной техники

М. БАРТОК, К. КОВАЧ и Н. И. ШУЙКИН

С помощью микрореакторной техники изучались превращения, наблюдаемые для смеси цис- и трансизомеров 2,4-диалкил-оксетанов (метил-этил, метил-н. бутил, метилциклогексил) на платиновых катализаторах, нанесенных на термолит или углерод, в присутствии гелия и водорода как газов-носителей, в интервале температур 200—350° С. В зависимости от экспериментальных условий — катализатор, температура, газноситель, структура оксетана — изучались степень превращения оксетанов и направление протекающих процессов. Основными направлениями превращений 2,4-диалкилоксетанов в изученных условиях являются образование изомерных кетонов в результате разрыва двух С—О связей (60—70%), а также термическое разложение, связанное с образованием олефинов и соответствующих альдегидов (30—40%). Первичные процессы — в зависимости от экспериментальных условий — могут сопровождаться некоторыми вторичными превращениями.

Бензазепины, II.

К. ХИДЕГ и О. Х. ХАНКОВСКИ

Описывается общий синтез 2,3-дигидро-6,7-бензо(1,5)-тиазепинов. Орто-аминотиофенол реагирует с аминокетонами с открытой цепочкой или с алициклическим кольцом, получаемыми по реакции Манниха, с хорошим выходом, причём образуется с выделением воды и соли амина дигидро-тиазепин. При восстановлении дигидро-производных с помощью $NaBH_4$ и $LiAlH_4$ получаются 2,3,4,5-тетрагидропроизводные. Восстановленные продукты могут быть ацигированы хлоридами кислот до 5-ацил-производных. Тетрагидробензтиазепин в 1,1-диокси-2,3,4,5-тетрагидро-бензтиазепин с помощью H_2O_2 окисляется.

Окисление альдегидов с помощью акво-ионов церия в хлорной кислоте

М. РАНГАСВАМИ и М. САНТАППА

Изучалась кинетика окисления ацетальдегида (при 13, 20 и 25° С) и хлоральгидрата (при 40, 45 и 50° С) под действием перхлората церия в хлорнокислой среде ($[H^+]$ — 0,1—1,0 М). За реакцией следили, определяя скорости исчезновения церия при различных концентрациях $[Ce^{4+}]$, [альдегид], $[H^+]$, а также при различных ионной силе μ, температуре и т. д. Проводился анализ продуктов и была определена стехиометрия $\Delta Ce^4 / \Delta$ ацетальдегид ≈ 2. Было найдено, что эта реакция является реакцией второго порядка — и первого порядка по отношению к отдельным $[Ce^{4+}]$ и [альдегид]. Не было найдено никаких доказательств существования комплекса между Ce^{4+} и альдегидами. Полагалось, что активными частицами являются Ce^{4+} (aq) и диол альдегида. Изменения скорости окисления сопоставлялись со структурой. Были рассчитаны и обсуждались константы скорости и их термодинамические параметры. Данная работа по окислению формальдегида с помощью Ce^{4+} в $HClO_4$ является продолжением и расширением работ Харгревса и Сатклиффа, особенно в отношении оценки скоростей и термодинамических данных.

The Acta Chimica publish papers on chemistry in English, German, French and Russian.

The Acta Chimica appear in volumes consisting of four parts of varying size, 4 volumes being published a year.

Manuscripts should be addressed to

Acta Chimica
Budapest 502, Postafiók 32.

Correspondence with the editors should be sent to the same address.

The rate of subscription is 165 forints a volume. Orders may be placed with "*Kultúra*" Foreign Trade Company for Books and Newspapers (Budapest I., Fő utca 32. Account No. 43-790-057-181) or with representatives abroad.

Les Acta Chimica paraissent en français, allemand, anglais et russe et publient des mémoires du domaine des sciences chimiques.

Les Acta Chimica sont publiés sous forme de fascicules. Quatre fascicules seront réunis en un volume (4 volumes par an).

On est prié d'envoyer les manuscrits destinés à la rédaction à l'adresse suivante:

Acta Chimica
Budapest 502, Postafiók 32.

Toute correspondance doit être envoyée à cette même adresse.

Le prix de l'abonnement est de 165 forints par volume.

On peut s'abonner à l'Entreprise pour le Commerce Extérieur de Livres et Journaux «*Kultúra*» (Budapest I., Fő utca 32. Compte-courant No. 43-790-057-181) ou à l'étranger chez tous les représentants ou dépositaires.

«*Acta Chimica*» издают трактаты из области химической науки на русском, французском, английском и немецком языках.

«*Acta Chimica*» выходят отдельными выпусками разного объема. 4 выпуска составляют один том. 4 тома публикуются в год.

Предназначенные для публикации рукописи следует направлять по адресу:

Acta Chimica
Budapest 502, Postafiók 32.

По этому же адресу направлять всякую корреспонденцию для редакции.

Подписная цена «*Acta Chimica*» — 165 форинтов за том. Заказы принимает предприятие по внешней торговле книг и газет «*Kultúra*» (Budapest I., Fő utca 32. Текущий счет № 43-790-057-181) или его заграничные представительства и уполномоченные.

44,— Ft

Reviews of the Hungarian Academy of Sciences are obtainable at the following addresses:

ALBANIA

Ndermarja Shtetnore e Botimeve
Tirana

AUSTRALIA

A. Keesing
Box 4886, GPO
Sydney

AUSTRIA

Globus Buchvertrieb
Salzgries 16
Wien I

BELGIUM

Office International de Librairie
30, Avenue Marnix
Bruxelles 5

Du Monde Entier
5, Place St. Jean
Bruxelles

BULGARIA

Raznoiznos
1, Tzar Assen
Sofia

CANADA

Pannonia Books
2, Spadina Road
Toronto 4, Ont.

CHINA

Waiwen Shudian
Peking
P. O. B. 88

CZECHOSLOVAKIA

Artia
Ve Směčkách 30
Praha 2

Poštová Novinová Služba
Dovoz tisku
Vinohradská 46
Praha 2

Mad'arská Kultura
Václavské nám. 2
Praha I

Poštová Novinová Služba
Dovoz tlače
Leningradská 14
Bratislava

DENMARK

Ejnar Munksgaard
Nörregade 6
Copenhagen

FINLAND

Akateeminen Kirjkauppa
Keskuskatu 2
Helsinki

FRANCE

Office International de Documentation et Librairie
48, rue Gay Lussac
Paris 5

GERMAN DEMOCRATIC REPUBLIC

Deutscher Buch-Export und Import
Leninstraße 16
Leipzig 701

Zeitungsvertriebsamt
Clara Zetkin Straße 62
Berlin N. W.

GERMAN FEDERAL REPUBLIC

Kunst und Wissen
Erich Bieber
Postfach 46
7 Stuttgart S.

GREAT BRITAIN

Collet's Holdings Ltd.
Dennington Estate
London Rd.
Wellingborough. Northants.

Robert Maxwell and Co. Ltd.
Waynflete Bldg. The Plain
Oxford

HOLLAND

Swetz and Zeitlinger
Keizersgracht 471—487
Amsterdam C.

Martinus Nijhof
Lange Voorhout 9
The Hague

INDIA

Current Technical Literature
Co. Private Ltd.
India House OPP
GPO Post Box 1374
Bombay I

ITALY

Santo Vanasia
Via M. Macchi 71
Milano

Libreria Commissionaria Sansoni
Via La Marmora 45
Firenze

JAPAN

Nauka Ltd.
92, Ikebukur O-Higashi 1-chome
Toshima-ku
Tokyo

Maruzen and Co. Ltd.
P. O. Box 605
Tokyo-Central

Far Eastern Booksellers
Kanda P. O. Box 72
Tokyo

KOREA

Chulpanmul
Phenjan

NORWAY

Johan Grundt Tanum
Karl Johansgatan 43
Oslo

POLAND

RUCH
ul. Wronia 23
Warszawa

ROUMANIA

Cartimex
Str. Aristide Briand 14—18
Bucureşti

SOVIET UNION

Mezhdunarodnaya Kniga
Moscow G—200

SWEDEN

Almquist and Wiksell
Gamla Brogatan 26
Stockholm

USA

Stechert Hafner Inc.
31, East 10th Street
New York, N. Y. 10003

Walter J. Johnson
111, Fifth Avenue
New York, N. Y. 10003

VIETNAM

Xunhasaba
19, Tran Quoc Toan
Hanoi

YUGOSLAVIA

Forum
Vojvode Mišića broj 1
Novi Sad

Jugoslovenska Knjiga
Terazije 27
Beograd

18. VII. 1968. Index: 26.007